q-deformed LQG in three dimensional space-time

by

Qiaoyin Pan

A thesis
presented to the University of Waterloo
in fulfillment of the
thesis requirement for the degree of
Doctor of Philosophy
in
Applied Mathematics

Waterloo, Ontario, Canada, 2022

Examining Committee Membership

The following served on the Examining Committee for this thesis. The decision of the Examining Committee is by majority vote.

External Examiner: **Eugenio Bianchi**
Associate Professor, Dept. of Physics
Pennsylvania State University

Supervisors: **Maïté Dupuis**
Research Assistant Professor, Dept. of Applied Mathematics
University of Waterloo

Florian Girelli
Associate Professor, Dept. of Applied Mathematics
University of Waterloo

Internal Member: **Eduardo Martín-Martínez**
Associate Professor, Dept. of Applied Mathematics
University of Waterloo

Ghazal Geshnizjani
Research Assistant Professor, Dept. of Applied Mathematics
University of Waterloo

Internal-External Member: **Bianca Dittrich**
Faculty, Perimeter Institute for Theoretical Physics
Adjunct Faculty, Department of Physics and Astronomy
University of Waterloo

Author's Declaration

This thesis consists of material all of which I authored or co-authored: see Statement of Contributions included in the thesis. This is a true copy of the thesis, including any required final revisions, as accepted by my examiners.

I understand that my thesis may be made electronically available to the public.

Statement of Contributions

Section 2.3 – 2.4 and part of Section 2.5 are based on [77] co-authored with Maïté Dupuis and Etera Livine.

Section 2.3, Chapter 3 – 5 are based on [41] co-authored with Valentin Bonzom, Maïté Dupuis and Florian Girelli.

Chapter 6 is based on [42] co-authored with Valentin Bonzom and Maïté Dupuis.

Chapter 7 is based on a not-yet-published work [137] with Etera Livine.

Abstract

Loop quantum gravity (LQG) is a canonical, background-independent and non-perturbative approach to quantum gravity. This thesis is devoted to studying three-dimensional (3D) quantum gravity with a non-vanishing cosmological constant Λ in the LQG approach. In particular, we focus on the case of Λ negative in the Euclidean signature where the isometry group is $\mathrm{SL}(2,\mathbb{C})$. We construct the *q-deformed LQG model* with the real deformation parameter q encoding the value of $|\Lambda|$. In this model, the kinematical and physical Hilbert spaces of gravity exhibit the quantum group symmetries consistent with other approaches to 3D quantum gravity. The LQG model with $\Lambda = 0$ is recovered at $q \to 1$. This quantum gravity model is derived from the classical theory using the standard canonical quantization program *à la* Dirac and the mathematical connection between quantum groups and Lie bialgebras. We establish this model first in terms of the holonomy-flux algebra and then in terms of spinors, which are purely geometrical objects. We write the quantum Hamiltonian constraint with spinors and recover the Turaev-Viro amplitudes defined in the spinfoam model, which is a covariant approach to quantum gravity written in a discrete path integral formalism. We also use spinors to reconstruct the spinfoam model in a way that the local building blocks to construct global 3D geometry are conformal. This is done for the $\Lambda = 0$ case as a first step. The q-deformed LQG model is topological and describes the curved geometries in 3D as well as on 2D spatial surfaces. It is expected to serve as a better starting point to connect LQG with other quantum gravity approaches and generalize to 4D LQG with a non-vanishing Λ.

Acknowledgements

First of all, I would like to express my deepest gratitude to my supervisors Maïté and Etera Livine. Maïté has been giving me great support at every step throughout my Ph.D., both academically and mentally. This journey would have been much harder without her help, encouragement and kindness. Etera is not listed as my official supervisor but it is his continuous supervision that pushes me to dig into math and physics deeper and deeper. I am often inspired by his insights and perspective on quantum gravity and more generally physics. Every time I discussed with Etera, I learned new things and/or realized my ignorance of some knowledge I thought I understood. Etera has been guiding me in many ways and words can not express my gratefulness.

I would also like to thank my co-supervisor Florian. Discussing with him is always joyful and I often learned from his intuitions about math and physics. He has been helping me a lot in writing this thesis and preparing for talks.

Thanks should also go to all my examination committee members Eduardo Martin-Martinez, Ghazal Geshnizjani, Bianca Dittrich and Eugenio Bianchi for taking the time to read this thesis and for constructive criticism.

Many thanks to my collaborator Valentin Bonzom. Every Zoom meeting with him is fun. I am really appreciative that he spent time discussing many details about our work and checked carefully my calculations to help me ensure their correctness.

Also thanks to the quantum gravity research group at Perimeter Institute. The group meetings and seminars have been very well organized and they always remind me of many fundamental questions on quantum gravity and keep me up with the frontiers of the field. Thanks to my peers Johanna Borissova, Ding Jia and José de Jesús Padua Argüelles for organizing and joining the quantum gravity journal club, which has been very interesting and helpful.

And of course thanks to my colleagues and friends at PI especially Lei, Finn and Victor. I had a very enjoyable time every time of our gathering. Their friendship makes my life in Waterloo more fun. Also thanks to Christophe Goeller and Qian Chen for accompanying and support during my time in Lyon. Special thanks to Ue-Li who often treat me to good food and gave me the unicycle.

Lastly, thanks to my family for all-time support despite the long departure. Finally, thanks to my boyfriend Qizhong. He has been able to cheer me up an endless amount of times during my Ph.D without fading out. His support makes me what I am today.

Table of Contents

Chapter 0

Introduction

In search of Quantum Gravity

The development of quantum mechanics and quantum field theories conveys a message that nature is fundamentally quantum. Within the framework of these quantum theories, electromagnetism, weak interactions and strong interactions can be described consistently. Moreover, the quantum theories of these three interactions are successful in describing the standard model of elementary particle physics, which is proven in experiments with high accuracy. In the spirit of unification, gravity, as the fourth interaction, ought to be described within the quantum framework hence by a quantum gravity theory.

The search for quantum gravity is not only to fulfill the unification dream but also necessary to understand some of the most challenging problems in physics. Some concrete yet far-from-complete arguments that motivate the necessity of searching for quantum gravity are listed in the following. Interested readers can refer to *e.g.* [202, 134, 138] for other motivations and *e.g.* [181] for a historical review on the search of quantum gravity.

- **Incompleteness within general relativity**

  Gravity is a field theory of spacetime metrics. According to Lovelock's theorem [146], in three and four dimensions, the only possible equation of motion from a second-order Lagrangian of metrics is the Einstein equation. This picks out general relativity to be the classical theory of gravity at least in three and four dimensions. General relativity itself is an incomplete theory due to the existence of singularities, where curvature blows up. Examples include the Big Bang, which is believed to be the origin of the universe, and the singularity inside black holes. Non-negligible quantum

fluctuations and gravitational effects are expected to occur in these spacetime regions. It is believed that a valid quantum gravity theory can explain the physics within the Planckian regime, where quantum effects are comparable to gravitational effects.

In recent years, the searching for quantum gravity effects is not only on short distances and the UV regime but also on long distances and the IR regime [94, 32]. For instance, the programs of celestial holography [176] and the infrared triangle program for low-energy gravity relating the asymptotic symmetries, gravitational memory effect and soft theorem developed in recent years [195] could predict low-energy quantum gravity signatures.

- **Failure to apply perturbative quantum field theory on flat spacetime**

  On the other hand, in quantum field theory, divergencies appear when one does perturbation theory. Renormalization methods can address this problem, which absorbs the infinities by redefining a few measurable quantities. These methods work for all the operators relevant to the standard model of particle physics. However, when one attempts to construct a field theory for gravity perturbatively in the same way, *i.e.* treating the metric as a perturbation of the Minkowski metric, the correlation functions turn out to be nonrenormalizable [197, 198, 64]. This means one needs to determine infinitely many parameters to define quantum gravity perturbatively.

  Secondly, general relativity is a geometric theory of spacetime. However, the conventional quantum field theories inevitably rely on a background spacetime which is taken classically. Following this idea, quantizing gravity means quantizing the background itself which is difficult to interpret physically, hence a background-dependent quantization seems to be a blind alley. Thirdly, the symmetry of gravity is diffeomorphism invariance. This means observables can be non-local, which are not defined in local field theories like the quantum field theories. Last but not least, in the framework of quantum field theory, the evolution of a field is governed by the Hamiltonian. However, the naturally defined Hamiltonian of gravity is zero on-shell, making the evolution of a gravitational system ill-defined conventionally. These problems suggest that a more indirect way of quantizing gravity is needed.

- **Black hole issues**

  It was proven in the 70s that a black hole solution to the Einstein-Maxwell equation in general relativity can be completely characterized by its mass, angular momentum and charge, and all other information is hidden behind the horizon. This is the well-known *No-hair Theorem* [154]. This implies that information would disappear by being swallowed by a black hole, which violates the inference from the unitarity

postulate that information carried by wave functions should be conserved quantum mechanically. It was later discovered that black holes can have "soft hair" containing an infinite number of conserved charges [131, 130]. However, the information paradox is still unsolved. This puzzle suggests that a resolution should come from a theory combining quantum theory and general relativity. In this sense, black holes can serve as a testing ground to test quantum gravity theory candidates.

The recent experimental results on detecting gravitational waves and imaging black holes [1, 4, 5] encourage that testing quantum gravity experimentally is not far from being possible. It brings excitement to the research of quantum gravity in the current era.

Due to the fact that general relativity and quantum theory are in conflict with each other at the fundamental level, it is necessary to place both theories in the same framework, with the recovery of either theory in some limits. Different approaches have been proposed to reach this goal, *e.g. string theory* [31, 171, 172], *Anti-de Sitter/conformal field theory* (AdS/CFT) [211, 65, 156], *loop quantum gravity* (LQG) [200, 182, 16], *spinfoam models* [21, 168, 138], *non-commutative geometry* [57, 56], *causal dynamical triangulations* [9, 145], *causal sets* [196, 70], *asymptotic safty* [208, 157] *etc.* Reviewing all of these approaches is out of the scope of this thesis. See *e.g.* [164, 11] for reviews and talks from experts in different fields.

Loop quantum gravity and spinfoam models

The focus of this thesis is mainly on the LQG approach and we will also discuss a particular application of the spinfoam model. In fact, these two approaches are highly entangled and some literature views spinfoam models as part of the LQG framework. LQG and spinfoam merge the principles of quantum theory and general relativity harmonically, taking the principles of both theories to be fundamental and building quantum gravity theories on top of it. By considering gravity as being dynamical, they attempt to quantize the spacetime geometry and describe spacetime dynamics quantum mechanically. They preserve the main feature of general relativity — background independence, and they are non-perturbative approaches. The main difference between these two approaches is that LQG follows the canonical description of quantum mechanics while spinfoam models follow the path integral description and hence are covariant formalisms. Canonical means we take a space-time splitting and first construct the kinematical structure on the spatial surface then analyze its dynamics along time.

The main merit of LQG is that it provides a mathematically well-defined and rigorous framework to build up the Hilbert space and states of quantum geometry. It leads to the

prediction that spacetime geometries are intrinsically distinct at the Planck scale. The method of LQG has been applied to cosmology (called *loop quantum cosmology* or LQC), one inviting result of which is the avoidance of curvature singularity at the origin of the universe, replaced by a "bounce". (See [36, 18] for reviews.) However, LQG is still far from complete. There are many important pieces to be given, for instance, the precise form of the quantum hamiltonian, a proper (semi-)classical limit recovering the low energy physics, and practical measurable observables. For reviews, see *e.g.* [201, 17]. Many of the unsolved questions are due to the complexity of 4D spacetime. It is then natural to work on a simpler system that captures the important features of 4D gravity while reducing the computational difficulties. The hope is that studying such a simple gravitational system could help us understand the conceptual problems and teach us new techniques to analyze the real physical system. 3D gravity with 2 dimensions in space and 1 dimension in time is such a candidate.

3D gravity and 3D LQG

As a topological theory, 3D gravity is simple enough to allow us to do exact computations. The main drawback is that the dynamics of 3D gravity is authentically different from that of 4D gravity since there are no local degrees of freedom, or gravitational waves, in 3D gravity. On the other hand, it still carries many of the fundamental issues of quantum gravity *e.g.* the problem of time, the construction of quantum states and observables, inclusion of a cosmological constant and relations between different quantization approaches. 3D gravity has been proving instructive insights for the development of LQG and the spinfoam models.

The vast interest to study 3D gravity was first brought by the seminal work [63, 62] of Deser, Jackiw and 't Hooft, where they studied particles coupling with gravity and particle interactions in the gravitational field with and without a cosmological constant. It was later discovered by Achúcarro and Townsend [2] then elaborated by Witten [209] that 3D gravity can be written as a Chern-Simons action. Quantizing 3D gravity can then refer to the quantization techniques of Chern-Simons theory developed in mathematics and condensed matter.

On the other hand, 3D gravity in the absence of a cosmological constant Λ, up to the second-order derivative of metric and boundary terms, can also be formulated as a BF action [133, 35, 34], which also describes a topological invariant theory. The BF formulation of 3D gravity is the starting point of 3D LQG and spinfoam models. The isometry group of 3D gravity with $\Lambda = 0$ in Lorentzian signature is $\mathrm{ISO}(2,1)$. However, the non-compactness of $\mathrm{ISO}(2,1)$ makes it complicated to construct a quantum representation

theory. It is then common to work in the Euclidean signature instead, which is to treat the spacial and temporal dimensions equally. This turns the isometry group to ISO(3) which is isomorphic to $\mathrm{SO}(3) \ltimes \mathbb{R}^3$. Furthermore, in building the quantum theory, one makes use of the irreducible representations of the compact subgroup SO(3), which are integer spin representations $j = 0, 1, 2, \cdots$. In order for fermions to couple with the framework, one also considers the double cover SU(2) of SO(3) so that the irreducible representation runs over all half integers. This is a common treatment in physics and is also what we will apply in this thesis. Therefore, for the case of $\Lambda = 0$ in the Euclidean signature, we deal with the Poincaré group ISU(2).

In the LQG framework, a Hilbert space of a graph *i.e.* collections of 0D nodes, 1D links and 2D faces embedded on a 2D spacial surface is constructed at the kinematical level. This Hilbert space is spanned by the so-called *spin network states* which are labelled by spins associated to all the links of the graph. In the past two decades, many works *e.g.* [104, 105, 97, 162, 161, 152, 189] have been done to understand the kinematical and dynamical aspects of 3D LQG with $\Lambda = 0$, its geometrical interpretation and its relation to spinfoam models.

Inclusion of a non-vanishing cosmological constant

However, the appearance of the cosmological constant Λ which is taken as a coupling constant in both LQG and spinfoam models, adds a volume term in the BF action. It complexifies the structure and brings obstacles to quantization. Nevertheless, it is essential to include a $\Lambda \neq 0$ in a quantum gravity model in order to give an instructive guide for applying it to the cosmological model. This is because observations have established that our universe is acceleratedly expanding. This result is under the framework of the ΛCDM model with a positive Λ. Moreover, since 3D LQG provides a clear mathematical framework for constructing dynamics of quantum gravity and it can be extended to 4D, it is important to understand how a non-zero Λ is incorporated in the 3D LQG framework.

Before we dig into the LQG construction, one can take lessons from other approaches of 3D quantum gravity with $\Lambda \neq 0$ and gain insights from them. The most successful way to quantize 3D gravity is based on the Chern-Simons formalism, which is so powerful that it provides a uniform formulation for Euclidean and Lorentzian signatures and different signs of cosmological constants. The quantization has been performed through the path integral method [210, 177] or the combinatorial quantization method [7, 8]. Both results have revealed that quantum group [149, 58] structures show up when $\Lambda \neq 0$ as the deformation of group symmetries in the $\Lambda = 0$ theory and Λ is encoded in the deformation parameter. This is consistent with the results from the first-ever spinfoam model for 3D Euclidean

gravity with a $\Lambda \neq 0$ — the *Turaev-Viro model* [204], which is a deformed version of the *Ponzano-Regge model* [174] for $\Lambda = 0$. These results provide some guidances for the LQG model we are looking for.

Inspired by this prospect, it was proposed in [158, 159] to define non-commutative quantum operators in constructing the quantum dynamics within the LQG framework, which does lead to desired quantum group feature. However, it appears as regularization and it is not clear from what principles one should introduce such a deformation. A few years later, a revisit of the kinematical (discrete) phase space in the work of [40] conveyed the idea that one can study the "classical limit" of some quantum groups — Lie bialgebra and reformulate the classical theory in this new mathematical framework. This successfully reproduces the quantum group symmetry in the Turaev-Viro model upon a natural quantization process [39]. It was recently realized [72] that one can even start from the action principle and go through the steps in the LQG scheme to obtain the known quantum group structures. The theme of this thesis is to further develop this approach and understand both the classical and quantum structures of this framework. We call this framework the q-deformed LQG, where q is a deformation parameter encoding the value of the cosmological constant.

Spin and spinor representations of LQG

Returning to the case of $\Lambda = 0$, the quantum theory of the original LQG relies on the SU(2) irreducible representations — spins. These spins give the eigenvalues of link operators. In the geometrical picture, the building blocks of global geometry are the Planck-scale links. This can be extended to the $\Lambda \neq 0$ case which is the perspective taken in the work of [40, 39]. In this formalism, the basic variables are holonomies on links and their conjugated momentum — fluxes.

Alternatively, one can describe the same quantum geometries for $\Lambda = 0$ in terms of a pair of harmonic oscillators which defines (quantum) spinors [118, 142, 143]. The spinors here are purely geometrical objects and should not be confused with the spinors used in describing particles. To emphasize this point, we refer to this reformulation of LQG as the spinorial, or spinor, representation. Contrary to spins, the use of spinors allows us to shift the view to building up global geometry with Plank-scale 3D blocks. This viewpoint has been established in the U(n) formalism of LQG [98, 99, 50]. These spinors are also useful tools to define the so-called SU(2) *coherent states*, which have shown advantages in constructing the spinfoam model and studying the semi-classical limit [82, 96, 141]. In addition, the fact that spinors are associated to nodes instead of links brings benefits

in constructing local observables which form a closed algebra [98, 144, 120]. These local observables have been used to formulate the dynamics of LQG [44].

Keeping these upsides of spinor representation in mind, we would like to extend them to the $\Lambda \neq 0$ case that is compatible with the framework of [40, 39]. This has been initiated in the work of [79], which focused on the classical aspect. The quantum spinors and observables constructed with them have nevertheless been considered in some previous works [80, 81]. The derivation of them from the classical spinors is one of the key results of this thesis. Studying these spinors could potentially provide a route to relate LQG with other approaches when $\Lambda \neq 0$ and deepen our understanding of the quantum nature of geometries.

Plan of this thesis

This thesis is organized into seven chapters as follows.

Chapter 1-3 describe the classical aspects. In Chapter 1, we briefly review general relativity with a cosmological constant included. We focus on the first-order formalism — BF action of 3D gravity and perform the canonical analysis on this action. We also concisely review the Chern-Simons formalism of 3D gravity as a prelude to some analysis in later chapters. Chapter 2 describes the classical structure of the q-deformed LQG framework. We start by reviewing the derivation from the first-order action, then focus on illustrating the discrete phase space structure of the classical model in terms of the deformed fluxes and holonomies. We also build an exact link to the classical phase space in the combinatorial quantization approach in an explicit setup. This is based on [77]. In Chapter 3, we revisit the classical phase space of the q-deformed LQG in the spinor representation. We introduce the deformed spinors and use them to construct (kinematical) local observables. This chapter is mainly based on [41].

Chapter 4-6 describe the quantum theory of the q-deformed LQG. In Chapter 4, we first summarize the definitions and necessary mathematical properties of the quantum groups relevant to this model. We then apply the natural quantization on the classical deformed fluxes and holonomies described in Chapter 2 and construct the kinematical Hilbert space. In parallel with this, Chapter 5 is on the quantization of the classical structure in Chapter 3. Apart from constructing the quantum deformed spinors and building quantum observables out of them, we extract the geometrical interpretation of the $\mathcal{R}$-matrix, which is an inbuilt mathematical structure for some quantum group, within the spinorial representation of the q-deformed LQG. This is a new discovery at least to the LQG community. Chapter 4 and 5 are mainly based on [41]. Chapter 6 focuses on the dynamics of the q-deformed LQG. We

specify the quantum Hamiltonian constraint in terms of the spinor representation. We then solve the constraint for the physical states in the physical Hilbert space. We examine these states by showing their invariance under the Pachner moves, which is a discrete version of diffeomorphism. This chapter is based on [42].

Finally, Chapter 7 is about an application of quantum spinors in the spinfoam model. The goal is to construct the spinfoam model purely with spinors. In this chapter, we consider the $\Lambda = 0$ case which has not been established in the literature yet. As the spinfoam model was not described in detail before this chapter, we start with a short review of the Ponzano-Regge model which is formulated as a state-sum in terms of spin representations of SU(2). It is followed by the introduction of the coherent states defined with (non-deformed) spinors. We end up with a state-integral reformulation of the Ponzano-Regge model where spins are all eliminated and only spinors are involved. We prove the topological invariance of this formalism and study its geometrical interpretation. This chapter is based on [137].

This thesis is supplied with two appendix chapters. Appendix A contains the concise summaries of the mathematical frameworks for the classical phase space and the quantum Hilbert space of the q-deformed LQG model. Appendix B collects some lengthy calculation details and a toy model example of the q-deformed LQG phase space.

Chapter 1

3D gravity with a cosmological constant

General relativity is a highly nonlinear theory, which brings obstacles to quantization compared to other systems *e.g.* electrodynamics. Therefore, it is natural to consider a computation-wise simpler system that allows us to tackle conceptual questions relevant to quantum gravity such as the problem of time, unitarity, causality, topology change and to study the relation between different quantization approaches. Three-dimensional (3D) gravity, as a topological field theory, is such a system.

3D gravity can be written, at the first (derivative) order of the metric, as a *BF theory* [133, 34, 35]. BF theory is a class of topological field theory that has been extensively studied, especially for gravity, since it provides an arena for different quantization approaches of gravity such as LQG (see *e.g.* books [200, 182] and a recent review [15]), spinfoam models (see *e.g.* [21, 168, 138] for review) and the group field theory approach (see *e.g.* [165, 87, 166]).

In this section, we review classical gravity theory with a non-vanishing cosmological constant. We start from the Einstein-Hilbert action in Section 1.1, then define its first-order formulation in the 3D case in Section 1.2. In Section 1.3, we apply the Hamiltonian analysis to the first-order system and extract the constraint algebra in the standard manner (compared to the treatment in Chapter 2). We close this chapter, with Section 1.4, rewriting 3D gravity into the Chern-Simons formulation, which builds the classical connection between the LQG formalism and the combinatorial quantization [85, 7, 8] of 3D quantum gravity.

1.1 General relativity with a cosmological constant

We start from the Einstein-Hilbert action for a D-dimensional manifold $\mathcal{M}$ (without matter or boundaries). For unification purposes, we write the action for both Lorentzian ($s = -$) and Euclidean ($s = +$) signatures.

$$S_{\mathrm{EH}}[g_{\mu\nu}] = \frac{1}{16\pi \mathrm{G}} \int_{\mathcal{M}} \mathrm{d}^D x \sqrt{sg}(R - 2\Lambda)\,, \tag{1.1}$$

where G is the gravitational constant (for D-dimensional gravitational system), R is the Ricci scalar and Λ is the cosmological constant.

Consider a boundary $\partial\mathcal{M}$ of the manifold $\mathcal{M}$. Denote the induced metric on $\partial\mathcal{M}$ by $h_{\mu\nu}$ and its determinant by h. A boundary term

$$S_{\partial\mathcal{M}} = \int_{\partial\mathcal{M}} \mathrm{d}^{D-1} x \sqrt{sh}\mathcal{L}_{\partial\mathcal{M}}$$

should be added to the action (1.1), whose form reveals the choice of boundary condition. A common choice is to keep the variation of the metric vanishing on the boundary, *i.e.* $\delta g_{\mu\nu}|_{\partial\mathcal{M}} = 0$, which corresponds to the Gibbons-Hawking-York (GHY) boundary action [115, 212]:

$$S_{\partial\mathcal{M}}[h_{\mu\nu}] = \frac{1}{8\pi \mathrm{G}} \int_{\partial\mathcal{M}} \mathrm{d}^{D-1} x \sqrt{sh} K\,, \tag{1.2}$$

where K is the extrinsic curvature. On the other hand, when considering the physical theory *i.e.* $D = 4, s = -1$ with some matter field Ψ, the action for the matter field $S_{\mathrm{m}}[\Psi] = \int \mathrm{d}^4 x \sqrt{-g}\mathcal{L}_{\mathrm{m}}[\Psi]$ should also be taken into account.

In the general relativity framework, one sets the torsion tensor to be zero and thus describes the geometry of the space-time manifold through probing the Riemann tensor, also called the curvature tensor, $R_{\mu\nu\rho\gamma}$, which is fully characterized by the metric and its derivatives. The equations of motion given by the variation of the metric, $\delta g_{\mu\nu}$, of the action (1.1), is the Einstein equation

$$R_{\mu\nu} - \frac{1}{2}(R - 2\Lambda) g_{\mu\nu} = 8\pi \mathrm{G} T_{\mu\nu}\,, \tag{1.3}$$

where $R_{\mu\nu}$ is the Ricci tensor and $T_{\mu\nu}$ is the energy-momentum tensor determined by the matter field.

In this thesis, we mainly focus on the case of a manifold with no boundaries and pure gravity, *i.e.* $T_{\mu\nu} = 0$ identically.

Solving the Einstein equation $R_{\mu\nu} - \frac{1}{2}(R - 2\Lambda)g_{\mu\nu} = 0$, one gets the vacuum metrics. The maximally symmetric solutions are called the *de Sitter* (dS) spacetime if $\Lambda > 0$ and the *Anti-de Sitter* (AdS) spacetime if $\Lambda < 0$ respectively. Define a so-called dS/AdS length scale l by $\Lambda = \sigma\frac{(D-1)(D-2)}{2l^2}$ where $\sigma = \text{sign}(\Lambda)$ denotes the sign of Λ. The dS/AdS metric can be jointly written as

$$\mathrm{d}s^2 = s\left(1 - \sigma\frac{r^2}{l^2}\right)\mathrm{d}t^2 + \frac{1}{\left(1 - \sigma\frac{r^2}{l^2}\right)}\mathrm{d}r^2 + r^2\mathrm{d}\Omega_{D-1}^2\,, \tag{1.4}$$

where Ω_{D-1} is the angular coordinate of the $(D-1)$-dimensional sphere. For instance, $\mathrm{d}\Omega_2^2 = \mathrm{d}\theta^2 + \sin^2\theta\mathrm{d}\phi^2$ (with $\theta = [0, \pi], \phi = [0, 2\pi)$) covers the 2-sphere for the 3D gravity case. Indeed, $l^2 \to +\infty$ is equivalent to $\Lambda \to 0$. AdS spacetime has been enormously studied since the inspiring work [51] by Brown and Henneaux, where they discovered that the asymptotic symmetry of the AdS_3 spacetime is captured by two commuting copies of Virasoro algebras, which is the symmetry algebra of 2D *conformal field theory* (CFT). This work turned out to be the precursor of the field *holographic duality*.

Taking the trace of the (1.3) (and considering $T_{\mu\nu} = 0$), the Ricci scalar is determined by the cosmological constant as $R = \frac{2D\Lambda}{D-2}$ hence the Ricci tensor is proportional to the metric: $R_{\mu\nu} = \frac{2\Lambda}{D-2}g_{\mu\nu}$. The curvature tensor can be separated into a traceless part $W_{\mu\nu\rho\gamma}$ called the Weyl tensor and a part described by the Ricci tensor and Ricci scalar:

$$\begin{aligned} &R_{\mu\nu\rho\gamma} \\ &= W_{\mu\nu\rho\gamma} + \frac{1}{D-2}(g_{\mu\rho}R_{\nu\gamma} + g_{\nu\gamma}R_{\mu\rho} - g_{\mu\gamma}R_{\nu\rho} - g_{\nu\rho}R_{\mu\gamma}) - \frac{1}{(D-1)(D-2)}(g_{\mu\gamma}g_{\nu\rho} - g_{\mu\rho}g_{\nu\gamma})R\,. \end{aligned} \tag{1.5}$$

The Riemann tensor is antisymmetric on the exchange of the first two components as well as on the exchange of the last two components and it satisfies the Bianchi identity, which restricts $R_{\mu\nu\rho\gamma}$ to have $\frac{D^2(D^2-1)}{12}$ independent components. On the other hand, the Ricci tensor $R_{\mu\nu}$ is symmetric on the exchange of the two components thus it has $\frac{D(D+1)}{2}$ independent components. Therefore, it is apparent that when the manifold is three-dimensional, the Riemann tensor (1.5) can be completely determined by the Ricci tensor hence the Weyl tensor vanishes.

On the other hand, one can count the physical (local) degrees of freedom of gravity by taking the space-time decomposition $\mathcal{M} = \Sigma \times \mathbb{R}$ of the manifold and considering it as an initial value problem. The *Arnowitt-Deser-Misner (ADM) formalism* [12, 155] is such a formalism. It describes the canonical structure of the gravitational phase space and the

evolution of the spatial geometries given by its Hamiltonian. Indeed, in D-dimensions, the gravitational phase space is described by the spatial metric $h_{\mu\nu}$, which contains $\frac{D(D-1)}{2}$ components, and its conjugate momentum, which contains another $\frac{D(D-1)}{2}$ components. Among them, there are D constraints on the initial conditions and another D unphysical degrees of freedom for the choice of coordinates. Therefore, there are $D(D-3)$ physical degrees of freedom left. [55]. In the case of 3D gravity, there are no local, but only global degrees of freedom depending on the topology of $\mathcal{M}$. In this sense, 3D gravity is a topological theory.

Despite its simplicity in terms of physical degrees of freedom, the Einstein-Hilbert action (1.1) is nonlinear since the curvature tensor contains a second derivative of the metric. The nonlinear nature of the Einstein-Hilbert action brings difficulties in quantizing gravity. We will adopt another formulation — the BF formulation, which is the first-order formalism of 3D gravity.

1.2 First-order formalism — the BF theory

In this section, we review and study the first-order formalism of 3D gravity with a cosmological constant Λ, which is the starting point of the LQG program. We first briefly define the BF theory in D dimensions, then rewrite the Einstein-Hilbert action (1.1) in a form of the 3D BF action by "relaxing" some constraints. A side note is that the GHY action (1.2) can also be written in the first-order formalism which turns out to be the same one as in the Chern-Simons formalism we derive later. Finally, we analyze the symmetries and constraints in the BF formalism of 3D gravity.

The BF theory, first discovered by Horowitz [133] and named by Blau and Thompson [35, 34], is a topological field theory defined on the principal G-bundle[1] on a D-dimensional manifold $\mathcal{M}$. Here, B is a $(D-2)$-form in value of the Lie algebra $\mathfrak{g}$ of the group G and F is a curvature two-form of some connection one-form ω in $\mathfrak{g}$, *i.e.* $F = \mathrm{d}\omega + [\omega \wedge \omega]$. The BF action is

$$S[B, \omega] = \int_{\mathcal{M}} \mathrm{Tr}(B \wedge F[\omega]) \,, \tag{1.6}$$

where the trace is taken as the invariant non-degenerate bilinear form over $\mathfrak{g}$. Since (1.6) is written in a form independent of the metric on $\mathcal{M}$, it is a natural topological theory.

[1] We remind the readers of the notation difference between G - the gravitational constant - and G - the group - used in this thesis.

Due to its simplicity, the BF theory is also a good testing ground to explore and compare different quantization schemes.

For purpose of compactness, we denote $\mathfrak{su}(+) := \mathfrak{su}(2)$ while $\mathfrak{su}(-) := \mathfrak{su}(1,1) \cong \mathfrak{sl}(2,\mathbb{R})$[2]. Denote the basis of $\mathfrak{su}(s)$ by τ^a $(a = 1,2,3)$ with commutation relations $[\tau^a, \tau^b] = \epsilon^{ab}{}_c \tau^c$ where we fix $\epsilon^{123} = s$ and $\epsilon_{123} = 1$ [3]. General relativity in 2+1 dimensions can be written as a BF action with B given by the *triad* field $\mathbf{e} = \mathbf{e}^a \tau_a = \mathbf{e}^a_\mu \tau_a \mathrm{d}x^\mu$ — a one-form in $\mathfrak{su}(s)$ — and the connection one-form given by the *spin connection* $\tilde{\omega} = \tilde{\omega}^a \tau_a = \frac{1}{2}\epsilon^{abc}\tilde{\omega}_{\mu cb}\tau_a \mathrm{d}x^\mu$[4] as we now describe.

The triad or frame field satisfies

$$g_{\mu\nu} = \eta^s_{ab} e^a_\mu e^b_\nu \,, \quad \eta^{ab}_s = g^{\mu\nu} e^a_\mu e^b_\nu \,, \tag{1.7}$$

where the internal metric $\eta^s = \eta_s = \mathrm{diag}(+,+,s)$. We use the latin letters a, b, c, etc to denote the local frame coordinate, or the internal indices, and the Greek letters μ, ν, ρ, etc to denote the spacetime indices. Just like that the Levi-Civita connection $\Gamma^\rho_{\mu\nu}$ is used to describe the covariant derivative of a vector with spacetime index, the spin connection is used to describe the gauge-covariant derivative of a vector with internal index. For a given vector v^a_ν, its total covariant derivative is

$$\mathrm{D}_\mu v^a_\nu = \partial_\mu v^a_\nu - \Gamma^\rho_{\mu\nu} v^a_\rho + \tilde{\omega}^a_{\mu b} v^b_\nu = \nabla_\mu v^a_\nu + \tilde{\omega}^a_{\mu b} v^b_\nu \,. \tag{1.8}$$

In the first-order formalism, e^a and ω^a are treated as independent variables. The curvature two-form $\tilde{F}^a = \frac{1}{2}\epsilon^{abc}\tilde{F}_{\mu\nu cb}\mathrm{d}x^\mu \wedge \mathrm{d}x^\nu$ is given in terms of the spin connection by

$$\tilde{F}_{ab} = \mathrm{d}\tilde{\omega}_{ab} + \tilde{\omega}_a{}^c \wedge \tilde{\omega}_{cb} \,, \quad \text{or} \quad \tilde{F}_a = \mathrm{d}\tilde{\omega}_a - \frac{s}{2}[\tilde{\omega} \wedge \tilde{\omega}]_a \,, \tag{1.9}$$

where the commutator acts on the $\mathfrak{su}(s)$ generators, that is, $[\tilde{\omega} \wedge \tilde{\omega}] = \tilde{\omega}^b \wedge \tilde{\omega}^c [\tau_b \,, \tau_c]$. To have a curvature 2-form independent of the signature, we will instead work on the rescaled connection ω and the curvature F defined by

$$F = -s\tilde{F} \,, \quad \omega = -s\tilde{\omega} \quad \Longrightarrow \quad F_a = \mathrm{d}\omega_a + \frac{1}{2}[\omega \wedge \omega]_a \,. \tag{1.10}$$

[2] $\cong$ denotes "isomorphic to". Note the difference from $\simeq$ used in other context in this thesis.

[3] The generators of $\mathfrak{su}(2)$ and $\mathfrak{sl}(2,\mathbb{R})$ can both represented in terms of the Pauli matrices $\sigma_x = \begin{pmatrix} 0 & 1 \\ 1 & 0 \end{pmatrix}, \sigma_y = \begin{pmatrix} 0 & -i \\ i & 0 \end{pmatrix}, \sigma_z = \begin{pmatrix} 1 & 0 \\ 0 & -1 \end{pmatrix}$. For the Euclidean signature, $\tau^1 = \frac{\sigma_x}{2i}, \tau^2 = \frac{\sigma_y}{2i}, \tau^3 = \frac{\sigma_z}{2i}$, while for the Lorentzian signature, $\tau^1 = \frac{\sigma_z}{2}, \tau^2 = \frac{\sigma_x}{2}, \tau^3 = \frac{\sigma_y}{2i}$. The commutation relations defining the $\mathfrak{su}(2)$ and $\mathfrak{sl}2,\mathbb{R})$ Lie algebra are explicitly $[\tau^1, \tau^2] = \tau^3 = s\tau_3 = s[\tau_1, \tau_2], [\tau^2, \tau^3] = \tau^1 = \tau_1 = [\tau_2, \tau_3], [\tau^3, \tau^1] = \tau^2 = \tau_2 = [\tau_3, \tau_1]$. We therefore have $\epsilon^{abc}\epsilon_{afg} = s(\delta^b_f \delta^c_g - \delta^b_g \delta^c_f)$.

[4] Conversely, $\tilde{\omega}_{bc} = s\epsilon_{abc}\tilde{\omega}^a$.

Its relation to the Riemann curvature tensor is obtained by first solving the spin connection in terms of the triads by demanding $\mathrm{D}_\mu e^a_\nu = 0$, that is

$$\nabla_\mu \mathbf{e}^a_\nu = s\omega^a_{\mu b}\mathbf{e}^b_\nu \quad \text{hence} \quad \omega^a_\mu = -\frac{s}{2}\epsilon^a{}_b{}^c\mathbf{e}^\nu_c\nabla_\mu\mathbf{e}^b_\nu\,. \tag{1.11}$$

By examining the commutator $R_{\mu\nu\rho}{}^\sigma v_\sigma = [\mathrm{D}_\mu, \mathrm{D}_\nu](\mathbf{e}^a_\sigma v_a)$, one gets $R_{\mu\nu\rho}{}^\sigma = -s\mathbf{e}^a_\rho\mathbf{e}^{\sigma b}F_{\mu\nu ab}$. We assume that the triad field is non-degenerate[5], then one can rewrite the Ricci scalar as

$$R = R_{\mu\nu}g^{\mu\nu} = -s\mathbf{e}^\mu_a\mathbf{e}^\nu_b F^{ab}_{\mu\nu} = -\mathbf{e}^\mu_a\mathbf{e}^\nu_b\epsilon^{abc}F_{\mu\nu c}\,. \tag{1.12}$$

Furthermore, the volume form $\sqrt{sg}\mathrm{d}^3x = \det(\mathbf{e}^a_\mu)\mathrm{d}^3x = \frac{1}{3!}\mathrm{Tr}(\mathbf{e}\wedge[\mathbf{e}\wedge\mathbf{e}])$[6] with the trace acting on the $\mathfrak{su}(s)$ generators. Putting these ingredients together, one can prove the equivalence of the Einstein-Hilbert action and the BF action

$$\begin{aligned}\frac{1}{16\pi\mathrm{G}}\int_{\mathcal{M}}\mathrm{d}^3x\sqrt{sg}(R-2\Lambda) &= -\frac{s}{8\pi\mathrm{G}}\int_{\mathcal{M}}\mathbf{e}^a\wedge F_a + s\frac{\Lambda}{6}\epsilon_{abc}\mathbf{e}^a\wedge\mathbf{e}^b\wedge\mathbf{e}^c \\ &= -\frac{s}{8\pi\mathrm{G}}\int_{\mathcal{M}}\mathrm{Tr}\left((\mathbf{e}\wedge(F+s\frac{\Lambda}{3}E)\right)\,,\end{aligned} \tag{1.13}$$

where we denote $E = \frac{1}{2}[\mathbf{e}\wedge\mathbf{e}] = \frac{1}{2}\epsilon_{abc}\mathbf{e}^b\wedge\mathbf{e}^c\tau^a$ to be the area flux two-form. Clearly, when the cosmological constant is vanishing, (1.13) takes the form of the BF action (1.6).

Let us take $\frac{s}{8\pi\mathrm{G}} = 1$ for simplicity in the rest of the thesis unless specified, then the first-order action of 3D gravity with a cosmological constant, denoted as $S_{\Lambda\mathrm{BF}}$, is

$$S_{\Lambda\mathrm{BF}}[\mathbf{e},\omega] = -\int_{\mathcal{M}}\mathrm{Tr}\left((\mathbf{e}\wedge(F[\omega]+s\frac{\Lambda}{3}E[\mathbf{e}])\right)\,. \tag{1.14}$$

The field variation of the action then gives[7]

$$\delta S_{\Lambda\mathrm{BF}}[\mathbf{e},\omega] = -\int_{\mathcal{M}}\mathrm{Tr}\left(\delta\mathbf{e}\wedge(F+s\Lambda E)+\delta\omega\wedge\mathrm{d}_\omega\mathbf{e}\right) - \int_{\partial\mathcal{M}}\mathrm{Tr}\left(\mathbf{e}\wedge\delta\omega\right)\,, \tag{1.15}$$

where $\mathrm{d}_\omega\cdot \equiv \mathrm{d}\cdot + [\omega,\cdot]$ is the gauge covariant derivative. Therefore, the variations of the $\mathbf{e}$ field and the ω field give respectively the equations of motion in terms of the curvature and the torsion

$$\begin{aligned}\tfrac{\delta S_{\Lambda\mathrm{BF}}}{\delta\mathbf{e}} \quad &\Longrightarrow \quad \mathcal{C} = F + s\Lambda E \simeq 0\,, \\ \tfrac{\delta S_{\Lambda\mathrm{BF}}}{\delta\omega} \quad &\Longrightarrow \quad \mathcal{T} = \mathrm{d}_\omega\mathbf{e} \simeq 0\,,\end{aligned} \tag{1.16}$$

[6] Tr is the normalized trace thus $\mathrm{Tr}(\tau_a\tau_b) = \delta_{ab}$.

[6] We require $\mathbf{e}$ to be non-degenerate because in the derivation to get the second equation of (1.12), one uses the inverse of $\det(\mathbf{e}^a_\mu)$. It cancels out the determinant in the volume form written in terms of the triads thus the integrand of (1.13) includes simply a trace term. See also [95].

[7] We have used the fact that $\frac{1}{3}\delta\mathrm{Tr}(\mathbf{e}\wedge E) = \frac{1}{6}\epsilon_{abc}\delta\mathrm{Tr}(\mathbf{e}^a\wedge\mathbf{e}^b\wedge\mathbf{e}^c) = \frac{1}{2}\epsilon_{abc}\mathrm{Tr}(\delta\mathbf{e}^a\wedge\mathbf{e}^b\wedge\mathbf{e}^c) = \mathrm{Tr}(\delta\mathbf{e}\wedge E)$ due to the antisymmetry of the wedge operations.

where $\simeq$ denotes the on-shell condition. Solving the torsion-free equation of motion $\mathcal{T}=0$, one gets the spin connection ω in terms of $\mathbf{e}$, *i.e.* (1.11).

Notice that when the manifold $\mathcal{M}$ has a boundary $\partial\mathcal{M}$, the boundary term $\int_{\partial\mathcal{M}}\mathrm{Tr}\,(\mathbf{e}\wedge\delta\omega)$ does not vanish. In fact, when taking the boundary condition to be a fixed metric hence $\delta\mathbf{e}|_{\partial\mathcal{M}}=0$, such a boundary term is given by the symplectic potential $\Theta=\delta\int_{\partial\mathcal{M}}\mathrm{Tr}(\mathbf{e}\wedge\omega)$. This is nothing but the variation of the first-order formalism of the GHY boundary term at $D=3$, which we now show.

Let us impose the torsion-free condition of the connection (1.11). We choose a gauge for the triad $\mathbf{e}^3_\mu=n_\mu$ on the boundary $\partial\mathcal{M}$, where $\vec{n}$ is the vector normal to $\partial\mathcal{M}$, which links the metric $g_{\mu\nu}$ and the induced metric $h_{\mu\nu}$ on the boundary by

$$g_{\mu\nu}=h_{\mu\nu}+n_\mu n_\nu\,. \tag{1.17}$$

The torsion-free connection on the boundary can thus be written as $\omega^a_\mu=-s\epsilon^{ab0}n^\nu\nabla_\mu\mathbf{e}^b_\nu-s\epsilon^{a0c}\mathbf{e}^\nu_c\nabla_\mu n_\nu=2s\epsilon^{ab}\mathbf{e}^\nu_b\nabla_\mu n_\nu$. Therefore, the boundary term $\int_{\partial\mathcal{M}}\mathrm{Tr}(\mathbf{e}\wedge\omega)$ reads explicitly

$$\begin{aligned}\int_{\partial\mathcal{M}}\mathrm{d}^2x\,\epsilon^{\mu\nu\rho}\mathbf{e}^a_\mu\omega_{\nu a}\hat{n}_\rho&=2s\int_{\partial\mathcal{M}}\mathrm{d}^2x\,\epsilon^{\mu\nu\rho}\epsilon^{ab}\mathbf{e}_{\mu a}\mathbf{e}^\lambda_b\hat{n}_\rho\nabla_\nu n_\lambda\\&=2\int_{\partial\mathcal{M}}\det(\mathbf{e}^a_\mu)\,\nabla_\mu n^\mu=2\int_{\partial\mathcal{M}}\mathrm{d}^2x\,\sqrt{sh}K\,,\end{aligned} \tag{1.18}$$

which recovers the GHY boundary term (1.2). $\vec{\hat{n}}$ is a dimensionless normal direction vector to $\partial\mathcal{M}$ that is proportional to $\vec{n}$, say $\vec{n}=N\vec{\hat{n}}$ [8]. On the other hand, the variation of the symplecitc potential gives the boundary term of (1.15) upon the Dirichlet boundary condition $\delta\mathbf{e}^a_\mu|_{\partial\mathcal{M}}=0$, which is consistent with the boundary condition $\delta g_{\mu\nu}|_{\partial\mathcal{M}}=0$ of the action Einstein-Hilbert action (1.1) when considering the GHY boundary term (1.2) [115, 212].

There are two types of gauge symmetries of the action (1.13), namely the local Lorentz transformation $\delta^{\mathrm{L}}_\alpha$, infinitesimally parametrized by a scalar field $\alpha=\alpha^a\tau_a$, and the local translation transformation δ^{t}_ϕ, infinitesimally parametrized by a scalar field $\phi=\phi^a\tau_a$,

$$\delta^{\mathrm{L}}_\alpha\mathbf{e}=[\mathbf{e},\alpha]\,,\quad\delta^{\mathrm{L}}_\alpha\omega=\mathrm{d}_\omega\alpha\,,\quad\delta^{\mathrm{t}}_\phi\mathbf{e}=\mathrm{d}_\omega\phi\,,\quad\delta^{\mathrm{t}}_\phi\omega=s\Lambda[\mathbf{e},\phi]\,. \tag{1.19}$$

One can also consider the finite Lorentz transformation performed by an $\mathrm{SU}(s)$ element g which is the exponential of a Lie algebra $\mathfrak{su}(s)$, and the finite translation performed by a

[8] It is important to note the difference between n_μ and $\hat{n}_\mu$. As the metric carries square of length dimensions, n_μ is with dimension of length according to (1.17) while $\hat{n}_\mu$ is dimensionless, the dimension of the boundary action (1.18) is correct.

scalar field Φ. Then the finite Lorentz transformation and translation laws read

$$\left|\begin{array}{rcl} e & \mapsto & geg^{-1} \\ \omega & \mapsto & g\omega g^{-1} + g\,\mathrm{d}g^{-1} \end{array}\right. , \qquad \left|\begin{array}{rcl} e & \mapsto & e + \mathrm{d}_\omega \Phi \\ \omega & \mapsto & \omega + s\Lambda[\mathbf{e}, \Phi] \end{array}\right. . \tag{1.20}$$

The equations of motion are indeed invariant under these gauge transformations:

$$\delta_\alpha \mathcal{T} = [\mathcal{T}, \alpha] \simeq 0\,, \quad \delta_\alpha \mathcal{C} = [\mathcal{C}, \alpha] \simeq 0\,, \quad \delta_\phi \mathcal{T} = [\mathcal{C}, \phi] \simeq 0\,, \quad \delta_\phi \mathcal{C} = s\Lambda[\mathcal{T}, \phi] \simeq 0\,. \tag{1.21}$$

As an example, the first transformation is calculated as

$$\begin{aligned} \delta_\alpha \mathcal{T} &= \delta_\alpha(\mathrm{d}\mathbf{e} + [\omega \wedge \mathbf{e}]) = \mathrm{d}[\mathbf{e}, \alpha] + [\mathrm{d}_\omega \alpha, \mathbf{e}] + [\omega \wedge [\mathbf{e}, \alpha]] \\ &= \mathrm{d}[\mathbf{e}, \alpha] + \mathrm{d}[\alpha, \mathbf{e}] - [\alpha, \mathrm{d}\mathbf{e}] + [[\omega, \alpha] \wedge \mathbf{e}] - [\alpha, [\omega \wedge \mathbf{e}]] + [\mathbf{e} \wedge [\alpha, \omega]] = [\mathrm{d}_\omega \mathbf{e}, \alpha]\,, \end{aligned} \tag{1.22}$$

where the Jacobi identity $[\omega \wedge [\mathbf{e}, \alpha]] + [\alpha, [\omega \wedge \mathbf{e}]] - [\mathbf{e} \wedge [\alpha, \omega]] = 0$ was used[9]. The rest of gauge transformations in (1.22) follow with similar calculations.

In fact, there is another symmetry — diffeomorphism invariance — in the action (1.13). The diffeomorphism transformation δ^{d}_ξ is described by the Lie derivative $\mathcal{L}_\xi$ along a vector field $\xi = \xi_\mu \mathrm{d}x^\mu$. It, however, can be written on-shell in terms of the field-dependent translation and field-dependent gauge transformation. For the triad and the connection[10],

$$\begin{aligned} \delta^{\mathrm{d}}_\xi \mathbf{e} = \mathcal{L}_\xi \mathbf{e} = \mathrm{d}(\iota_\xi \mathbf{e}) + \iota_\xi \mathrm{d}\mathbf{e} &= \mathrm{d}_\omega(\iota_\xi \mathbf{e}) - [\omega, \iota_\xi \mathbf{e}] + \iota_\xi(\mathrm{d}_\omega \mathbf{e}) - \iota_\xi[\omega \wedge \mathbf{e}] \\ &= \mathrm{d}_\omega(\iota_\xi \mathbf{e}) + [\mathbf{e}, \iota_\xi \omega] + \iota_\xi(\mathrm{d}_\omega \mathbf{e}) \\ &= \delta^{\mathrm{t}}_{\iota_\xi \mathbf{e}} \mathbf{e} + \delta^{\mathrm{L}}_{\iota_\xi \omega} \mathbf{e} + \iota_\xi \mathcal{T}\,, \end{aligned} \tag{1.23a}$$

$$\begin{aligned} \delta^{\mathrm{d}}_\xi \omega = \mathcal{L}_\xi \omega = \mathrm{d}(\iota_\xi \omega) + \iota_\xi \mathrm{d}\omega &= \mathrm{d}_\omega(\iota_\xi \omega) - [\omega, \iota_\xi \omega] + \iota_\xi F + \frac{1}{2}\iota_\xi[\omega \wedge \omega] \\ &= \mathrm{d}_\omega(\iota_\xi \omega) + s\Lambda[\mathbf{e}, \iota_\xi \mathbf{e}] + \iota_\xi(F + s\Lambda E) \\ &= \delta^{\mathrm{L}}_{\iota_\xi \omega} \omega + \delta^{\mathrm{t}}_{\iota_\xi \mathbf{e}} \omega + \iota_\xi \mathcal{C}\,. \end{aligned} \tag{1.23b}$$

[9] In general, for A, B, C which are m, n, p-forms respectively, the Jacobi identity is

$$[A \wedge [B \wedge C]] + (-1)^{m(n+p)}[B \wedge [C \wedge A]] + (-1)^{p(m+n)}[C \wedge [A \wedge B]] = 0\,.$$

Also note that $[A \wedge B] = -(-1)^{mn}[B \wedge A]$ and $\mathrm{d}[A \wedge B] = [\mathrm{d}A \wedge B] + (-1)^m[A \wedge \mathrm{d}B]$.

As LQG is a canonical quantization approach, the next step of the program is to apply the Hamiltonian analysis based on a space-time splitting, that is to formulate the time evolution of the spatial geometries.

1.3 Hamiltonian analysis

We now perform the Hamiltonian analysis of the action (1.13) using the covariant phase space formalism. Consider the space-time foliation $\mathcal{M} = \Sigma \times [t_i, t_f]$[11] where Σ is a two-dimensional space surface with boundary $S = \partial\Sigma$ and is future oriented, as shown in fig.1.1. The symplectic form is defined as $\Omega_\Sigma = \int_\Sigma \delta\Theta$, that is

$$\Omega_\Sigma = -\int_\Sigma \mathrm{Tr}\left(\delta\omega \curlywedge \delta\mathbf{e}\right) . \tag{1.24}$$

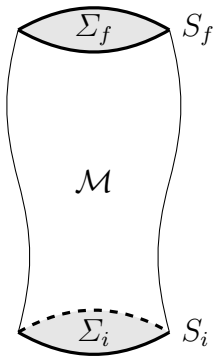

Figure 1.1: The space-time decomposition of a 3D manifold $\mathcal{M}$ into $\Sigma \times [t_i, t_f]$. The initial (*resp.* final) spatial surface at t_i (*resp.* t_f) is Σ_i (*resp.* Σ_f) (*in grey*) with the boundary S_i (*resp.* S_f) (*thick loops*).

[10] We have used the Cartan formula in (1.23)

$$\mathcal{L}_X \theta = \mathrm{d}(\iota_X \theta) + \iota_X \mathrm{d}\theta \, .$$

where X is a vector field and θ is a p-form.

[11] When considering inifite time, $\mathcal{M} = \Sigma \times \mathbb{R}$.

Here, $\curlywedge$ is the extension of the wedge product to variational forms hence $\mathrm{Tr}\,(\delta\omega \curlywedge \delta\mathbf{e}) = \mathrm{Tr}\,(\delta\mathbf{e} \curlywedge \delta\omega)$[12]. The gauge transformation of the symplectic form generates the boundary symmetry charges. In particular, when the coefficients α and ϕ are field independent,

$$\begin{aligned}
\iota_{\delta^{\mathrm{L}}_\alpha}\Omega_\Sigma &= -\int_\Sigma \mathrm{Tr}\left(\delta^{\mathrm{L}}_\alpha\omega \wedge \delta\mathbf{e} - \delta\omega \wedge \delta^{\mathrm{L}}_\alpha\mathbf{e}\right)\\
&= -\int_\Sigma \left(\mathrm{d}_\omega\alpha_a \wedge \delta\mathbf{e}^a - \epsilon^a{}_{bc}\delta\omega_a \wedge \mathbf{e}^b\alpha^c\right)\\
&= -\int_\Sigma \left(\mathrm{d}\alpha_a \wedge \delta\mathbf{e}^a + \epsilon^a{}_{bc}\omega_a\alpha^b \wedge \delta\mathbf{e}^c - \epsilon^a{}_{bc}\delta\omega_a \wedge \mathbf{e}^b\alpha^c\right)\\
&= -\delta\mathrm{d}\int_\Sigma \alpha_a\mathbf{e}^a + \delta\int_\Sigma \left(\alpha_a\mathrm{d}\mathbf{e}^a + \epsilon^a{}_{bc}\omega^a \wedge \mathbf{e}^b\alpha^c\right)\\
&= -\delta\left(-\int_\Sigma \alpha_a\mathrm{d}_\omega\mathbf{e}^a + \int_S \alpha_a\mathbf{e}^a\right) = -\delta J_\alpha\,.
\end{aligned} \tag{1.25}$$

and

$$\begin{aligned}
\iota_{\delta^{\mathrm{t}}_\phi}\Omega_\Sigma &= -\int_\Sigma \mathrm{Tr}\left(\delta^{\mathrm{t}}_\phi\omega \wedge \delta\mathbf{e} - \delta\omega \wedge \delta^{\mathrm{t}}_\phi\mathbf{e}\right)\\
&= -\int_\Sigma \left(s\Lambda\epsilon_{abc}\mathbf{e}^a\phi^b \wedge \delta\mathbf{e}^c - \delta\omega_a \wedge \mathrm{d}_\omega\phi^a\right)\\
&= \int_\Sigma \left(s\Lambda\epsilon_{abc}\mathbf{e}^a \wedge \delta\mathbf{e}^b\phi^c + \delta\omega_a \wedge \mathrm{d}\phi^a + \epsilon^{abc}\delta_a \wedge \omega_b\phi_c\right)\\
&= -\delta\mathrm{d}\int_\Sigma \phi^a\omega_a + \delta\int_\Sigma \phi^a(\mathrm{d}\omega_a + \frac{1}{2}\epsilon^{abc}\omega_b \wedge \omega_c + \frac{s}{2}\Lambda\epsilon_{abc}\mathbf{e}^b \wedge \mathbf{e}^c)\\
&= -\delta\left(-\int_\Sigma \phi^a\left(F_a + s\Lambda E_a\right) + \int_S \phi^a\omega_a\right) = -\delta P_\phi\,.
\end{aligned} \tag{1.26}$$

Therefore, the boundary charges are given by

$$J_\alpha = -\int_\Sigma \alpha_a\mathrm{d}_\omega\mathbf{e}^a + \int_S \alpha_a\mathbf{e}^a \simeq \int_S \alpha_a\mathbf{e}^a\,, \tag{1.27}$$

$$P_\phi = -\int_\Sigma \phi^a\left(F_a + s\Lambda E_a\right) + \int_S \phi^a\omega_a \simeq \int_S \phi^a\omega_a\,. \tag{1.28}$$

[12]For n-form α and m-form β, we have

$$\alpha \curlywedge \beta = \alpha \wedge \beta\,, \quad \alpha \curlywedge \delta\beta = \alpha \wedge \delta\beta\,, \quad \delta\alpha \curlywedge \delta\beta = -(-1)^{mn}\delta\beta \curlywedge \delta\alpha\,.$$

The Hamiltonian H_ξ of gravity is defined, in the covariant phase space formalism, as the diffeomorphism charge, generated by the diffeomorphism transformation $\delta^{\rm d}_\xi$. Then one can straightforwardly compute that

$$\begin{aligned}
\iota_{\delta^{\rm d}_\xi}\Omega_\Sigma &= -\int_\Sigma \mathrm{Tr}\left(\delta^{\rm d}_\xi\omega\wedge\delta\mathbf{e}-\delta\omega\wedge\delta^{\rm d}_\xi\mathbf{e}\right)\\
&= -\delta J_{\iota_\xi\omega}-\delta P_{\iota_\xi\mathbf{e}}-\int_\Sigma\left((\iota_\xi\mathcal{C})_a\delta\mathbf{e}^a+(\iota_\xi\mathcal{T})^a\delta\omega_a\right)\\
&\simeq \int_S \mathrm{Tr}\left(\iota_\xi\omega\,\delta\mathbf{e}+\iota_\xi\mathbf{e}\,\delta\omega_a\right)\\
&= -\delta\int_S\mathrm{Tr}\left(\iota_\xi\omega\,\mathbf{e}\right)+\iota_\xi\int_\Sigma\mathrm{Tr}(\delta\omega\wedge\mathbf{e}) = -\delta Q_\xi+\iota_\xi\Theta\equiv-\delta H_\xi\,,
\end{aligned}\tag{1.29}$$

where Q_ξ is the diffeomorphism Noether charge [128].

The symplectic form (1.24) generates the Poisson brackets ($i,j\in\{1,2\}$ denotes the spacetime indices tangent to Σ and x,y are points on Σ.)

$$\{\omega^i_a(x),\mathbf{e}^b_j(y)\}=\epsilon_i{}^j\eta^a{}_b\delta^2(x-y)\,,\quad \{\omega^i_a(x),\omega^j_b(y)\}=\{\mathbf{e}^a_i(x),\mathbf{e}^b_j(y)\}=0\,.\tag{1.30}$$

One can thus compute the boundary symmetry algebra

$$\{J_\alpha,J_\beta\}=J_{[\alpha,\beta]}\,,\quad \{P_\phi,P_\psi\}=s\Lambda J_{[\phi,\psi]}\,,\quad \{J_\alpha,P_\phi\}=P_{[\alpha,\phi]}+\int_S\phi^a\mathrm{d}\alpha_a\,.\tag{1.31}$$

One the other hand, (1.27) and (1.28) mean that the generators J_α and P_ϕ generate canonical transformation

$$\delta^L_\alpha\cdot=\{J_\alpha,\cdot\}\,,\quad \delta^t_\phi\cdot=\{P_\phi,\cdot\}\,,\tag{1.32}$$

which can also be used to compute (1.31).

As an explicit example, we consider the manifold as a solid cylinder and parametrize the coordinate as (t,r,θ) where $t\in[t_i,t_f]\,,r\in[0,R]$ and $\theta\in[0,2\pi]$. The boundary S is then located at $t=t_0,r=R$. The symmetry current are given by $(j(\theta),p(\theta))=(\omega^\theta,\mathbf{e}_\theta)$. (1.31) can be written as the Poisson brackets of the currents[13]:

$$\{j^a(\theta),j^b(\theta')\}=\epsilon^{ab}{}_c\delta(\theta-\theta')j^c(\theta)\,,\tag{1.33a}$$

$$\{j^a(\theta),p_b(\theta')\}=\epsilon^a{}_b{}^c\delta(\theta-\theta')p_c(\theta)-\delta^a_b\partial_\theta\delta(\theta-\theta')\,,\tag{1.33b}$$

$$\{p_a(\theta),p_b(\theta)\}=s\Lambda\epsilon_{abc}\delta(\theta-\theta')j^c(\theta)\,.\tag{1.33c}$$

We define their Fourier transformation

$$J_n^a \approx \int_S e^{-in\theta} j^a(\theta)\mathrm{d}\theta\,, \quad P_m^a \approx \int_S e^{-in\theta} p_a(\theta)\mathrm{d}\theta\,, \tag{1.34}$$

with the normalized measure on the circle $\int_S \mathrm{d}\theta = 1$. Then the Poisson brackets of the Fourier modes are

$$\{J_n^a, J_m^b\} = \epsilon^{ab}{}_c J_{n+m}^c\,, \quad \{P_n^a, P_m^b\} = s\Lambda\epsilon^{ab}{}_c J_{n+m}^c\,, \quad \{J_n^a, P_m^b\} = \epsilon^{ab}{}_c P_{m+n}^c - in\delta^{ab}\delta_{n+m,0}\,. \tag{1.35}$$

When $\Lambda = 0$, (1.31) is the Poincaré loop algebra $L(\mathfrak{isu}(2))$ with central extension, with the BMS group as the subgroup. Understanding how the Poincaré loop algebra can be discretized is an open question. In [92], the authors proposed a limit starting from the discrete picture to recover this loop algebra, when $\Lambda = 0$. The generalization to the $\Lambda \neq 0$ case is under investigation.

1.4 Chern-Simons formalism

Another formulation often used to study 3D gravity is *Chern-Simons formulation* [60]. It is a 3D topological field theory intensively studied in mathematics and condensed matter physics (*e.g.* knots invariants [210], (extended) topological quantum field theory [86], fractional quantum hall effects [213]). The Chern-Simon action on a 3D manifold $\mathcal{M}$ for a gauge group G, whose Lie algebra is denoted as $\mathfrak{g}$, is defined as

$$S_{\mathrm{CS}}[\mathcal{A}] = \frac{k}{4\pi}\int_{\mathcal{M}} \mathrm{Tr}(\mathcal{A}\wedge\mathrm{d}\mathcal{A} + \frac{1}{3}\mathcal{A}\wedge[\mathcal{A}\wedge\mathcal{A}])\,, \tag{1.36}$$

[13] Here we give the calculation of the Poisson bracket (1.33b). The other two in (1.33) can be obtained in a similar way. We parametrize the boundary charges as $J_\alpha \approx \int_0^{2\pi}\alpha_a(\theta)j^a(\theta)\mathrm{d}\theta$ and $P_\phi \approx \int_0^{2\pi}\phi^a(\theta)p_a(\theta)\mathrm{d}\theta$. Then the last Poisson bracket in (1.31), as an example, can be written as

$$\begin{aligned}
\{J_\alpha, P_\phi\} &= \int_0^{2\pi}\int_0^{2\pi}\alpha_a(\theta)\phi^b(\theta')\{j^a(\theta), p_b(\theta')\}\mathrm{d}\theta\mathrm{d}\theta' = \int_0^{2\pi}\epsilon^a{}_b{}^c\alpha_a(\theta)\phi^b(\theta)p_c(\theta)\mathrm{d}\theta + \int_0^{2\pi}\phi^a(\theta)\partial_\theta\alpha_a(\theta)\mathrm{d}\theta \\
&= \int_0^{2\pi}\int_0^{2\pi}\alpha_a(\theta)\phi^b(\theta')\epsilon^a{}_b{}^c\delta(\theta-\theta')p_c(\theta)\mathrm{d}\theta\mathrm{d}\theta' + \int_0^{2\pi}\int_0^{2\pi}\partial_\theta\alpha_b(\theta)\phi^a(\theta')\delta_b^a\delta(\theta-\theta')\mathrm{d}\theta\mathrm{d}\theta' \\
&= \int_0^{2\pi}\int_0^{2\pi}\alpha_a(\theta)\phi^b(\theta')\epsilon^a{}_b{}^c\left(\epsilon^a{}_b{}^c\delta(\theta-\theta')p_c(\theta) - \delta_b^a\partial_\theta\delta(\theta-\theta')\mathrm{d}\theta\mathrm{d}\theta'\right)\,,
\end{aligned}$$

which gives $\{j^a(\theta), p_b(\theta')\} = \epsilon^a{}_b{}^c\delta(\theta-\theta')p_c(\theta) - \delta_b^a\partial_\theta\delta(\theta-\delta')$ as given in (1.33b).

where $\mathcal{A}$ is a $\mathfrak{g}$-valued one-form, k is the level of energy and Tr is the Ad-invariant invariant bilinear form on $\mathfrak{g}$. The equation of motion of the Chern-Simons action is the flatness condition

$$\mathrm{d}\mathcal{A} + \frac{1}{2}[\mathcal{A} \wedge \mathcal{A}] = 0\,. \tag{1.37}$$

It was first discovered by Achúcarro and Townsend [2] then elaborated by Witten in his seminal paper [209] that 3D gravity can be written as a Chern-Simons action with the gauge group given by the isometry group of gravity which depends on the signature under study and the sign of the cosmological constant. Consider $\mathfrak{g}$ to be a 6-dimensional Lie algebra with generators $J^a, P_a\,, a = 1, 2, 3$ satisfying the commutator

$$[J^a, J^b] = \epsilon^{ab}{}_c J^c\,, \quad [J^a, P_b] = \epsilon^a{}_b{}^c P_c\,, \quad [P_a, P_b] = \epsilon_{abc} s\Lambda J^c\,. \tag{1.38}$$

Note that we are using the same convention $\epsilon^a{}_b{}^c = s$ as is in Section 1.2. The Ad-invariant bilinear form for the generators is defined as

$$\mathrm{Tr}(J^a J^b) = 0\,, \quad \mathrm{Tr}(P_a P_b) = 0\,, \quad \mathrm{Tr}(P_a J^b) = \eta^s{}_a{}^b\,. \tag{1.39}$$

First, let us analyze this gauge group for different cases - Euclidean/Lorentzian signature and $\Lambda = 0\,, \Lambda > 0\,, \Lambda < 0$. The first commutator in (1.38) implies that J^a's are generators of $\mathrm{SU}(s)$. When $\Lambda = 0$, the commutators of P_a's vanish thus P_a are generators of $\mathbb{R}^3$. That the second commutator gives only P_c on the right hand side means that there is only action of J^a's on P_a's but not the other way around, which translates into a semi-direct product structure in constructing G. When $\Lambda \neq 0$, we consider $s\Lambda < 0$ and $s\Lambda > 0$ separately. When $s\Lambda < 0$, one takes $P_a = i\sqrt{|\Lambda|}J^a$ then the second and third commutators in (1.38) follow from the first one, which implies that G is the complexification of $\mathrm{SU}(s)$. In the case of $s\Lambda > 0$, on the other hand, one can take $P_a = \sqrt{|\Lambda|}J^a$ to realize these commutators hence $\mathfrak{g}$ is the double copy of $\mathrm{SU}(s)$. The isometry group associated to (1.38) is summarized in Table 1.1.

G	$s = +$	$s = -$
$\Lambda = 0$	$\mathrm{SU}(2) \ltimes \mathbb{R}^3$	$\mathrm{SL}(2,\mathbb{R}) \ltimes \mathbb{R}^3$
$\Lambda < 0$	$\mathrm{SL}(2,\mathbb{C})$	$\mathrm{SL}(2,\mathbb{R}) \times \mathrm{SL}(2,\mathbb{R})$
$\Lambda > 0$	$\mathrm{SU}(2) \times \mathrm{SU}(2)$	$\mathrm{SL}(2,\mathbb{C})$

Table 1.1: The isometry group of 3D gravity for Euclidean ($s = +$) and Lorentzian ($s = -$) signatures and for different signs of the cosmological constant.

Let the gauge group element $\mathcal{A}$ take value in the triads and the spin connections in the way of

$$\mathcal{A} = \mathbf{e}^a P_a + \omega_a J^a \,, \tag{1.40}$$

and take $k = \frac{1}{4\mathrm{G}}$[14], then the Chern-Simons action can be equivalently written as

$$S_{\mathrm{CS}}[\mathbf{e}, \omega] = \int_{\mathcal{M}} \mathrm{Tr}\left(\mathbf{e} \wedge (\mathrm{d}\omega + \frac{1}{2}[\omega \wedge \omega] + s\frac{\Lambda}{3}[\mathbf{e} \wedge \mathbf{e}])\right) + \int_{\partial\mathcal{M}} \mathrm{Tr}\left(\mathbf{e} \wedge \omega\right) \,, \tag{1.41}$$

which is identical to (1.14) up to a boundary term which is the first-order formulation of the GHY action. The equation of motion (1.37) can also be separated, using (1.40), into the torsion-free and curvature-free equations of motion (1.16).

The Chern-Simons formulation is a powerful tool to construct, in a unified way, 3D gravity in different signatures, with or without a cosmological constant and even for introducing particles (*e.g.* [61]).The vast amount of study and results on the Chern-Simons theory makes this formulation of 3D gravity an inviting starting point for quantizing gravity as the concepts and methods in gauge theories and quantum topological theories can be naturally applied (*e.g.* [209, 19, 7, 8, 27]). Despite the benefits of using the Chern-Simons formulation of gravity mentioned above, its use to generalize to 4D gravity and hence 4D quantum gravity is limited since 4D gravity can not be formulated into a Chern-Simons action (see however [125, 126] for recent works relating $\mathrm{SL}(2,\mathbb{C})$ Chern-Simons theory to 4D quantum gravity in the path integral approach).

3D gravity action written in terms of the triads and connections can also be generalized to the most general form that is diffeomorphism and Lorentz invariant, called the Mielke-Baekler action [153, 20]. See a recent work [113] of the analysis of this action. On the other hand, adding a boundary term to gravity, as we did in this chapter for general consideration, turns the gauge symmetries in the bulk into physical symmetries possessing non-vanishing charges on the boundaries. The boundary symmetry algebra depends on the location of the boundaries, the type of boundaries and the boundary conditions imposed. (See [124, 123] for works on the most general boundary condition in 3D gravity.) Over the years, massive works have been done to unfold the boundary symmetry algebras of gravity and possible physical applications. (See *e.g.* recent works [101, 88, 89, 90, 107, 106] and references therein.) One of the most important applications is in the context of black holes, for instance, to define the black hole states and compute the black hole entropy (see

[14] When taking the dimension of G, which is the dimension of the plank length ℓ_{p}, into account, $k = \frac{\ell_{\mathrm{p}}}{4\mathrm{G}}$. One can assign a dimension of length to $\mathbf{e}$ and make ω hence F dimensionless. In this way, (1.40) would become $\mathcal{A} = \ell_{\mathrm{p}}^{-1}\mathbf{e}^a P_a + \omega^a J_a$.

e.g. [14, 25, 54, 83, 114]). This requires understanding the quantum gravity theory in the presence of boundaries. We leave the discussion on the quantum theory to the second half of the thesis.

In the context of LQG, the starting point to quantize the 3D gravity is the BF formulation. Our goal for the next chapter is to construct the phase space by carefully choosing the basic variables which form dual pairs well-fitted in the Poisson-Lie group language. Such a representation is powerful in constructing the kinematical and dynamical phase space as well as quantizing the theory.

Chapter 2

Deformed loop gravity

To quantize 3D gravity from the BF formalism (1.14), one needs to regularize the degrees of freedom in order to obtain a Poisson bracket forming an algebra which is not distributional. Indeed, the basic variables $(\omega_\nu^j(\vec{x}), e_\mu^i(\vec{x}))$ are functions of the spatial position $\vec{x} \in \Sigma$. Therefore, the direct quantization of their Poisson brackets into commutators would lead to operator-valued distribution which is singular and does not form a closed algebra. One natural way, stemming from quantizing the Yang-Mills theory [151, 111, 66, 112], is to work on path-dependent states or, more precisely, loop-dependent states. This motivates the use of holonomies - G-valued variables - provided that the connection values in $\mathfrak{g}$, the Lie algebra of G. The holonomy can be viewed as a smeared[1] function of the connection along a path over the spatial sub-manifold. Such a smearing process can also be performed for its conjugate variables, the densitized triad, and can be generalized to 4D gravity.

To start with, one needs to decide which (pair of) group-valued basic variables to take to define the kinematical phase space. Let us first consider the $\Lambda = 0$ case. The smeared function along some path of $\omega_\nu^j(\vec{x})$ gives rise to an SU(2) holonomy and the smeared function of $e_\mu^i(\vec{x}))$ leads to an $\mathbb{R}^3$ flux which is the conjugate momentum of the holonomy. They form the so-called *loop gravity* phase space with Poisson structure emerging from (1.30) [200, 182]. We will review this phase space in Section 2.5. The holonomy and flux variables are turned into operators in the quantization process, which capture nicely the quantum

[1]For a field $\phi(\vec{x})$ valued at point $\vec{x}$ in a manifold D-dimensional $\mathcal{M}$, a smeared field with a smooth and compactly supported function $f(\vec{x})$ is defined as

$$\phi[f] = \int_{\mathcal{M}} \mathrm{d}^D x f(\vec{x})\phi(\vec{x})\,.$$

flat geometries. This establishes that $(\omega^j_\nu(\vec{x}), e^i_\mu(\vec{x}))$ is a good pair of basic variables to start with. When $\Lambda \neq 0$, we want to address the same question. The most natural choice of basic variables would be still $(\omega^j_\nu(\vec{x}), e^i_\mu(\vec{x}))$, identical to the $\Lambda = 0$ case. Then one only needs to smear the Poisson algebra and constraints described in Chapter 1. Such a choice was the first one used in the literature but leads to an anomaly when considering the (regularized) curvature constraint [169].

A useful guide comes from the existing quantum theories of 3D gravity. It was first discovered in the Chern-Simons formalism of gravity by Witten in [210] that the topological invariant quantum observable is described by some quantum group. Shortly later, this topological invariance was constructed mathematically rigorously using quantum group theory by Reshetikhin and Turaev [177], and soon re-discovered in the so-called *Turaev-Viro model* [204]. This is known as a spinfoam model for 3D quantum gravity with a non-vanishing cosmological constant in the Euclidean signature. One lesson from this model is that the cosmological constant deforms the symmetry group of the flat ($\Lambda = 0$) case into a quantum group. Last but not least, also based on the Chern-Simons formulation, the combinatorial quantization approach [7, 8] points out that the gauge symmetry is deformed when $\Lambda \neq 0$.

Inspired by this idea, it was later proposed to use new connections $A_\pm = \omega \pm \sqrt{\Lambda}\mathbf{e}$ (in the case of $\Lambda > 0$) which are quantized to non-commutative holonomy operators [158, 159]. In this approach (and other approaches that we will mention in the quantum part of the thesis), the triads are kept unchanged thus the Gauss constraint expressed solely in terms of the triads is the same as the $\Lambda = 0$ case. From the geometrical perspective, this amounts to taking 2D flat geometries as the building blocks in constructing the global 3D geometry [43]. In this way, the quantum group features come as the regularization in the quantization process and are put by hand. It is, therefore, unnatural to extract the physical (or geometrical) meaning of such a non-commutativity within these frameworks.

Another way is to perform the *deformation* at the kinematical level. This means one considers a different definition of triads which stores curved geometry information. This was first realized at the discrete and quantum level [40, 39]. The spirit is to first realize that the quantum symmetry can be described by the Drinfeld double, which is not apparent in the flat case (see however the early works on the Ponzano-Regge model [104, 105, 160, 152] with a discussion on the Drinfeld double), and secondly that the Drinfeld double is mathematically linked to the Poisson-Lie group and Poisson-Lie algebra [135] at the classical level. It was only recently that such symmetries were derived in the continuous theory [72]. From the geometrical point of view, such an approach is also in accordance with the claim that, in the case of $\Lambda \neq 0$, taking the discrete curved geometry instead of the flat ones as the building blocks to build the global geometry could simplify the

quantization process and better approximate the continuous (diffeomorphism) symmetry [67, 23, 24].

In this chapter, we start reviewing the work of [72] in Section 2.1. We define a new pair of triad and connection which form a dual pair in the sense of a Poisson-Lie algebra. It follows with a discretization process to truncate the degrees of freedom, which we summarize in Section 2.2 following [72]. It leads to the notion of *q-deformed loop gravity phase space*[2] after the standard discretization process, which we describe in Section 2.3. Already at this level, we are able to connect the LQG approach with another quantum gravity approach - the combinatorial quantization [7, 8]. We will describe in Section 2.4 how we can rebuild the q-deformed loop gravity phase space from that discovered by Fock and Rosly [85]. To analyze the relation explicitly, we focus on an example when Σ is a torus. The q-deformed loop gravity phase space for this toy model is given in Appendix B.2. These results were published in [78]. Finally, in Section 2.5, we take the $\Lambda \to 0$ limit of the q-deformed loop gravity model and rewrite the standard loop gravity phase space in the different mathematical framework.

2.1 Change of variables

We first realize that, as in the Turaev-Viro model, the quantum group structure can be seen as the deformation of some group structure with a deformation parameter depending on the value of Λ. Classically, the geometry, solution of the constraints, is curved in the presence of a non-vanishing cosmological constant. However, the torsion constraint, which encodes the gauge symmetries does not depend on the cosmological constant. To have a deformed symmetry realization at the quantum level means that some *ad hoc* treatment needs to be done in the quantization process.

It is therefore natural to look for a different formulation of the theory such that the torsion constraint encoding the gauge symmetry is depending on the cosmological constant, already at the classical level.

We want to identify at the classical level a new pair of variables leading to a new set of constraints all depending on Λ, from which the quantum group structure will eventually emerge naturally.

[2] In fact, as we will see in Section 2.3, the deformation parameter we use in the classical theory is κ. q encodes both κ and reduced Planck constant $\hbar$ and is used in the quantum theory. The term "q-deformed" is used here to be consistent with the quantum theory.

This can be done by implementing a canonical transformation generated by a boundary term to the action. Such an added boundary term keeps the equations of motion unchanged but deforms the notion of torsion. The deformation parameter was actually proposed [72] after the construction of the discrete theory [40] and the quantum theory [39]. We will see in Section 2.5 then Chapter 4 that the desired quantum group symmetries show up after the *standard* quantization process due to precisely our particular choice of new variables.

2.1.1 The new action

We now review the canonical transformation introduced in [72]. We introduce a constant vector $\mathbf{n} = \mathbf{n}^a\tau_a$ whose norm is constrained to be given by the cosmological constant *i.e.* $\mathbf{n}^2 = -\Lambda$. We also demand that $\mathrm{d}\mathbf{n} = 0$ and that $\mathbf{n}$ is constant under the variations *i.e.* $\delta\mathbf{n} = 0$. We add a boundary term to the action (1.14) as follows.

$$\begin{aligned} S'_{\Lambda\mathrm{BF}}[\mathbf{e},\omega] &= -\int_{\mathcal{M}} \mathbf{e}^a \wedge \left(F_a + s\frac{\Lambda}{3}E_a\right) - \int_{\partial\mathcal{M}} \mathrm{d}^2x\, E_a\mathbf{n}^a \\ &= -\int_{\mathcal{M}} \mathrm{Tr}\left(\mathbf{e}\wedge(F + s\frac{\Lambda}{3}E)\right) + \mathrm{d}\left(E\cdot\mathbf{n}\right). \end{aligned} \tag{2.1}$$

Consider the foliation $\mathcal{M} = \Sigma\times\mathbb{R}$, the variation of the new action

$$\begin{aligned} \delta S'_{\Lambda\mathrm{BF}} = -\int_{\mathcal{M}} \mathrm{Tr}\left(\delta\mathbf{e}\wedge(F + s\Lambda E) + \delta\omega\wedge \mathrm{d}_\omega\mathbf{e}\right) - \int_\Sigma \Theta', \\ \Theta' = (\delta\omega_a\wedge\mathbf{e}^a + [\delta\mathbf{e}\wedge\mathbf{e}]_a\mathbf{n}^a) = \left(\delta(\omega_a - \epsilon_{abc}\mathbf{e}^b\mathbf{n}^c)\wedge\mathbf{e}^a\right) \end{aligned} \tag{2.2}$$

leads to a new symplectic potential which reads

$$\Theta' = \mathrm{Tr}\left(\delta A\wedge\mathbf{e}\right), \quad A[\omega,\mathbf{e}] \equiv \omega - [\mathbf{e},\mathbf{n}], \tag{2.3}$$

where A is the new connection. The change of variables $(\omega,\mathbf{e})\to(A,\mathbf{e})$ can be viewed as a canonical transformation, which is generated by the boundary term $\int_{\partial\mathcal{M}}\mathrm{Tr}(E\cdot\mathbf{n})$. Note that we still demand the boundary condition $\delta e|_\Sigma = 0$ in the new variable analysis. One can thus re-express the curvature $F[\omega]$ in terms of the new connection,

$$\begin{aligned} F[\omega] =& \mathrm{d}(A + [\mathbf{e},\mathbf{n}]) + \frac{1}{2}[(A + [\mathbf{e},\mathbf{n}])\wedge(A + [\mathbf{e},\mathbf{n}])] \\ &= F[A] + \mathrm{d}[\mathbf{e},\mathbf{n}] + [A\wedge[\mathbf{e},\mathbf{n}]] + \frac{1}{2}[[\mathbf{e},\mathbf{n}]\wedge[\mathbf{e},\mathbf{n}]] \\ &= F[A] + \mathrm{d}_A[\mathbf{e},\mathbf{n}] + \frac{1}{2}[[\mathbf{e},\mathbf{n}]\wedge[\mathbf{e},\mathbf{n}]]. \end{aligned} \tag{2.4}$$

Let us denote $F[A]$ by F' for short. Then the new action (2.1) can be re-expressed in terms of the new pair of variables $(\mathbf{e}, A)$ as

$$S'_{\Lambda\text{BF}}[\mathbf{e}, A] = -\int_{\mathcal{M}} \text{Tr}\left(\mathbf{e}\wedge F' + \mathbf{e}\wedge \text{d}_A[\mathbf{e},\mathbf{n}] + \frac{1}{2}\mathbf{e}\wedge[[\mathbf{e},\mathbf{n}]\wedge[\mathbf{e},\mathbf{n}]] \right.$$
$$\left. + s\frac{\Lambda}{6}\mathbf{e}\wedge[\mathbf{e}\wedge\mathbf{e}] + \frac{1}{2}\text{d}\left([\mathbf{e}\wedge\mathbf{e}]\mathbf{n}\right)\right) . \quad (2.5)$$

This expression can be dramatically simplified. Firstly, the third and fourth terms cancel according to the identities

$$\begin{aligned}\text{Tr}\left(\mathbf{e}\wedge[[\mathbf{e},\mathbf{n}]\wedge[\mathbf{e},\mathbf{n}]]\right) &= \epsilon_{abc}\epsilon^{b}{}_{lm}\epsilon^{c}{}_{pq}\mathbf{e}^a\wedge\mathbf{e}^l\wedge\mathbf{e}^p\mathbf{n}^m\mathbf{n}^q \\ &= s\epsilon^{b}{}_{lm}\mathbf{e}^a\wedge\mathbf{e}^l\wedge(\mathbf{e}^a\mathbf{n}^m\mathbf{n}^b - \mathbf{e}^b\mathbf{n}^m\mathbf{n}^a) \\ &= s\text{Tr}(\mathbf{e}\wedge\mathbf{e})\text{Tr}(\mathbf{e}\wedge[\mathbf{n},\mathbf{n}]) - \frac{1}{3}s\text{Tr}(\mathbf{nn})\text{Tr}(\mathbf{e}\wedge[\mathbf{e}\wedge\mathbf{e}]) \\ &= -s\frac{\Lambda}{3}\text{Tr}(\mathbf{e}\wedge[\mathbf{e}\wedge\mathbf{e}]) .\end{aligned} \quad (2.6)$$

The second and last terms combine to give[3]

$$\text{Tr}\left(\mathbf{e}\wedge\text{d}[\mathbf{e},\mathbf{n}] + \mathbf{e}\wedge[A\wedge[\mathbf{e},\mathbf{n}]] + \frac{1}{2}\text{d}([\mathbf{e}\wedge\mathbf{e}]\mathbf{n})\right) = -\text{Tr}\left(E\wedge\text{d}_A\mathbf{n}\right) \quad (2.7)$$

Therefore, when using the new connection, the action takes a simple form

$$S'_{\Lambda\text{BF}}[\mathbf{e}, A] = -\int_{\mathcal{M}} \text{Tr}\left(\mathbf{e}\wedge F' - E\wedge\text{d}_A\mathbf{n}\right) . \quad (2.8)$$

We now take $\mathbf{e}$ and A to be independent variables. The variation of (2.8) gives the equations of motion

$$\begin{aligned}\tfrac{\delta S'_{\Lambda\text{BF}}}{\delta\mathbf{e}} \quad &\Longrightarrow \quad \mathcal{C}' = F' - [\mathbf{e}\wedge\text{d}_A\mathbf{n}] \simeq 0 , \\ \tfrac{\delta S'_{\Lambda\text{BF}}}{\delta A} \quad &\Longrightarrow \quad \mathcal{T}' = \text{d}_A\mathbf{e} + [E,\mathbf{n}] \simeq 0 .\end{aligned} \quad (2.9)$$

The symplectic form can be written as

$$\Omega_\Sigma = -\int_\Sigma \text{Tr}\left(\delta A\wedge\delta\mathbf{e}\right) . \quad (2.10)$$

[3]To show that the second and last terms in (2.5) combine to give (2.7), we apply the cyclic symmetry for the expression $\text{Tr}(A\wedge[B\wedge C]) = (-1)^{m(n+p)}\text{Tr}(B\wedge[C\wedge A]) = (-1)^{p(m+n)}\text{Tr}(C\wedge[A\wedge B])$ where A is an m-form, B is an n-form and C is a p-form. Also note that $\mathbf{n}$ is a 0-form so we dropped the $\wedge$ to simplify the expression.

With this new symplectic form at hand, one can study the algebra of symmetries by performing the same analysis as we did in Chapter 1. We describe this analysis in a concise manner in the next subsection.

2.1.2 The new symmetry algebra and the Manin pair

Let us now study the local Lorentz transformation $\delta'^{\mathrm{L}}_\alpha$ and local translation $\delta'^{\mathrm{t}}_\phi$ of the new pair of variables, compared to (1.19). Note that since $\mathbf{n}$ is taken to be kinematical, $\delta'^{\mathrm{L}}_\alpha \mathbf{n} = \delta'^{\mathrm{t}}_\phi \mathbf{n} = 0$.

$$\delta'^{\mathrm{L}}_\alpha \mathbf{e} = [\mathbf{e}, \alpha]\,, \quad \delta'^{\mathrm{L}}_\alpha A = \mathrm{d}_A \alpha + [\mathbf{e}, [\mathbf{n}, \alpha]]\,, \quad \delta'^{\mathrm{t}}_\phi \mathbf{e} = \mathrm{d}_A \phi + [[\mathbf{e}, \phi], \mathbf{n}]\,, \quad \delta'^{\mathrm{t}}_\phi A = [\phi, \mathrm{d}_A \mathbf{n}]\,. \tag{2.11}$$

Only the Lorentz transformation of the triad is unchanged and the other transformations have different shapes. Therefore, we expect a new Poisson structure of the boundary charges (J'_α, P'_ϕ).

We first apply the contraction for the symplectic form with the transformation vectors to get the boundary charges

$$\begin{aligned} \iota_{\delta'^{\mathrm{L}}_\alpha} \Omega_\Sigma = -\delta J'_\alpha \quad &\Longrightarrow \quad J'_\alpha = -\textstyle\int_\Sigma \alpha_a \left(\mathrm{d}_A \mathbf{e} + [E, \mathbf{n}]\right) + \int_S \alpha_a \mathbf{e}^a \simeq \int_S \alpha_a \mathbf{e}^a\,, \\ \iota_{\delta'^{\mathrm{t}}_\phi} \Omega_\Sigma = -\delta P'_\phi \quad &\Longrightarrow \quad P'_\phi = -\textstyle\int_\Sigma \phi^a \left(F'_a - [\mathbf{e} \wedge \mathrm{d}_A \mathbf{n}]_a\right) + \int_S \phi^a A_a \simeq \int_S \phi^a A_a\,. \end{aligned} \tag{2.12}$$

Indeed, the symplectic form generates the new Poisson brackets

$$\{A^i_a(x), \mathbf{e}^b_j(y)\} = \epsilon_i{}^j \delta^a{}_b \delta^2(x-y)\,, \quad \{A^i_a(x), A^j_b(y)\} = \{\mathbf{e}^a_i(x), \mathbf{e}^b_j(y)\} = 0\,, \tag{2.13}$$

from which the Poisson algebra of the symmetry charges read

$$\{J'_\alpha, J'_\beta\} = J'_{[\alpha,\beta]} \tag{2.14a}$$

$$\{P'_\phi, P'_\psi\} = P'_{[[\phi,\psi],\mathbf{n}]} + \int_S \mathrm{Tr}\left([\phi, \psi]\mathrm{d}\mathbf{n}\right)\,, \tag{2.14b}$$

$$\{J'_\alpha, P'_\phi\} = P'_{[\alpha,\phi]} + J'_{[\phi,[\alpha,\mathbf{n}]]} + \int_S \mathrm{Tr}\left(\phi \mathrm{d}\alpha\right)\,. \tag{2.14c}$$

Let us now compare this Poisson algebra and (1.31). Firstly, the subalgebra (2.14a) of $\{J'_\alpha\}$ is the same as that of $\{J_\alpha\}$. Recall that we imposed $\mathrm{d}\mathbf{n} = 0$. We also assume that $\mathrm{d}\alpha|_S = 0$ so that the central charges in (2.14) vanish. In this way, the charges $\{P'_\phi\}$ form a closed algebra (depending on the vector $\mathbf{n}$), which is the major difference from the case

of the algebra for $\{P_\phi\}$. Finally, the mixed Poisson bracket (2.14c) is expressed in terms of both charges J'_α and P'_ϕ with a structure related to the notion of a Manin pair, in the language of Lie bialgebra [135]. We refer readers to [72] for more details. A brief review of the Lie bialgebra for a general Lie group is given in Appendix A.1.

Since the algebra of $\{P'_\phi\}$ depends on $\mathbf{n}$, it is convenient to choose a specific direction for $\mathbf{n}$. We denote the sign of Λ by σ. For the Euclidean signature with a positive Λ, we choose $\mathbf{n}^a = (0, 0, i\sqrt{|\Lambda|})$ and the metric $\eta = (+, +, +)$, while for other cases, we take $\mathbf{n}^a = (0, 0, -\sigma s\sqrt{|\Lambda|})$ and the metric $\eta = (+, -\sigma s, -\sigma)$ [72]. They all give $\mathbf{n}^a\mathbf{n}_a = -\Lambda$. Specifically, when $\Lambda = 0$, $\mathbf{n} = 0$ or $\mathbf{n}$ is null (*resp.* Grasmannian) in the Lorentzian (*resp.* Euclidean) case.

We notice that the on-shell version of the symmetry charges (2.12) are

$$J'_\alpha \simeq \int_S \mathrm{Tr}(\alpha\mathbf{e}) = J_\alpha\,, \quad P'_\phi \simeq \int_S \mathrm{Tr}(\phi A) = \int_S \mathrm{Tr}(\phi(\omega + [\mathbf{n}, \mathbf{e}]))\,, \tag{2.15}$$

which can be quantized to be the generators

$$J'_{\alpha_a} \to J^a \equiv \tau^a\,, \quad P'_{\phi^a} \to P_a + \epsilon_{abc}\mathbf{n}^b J^c =: \rho_a\,, \tag{2.16}$$

where J^a, P^a satisfy the commutation relations (1.38). (To be consistent with literatures [41, 42], we will use τ^a and ρ_a to denote the generators and also denote $\kappa = \sqrt{|\Lambda|}$.) They satisfy the Lie brackets

$$\begin{aligned} &[\tau^a, \tau^b] = \alpha^{ab}_c\tau^c \\ &[\rho_a, \rho_b] = \beta^c_{ab}\rho_c \\ &[\tau^a, \rho_b] = \beta^a_{bc}\tau^c - \alpha^{ca}_b\rho_c \end{aligned} \quad, \quad \text{where} \quad \left| \begin{aligned} &\alpha^{ab}_c = \epsilon^{ab}{}_c \\ &\beta^c_{ab} = s(\mathbf{n}_b\delta^c_a - \mathbf{n}_a\delta^c_b) \end{aligned} \right. . \tag{2.17}$$

We recognize the Lie algebra structure of the classical double[4] $\mathfrak{d}_s = \mathfrak{su}(s) \bowtie \mathfrak{an}(2)$. In other words, $\mathfrak{su}(s)$ and $\mathfrak{an}(2)$ form a Manin pair. Another important structure of a Manin pair is a bilinear dual map $\langle\,,\,\rangle : \mathfrak{su}(2) \otimes \mathfrak{an}(2) \to \mathbb{C}$ such that

$$\langle\tau^a, \rho_b\rangle = \langle\rho_b, \tau^a\rangle = \delta^a_b\,, \quad \langle\tau^a, \tau^b\rangle = \langle\rho_a, \rho_b\rangle = 0\,. \tag{2.18}$$

The simplest case among the four cases is the Euclidean signature with a negative cosmological constant, *i.e.* $(s = +, \sigma = -)$, as τ^a's are generators of SU(2) which is a

[3]The reason that we need to single out the parametrization for the case of $(s = +, \Lambda > 0)$ is that the isometry group $\mathfrak{so}(4)$ does not possess an Iwasawa decomposition.

compact group and $\mathfrak{sl}(2,\mathbb{C}) \cong \mathfrak{su}(2) \bowtie \mathfrak{an}(2)$ admits an Iwasawa decomposition. We will focus on this specific case in the rest of this thesis.

Therefore, by performing the canonical transformation, the new connection A is still $\mathfrak{su}(2)$valued while the triad $\mathbf{e}$ now takes value in $\mathfrak{an}(2)$. Since the torsion constraint $\mathcal{T}'$ (2.9) is written in terms of the triads and $\mathbf{n}$, this implies that the gauge symmetries are deformed by the cosmological constant. We will see this will result in the deformed kinematical phase space in loop gravity upon a proper discretization process which we now briefly describe. More details can be found in [72].

2.2 Discretization of variables

In this section, we briefly summarize the discretization procedure from the new continuous variables $(A(\vec{x}), \mathbf{e}(\vec{x}))$ on Σ we just obtained to discrete variables living on graphs, which was detailly described in [72]. (The $\Lambda = 0$ case was illustrated in more details in [91, 189]). It leads to the basic discrete variables for the q-deformed loop gravity phase space. The discretization process can be separated into two steps. The first step is to consider a triangulation[5] of the manifold Σ, from which one can construct a graph dual to it. The second step is to truncate the infinite number of degrees of freedom on Σ to a finite number of degrees of freedom on the graph by solving the constraints within each triangle.

Let us now fix the terminology and notation as follows. In the triangulation picture, a 2-simplex, or 2-skeleton, is a triangle, denoted as $\triangle$; a 1-simplex is an edge, denoted as $\bar{e}$; and a 0-simplex is a vertex, denoted as $\bar{v}$. The boundary of a $\triangle$, composed of three edges, is denoted by $\partial\triangle$. We will also consider the oriented dual 2-complex of the triangulation embedded in Σ, which we call the *graph* and is denoted as Γ. Γ is composed with faces f's, links e's and nodes v's. Indeed, such a graph is 3-valent, meaning that each node is attached to three links. When e is incident to v, we denote $e \in v$. When e is on the boundary of f, we denote $e \in \partial f$. One face f is dual to one vertex $\bar{v}$; one oriented link e is dual to one edge $\bar{e}$; and one node v is dual to one triangle $\triangle$. By Γ being oriented, we mean that f's are oriented to the orientation of Σ and that each e is given an orientation. In this way, we can also fix the orientation of all the edges $\bar{e}$'s in the triangulation by demanding that the orientations of e_i, $\bar{e}_i$ and Σ satisfy the right-hand rule, where e_i is dual to $\bar{e}_i$. An example is illustrated in fig.2.1.

[4]The symbol "$\bowtie$" means there is mutual action between the two subalgebras $\mathfrak{su}(s)$ and $\mathfrak{an}(2)$. See the explicit action *e.g.* in [72].

[5]More generally, one can consider the cell decomposition of Σ, where each 2-cell is isomorphic to a

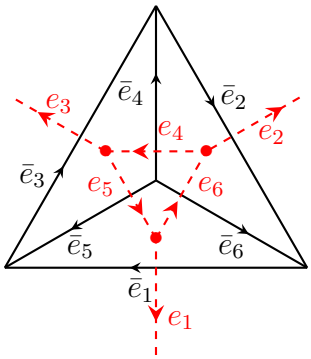

Figure 2.1: Trianglulation (*in black solid*) for Σ composed of three tiangles and its oriented dual graph Γ (*in red dashed*). Each link e_i is dual to the edge $\bar{e}_i$. The orientation of Σ is pointing out of the paper. Then the orientations of e_i, $\bar{e}_i$ and Σ satisfy the right-hand rule.

The triangulation described above is the first step of the distretization process. The next step is to truncate the degrees of freedom to edges and vertices. This is done by solving the equations of motion (2.9) within each triangle. The solution gives $\mathcal{A}_\triangle = A_\triangle + \mathbf{e}_\triangle \in \mathfrak{sl}(2,\mathbb{C})$ associated to each $\partial\triangle$, or equivalently $\mathcal{A}_v = A_v + \mathbf{e}_v$ associated to the node v dual to $\triangle$ in the graph picture. The solution $\mathcal{A}_v$ is parametrized by an $\mathrm{SL}(2,\mathbb{C})$ element G_v, which can be written, by the *Iwasawa decomposition*, into the product of an $\mathrm{AN}(2)$[6] element x_v and $\mathrm{SU}(2)$ element h_v, *i.e.* $G_v = x_v h_v$ [72]. Explicitly,[7]

$$\mathcal{A}_v = G_v^{-1}\mathrm{d}G_v = (x_v h_v)^{-1}\mathrm{d}(x_v h_v) \quad \Longrightarrow \quad \left| \begin{array}{l} A_v = h_v^{-1}\mathrm{d}h_v + (h_v^{-1}(x_v^{-1}\mathrm{d}x_v)h_v)_{\mathfrak{su}(2)} \\ \mathbf{e}_v = (h_v^{-1}(x_v\mathrm{d}x_v)h_v)_{\mathfrak{an}(2)} \end{array} \right. , \tag{2.19}$$

where the subscript $\mathfrak{su}(2)$ means taking the $\mathfrak{su}(2)$ part of the $\mathfrak{sl}(2,C)$-value variable $h_v^{-1}(x_v^{-1}\mathrm{d}x_v)h_v$. Likewise for the subscript $\mathfrak{an}(2)$. As we have solved the constraints at any point, say $p \in \Sigma$,

polygon. For each n-gon, one can add $n-3$ edges connecting a randomly selected vertex and all other vertices to decompose it into $n-2$ triangles, each of which has at least one side coming from the original n-gon. Thus triangulation can be viewed as the most elementary cell decomposition.

[6] In some literature, $\mathrm{AN}(2)$ is also denoted as $\mathrm{SB}(2,\mathbb{C})$ standing for the special Borel group. We will describe more details on this group in Section 2.3.

[7] Consider the gauge transformation by G_v of the connection $\mathcal{A}_v^0$,

$$\mathcal{A}_v^0 \to \mathcal{A}_v = G_v^{-1}\mathcal{A}_v^0 G_v + G_v^{-1}\mathrm{d}G_v\,.$$

Since $\mathcal{A}_v^0 = 0$ is a solution to the flatness $F[\mathcal{A}_v] = 0$. One can gauge fix $\mathcal{A}_v^0$ to 0 then the expression of $\mathcal{A}_v = G_v^{-1}\mathrm{d}G_v$ is the gauge transformation of the connection at 0 which preserves the constraint

within $\triangle$, the solution $\mathcal{A}_v$ in general can be written as a function $\mathcal{A}_v(p) = (G_v^{-1}\mathrm{d}G_v)(p)$ of the point p. When p is v, we gauge fix $G_v(v)$ to be $\mathbb{I}$, then it is natural to view $G_v(p) \equiv G_{vp}$ as the holonomy along a path from v to p. We also take the convention that $G_{pv} = G_{vp}^{-1}$. The symplectic form (2.10) on Σ can thus be written as the the sum of that on each triangle $\triangle$ (or its dual v), each of which can be shown to be equal to the sum of the symplectic form on the boundary edges $\bar{e} \in \partial\triangle$ [72], that is

$$\Omega_\Sigma = \sum_v \Omega_v = \sum_v \sum_{\bar{e}\in\partial\triangle} \Omega_v^{\bar{e}} = -\frac{1}{2}\sum_v \int_v \mathrm{Tr}(\delta\mathcal{A}_v \wedge \delta\mathcal{A}_v)\,. \tag{2.20}$$

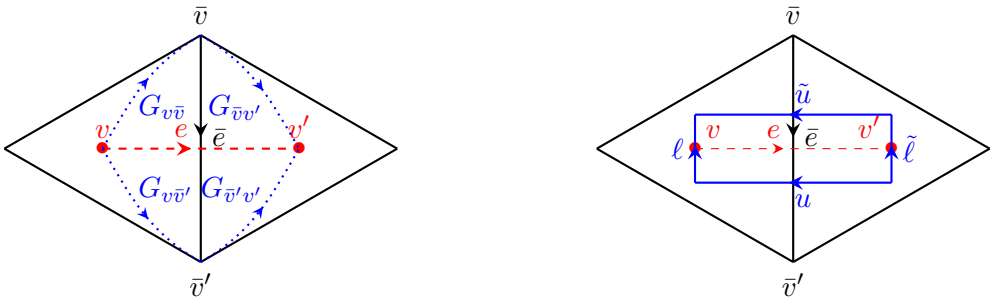

Figure 2.2: *(a)* Two adjacent triangles $\triangle$ (*left*, dual to node v) and $\triangle'$ (it right, dual to node v') sharing one edge $\bar{e}$ whose source and target vertices are $s(\bar{e}) = \bar{v}$ and $t(\bar{e}) = \bar{v}'$ respectively. The $\mathrm{SL}(2,\mathbb{C})$ holonomies $G_{v\bar{v}}, G_{\bar{v}v'}, G_{v\bar{v}'}, G_{\bar{v}'v'}$ (*in dotted blue*) are constrainted by the relation $G_{v\bar{v}}G_{\bar{v}v'} = G_{v\bar{v}'}G_{\bar{v}'v'}$. *(b)*Taking the Iwasawa decomposition of the $\mathrm{SL}(2,\mathbb{C})$ holonomies given in (a), the relation $G_{v\bar{v}}G_{\bar{v}v'} = G_{v\bar{v}'}G_{\bar{v}'v'}$ can be rewitten as $\ell u = \tilde{u}\tilde{\ell}$ where these elements are defined in (2.24).

Now we consider two triangles $\triangle$ - dual to node v - and $\triangle'$ - dual to node v' - who share one edge $\bar{e}$ as illustrated in fig.2.2. For sake of continuity, we demand that $\mathcal{A}(p)$ defined in the frames $\triangle$ and $\triangle'$ share the same value on $\bar{e}$, that is

$$\mathcal{A}_v(p) = \mathcal{A}_{v'}(p) \quad \Longleftrightarrow \quad G_{pv}\mathrm{d}G_{vp} = G_{pv'}\mathrm{d}G_{v'p}\,, \quad \forall p \in \bar{e}\,. \tag{2.21}$$

Let $G_{pv'} = G_{pv}G_{vv'}$. Pluging in the right equation of (2.21), one arrives at $G_{vv'}$ being a constant. This implies that

$$G_{v\bar{v}}G_{\bar{v}v'} = G_{v\bar{v}'}G_{\bar{v}'v'}\,. \tag{2.22}$$

This is illustrated in fig.2.2a. Taking the Iwasawa decomposition $G_{vp} = x_{vp}h_{vp}$ while $G_{pv} = h_{pv}x_{pv}$ (like wise for $G_{v'p}$ and $G_{pv'}$), (2.22) is equivalent to

$$x_{v\bar{v}}h_{v\bar{v}}h_{\bar{v}v'}v_{\bar{v}v'} = x_{v\bar{v}'}h_{v\bar{v}'}h_{\bar{v}'v'}x_{\bar{v}'v'} \quad \Longleftrightarrow \quad x_{\bar{v}'v}x_{v\bar{v}}h_{v\bar{v}}h_{\bar{v}v'} = h_{v\bar{v}'}h_{\bar{v}'v'}x_{\bar{v}'v'}v_{v'\bar{v}}\,. \tag{2.23}$$

If we define the group valued variables

$$(\ell, \tilde{\ell}) := (x_{\bar{v}'v}x_{v\bar{v}}, x_{\bar{v}'v'}x_{v'\bar{v}}) \in \mathrm{AN}(2)\,, \quad (u, \tilde{u}) := (h_{v\bar{v}}h_{\bar{v}v'}, h_{v\bar{v}'}h_{\bar{v}'v'}) \in \mathrm{SU}(2)\,, \tag{2.24}$$

then (2.22) is equivalent to the constraint

$$\ell u = \tilde{u}\tilde{\ell}\,, \tag{2.25}$$

as illustrated in fig.2.2b. The variables $\ell, \tilde{\ell}, u, \tilde{u}$ are used to contruct the q-deformed loop gravity phase space which we will describe in Section 2.3, and (2.25) is essential to define the so-called "ribbon structure" therein. A key question is whether such a phase space can be deduced from the symplectic from (2.10). It was shown in [72] that it is indeed the case. In particular, it was proven in [72] that the symplectic form for the shared edge $\bar{e}$ of two triangles $\triangle, \triangle'$ (whose dual nodes are v and v' respectively) gains contribution from both triangles and takes the form of [8]

$$\Omega^{\bar{e}} = \Omega_v'^{\bar{e}} - \Omega_{v'}^{\bar{e}} = -\frac{1}{2}\int \mathrm{Tr}\left(\delta\tilde{u}\tilde{u}^{-1} \wedge \delta\ell\ell^{-1} + u^{-1}\delta u \wedge \tilde{\ell}^{-1}\delta\tilde{\ell}\right)\,. \tag{2.26}$$

On the other hand, the Poisson bracket between the variables $\ell, \tilde{\ell}, u, \tilde{u}$ can be obtained in the covariant phase space formalism using the new symplectic form (2.20) as we did in Chapter 1. A systematic but lengthy calculation gives rise to the Poisson brackets neatly written in the Poisson-Lie group language which we describe in the next subsection (see (2.35) and (2.36)). We refer to [72] for more details. See also a similar discretization process for the flat case in [91, 189, 188].

At the end of the day, the truncation of degrees of freedom leads us from a phase space on Σ to a phase space on Γ, which contains a finite number of degrees of freedom at the kinematical level. Note that SU(2) and AN(2), as subgroups of $\mathrm{SL}(2,\mathbb{C})$, are of the same footing, hence one can decide at this point which subgroup we choose as the configuration space then the other subgroup would describe the conjugate momentum space. This is called the *choice of polarization* [71]. To emphasize the notion of *deformed* loop gravity, we choose SU(2) to describe the configuration space, which is the same as in loop gravity. Then the momentum space is given by the AN(2) group, which can be seen as a deformation of $\mathbb{R}^3$, the momentum space of loop gravity with $\Lambda = 0$.

[8] The minus sign before $\Omega_{v'}'^{\bar{e}}$ is due to the fact that the edge $\bar{e}$ is oriented oppositely relative to the triangles $\triangle$ and $\triangle'$, as shown in fig.2.2a.

2.3 q-deformed loop gravity phase space

In this section, we construct the phase space of the q-deformed loop gravity for the case of Euclidean signature with $\Lambda < 0$ in terms of the SU(2) and AN(2) discrete variables we obtain in the discretization procedure. It was first introduced in [40] and later developed in a series of works by Bonzom, Dupuis, Girelli, Livine and the author [39, 73, 77, 42]. The discrete variables we work with are different from those defined in [158, 159]. We will see that our discrete variables are elements of a pair of groups forming a Heisenberg double, which possesses a symplectic structure by definition and hence can be used to describe a phase space. A toy model for a simple graph embedded on the torus is summarized in Appendix B.2, which was illustrated in more detail in our published work [77].

2.3.1 Ribbon for one link

We first consider a single graph link, whose phase space is described by $\mathrm{SL}(2,\mathbb{C})$ as a group. The relevant mathematical frameworks are the *classical double* (at the Lie algebra level) and the *Heisenberg double* (at the group level), which we review in Appendix A.1. Provided the symplectic structure, $\mathrm{SL}(2,\mathbb{C})$ is equivalent to a Heisenberg double $\mathcal{D}(\mathrm{SU}(2))$ of SU(2) with the dual group $\mathrm{SU}(2)^* = \mathrm{AN}(2)$, the group of 2×2 lower triangular matrices with positive real diagonal entries and determinant 1. We parametrize an AN(2) element ℓ as

$$\ell = \begin{pmatrix} \lambda & 0 \\ z & \lambda^{-1} \end{pmatrix}, \quad \lambda \in \mathbb{R}^+, z \in \mathbb{C}. \tag{2.27}$$

We write $\mathcal{D}(\mathrm{SU}(2)) \cong \mathrm{SU}(2) \bowtie \mathrm{AN}(2)$ with $\bowtie$ inheriting from the Lie algebra mutual action. Their duality and the Poisson structure are also built from the Lie algebra level.

Since we fixed the signature and the sign of Λ, we can now write out explicitly the SU(2) and AN(2) generators

$$\begin{aligned} &\tau^a = \frac{\sigma^a}{2i} \in \mathfrak{su}(2), \quad \rho^a = i\kappa(\tau^a - i[\tau^3, \tau^a]) \in \mathfrak{an}(2) \\ \Longrightarrow\ &\tau^1 = \tfrac{1}{2}\begin{pmatrix} 0 & -i \\ -i & 0 \end{pmatrix}, \quad \tau^2 = \tfrac{1}{2}\begin{pmatrix} 0 & -1 \\ 1 & 0 \end{pmatrix}, \quad \tau^3 = \tfrac{1}{2}\begin{pmatrix} -i & 0 \\ 0 & i \end{pmatrix} \\ &\rho^1 = i\kappa\tau^- = \kappa\begin{pmatrix} 0 & 0 \\ 1 & 0 \end{pmatrix}, \quad \rho^2 = -\kappa\tau^- = \kappa\begin{pmatrix} 0 & 0 \\ i & 0 \end{pmatrix}, \quad \rho^3 = i\kappa\tau^3 = \tfrac{\kappa}{2}\begin{pmatrix} 1 & 0 \\ 0 & -1 \end{pmatrix}. \end{aligned} \tag{2.28}$$

Mathematically, the Lie algebra structure of $\mathfrak{an}(2)$ is determined by a cocycle δ, which is a map $\delta : \mathfrak{su}(2) \to \mathfrak{su}(2) \otimes \mathfrak{su}(2)$. This defines a Lie bialgebra $(\mathfrak{su}(2), \delta)$. On the other hand, adding a cocycle $\delta_* : \mathfrak{an}(2) \to \mathfrak{an}(2) \otimes \mathfrak{an}(2)$ to $\mathfrak{an}(2)$ Lie algebra that determines the Lie algebra structure of $\mathfrak{su}(2)$ defines the Lie bialgebra $(\mathfrak{an}(2), \delta_*)$. These cocycles act explicitly on the generators as

$$\delta(\tau^c) = \kappa(\delta^c_a\delta^3_b - \delta^3_a\delta^c_b)\tau^a \otimes \tau^b\,, \quad \delta_*(\rho_c) = \epsilon^{ab}{}_c \rho_a \otimes \rho_b \quad \longrightarrow \quad \left| \begin{array}{l} [\tau^a, \tau^b] = \epsilon^{ab}{}_c \tau^c \\ [\rho_a, \rho_b] = \kappa(\delta^c_a\delta^3_b - \delta^3_a\delta^c_b)\rho_c \end{array} \right. , \tag{2.29}$$

where the Lie algebra (2.17) of $\mathfrak{su}(2)$ and $\mathfrak{an}(2)$ introduced before with the chosen parametrization $\mathbf{n} = (0, 0, \kappa)$ is recovered. The bilinear form dualizing $\mathfrak{su}(2)$ and $\mathfrak{an}(2)$ is

$$\langle M, N\rangle := -\frac{1}{2\kappa}\mathrm{Im}(\mathrm{Tr}(MN))\,, \quad M, N \in \mathfrak{sl}(2, \mathbb{C})\,, \tag{2.30}$$

thus $\langle \rho_a, \tau^b\rangle = \delta^b_a\,, \langle \rho_a, \rho_b\rangle = \langle \tau^a, \tau^b\rangle = 0$ as desired. Given the representation of the generators, one can also compute

$$[\tau^a, \rho_b] = \kappa(\delta^a_b\delta^c_3 - \delta^3_b\delta^c_a)\tau^c + \epsilon^a{}_b{}^c\rho_c\,, \tag{2.31}$$

which is consistent with (2.17). Together with (2.29), they are precisely the Lie bialgebra structure of the classical double $(\mathfrak{d}(\mathfrak{su}(2)), \delta_\mathfrak{d})$ which is a quasitriangular Lie bialgebra with the Lie algebra $\mathfrak{d}(\mathfrak{su}(2)) = \mathfrak{su}(2) \bowtie \mathfrak{an}(2)$ and the cocycle $\delta_\mathfrak{d}$ (See (A.13) for its action on the Lie algebra objects). It is called quasitriangular in the sense that the cocycle $\delta_\mathfrak{d}$ is a coboundary $\delta_\mathfrak{d} = \partial r$ of some cochain such that satisfies a so-called *classical Yang-Baxter equation*. Such a cochain $r \in \mathfrak{d} \otimes \mathfrak{d}$ is also called the *classical r-matrix*, or r-matrix for short.[9] We denote $r \equiv r_{12} = \sum r_{[1]} \otimes r_{[2]}$, $r_{21} := \sum r_{[2]} \otimes r_{[1]}$. More generally, r_{ij} means that $r_{[1]}$ is in the i-th vector space, $r_{[2]}$ is in the j-th vector space and all other vector spaces are identity. Using this notation, the classical Yang-Baxter equation is expressed as

$$[r_{12}, r_{13}] + [r_{12}, r_{23}] + [r_{13}, r_{23}] = 0\,. \tag{2.32}$$

In the fundamental representation, an r-matrix for $\mathfrak{d}(\mathfrak{su}(2))$ giving rise to the commutators (2.29) and (2.31) can be written as a 4×4 matrix

$$r = -\sum_a \tau^a \otimes \rho_a = \frac{i\kappa}{4}\begin{pmatrix} 1 & 0 & 0 & 0 \\ 0 & -1 & 4 & 0 \\ 0 & 0 & -1 & 0 \\ 0 & 0 & 0 & 1 \end{pmatrix} \in \mathfrak{su}(2) \otimes \mathfrak{an}(2) \subset \mathfrak{d} \otimes \mathfrak{d}\,. \tag{2.33}$$

[9] See Definition A.1.2 for an alternative but equivalent way to define a quasitriangular Lie bialgebra that is the classical version of the definition A.2.1 of a quasitriangular Hope algebra.

Exponentiating the Lie subalgebras $\mathfrak{su}(2)$ and $\mathfrak{an}(2)$ of $\mathfrak{d}(\mathfrak{su}(2))$, one obtains the Heisenberg double $(\mathcal{D}(\mathrm{SU}(2)), \pi_H)$, whose Poisson structure π_H is fully determined by the r-matrix inheriting from $\mathfrak{d}(\mathfrak{su}(2))$. Explicitly, the Poisson bracket is given by

$$\{d_1, d_2\} = -r_{21} d_1 d_2 + d_1 d_2 r = r d_1 d_2 - d_1 d_2 r_{21} \,, \quad \forall d \in \mathrm{SL}(2,\mathbb{C}) \,, \tag{2.34}$$

where we have used the standard notation $d_1 = d \otimes \mathbb{I}$, $d_2 = \mathbb{I} \otimes d$. The last equality in (2.34) is guaranteed by the fact that the symmetric part $r_s = \frac{1}{2}(r + r_{21})$ of the r-matrix is a Casimir hence $[r_s, d_1 d_2] = 0$

On the other hand, since the two subgroups SU(2) and AN(2) are of the same footing, one can equivalently write the phase space as the Heisenberg double $\mathcal{D}(\mathrm{AN}(2))$ of AN(2) with a different r-matrix $\tilde{r} \in \mathfrak{an}(2) \otimes \mathfrak{su}(2)$ exchanging the generators on the two subspaces from (2.33) in the fundamental representation, *i.e.* $\tilde{r} = r_{21}, \tilde{r}_{21} = r$. The two different ways of viewing the phase space $\mathrm{SL}(2,\mathbb{C})$ correspond to the only two possible *Iwasawa decompositions* of a given $\mathrm{SL}(2,\mathbb{C})$ element d. We refer the decomposition $d = \ell u$ with $\ell \in \mathrm{AN}(2), u \in \mathrm{SU}(2)$ to be the left Iwasawa decomposition and $d = \tilde{u}\tilde{\ell}$ with $\tilde{\ell} \in \mathrm{AN}(2), \tilde{u} \in \mathrm{SU}(2)$ to be the right Iwasawa decomposition. Then from (2.34), we can deduce the Poisson brackets between ℓ and u [40]:

$$\{\ell_1, \ell_2\} = -[r_{21}, \ell_1 \ell_2] \,, \quad \{\ell_1, u_2\} = -\ell_1 r_{21} u_2 \,, \quad \{u_1, \ell_2\} = \ell_2 r u_1 \,, \quad \{u_1, u_2\} = -[r, u_1 u_2] \,, \tag{2.35}$$

and the Poisson brackets between $\tilde{\ell}$ and $\tilde{u}$:

$$\{\tilde{\ell}_1, \tilde{\ell}_2\} = [r_{21}, \tilde{\ell}_1 \tilde{\ell}_2] \,, \quad \{\tilde{\ell}_1, \tilde{u}_2\} = -\tilde{u}_2 r_{21} \tilde{\ell}_1 \,, \quad \{\tilde{u}_1, \tilde{\ell}_2\} = \tilde{u}_1 r \tilde{\ell}_2 \,, \quad \{\tilde{u}_1, \tilde{u}_2\} = [r, \tilde{u}_1 \tilde{u}_2] \,. \tag{2.36}$$

It is easy to check that the equivalence of the left and right Iwasawa decomposition forms a second class constraint (meaning that they do not close under Poisson brackets), which we call the "ribbon constraint"

$$\mathcal{C} = \ell u \tilde{\ell}^{-1} \tilde{u}^{-1} \,. \tag{2.37}$$

The name "ribbon" will become clear when we represent graphically these two equal Iwasawa decompositions. Concretely, a link e is thickened into a ribbon $R(e)$ with

- long links, parallel to e, carrying SU(2) elements $u, \tilde{u}$ called *holonomies*
- short links carrying AN(2) elements $\ell, \tilde{\ell}$ and called *fluxes* [40].

This is represented in fig.2.3 together with a choice of orientations (detailed below). We have fixed the orientation of the long ribbon links decorated with u and $\tilde{u}$ to be opposite

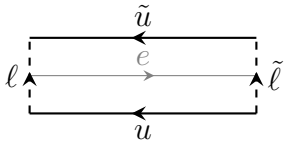

Figure 2.3: The ribbon graph associated to the ribbon constraint. The ribbon carries two pairs of variables (ℓ, u) and $(\tilde{\ell}, \tilde{u})$. The ribbon constraint associated to a ribbon is represented as the trivialization of the ribbon loop $\ell u \tilde{\ell}^{-1} \tilde{u}^{-1}$.

to that of the link, which automatically fixes the orientation of the two short links of a ribbon to have the ribbon constraint (2.37) satisfied.

By solving the ribbon constraint, we obtain the Poisson brackets between $(\tilde{\ell}, \tilde{u})$ and (ℓ, u):

$$\begin{aligned} &\{\ell_1, \tilde{u}_2\} = -r_{21}\ell_1\tilde{u}_2\,, \quad \{\tilde{\ell}_1, u_2\} = -\tilde{\ell}_1 u_2 r_{21}\,, \quad \{u_1, \tilde{\ell}_2\} = \tilde{\ell}_2 u_1 r,\,, \quad \{\tilde{u}_1, \ell_2\} = r\tilde{u}_1\ell_2\,, \\ &\{\tilde{\ell}_1, \ell_2\} = 0\,, \qquad\qquad \{\tilde{u}_1, u_2\} = 0\,. \end{aligned} \tag{2.38}$$

Consider the fundamental represenation of SU(2) and AN(2) variables, each of the Poisson brackets written in the form of (2.35), (2.36) and (2.38) is a 4×4 matrix of Poisson brackets. Writing out the matrix elements of $\ell, u, \tilde{\ell}$ and $\tilde{u}$, one can write out the explicit Poisson brackets of these matrix elements. We collect these Poisson brackets in Appendix B.1. The dimension of the phase space for a ribbon is $12-6=6$ upon imposing the ribbon constraint, thus consistent with the dimension of $\mathrm{SL}(2,\mathbb{C})$.

It is important to notice that there is another version of the ribbon constraint available. Indeed, in the definition, we used the lower triangular matrices. But instead, we could use the upper triangular matrices. The equivalence between the two formulations can be seen by using the composition of the adjoint and inverse on the ribbon constraint,

$$\mathcal{C} = \ell u \tilde{\ell}^{-1} \tilde{u}^{-1} \to \mathcal{C}^{-1\dagger} = \ell^{-1\dagger} u \tilde{\ell}^{\dagger} \tilde{u}^{-1}, \tag{2.39}$$

which amounts to replacing ℓ and $\tilde{\ell}$ with respectively $\ell^{-1\dagger}$ and $\tilde{\ell}^{-1\dagger}$ (and similarly with $u, \tilde{u}$ but obviously $u^{-1\dagger} = u$ for any $u \in \mathrm{SU}(2)$). Therefore, only the short link structure is changed, as in fig.2.4. The associated transformation preserving the Lie algebra $\mathfrak{an}(2)$ is given by $\rho^i \to -(\rho^i)^\dagger$. As a consequence, one switches the r-matrix by $r \to -r^\dagger = r_{21}$. All Poisson brackets are given in Appendix B.1.

Deformed flux vectors. Combing the two parametrizations together, we construct the Hermitian matrices $\ell\ell^\dagger =: X = \kappa X_0 \mathbb{I} - \kappa \vec{X} \cdot \vec{\sigma}$ and $\ell^\dagger \ell =: X^{\mathrm{op}} = \kappa X_0^{\mathrm{op}} \mathbb{I} - \kappa \vec{X}^{\mathrm{op}} \cdot \vec{\sigma}$

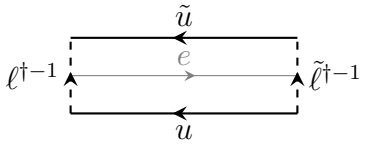

Figure 2.4: The conjugate ribbon structure defined in terms of upper triangular matrices.

where the traceless parts give components of vectors $\vec{X}$ and $\vec{X}^{\rm op}$. Written in terms of the parametrization (2.27), they read explicitly

$$\begin{aligned} X = \ell\ell^\dagger = \begin{pmatrix} \lambda^2 & \lambda\bar{z} \\ \lambda z & \lambda^{-2}+|z|^2 \end{pmatrix}, \quad & \left| \begin{array}{l} X_0 = \frac{1}{2\kappa}\mathrm{Tr}(\ell\ell^\dagger) = \frac{1}{2\kappa}(\lambda^2+\lambda^{-2}+|z|^2) \\ \vec{X} = -\frac{1}{2\kappa}\mathrm{Tr}(\ell\ell^\dagger\vec{\sigma}) \end{array} \right. , \\ X^{\rm op} = \ell^\dagger\ell = \begin{pmatrix} \lambda^2+|z|^2 & \lambda^{-1}\bar{z} \\ \lambda^{-1}z & \lambda^{-2} \end{pmatrix}, \quad & \left| \begin{array}{l} X_0^{\rm op} = X_0 \\ \vec{X}^{\rm op} = -\frac{1}{2\kappa}\mathrm{Tr}(\ell^\dagger\ell\vec{\sigma}) \end{array} \right. , \end{aligned} \tag{2.40}$$

where the 4-vector $X^\mu(\mu = 0,1,2,3)$ lives on the space-like 3-hyperboloid in the 3+1 Minkowski space, $X^\mu X_\mu = X_0^2 - \vec{X}^2 = \kappa^{-2}$. The deformation parameter κ clearly plays the role of the curvature. The 3D component of X^μ defines the flux vector X at the ribbon source.

Similarly, $\tilde{X}$ and $\tilde{X}^{\rm op}$ can be written in terms of the tilde spinors in the same way. They are stable under the adjoint action of SU(2),

$$\tilde{X} = \tilde{u}^{-1}X\tilde{u}\,, \quad u^{-1}X^{\rm op}u = \tilde{X}^{\rm op}\,, \tag{2.41}$$

which is the same transformation of the flux vectors in the flat case as we will see in Section 2.5. They capture the deformed geometry of the discretization of Σ, which possesses the hyperbolic nature [40]. In particular, the Gauss constraint for a three-valent node describes the closure of a hyperbolic triangle, whose side lengths are given by the vector X's or $X^{\rm op}$'s for the corresponding side (see [40]).

SU(2) **transformations.** Write $w = \mathbb{I}+i\vec{\epsilon}\cdot\vec{\sigma}$ an infinitesimal SU(2) group element. Then, the variation of a phase space function h under a left infinitesimal SU(2) transformation is given by [40]:

$$\delta_\epsilon h = -\lambda^{-2}\kappa^{-1}\{\mathrm{Tr}WX, h\} = -\lambda^{-2}\kappa^{-1}\{2\epsilon_z\lambda^2 + \epsilon_-\lambda z + \epsilon_+\lambda\bar{z}, h\}\,, \tag{2.42}$$

where $W = \epsilon_z(\mathbb{I}+\sigma_z) + \epsilon_-\sigma_+ + \epsilon_+\sigma_-$ and X is the flux vector defined in (2.40).

Change of edge orientations. The way we associate variables to the sides of a ribbon has been described above, as in fig.2.3. Changing the orientation of an edge is an involution $\mathfrak{m}$ which has the following effects on the variables,

$$\mathfrak{m} : u \mapsto \tilde{u}^{-1}\,, \quad \mathfrak{m} : \ell \mapsto \tilde{\ell}^{-1} \tag{2.43}$$

and since it is an involution, $\mathfrak{m}(\tilde{u}) = u^{-1}$ and $\mathfrak{m}(\tilde{\ell}) = \ell^{-1}$.

2.3.2 Ribbon graph and the first-class constraints

Considering now a full graph Γ embedded in Σ, we thicken it into a ribbon graph $\Gamma_{\rm r}$ by thickening every link into a ribbon in the same way as in fig.2.3, where all ribbons are embedded in Σ. An example is given in fig.2.5.

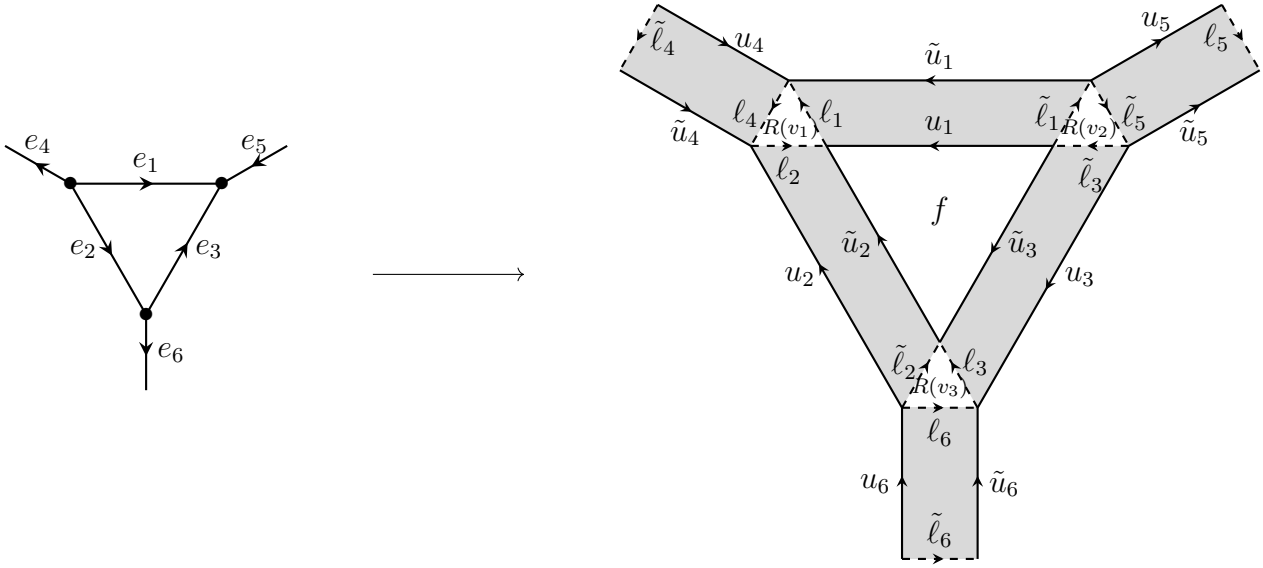

Figure 2.5: A graph Γ (*on the left*) and its correspondent ribbon graph $\Gamma_{\rm r}$(*on the right*).

As such, a ribbon graph contains three types of simple faces (with no links inside):

i. faces within the ribbon $R(e)$'s for which the ribbon constraints are imposed - these are the faces in grey in fig.2.5;

ii. faces surrounded by the short links of the ribbons decorated with fluxes only - these are fat nodes - we call them ribbon nodes. If v is a node of Γ, then let $R(v)$ be the the corresponding ribbon node in $\Gamma_{\rm r}$. In fig.2.5, these are faces $R(v_1), R(v_2)$ and $R(v_3)$.

iii. faces surrounded by the long links of the ribbons - these are the faces from the original graph. There is one such face - f in fig.2.5.

Within each ribbon $R(e)$, the holonomies and fluxes satisfy the Poisson brackets (2.35), (2.36) and (2.38), while variables from different ribbons commute. Apart from the ribbon constraints, we also have two sets of first-class constraints, namely the Gauss constraints which are associated to nodes and the flatness constraints[10] which are associated to faces.

The Gauss constraints and the kinematical phase space. For an n-valent node v, the Gauss constraint imposes that the ordered product of the fluxes along the short links of $R(v)$ is trivial. Explicitly, the Gauss constraint reads

$$\mathcal{G}_v = \overrightarrow{\prod}_i^n \ell_{e_i,v}\,, \quad \ell_{e_i,v} = \begin{cases} \ell_i & \text{if} \quad o_i = 1 \\ \tilde{\ell}_i^{-1} & \text{if} \quad o_i = -1 \end{cases}, \tag{2.44}$$

where $o_i = 1$ corresponds to an outgoing link and $o_i = -1$ corresponds to an incoming link. For instance, the Gauss constraint for $R(v_3)$ in fig.2.5 is $\mathcal{G}_{v_3} = \tilde{\ell}_2^{-1}\ell_6\ell_3 \simeq \mathbb{I}$.

The Gauss constraint generates SU(2) transformations. A phase space function h transforms under the infinitesimal rotation parametrized by a infinitesimal vector $\vec{\epsilon}$ as [40]

$$\delta_\epsilon h = -\kappa^{-1} \prod_{i=1}^n \Lambda_i^{-2} \{\mathrm{Tr}(W\mathcal{G}_v\mathcal{G}_v^\dagger), h\}\,, \quad \text{with } W = \begin{pmatrix} 2\epsilon_z & \epsilon_- \\ \epsilon_+ & 0 \end{pmatrix}, \tag{2.45}$$

where Λ_i is the first diagonal element of the matrix (2.27) of the i-th flux, $\ell_{e_i,v}$, in $\mathcal{G}_v$, that is λ_i or $\tilde{\lambda}_i^{-1}$.

Alternatively, one can use the parametrization with $\ell^\dagger$ and $\tilde{\ell}^\dagger$ for the fluxes as in fig.2.4. Then the Gauss constraint is transformed accordingly

$$\mathcal{G}_v \to \mathcal{G}_v^{\dagger -1}, \tag{2.46}$$

and we have the same action in terms of the symmetry if we consider

$$\delta_\epsilon h = -\frac{1}{\kappa} \prod_{i=1}^n \Lambda_i^{-2} \{\mathrm{Tr}(\tilde{W}\left(\mathcal{G}_v\mathcal{G}_v^\dagger\right)^{-1}), h\}\,, \quad \text{with } \tilde{W} = \begin{pmatrix} 0 & -\epsilon_- \\ -\epsilon_+ & 2\epsilon_z \end{pmatrix}, \tag{2.47}$$

[10] We call them the flatness constraints to match the notion in loop gravity, but they do not impose the zero curvature but a constant curvature. In other words, curvature excitation is defined on top of the constant curvature given by the cosmological constant.

where Λ_i is still λ_i or $\tilde{\lambda}_i^{-1}$ according to the orientation of the link e_i.

In fact, such a parametrization is not only an alternative one but a necessary piece for constructing the complete kinematical phase space as ℓ and $\tilde{\ell}$ only contain z and $\tilde{z}$ in their matrix elements, while one also needs access to their complex conjugate counterparts $\bar{z}$ and $\bar{\tilde{z}}$ which are stored in $\ell^{-1\,\dagger}$ and $\tilde{\ell}^{\dagger}$ respectively. We will see in Chapter 4 that both z and $\bar{z}$ (as well as $\tilde{z}$ and $\bar{\tilde{z}}$) are needed to construct the $\mathcal{U}_q(\mathfrak{su}(2))$ generators upon quantization.

Gauss constraints generate local SU(2) transformations through the Poisson brackets [40, 41]. As usual in symplectic geometry, first-class constraints are not only imposed but one also needs to quotient out the phase space by the orbits they generate. This is called the symplectic quotient. Here, one obtains $\mathcal{P}_{\text{kin}} = \text{SL}(2,\mathbb{C})^E//\text{SU}(2)^V$ which is called the *kinematical phase space*, where E and V denotes the number of links and nodes in Γ.

It was shown in [40] that the Gauss constraint for a trivalent node geometrically represents the hyperbolic cosine law, implying that the kinematical phase space describes hyperbolic discrete geometries (more particularly hyperbolic triangles in that case).

The flatness constraints and the physical phase space. For a face surrounded by m long links, the flatness constraint imposes that the ordered product of the holonomies along the long links of ribbons is trivial. It is expressed in a similar way as the Gauss constraint,

$$\mathcal{F}_f = \overrightarrow{\prod_i^m} u_{e_i,f}\,, \quad u_{e_i,f} = \begin{cases} u_i & \text{if} \quad o_i = 1 \\ \tilde{u}_i^{-1} & \text{if} \quad o_i = -1 \end{cases}, \tag{2.48}$$

where the orientation is relative to the orientation of f, which is naturally generated by the orientation of Σ. Flatness constraints generate (deformed) translations [40]. The *physical phase space* is then obtained via the symplectic quotient of the kinematical phase space by the flatness constraints, $\mathcal{P}_{\text{phys}} = \mathcal{P}_{\text{kin}}//\text{AN}(2)^F$ with F the number of the faces in Γ.

We also give an explicit example of the phase space for a simple group embedded on a torus in Appendix B.2 and construct with the holonomies and fluxes of the ribbon graph the physical observables which form the Goldman brackets [122]. This will be compared to the Fock-Rosly phase space structure which we will describe in the next section. We also refer to [77] for more details.

Up to now, we have developed the q-deformed loop gravity phase space in terms of the holonomy and flux variables. The use of the r-matrix is reminiscent of the phase space constructed by Fock and Rosly [85], which became well-known after it was used by Alekeev, Grosse and Schomerus to define the combinatorial quantization of the Chern-Simons theory

[7, 8]. This hints that there may be an explicit relation between our deformed phase space and the Fock-Rosly one. This is indeed the case as shown in [77], which we describe in the next section.

2.4 Relation with the Fock-Rosly construction

As illustrated in Chapter 1, 3D Euclidean gravity with $\Lambda < 0$ can be reformulated as an $\mathrm{SL}(2,\mathbb{C})$ Chern-Simons theory. The symplectic structure of the moduli space of flat $\mathrm{SL}(2,\mathbb{C})$ graph connections up to $\mathrm{SL}(2,\mathbb{C})$ gauge transformations can be described by the so-called Fock-Rosly brackets. Quantizing this bracket and promoting it to commutators of operators leads to the combinatorial quantization of Chern-Simons theory [7, 8, 53]. The question we want to explore is whether the 3D q-deformed loop gravity framework could be reconciled with the Fock-Rosly phase space. This can be seen as a first step to understanding the relation between the LQG approach and the quantum Chern-Simons theory. To be explicit, we work on a toy model when Σ is a torus. This is the simplest compact 2D manifold with a non-trivial topology, which allows us to construct non-trivial global observables.

2.4.1 Fock-Rosly construction

Let us first briefly review the Fock-Rosly construction introduced in [85]. It is built on a compact, oriented Riemann surface. We consider a cell decomposition of that surface and focus on the graph defined by its 1-skeleton. We consider a Riemann surface with no boundaries for simplicity[11]. We define a graph connection, as in lattice gauge theory, by assigning an $\mathrm{SL}(2,\mathbb{C})$ group element, or holonomy, to each oriented link of the graph. The Fock-Rosly construction provides the space of flat graph connections with a symplectic structure compatible with gauge transformations. More precisely, we impose the flatness of the $\mathrm{SL}(2,\mathbb{C})$ connection around every face of the graph and consider equivalence classes under $\mathrm{SL}(2,\mathbb{C})$ gauge transformations at every node of the graph.

For this purpose, we introduce another combinatorial structure to the graph, a linear order, denoted as $\prec$, of the links around each node. This is visually realized by adding a cilium at each node, separating the links of the lowest and highest order. For each link α, we denote as $\alpha_{(s)}$ the half-link incident to the source and $\alpha_{(t)}$ the opposite half-link incident to the target. When two links α and β are incident to a same node v, *i.e.* $\alpha, \beta \in v$, $\alpha \prec \beta$

[11] Fock-Rosly phase space is also defined for Riemann surfaces with boundaries [85].

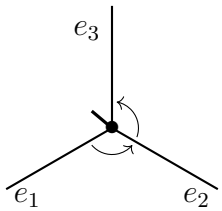

Figure 2.6: One node with three incident links e_1, e_2, e_3. The thick short strand represents the cilium sitting at the node. The linear order of three links reads $e_1 \prec e_2 \prec e_3$.

(or equivalent $\beta \succ \alpha$) represents that link β is of higher order than α relative to the node v. (When the orientation is specified, say $\alpha_{(s)}, \beta_{(t)} \in v$, it is clearer to say $\alpha_{(s)} \prec \beta_{(t)}$.) It means when one sweeps the cilium sitting on v in the direction induced by the orientation of Σ, the cilium meets with α before β. An example is shown in fig.2.6. A graph with a linear order on each node is called a *ciliated graph*. On a ciliated graph, we further assign an r-matrix $r(v)$ to each node v. Each r-matrix is decomposed as $r(v) = r_s + r_a(v)$ in terms of its symmetric part $r_s = \frac{1}{2}(r(v) + r_{21}(v))$ and its antisymmetric part $r_a = \frac{1}{2}(r(v) - r_{21}(v))$. As the notation suggests, we require that the symmetric parts r_s of the r-matrices are all the same and do not depend on the nodes, while their antisymmetric parts $r_a(v)$ are left free. This allows us to define a Poisson structure on the space of graph connections by the following bivector [85]:

$$\pi_{\mathrm{FR}} = \sum_v \left(\sum_{\alpha,\beta \in v; \alpha \prec \beta} r^{ij}(v) X_i^\alpha \wedge X_j^\beta + \frac{1}{2} \sum_{\alpha \in v} r^{ij}(v) X_i^\alpha \wedge X_j^\alpha \right) , \tag{2.49}$$

where $X_i^\alpha = L_i^\alpha + R_i^\alpha$ is the sum of the right-invariant vector R_i^α and the left-invariant vector L_i^α associated to the $\mathrm{SL}(2,\mathbb{C})$ group element on link α and the basis $t_i \in \mathfrak{sl}(2,\mathbb{C})$. They act on functions $\mathcal{F} \in C^\infty(\mathrm{SL}(2,\mathbb{C})^E)$ as

$$L_i^\alpha f(g_\alpha, \cdots) = \frac{\mathrm{d}}{\mathrm{d}\nu}\bigg|_{\nu=0} f(e^{-\nu t_i} g_\alpha, \cdots) , \quad R_i^\alpha f(g_\alpha, \cdots) = \frac{\mathrm{d}}{\mathrm{d}\nu}\bigg|_{\nu=0} f(g_\alpha\, e^{\nu t_i}, \cdots) . \tag{2.50}$$

The bivector π_{FR} defines the Poisson brackets for all configurations. It would be clearer to write the Poisson brackets for different cases out. Let us call $G^e \in \mathrm{SL}(2,\mathbb{C})$ the holonomy along the link e. We call $s(e)$ and $t(e)$ respectively the source and target nodes of the link e. Then the Fock-Rosly bracket $\{G_1^e, G_2^{e'}\}_{\mathrm{FR}}$ between the holonomies along the two links e and e' is defined by distinguishing the various configurations (the list below is not exhaustive but representative):

- For a single link e with distinct source and target, *i.e.* $s(e) \neq t(e)$:

$$\{G_1^e, G_2^e\}_{\mathrm{FR}} = r_a(s(e))G_1^e G_2^e + G_1^e G_2^e r_a(t(e))\,. \tag{2.51a}$$

- For a single closed curve e oriented counterclockwise, *i.e.* $s(e) = t(e)$ and $e_{(s)} \prec e_{(t)}$:

$$\{G_1^e, G_2^e\}_{\mathrm{FR}} = r_a G_1^e G_2^e + G_2^e G_1^e r_a + G_2^e r_{21} G_1^e - G_1^e r G_2^e\,. \tag{2.51b}$$

- For a single closed curve e oriented counterclockwise, *i.e.* $s(e) = t(e)$ and $e_{(t)} \prec e_{(s)}$:

$$\{G_1^e, G_2^e\}_{\mathrm{FR}} = r_a G_1^e G_2^e + G_2^e G_1^e r_a + G_1^e r_{21} G_2^e - G_2^e r G_1^e\,. \tag{2.51c}$$

- For two links e, e' with the same source but different targets distinct from the source, *i.e.* $s(e) = s(e')$ but $s(e)$, $t(e)$, $t(e')$ all three distinct, and $e_{(s)} \prec e'_{(s)}$:

$$\{G_1^e, G_2^{e'}\}_{\mathrm{FR}} = r G_1^e G_2^{e'}\,. \tag{2.51d}$$

- For two closed loops e, e' intersecting at a single node, *i.e.* $s(e) = s(e') = t(e) = t(e')$, with the order $e_{(s)} \prec e'_{(s)} \prec e_{(t)} \prec e'_{(t)}$:

$$\{G_1^e, G_2^{e'}\}_{\mathrm{FR}} = r G_1^e G_2^{e'} + G_1^e G_2^{e'} r + G_2^{e'} r_{21} G_1^e - G_1^e r G_2^{e'}\,. \tag{2.51e}$$

All the Poisson brackets between two non-intersecting links vanish. Then the gauge transformations at nodes, $G^e \mapsto H_{s(e)} G^e H_{t(e)}^{-1}$ for $H_v \in \mathrm{SL}(2,\mathbb{C})$, is a Poisson map leaving the Fock-Rosly bracket invariant [85]. This confirms that the Fock-Rosly brackets provide the moduli space of flat graph connection up to gauge transformations with a symplectic structure. One can further show that the definition of the Fock-Rosly bracket is stable under contraction and deletion of links and leads to the so-called Goldman bracket [85].

If we compare the Fock-Rosly Poisson brackets (2.51) and those of the q-deformed loop gravity ((2.35), (2.36) and (2.38)) on the same ribbon graph Γ_{r}, they look very different. Apparently, in the q-deformed loop gravity phase space, variables from different ribbons Poisson commute even though they are assigned on two ribbon links intersecting to the same node in Γ_{r}. This is not the case in the Fock-Rosly phase space. In fact, we will explain below that one needs to go one step further and introduce a "*fat graph*" Γ_{fat} and that the q-deformed loop gravity on Γ_{r} turns out to result from the Fock-Rosly structure on Γ_{fat} by a partial gauge-fixing.

2.4.2 Gauge fixing of Fock-Rosly on the torus

In this subsection, we show that the loop gravity phase space for a given graph can be obtained from the Fock-Rosly phase space through a particular gauge fixing. We will start from the Fock-Rosly setup on a fat graph Γ_{fat} fattened from a ribbon graph Γ_{r} with special assignments of r-matrices and cilia on nodes. Then we apply some particular gauge-fixing to the holonomies on links by acting with some gauge transformations on the nodes one after the other one. The gauge fixing process can change the values of the holonomies to our preference but does not change the Poisson brackets. It allows us to fix the holonomies on the auxiliary links to be the identity, which means one can shrink these auxiliary links and change Γ_{fat} to Γ_{r}. In this way, we get a ribbon graph with the loop gravity phase space structure from a bigger graph with the Fock-Rosly phase space structure.

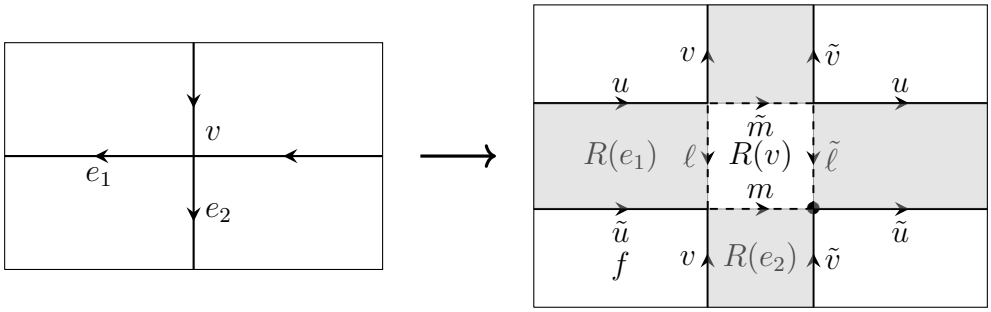

Figure 2.7: *(left)* Basic graph for the 2-torus, with two links e_1, e_2 wrapping around the torus meeting at a single node v and surrounding a single face f. *(right)* The corresponding ribbon graph on the torus, parametrized by $\ell, \tilde{\ell}, m, \tilde{m} \in \text{AN}(2)$ and $u, \tilde{u}, v, \tilde{v} \in \text{SU}(2)$. The ribbons, shaded in grey, are the thickened graph links.

To be explicit, we consider the ribbon graph as shown in fig.2.7, which is analyzed in more detail in Appendix B.2. What we do here is to unfold the four 4-valent nodes of the ribbon graph fig.2.7 into pairs of 3-valent nodes by adding an intermediate link. This leads to a graph with twelve links, each decorated with $\text{SL}(2,\mathbb{C})$ holonomies. This is the fat graph on which we apply the Fock-Rosly structure. We note $L, U, \tilde{L}, \tilde{U}, M, V, \tilde{M}, \tilde{V}$ the eight group elements along the ribbon links, and P, Q, S, T the four group elements on the new intermediate links. To simplify the notations, we refer to the link through the $\text{SL}(2,\mathbb{C})$ group element it carries.

In order to recover the loop gravity Poisson structure, we assign the r-matrix r_{21} to the source nodes of the intermediate links $s(P)$, $s(Q)$, $s(S)$ and $s(T)$, while we assign the r-matrix r to their target nodes $t(P)$, $t(Q)$, $t(S)$ and $t(T)$. We further choose all the cilia

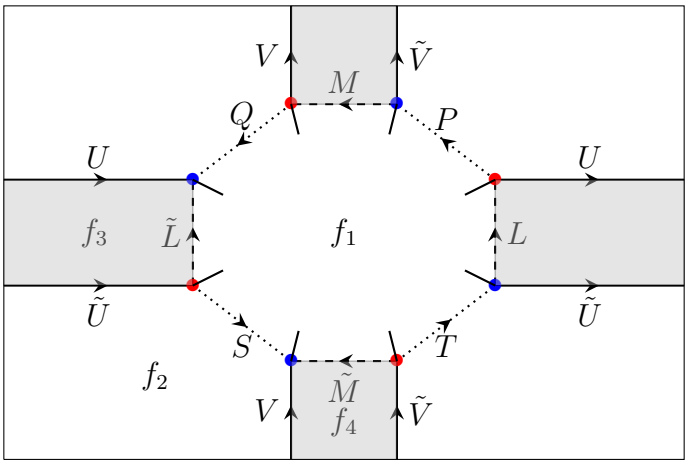

Figure 2.8: A fat graph on the torus. Nodes $s(P)$, $s(Q)$, $s(S)$ and $s(T)$ (*in red*) are assigned the r-matrix r_{21}, while nodes $t(P)$, $t(Q)$, $t(S)$ and $t(T)$ (*in blue*) are assigned r. On each node, a cilium is introduced to fix the linear order of the links around this node. The cilia are chosen to all look into the face f_1.

looking inwards to the face f_1 to fix the convention. A different choice of cilia would still lead to the loop gravity phase space.

The Fock-Rosly brackets can be read directly from their definition (2.51a)-(2.51d) applied to the fat graph shown in fig.2.8. All the non-vanishing Fock-Rosly brackets related to P are

$$\begin{aligned}
&\{P_1, L_2\}_{\text{FR}} = L_2 r P_1\,, \quad \{L_1, P_2\}_{\text{FR}} = -L_1 r_{21} P_2\,, \quad \{P_1, U_2\}_{\text{FR}} = -r P_1 U_2\,,\\
&\{U_1, P_2\}_{\text{FR}} = r_{21} U_1 P_2\,, \quad \{P_1, M_2\}_{\text{FR}} = P_1 r M_2\,, \quad \{M_1, P_2\}_{\text{FR}} = -P_2 r_{21} M_1\,,\\
&\{P_1, \tilde{V}_2\}_{\text{FR}} = P_1 r \tilde{V}_2\,, \quad \{\tilde{V}_1, P_2\}_{\text{FR}} = -P_2 r_{21} \tilde{V}_1\,, \quad \{P_1, P_2\}_{\text{FR}} = [r_{21}, P_1 P_2]\,.
\end{aligned} \tag{2.52}$$

The Fock-Rosly phase space is defined on top of the Poisson brackets given above by imposing the flatness of the $\mathrm{SL}(2,\mathbb{C})$ connection around the four faces of the fatter graph:

$$\mathcal{C}^{f_1} = TLPMQ\tilde{L}^{-1}S\tilde{M}^{-1}\,, \tag{2.53a}$$
$$\mathcal{C}^{f_2} = UQ^{-1}VS^{-1}\tilde{U}^{-1}T^{-1}\tilde{V}^{-1}P^{-1}\,, \tag{2.53b}$$
$$\mathcal{C}^{f_3} = LU\tilde{L}^{-1}\tilde{U}^{-1}\,, \tag{2.53c}$$
$$\mathcal{C}^{f_4} = MV\tilde{M}^{-1}\tilde{V}^{-1}\,, \tag{2.53d}$$

and quotienting the $\mathrm{SL}(2,\mathbb{C})$ group action at the eight nodes of the graph.

If we look at the Fock-Rosly brackets for the eight group elements $L, U, \tilde{L}, \tilde{U}, M, V, \tilde{M}, \tilde{V}$, they are the same Poisson brackets as for the loop gravity phase space parametrized by the group elements $\ell, u, \tilde{\ell}, \tilde{u}, m, v, \tilde{m}, \tilde{v}$. The only difference is that the Fock-Rosly brackets involve $\mathrm{SL}(2,\mathbb{C})$ group elements, while the loop gravity group elements live alternatively in the subgroups $\mathrm{SU}(2)$ and $\mathrm{AN}(2)$. Thus, in order to recover the loop gravity phase space, we perform a partial gauge fixing of these $\mathrm{SL}(2,\mathbb{C})$ group elements. We start at the node $t(T) = s(L) = s(\tilde{U})$ and will go around the face f_1. We use the $\mathrm{SL}(2,\mathbb{C})$ gauge invariance at that node to fix $T = \mathbb{1}$. Then moving to the following node $t(L) = s(U) = s(P)$, we use the Iwasawa decompositions $L = \ell u^L$ and $U = \ell^U u$ and perform a gauge transformation:

$$u^L \ell^U = \ell' u' \,, \quad G = (\ell')^{-1} u^L \,, \qquad \left| \begin{array}{lllll} L & \mapsto & LG^{-1} & = \ell\ell' & \in \mathrm{AN}(2)\,, \\ U & \mapsto & GU & = u'u & \in \mathrm{SU}(2)\,, \\ P & \mapsto & GP & = (\ell')^{-1} u^L P\,, & \end{array} \right. \tag{2.54}$$

thus gauge fixing L to live in $\mathrm{AN}(2)$ and U to live in $\mathrm{SU}(2)$.

Next, at the following node, $t(P) = s(M) = s(\tilde{V})$, we perform an $\mathrm{SL}(2,\mathbb{C})$ gauge transformation to gauge fix to $P = \mathbb{1}$. Then we repeat this pair of gauge fixings all around the central face f_1. So at the node $t(M) = s(V) = s(Q)$, we gauge fix to $M \in \mathrm{AN}(2)$ and $V \in \mathrm{SU}(2)$. At the node $t(Q) = t(U) = t(\tilde{L})$ we gauge fix to $Q = \mathbb{1}$. At the node $s(S) = s(\tilde{L}) = t(\tilde{U})$, we gauge fix to $\tilde{L} \in \mathrm{AN}(2)$ and $\tilde{U} \in \mathrm{SU}(2)$. At the node $t(S) = t(V) = t(\tilde{M})$, we gauge fix to $S = \mathbb{1}$.

Finally at the last node $s(T) = s(\tilde{M}) = t(\tilde{V})$, we do not do anything. The flatness condition around the face f_1 automatically implies that the group element $\tilde{M}$ lives in $\mathrm{AN}(2)$ while the flatness condition around the face f_2 automatically implies that the group element $\tilde{V}$ lives in the $\mathrm{SU}(2)$ subgroup. Since we do not gauge-fix the group action at the last node of the graph, we are left with a single $\mathrm{SL}(2,\mathbb{C})$ gauge invariance of our partially gauge-fixed group variables.

This reproduces exactly the setting of the q-deformed loop gravity variables on the ribbon graph, with the group elements $\ell, \tilde{\ell}, m, \tilde{m} \in \mathrm{AN}(2)$ and $u, \tilde{u}, v, \tilde{v} \in \mathrm{SU}(2)$ satisfying the flatness constraints around the 4 faces of the graph:

$$\mathcal{C}^{f_1} = uv\tilde{u}^{-1}\tilde{v}^{-1}\,, \quad \mathcal{C}^{f_2} = \ell m \tilde{\ell}^{-1}\tilde{m}^{-1}\,, \quad \mathcal{C}^{f_3} = \ell u \tilde{\ell}^{-1}\tilde{u}^{-1}\,, \quad \mathcal{C}^{f_4} = mv\tilde{m}^{-1}\tilde{v}^{-1}\,. \tag{2.55}$$

Since the $\mathrm{SL}(2,\mathbb{C})$ group action at the nodes is a Poisson map for the Fock-Rosly symplectic structure [85], it is straightforward to check that the Fock-Rosly brackets on the original $\mathrm{SL}(2,\mathbb{C})$ group elements $L, U, \tilde{L}, \tilde{U}, M, V, \tilde{M}, \tilde{V}$ directly descend to Poisson brackets on the

gauge-fixed group variables $\ell, u, \tilde{\ell}, \tilde{u}, m, v, \tilde{m}, \tilde{v}$:

$$\begin{aligned}
&\{\ell_1,\ell_2\}_{\rm FR}=-[r_{21},\ell_1\ell_2]\,, && \{u_1,u_2\}_{\rm FR}=-[r,u_1u_2]\,, && \{\tilde{\ell}_1,\tilde{\ell}_2\}_{\rm FR}=[r_{21},\tilde{\ell}_1\tilde{\ell}_2]\,,\\
&\{\tilde{u}_1,\tilde{u}_2\}_{\rm FR}=[r,\tilde{u}_1\tilde{u}_2]\,, && \{m_1,m_2\}_{\rm FR}=-[r_{21},m_1m_2]\,, && \{v_1,v_2\}_{\rm FR}=-[r,v_1v_2]\,,\\
&\{\tilde{m}_1,\tilde{m}_2\}_{\rm FR}=[r_{21},\tilde{m}_1\tilde{m}_2]\,, && \{\tilde{v}_1,\tilde{v}_2\}_{\rm FR}=[r,\tilde{v}_1\tilde{v}_2]\,, && \{\ell_1,u_2\}_{\rm FR}=-\ell_1 r_{21}u_2\,,\\
&\{\tilde{\ell}_1,\tilde{u}_2\}_{\rm FR}=-\tilde{u}_2 r_{21}\tilde{\ell}_1\,, && \{m_1,v_2\}_{\rm FR}=-m_1 r_{21}v_2\,, && \{\tilde{m}_1,\tilde{v}_2\}_{\rm FR}=-\tilde{v}_2 r_{21}\tilde{m}_1\,.
\end{aligned} \tag{2.56}$$

These are precisely the (flat or q-deformed) loop gravity Poisson brackets. $\mathcal{C}^{f_1}$ and $\mathcal{C}^{f_2}$ are still first class constraints generating respectively the gauge invariance under AN(2) translation and SU(2) rotations, while $\mathcal{C}^{f_3}$ and $\mathcal{C}^{f_4}$ are second class constraints directly hardcoded in the Poisson brackets. This explicitly shows that the loop gravity phase space can be reconstructed from the Fock-Rosly description by a specific gauge fixing.

Let us stress that the partial gauge fixing introduced here mapping the Fock-Rosly phase space to the q-deformed loop gravity phase space is very different from the gauge fixing usually done in the Fock-Rosly approach to go from a refined graph to a coarse-grained graph (subgraph of the original graph) by simply setting all the extra $\mathrm{SL}(2,\mathbb{C})$ group elements to the identity. These different gauge fixings produce different intermediate Poisson brackets, which nevertheless all lead to the same Goldman brackets on the $\mathrm{SL}(2,\mathbb{C})$ gauge-invariant variables. See [77] for more discussion. These analysis and results can be generalized to graphs on a general 2D manifold with no boundaries. For a given graph, one merely needs to start from a corresponding fat graph with the Fock-Rosly Poisson structure and apply the same gauge fixing procedure to obtain the ribbon graph with the Poisson structure of the deformed loop gravity. For manifolds with boundaries, we need to specify the ribbon configurations on the boundaries for the ribbon graph depending on the boundary conditions and be careful on the gauge fixing procedure located at the boundaries for the corresponding fat graph. We leave it for future investigation.

With such an explicit relation, it follows that the observable algebra constructed in the Fock-Rosly phase space and the loop gravity phase space coincide. This relation builds a bridge between the LQG quantization approach and the combinatorial quantization approach at the classical level, while the complete relation at the quantum level remains to be explored.

2.5 The $\Lambda = 0$ case: loop gravity

Finally, we end this chapter by considering the $\Lambda \to 0$ limit of the q-deformed loop gravity model developed above. To deserve the name of "q-deformation", one needs to recover

the standard 3D loop gravity structure. To this end, we first review the $\Lambda = 0$ case of 3D gravity in the standard description in Subsection 2.5.1. It turns out that it can be rewritten in the Heisenberg double framework (Subsection 2.5.2) as we did in the q-deformed loop gravity but defined with a different r-matrix and a different group. This gives a unified construction of the discrete phase space for gravity with or without cosmological constant, and the q-deformed phase space is then really a deformed version of the standard loop gravity phase space. Conversely, one can also directly take the $\Lambda \to 0$ limit of the variables in the q-deformed loop gravity model to recover those in the flat case. We perform this analysis in Subsection 2.5.3. This can be seen as a consistency check to further confirm the notion of deformation. It will also be useful as a reference when we build the spinorial phase space in the next chapter.

2.5.1 The standard phase space for 3D loop gravity

The phase space for canonical 3D loop gravity encodes the basic geometrical degrees of freedom of a discretized 2D surface (see [71, 91] for a thorough and careful discretization). Considering an oriented graph Γ, the basic building block is a $T^*\mathrm{SU}(2) \cong \mathrm{ISU}(2)$ phase space associated to each link $e \in \Gamma$. For each oriented link, we define a group element $g_e \in \mathrm{SU}(2)$ along the link and a vector $\vec{x}_e \in \mathbb{R}^3$ thought of as living on the source node $s(e)$ of the link e, as illustrated on fig.2.9. We identify this vector with an $\mathfrak{su}(2)$-Lie algebra valued element $x_e := x_e^a \sigma^a$. The group element g_e gives the holonomy of the SU(2) connection along the link while the vector x_e is the discretized geometric flux transverse to that link, defined as the integrated triad along the edge of a 2D triangulation dual to the graph.

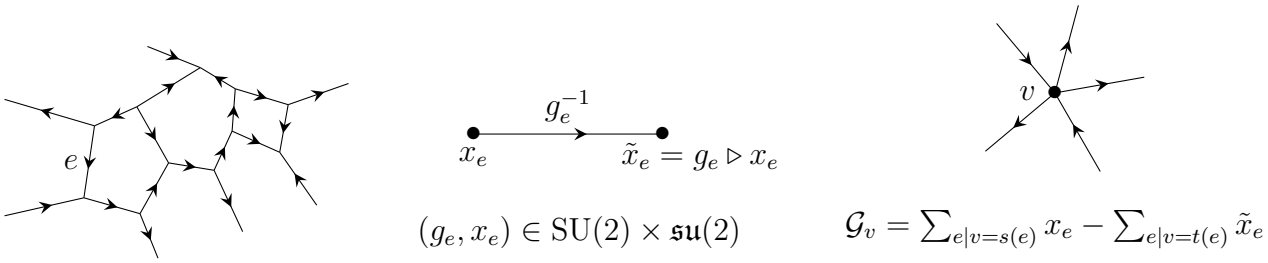

(a) Oriented graph Γ.

(b) $T^*\mathrm{SU}(2)$ phase space on the link e.

(c) Gauss constraint at a node v.

Figure 2.9: Holonomy-flux phase space for 3D loop gravity on a graph Γ.

Decomposing the flux vector on the Pauli matrix basis for Hermitian matrices, $x_e =$

$x_e^a \sigma^a$ $(a = 1, 2, 3)$, the $T^*\mathrm{SU}(2)$ symplectic structure is explicitly given by the Poisson brackets:

$$\{x_e^a, g_e\} = \frac{i}{2}\sigma^a g_e\,, \quad \{x_e^a, x_e^b\} = \epsilon^{abc} x_e^c\,, \quad \{g_e, g_e\} = 0\,. \tag{2.57}$$

We also define the flux vector at the target node $t(e)$ by parallel transporting x_e by the SU(2) holonomy g_e, $\tilde{x}_e = g_e \triangleright x_e = g_e^{-1} x_e g_e$, satisfying flipped $\mathfrak{su}(2)$ algebra Poisson brackets:

$$\{x_e^a, \tilde{x}_e^b\} = 0\,, \quad \{\tilde{x}_e^a, g_e\} = \frac{i}{2} g_e \sigma^a\,, \quad \{\tilde{x}_e^a, \tilde{x}_e^b\} = -\epsilon^{abc}\tilde{x}_e^c\,. \tag{2.58}$$

We now consider the graph Γ with E links. The loop gravity phase space on Γ is defined by considering the collection of the independent $T^*\mathrm{SU}(2)$ phase spaces living on each link $e \in \Gamma$ and coupling them at the graph nodes by a Gauss constraint. At each node $v \in \Gamma$,

$$\mathcal{G}_v^a = \sum_{e|v=s(e)} x_e^a - \sum_{e|v=t(e)} \tilde{x}_e^a \simeq 0\,. \tag{2.59}$$

Imposing $\vec{\mathcal{G}}_v = \vec{0}$ amounts to requiring that the incoming flux at the node v equals the outgoing flux. This Gauss constraint generates the gauge invariance under SU(2) transformations around the node:

$$\{\mathcal{G}^a, \mathcal{G}^b\} = \epsilon^{abc}\mathcal{G}^c\,, \qquad \begin{aligned} &\forall e\,|\,v = s(e)\,, \quad \{\mathcal{G}^a, x_e^b\} = \epsilon^{abc} x_e^c\,, \\ &\forall e\,|\,v = t(e)\,, \quad \{\mathcal{G}^a, \tilde{x}_e^b\} = \epsilon^{abc}\tilde{x}_e^c\,. \end{aligned} \tag{2.60}$$

The symplectic quotient of the product of the link phase spaces $T^*\mathrm{SU}(2)^E$ by the Gauss constraint defines the kinematical phase space of 3D loop gravity on the graph Γ. In the context of loop gravity in 3+1 dimensions, this holonomy-flux phase space is interpreted as discrete three-dimensional twisted geometries [108] (see also [78, 109, 100]). Here, in 3D space-time dimensions, these are meant to represent 2D discrete geometries. This becomes explicit once we impose the Hamiltonian constraints for 3D loop quantum gravity, implemented as flatness constraints for the SU(2) holonomies around loops of the graph, which implies that we can reconstruct a 2D geometric triangulation dual to the graph (see e.g. [43, 44, 38]).

2.5.2 Poincaré group as a Heisenberg double

In fact, the Poincaré group as a phase space can also be written as a Heisenberg double, which was not realized until the work of [40] (see also [77]). This allows us to view the

loop gravity phase space as the $\Lambda \to 0$ limit of that of the q-deformed loop gravity in the same framework. Indeed, when $\kappa = 0$, the Lie brackets (2.29) for ρ^a vanish hence the Lie algebra for the fluxes becomes $\mathbb{R}^3$ and the group of the phase space becomes the Poincaré group $\mathrm{ISU}(2) = \mathrm{SU}(2) \ltimes \mathbb{R}^3$. In this subsection, we will see that considering the Poincaré group as a Heisenberg double, the Poisson structure of $\mathrm{ISU}(2)$ is encoded in the r-matrix given as the tensor product of the generators of $\mathrm{SU}(2)$ and $\mathbb{R}^3$ (see e.g. [3, 135]).

We start by representing Poincaré group elements $(g, x) \in \mathrm{SU}(2) \times \mathbb{R}^3$ in terms of 4×4 matrices written as 2×2 block matrices[12]:

$$(g, x) = \left(\begin{array}{c|c} g & ixg \\ \hline 0 & g \end{array}\right) , \tag{2.61}$$

where $g \in \mathrm{SU}(2)$ is represented in its fundamental representation as a 2×2 unitary matrix and $x = \vec{x} \cdot \vec{\sigma} \in \mathfrak{su}(2)$ is represented as a 2×2 traceless Hermitian matrix. For $x \neq 0$, the expression xg is the polar decomposition of an arbitrary 2×2 invertible complex matrix. These provide a representation of the Poincaré group multiplication:

$$\begin{aligned}(g_1, x_1)(g_2, x_2) &= \left(\begin{array}{c|c} g_1 & ix_1g_1 \\ \hline 0 & g_1 \end{array}\right)\left(\begin{array}{c|c} g_2 & ix_2g_2 \\ \hline 0 & g_2 \end{array}\right) \\ &= \left(\begin{array}{c|c} g_1g_2 & i(x_1 + g_1x_2g_1^{-1})g_1g_2 \\ \hline 0 & g_1g_2 \end{array}\right) = (g_1g_2, x_1 + g_1x_2g_1^{-1}) . \end{aligned} \tag{2.63}$$

Each Poincaré group element admits a unique decomposition as the product of a translation and a rotation:

$$\begin{aligned}(g, x) = \left(\begin{array}{c|c} g & ixg \\ \hline 0 & g \end{array}\right) = \left(\begin{array}{c|c} \mathbb{I} & ix \\ \hline 0 & \mathbb{I} \end{array}\right)\left(\begin{array}{c|c} g & 0 \\ \hline 0 & g \end{array}\right) = (\mathbb{I}, x)(g, 0) = \ell u \\ \text{with} \quad \ell = (\mathbb{I}, x) \quad \text{and} \quad u = (g, 0) . \end{aligned} \tag{2.64}$$

[12] Another parametrization of Poincaré group elements was used in [40], the spin-1 representation for the $\mathrm{SU}(2)$ group elements instead of the spin-$\frac{1}{2}$ used here. It still led to 4×4 matrices, but the $\mathrm{SU}(2)$ group elements were encoded in a 3×3 block while the $\mathfrak{su}(2)$ vectors were written as 3-vectors:

$$(g, x) = \left(\begin{array}{c|c} D^1(g) & \vec{x} \\ \hline 0 & 1 \end{array}\right) , \tag{2.62}$$

with $D^1(g)$ the 3×3 Wigner matrix representing the $\mathrm{SU}(2)$ group element as a 3D rotation acting on 3-vectors.

The generators of the Poincaré Lie algebra are the J^a's for the SU(2) subgroup and E^a for the $\mathfrak{su}(2)$ subgroup :

$$J^a = \frac{1}{2}\left(\begin{array}{c|c} \sigma^a & 0 \\ \hline 0 & \sigma^a \end{array}\right), \quad u = e^{iv^a J^a} = \left(\begin{array}{c|c} g & 0 \\ \hline 0 & g \end{array}\right) \quad \text{with} \quad g = e^{\frac{i}{2}v^a\sigma^a}, \tag{2.65}$$

$$E^a = \left(\begin{array}{c|c} 0 & \sigma^a \\ \hline 0 & 0 \end{array}\right), \quad E^aE^b = 0\,,\ \forall a,b\,, \qquad \ell = e^{ix^aE^a} = \mathbb{I} + ix^aE^a = \left(\begin{array}{c|c} \mathbb{I} & ix \\ \hline 0 & \mathbb{I} \end{array}\right), \tag{2.66}$$

which satisfies the Poincaré algebra commutators:

$$[J^a, J^b] = i\epsilon^{abc}J^c\,, \qquad [J^a, E^b] = i\epsilon^{abc}E^c\,, \qquad [E^a, E^b] = 0\,. \tag{2.67}$$

Provided with the bilinear form on the Lie algebra $\mathfrak{isu}(2)$ spanned by the E^a and J^a,

$$\mathcal{B}(M,N) := \mathrm{Tr}\left[MN\left(\begin{array}{c|c} 0 & \mathbb{I} \\ \hline \mathbb{I} & 0 \end{array}\right)\right], \quad \forall M,N \in \mathfrak{isu}(2)\,, \tag{2.68}$$

which defines a pairing between the rotation and translation generators, $\mathcal{B}(E^a, J^b) = \delta^{ab}$, $\mathcal{B}(E^a, E^b) = \mathcal{B}(J^a, J^b) = 0$, the Heisenberg double structure defines a r-matrix:

$$r = \sum_a J^a \otimes E^a\,, \qquad r_{21} = \sum_a E^a \otimes J^a\,, \tag{2.69}$$

which naturally satisfies the classical Yang-Baxter equation [77].

Moreover, this r-matrix defines a Poisson bracket on the Poincaré group ISU(2) endowing it with a phase space structure:

$$\{\ell_1, \ell_2\} = -[r_{21}, \ell_1\ell_2]\,, \quad \{u_1, u_2\} = -[r, u_1u_2]\,, \quad \{\ell_1, u_2\} = -\ell_1 r_{21} u_2\,, \quad \{u_1, \ell_2\} = \ell_2 r u_1\,, \tag{2.70}$$

which takes exactly the same form as (2.35). It can also be directly written in a compact form as a Poisson bracket for an arbitrary Poincaré group element :

$$d \equiv (g, x) = \ell u\,, \qquad \{d_1, d_2\} = rd_1d_2 - d_1d_2r_{21}\,, \tag{2.71}$$

which reproduces the form of (2.34). Explicitly computing the Poisson brackets between ℓ and u leads back to the T^*SU(2) brackets of the 3D loop gravity phase space structure for the variables on a link:

$$\{g, g\} = 0\,, \qquad \{x^a, g\} = \frac{i}{2}\sigma^a g\,, \qquad \{x^a, x^b\} = \epsilon^{abc}x^c \tag{2.72}$$

as was given in (2.57). In particular, it is interesting that the Poisson bracket $\{u_1, u_2\}$ vanishes because $u \otimes u$ commutes with r for $u \in \mathrm{SU}(2)$. We have seen that this Poisson bracket becomes non-trivial in the deformed case accounting for a non-vanishing cosmological constant.

We now want to get the Poisson bracket for the target flux $\tilde{x}$. We assume that the parallel transport equation along the link amounts to switching the decomposition as follows.

$$d = (g, x) = (\mathbb{1}, x)(g, 0) = (g, 0)(\mathbb{1}, \tilde{x})\,. \tag{2.73}$$

Then decomposing the Poincaré group element $d = \tilde{u}\tilde{\ell}$ with actually $\tilde{u} = u \equiv (g, 0)$ gives similar Poisson brackets:

$$\{\tilde{\ell}_1, \tilde{\ell}_2\} = [r_{21}, \tilde{\ell}_1\tilde{\ell}_2]\,, \quad \{\tilde{\ell}_1, \tilde{u}_2\} = -\tilde{u}_2 r_{21}\tilde{\ell}_1\,, \quad \{\tilde{u}_1, \tilde{\ell}_2\} = \tilde{u}_1 r\tilde{\ell}_2\,, \quad \{\tilde{u}_1, \tilde{u}_2\} = [r, \tilde{u}_1\tilde{u}_2]\,, \tag{2.74}$$

which leads to the switched $T^*\mathrm{SU}(2)$ brackets for $\tilde{g} = g$ and $\tilde{x}$:

$$\{g, g\} = 0\,, \quad \{\tilde{x}^a, g\} = \frac{i}{2} g\sigma^a\,, \quad \{\tilde{x}^a, \tilde{x}^b\} = -\epsilon^{abc}\tilde{x}^c\,, \tag{2.75}$$

where we recognize (2.36). (2.73) can be graphically represented flatnss constraint for a ribbon as shown in fig.2.10.

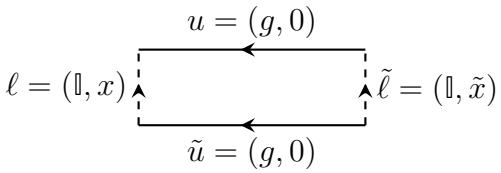

Figure 2.10: The ribbon graph for loop gravity with $\ell, \tilde{\ell} \in \mathfrak{su}(2)$ and $u = ut \in \mathrm{SU}(2)$. The ribbon constraint can be written as $\ell u\tilde{\ell}^{-1}\tilde{u}^{-1}$, hence in the same form of the q-deformed case.

This allows us to reformulate the Poisson bracket for the ISU(2) holonomy $d = (g, x)$ going along the ribbon in terms of the r-matrix for the Poincaré group seen as a Heisenberg double hence establishing that the q-deformed loop gravity structure is really a *q-deformed* loop gravity.

2.5.3 $\kappa \to 0$ limit of the deformed flux vectors

One can also take the $\kappa \to 0$ limit of the q-deformed variables $\vec{X}$ defined in (2.40) and likewise for $\vec{\tilde{X}}$, which would recover the flat flux vectors $\vec{x}$ and $\vec{\tilde{x}}$ and the Poisson brackets (2.35) and (2.36) would recover (2.57) and (2.58). We now establish these.

Recall that

$$\left|\begin{array}{l} X^0 = \frac{1}{2\kappa}(\lambda^2 + \lambda^{-2} + |z|^2) \\ X^1 = -\frac{1}{2\kappa}\lambda(z+\bar{z}) \\ X^2 = -\frac{i}{2\kappa}\lambda(\bar{z}-z) \\ X^3 = -\frac{1}{2\kappa}(\lambda^2 - \lambda^{-2} - |z|^2) \end{array}\right. , \quad \left|\begin{array}{l} \tilde{X}^0 = \frac{1}{2\kappa}(\tilde{\lambda}^2 + \tilde{\lambda}^{-2} + |\tilde{z}|^2) \\ \tilde{X}^1 = -\frac{1}{2\kappa}\tilde{\lambda}(\tilde{z}+\bar{\tilde{z}}) \\ \tilde{X}^2 = -\frac{i}{2\kappa}\tilde{\lambda}(\bar{\tilde{z}}-\tilde{z}) \\ \tilde{X}^3 = -\frac{1}{2\kappa}(\tilde{\lambda}^2 - \tilde{\lambda}^{-2} - |\tilde{z}|^2) \end{array}\right. . \tag{2.76}$$

We first write the Poisson brackets (2.35), (2.36) and (2.38) explicitly in terms of the deformed flux vectors X^μ and $\tilde{X}^\mu$:

$$\left|\begin{array}{l} \{X^a, X^b\} = \epsilon_{abc}\kappa(X^0 - X^3)X^c\,, \\ \{X^1, \tilde{u}\} = \frac{i}{2}\kappa(X^0 - X^3)\sigma^1\tilde{u}\,, \\ \{X^2, \tilde{u}\} = \frac{i}{2}\kappa(X^0 - X^3)\sigma^2\tilde{u}\,, \\ \{X^3 + X^0, \tilde{u}\} = \frac{i}{2}\kappa(X^0 - X^3)\sigma^3\tilde{u}\,, \end{array}\right. \quad \left|\begin{array}{l} \{\tilde{X}^a, \tilde{X}^b\} = -\epsilon_{abc}\kappa(\tilde{X}^0 - \tilde{X}^3)\tilde{X}^c\,, \\ \{\tilde{X}^1, \tilde{u}\} = \frac{i}{2}\kappa(\tilde{X}^0 - \tilde{X}^3)\tilde{u}\sigma^1\,, \\ \{\tilde{X}^2, \tilde{u}\} = \frac{i}{2}\kappa(\tilde{X}^0 - \tilde{X}^3)\tilde{u}\sigma^2\,, \\ \{\tilde{X}^3 + \tilde{X}^0, \tilde{u}\} = \frac{i}{2}\kappa(\tilde{X}^0 - \tilde{X}^3)\tilde{u}\sigma^3\,, \end{array}\right. \tag{2.77}$$

$$\{X^0, X^a\} = \{\tilde{X}^0, \tilde{X}^a\} = \{X^a, \tilde{X}^b\} = 0\,.$$

The difference with the standard flat holonomy-flux brackets of the $T^*\mathrm{SU}(2)$ phase space, given in (2.57) and (2.58), are the rescaling factors $\lambda^2 = \kappa(X^0 - X^3)$ and $\tilde{\lambda}^2 = \kappa(\tilde{X}^0 - \tilde{X}^3)$. The flat limit $\kappa \to 0$ is an inhomogeneous scaling of the flux 4-vector. As κ is sent to 0, the hyperboloid $X_0^2 - \vec{X}^2 = \kappa^{-2}$ becomes the flat $\mathbb{R}^3$ space, with the inhomogeneous limit $\kappa X^0 \to 1$, with $X^0 \sim \kappa^{-1}$ sent to $+\infty$, while the 3D flux vector X^a remains finite. This actually sends the $\mathrm{SL}(2,\mathbb{C})$ Poisson brackets written above to the $T^*\mathrm{SU}(2)$ Poisson brackets of the standard "flat" loop gravity, given in (2.57) and (2.58).

To avoid the subtleties of the inhomogeneous re-scaling limit, we can take the Euler parametrization of the AN(2) fluxes in terms of the AN(2) generators [40, 77]:

$$\ell = e^{-j^3\rho^3}e^{-j^1\rho^1}e^{-j^2\rho^2}\,, \quad \lambda = e^{-\frac{\kappa}{2}j^3}\,, \quad z = -\kappa e^{\frac{\kappa}{2}j^3}(j^1 + ij^2) = -e^{\frac{\kappa}{2}j^3}\kappa j^+\,, \quad \bar{z} = -e^{\frac{\kappa}{2}j^3}\kappa j^-\,, \tag{2.78}$$

where $j^a \in \mathbb{R}^3$ is an arbitrary 3-vector. The flat limit $\kappa \to 0$ is taken keeping the 3-vector j^a finite:

$$\left|\begin{array}{l} \kappa X^0 = \cosh\kappa j^3 + \frac{\kappa^2}{2}e^{\kappa j^3}j^+j^- \xrightarrow{\kappa\to 0} 1\,, \\ X^3 = \frac{\sinh\kappa j^3}{\kappa} - \frac{\kappa}{2}e^{\kappa j^3}j^+j^- \xrightarrow{\kappa\to 0} j^3\,, \end{array}\right. \quad \left|\begin{array}{l} X^1 = j^1\,, \\ X^2 = j^2\,. \end{array}\right. \tag{2.79}$$

Similarly defining the 3-vector $\tilde{j}^a$ for the target flux $\tilde{\ell}$, we recover the $T^*\mathrm{SU}(2)$ Poisson brackets (2.57) and (2.58) of flat loop gravity in the limit $\kappa \to 0$:

$$\begin{aligned} &\{j^a, j^b\} \to \epsilon_{abc} j^c \,, \qquad &&\{j^a, \tilde{u}\} \to \tfrac{i}{2}\sigma^a \tilde{u} \,, \qquad &&\{\tilde{u}, \tilde{u}\} \to 0 \,, \\ &\{\tilde{j}^a, \tilde{j}^b\} \to -\epsilon_{abc} \tilde{j}^c \,, \qquad &&\{\tilde{j}^a, \tilde{u}\} \to \tfrac{i}{2}\tilde{u}\sigma^a \,, \qquad &&\{j^a, \tilde{j}^b\} = 0 \,. \end{aligned} \tag{2.80}$$

Reciprocally, the $\mathrm{SL}(2,\mathbb{C})$ Poisson brackets (2.77) define the curved deformation of the $T^*\mathrm{SU}(2)$ Poisson brackets extending them to take into account a non-vanishing cosmological constant. This establishes that the q-deformed loop gravity phase space variables and the Poisson structures are the deformations of the Poincaré phase space counterpart, with the deformation parameter determined by the value of the cosmological constant.

To summarize, we have reviewed in this section the loop gravity phase space with $\Lambda = 0$ in terms of the holonomy and flux vectors. As we will start introducing the notion of spinors in the next chapter from the flat case, the holonomy-flux algebra described here serves as a reference to justify the construction of spinors. We have also related the loop gravity phase space to the q-deformed phase space illustrated in Section 2.3 in two ways - firstly by reformulating the loop gravity phase space in the Heisenberg double framework and secondly by taking the $\kappa \to 0$ limit of the phase space variables in the q-deformed phase space to recover the holonomy and flux vectors in the loop gravity phase space. A unified description of the phase space for $\Lambda = 0$ and $\Lambda \neq 0$ cases could be useful for building the relation to the Chern-Simons quantization in a more systematic manner, which is left for future investigation. This construction can also be generalized to 4D gravity. This has been initiated in recent works [121, 117], where the Drinfeld double was generalized to the notion of 2-Drinfeld double in terms of 2-groups.

Chapter 3

Spinorial representation for loop gravity

We described in the previous chapter the loop gravity phase space using the holonomy-flux variables in the flat ($\Lambda = 0$) case and the q-deformed case with the corresponding deformed variables. These phase spaces can be equivalently represented by the (deformed) SU(2)-covariant *spinors*. A spinor is a pair of complex variables transforming covariantly under SU(2). They live on the half-links of the lattice and thus will make it easier to construct *local*, gauge-invariant quantities, *i.e.* observables. Note that these spinors do not encode matter degrees of freedom, they are just a different parametrization of the phase-space. There were initially introduced in the LQG formalism as a different parametrization of the T^*SU(2) phase space [118, 98, 99, 142, 44, 75, 74]. The benefits of using spinors will be fully revealed at the quantum level, which we will explore in Chapter 7.

In this chapter, we intend to construct the deformed spinors which provide an alternative parametrization of the deformed holonomy-flux phase space, which will allow us to construct the (deformed) notion of observables for this setup. We start by introducing spinors in the flat case in Section 3.1, which reproduce the holonomy-flux phase space for $\Lambda = 0$. We then perform a κ-deformation on these spinors, which is helpful to recover the AN(2) parametrization, *e.g.* z, λ in (2.27). However, these deformed versions of spinors are not covariant under SU(2). We are then led to further deform them to be the SU(2)-covariant ones. These SU(2)-covariant spinors are the key objects we will use to construct the quantum theory. Their definitions are in fact highly hinted by the quantum spinors [33, 148] which will be clear when we introduce them in Chapter 5.

3.1 Spinors as geometrical objects

In this section, we review the definition of spinors and use it to construct the spinorial phase space of loop gravity, which is isomorphic to the holonomy-flux phase space described in Section 2.5.

Let us introduce the spinor components $\zeta_A \in \mathbb{C}\,(A = \pm\frac{1}{2})$ and their complex conjugate $\bar{\zeta}_A$ where the subscripts are denoted as $\pm$ for short. (The same subscript notation will be used for the deformed spinors and their quantizations.) Then a spinor is defined as

$$|\zeta\rangle := \begin{pmatrix} \zeta_- \\ \zeta_+ \end{pmatrix}, \quad \langle\zeta| := \begin{pmatrix} \bar{\zeta}_-, & \bar{\zeta}_+ \end{pmatrix}. \tag{3.1}$$

We also introduce the dual spinor by a dual map ς

$$|\zeta] \equiv |\varsigma\zeta\rangle := \begin{pmatrix} 0 & -1 \\ 1 & 0 \end{pmatrix} |\bar{\zeta}\rangle = \begin{pmatrix} -\bar{\zeta}_+ \\ \bar{\zeta}_- \end{pmatrix}, \quad [\zeta| \equiv \langle\varsigma\zeta| := \langle\bar{\zeta}| \begin{pmatrix} 0 & 1 \\ -1 & 0 \end{pmatrix} = \begin{pmatrix} -\zeta_+, & \zeta_- \end{pmatrix}. \tag{3.2}$$

A spinor and its corresponding *dual spinor* share the same norm, which we denote as $N = \langle\zeta|\zeta\rangle = [\zeta|\zeta] = N_- + N_+ \equiv \zeta_-\bar{\zeta}_- + \zeta_+\bar{\zeta}_+$. A spinor transforms covariantly under the SU(2) action $|\zeta\rangle \to g|\zeta\rangle$ ($g \in \mathrm{SU}(2)$) in the fundamental representation of SU(2). Thus the SU(2)-, hence $\mathrm{SL}(2,\mathbb{C})$- by complexification, invariant objects can be naturally formed by the inner product of two spinors, say $|\zeta\rangle$ (or $|\zeta]$) and $|\gamma\rangle$ (or $|\gamma]$)

$$\langle\gamma|\zeta\rangle = [\zeta|\gamma] = \sum_{A=\pm 1/2} \bar{\gamma}_A\zeta_A\,, \quad [\gamma|\zeta\rangle = -\gamma_+\zeta_- + \gamma_-\zeta_+\,, \quad \langle\gamma|\zeta] = -\bar{\gamma}_-\bar{\zeta}_+ + \bar{\gamma}_+\bar{\zeta}_-\,. \tag{3.3}$$

$|\zeta]$ is dual to $|\zeta\rangle$ in the sense that they are orthogonal via the inner product, *i.e.* $[\zeta|\zeta\rangle \equiv 0$.

Now we want to use some copies of these spinors to reconstruct the loop gravity phase space structure for one link. Consider a pair of spinors $\{|\zeta\rangle, |\tilde{\zeta}\rangle\}$, whose components are provided with the Poisson brackets

$$\{\zeta_A, \bar{\zeta}_B\} = \{\tilde{\zeta}_A, \bar{\tilde{\zeta}}_B\} = -i\delta_{AB}\,, \quad A, B = \pm 1/2\,, \tag{3.4}$$

and all the non-tilde spinors commute with the tilde spinors. As for the non-tilde spinors, we denote the norm $\tilde{\zeta}_A\bar{\tilde{\zeta}}_A$ of $\tilde{\zeta}_A$ as $\tilde{N}_A$ and $\tilde{N} = \tilde{N}_- + \tilde{N}_+ = \langle\tilde{\zeta}|\tilde{\zeta}\rangle = [\tilde{\zeta}|\tilde{\zeta}]$. We assign this pair of spinors on a link as in fig.3.1.

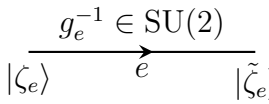

Figure 3.1: The spinors associated to a link e and related by parallel transport by an SU(2) group element g_e^{-1}. The non-tilde spinor $|\zeta_e\rangle$ is assigned to the source of the link and the tilde spinor $|\tilde{\zeta}]$ is assigned to the target of the link.

This pair of spinors reproduce the holonomy and flux $(g, \vec{x}) \in \mathrm{SU}(2) \ltimes \mathbb{R}^3$ (or equivalently $(g, \vec{\tilde{x}}) \in \mathrm{SU}(2) \ltimes \mathbb{R}^3$) in the flat case as follows. We introduce the Hermitian matrices $\mathbf{x} := |\zeta\rangle\langle\zeta|$ and $\tilde{\mathbf{x}} := |\tilde{\zeta}\rangle\langle\tilde{\zeta}|$, then project them onto the identity and the Pauli matrices

$$\begin{aligned} |\zeta\rangle\langle\zeta| &= x_0 \, \mathbb{I} - \vec{x} \cdot \vec{\sigma} \quad \text{with} \quad x_0 \equiv |\vec{x}| \equiv \tfrac{1}{2}\langle\zeta|\zeta\rangle \,, \quad \vec{x} \equiv \tfrac{1}{2}\langle\zeta|\vec{\sigma}|\zeta\rangle \in \mathbb{R}^3 \,, \\ |\tilde{\zeta}][\tilde{\zeta}| &= \tilde{x}_0 \, \mathbb{I} - \vec{\tilde{x}} \cdot \vec{\sigma} \quad \text{with} \quad \tilde{x}_0 \equiv |\vec{\tilde{x}}| \equiv \tfrac{1}{2}[\tilde{\zeta}|\tilde{\zeta}] \,, \quad \vec{\tilde{x}} \equiv \tfrac{1}{2}[\tilde{\zeta}|\vec{\sigma}|\tilde{\zeta}] \in \mathbb{R}^3 \,, \end{aligned} \tag{3.5}$$

where $|\vec{x}|$ (*resp.* $|\vec{\tilde{x}}|$) is the norm of the vector $\vec{x}$ (*resp.* $\vec{\tilde{x}}$). The vectors $\vec{x}$ and $\vec{\tilde{x}}$ are the flux vectors we introduced in the holonomy-flux representation.

We now relate the non-tilde spinor variables and the tilde spinor variables by an SU(2) action

$$g^{-1}|\zeta\rangle = |\tilde{\zeta}] \,, \quad g^{-1}|\zeta] = -|\tilde{\zeta}\rangle \,, \quad g \in \mathrm{SU}(2) \,. \tag{3.6}$$

The first relation is illustrated in fig.3.1. Then one can deduce that the matrices $\mathbf{x}$ and $\tilde{\mathbf{x}}$ are related by an SU(2) adjoint action: $\tilde{\mathbf{x}} = g^{-1}\mathbf{x}g$. (3.6) determines the SU(2) group element g uniquely to be[1]

$$g = \frac{|\zeta\rangle[\tilde{\zeta}| - |\zeta]\langle\tilde{\zeta}|}{\sqrt{\langle\zeta|\zeta\rangle\langle\tilde{\zeta}|\tilde{\zeta}\rangle}} \,, \tag{3.7}$$

which is the reconstruction of the holonomy in the loop gravity phase space. (3.7) also implies that the spinors $|\zeta\rangle$ and $|\tilde{\zeta}\rangle$ satisfy a norm matching constraint

$$\mathcal{N} := \langle\zeta|\zeta\rangle - \langle\tilde{\zeta}|\tilde{\zeta}\rangle \,, \tag{3.8}$$

which generates a U(1) transformation on spinors $\{\mathcal{N}, |\zeta\rangle\} = i|\zeta\rangle$, $\{\mathcal{N}, |\tilde{\zeta}\rangle\} = -i|\tilde{\zeta}\rangle$. The finite gauge transformation reads

$$|\zeta\rangle \xrightarrow{\mathrm{U}(1)} e^{i\theta}|\zeta\rangle \,, \quad |\tilde{\zeta}\rangle \xrightarrow{\mathrm{U}(1)} e^{-i\theta}\,|\tilde{\zeta}\rangle \,, \quad \langle\zeta| \xrightarrow{\mathrm{U}(1)} e^{-i\theta}\langle\zeta| \,, \quad \langle\tilde{\zeta}| \xrightarrow{\mathrm{U}(1)} e^{i\theta}\langle\tilde{\zeta}| \,. \tag{3.9}$$

[1]Note that $\langle\zeta|\zeta\rangle \equiv [\zeta|\zeta]$ and $\langle\tilde{\zeta}|\tilde{\zeta}\rangle \equiv [\tilde{\zeta}|\tilde{\zeta}]$.

One can not only reproduce the holonomy and flux variables, but also the Poisson brackets between them. Using (3.4), the variables $(\vec{x}, g)$ (or equivalently $(\vec{\tilde{x}}, g)$) defined in (3.5) and (3.7) indeed satisfy

$$\begin{aligned} &\{x^a, g\} = \tfrac{i}{2}\sigma^a g\,, \quad \{x^a, x^b\} = \epsilon^{abc}x^c\,, \qquad \{g, g\} \overset{\mathcal{N}=0}{\simeq} 0\,, \\ &\{\tilde{x}^a, g\} = \tfrac{i}{2} g\sigma^a\,, \quad \{\tilde{x}^a, \tilde{x}^b\} = -\epsilon^{abc}\tilde{x}^c\,, \quad \{x^a, \tilde{x}^b\} = 0\,, \end{aligned} \tag{3.10}$$

which are the Poisson structure of the loop gravity phase space with $\Lambda = 0$, *i.e.* the $T^*\mathrm{SU}(2)$ phase space described in Section 2.5. Note that (x, g) are invariant under the U(1) transformation (3.9), thus the loop gravity phase space can be reconstructed completely as a symplectic reduction of the spinor phase space $\mathbb{C}^2 \times \mathbb{C}^2$:

$$T^*\mathrm{SU}(2)\backslash\{|\vec{x}| = 0\} = \mathbb{C}^2 \times \mathbb{C}^2 \backslash \{\langle\zeta|\zeta\rangle = 0, \langle\tilde{\zeta}|\tilde{\zeta}\rangle = 0\}//\mathrm{U}(1)\,. \tag{3.11}$$

Let us now consider an oriented graph Γ with E links and V nodes. For each link e, we assign a non-tilde spinors $|\zeta_e\rangle$ to its source node $s(e)$ and a tilde spinors $|\tilde{\zeta}_e]$ to its target node $t(e)$. They are related by an SU(2) action thus satisfy the norm matching constraint

$$g_e^{-1}|\zeta_e\rangle = |\tilde{\zeta}_e]\,, \quad \langle\zeta_e|\zeta_e\rangle = [\tilde{\zeta}_e|\tilde{\zeta}_e]\,. \tag{3.12}$$

g_e's can be viewed as an assignment to the links. The kinematical phase space of Γ is defined as the collection of $(\zeta_e, \tilde{\zeta}_e) \in \mathbb{C}^2 \times \mathbb{C}^2$ for each link imposing the closure constraints $\vec{\mathcal{C}}_v$ for each node:

$$\vec{\mathcal{C}}_v = \sum_{e|v=s(e)} \langle\zeta_e|\vec{\sigma}|\zeta_e\rangle - \sum_{e|v=t(e)} [\tilde{\zeta}_e|\vec{\sigma}|\tilde{\zeta}_e]\,. \tag{3.13}$$

The phase space defined with spinors allows us to have a U(n) reformulation of LQG after quantization [98, 99, 50]. The essential idea, from the geometrical point of view, is to change the building blocks from degrees of freedom on links (which are holonomies or fluxes) to those on nodes (which are spinors). For each (n-valent) node v, we define an $n \times n$ symmetric matrix $\mathbf{E}$ and two $n \times n$ asymmetric matrices $\mathbf{F}$ and $\mathbf{G}$ with complex entries representing the correlation of spinors associated to different half-links incident to the same node. (we will use the Latin indices i, j, k, l in the subscript to label the legs of the node):

$$\begin{aligned} &E_{ij} = \langle\zeta_i|\zeta_j\rangle\,, && E_{ji} = \overline{E}_{ij}\,, \\ &F_{ij} = [\zeta_i|\zeta_j\rangle\,, && F_{ji} = -F_{ij}\,, \\ &G_{ij} = \overline{F}_{ij} \equiv \langle\zeta_j|\zeta_i]\,, && G_{ji} = -G_{ij}\,, \end{aligned} \tag{3.14}$$

where the bar denotes the complex conjugate. These SU(2) observables form a closed algebra. With no loss of generality, consider that all the links incident to the node v are outgoing, then the Poisson brackets of the components read

$$\begin{aligned}
&\{E_{ij}, E_{kl}\} = i(\delta_{il}E_{kj} - \delta_{jk}E_{il})\,, \quad \{E_{ij}, F_{kl}\} = i(\delta_{il}F_{jk} - \delta_{ik}F_{jl})\,,\\
&\{E_{ij}, G_{kl}\} = i(\delta_{jl}G_{ik} - \delta_{jk}G_{il})\,, \quad \{F_{ij}, F_{kl}\} = 0\,, \quad \{G_{ij}, G_{kl}\} = 0\,,\\
&\{F_{ij}, G_{kl}\} = i(\delta_{ik}E_{lj} - \delta_{il}E_{kj} + \delta_{jl}E_{ki} - \delta_{jk}E_{li})\,.
\end{aligned} \tag{3.15}$$

It can be seen from the first Poisson bracket that the components of the matrix $\mathbf{E}$ form a $\mathfrak{u}(n)$ Poisson algebra and the components of $\mathbf{E}, \mathbf{F}, \mathbf{G}$ together form a $\mathfrak{so}^*(2n)$ Poisson algebra [120]. We will use the spinors defined in this subsection to define a spinfoam model for 3D quantum gravity with $\Lambda = 0$ in Chapter 7 whose building blocks capture the conformal geometries, different from the standard spinfoam model. On the other hand, to recover the q-deformed loop gravity phase space, one needs to deform the spinors and their Poisson brackets (3.4). We will describe below how this deformation is performed, which also lead to the deformation of the algebras (3.15).

3.2 q-deformed spinors

We aim to find the spinors that transform covariantly under the SU(2) gauge transformation (2.45) (or (2.47)) in the q-deformed phase space. To this end, one needs to start from the correct spinor variables. Indeed, the spinor variables ζ_A and $\tilde{\zeta}_A$ capture only the flat geometries as they reproduce the loop gravity phase space and no Λ information is encoded. We will perform a deformation of these spinor variables in two consecutive steps to arrive at the SU(2)-covariant spinors in the q-deformed picture. Graphically, spinors are assigned to the half links of each link. After the deformation, each SU(2)-covariant spinor is associated to the two half ribbon links meeting at the same node of a ribbon. The deformation process can be summarized as in fig.3.2, with the spinors therein defined in the main text. Some of the initial results have been given in [73], and the main part of the rest of this chapter is from the work in [41] by the author and collaborators.

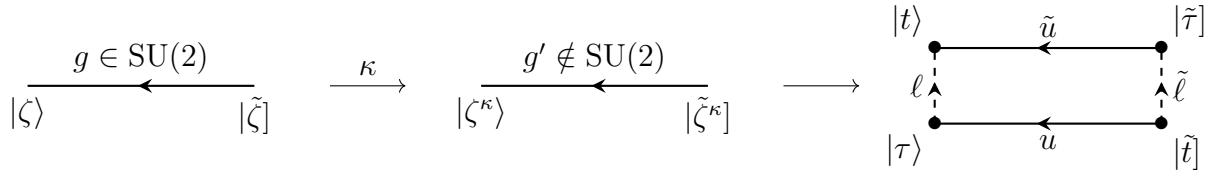

Figure 3.2: Two consecutive deformations of the spinors in the flat case to arrive at the SU(2)-covariant spinors in the ribbon picture.

3.2.1 Basic variables

We can now define the κ-deformed spinor $|\zeta^\kappa\rangle$ from $|\zeta\rangle$, with its dual $\langle\zeta^\kappa|$ and norm $\langle\zeta^\kappa|\zeta^\kappa\rangle$ [73] (Recall that $\kappa = \sqrt{|\Lambda|}$):

$$\zeta^\kappa_A := \zeta_A \sqrt{\frac{\sinh(\frac{\kappa}{2}N_A)}{\frac{\kappa}{2}N_A}}\,, \quad \bar{\zeta}^\kappa_A \equiv \overline{\zeta^\kappa_A}\,, \qquad \text{with } N_A = \bar{\zeta}_A\zeta_A\,, \tag{3.16}$$

$$\langle\zeta^\kappa|\zeta^\kappa\rangle = \sum_A \bar{\zeta}^\kappa_A\zeta^\kappa_A \;=\; \sum_A \frac{2}{\kappa}\sinh(\frac{\kappa N_A}{2}) \;=\; \frac{1}{\kappa}\sum_A \left(e^{\frac{\kappa N_A}{2}} - e^{\frac{-\kappa N_A}{2}}\right) \geq 0\,, \tag{3.17}$$

These κ-deformed spinors satisfy the following Poisson brackets

$$\{\zeta^\kappa_A, \bar{\zeta}^\kappa_B\} = -i\,\delta_{AB}\,\cosh(\frac{\kappa N_A}{2}), \quad \{N_A, \zeta^\kappa_B\} = i\,\delta_{AB}\,\zeta^\kappa_A, \quad \{N_A, \bar{\zeta}^\kappa_B\} = -i\,\delta_{AB}\,\bar{\zeta}^\kappa_A\,. \tag{3.18}$$

It is easy to check that we recover the undeformed Poisson brackets (3.4) when $\kappa \to 0$. The deformed variable $|\tilde{\zeta}^\kappa\rangle$ is defined from $|\tilde{\zeta}\rangle$ by (3.16) and (3.17) where all ζ_A are replaced by $\tilde{\zeta}_A$.

Change of link orientations. Since there are no differences between $|\zeta^\kappa\rangle$ and $|\tilde{\zeta}^\kappa\rangle$, and since changing the orientation of a link exchanges the two sectors, it is natural to lift the involution $\mathfrak{m}$ to the spinor space as follows,

$$\mathfrak{m}(\zeta^\kappa_A) = \tilde{\zeta}^\kappa_A, \qquad \mathfrak{m}(\tilde{\zeta}^\kappa_A) = \zeta^\kappa_A\,, \quad \text{for } A = \pm 1/2\,. \tag{3.19}$$

Reconstructing the fluxes. We will use $\zeta^\kappa_\pm$ to reconstruct ℓ and $\tilde{\zeta}^\kappa_\pm$ to reconstruct $\tilde{\ell}$. Since the spinors in the tilde and non-tilde sectors are identical whereas $\mathfrak{m}(\ell) \neq \tilde{\ell}$, ℓ can

not be the same function of $\zeta^\kappa_\pm$ as $\tilde{\ell}$ is of $\tilde{\zeta}^\kappa_\pm$. We use

$$\begin{aligned} \lambda &\equiv \exp(\tfrac{\kappa}{4}(N_+ - N_-))\,, \quad z \equiv -\kappa\bar{\zeta}^\kappa_-\zeta^\kappa_+\,, \\ \tilde{\lambda} &\equiv \exp(\tfrac{\kappa}{4}(\tilde{N}_- - \tilde{N}_+))\,, \quad \tilde{z} \equiv \kappa\bar{\tilde{\zeta}}^\kappa_-\tilde{\zeta}^\kappa_+\,. \end{aligned} \tag{3.20}$$

By applying $\mathfrak{m}$ to (3.20), we recover as expected that $\mathfrak{m}(\lambda) = \tilde{\lambda}^{-1}$ and $\mathfrak{m}(z) = -\tilde{z}$. The AN(2) matrices ℓ and $\tilde{\ell}$ become functions of the spinors,

$$\ell(\zeta^\kappa_\pm, \bar{\zeta}^\kappa_\pm) = \begin{pmatrix} \lambda & 0 \\ z & \lambda^{-1} \end{pmatrix}\,, \quad \tilde{\ell}(\tilde{\zeta}^\kappa_\pm, \bar{\tilde{\zeta}}^\kappa_\pm) = \begin{pmatrix} \tilde{\lambda} & 0 \\ \tilde{z} & \tilde{\lambda}^{-1} \end{pmatrix}\,, \tag{3.21}$$

and $\mathfrak{m}(\ell) = \tilde{\ell}^{-1}$. It is easy to check that these AN(2) matrix elements do satisfy the expected explicit Poisson brackets (B.4). Let us point out that z, $\bar{z}$, λ all commute with $N = N_- + N_+$, $\{N, \bar{z}\} = \{N, \lambda\} = \{N, z\} = 0$.

While the deformed variables $|\zeta^\kappa\rangle$ and $|\tilde{\zeta}^\kappa\rangle$ are important in parametrizing the AN(2) elements and generating the (infinitesimal) rotation transformations [40], they are not yet the spinors we will use to reconstruct the holonomy-flux phase space, because they do *not* transform covariantly under the SU(2) action.

3.2.2 Covariant Spinors

Let us now define the variables which transform covariantly as spin 1/2 under SU(2), *i.e.* either (2.45) or (2.47), depending on if we consider the ribbon variable ℓ or $\ell^{-1\dagger}$. We consider the first case, where we deal with ℓ. We recall that $X = \ell\ell^\dagger$ with ℓ an AN(2) element now parametrized as in (3.21) whose entries are defined in terms of the spinor variables given in (3.20).

Covariant spinor. An SU(2)-covariant spinor (henceforth spinor) $|T\rangle$ is defined by the transformation law

$$\delta_\epsilon|T\rangle \equiv (w - \mathbb{I})|T\rangle = i\begin{pmatrix} \epsilon_z & \epsilon_- \\ \epsilon_+ & -\epsilon_z \end{pmatrix}|T\rangle\,. \tag{3.22}$$

As shown in [79], the only two independent solutions (up to normalization) to equating the RHS of (3.22) with the RHS of (2.42) are $|t\rangle$ and its dual $|t]$ defined as

$$|t\rangle = \begin{pmatrix} t_- \\ t_+ \end{pmatrix} = \begin{pmatrix} e^{\frac{\kappa N_+}{4}}\zeta^\kappa_- \\ e^{-\frac{\kappa N_-}{4}}\zeta^\kappa_+ \end{pmatrix}\,, \qquad |t] = \begin{pmatrix} 0 & -1 \\ 1 & 0 \end{pmatrix}|\bar{t}\rangle = \begin{pmatrix} -\bar{t}_+ \\ \bar{t}_- \end{pmatrix} = \begin{pmatrix} -e^{-\frac{\kappa N_-}{4}}\bar{\zeta}^\kappa_+ \\ e^{\frac{\kappa N_+}{4}}\bar{\zeta}^\kappa_- \end{pmatrix}\,, \tag{3.23}$$

The norm is a function of the non-deformed norm N,

$$\langle t|t\rangle = [t|t] = \frac{2}{\kappa}\sinh\left(\frac{\kappa}{2}N\right) .$$

The Poisson brackets of the components are

$$\begin{array}{lll} \{t_-, t_+\} = \frac{i\kappa}{2}\, t_-\, t_+ , & \{t_-, \bar{t}_-\} = \frac{i\kappa}{2}\left(t_-\, \bar{t}_- - \frac{2}{\kappa}e^{\frac{\kappa}{2}N}\right) , & \{t_-, \bar{t}_+\} = 0 , \\ \{\bar{t}_-, \bar{t}_+\} = -\frac{i\kappa}{2}\, \bar{t}_-\, \bar{t}_+ , & \{t_+, \bar{t}_+\} = -\frac{i\kappa}{2}\left(t_+\, \bar{t}_+ + \frac{2}{\kappa}e^{-\frac{\kappa}{2}N}\right) , & \{t_+, \bar{t}_-\} = 0 . \end{array} \tag{3.24}$$

Braided covariant spinor. The spinor $|t\rangle$ can be "parallell transported" by ℓ^{-1}, which produces another spinor, whose transformation law under SU(2) is called *braided*. Explicitly, using (3.20), we have

$$\ell^{-1}\,|t\rangle = \begin{pmatrix} \lambda^{-1} & 0 \\ -z & \lambda \end{pmatrix} \begin{pmatrix} e^{\frac{\kappa N_+}{4}}\zeta^\kappa_- \\ e^{-\frac{\kappa N_-}{4}}\zeta^\kappa_+ \end{pmatrix} = e^{\frac{\kappa N}{4}} \begin{pmatrix} e^{-\frac{\kappa N_+}{4}}\zeta^\kappa_- \\ e^{\frac{\kappa N_-}{4}}\zeta^\kappa_+ \end{pmatrix} , \tag{3.25}$$

which prompts the definition of the following spinor[2],

$$|\tau\rangle \equiv e^{-\frac{\kappa N}{4}}\ell^{-1}\,|t\rangle. \tag{3.26}$$

The dual of $|\tau\rangle$ is

$$|\tau] = \begin{pmatrix} 0 & -1 \\ 1 & 0 \end{pmatrix} |\bar{\tau}\rangle = \begin{pmatrix} -\bar{\tau}_+ \\ \bar{\tau}_- \end{pmatrix} = \begin{pmatrix} -e^{\frac{\kappa N_-}{4}}\bar{\zeta}^\kappa_+ \\ e^{-\frac{\kappa N_+}{4}}\bar{\zeta}^\kappa_- \end{pmatrix} = e^{\frac{\kappa}{4}N}\ell^{-1}|t] .$$

On the other hand, as the ribbon structure can be equivalently represented by either ℓ or $\ell^{-1\,\dagger}$ as shown in (2.39), one expects that $|\tau\rangle$ can also be defined by parallelly transporting $|t\rangle$ with $\ell^\dagger$. This is indeed the case,

$$|\tau\rangle = e^{\frac{\kappa N}{4}}\ell^\dagger|t\rangle , \quad |\tau] = e^{-\frac{\kappa N}{4}}\ell^\dagger|t] . \tag{3.27}$$

Hence whether we use ℓ or $\ell^{-1\dagger}$ we get essentially the same object.

The Poisson brackets of the components of $|\tau\rangle$ are the same as those of $|t\rangle$ and $|t]$ with τ_A replacing t_{-A} and $\bar{\tau}_A$ replacing $\bar{t}_{-A}$, *i.e.*

$$\begin{array}{lll} \{\tau_-, \tau_+\} = -\frac{i\kappa}{2}\tau_-\tau_+ , & \{\tau_-, \bar{\tau}_-\} = -\frac{i\kappa}{2}(\tau_-\bar{\tau}_- + \frac{2}{\kappa}e^{-\kappa N}) , & \{\tau_-, \bar{\tau}_+\} = 0 , \\ \{\bar{\tau}_-, \bar{\tau}_+\} = \frac{i\kappa}{2}\bar{\tau}_-\bar{\tau}_+ , & \{\tau_+, \bar{\tau}_+\} = \frac{i\kappa}{2}(\tau_+\bar{\tau}_+ - \frac{2}{\kappa}e^{\kappa N}) , & \{\bar{\tau}_-, \tau_+\} = 0 . \end{array} \tag{3.28}$$

[2]It differs from the spinor $|\tau\rangle$ of [79] by its normalization.

$|\tau\rangle$ defines what we call a *braided spinor*. Indeed, it transforms as a spinor under the SU(2) transformations generated by (2.42), but with a group element w' related to w through ℓ. Since triangular matrices are not stable under conjugation by SU(2) group elements, we need to introduce another SU(2) group element to stabilize the transformation. Let ${}^{(w)}\ell \in \mathrm{AN}(2)$ and $w' \in \mathrm{SU}(2)$ be defined by the Iwasawa decomposition

$$w\ell = {}^{(w)}\ell w' \,. \tag{3.29}$$

Then we say that ℓ transforms as

$$\ell \quad \xrightarrow{w\in \mathrm{SU}(2)} \quad {}^{(w)}\ell = w\ell w'^{-1} \in \mathrm{AN}(2)\,. \tag{3.30}$$

Going at the infinitesimal level [40],

$$w \sim \mathbb{I} + i\vec{\epsilon}\cdot\vec{\sigma} = \mathbb{I} + i\begin{pmatrix} \epsilon_z & \epsilon_- \\ \epsilon_+ & -\epsilon_z \end{pmatrix}, \quad w' \sim \mathbb{I} + i\vec{\epsilon'}\cdot\vec{\sigma} = \mathbb{I} + i\begin{pmatrix} \epsilon'_z & \epsilon'_- \\ \epsilon'_+ & -\epsilon'_z \end{pmatrix}, \tag{3.31}$$

the relation between $\vec{\epsilon}$ and $\vec{\epsilon'}$ is given by

$$\epsilon'_\pm = \lambda^{-2}\epsilon_\pm\,, \quad \epsilon'_z = \epsilon_z + 1/2(\lambda^{-1}z\epsilon_- + \lambda^{-1}\bar{z}\epsilon_+)\,. \tag{3.32}$$

One can then check that, remarkably, the transformation generated by (2.42) is a rotation by (the infinitesimal version of) w'

$$\delta_\epsilon|\tau\rangle = -\lambda^{-2}\kappa^{-1}\{\mathrm{Tr}WX, |\tau\rangle\} = i\begin{pmatrix} \epsilon'_z\tau_- + \epsilon'_-\tau_+ \\ \epsilon'_+\tau_- - \epsilon'_z\tau_+ \end{pmatrix} \sim (w' - \mathbb{I})|\tau\rangle\,, \tag{3.33}$$

$|\tau]$ is also a braided covariant spinor. The transformation (3.33) can also be written as a non-braided one, but generated with $X^{\mathrm{op}} := \ell^\dagger\ell$ instead of X,

$$\delta_\epsilon|\tau\rangle = \lambda^2\kappa^{-1}\{\mathrm{Tr}W'(X^{\mathrm{op}})^{-1}, |\tau\rangle\} = \lambda^2\kappa^{-1}\{2\epsilon'_z\lambda^{-2} - \epsilon'_-\lambda^{-1}z - \epsilon'_+\lambda^{-1}\bar{z}, |\tau\rangle\} = (w' - \mathbb{I})|\tau\rangle\,, \tag{3.34}$$

with $W' = \epsilon'_z(\mathbb{I} + \sigma_z) + \epsilon'_-\sigma_+ + \epsilon'_+\sigma_-$.

3.2.3 The tilde spinors

Covariant spinors and braided covariant spinors for the tilde sector, the "tilde covariant spinors", are defined in a similar way as the non-tilde ones. We have

$$|\tilde{t}\rangle = \mathfrak{m}(|t\rangle) = \begin{pmatrix} \tilde{t}_- \\ \tilde{t}_+ \end{pmatrix} = \begin{pmatrix} e^{\frac{\kappa\tilde{N}_+}{4}}\tilde{\zeta}^\kappa_- \\ e^{-\frac{\kappa\tilde{N}_-}{4}}\tilde{\zeta}^\kappa_+ \end{pmatrix}, \quad |\tilde{t}] = \begin{pmatrix} -\bar{\tilde{t}}_+ \\ \bar{\tilde{t}}_- \end{pmatrix} = \begin{pmatrix} -e^{-\frac{\kappa\tilde{N}_-}{4}}\bar{\tilde{\zeta}}^\kappa_+ \\ e^{\frac{\kappa\tilde{N}_+}{4}}\bar{\tilde{\zeta}}^\kappa_- \end{pmatrix}, \tag{3.35}$$

$$|\tilde{\tau}\rangle = \mathfrak{m}(|\tau\rangle) = \begin{pmatrix} \tilde{\tau}_- \\ \tilde{\tau}_+ \end{pmatrix} = \begin{pmatrix} e^{-\frac{\kappa\tilde{N}_+}{4}}\tilde{\zeta}^\kappa_- \\ e^{\frac{\kappa\tilde{N}_-}{4}}\tilde{\zeta}^\kappa_+ \end{pmatrix}, \quad |\tilde{\tau}] = \begin{pmatrix} -\bar{\tilde{\tau}}_+ \\ \bar{\tilde{\tau}}_- \end{pmatrix} = \begin{pmatrix} -e^{\frac{\kappa\tilde{N}_-}{4}}\bar{\tilde{\zeta}}^\kappa_+ \\ e^{-\frac{\kappa\tilde{N}_+}{4}}\bar{\tilde{\zeta}}^\kappa_- \end{pmatrix}, \tag{3.36}$$

whose norms are given by

$$\langle\tilde{t}|\tilde{t}\rangle = [\tilde{t}|\tilde{t}] = \langle\tilde{\tau}|\tilde{\tau}\rangle = [\tilde{\tau}|\tilde{\tau}] = \frac{2}{\kappa}\sinh\left(\frac{\kappa}{2}\tilde{N}\right). \tag{3.37}$$

They are independent of the non-tilde spinors, *i.e.* all the components Poisson commute with those of the non-tilde spinors. The Poisson brackets of the tilde spinor components are the same as the non-tilde ones:

$$\begin{aligned} &\{\tilde{t}_-,\tilde{t}_+\} = \tfrac{i\kappa}{2}\tilde{t}_-\tilde{t}_+, && \{\tilde{t}_-,\bar{\tilde{t}}_-\} = \tfrac{i\kappa}{2}\left(\tilde{t}_-\bar{\tilde{t}}_- - \tfrac{2}{\kappa}e^{\frac{\kappa}{2}N}\right), && \{\tilde{t}_-,\bar{\tilde{t}}_+\} = 0, \\ &\{\bar{\tilde{t}}_-,\bar{\tilde{t}}_+\} = -\tfrac{i\kappa}{2}\bar{\tilde{t}}_-\bar{\tilde{t}}_+, && \{\tilde{t}_+,\bar{\tilde{t}}_+\} = -\tfrac{i\kappa}{2}\left(\tilde{t}_+\bar{\tilde{t}}_+ + \tfrac{2}{\kappa}e^{-\frac{\kappa}{2}N}\right), && \{\bar{\tilde{t}}_-,\tilde{t}_+\} = 0, \end{aligned} \tag{3.38}$$

$$\begin{aligned} &\{\tilde{\tau}_-,\tilde{\tau}_+\} = -\tfrac{i\kappa}{2}\tilde{\tau}_-\tilde{\tau}_+, && \{\tilde{\tau}_-,\bar{\tilde{\tau}}_-\} = -\tfrac{i\kappa}{2}\left(\tilde{\tau}_-\bar{\tilde{\tau}}_- + \tfrac{2}{\kappa}e^{-\frac{\kappa}{2}\tilde{N}}\right), && \{\tilde{\tau}_-,\bar{\tilde{\tau}}_+\} = 0, \\ &\{\bar{\tilde{\tau}}_-,\bar{\tilde{\tau}}_+\} = \tfrac{i\kappa}{2}\bar{\tilde{\tau}}_-\bar{\tilde{\tau}}_+, && \{\tilde{\tau}_+,\bar{\tilde{\tau}}_+\} = \tfrac{i\kappa}{2}\left(\tilde{\tau}_+\bar{\tilde{\tau}}_+ - \tfrac{2}{\kappa}e^{\frac{\kappa}{2}\tilde{N}}\right), && \{\bar{\tilde{\tau}}_-,\tilde{\tau}_+\} = 0. \end{aligned} \tag{3.39}$$

Note however that $\tilde{\ell}$ is not the same function of $\tilde{\zeta}^\kappa_\pm$ as ℓ is of $\zeta^\kappa_\pm$, see (3.20), (3.21). In fact , we have $\mathfrak{m}(\ell) = \tilde{\ell}^{-1}$ where we recall that $\mathfrak{m}$ defined in (3.19) is an operator which adds tildes to $\zeta^\kappa_\pm$ and their complex conjugates. As a consequence, the relation between $|\tilde{t}\rangle$ and $|\tilde{\tau}\rangle$ is not obtained by adding tildes to $|\tau\rangle = e^{-\frac{\kappa N}{4}}\ell^{-1}|t\rangle = e^{\frac{\kappa N}{4}}\ell^\dagger|t\rangle$. Instead we act with $\mathfrak{m}$ to get

$$|\tilde{\tau}\rangle = e^{-\frac{\kappa\tilde{N}}{4}}\tilde{\ell}|\tilde{t}\rangle = e^{\frac{\kappa\tilde{N}}{4}}\tilde{\ell}^{-1\dagger}|\tilde{t}\rangle. \tag{3.40}$$

Since the Poisson brackets of the tilde spinors are the same (with tildes) as the non-tilde ones, the generator of SU(2) transformations for the tilde spinors is given by

$$\mathfrak{m}\big(-\lambda^{-2}\kappa^{-1}\mathrm{Tr}(WX)\big) = -\tilde{\lambda}^2\kappa^{-1}\mathrm{Tr}W(\tilde{X}^{\mathrm{op}})^{-1}, \tag{3.41}$$

where $\tilde{X}^{\mathrm{op}} = \tilde{\ell}^\dagger\tilde{\ell}$. This is consistent with the Gauss constraint (2.44), which is a product of ℓ and $\tilde{\ell}^{-1}$ depending on the orientations of the ribbons. Explicitly, we can expand $\mathrm{Tr}W(\tilde{X}^{\mathrm{op}})^{-1}$ as

$$\mathrm{Tr}W(\tilde{X}^{\mathrm{op}})^{-1} = 2\epsilon_z\tilde{\lambda}^{-2} - \epsilon_-\tilde{\lambda}^{-1}\tilde{z} - \epsilon_+\tilde{\lambda}^{-1}\bar{\tilde{z}}. \tag{3.42}$$

It is then straightforward using the Poisson brackets from Appendix B.1 to show that the tilde spinors (3.36) satisfy the following equations

$$\delta_\epsilon|\tilde{t}\rangle = -\tilde{\lambda}^2\kappa^{-1}\{\mathrm{Tr}(W(\tilde{X}^{\mathrm{op}})^{-1}), |\tilde{t}\rangle\} = (w-\mathbb{1})|\tilde{t}\rangle\,, \tag{3.43a}$$

$$\delta_\epsilon|\tilde{t}] = -\tilde{\lambda}^2\kappa^{-1}\{\mathrm{Tr}(W(\tilde{X}^{\mathrm{op}})^{-1}), |\tilde{t}]\} = (w-\mathbb{1})|\tilde{t}]\,, \tag{3.43b}$$

$$\delta_\epsilon|\tilde{\tau}\rangle = -\tilde{\lambda}^2\kappa^{-1}\{\mathrm{Tr}(W(\tilde{X}^{\mathrm{op}})^{-1}), |\tilde{\tau}\rangle\} = (w''-\mathbb{1})|\tilde{\tau}\rangle\,, \tag{3.43c}$$

$$\delta_\epsilon|\tilde{\tau}] = -\tilde{\lambda}^2\kappa^{-1}\{\mathrm{Tr}(W(\tilde{X}^{\mathrm{op}})^{-1}), |\tilde{\tau}]\} = (w''-\mathbb{1})|\tilde{\tau}]\,, \tag{3.43d}$$

where the infinitesimal SU(2) elements $w = \mathbb{1} + i\vec{\epsilon}\cdot\vec{\sigma}$ and $w'' = \mathbb{1} + i\vec{\epsilon''}\cdot\vec{\sigma}$ are related by the right SU(2) transformation of $\tilde{\ell}$, *i.e.*

$$\tilde{\ell} \xrightarrow{w\in\mathrm{SU}(2)} \tilde{\ell}^{(w)} = w''^{-1}\tilde{\ell}w \in \mathrm{AN}(2)\,, \quad \left| \begin{array}{l} w \sim \mathbb{1} + i\vec{\epsilon}\cdot\vec{\sigma} = \mathbb{1} + i\begin{pmatrix} \epsilon_z & \epsilon_- \\ \epsilon_+ & -\epsilon_z \end{pmatrix} \\ w'' \sim \mathbb{1} + i\vec{\epsilon''}\cdot\vec{\sigma} = \mathbb{1} + i\begin{pmatrix} \epsilon''_z & \epsilon''_- \\ \epsilon''_+ & -\epsilon''_z \end{pmatrix} \end{array} \right. . \tag{3.44}$$

Thus the two infinitesimal parameters $\vec{\epsilon}$ and $\vec{\epsilon''}$ are related by

$$\epsilon''_\pm = \tilde{\lambda}^2\epsilon_\pm\,, \quad \epsilon''_z = \epsilon_z - 1/2(\tilde{\lambda}z\epsilon_- + \lambda\bar{\tilde{z}}\epsilon_+)\,. \tag{3.45}$$

Just like there are two ways to write the transformations of $|\tau\rangle$ and $|\tau]$, there are also two for $|\tilde{\tau}\rangle$ and $|\tilde{\tau}]$. While we have seen above the equivalent of (3.33), the equivalent of (3.34) is

$$\delta_\epsilon|\tilde{\tau}\rangle = \mathfrak{m}\big(\lambda^2\kappa^{-1}\big)\{\mathrm{Tr}(W''\mathfrak{m}(X^{\mathrm{op}\,-1}))\,, |\tilde{\tau}\rangle\} = \tilde{\lambda}^{-2}\kappa^{-1}\{\mathrm{Tr}(W''\tilde{X}), |\tilde{\tau}\rangle\}\,, \tag{3.46a}$$

$$\delta_\epsilon|\tilde{\tau}] = \tilde{\lambda}^{-2}\kappa^{-1}\{\mathrm{Tr}(W''\tilde{X}), |\tilde{\tau}]\}\,, \tag{3.46b}$$

and it is clear that $|\tilde{\tau}\rangle$ and $|\tilde{\tau}]$ are braided spinors in the same sense as $|\tau\rangle, |\tau]$.

There is a nice geometric interpretation of the relations (3.26) and (3.40) which define the braided covariant spinors. If we consider $|t\rangle$ to sit at a node of Γ_{r} which is the target of the short link carrying ℓ, then $|\tau\rangle = e^{-\frac{\kappa N}{4}}\ell^{-1}\,|t\rangle$ sits on the node of Γ_{r} at the source of the short link carrying ℓ. In other words, $|\tau\rangle$ results from parallelly transporting $|t\rangle$ by ℓ^{-1}. Similarly $|\tilde{\tau}\rangle$ is the result of parallelly transporting $|\tilde{t}\rangle$ by $\tilde{\ell}$. This is represented in fig.3.2.

3.3 Recovering the q-deformed holonomy-flux variables

Now that we have defined the two pairs of spinors $(|t\rangle, |\tau\rangle)$ and $(|\tilde{\tau}], |\tilde{t}])$, each pair of which are related by the flux ℓ or $\tilde{\ell}$, it is natural to assign them to the corners (that is the nodes on a ribbon) of the ribbon link as in fig.3.3.

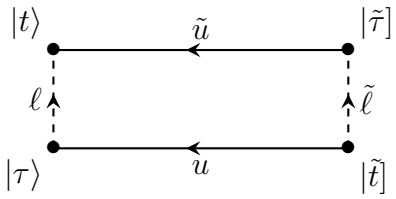

Figure 3.3: Ribbon graph for a link with one spinor on each corner.

We assume the norm matching condition $N = \tilde{N}$ so that the tilde spinors and their corresponding non-tilde spinors have the same norm:

$$\langle t|t\rangle = [\tilde{\tau}|\tilde{\tau}] = \frac{2}{\kappa}\sinh\frac{\kappa N}{2}\,. \tag{3.47}$$

The holonomies $u, \tilde{u} \in \mathrm{SU}(2)$ can be parametrized in terms of these spinors

$$u = \frac{|\tau\rangle[\tilde{t}| - |\tau]\langle\tilde{t}|}{\sqrt{\langle\tau|\tau\rangle\langle\tilde{t}|\tilde{t}\rangle}}\,, \quad \tilde{u} = \frac{|t\rangle[\tilde{\tau}| - |t]\langle\tilde{\tau}|}{\sqrt{\langle t|t\rangle\langle\tilde{\tau}|\tilde{\tau}\rangle}}\,, \qquad \text{with } N = \tilde{N}\,, \tag{3.48}$$

so that the following parallel transport relations are satisfied,

$$\begin{aligned} &u|\tilde{t}] = |\tau\rangle\,, \quad u|\tilde{t}\rangle = -|\tau]\,, \quad u^{-1}|\tau\rangle = |\tilde{t}]\,, \quad u^{-1}|\tau] = -|\tilde{t}\rangle\,, \\ &\tilde{u}|\tilde{\tau}\rangle = -|t]\,, \quad \tilde{u}|\tilde{\tau}] = |t\rangle\,, \quad \tilde{u}^{-1}|t] = -|\tilde{\tau}\rangle\,, \quad \tilde{u}^{-1}|t\rangle = |\tilde{\tau}]\,. \end{aligned} \tag{3.49}$$

Therefore, the ribbon graph fig.3.2 illustrates the full transport relations of the four spinors. Finally, they solve the ribbon constraint:

$$\begin{cases} \ell u|\tilde{t}] = \ell|\tau\rangle = e^{-\frac{\kappa N}{4}}|t\rangle \\ \tilde{u}\tilde{\ell}|\tilde{t}] = e^{-\frac{\kappa N}{4}}\tilde{u}|\tilde{\tau}] = e^{-\frac{\kappa N}{4}}|t\rangle \end{cases} \quad \Longrightarrow \quad \mathcal{C} \equiv \ell u\tilde{\ell}^{-1}\tilde{u}^{-1} = \mathbb{1}\,, \tag{3.50}$$

and the same can be done with the equivalent ribbon constraint $\ell^{-1\dagger}u\tilde{\ell}^{\dagger}\tilde{u}^{-1} = \mathbb{1}$. These spinors thus live on the constraint surface generated by the ribbon constraint $\mathcal{C}$. The matrix components defined in (3.48) also satisfy the desired Poisson brackets (see (B.4)).

Deformed flux variables in terms of the deformed spinors. We furthermore write the flux vectors $\ell\ell^{\dagger} = X \equiv \kappa X_0\mathbb{1} - \kappa\vec{X}\cdot\vec{\sigma}$ and $\ell^{\dagger}\ell \equiv X^{\mathrm{op}} = \kappa X_0^{\mathrm{op}}\mathbb{1} - \kappa\vec{X}^{\mathrm{op}}\cdot\vec{\sigma}$ defined in

(2.40) in terms of the spinors. Their components can be represented in term of the spinors $|t\rangle$ and $|\tau\rangle$,

$$X_0 = \frac{1}{\kappa}\sqrt{1+\frac{\kappa^2}{4}\langle t|t\rangle^2} = X_0^{\rm op} = \frac{1}{\kappa}\sqrt{1+\frac{\kappa^2}{4}\langle \tau|\tau\rangle^2}, \quad \vec{X} = \frac{1}{2}\langle t|\vec{\sigma}|t\rangle, \quad \vec{X}^{\rm op} = \frac{1}{2}\langle \tau|\vec{\sigma}|\tau\rangle. \tag{3.51}$$

Similarly, $\tilde{\ell}\tilde{\ell}^\dagger \equiv \tilde{X} = \kappa\tilde{X}_0 \mathbb{I} - \kappa\vec{\tilde{X}}\cdot\vec{\sigma}$ and $\tilde{\ell}^\dagger\tilde{\ell} \equiv \tilde{X}^{\rm op} = \kappa\tilde{X}_0^{\rm op}\mathbb{I} - \kappa\vec{\tilde{X}}^{\rm op}\cdot\vec{\sigma}$ can be written with the tilde spinors but the dual sectors. Explicitly,

$$\tilde{X}_0 = \frac{1}{\kappa}\sqrt{1+\frac{\kappa^2}{4}[\tilde{\tau}|\tilde{\tau}]^2} = \tilde{X}_0^{\rm op} = \frac{1}{\kappa}\sqrt{1+\frac{\kappa^2}{4}[\tilde{t}|\tilde{t}]^2}\,, \quad \vec{\tilde{X}} = \frac{1}{2}[\tilde{\tau}|\vec{\sigma}|\tilde{\tau}]\,, \quad \vec{\tilde{X}}^{\rm op} = \frac{1}{2}[\tilde{t}|\vec{\sigma}|\tilde{t}]\,. \tag{3.52}$$

These objects transform as vectors under the SU(2) transformation as $\tilde{X} = \tilde{u}^{-1}X\tilde{u}$ and $u^{-1}X^{\rm op}u = \tilde{X}^{\rm op}$, consistently with (3.49), and as such can be seen as the deformation of the flat flux vectors (see (3.5)).

When $\kappa \to 0$, $|t\rangle, |\tilde{t}]$ is identical to $|\tau\rangle, |\tilde{\tau}]$ respectively, as it can be directly seen from their definition (3.23), (3.26) and (3.36). We recover then the flat case where there is only one pair of spinors associated to each link. The flux vectors $\vec{X}$ and $\vec{\tilde{X}}$ become the standard flat flux vectors which we denote $\vec{x}$ and $\vec{\tilde{x}}$ respectively. As a consistency check, one can take the $\kappa \to 0$ limit for X (3.51) and $\tilde{X}$ (3.52) defined in terms of the spinors, or more explicitly in terms of the κ-deformed spinor variables as in (3.20). Let us rewrite

$$\begin{aligned}
X = \begin{pmatrix} \lambda^2 & \lambda\bar{z} \\ \lambda z & \lambda^{-2}+|z|^2 \end{pmatrix} &= \begin{pmatrix} e^{\frac{\kappa(N_+-N_-)}{2}} & -\kappa e^{\frac{\kappa(N_+-N_-)}{4}}\zeta_-^\kappa\bar{\zeta}_+^\kappa \\ -\kappa e^{\frac{\kappa(N_+-N_-)}{4}}\zeta_+^\kappa\bar{\zeta}_-^\kappa & e^{\frac{\kappa(N_--N_+)}{2}} + 4\sinh\frac{\kappa N_+}{2}\sinh\frac{\kappa N_-}{2} \end{pmatrix} \\
&\xrightarrow{\kappa\to 0} \begin{pmatrix} 1+\frac{\kappa(N_+-N_-)}{2} & -\kappa\zeta_-\bar{\zeta}_+ \\ -\kappa\zeta_+\bar{\zeta}_- & 1+\frac{\kappa(N_--N_+)}{2} \end{pmatrix} = (1+\tfrac{\kappa N}{2})\mathbb{I} - \kappa\vec{x}\cdot\vec{\sigma}\,, \\
\tilde{X} = \begin{pmatrix} \tilde{\lambda}^2 & \tilde{\lambda}\bar{\tilde{z}} \\ \tilde{\lambda}\tilde{z} & \tilde{\lambda}^{-2}+|\tilde{z}|^2 \end{pmatrix} &= \begin{pmatrix} e^{\frac{\kappa(\tilde{N}_--\tilde{N}_+)}{2}} & \kappa e^{\frac{\kappa(\tilde{N}_--\tilde{N}_+)}{4}}\tilde{\zeta}_-^\kappa\bar{\tilde{\zeta}}_+^\kappa \\ \kappa e^{\frac{\kappa(\tilde{N}_--\tilde{N}_+)}{4}}\tilde{\zeta}_+^\kappa\bar{\tilde{\zeta}}_-^\kappa & e^{\frac{\kappa(\tilde{N}_+-\tilde{N}_-)}{2}} + 4\sinh\frac{\kappa\tilde{N}_+}{2}\sinh\frac{\kappa\tilde{N}_-}{2} \end{pmatrix} \\
&\xrightarrow{\kappa\to 0} \begin{pmatrix} 1+\frac{\kappa(\tilde{N}_--\tilde{N}_+)}{2} & \kappa\tilde{\zeta}_-\bar{\tilde{\zeta}}_+ \\ \kappa\tilde{\zeta}_+\bar{\tilde{\zeta}}_- & 1+\frac{\kappa(\tilde{N}_+-\tilde{N}_-)}{2} \end{pmatrix} = (1+\tfrac{\kappa\tilde{N}}{2})\mathbb{I} - \kappa\vec{\tilde{x}}\cdot\vec{\sigma}\,,
\end{aligned} \tag{3.53}$$

where $\vec{x}$ and $\vec{\tilde{x}}$ are defined in (3.5). Therefore, the $\kappa \to 0$ limit of the flux vectors $\vec{X}$ and $\vec{\tilde{X}}$ (2.40) recover the flat fluxes

$$\vec{X} = -\frac{1}{2\kappa}{\rm Tr}(X\vec{\sigma}) \xrightarrow{\kappa\to 0} \vec{x}\,, \quad \vec{\tilde{X}} = -\frac{1}{2\kappa}{\rm Tr}(\tilde{X}\vec{\sigma}) \xrightarrow{\kappa\to 0} \vec{\tilde{x}}\,. \tag{3.54}$$

The same limit can be achieved for $\vec{X}^{\rm op}$ and $\vec{\tilde{X}}^{\rm op}$ as $|t\rangle \overset{\kappa\to 0}{\longleftrightarrow} |\tau\rangle$ and $|\tilde{t}] \overset{\kappa\to 0}{\longleftrightarrow} |\tilde{\tau}]$.

As shown in [73], the phase space $\mathrm{SL}(2,\mathbb{C})$ with the Poisson structure (2.34) for one ribbon is equivalent to $\mathcal{S}_\kappa \times \tilde{\mathcal{S}}_\kappa //\mathcal{M}$, with $\mathcal{S}_\kappa = \{|t\rangle \in \mathbb{C}^2 \backslash \{\langle t|t\rangle = 0\}\}$ the spinor phase space with the Poisson structure (3.24), $\tilde{\mathcal{S}}_\kappa = \{|\tilde{t}\rangle \in \mathbb{C}^2 \backslash \{\langle \tilde{t}|\tilde{t}\rangle = 0\}\}$ the phase space with the Poisson structure (3.38), and $\mathcal{M} := N - \tilde{N}$ the norm matching constraint. It is a simple check that the dimension of such a phase space is $8 - 2 = 6$, matching that of the holonomy-flux phase space constructed in Section 2.3.

3.4 Spinorial observables

3.4.1 The spinorial phase space

For a given graph, we take the Cartesian product of the spinor phase space over all links of Γ. A link e carries variables spinors $|t_e\rangle, |\tau_e\rangle, |\tilde{t}_e\rangle, |\tilde{\tau}_e\rangle$ and their duals. We have already seen in Section 3.3 that those variables reconstruct the holonomy-flux variables in a way which automatically solves the ribbon constraint in each ribbon. We are thus left with imposing the Gauss constraint at each node of Γ.

Let us consider an n-valent node v of Γ. We then pick an arbitrary link incident to it, which we denote by e_1, and then going counterclockwise starting from e_1, we label the other incident links by $e_2, \cdots, e_n$ and identify $e_{n+1} \equiv e_1$. In the ribbon graph $\Gamma_{\rm r}$, v gives rise to an n-gon $R(v)$ and each link e_i to a ribbon $R(e_i)$. Each of them shares a node with its two neighbor ribbons, one clockwise and one counter-clockwise.

It is convenient to unify the notation for spinors as follows,

$$\begin{array}{llll} t^- = |t\rangle & t^+ = |t] & \tau^- = |\tau\rangle & \tau^+ = |\tau] \\ \tilde{t}^- = |\tilde{t}\rangle & \tilde{t}^+ = |\tilde{t}] & \tilde{\tau}^- = |\tilde{\tau}\rangle & \tilde{\tau}^+ = |\tilde{\tau}]\,, \end{array} \tag{3.55}$$

or component-wise

$$\begin{array}{llll} t^-_A = t_A\,, & t^+_A = (-1)^{\frac{1}{2}-A}\bar{t}_{-A}\,, & \tau^-_A = \tau_A\,, & \tau^+_A = (-1)^{\frac{1}{2}-A}\bar{\tau}_{-A}\,, \\ \tilde{t}^-_A = \tilde{t}_A\,, & \tilde{t}^+_A = (-1)^{\frac{1}{2}-A}\bar{\tilde{t}}_{-A}\,, & \tilde{\tau}^-_A = \tilde{\tau}_A\,, & \tilde{\tau}^+_A = (-1)^{\frac{1}{2}-A}\bar{\tilde{\tau}}_{-A}\,, \quad A = \pm\tfrac{1}{2}\,. \end{array} \tag{3.56}$$

We use the same notation as in (2.48) to denote the fluxes on the boundary links of $R(v)$ as $\ell_{e_i,v}$. Denote the spinor sitting at the source node of $\ell_{e_i,v}$ to be $t^\epsilon_{e_i v}$ and that sitting at its target is $\tau^\epsilon_{e_i v}$. Referring to fig.3.2, they are explicitly

$$\left|\begin{array}{l} t^\epsilon_{e_i v} = t^\epsilon_i \\ \tau^\epsilon_{e_i v} = \tau^\epsilon_i \end{array}\right. \text{if } o_i = +\,, \qquad \left|\begin{array}{l} t^\epsilon_{e_i v} = \tilde{t}^\epsilon_i \\ \tau^\epsilon_{e_i v} = \tilde{\tau}^\epsilon_i \end{array}\right. \text{if } o_i = -\,. \tag{3.57}$$

Indeed, each node in $\Gamma_{\rm r}$ is assigned two spinors from two different ribbons. For instance, the spinors $\tau^{\epsilon}_{e_{i+1}v}$ and $t^{\epsilon}_{e_iv}$ sit at the node where $\ell_{e_i,v}$ and $\ell_{e_{i+1},v}$ intersect. The following proposition shows that these two spinors, except $t^{\epsilon}_{e_n}$ sitting at the base node, are all braided-covariant under the SU(2) transformation generated by the Gauss constraint.

Proposition 3.4.1. *The spinors $\tau^{\epsilon_{i+1}}_{e_{i+1},v}$ and $t^{\epsilon_i}_{e_i,v}$ $(i=1,\cdots,n)$ on the node of Γ_r are braided-covariant under the* SU(2) *transformation defined in (2.45) by the same braided infinitesimal* SU(2) *parameter denoted by $w^{(i)}=\mathbb{I}+i\begin{pmatrix}\epsilon_z^{(i)} & \epsilon_-^{(i)}\\ \epsilon_+^{(i)} & \epsilon_z^{(i)}\end{pmatrix}$. Parametrize $\ell_{e_i,v}=\begin{pmatrix}\Lambda_i & 0\\ \mathfrak{z}_i & \Lambda_i^{-1}\end{pmatrix}$, then the transformation reads*

$$\delta_\epsilon t^{\epsilon}_{e_iv}=-\kappa^{-1}\left(\prod_{k=1}^{n}\Lambda_k^{-2}\right)\{TrW\mathcal{G}\mathcal{G}^\dagger,t^{\epsilon}_{e_iv}\}=(w^{(i+1)}-\mathbb{I})t^{\epsilon}_{e_iv}\,, \tag{3.58a}$$

$$\delta_\epsilon \tau^{\epsilon}_{e_iv}=-\kappa^{-1}\left(\prod_{k=1}^{n}\Lambda_k^{-2}\right)\{TrW\mathcal{G}\mathcal{G}^\dagger,\tau^{\epsilon}_{e_iv}\}=(w^{(i)}-\mathbb{I})\tau^{\epsilon}_{e_iv}\,, \tag{3.58b}$$

where parameters in $w^{(i)}$ are defined by induction as

$$\left|\begin{array}{l}\epsilon_\pm^{(i)}=\Lambda_i^{-2}\epsilon_\pm^{(i+1)}\\ \epsilon_z^{(i)}=\epsilon_z^{(i+1)}+\frac{1}{2}\left(\Lambda_i^{-1}\mathfrak{z}_i\epsilon_-^{(i+1)}+\Lambda_i^{-1}\bar{\mathfrak{z}}_i\epsilon_+^{(i+1)}\right)\end{array}\right. \quad , \quad \textit{and} \quad \left|\begin{array}{l}\epsilon_\pm^{(n+1)}\equiv\epsilon_\pm\\ \epsilon_z^{(n+1)}\equiv\epsilon_z\end{array}\right. \quad , .i=1,\cdots,n\,. \tag{3.59}$$

The proof is given in Proof B.3.1.

3.4.2 Scalar products of spinors

We will build local invariant quantities by taking scalar products between spinors from different links which meet at the same node of Γ. Due to the ribbon structure, they might meet at the same node in $\Gamma_{\rm r}$ or at different nodes in $\Gamma_{\rm r}$. In the latter case, parallel transport around the ribbon node is required to evaluate the scalar product at a common node in $\Gamma_{\rm r}$. An example of the situation is given for a 3-valent node in fig.3.4. One can form (quadratic) scalar products of spinors from two adjacent links e_i and e_{i+1}. The symmetry transformation is induced at the node where the ribbons meet and if they sit at the same node, this ensures that the scalar product is invariant. One can also define observables for spinors not sitting at the same node. But in this case, it is necessary to parallel transport one spinor to the other in order to ensure invariance.

Invariants from spinors sitting at the same node in $\Gamma_{\mathbf{r}}$. The spinors $t^{\epsilon_i}_{e_i v}$ and $\tau^{\epsilon_{i+1}}_{e_{i+1} v}$ sit at the same node in Γ_{r}. One can build directly the quadratic observables denoted $E^{\epsilon_i,\epsilon_{i+1}}_{i,i+1}$ with these two spinors by forming their scalar products

$$\begin{aligned} E^{\epsilon_i,\epsilon_{i+1}}_{i,i+1} &= \epsilon_i \sum_{A=\pm 1/2} (-1)^{\frac{1}{2}+A} t^{\epsilon_i}_{e_i v,-A} \tau^{\epsilon_{i+1}}_{e_{i+1} v,A} \\ &= \begin{cases} \epsilon_i \sum_{A=\pm 1/2} (-1)^{\frac{1}{2}+A} t^{\epsilon_i}_{i,-A} \tau^{\epsilon_{i+1}}_{i+1,A} \,, & \text{for} \quad o_i = o_{i+1} = 1 \\ \epsilon_i \sum_{A=\pm 1/2} (-1)^{\frac{1}{2}+A} t^{\epsilon_i}_{i,-A} \tilde{\tau}^{\epsilon_{i+1}}_{i+1,A} \,, & \text{for} \quad o_i = -o_{i+1} = 1 \\ \epsilon_i \sum_{A=\pm 1/2} (-1)^{\frac{1}{2}+A} \tilde{t}^{\epsilon_i}_{i,-A} \tau^{\epsilon_{i+1}}_{i+1,A} \,, & \text{for} \quad -o_i = o_{i+1} = 1 \\ \epsilon_i \sum_{A=\pm 1/2} (-1)^{\frac{1}{2}+A} \tilde{t}^{\epsilon_i}_{i,-A} \tilde{\tau}^{\epsilon_{i+1}}_{i+1,A} \,, & \text{for} \quad o_i = o_{i+1} = -1 \end{cases} . \end{aligned} \tag{3.60}$$

Consider for instance $o_i = o_{i+1} = 1$, $E^{\epsilon_i,\epsilon_{i+1}}_{i,i+1}$ encodes four possible options of scalar products depending on the signs of $\epsilon_i = \pm$ and $\epsilon_{i+1} = \pm$.

$$\epsilon_i \sum_{A=\pm 1/2} (-1)^{\frac{1}{2}+A} t^{\epsilon_i}_{i,-A} \tau^{\epsilon_{i+1}}_{i+1,A} = \begin{cases} [t^{\epsilon_i}|\tau^{\epsilon_{i+1}}\rangle & \text{for} \quad \epsilon_i = \epsilon_{i+1} = - \\ [t^{\epsilon_i}|\tau^{\epsilon_{i+1}}] & \text{for} \quad \epsilon_i = -, \epsilon_{i+1} = + \\ \langle t^{\epsilon_i}|\tau^{\epsilon_{i+1}}\rangle & \text{for} \quad \epsilon_i = +, \epsilon_{i+1} = - \\ \langle t^{\epsilon_i}|\tau^{\epsilon_{i+1}}] & \text{for} \quad \epsilon_i = \epsilon_{i+1} = + \end{cases} . \tag{3.61}$$

They are by definition invariant under the SU(2) transformation acting on the node of Γ_{r} where the two spinors meet. Indeed, under an SU(2) transformation with $g \in \mathrm{SU}(2)$, $[t^{\epsilon_i}| \to [t^{\epsilon_i}|g^{-1}\,, \langle t^{\epsilon_i}| \to \langle t^{\epsilon_i}|g^{-1}\,, |\tau^{\epsilon_{i+1}}\rangle \to g|\tau^{\epsilon_{i+1}}\rangle\,, |\tau^{\epsilon_{i+1}}] \to g|\tau^{\epsilon_{i+1}}]$ and so clearly all $E^{\epsilon_i,\epsilon_{i+1}}_{i,i+1}$ defined in (3.61) are invariant under SU(2) transformations. Since those transformations are generated by the Gauss constraint as shown in Proposition 3.4.1, we find directly the following corollary.

Corollary 3.4.2. *The scalar product $E^{\epsilon_i,\epsilon_{i+1}}_{i,i+1}$ defined in (3.60) is invariant under the infinitesimal gauge transformation δ_ϵ generated by the Gauss constraint defined in (2.45), i.e.*

$$\delta_\epsilon E^{\epsilon_i,\epsilon_{i+1}}_{i,i+1} = 0\,. \tag{3.62}$$

Invariants from spinors sitting at different nodes in $\Gamma_{\mathbf{r}}$. We now explain how to build invariants for an arbitrary pair of links $i, j = 1, \dots, n$ incident to an n-valent node. As before, we can work with the ribbon decorated with $\ell, \tilde{\ell}$ or $\ell^{-1\dagger}, \tilde{\ell}^{-1\dagger}$. We choose to explicit the case where we use $\ell, \tilde{\ell}$, and the other case is obtained in a similar way.

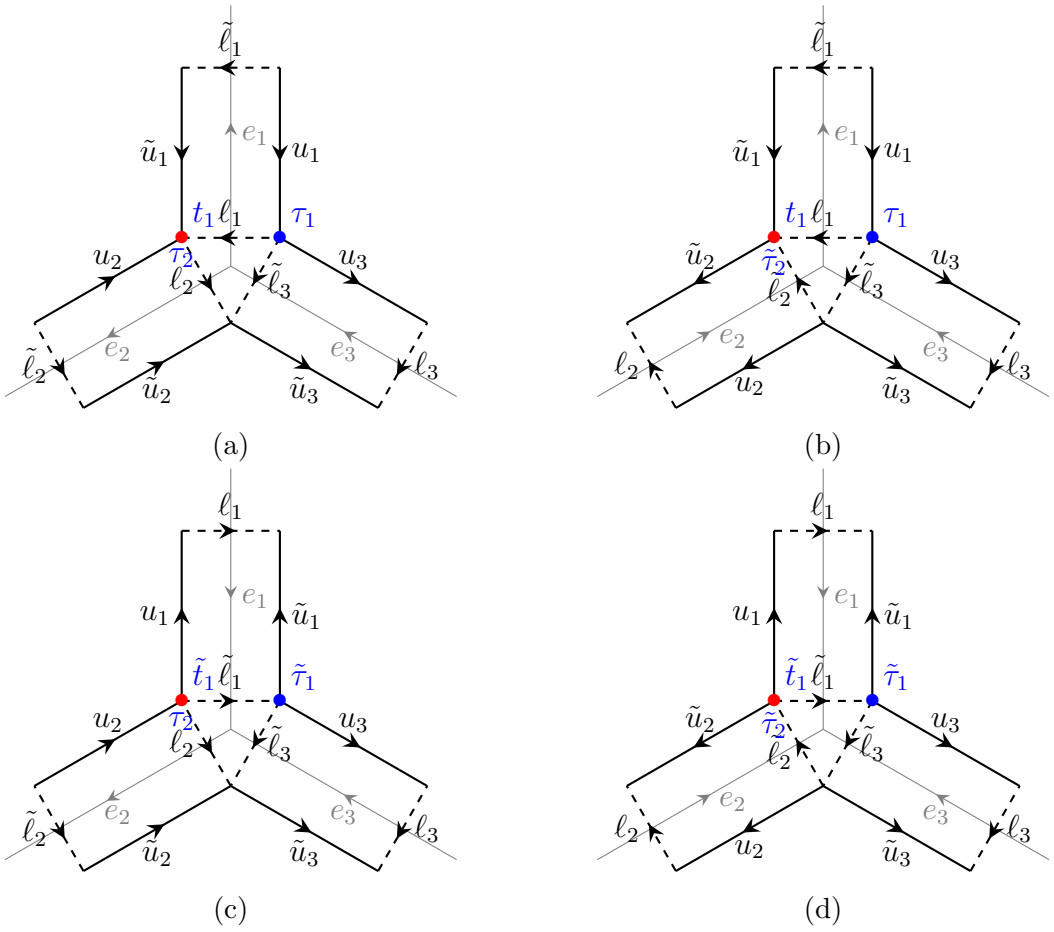

Figure 3.4: A node with three incident links e_1, e_2, e_3 (*in gray*) and the correspondent ribbon graph. The four possible orientations for e_1 and e_2 with a fix orientation $o_3 = -1$ for e_3 are illustrated separately. The spinors defining the scalar product $E^{\epsilon_1,\epsilon_2}_{12}$ can be read at the common corner (*in red*) of the ribbons associated to e_1 and e_2.

Consider first $j = i + 1$ so that the links share a node in $\Gamma_{\rm r}$. Then we know of the invariant $E^{\epsilon_i,\epsilon_{i+1}}_{i,i+1}$. We can also try to define an observable in terms of τ_i and τ_{i+1}. We have showed that the scalar product of t_i and τ_{i+1} is an observable. On the other hand, we know that t_i is the result of transporting τ_i by $\ell_{e_i v}$, see (3.26), (3.40) ($\ell_{e_i v}$ is defined in (2.44)). Therefore we can in fact transport τ_{i+1} by $\ell_{e_i v}$ so that it sits at the same node as τ_i in $\Gamma_{\rm r}$. Obviously one gets the same invariant as in (3.60). To be explicit, we focus on the scalar product $E^{\epsilon_1,\epsilon_2}_{12}$ with no loss of generality.

Proposition 3.4.3. *Up to a coefficient* $e^{\pm\frac{\kappa N_1}{4}}$*, we have that*

$$E_{12}^{\epsilon_1,\epsilon_2}$$
$$= \begin{cases} \epsilon_1 \sum\limits_{A=\pm\frac{1}{2}} (-1)^{\frac{1}{2}+A} \tau_{1,-A}^{\epsilon_1} \left(\ell_1^{-1}\tau_2^{\epsilon_2}\right)_A \sim \epsilon_1 \sum\limits_{A=\pm\frac{1}{2}} (-1)^{\frac{1}{2}+A} \tau_{1,-A}^{\epsilon_1} \left(\ell_1^{\dagger}\tau_2^{\epsilon_2}\right)_A \,, \text{if } o_1 = o_2 = 1 \\ \epsilon_1 \sum\limits_{A=\pm\frac{1}{2}} (-1)^{\frac{1}{2}+A} \tau_{1,-A}^{\epsilon_1} \left(\ell_1^{-1}\tilde{\tau}_2^{\epsilon_2}\right)_A \sim \epsilon_1 \sum\limits_{A=\pm\frac{1}{2}} (-1)^{\frac{1}{2}+A} \tau_{1,-A}^{\epsilon_1} \left(\ell_1^{\dagger}\tilde{\tau}_2^{\epsilon_2}\right)_A \,, \text{if } o_1 = -o_2 = 1 \\ \epsilon_1 \sum\limits_{A=\pm\frac{1}{2}} (-1)^{\frac{1}{2}+A} \tilde{\tau}_{1,-A}^{\epsilon_1} \left(\tilde{\ell}_1\tau_2^{\epsilon_2}\right)_A \sim \epsilon_1 \sum\limits_{A=\pm\frac{1}{2}} (-1)^{\frac{1}{2}+A} \tilde{\tau}_{1,-A}^{\epsilon_1} \left(\tilde{\ell}_1^{-1\,\dagger}\tau_2^{\epsilon_2}\right)_A \,, \text{if } -o_1 = o_2 = 1 \\ \epsilon_1 \sum\limits_{A=\pm\frac{1}{2}} (-1)^{\frac{1}{2}+A} \tilde{\tau}_{1,-A}^{\epsilon_1} \left(\tilde{\ell}_1\tilde{\tau}_2^{\epsilon_2}\right)_A \sim \epsilon_1 \sum\limits_{A=\pm\frac{1}{2}} (-1)^{\frac{1}{2}+A} \tilde{\tau}_{1,-A}^{\epsilon_1} \left(\tilde{\ell}_1^{-1\,\dagger}\tilde{\tau}_2^{\epsilon_2}\right)_A \,, \text{if } o_1 = o_2 = -1 \,. \end{cases} \tag{3.63}$$

Proof. Consider the definition (3.60) and focus on the first case, with $o_1 = o_2 = 1$. Then, we apply (3.26), $(\ell_1\tau_1^{\epsilon_1})_A \propto t_{1,A}^{\epsilon_1}$ and that $\left(\ell_1^{-1\,\dagger}\tau_1^{\epsilon_1}\right)_A \propto t_{1,A}^{\epsilon_1}$ up to coefficients $e^{\pm\frac{\kappa N_1}{4}}$. We further have

$$\left(\ell^{-1}\right)_{AB} = (-1)^{B-A}\ell_{-B-A}\,, \quad \left(\ell^{\dagger}\right)_{AB} = (-1)^{B-A}\left(\ell^{-1\,\dagger}\right)_{-B-A}\,. \tag{3.64}$$

Putting these equalities together, we get the proposition. □

In the quantization scheme, since we need to order the Hilbert spaces, and build the spinor operators using some braided permutation to the following Hilbert space we will need to set up a reference point. We will see that the notion of braided permutation is nothing else than the quantum version of the parallel transport we are discussing. As a consequence, the notion of quantum observable based on the braiding will be associated to the formulation (3.63) instead of (3.60).

We generalize this construction to links e_i, e_j incident to the same node in Γ but with $j \neq i+1$. To simplify the notations of (3.57), we denote $\tau_i^{\epsilon_i} \equiv \tau_{e_i v}^{\epsilon_i}$ and similarly for other spinors. Up to parallel transport by $\ell_{e_i v}, \ell_{e_j v}$, we can always build our observables from the spinors $\tau_i^{\epsilon_i}, \tau_j^{\epsilon_j}$. The recipe is to parallel transport $\tau_j^{\epsilon_j}$ around the ribbon node to meet $\tau_i^{\epsilon_i}$ at the same node in Γ_{r}. This is done by introducing $\mathcal{L}_{ij}$ (resp. $\mathcal{L}_{ij}^{-1\dagger}$), the AN(2) holonomy consisting of the product of ℓ^{-1} and $\tilde{\ell}$ (resp. $\ell^{\dagger}$ and $\tilde{\ell}^{-1\dagger}$) clockwise around $R(v)$ from j to i,

Proposition 3.4.4. *The quantity*

$$E_{ij}^{\epsilon_i,\epsilon_j} = \begin{cases} \sum_{A=\pm\frac{1}{2}} (-1)^{\frac{1}{2}+A} \tau_{i,-A}^{\epsilon_i} \left(\mathcal{L}_{ij}\tau_j^{\epsilon_j}\right)_A \sim \sum_{A=\pm\frac{1}{2}} (-1)^{\frac{1}{2}+A} \tau_{i,-A}^{\epsilon_i} \left(\mathcal{L}_{ij}^{-1\,\dagger}\tau_j^{\epsilon_j}\right)_A, \text{if } o_i = o_j = 1 \\ \sum_{A=\pm\frac{1}{2}} (-1)^{\frac{1}{2}+A} \tau_{i,-A}^{\epsilon_i} \left(\mathcal{L}_{ij}\tilde{\tau}_j^{\epsilon_j}\right)_A \sim \sum_{A=\pm\frac{1}{2}} (-1)^{\frac{1}{2}+A} \tau_{i,-A}^{\epsilon_i} \left(\mathcal{L}_{ij}^{-1\,\dagger}\tilde{\tau}_j^{\epsilon_j}\right)_A, \text{if } o_i = -o_j = 1 \\ \sum_{A=\pm\frac{1}{2}} (-1)^{\frac{1}{2}+A} \tilde{\tau}_{i,-A}^{\epsilon_i} \left(\mathcal{L}_{ij}\tau_j^{\epsilon_j}\right)_A \sim \sum_{A=\pm\frac{1}{2}} (-1)^{\frac{1}{2}+A} \tilde{\tau}_{i,-A}^{\epsilon_i} \left(\mathcal{L}_{ij}^{-1\,\dagger}\tau_j^{\epsilon_j}\right)_A, \text{if } -o_i = o_j = 1 \\ \sum_{A=\pm\frac{1}{2}} (-1)^{\frac{1}{2}+A} \tilde{\tau}_{i,-A}^{\epsilon_i} \left(\mathcal{L}_{ij}\tilde{\tau}_j^{\epsilon_j}\right)_A \sim \sum_{A=\pm\frac{1}{2}} (-1)^{\frac{1}{2}+A} \tilde{\tau}_{i,-A}^{\epsilon_i} \left(\mathcal{L}_{ij}^{-1\,\dagger}\tilde{\tau}_j^{\epsilon_j}\right)_A, \text{if } o_i = o_j = -1 \end{cases} \tag{3.65}$$

is an observable, i.e. $\delta_\epsilon E_{e_ie_j}^{\epsilon_i,\epsilon_j} = 0$.

As in the case of the adjacent links, we can have different expressions of the same observable, depending on where we set the reference node in the ribbon. (For instance, referring to fig.3.4, one can take the node in red or the node in blue as the reference node on the ribbon of e_1.)

Now that we have defined observables we could discuss the algebra they form. Unlike the previous works [73], the definition of the observables seems to depend on the orientation of the links. Given some choice of orientation, we can determine the algebra the observables satisfy. Instead of doing so, we will first look at the quantization of this algebra in Chapter 5. We will see that each case of orientation is actually quantized in the same way, so that there is a unique quantum observable for the different orientations. Said otherwise, the natural quantum observables do not depend on the orientation, hence we can recover a unique deformed quantum algebra. This means in particular that the apparent different formulations (in terms of the spinors/orientation of the links) of the observables just give different representations of the same Poisson algebra.

Chapter 4

Quantization: q-deformed LQG

Having constructed the classical phase space, the Poisson algebra and the constraint algebra, we are now ready to quantize the classical structure to construct the Hilbert space, following the Dirac quantization programme. The quantum theory in the following few chapters is the core of this thesis and contains most of the original work of the author. This chapter is based on [41]. Before we describe the quantization process, let us emphasize the physical and mathematical guidelines.

As has been mentioned a few times above, we take it as hints that the quantum theory of 3D gravity with a $\Lambda \neq 0$ captures quantum group [58, 148] symmetries. This has been shown to be the case in the quantization based on the Chern-Simons formulation of 3D gravity either through the path integral method [210, 177] or the combinatorial quantization approach [7, 8] as well as the spinfoam approach [204]. The quantum groups describing the quantum gravity theories in these existing models are all formulated as deformations of some Lie groups that describe the classical features with deformation parameters determined by Λ. Our goal is to re-produce these quantum group symmetries in the LQG framework starting from the classical theory defined in terms of the Lie bialgebra as described in chapter 2. This relies on the deep mathematical correspondence between Lie bialgebras and Hopf algebras, which are the general notion of quantum groups.

Mathematically, there are (at least) two ways to understand the quantization process if one considers the relation between classical mechanics and quantum mechanics. One way is to replace the Poisson algebra of functions on group, say $\{A, B\}$, in classical mechanics into a (non-commutative) quantum algebra $[\hat{A}, \hat{B}] = i\hbar\widehat{\{A, B\}}$ where $\hat{A}$ and $\hat{B}$ are (non-commutative) *operators*. Another way is to introduce an auxiliary parameter, say t (which can contain the information of $\hbar$), and use it to parametrize a deformation, which deforms

the classical Poisson algebra into a non-commutative one. We require that the $t \to 0$ limit recovers the classical Poisson algebra at the first t-order [148]. Mathematically, this is how a Lie bialgebra can be recovered as the infinitesimal notion of a Hopf algebra, in an analogous way that a Lie algebra is an infinitesimal notion of a Lie group. In fact, this is the reason why we construct in Chapter 4 the classical continuous and discrete theory in the language of Lie bialgebra. The deformation parameter κ introduced in Chapter 2 and also used in Chapter 3 can be promoted by exponentiation to a deformation parameter $q \equiv e^{\kappa\hbar}$ which combines the value of the cosmological constant and quantum parameter $\hbar$.

We now mention the mathematical ingredients we need for quantizing the classical kinematical phase space of a ribbon graph into a Hilbert space. The Hilbert space structure is based on two dual pairs of Hopf algebras $(\mathcal{U}_q(\mathfrak{su}(2)), \mathrm{SU}_q(2))$ and $(\mathcal{U}_{q^{-1}}(\mathfrak{su}(2)), \mathrm{SU}_{q^{-1}}(2))$ with q real. They are dual pairs in the sense of Hopf algebra duality [148]. $\mathcal{U}_q(\mathfrak{su}(2))$ (*resp.* $\mathcal{U}_{q^{-1}}(\mathfrak{su}(2))$) is isomorphic to q-deformed function $F_q(\mathrm{AN}(2))$ (*resp.* $F_{q^{-1}}(\mathrm{AN}(2))$) and gives the quantization of fluxes while $\mathrm{SU}_q(2)$ (*resp.* $\mathrm{SU}_{q^{-1}}(2)$) describes the q-deformation of the holonomies. More precisely, in the ribbon picture, the two fluxes on a ribbon are quantized to a $\mathcal{U}_q(\mathfrak{su}(2))$ element and a $\mathcal{U}_{q^{-1}}(\mathfrak{su}(2))$ element respectively, while the two holonomies are respectively quantized to an $\mathrm{SU}_q(2)$ element and an $\mathrm{SU}_{q^{-1}}(2)$ element. The Poisson structure of the classical phase space, as we will see, is precisely the first order in $\hbar$ of the defining commutation relations of the above two Hopf algebras. The main concepts used in this section are the *quasitriangular Hopf algebra* and the *dual quasitriangular Hopf algebra* which are different Hopf algebras with the same quantum $\mathcal{R}$*-matrix* [148][1]. The mathematical construction of the (dual) quasitriangular Hopf algebra for a general Hopf algebra is concisely reviewed in Appendix A.2.

In this chapter, we first summarize in Section 4.1 the definitions and properties of the Hopf algebra $\mathcal{U}_q(\mathfrak{su}(2))$ and $\mathrm{SU}_q(2)$. With this mathematical knowledge, we give a complete quantization of the kinematical phase space in Section 4.2. It was first introduced in [39] but the $\mathcal{U}_{q^{-1}}(\mathfrak{su}(2))$ part of the structure was not realized therein. We completed this structure in [41]. We also realize, in the LQG framework, that one can extract the geometrical meaning of the quantum $\mathcal{R}$-matrix, which was understood as a mathematical "structure constant" in Hopf algebra. Finally in Section 4.3, we quantize the Gauss constraint and solve for the intertwiners as the states invariant under the quantum Gauss constraint.

[1] We remind the reader that, despite their similar names, the quasitriangular Hopf algebra and the dual quasitriangular Hopf algebra are two distinct mathematical concepts (see Appendix A.2), following [148]. They are named as such because the two Hopf algebras therein form a dual pair. The correspondent classical objects are the quasitriangular Lie bialgebra and the dual quasitriangular Lie bialgebra as described in Appendix A.1, see also [148].

4.1 $\mathcal{U}_q(\mathfrak{su}(2))$ and $\mathrm{SU}_q(2)$

Introduce a real deformation parameter $q = e^{\kappa\hbar}$ which includes the quantum parameter $\hbar$ and the cosmological constant information encoded in κ. The key point is to realize that the classical dual pair $(\mathrm{SU}(2)^* \equiv \mathrm{AN}(2), \mathrm{SU}(2))$ whose Lie bialgebra structures are given by the classical r-matrix can be q-deformed into the pair formed by the quasitriangular Hopf algebra $(\mathcal{U}_q(\mathfrak{su}(2)), \mathcal{R})$ and by the dual quasitriangular Hopf algebra $(\mathrm{SU}_q(2), \mathcal{R})$. Let us first recall the mathematical facts of these two Hopf algebras. We refer to quantum group textbooks *e.g.* [148, 58] for more details on these two Hopf algebras.

Definition 4.1.1 ($(\mathcal{U}_q(\mathfrak{su}(2)), \mathcal{R})$)**.** *The quasitriangular Hopf algebra $(\mathcal{U}_q(\mathfrak{su}(2)), \mathcal{R})$ is generated by the identity and $J_\pm, K = q^{\frac{J_z}{2}}$ with the relations*

$$K J_\pm K^{-1} = q^{\pm\frac{1}{2}} J_\pm \,, \quad [J_+, J_-] = [2J_z] \,, \qquad \text{with } [n] \equiv \frac{q^{\frac{n}{2}} - q^{-\frac{n}{2}}}{q^{\frac{1}{2}} - q^{-\frac{1}{2}}} \,. \tag{4.1}$$

This form a Hopf algebra with the coproduct $\triangle : \mathcal{U}_q(\mathfrak{su}(2)) \to \mathcal{U}_q(\mathfrak{su}(2)) \otimes \mathcal{U}_q(\mathfrak{su}(2))$, antipode $S : \mathcal{U}_q(\mathfrak{su}(2)) \to \mathcal{U}_q(\mathfrak{su}(2))$ and counit $\epsilon : \mathcal{U}_q(\mathfrak{su}(2)) \to \mathbb{C}$ which act on the generators as

$$\begin{aligned} &\triangle(J_\pm) := J_\pm \otimes K + K^{-1} \otimes J_\pm \,, && S(J_\pm) := -q^{\pm\frac{1}{2}} J_\pm \,, && \epsilon(K) = 1 \,, \\ &\triangle(K) := K \otimes K \,, && S(K) := K^{-1} \,, && \epsilon(J_\pm) = 0 \,. \end{aligned} \tag{4.2}$$

This Hopf algebra is quasitriangular with an $\mathcal{R}$-matrix $\mathcal{R} \in \mathcal{U}_q(\mathfrak{su}(2)) \otimes \mathcal{U}_q(\mathfrak{su}(2))$:

$$\mathcal{R} = q^{J_z \otimes J_z} \sum_{n=0}^{\infty} \frac{(1-q^{-1})^n}{[n]!} q^{\frac{n(n-1)}{4}} \left(q^{\frac{J_z}{2}} J_+\right)^n \otimes \left(q^{-\frac{J_z}{2}} J_-\right)^n \,. \tag{4.3}$$

A number $[n]$ defined as in (4.1) is called the q-number. The $\mathcal{R}$-matrix is the quantum version of the classical r-matrix and it satisfies the *quantum Yang-Baxter equation* (QYBE)

$$\mathcal{R}_{12}\mathcal{R}_{13}\mathcal{R}_{23} = \mathcal{R}_{23}\mathcal{R}_{13}\mathcal{R}_{12} \,, \tag{4.4}$$

where we have used the standard notation $\mathcal{R}_{12} = \sum \mathcal{R}_{(1)} \otimes \mathcal{R}_{(2)} \otimes \mathbb{I}, \mathcal{R}_{23} = \mathbb{I} \otimes \mathcal{R}_{(1)} \otimes \mathcal{R}_{(2)}, \mathcal{R}_{13} = \mathcal{R}_{(1)} \otimes \mathbb{I} \otimes \mathcal{R}_{(2)}$. In the fundamental representation ($j = 1/2$), the generators are represented as 2×2 matrices

$$J_-|_{j=1/2} = \begin{pmatrix} 0 & 0 \\ 1 & 0 \end{pmatrix} \,, \quad J_+|_{j=1/2} = \begin{pmatrix} 0 & 1 \\ 0 & 0 \end{pmatrix} \,, \quad K|_{j=1/2} = \begin{pmatrix} q^{\frac{1}{4}} & 0 \\ 0 & q^{-\frac{1}{4}} \end{pmatrix} \,. \tag{4.5}$$

We denote the $\mathcal{R}$-matrix (4.3) in the fundamental representation by R, which is a 4×4 matrix that takes the form

$$R=\begin{pmatrix} q^{\frac{1}{4}} & 0 & 0 & 0\\ 0 & q^{-\frac{1}{4}} & q^{-\frac{1}{4}}(q^{\frac{1}{2}}-q^{-\frac{1}{2}}) & 0\\ 0 & 0 & q^{-\frac{1}{4}} & 0\\ 0 & 0 & 0 & q^{\frac{1}{4}} \end{pmatrix} \equiv \mathcal{R}|_{j=1/2}\,. \tag{4.6}$$

Clearly, the first $\hbar$-order of R recovers the classical r-matrix (2.33) in the fundamental representation, *i.e.*

$$R=\mathbb{I}\otimes\mathbb{I}+i\hbar r+O(\hbar^2)\,. \tag{4.7}$$

We are particularly interested in the 2×2 matrix operators, denoted as $Q^{\pm}$, whose elements $(q^{\pm})^i{}_j (i,j=\pm)$ are given by the $\mathcal{U}_q(\mathfrak{su}(2))$ elements [148]. They are defined as

$$Q^{+}=\begin{pmatrix} K & 0\\ q^{-\frac{1}{4}}(q^{\frac{1}{2}}-q^{-\frac{1}{2}})J_{+} & K^{-1}\end{pmatrix}\,,\quad Q^{-}=\begin{pmatrix} K^{-1} & -q^{\frac{1}{4}}(q^{\frac{1}{2}}-q^{-\frac{1}{2}})J_{-}\\ 0 & K\end{pmatrix}\,. \tag{4.8}$$

The coproduct and counit of $Q^{\pm}$ are given by

$$\triangle(Q^{\pm})=Q^{\pm}\otimes Q^{\pm}\,,\quad \epsilon(Q^{\pm})=\mathbb{I}\,,\quad i.e.\ \ \triangle((q^{\pm})^i{}_j)=\sum_k (q^{\pm})^i{}_k\otimes(q^{\pm})^k{}_j\,,\quad \epsilon((q^{\pm}))^i=\delta^i_j\,. \tag{4.9}$$

They satisfy

$$Q_1^{\pm}Q_2^{\pm}R=RQ_2^{\pm}Q_1^{\pm}\,,\quad Q_1^{-}Q_2^{+}R=RQ_2^{+}Q_1^{-}\,, \tag{4.10}$$

with $Q_1^{\pm}=Q^{\pm}\otimes\mathbb{I}$ and $Q_2^{\pm}=\mathbb{I}\otimes Q^{\pm}$.

$\mathcal{U}_{q^{-1}}(\mathfrak{su}(2))$ is generated by the same generators as $\mathcal{U}_q(\mathfrak{su}(2))$ with the same commutation relations (4.1) but possessing a different coproduct denoted as $\overline{\triangle}$ and a different antipode denoted as $\overline{S}$. They act on the generators as

$$\overline{\triangle}(J_{\pm}):=J_{\pm}\otimes K^{-1}+K\otimes J_{\pm}\,,\quad \overline{\triangle}(K):=K\otimes K\,,\quad \overline{S}(J_{\pm}):=-q^{\mp\frac{1}{2}}J_{\pm}\,,\quad \overline{S}(K):=K^{-1}\,. \tag{4.11}$$

The two coproducts and two antipodes are related by

$$\overline{\triangle}=\sigma\circ\triangle\,,\quad \overline{S}=S^{-1}\,,$$

where σ is the permutation operator acting on the tensor space as $\sigma(a\otimes b)=b\otimes a$.

Definition 4.1.2 ($(\mathrm{SU}_q(2),\mathcal{R})$). *The dual quasitriangular Hopf algebra* $(\mathrm{SU}_q(2),\mathcal{R})$ *is generated by identity and the coordinate functions* $T=\begin{pmatrix} t_{--} & t_{-+} \\ t_{+-} & t_{++}\end{pmatrix}$ *on the space of* 2×2 *matrices satisfying*

$$RT_1T_2 = T_2T_1R\,, \tag{4.12}$$

where R *is defined in* (4.6)*, and quotient with the* q*-determinant* $\det_q T := t_{--}t_{++} - q^{-\frac{1}{2}}t_{-+}t_{+-} = \mathbb{I}$*. The antipode, coproduct and counit are given by*

$$\begin{aligned} &S(T)=\begin{pmatrix} t_{++} & -q^{\frac{1}{2}}t_{-+} \\ -q^{-\frac{1}{2}}t_{+-} & t_{--}\end{pmatrix} \quad \triangle(T)=T\otimes T\,, \quad \epsilon(T)=\mathbb{I}\,,\\ &i.e.\ \ \triangle(t^i{}_j)=\sum_{k=\pm} t^i{}_k\otimes t^k{}_j\,, \quad \epsilon(t^i{}_j)=\delta^i_j\,, \quad i,j=\pm\,. \end{aligned} \tag{4.13}$$

This Hopf algebra is dual quasitriangular with the $\mathcal{R}$*-matrix defined in* (4.3) *which is viewed as a map* $\mathcal{R}:\mathrm{SU}_q(2)\otimes\mathrm{SU}_q(2)\to\mathbb{C}$*.*

The commutation relation (4.12) is equivalent to the following relations.

$$\begin{aligned} &t_{--}t_{-+}=q^{-\frac{1}{2}}t_{-+}t_{--}\,, \quad t_{--}t_{+-}=q^{-\frac{1}{2}}t_{+-}t_{--}\,, \quad t_{-+}t_{++}=q^{-\frac{1}{2}}t_{++}t_{-+}\,,\\ &t_{+-}t_{++}=q^{-\frac{1}{2}}t_{++}t_{+-}\,, \quad t_{-+}t_{+-}=t_{+-}t_{-+}\,, \quad [t_{--},t_{++}]=-(q^{\frac{1}{2}}-q^{-\frac{1}{2}})t_{-+}t_{+-}\,. \end{aligned} \tag{4.14}$$

The duality between $\mathcal{U}_q(\mathfrak{su}(2))$ and $\mathrm{SU}_q(2)$ can be represented by the bilinear map between the operator matrices $Q^{\pm}$ and T as follows [148]. (See *e.g.* [58] for a more detailed proof of the duality relation)

$$\langle T_1, Q_2^+\rangle = R\,, \quad \langle T_1, Q_2^-\rangle = R_{21}^{-1}\,, \quad i.e.\ \ \langle t^i{}_j, (q^+)^k{}_l\rangle = R^{i\ k}_{\ j\ l}\,, \quad \langle t^i{}_j, (q^-)^k{}_l\rangle = (R^{-1})^{i\ k}_{\ j\ l}\,, \tag{4.15}$$

where $R_{21}=\sigma\circ R=\sum R_{(2)}\otimes R_{(1)}$.

4.2 From phase space to Hopf algebras

We are interested in the quantization of the Poisson brackets (2.35) and (2.36) for a single ribbon. To this aim, we construct the operators associated to the classical variables (the holonomy-flux algebra) and introduce the Hilbert space structure on which we represent these operators.

4.2.1 Poisson bracket quantization

As a first step, we introduce the deformation parameter, $q = e^{\hbar\kappa}$. Then the classical r-matrix is quantized as $r \to R$ according to the relation (4.7). Note that one obtains the inverse matrix R^{-1} if one replaces q by q^{-1}. We quantize the holonomies and fluxes to be matrices of operators $\ell \to L\,, u \to U\,, \tilde{\ell} \to \tilde{L}\,, \tilde{u} \to \tilde{U}$. The quantization of the Poisson brackets (2.35) and (2.36) gives the following commutation relations for the matrices of operators [194, 6]

$$\begin{array}{llll} R_{21}U_1U_2 = U_2U_1R_{21}\,, & RL_1L_2 = L_2L_1R\,, & L_1R_{21}^{-1}U_2 = U_2L_1\,, & L_2R^{-1}U_1 = U_1L_2\,, \\ R_{21}^{-1}\tilde{U}_1\tilde{U}_2 = \tilde{U}_2\tilde{U}_1R_{21}^{-1}\,, & R^{-1}\tilde{L}_1\tilde{L}_2 = \tilde{L}_2\tilde{L}_1R^{-1}\,, & \tilde{U}_2R_{21}\tilde{L}_1 = \tilde{L}_1\tilde{U}_2\,, & \tilde{U}_1R\tilde{L}_2 = \tilde{L}_2\tilde{U}_1\,, \\ \tilde{L}_1U_2R_{21}^{-1} = U_2\tilde{L}_1\,, & R\tilde{U}_1L_2 = L_2\tilde{U}_1\,, & R_{21}^{-1}L_1\tilde{U}_2 = \tilde{U}_2L_1\,, & U_1\tilde{L}_2R = \tilde{L}_2U_1\,, \end{array} \tag{4.16}$$

The Poisson brackets (2.35), (2.36) and (2.38) are recovered at the first order through the map $[\hat{A}, \hat{B}] = i\hbar\widehat{\{A, B\}}$. Note that R^{-1} appears because of the minus sign difference between the classical Poisson structures respectively defined in (2.35) and in (2.36).

The classical Casimir $r + r_{21}$ can be quantized as $R_{21}R$ and requesting this operator to be a Casimir implies that

$$[R_{21}R, L_1L_2] \,=\, [R_{21}R, U_2U_1] \,=\, [R_{21}R, \tilde{L}_2\tilde{L}_1] \,=\, [R_{21}R, \tilde{U}_1\tilde{U}_2] = 0\,. \tag{4.17}$$

Using this in (4.16) leads to the following equivalent commutation relations

$$\begin{array}{rcl} R_{21}U_1U_2 = U_2U_1R_{21} & \Longleftrightarrow & R^{-1}U_1U_2 = U_2U_1R^{-1}\,, \\ R_{21}^{-1}\tilde{U}_1\tilde{U}_2 = \tilde{U}_2\tilde{U}_1R_{21}^{-1} & \Longleftrightarrow & R\tilde{U}_1\tilde{U}_2 = \tilde{U}_2\tilde{U}_1R\,. \end{array} \tag{4.18}$$

Note that the $\mathcal{R}$-matrix for $\mathcal{U}_{q^{-1}}(\mathfrak{su}(2))$ is simply the inverse of the $\mathcal{R}$-matrix for $\mathcal{U}_q(\mathfrak{su}(2))$. Comparing to the defining commutation relations (4.10) and (4.12) for $\mathcal{U}_q(\mathfrak{su}(2))$ and $\mathrm{SU}_q(2)$ respectively, one realizes that the commutation relations (4.18) of the quantum holonomies with themselves and those of the quantum fluxes with themselves included in (4.16) imply that the holonomies and fluxes can be quantized as

$$\left|\begin{array}{lcl} \ell \in \mathrm{AN}(2) & \to & L \in \mathrm{Fun}_{q^{-1}}(\mathrm{AN}(2)) \cong \mathcal{U}_{q^{-1}}(\mathfrak{su}(2)) \\ u \in \mathrm{SU}(2) & \to & U \in \mathrm{SU}_{q^{-1}}(2) \\ \tilde{\ell} \in \mathrm{AN}(2) & \to & \tilde{L} \in \mathrm{Fun}_q(\mathrm{AN}(2)) \cong \mathcal{U}_q(\mathfrak{su}(2)) \\ \tilde{u} \in \mathrm{SU}(2) & \to & \tilde{U} \in \mathrm{SU}_q(2) \end{array}\right. . \tag{4.19}$$

We have in particular

$$L = \begin{pmatrix} K^{-1} & 0 \\ -q^{\frac{1}{4}}(q^{\frac{1}{2}} - q^{-\frac{1}{2}})J_+ & K \end{pmatrix}\,, \quad \tilde{L} = \begin{pmatrix} \tilde{K} & 0 \\ q^{-\frac{1}{4}}(q^{\frac{1}{2}} - q^{-\frac{1}{2}})\tilde{J}_+ & \tilde{K}^{-1} \end{pmatrix}\,, \tag{4.20}$$

where $(\tilde{J}_\pm, \tilde{K})$ are another copy of the $\mathcal{U}_q(\mathfrak{su}(2))$ generators commuting with the non-tilde pieces. The antipodes $\overline{S}(L)$ and $S(\tilde{L})$ are given by acting the correspondent antipodes on all the matrix elements. That is

$$\overline{S}(L) = \begin{pmatrix} \overline{S}(K^{-1}) & 0 \\ -q^{\frac{1}{4}}(q^{\frac{1}{2}} - q^{-\frac{1}{2}})\overline{S}(J_+) & \overline{S}(K) \end{pmatrix} = \begin{pmatrix} K & 0 \\ q^{-\frac{1}{4}}(q^{\frac{1}{2}} - q^{-\frac{1}{2}})J_+ & K^{-1} \end{pmatrix}, \tag{4.21}$$

$$S(\tilde{L}) = \begin{pmatrix} S(\tilde{K}) & 0 \\ q^{-\frac{1}{4}}(q^{\frac{1}{2}} - q^{-\frac{1}{2}})S(\tilde{J}_+) & S(\tilde{K}^{-1}) \end{pmatrix} = \begin{pmatrix} \tilde{K}^{-1} & 0 \\ -q^{\frac{1}{4}}(q^{\frac{1}{2}} - q^{-\frac{1}{2}})\tilde{J}_+ & \tilde{K} \end{pmatrix}. \tag{4.22}$$

Neither of these antipodes is an involution. However, they are the inverse of each other: $\overline{S} \circ S = S \circ \overline{S} = \mathbb{I}$. Also notice that the antipode acting on the quantum holonomies and quantum fluxes plays the role of exchanging $q \leftrightarrow q^{-1}$. That is, $\overline{S}(U) \in \mathrm{SU}_q(2), S(\tilde{U}) \in \mathrm{SU}_{q^{-1}}(2), \overline{S}(L) \in \mathcal{U}_q(\mathfrak{su}(2)), S(\tilde{L}) \in \mathcal{U}_{q^{-1}}(\mathfrak{su}(2))$. Thus when the antipode acts twice on the same quantum holonomy/flux, both $\overline{S}$ and S need to be used which leads to the original object.

We note that the left Iwasawa decomposition leads to elements in the Hopf algebras, $\mathcal{U}_{q^{-1}}(\mathfrak{su}(2))$ and $\mathrm{SU}_{q^{-1}}(2)$ while the right decomposition leads to elements in the Hopf algebras, $\mathcal{U}_q(\mathfrak{su}(2))$ and $\mathrm{SU}_q(2)$. At the classical level, this is reflected in the presence of the minus sign difference between (2.35), (2.36), the Poisson structures respectively for the elements u, ℓ of the left Iwasawa decomposition and for the elements $\tilde{u}$, $\tilde{\ell}$ of the right Iwasawa decomposition.

One can also quantize the phase space element $d = \ell u \in \mathrm{SL}(2,\mathbb{C})$ into an operator matrix. At first glance, it would lead to $\mathrm{SL}_q(2,\mathbb{C})$[2]. However, since the Heisenberg double is not a Poisson-Lie group, its quantization does not lead to a Hopf algebra either[3]. Nevertheless, one can form the objects LU and $\tilde{U}\tilde{L}$ whose commutation relation would give the quantization of the Poisson bracket (2.34). They are not necessarily equal as the q-determinant is not preserved under matrix multiplication, *i.e.* $\det_q(\tilde{U}\tilde{L}) \neq \det_q(\tilde{U}) \det_q(\tilde{L})$ and $\det_{q^{-1}}(LU) \neq \det_{q^{-1}} L \det_{q^{-1}} U$. To fix the coefficient, we define

$$D = c_L(q) LU = c_R(q) \tilde{U}\tilde{L} \tag{4.23}$$

such that $\det_q D = \mathbb{I}$, where $c_L(q)$ and $c_R(q)$ are q-dependent constants whose $q \to 1$ limit are both one. This will guarantee that the classical limit gives back (2.34). These constants

[2] $\mathrm{SL}_q(2,\mathbb{C})$ is defined in the same way as in Definition 4.1.2 but with q complex.

[3] On the other hand, the Drinfeld double $(\mathrm{SL}(2,\mathbb{C}), \pi_D)$ as a Poisson-Lie group is expected to be quantized to the Hopf algebra $\mathrm{SL}_q(2,\mathbb{C})$ and describes quantum symmetries of the system. We leave this for future investigation. See [170] for the Iwasawa decomposition of a $\mathrm{SL}_q(2,\mathbb{C})$ into $\mathrm{SU}_q(2)$ and $\mathrm{AN}_q(2)$, in which the commutation relations of the two quantum subgroups are the quantization of the Drinfeld double Poisson structure (A.17).

will not affect the commutation relations. We then can write the quantum version of the ribbon constraint as

$$LU = \frac{c_L(q)}{c_R(q)}\tilde{U}\tilde{L}\,. \tag{4.24}$$

Coupling the commutation relations in (4.16), one finds that the quantization of the Poisson bracket (2.34) gives the following equivalent commutation relations.

$$RD_1D_2 = D_2D_1R_{21} \quad \Longleftrightarrow \quad R_{21}^{-1}D_1D_2 = D_2D_1R^{-1}\,. \tag{4.25}$$

The equivalence of these two equations can be shown by using the Casimir property (4.17) of $R_{21}R$. Corresponding to the matrix elements of $D = \begin{pmatrix} \hat{a} & \hat{b} \\ \hat{c} & \hat{d} \end{pmatrix}$, (4.25) is equivalent to the following relations:

$$\begin{aligned} &\hat{a}\hat{b} = q^{\frac{1}{2}}\hat{b}\hat{a}\,, \quad \hat{c}\hat{d} = q^{\frac{1}{2}}\hat{d}\hat{c}\,, \quad \hat{a}\hat{c} = q^{-\frac{1}{2}}\hat{c}\hat{a}\,, \quad \hat{b}\hat{d} = q^{-\frac{1}{2}}\hat{d}\hat{b}\,, \\ &\hat{a}\hat{d} = \hat{d}\hat{a}\,, \quad \hat{b}\hat{c} - \hat{c}\hat{b} = -(q^{\frac{1}{2}} - q^{-\frac{1}{2}})\hat{a}\hat{d}\,. \end{aligned} \tag{4.26}$$

This shows clearly that $D \notin \mathrm{SL}_q(2,\mathbb{C})$.

Lastly, the matrix R also captures completely the duality in the sense of Hopf algebra between the quantum holonomies and quantum fluxes according to (4.15). Denote the matrices $U = \begin{pmatrix} U_{--} & U_{-+} \\ U_{+-} & U_{++} \end{pmatrix}$, $\tilde{U} = \begin{pmatrix} \tilde{U}_{--} & \tilde{U}_{-+} \\ \tilde{U}_{+-} & \tilde{U}_{++} \end{pmatrix}$ and use the parametrization (4.20) of L, $\tilde{L}$. Then the dualities between L, U and between $\tilde{L}$, $\tilde{U}$ mean

$$\begin{aligned} &\langle U_{--}, K^{\pm}\rangle = q^{\pm\frac{1}{4}}\,, \quad \langle U_{-+}, J_+\rangle = \langle U_{-+}, J_-\rangle = 1\,, \quad \langle U_{++}, K^{\pm}\rangle = q^{\mp\frac{1}{4}}\,, \\ &\langle \tilde{U}_{--}, \tilde{K}^{\pm}\rangle = q^{\pm\frac{1}{4}}\,, \quad \langle \tilde{U}_{-+}, \tilde{J}_+\rangle = \langle \tilde{U}_{-+}, \tilde{J}_-\rangle = 1\,, \quad \langle \tilde{U}_{++}, \tilde{K}^{\pm}\rangle = q^{\mp\frac{1}{4}}\,, \end{aligned} \tag{4.27}$$

and other bilinear maps vanish.

In this section, we have fully quantized the Poisson brackets (2.34), (2.35) and (2.36) and extend the duality between the classical fluxes and holonomies in the sense of Lie bialgebra to the duality between the quantum fluxes and quantum holonomies in the sense of Hopf algebra. We have found that the quantum symmetry of 3D gravity with a (negative) cosmological constant is captured by the quantum groups $\mathcal{U}_q(\mathfrak{su}(2))$ and $\mathrm{SU}_q(2)$ (if taking $\mathcal{U}_{q^{-1}}(\mathfrak{su}(2))$ and $\mathrm{SU}_{q^{-1}}(2)$ as the isomorphism of $\mathcal{U}_q(\mathfrak{su}(2))$ and $\mathrm{SU}_q(2)$ respectively). This is consistent with the results in the literature from other approaches [204, 53, 185]. The advantage here is that we derive these results starting from first principle and following the loop quantization program. It is thus encouraging to apply the flux and holonomy we defined in this model for future developments of the quantum theory and to generalize to higher dimensions.

4.2.2 The $\mathcal{R}$-matrix contains the information about fluxes and holonomies

Let us add some additional comments on the defining relations

$$L_1 L_2 R^{-1} = R^{-1} L_2 L_1 \,, \quad R^{-1} U_1 U_2 = U_2 U_1 R^{-1} \,, \quad \tilde{L}_1 \tilde{L}_2 R = R \tilde{L}_2 \tilde{L}_1 \,, \quad R \tilde{U}_1 \tilde{U}_2 = \tilde{U}_2 \tilde{U}_1 R \tag{4.28}$$

for the quantum fluxes and quantum holonomies. It is well-known [184] that they can be obtained from the (QYBE) (4.4), which in components is written as

$$\sum_{k_1,k_2,k_3} \mathcal{R}^{i_1\ i_2}_{\ k_1\ k_2} \mathcal{R}'^{k_1\ i_3}_{\ j_1\ k_3} \mathcal{R}''^{k_2\ k_3}_{\ j_2\ j_3} = \sum_{k_1,k_2,k_3} \mathcal{R}''^{i_2\ i_3}_{\ k_2\ k_3} \mathcal{R}'^{i_1\ k_3}_{\ k_1\ j_3} \mathcal{R}^{k_1\ k_2}_{\ j_1\ j_2} \,. \tag{4.29}$$

Here, $\mathcal{R}, \mathcal{R}', \mathcal{R}''$ are different copies of the $\mathcal{R}$-matrix. The first two indices (i,j) of $\mathcal{R}^{i\ k}_{\ j\ l}$ are the indices for $\mathcal{R}_{(1)}$ and the last two indices (k,l) are the indices for $\mathcal{R}_{(2)}$ given the decomposition $\mathcal{R} = \sum \mathcal{R}_{(1)} \otimes \mathcal{R}_{(2)}$.

Let us fix the representation of $\mathcal{R}_{(2)}, \mathcal{R}'_{(2)}$ and $\mathcal{R}''$ to be the fundamental representation of $\mathcal{U}_q(\mathfrak{su}(2))$, then the indices $(i_2,i_3),(j_2,j_3),(k_2,k_3) \in \{-\frac{1}{2},\frac{1}{2}\}$ in (4.29). In this representation, we then have

$$(\tilde{L}^k_{\ l})^\alpha_{\ \beta} = \mathcal{R}^{\alpha\ k}_{\ \beta\ l} \tag{4.30}$$

where the indices $k,l = \pm\frac{1}{2}$ are the indices labelling the matrix elements of $\tilde{L}$, while α,β are the indices of the $\mathcal{U}_q(\mathfrak{su}(2))$ generators in any representation. The QYBE (4.29) thus can be written as $\tilde{L}_1 \tilde{L}_2 R = R \tilde{L}_2 \tilde{L}_1$, which is the third relation of (4.28).

On the other hand, fixing the representation of $\mathcal{R}, \mathcal{R}'_{(1)}$ and $\mathcal{R}''_{(1)}$ to be the fundamental representation and using that

$$(\tilde{U}^i_{\ j})^\alpha_{\ \beta} = \mathcal{R}^{i\ \alpha}_{\ j\ \beta} \tag{4.31}$$

when $i,j \in \{-\frac{1}{2},\frac{1}{2}\}$, the QYBE can be written as $R \tilde{U}_1 \tilde{U}_2 = \tilde{U}_2 \tilde{U}_1 R$, which reproduce the last relation in (4.28).

In the same spirit, the first two equations in (4.28) are the QYBE for the $\mathcal{R}$-matrix of $\mathcal{U}_{q^{-1}}(\mathfrak{su}(2))$ (which is the inverse of the $\mathcal{R}$-matrix of $\mathcal{U}_q(\mathfrak{su}(2))$) in a given representation. Therefore, the $\mathcal{R}$-matrix captures the quantum holonomy and quantum flux information in its two sub-spaces. This gives a more geometrical interpretation to the $\mathcal{R}$-matrix in terms of quantum "holonomies" either in some deformation of AN(2) or SU(2)[4].

[4] Although we stick to the terminology that ℓ and $\tilde{\ell}$ are called fluxes, they are AN(2) holonomies in the ribbon picture as each is assigned to a side of the ribbon.

The construction of tensor operators (such as spinor and vector operators) usually requires some braiding defined in terms of the $\mathcal{R}$-matrix to transform appropriately [179, 175]. We will show in Chapter 5 how this braiding can be re-interpreted in a more geometrical setting, *i.e.* in terms of parallel transport. Last but not least, as the $\mathcal{R}$-matrix has been intensively used and studied in the integrable lattice model (see *e.g.* [147, 84] and a recent lecture note [178] and reference therein), we expect that the methodology and analysis therein can offer lessons on understanding the quantum structure of LQG. We leave this for future investigation.

4.3 Kinematical Hilbert space intertwiners

Let us consider a node v with n ($n \geq 3$) incident links. A quantum state on this node lives in the tensor product of the n vector spaces or dual vector spaces for the incident links depending on their orientations. The quantized Gauss constraint, as an operator on such a space, is provided by the coproduct of $\mathcal{U}_q(\mathfrak{su}(2))$ and $\mathcal{U}_{q^{-1}}(\mathfrak{su}(2))$. In this section, we construct the quantized Gauss constraint and solve it. The solutions are the so-called intertwiner states. It was first given in [39], in which different definitions of the quantum fluxes were used.

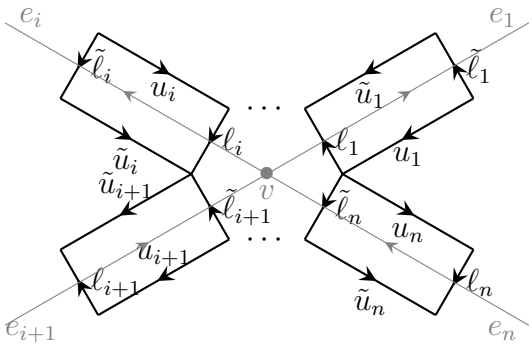

Figure 4.1: An n-valent node v (*in gray*) with incident links $e_1, e_2, \cdots, e_n$ attached on v in a cyclic order and its corresponding ribbon graph.

Denote the incident links by $e_1, e_2, \cdots, e_n$ in a cyclic order in the counterclockwise orientation as shown in fig.4.1. We rewrite the classical Gauss constraint on v (in an inverse way compared to (2.44)) as $\mathcal{G}_v = \mathcal{L}_1\mathcal{L}_2\cdots\mathcal{L}_n$ with $\mathcal{L}_i = \tilde{\ell}_i$ if $o_i = -1$ and $\mathcal{L}_i = \ell^{-1}$ if $o_i = 1$.

Upon quantization, $\tilde{\ell}$ is quantized to $\tilde{L}$ and ℓ^{-1} is quantized to $L^{-1} := \overline{S}(L)$. The change of orientation for a link leads to the exchange of $\tilde{L}$ and L in the quantized Gauss constraint thus the exchange of $\mathcal{U}_q(\mathfrak{su}(2))$ and $\mathcal{U}_{q^{-1}}(\mathfrak{su}(2))$ operators. Moreover, the change of orientation results in the exchange between the representation on the vector space and the dual representation[5] on the dual vector space. We can thus define the associated quantum state for an incoming link in the representation space of $\mathcal{U}_q(\mathfrak{su}(2))$ and the associated state for an outgoing link in the dual representation space of $\mathcal{U}_{q^{-1}}(\mathfrak{su}(2))$. Combining these ideas, we consider the representation $\Pi(\tilde{L}) = \tilde{L}$ of $\mathcal{U}_q(\mathfrak{su}(2))$ in the quantized Gauss constraint for an incoming link, while for an outgoing link we need to consider the dual representation $\Pi^*(\overline{S}(L)) \equiv S \circ \overline{S}(L) = L$ of $\mathcal{U}_q(\mathfrak{su}(2))$. The quantized Gauss constraint on v is thus

$$\hat{\mathcal{G}}_v = \triangle^{(n-1)}(\hat{\mathcal{L}})\,, \text{ with } \triangle^{(n-1)} = (\triangle \otimes \mathbb{I}) \circ \triangle^{(n-2)}\,, \quad \triangle(\hat{\mathcal{L}}_{ij}) = \sum_{k=\pm} \hat{\mathcal{L}}_{1,ik} \otimes \hat{\mathcal{L}}_{2,kj}\,,\ i,j = \pm\,. \tag{4.32}$$

On the right hand side of the last equation, $\hat{\mathcal{L}}_\alpha = \tilde{L}$ if $o_\alpha = -1$ and $\hat{\mathcal{L}}_\alpha = L$ if $o_\alpha = 1$ with $\alpha = 1, 2$ denoting the incident links.

4.3.1 Kinematical Hilbert space

Let us now construct the Hilbert space, more particularly the kinematical Hilbert space, denoted as $\mathcal{H}_{\text{kin}}$, of the q-deformed LQG model. A Hilbert space is mathematically defined as a squared integrable space with a measure defining the inner product of states - elements in the Hilbert space. And the kinematical Hilbert space is spanned by the state invariant under the quantum Gauss constraint. These states are called the *spin network states*.

Let us first take a step back and consider the case $\Lambda = 0$. It is well-known that the kinematical Hilbert space for one link in 3D LQG is $L_2(\mathrm{SU}(2), \mathrm{d}g)$ with $\mathrm{d}g$ being the *Haar measure* of SU(2)[6]. According to the *Peter-Weyl theorem*, this Hilbert space can be written as the direct sum of the tensor products of all the irreducible (denoted by a half-integer, called spin j) vector spaces $\mathcal{V}^j$ and the irreducible dual vector spaces $\mathcal{V}^{*\,j}$, which is formally

[5] Given a representation (Π, V) of a Hopf algebra H, the dual representation of H is a pair (Π^*, V^*) consisting of a dual vector space $V^* = \mathrm{Hom}(V, \mathbb{C})$ and a homomorphism $\Pi^* : H \to \mathrm{End}(V^*)$ such that

$$\langle \Pi^*(h)\phi, v\rangle = \langle \phi, \Pi(S(h))v\rangle\,, \forall h \in H, \phi \in V^*\,, v \in V\,.$$

[6] A Haar measure of SU(2) is a measure invariant under the left and right SU(2) transformation, *i.e.* $\mathrm{d}g = \mathrm{d}(hg) = \mathrm{d}(gh), \forall h \in \mathrm{SU}(2)$.

written as

$$\mathcal{H}_e = L_2(\mathrm{SU}(2), \mathrm{d}g) = \bigoplus_{j=\mathbb{N}/2} \mathcal{V}^j \otimes \mathcal{V}^{*\,j}. \tag{4.33}$$

Before imposing any constraint, the Hilbert space for a graph Γ composed of E links is the E-times tensor product of the Hilbert space for a single link. Graphically, one can understand that $\mathcal{V}_e^j$ for a link e is the vector space associated to the half-link incident to the target node $t(e)$ and $\mathcal{V}^{*\,j}$ is the dual vector space associated to the half-link incident to the source node $s(e)$. It is common that instead of studying the whole Hilbert space, one specifies on certain irreducible[7] representations. In this spirit, we assign a spin j_e to each oriented link e, implying that we are picking the representation space $\mathcal{V}_e^j \otimes \mathcal{V}_e^{*\,j}$ for this link. Then a spin network state for an n-valent node v is a state invariant under the SU(2) transformation imposed on v. Such an SU(2)-invariant space is denoted as $\mathrm{Inv}\left(\bigotimes_{e|t(e)=v} \mathcal{V}_e^j \otimes \bigotimes_{e|s(e)=v} \mathcal{V}_e^{*\,j}\right)$. The basis of the kinematical Hilbert space $\mathcal{H}_{\mathrm{kin}}$ is given by the *intertwiners*, which by definition are states invariant under SU(2) transformations.

We now want to generalize the spin network states and hence the kinematical Hilbert space from the flat case to the q-deformed case by considering the irreducible representations of $\mathrm{SU}_q(2)$ (or of $\mathcal{U}_q(\mathfrak{su}(2))$ which are identical). The generalization is rather direct and we collect some ingredients needed for future illustration here [33]. To simplify the notation, we still denote the vector space and dual vector space of the spin j representation for $\mathrm{SU}_q(2)$ by $\mathcal{V}^j$ and $\mathcal{V}^{*\,j}$ in the rest of this section unless it brings confusion.

For the spin j representation space, we introduce an orthonormal basis called the *magnetic state basis* denoted as $|j, m\rangle \in \mathcal{V}^j$ by a spin j and a magnetic number m which can take $2j+1$ different values: $-j, \cdots, j$. Dualizing it, we get the corresponding magnetic state basis $\langle j, m| \in \mathcal{V}^{*\,j}$ for the dual representation space. It is an orthonormal basis in the sense that their inner product gives

$$\langle k, n | j, m\rangle = \delta_{jk}\delta_{mn}\,. \tag{4.34}$$

They form a complete basis for the vector space $\mathcal{V}^j \otimes \mathcal{V}^{*\,j}$, that is

$$\sum_m |j, m\rangle\langle j, m| = \mathbb{I}_{\mathcal{V}^j \otimes \mathcal{V}^{*\,j}}\,. \tag{4.35}$$

We now use these formulas to construct the $\mathcal{U}_q(\mathfrak{su}(2))$-invariant states in the kinematical Hilbert space of q-deformed LQG for a single node. Note that the flat case, which is more well-known, can be recovered at $q = 1$ for all these results.

[7] On physical ground, the representation should be irreducible because otherwise, we have closed subspaces which give superselection sectors [200].

4.3.2 Intertwiners for three-valent nodes

We are particularly interested in the case of $n = 3$ which corresponds to triangulation of Σ. We specify the quantum Gauss constraints for the different orientations in this case. Firstly, consider a node with three links e_1, e_2, e_3 incoming, as given in fig.3.4d. The quantum Gauss constraint reads

$$\hat{\mathcal{G}} = \triangle^{(2)}\tilde{L} = \begin{pmatrix} \tilde{K}\otimes\tilde{K}\otimes\tilde{K} & 0 \\ \begin{array}{c} q^{-\frac{1}{4}}(q^{\frac{1}{2}}-q^{-\frac{1}{2}})(\tilde{K}^{-1}\otimes\tilde{K}^{-1}\otimes\tilde{J}_+ \\ +\tilde{K}^{-1}\otimes\tilde{J}_+\otimes\tilde{K}+\tilde{J}_+\otimes\tilde{K}\otimes\tilde{K}) \end{array} & \tilde{K}^{-1}\otimes\tilde{K}^{-1}\otimes\tilde{K}^{-1} \end{pmatrix} . \tag{4.36}$$

An intertwiner $i_{j_1j_2j_3} \in \mathrm{Inv}(\mathcal{V}^{j_1}\otimes\mathcal{V}^{j_2}\otimes\mathcal{V}^{j_3})$ is defined as a state on a node invariant under the quantum Gauss constraint, that is the eigenstate for $\hat{\mathcal{G}} i_{j_1j_2j_3} = i_{j_1j_2j_3}$. Note that the generators act on the magnetic basis state $|j,m\rangle$ as

$$J_\pm|j,m\rangle = \sqrt{[j\pm m+1][j\mp m]}|j,m\pm1\rangle\,, \quad K|j,m\rangle = q^{\frac{m}{2}}|j,m\rangle\,, \tag{4.37}$$

and $\tilde{J}_\pm, \tilde{K}$ act in the same way. Using the recurrence relation of the q-Wigner-Clebsch–Gordan (WCG) coefficient ${}_qC^{j_1\ j_2\ j_3}_{m_1\,m_2\,m_3}$ [33]:

$$\begin{aligned} q^{\frac{m_2}{2}}\sqrt{[j_1\pm m_1][j_1\mp m_1+1]}\,{}_qC^{j_1\ j_2\ j_3}_{m_1\mp1\,m_2\,m_3} + q^{-\frac{m_1}{2}}\sqrt{[j_2\pm m_2][j_2\mp m_2+1]}\,{}_qC^{j_1\ j_2\ j_3}_{m_1\,m_2\mp1\,m_3} \\ -\sqrt{[j_3\mp m_3][j_3\pm m_3+1]}\,{}_qC^{j_1\ j_2\ j_3}_{m_1\,m_2\,m_3\pm1} = 0\,, \end{aligned} \tag{4.38}$$

we can solve the Gauss constraint, $\hat{\mathcal{G}} i_{j_1j_2j_3} = i_{j_1j_2j_3}$, and get the $\mathcal{U}_q(\mathfrak{su}(2))$ intertwiner defined as

$$i_{j_1j_2j_3} = \sum_{m_i} \frac{(-1)^{j_3+m_3}}{\sqrt{[d_{j_3}]}} q^{-\frac{m_3}{2}}\,{}_qC^{j_1\ j_2\ j_3}_{m_1\,m_2\,-m_3}|j_1,m_1\rangle\otimes|j_2,m_2\rangle\otimes|j_3,m_3\rangle\,. \tag{4.39}$$

When changing the orientation of any link, the correspondent intertwiner can be obtained by turning the representation, say j, associated to the orientation-changed link to the dual representation j^*. To do this, we make use of the $\mathcal{U}_q(\mathfrak{su}(2))$-invariant bilinear form, $\mathcal{B}_q : \mathcal{V}^j\otimes\mathcal{V}^j \to \mathbb{C}$, which is defined with the q-WCG coefficient projected on the trivial representation [33]. Explicitly, for two given vectors $w = \sum_m w_m|j,m\rangle, r = \sum_n r_n|j,n\rangle \in \mathcal{V}^j$,

$$\mathcal{B}_q(w,r) = \sum_m {}_qC^{j\ j\ 0}_{-m\,m\,0}\, w_{-m}r_m = \sum_m (-1)^{j+m}q^{-\frac{m}{2}}w_{-m}r_m\,. \tag{4.40}$$

One can thus define the dual vector w^* of w as

$$w^* \equiv \sum_m \langle j,m|w^*_m := \sum_m \langle j,m|q^{-\frac{m}{2}}(-1)^{j+m}w_{-m} \quad \Longrightarrow \quad w^*_m = q^{-\frac{m}{2}}(-1)^{j+m}w_{-m}\,. \tag{4.41}$$

Apparently, this dual operation is not involution. One can also define the dual vector with the $\mathcal{U}_{q^{-1}}(\mathfrak{su}(2))$-invariant bilinear form $\mathcal{B}_{q^{-1}}$, that is to replace q with q^{-1} in (4.41).

When link e_2 is outgoing and e_1, e_3 incoming, as given in fig.3.4c, one needs to dualize the vector on e_2, that is to change ${}_qC^{j_1\ j_2\ j_3}_{m_1\ m_2\ -m_3}|j_2,m_2\rangle \to {}_qC^{j_1\ j_2\ j_3}_{m_1\ -m_2\ -m_3}\langle j_2,m_2|$ and add $(-1)^{j_2+m_2}q^{-\frac{m_2}{2}}$ according to (4.41). Thus the correspondent intertwiner is

$$i_{j_1j_2^*j_3} = \sum_{m_i} \frac{(-1)^{j_3+m_3}}{\sqrt{[d_{j_3}]}} q^{-\frac{m_3+m_2}{2}}(-1)^{j_2+m_2}{}_qC^{j_1\ j_2\ j_3}_{m_1\ -m_2\ -m_3}|j_1,m_1\rangle\otimes\langle j_2,m_2|\otimes|j_3,m_3\rangle\,, \tag{4.42}$$

which can be checked to be the eigenstate for the quantum Gauss constraint

$$\hat{\mathcal{G}} = \tilde{L}\otimes L\otimes\tilde{L} = \begin{pmatrix} \tilde{K}\otimes K^{-1}\otimes\tilde{K} & 0 \\ q^{-\frac{1}{4}}(q^{\frac{1}{2}}-q^{-\frac{1}{2}})(\tilde{K}^{-1}\otimes K\otimes\tilde{J}_+ & \\ -q^{\frac{1}{2}}\tilde{K}^{-1}\otimes J_+\otimes\tilde{K}+\tilde{J}_+\otimes K^{-1}\otimes\tilde{K}) & \tilde{K}^{-1}\otimes K\otimes\tilde{K}^{-1} \end{pmatrix}. \tag{4.43}$$

When link e_1 is outgoing and e_2, e_3 incoming, as given in fig.3.4b, the intertwiner is obtained using the same dualization as in (4.42) but for j_1 and m_1. The last case for keeping e_3 unchanged is to switch both e_1 and e_2 to be outgoing, as given in fig.3.4a, then the same dualization should be applied to both (j_1,m_1) and (j_2,m_2).

What needs special care is when one switches the orientation of e_3, *i.e.* when e_3 is outgoing and e_1, e_2 incoming. In this case, one needs to dualize the vector on e_3 with a different rule. This is because the q-WCG coefficient ${}_qC^{j_1\ j_2\ j_3}_{m_1\ m_2\ m_3} = \langle j_1,m_1;j_2,m_2|(j_1j_2)j_3,m_3\rangle$ can be viewed as the coefficient w_{m_1} (*resp.* w_{m_2}) of a vector in $\mathcal{V}^{j_1}$ (*resp.* $\mathcal{V}^{j_2}$) or the coefficient $w^*_{m_3}$ of a dual vector in $\mathcal{V}^{j_3\,*}$ in the sense of the decomposition (4.41).

Note that the factor $(-1)^{j_3+m_3}q^{-\frac{m_3}{2}}$ in $i_{j_1j_2j_3}$ is the transformation factor from the coefficient w_m of a vector w to the coefficient w^*_m of a dual vector v^* as shown in (4.41), thus one needs to change $(-1)^{j_3+m_3}q^{-\frac{m_3}{2}}\,{}_qC^{j_1\ j_2\ j_3}_{m_1\ m_2\ -m_3}|j_3,m_3\rangle \to (-1)^{j_3-m_3}q^{\frac{m_3}{2}}\,{}_qC^{j_1\ j_2\ j_3}_{m_1\ m_2\ m_3}\langle j_3,m_3|$ and add $(-1)^{j_3-m_3}q^{-\frac{m_3}{2}}$ which is the factor of the inverse transformation of w^*. This leads to the intertwiner

$$i_{j_1j_2j_3^*} = \sum_{m_i} \frac{1}{\sqrt{[d_{j_3}]}}{}_qC^{j_1\ j_2\ j_3}_{m_1\ m_2\ m_3}|j_1,m_1\rangle\otimes|j_2,m_2\rangle\otimes\langle j_3,m_3|\,, \tag{4.44}$$

which is exactly the eigenstate for the quantum Gauss constraint

$$\hat{\mathcal{G}} = \tilde{L} \otimes \tilde{L} \otimes L = \begin{pmatrix} \tilde{K} \otimes \tilde{K} \otimes K^{-1} & 0 \\ \begin{array}{c} q^{-\frac{1}{4}}(q^{\frac{1}{2}} - q^{-\frac{1}{2}})(-q^{-\frac{1}{2}}\tilde{K}^{-1} \otimes \tilde{K}^{-1} \otimes J_+ \\ +\tilde{K}^{-1} \otimes \tilde{J}_+ \otimes K^{-1} + \tilde{J}_+ \otimes \tilde{K} \otimes K^{-1}) \end{array} & \tilde{K}^{-1} \otimes \tilde{K}^{-1} \otimes K \end{pmatrix}. \tag{4.45}$$

(4.44) can also be used to define the q-WCG coefficient

$${}_qC^{j_1\ j_2\ j_3}_{m_1\ m_2\ m_3} := \langle j_1, m_1| \otimes \langle j_2, m_2| i_{j_1 j_2 j_3^*} |j_3, m_3\rangle \,. \tag{4.46}$$

Indeed, when we change the orientation of e_3 again, we recovers the original intertwiner $i_{j_1 j_2 j_3}$ by adding the regular factor $(-1)^{j_3+m_3} q^{-\frac{m_3}{2}}$ as in obtaining $i_{j_1 j_2^* j_3}$ from $i_{j_1 j_2 j_3}$.

As the last example, we consider the case of three links outgoing, the correspondent intertwiner is

$$\begin{aligned} i_{j_1^* j_2^* j_3^*} =& \sum_{m_i} \frac{(-1)^{j_3-m_3}}{\sqrt{[d_{j_3}]}} q^{\frac{m_3}{2}} q^{-\frac{m_1+m_2+m_3}{2}} (-1)^{j_1+m_1}(-1)^{j_2+m_2}(-1)^{j_3-m_3} \\ & {}_qC^{\ j_1\ \ j_2\ \ j_3}_{-m_1\ -m_2\ m_3} \langle j_1, m_1| \otimes \langle j_2, m_2| \otimes \langle j_3, m_3| \\ =& \sum_{m_i} \frac{1}{\sqrt{[d_{j_3}]}} q^{\frac{m_3}{2}} (-1)^{j_1+m_1}(-1)^{j_2+m_2} {}_qC^{\ j_1\ \ j_2\ \ j_3}_{-m_1\ -m_2\ m_3} \langle j_1, m_1| \otimes \langle j_2, m_2| \otimes \langle j_3, m_3| \,. \end{aligned} \tag{4.47}$$

To summarize, we have clarified the quantization of the holonomy-flux algebra for one ribbon and the Gauss constraint for a three-valent node with incident links of any orientation and the corresponding intertwiner. These serve as the hints to quantize the deformed spinors that we will describe in Chapter 5 and the yardstick to measure the consistency of the results. Recall that the quantum fluxes defined in (4.20) can be defined from the $\mathcal{R}$-matrix of $\mathcal{U}_q(\mathfrak{su}(2))$ and $\mathcal{U}_{q^{-1}}(\mathfrak{su}(2))$ and form neat dualities with the quantum holonomies in terms of the $\mathcal{R}$-matrix, as given in (4.27). We thus believe that the intertwiners built from the quantized Gauss constraint with such quantum fluxes are more useful in constructing the kinematical Hilbert space and are more promising to link to the Turaev-Viro model. This is left for future investigation.

Chapter 5

Quantum spinorial representation of q-deformed LQG

The canonical quantization we did for holonomy and fluxes can also be performed on the classical deformed spinors we introduced in Chapter 3 and promote them to operators. These quantum deformed spinor operators, or quantum spinors for short, can recover the q-deformed LQG structure described in Chapter 4.

The use of quantum spinor in LQG was first introduced for the flat case ($q = 1$) [118, 98, 99, 142, 44, 75, 74]. One of the most appealing results is that the quantum spinors can be used as a tool to define the SU(2) *coherent states*, which build the U(N) formulation of LQG (see *e.g.* [98, 99, 50]). In this formalism, the focus of building quantum states is turned from the spin networks on links to the coherent intertwiners on nodes as, for a given graph, spins live on links while spinors live on nodes. The application of quantum spinors in the spinfoam model has also been much explored (*e.g.* [82, 96, 141]) See Chapter 7 for more discussion on the this topic.

The spinor operators that meet at an n-valent node can then define gauge invariant operators. Moreover, the latter form a $\mathfrak{u}(n)$ algebra of operators at each n-valent node. Later on [120], the larger algebra $\mathfrak{so}^*(2n)$ was identified as the full algebra of observables associated to n-valent nodes. These observables are the most fundamental ones since *any* other observable in the holonomy and flux variables, such as Wilson loops, can be rewritten as a function of those fundamental observables [144]. In other words, they parametrize the invariant subspace of the phase space.

The generalization to the quantum group case $\mathrm{SU}_q(2)$ was not fully understood until now and this is what we intend to achieve in this chapter (with q real). Here we quantize

the spinors directly, which gives rise to spinor operators. Those objects have already been developed quite extensively using the full algebraic apparatus of quantum groups [179, 175], such as the notion of braiding, induced by the quantum $\mathcal{R}$-matrix. Those algebraic considerations thus provide the guide lines to actually build local observables directly at the quantum level [80, 81]. However, since we are working on a graph, it is also natural to use the geometric picture to construct the observables in terms of quantum parallel transport. Note that in the non-deformed case, no parallel transport is involved in these local observables. However, in the deformed case, AN(2) elements play the role of holonomies to transport spinors around the ribbon structure of nodes. It was already noticed in [39] that one can find quantum invariants without using the braiding provided by the $\mathcal{R}$-matrix. In this chapter, we clarify this aspect and show that these two different approaches, *algebra versus geometry*, actually coincide beautifully. Indeed, *the notion of braided permutation used to construct the tensor operators can be understood as a specific parallel transport along the ribbons*. This interpretation in the context of loop quantum gravity is new to the best of our knowledge.

Quantizing the spinors leads to the quantization of the local observables which are built with them. The algebra of those observables around a node of valence n is shown to be a q-deformation of $\mathfrak{so}^*(2n)$ from [120], with a $\mathcal{U}_q(\mathfrak{u}(n))$ subalgebra. This is proved by reproducing the Serre-Chevalley relations from our quantized observables.

This chapter contains one of the key results of this thesis and it is based on [41] by the author and collaborators. In Section 5.1, we introduce the quantum spinor formalism. We provide the quantization rule to have the quantum deformed spinors. We then show in Section 5.2 that the quantum holonomy-flux algebra can be fully recovered by the quantum spinors in a geometrically clear way. In Section 5.4, we show that the action of the $\mathcal{R}$-matrix can be interpreted as parallel transport. This section contains the main original results of this chapter. Finally, in Section 5.5, Finally, we obtain the quantization of the local observables and prove that they form a deformation of $\mathfrak{so}^*(2n)$ in terms of the Serre-Chevalley relations. These observables will be used intensively in the next chapter for constructing the Hamiltonian constraint.

5.1 Quantizing the spinors

In this section, we quantize the deformed spinors $t^\epsilon, \tau^\epsilon, \tilde{t}^\epsilon, \tilde{\tau}^\epsilon$ defined in Section 3.2. We will describe their properties as quantum spinors. Let us first work on the non-tilde variables, then the tilde variables follow the same quantization law but give rise to an independent copy of operators.

The quantization of the deformed variables $\zeta_A^\kappa, \bar{\zeta}_A^\kappa, N_A$ will give rise to the q-deformation of the Jordan map for $\mathfrak{su}(2)$. Indeed these variables can be quantized as q-boson operators: the variables ζ_A^κ are quantized as q-boson annihilation operators, the variables $\bar{\zeta}_A^\kappa$ as q-boson creation operators and the variables N_A as number operators. Explicitly,

$$\begin{array}{lll} (\zeta_-^\kappa, \zeta_+^\kappa) \to (a, b)\,, & (\bar{\zeta}_-^\kappa, \bar{\zeta}_+^\kappa) \to (a^\dagger, b^\dagger)\,, & (N_-, N_+) \to (N_a, N_b)\,, \\ (\tilde{\zeta}_-^\kappa, \tilde{\zeta}_+^\kappa) \to (\tilde{a}, \tilde{b})\,, & (\bar{\tilde{\zeta}}_-^\kappa, \bar{\tilde{\zeta}}_+^\kappa) \to (\tilde{a}^\dagger, \tilde{b}^\dagger)\,, & (\tilde{N}_-, \tilde{N}_+) \to (\tilde{N}_a, \tilde{N}_b)\,. \end{array} \tag{5.1}$$

These q-harmonic oscillators obey the following commutation rules

$$aa^\dagger - q^{\mp\frac{1}{2}} a^\dagger a = q^{\pm\frac{N_a}{2}}\,, \quad a^\dagger a - q^{\pm\frac{1}{2}} aa^\dagger = -q^{\pm\frac{N_a+1}{2}}\,, \quad [N_a, a^\dagger] = a^\dagger\,, \quad [N_a, a] = -a\,, \tag{5.2}$$

from which one can deduce

$$q^{N_a/2} a^\dagger = q^{1/2} a^\dagger q^{N_a/2},\; q^{N_a/2} a = q^{-1/2} a q^{N_a/2}\,,\; a^\dagger a = [N_a] \equiv \frac{q^{N_a/2} - q^{-N_a/2}}{q^{\frac{1}{2}} - q^{-\frac{1}{2}}},\; aa^\dagger = [N_a + 1]\,. \tag{5.3}$$

Similar relations hold for the operators $(b,\, b^\dagger,\, N_b)$ and the tilde variables. The different sets of q-boson operators $(a, a^\dagger, N_a)$ $(b, b^\dagger, N_b)$, $(\tilde{a}, \tilde{a}^\dagger, \tilde{N}_a)$ and $(\tilde{b}, \tilde{b}^\dagger, \tilde{N}_b)$ all commute with each other.

States can be labeled by their occupation numbers, $|n_a\rangle = a^{\dagger n_a}|0\rangle/\sqrt{[n_a]}$ and $|n_b\rangle = b^{\dagger n_b}|0\rangle/\sqrt{[n_b]}$, and

$$|n_a, n_b\rangle_{\rm HO} = |n_a\rangle \otimes |n_b\rangle. \tag{5.4}$$

The q-deformed Jordan map is [33],

$$J_+ = a^\dagger b\,,\; J_- = ab^\dagger\,,\; K = q^{\frac{J_z}{2}} = q^{\frac{N_a - N_b}{4}}\,,\; \tilde{J}_+ = \tilde{a}^\dagger \tilde{b}\,,\; \tilde{J}_- = \tilde{a}\tilde{b}^\dagger\,,\; \tilde{K} = q^{\frac{\tilde{J}_z}{2}} = q^{\frac{\tilde{N}_a - \tilde{N}_b}{4}}\,. \tag{5.5}$$

Indeed, with the quantization map (5.1), we recover the classical generators $z, \bar{z}, \lambda$ and $\tilde{z}, \bar{\tilde{z}}, \tilde{\lambda}$ at the linear $\hbar$-order of the quantum fluxes (4.20) by taking $q = e^{\kappa\hbar} = 1 + \kappa\hbar + O(\hbar^2)$,

$$\left| \begin{array}{lll} -q^{\frac{1}{4}}(q^{\frac{1}{2}} - q^{-\frac{1}{2}}) J_+ & \to & z = -\kappa \bar{\zeta}_-^\kappa \zeta_+^\kappa \\ K^{-1} & \to & \lambda = \exp(\frac{\kappa}{4}(N_+ - N_-)) \end{array} \right| , \quad \left| \begin{array}{lll} q^{\frac{1}{4}}(q^{\frac{1}{2}} - q^{-\frac{1}{2}}) \tilde{J}_+ & \to & \tilde{z} = \kappa \bar{\tilde{\zeta}}_-^\kappa \tilde{\zeta}_+^\kappa \\ \tilde{K} & \to & \tilde{\lambda} = \exp(\frac{\kappa}{4}(\tilde{N}_- - \tilde{N}_+)) \end{array} \right| . \tag{5.6}$$

We define the right adjoint action[1], denoted as $\blacktriangleright$ (*resp.* $\overline{\blacktriangleright}$), of $\mathcal{U}_q(\mathfrak{su}(2))$ (*resp.*

$\mathcal{U}_{q^{-1}}(\mathfrak{su}(2))$) on some operator $\mathcal{O}$:

$$\begin{aligned} J_\pm \blacktriangleright \mathcal{O} &= S(J_\pm)\mathcal{O}K + S(K^{-1})\mathcal{O}J_\pm \\ &= -q^{\pm\frac{1}{2}} J_\pm \mathcal{O}K + K\mathcal{O}J_\pm \end{aligned}, \qquad \begin{aligned} K \blacktriangleright \mathcal{O} &= S(K)\mathcal{O}K \\ &= K^{-1}\mathcal{O}K \end{aligned}, \tag{5.7a}$$

$$\begin{aligned} J_\pm \overline{\blacktriangleright} \mathcal{O} &= \overline{S}(J_\pm)\mathcal{O}K^{-1} + \overline{S}(K)\mathcal{O}J_\pm \\ &= -q^{\mp\frac{1}{2}} J_\pm \mathcal{O}K^{-1} + K^{-1}\mathcal{O}J_\pm \end{aligned}, \qquad \begin{aligned} K \overline{\blacktriangleright} \mathcal{O} &= \overline{S}(K)\mathcal{O}K \\ &= K^{-1}\mathcal{O}K \end{aligned}. \tag{5.7b}$$

Let $\mathcal{V}^j$ be the irreducible representation of $\mathcal{U}_q(\mathfrak{su}(2))$ of dimension $2j+1$. The basis state $|j,m\rangle \in \mathcal{V}^j$ of fixed magnetic number m is the Fock state $|n_a, n_b\rangle_{\text{HO}}$,

$$|j,m\rangle = |j+m, j-m\rangle_{\text{HO}} \equiv \frac{\left(a^\dagger\right)^{j+m}\left(b^\dagger\right)^{j-m}}{\sqrt{[j+m]![j-m]!}}|0,0\rangle_{\text{HO}}\,, \tag{5.8}$$

i.e. $j = \frac{1}{2}(n_a+n_b)$ and $m = \frac{1}{2}(n_a - n_b)$. The q-bosons act on those states as

$$\begin{aligned} &a^\dagger|j,m\rangle = \sqrt{[j+m+1]}\,|j+\tfrac{1}{2}, m+\tfrac{1}{2}\rangle\,, \quad a|j,m\rangle = \sqrt{[j+m]}\,|j-\tfrac{1}{2}, m-\tfrac{1}{2}\rangle\,, \\ &b^\dagger|j,m\rangle = \sqrt{[j-m+1]}\,|j+\tfrac{1}{2}, m-\tfrac{1}{2}\rangle\,, \quad b|j,m\rangle = \sqrt{[j-m]}\,|j-\tfrac{1}{2}, m+\tfrac{1}{2}\rangle\,, \\ &N_a|j,m\rangle = (j+m)\,|j,m\rangle\,, \qquad\qquad N_b|j,m\rangle = (j-m)\,|j,m\rangle\,. \end{aligned} \tag{5.9}$$

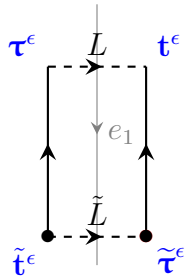

Figure 5.1: The reference ribbon. The spinor operators $\mathbf{t}^\epsilon$ and $\tilde{\mathbf{t}}^\epsilon$ are $\mathcal{U}_q(\mathfrak{su}(2))$ quantum spinors, while $\boldsymbol{\tau}^\epsilon$ and $\widetilde{\boldsymbol{\tau}}^\epsilon$ are $\mathcal{U}_{q^{-1}}(\mathfrak{su}(2))$ quantum spinors.

With the quantization map given above, we are now ready to define the $\mathcal{U}_q(\mathfrak{su}(2))$ and $\mathcal{U}_{q^{-1}}(\mathfrak{su}(2))$ quantum spinors, which decorate the ribbon as in fig.5.1. A $\mathcal{U}_q(\mathfrak{su}(2))$ (*resp.*

[1]Given a generator x of a Hopf algebra H with coproduct $\triangle(x) = \sum x_{(1)} \otimes x_{(2)}$, there are two kinds of adjoint actions on operators $\mathcal{O}$'s of H namely the left adjoint action $x \triangleright \mathcal{O} := \sum x_{(1)}\mathcal{O}S(x_{(2)})$ and the right adjoint action $x \blacktriangleright \mathcal{O} := \sum S(x_{(1)})\mathcal{O}x_{(2)}$.

$\mathcal{U}_{q^{-1}}(\mathfrak{su}(2))$) quantum spinor, denoted as $\mathbf{T} = \begin{pmatrix} \mathbf{T}_- \\ \mathbf{T}_+ \end{pmatrix}$, by definition should transform under the $\mathcal{U}_q(\mathfrak{su}(2))$ (*resp.* $\mathcal{U}_{q^{-1}}(\mathfrak{su}(2))$) adjoint action as a spinor, *i.e.*

$$J_\pm \bullet \mathbf{T}_\pm = 0\,, \quad J_\pm \bullet \mathbf{T}_\mp = \mathbf{T}_\mp\,, \quad K \bullet \mathbf{T}_\pm = q^{\mp\frac{1}{4}}\mathbf{T}_\pm\,, \tag{5.10}$$

where $\bullet$ is the right adjoint action (which can be either $\blacktriangleright$ or $\overline{\blacktriangleright}$).

Remark 5.1.1. *According to Biedenharn's terminology [33], the relations (5.10) define what he calls conjugate spinors. This is what we will call the right adjoint quantum spinors in this article. A left adjoint quantum spinor, or a quantum spinor according to Biedenharn's terminology, is defined by the $\mathcal{U}_q(\mathfrak{su}(2))$ or $\mathcal{U}_{q^{-1}}(\mathfrak{su}(2))$ left adjoint action. Denote uniformly the $\mathcal{U}_q(\mathfrak{su}(2))$ or $\mathcal{U}_{q^{-1}}(\mathfrak{su}(2))$ left adjoint action by $\circ$, then the left adjoint action of the generators on a left adjoint quantum spinor, say $\mathbf{T}'$, is*

$$J_\pm \circ \mathbf{T}'_\pm = 0\,, \quad J_\pm \circ \mathbf{T}'_\mp = \mathbf{T}'_\mp\,, \quad K \circ \mathbf{T}'_\pm = q^{\pm\frac{1}{4}}\mathbf{T}'_\pm\,.$$

Note the different behavior under the action of K compared to (5.10). A $\mathcal{U}_q(\mathfrak{su}(2))$ right adjoint quantum spinor ${}_q\mathbf{T}$ can be obtained via a $\mathcal{U}_{q^{-1}}(\mathfrak{su}(2))$ left adjoint quantum spinor ${}_{q^{-1}}\mathbf{T}'$ with the relation ${}_q\mathbf{T}_A = (-1)^{\frac{1}{2}-A}q^{\frac{A}{2}}{}_{q^{-1}}\mathbf{T}'_A$, while a $\mathcal{U}_{q^{-1}}(\mathfrak{su}(2))$ right adjoint quantum spinor ${}_{q^{-1}}\mathbf{T}$ can be obtained via an $\mathcal{U}_q(\mathfrak{su}(2))$ left adjoint quantum spinor ${}_q\mathbf{T}'$ with the relation ${}_{q^{-1}}\mathbf{T}_A = (-1)^{\frac{1}{2}-A}q^{-\frac{A}{2}}{}_q\mathbf{T}'_A$.

A spinor operator is a special example of a tensor operator $\mathbf{T}^{j=\frac{1}{2}}$. A tensor operator $\mathbf{T}^j$ associated with the representation j transforms under the adjoint action as an element of the representation j. The Wigner-Eckart theorem provides the matrix elements of any tensor operator $\mathbf{T}^j$.

Theorem 5.1.2 (Wigner-Eckart Theorem for $\mathcal{U}_q(\mathfrak{su}(2))$ [33])**.** *The matrix element of a tensor operator $\mathbf{T}^j$ of rank j with j an irreducible representation of $\mathcal{U}_q(\mathfrak{su}(2))$ is proportional to the q-WCG coefficient:*

$$\langle j_1, m_1|\mathbf{T}^j_m|j_2, m_2\rangle = N^j_{j_1 j_2}\,{}_qC^{j_1\ j\ j_2}_{m_1\,m\,m_2}\,, \tag{5.11}$$

where $\mathbf{T}^j_m$ is the m-th component of $\mathbf{T}^j$, ${}_qC^{j_1\ j\ j_2}_{m_1\,m\,m_2}$ is the q-WCG coefficient for coupling j_1 and j to get j_2 and $N^j_{j_1 j_2}$ is a constant independent of m, m_1, m_2.

The quantization map (5.1) leads to the quantum spinors defined as

$$|t\rangle = \begin{pmatrix} e^{\frac{\kappa N_+}{4}}\zeta^\kappa_- \\ e^{-\frac{\kappa N_-}{4}}\zeta^\kappa_+ \end{pmatrix} \to \mathbf{t}^- = \begin{pmatrix} \mathbf{t}^-_- \\ \mathbf{t}^-_+ \end{pmatrix} = \begin{pmatrix} q^{\frac{N_b}{4}}a \\ q^{-\frac{N_a}{4}}b \end{pmatrix}, \tag{5.12a}$$

$$|t] = \begin{pmatrix} -e^{-\frac{\kappa N_-}{4}}\bar{\zeta}^\kappa_+ \\ e^{\frac{\kappa N_+}{4}}\bar{\zeta}^\kappa_- \end{pmatrix} \to \mathbf{t}^+ = \begin{pmatrix} \mathbf{t}^+_- \\ \mathbf{t}^+_+ \end{pmatrix} = \begin{pmatrix} -b^\dagger q^{-\frac{N_a+1}{4}} \\ a^\dagger q^{\frac{N_b+1}{4}} \end{pmatrix}, \tag{5.12b}$$

$$|\tau\rangle = \begin{pmatrix} e^{-\frac{\kappa N_+}{4}}\zeta^\kappa_- \\ e^{\frac{\kappa N_-}{4}}\zeta^\kappa_+ \end{pmatrix} \to \boldsymbol{\tau}^- = \begin{pmatrix} \boldsymbol{\tau}^-_- \\ \boldsymbol{\tau}^-_+ \end{pmatrix} = \begin{pmatrix} q^{-\frac{N_b}{4}}a \\ q^{\frac{N_a}{4}}b \end{pmatrix}, \tag{5.12c}$$

$$|\tau] = \begin{pmatrix} -e^{\frac{\kappa N_-}{4}}\bar{\zeta}^\kappa_+ \\ e^{-\frac{\kappa N_+}{4}}\bar{\zeta}^\kappa_- \end{pmatrix} \to \boldsymbol{\tau}^+ = \begin{pmatrix} \boldsymbol{\tau}^+_- \\ \boldsymbol{\tau}^+_+ \end{pmatrix} = \begin{pmatrix} -b^\dagger q^{\frac{N_a+1}{4}} \\ a^\dagger q^{-\frac{N_b+1}{4}} \end{pmatrix}, \tag{5.12d}$$

$$|\tilde{t}\rangle = \begin{pmatrix} e^{\frac{\kappa \tilde{N}_+}{4}}\tilde{\zeta}^\kappa_- \\ e^{-\frac{\kappa \tilde{N}_-}{4}}\tilde{\zeta}^\kappa_+ \end{pmatrix} \to \tilde{\mathbf{t}}^- = \begin{pmatrix} \tilde{\mathbf{t}}^-_- \\ \tilde{\mathbf{t}}^-_+ \end{pmatrix} = \begin{pmatrix} q^{\frac{\tilde{N}_b}{4}}\tilde{a} \\ q^{-\frac{\tilde{N}_a}{4}}\tilde{b} \end{pmatrix}, \tag{5.12e}$$

$$|\tilde{t}] = \begin{pmatrix} -e^{-\frac{\kappa \tilde{N}_-}{4}}\bar{\tilde{\zeta}}^\kappa_+ \\ e^{\frac{\kappa \tilde{N}_+}{4}}\bar{\tilde{\zeta}}^\kappa_- \end{pmatrix} \to \tilde{\mathbf{t}}^+ = \begin{pmatrix} \tilde{\mathbf{t}}^+_- \\ \tilde{\mathbf{t}}^+_+ \end{pmatrix} = \begin{pmatrix} -\tilde{b}^\dagger q^{-\frac{\tilde{N}_a+1}{4}} \\ \tilde{a}^\dagger q^{\frac{\tilde{N}_b+1}{4}} \end{pmatrix}, \tag{5.12f}$$

$$|\tilde{\tau}\rangle = \begin{pmatrix} e^{-\frac{\kappa \tilde{N}_+}{4}}\tilde{\zeta}^\kappa_- \\ e^{\frac{\kappa \tilde{N}_-}{4}}\tilde{\zeta}^\kappa_+ \end{pmatrix} \to \widetilde{\boldsymbol{\tau}}^- = \begin{pmatrix} \widetilde{\boldsymbol{\tau}}^-_- \\ \widetilde{\boldsymbol{\tau}}^-_+ \end{pmatrix} = \begin{pmatrix} q^{-\frac{\tilde{N}_b}{4}}\tilde{a} \\ q^{\frac{\tilde{N}_a}{4}}\tilde{b} \end{pmatrix}, \tag{5.12g}$$

$$|\tilde{\tau}] = \begin{pmatrix} -e^{\frac{\kappa \tilde{N}_-}{4}}\bar{\tilde{\zeta}}^\kappa_+ \\ e^{-\frac{\kappa \tilde{N}_+}{4}}\bar{\tilde{\zeta}}^\kappa_- \end{pmatrix} \to \widetilde{\boldsymbol{\tau}}^+ = \begin{pmatrix} \widetilde{\boldsymbol{\tau}}^+_- \\ \widetilde{\boldsymbol{\tau}}^+_+ \end{pmatrix} = \begin{pmatrix} -\tilde{b}^\dagger q^{\frac{\tilde{N}_a+1}{4}} \\ \tilde{a}^\dagger q^{-\frac{\tilde{N}_b+1}{4}} \end{pmatrix}. \tag{5.12h}$$

The spinors t^ϵ and $\tilde{t}^\epsilon$ are quantized as $\mathcal{U}_q(\mathfrak{su}(2))$ spinor operators while the (braided) spinors τ^ϵ and $\tilde{\tau}^\epsilon$ are quantized as $\mathcal{U}_{q^{-1}}(\mathfrak{su}(2))$ spinor operators. Indeed, under the right adjoint action, these quantum spinors transform as desired:

$$\begin{aligned}
&J_\pm \blacktriangleright \mathbf{t}^\epsilon_\pm = 0, \quad J_\pm \blacktriangleright \mathbf{t}^\epsilon_\mp = \mathbf{t}^\epsilon_\pm, \quad K \blacktriangleright \mathbf{t}^\epsilon_\pm = q^{\mp\frac{1}{4}}\mathbf{t}^\epsilon_\pm\,, \\
&J_\pm \blacktriangleright \tilde{\mathbf{t}}^\epsilon_\pm = 0, \quad J_\pm \blacktriangleright \tilde{\mathbf{t}}^\epsilon_\mp = \tilde{\mathbf{t}}^\epsilon_\pm, \quad K \blacktriangleright \tilde{\mathbf{t}}^\epsilon_\pm = q^{\mp\frac{1}{4}}\tilde{\mathbf{t}}^\epsilon_\pm\,, \\
&J_\pm \overline{\blacktriangleright}\, \boldsymbol{\tau}^\epsilon_\pm = 0, \quad J_\pm \overline{\blacktriangleright}\, \boldsymbol{\tau}^\epsilon_\mp = \boldsymbol{\tau}^\epsilon_\pm, \quad K \overline{\blacktriangleright}\, \boldsymbol{\tau}^\epsilon_\pm = q^{\mp\frac{1}{4}}\boldsymbol{\tau}^\epsilon_\pm\,, \\
&J_\pm \overline{\blacktriangleright}\, \widetilde{\boldsymbol{\tau}}^\epsilon_\pm = 0, \quad J_\pm \overline{\blacktriangleright}\, \widetilde{\boldsymbol{\tau}}^\epsilon_\mp = \widetilde{\boldsymbol{\tau}}_\pm, \quad K \overline{\blacktriangleright}\, \widetilde{\boldsymbol{\tau}}^\epsilon_\pm = q^{\mp\frac{1}{4}}\widetilde{\boldsymbol{\tau}}^\epsilon_\pm\,.
\end{aligned} \tag{5.13}$$

As a consequence, the Wigner-Eckart theorem tells us that

$$\langle j_1, m_1|\mathbf{t}^\epsilon_m|j_2, m_2\rangle = \delta_{j_1,j_2+\epsilon/2}\sqrt{[d_{j_1}]}\,{}_qC^{j_1\ \frac{1}{2}\ j_2}_{m_1\ -m\ m_2}\,, \tag{5.14a}$$

$$\langle j_1, m_1|\boldsymbol{\tau}^\epsilon_m|j_2, m_2\rangle = \delta_{j_1,j_2+\epsilon/2}\sqrt{[d_{j_1}]}\,{}_{q^{-1}}C^{j_1\ \frac{1}{2}\ j_2}_{m_1\ -m\ m_2}\,, \tag{5.14b}$$

$$\langle j_1, m_1|\tilde{\mathbf{t}}^\epsilon_m|j_2, m_2\rangle = \delta_{j_1,j_2+\epsilon/2}\sqrt{[d_{j_1}]}\,{}_qC^{j_1\ \frac{1}{2}\ j_2}_{m_1\ -m\ m_2}\,, \tag{5.14c}$$

$$\langle j_1, m_1|\widetilde{\boldsymbol{\tau}}^\epsilon_m|j_2, m_2\rangle = \delta_{j_1,j_2+\epsilon/2}\sqrt{[d_{j_1}]}\,{}_{q^{-1}}C^{j_1\ \frac{1}{2}\ j_2}_{m_1\ -m\ m_2}\,. \tag{5.14d}$$

Therefore, as in the quantum fluxes, we again see both the $\mathcal{U}_q(\mathfrak{su}(2))$ and $\mathcal{U}_{q^{-1}}(\mathfrak{su}(2))$ structures appearing upon quantization. We decorate the ribbon with spinor operators as in fig.5.1. $\mathbf{t}^\epsilon$ and $\tilde{\mathbf{t}}^\epsilon$ are the $\mathcal{U}_q(\mathfrak{su}(2))$ quantum spinors, while $\boldsymbol{\tau}^\epsilon$ and $\widetilde{\boldsymbol{\tau}}^\epsilon$ are the $\mathcal{U}_{q^{-1}}(\mathfrak{su}(2))$ quantum spinors both in the sense of the right adjoint action. The quantum spinor components satisfy the commutation relations

$$\mathbf{t}^\epsilon_-\mathbf{t}^\epsilon_+ = q^{-\frac{1}{2}}\mathbf{t}^\epsilon_+\mathbf{t}^\epsilon_-\,,\quad \boldsymbol{\tau}^\epsilon_-\boldsymbol{\tau}^\epsilon_+ = q^{\frac{1}{2}}\boldsymbol{\tau}^\epsilon_+\boldsymbol{\tau}^\epsilon_-\,,\quad \tilde{\mathbf{t}}^\epsilon_-\tilde{\mathbf{t}}^\epsilon_+ = q^{-\frac{1}{2}}\tilde{\mathbf{t}}^\epsilon_+\tilde{\mathbf{t}}^\epsilon_-\,,\quad \widetilde{\boldsymbol{\tau}}^\epsilon_-\widetilde{\boldsymbol{\tau}}^\epsilon_+ = q^{\frac{1}{2}}\widetilde{\boldsymbol{\tau}}^\epsilon_+\widetilde{\boldsymbol{\tau}}^\epsilon_-\,,\quad \epsilon = \pm\,. \tag{5.15}$$

We define the inner products of the spinors with a bilinear form $\mathcal{B}_q$ determined by the q-WCG coefficient $\pm\sqrt{[2]}\,{}_qC^{\frac{1}{2}\ \frac{1}{2}\ 0}_{m\ n\ 0} = \pm\delta_{m,-n}(-1)^{1/2-m}q^{m/2}$ with q compatible with the spinor nature. $\mathcal{B}_q$ thus defines a (non-symmetric) metric on the spinors. We denote the inner products as spinor brackets in the following way

$$\begin{aligned}
\langle\mathbf{t}|\mathbf{t}\rangle &:= \mathcal{B}_q(\mathbf{t}^+,\mathbf{t}^-) = -\sqrt{[2]}\,{}_qC^{\frac{1}{2}\ \frac{1}{2}\ 0}_{m\ -m\ 0}\,\mathbf{t}^+_{-m}\mathbf{t}^-_m = [N]\,,\\
\langle\boldsymbol{\tau}|\boldsymbol{\tau}\rangle &:= \mathcal{B}_{q^{-1}}(\boldsymbol{\tau}^+,\boldsymbol{\tau}^-) = -\sqrt{[2]}\,{}_{q^{-1}}C^{\frac{1}{2}\ \frac{1}{2}\ 0}_{m\ -m\ 0}\,\boldsymbol{\tau}^+_{-m}\boldsymbol{\tau}^-_m = [N]\,,\\
\langle\tilde{\mathbf{t}}|\tilde{\mathbf{t}}\rangle &:= \mathcal{B}_q(\tilde{\mathbf{t}}^+,\tilde{\mathbf{t}}^-) = -\sqrt{[2]}\,{}_qC^{\frac{1}{2}\ \frac{1}{2}\ 0}_{m\ -m\ 0}\,\tilde{\mathbf{t}}^+_{-m}\tilde{\mathbf{t}}^-_m = [\tilde{N}]\,,\\
\langle\widetilde{\boldsymbol{\tau}}|\widetilde{\boldsymbol{\tau}}\rangle &:= \mathcal{B}_{q^{-1}}(\widetilde{\boldsymbol{\tau}}^+,\widetilde{\boldsymbol{\tau}}^-) = -\sqrt{[2]}\,{}_{q^{-1}}C^{\frac{1}{2}\ \frac{1}{2}\ 0}_{m\ -m\ 0}\,\widetilde{\boldsymbol{\tau}}^+_{-m}\widetilde{\boldsymbol{\tau}}^-_m = [\tilde{N}]\,,
\end{aligned} \tag{5.16}$$

as well as

$$\begin{aligned}
[\mathbf{t}|\mathbf{t}] &:= \mathcal{B}_q(\mathbf{t}^-,\mathbf{t}^+) = \sqrt{[2]}\,{}_qC^{\frac{1}{2}\ \frac{1}{2}\ 0}_{m\ -m\ 0}\,\mathbf{t}^-_{-m}\mathbf{t}^+_m = [N+2]\,,\\
[\boldsymbol{\tau}|\boldsymbol{\tau}] &:= \mathcal{B}_{q^{-1}}(\boldsymbol{\tau}^-,\boldsymbol{\tau}^+) = \sqrt{[2]}\,{}_{q^{-1}}C^{\frac{1}{2}\ \frac{1}{2}\ 0}_{m\ -m\ 0}\,\boldsymbol{\tau}^-_{-m}\boldsymbol{\tau}^+_m = [N+2]\,,\\
[\tilde{\mathbf{t}}|\tilde{\mathbf{t}}] &:= \mathcal{B}_q(\tilde{\mathbf{t}}^-,\tilde{\mathbf{t}}^+) = \sqrt{[2]}\,{}_qC^{\frac{1}{2}\ \frac{1}{2}\ 0}_{m\ -m\ 0}\,\tilde{\mathbf{t}}^-_{-m}\tilde{\mathbf{t}}^+_m = [\tilde{N}+2]\,,\\
[\widetilde{\boldsymbol{\tau}}|\widetilde{\boldsymbol{\tau}}] &:= \mathcal{B}_{q^{-1}}(\widetilde{\boldsymbol{\tau}}^-,\widetilde{\boldsymbol{\tau}}^+) = \sqrt{[2]}\,{}_{q^{-1}}C^{\frac{1}{2}\ \frac{1}{2}\ 0}_{m\ -m\ 0}\,\widetilde{\boldsymbol{\tau}}^-_{-m}\widetilde{\boldsymbol{\tau}}^+_m = [\tilde{N}+2]\,.
\end{aligned} \tag{5.17}$$

while it can be checked directly that the remaining vanish,

$$\begin{aligned}
[\mathbf{t}|\mathbf{t}\rangle &:= \mathcal{B}_q(\mathbf{t}^-,\mathbf{t}^-) = 0 = \mathcal{B}_q(\mathbf{t}^+,\mathbf{t}^+) =: \langle \mathbf{t}|\mathbf{t}]\,,\\
[\boldsymbol{\tau}|\boldsymbol{\tau}\rangle &:= \mathcal{B}_{q^{-1}}(\boldsymbol{\tau}^-,\boldsymbol{\tau}^-) = 0 = \mathcal{B}_{q^{-1}}(\boldsymbol{\tau}^+,\boldsymbol{\tau}^+) =: \langle \boldsymbol{\tau}|\boldsymbol{\tau}]\,,\\
[\tilde{\mathbf{t}}|\tilde{\mathbf{t}}\rangle &:= \mathcal{B}_q(\tilde{\mathbf{t}}^-,\tilde{\mathbf{t}}^-) = 0 = \mathcal{B}_q(\tilde{\mathbf{t}}^+,\tilde{\mathbf{t}}^+) =: \langle \tilde{\mathbf{t}}|\tilde{\mathbf{t}}]\,,\\
[\widetilde{\boldsymbol{\tau}}|\widetilde{\boldsymbol{\tau}}\rangle &:= \mathcal{B}_{q^{-1}}(\widetilde{\boldsymbol{\tau}}^-,\widetilde{\boldsymbol{\tau}}^-) = 0 = \mathcal{B}_{q^{-1}}(\widetilde{\boldsymbol{\tau}}^+,\widetilde{\boldsymbol{\tau}}^+) =: \langle \widetilde{\boldsymbol{\tau}}|\widetilde{\boldsymbol{\tau}}]\,.
\end{aligned} \tag{5.18}$$

Unlike in the classical case, the norms of the spinors and their duals are not equal, $\langle\cdot|\cdot\rangle \neq [\cdot|\cdot]$, due to the non-commutativity (5.15) of the spinor components. Furthermore, one can get $[N+1]$ or $[\tilde{N}+1]$ by the following inner products,

$$\begin{aligned}
[N+1] &= q^{-\frac{1}{4}}(\mathbf{t}^-_-\mathbf{t}^+_+ - \mathbf{t}^+_-\mathbf{t}^-_+) = q^{\frac{1}{4}}(\mathbf{t}^+_+\mathbf{t}^-_- - \mathbf{t}^-_+\mathbf{t}^+_-)\\
&= q^{-\frac{1}{4}}(\boldsymbol{\tau}^+_+\boldsymbol{\tau}^-_- - \boldsymbol{\tau}^-_+\boldsymbol{\tau}^+_-) = q^{\frac{1}{4}}(\boldsymbol{\tau}^-_-\boldsymbol{\tau}^+_+ - \boldsymbol{\tau}^+_-\boldsymbol{\tau}^-_+)\,,
\end{aligned} \tag{5.19}$$

$$\begin{aligned}
[\tilde{N}+1] &= q^{-\frac{1}{4}}(\tilde{\mathbf{t}}^-_-\tilde{\mathbf{t}}^+_+ - \tilde{\mathbf{t}}^+_-\tilde{\mathbf{t}}^-_+) = q^{\frac{1}{4}}(\tilde{\mathbf{t}}^+_+\tilde{\mathbf{t}}^-_- - \tilde{\mathbf{t}}^-_+\tilde{\mathbf{t}}^+_-)\\
&= q^{-\frac{1}{4}}(\widetilde{\boldsymbol{\tau}}^+_+\widetilde{\boldsymbol{\tau}}^-_- - \widetilde{\boldsymbol{\tau}}^-_+\widetilde{\boldsymbol{\tau}}^+_-) = q^{\frac{1}{4}}(\widetilde{\boldsymbol{\tau}}^-_-\widetilde{\boldsymbol{\tau}}^+_+ - \widetilde{\boldsymbol{\tau}}^+_-\widetilde{\boldsymbol{\tau}}^-_+)\,.
\end{aligned} \tag{5.20}$$

They are actually those we will use to reconstruct the quantum holonomies, which we will describe in the next section.

5.2 Recovering the quantum holonomy-flux algebra

Both the quantum fluxes and quantum holonomies can be built from the quantum spinors in a neat way as their classical counterparts (3.48).

Holonomies. We start with the following proposition.

Proposition 5.2.1. *Impose the norm matching constraint $N = \tilde{N}$. Then the operator matrix $U = \begin{pmatrix} U_{--} & U_{-+} \\ U_{+-} & U_{++} \end{pmatrix}$ whose matrix elements are given by*

$$U_{AB} = (-1)^{\frac{1}{2}-B} q^{\frac{B}{2}} \sum_{\epsilon=\pm} \boldsymbol{\tau}^\epsilon_A \tilde{\mathbf{t}}^\epsilon_{-B} \frac{1}{[N+1]} \tag{5.21}$$

is an $\mathrm{SU}_{q^{-1}}(2)$ quantum matrix. The operator matrix $\tilde{U} = \begin{pmatrix} \tilde{U}_{--} & \tilde{U}_{-+} \\ \tilde{U}_{+-} & \tilde{U}_{++} \end{pmatrix}$ whose matrix elements are given by

$$\tilde{U}_{AB} = \frac{1}{[\tilde{N}+1]} (-1)^{\frac{1}{2}+B} q^{-\frac{B}{2}} \sum_{\epsilon=\pm} \mathbf{t}^\epsilon_A \widetilde{\boldsymbol{\tau}}^\epsilon_{-B} \tag{5.22}$$

is an $\mathrm{SU}_q(2)$ *quantum matrix.*

In addition, together with the fluxes L *and* $\tilde{L}$ (4.20) *defined in terms of the* $\mathcal{U}_q(\mathfrak{su}(2))$ *generators given by the Jordan map* (5.5)*, the holonomies defined this way satisfy the commutation relations* (4.16)*.*

Proof. By repeatedly applying (5.15) – (5.20) and the commutation relation of the spinor components and the norm factor

$$\frac{1}{[N+1]}\mathbf{T}^{\epsilon}_{m} = \mathbf{T}^{\epsilon}_{m}\frac{1}{[N+1+\epsilon]}\,, \quad \frac{1}{[\tilde{N}+1]}\tilde{\mathbf{T}}^{\epsilon}_{m} = \tilde{\mathbf{T}}^{\epsilon}_{m}\frac{1}{[\tilde{N}+1+\epsilon]}\,, \quad \mathbf{T} = \mathbf{t}\,,\boldsymbol{\tau}\,, \quad \tilde{\mathbf{T}} = \tilde{\mathbf{t}}\,,\widetilde{\boldsymbol{\tau}}\,, \tag{5.23}$$

one can compute that

$$\begin{aligned}
&U_{--}U_{-+} = q^{\frac{1}{2}}U_{-+}U_{--}\,, \quad U_{--}U_{+-} = q^{\frac{1}{2}}U_{+-}U_{--}\,, \quad U_{-+}U_{++} = q^{\frac{1}{2}}U_{++}U_{-+}\,,\\
&U_{+-}U_{++} = q^{\frac{1}{2}}U_{++}U_{+-}\,, [U_{--},U_{++}] = -(q^{\frac{1}{2}}-q^{-\frac{1}{2}})U_{-+}U_{+-}\,, \quad [U_{-+},U_{+-}] = 0\,,\\
&\det\nolimits_{q^{-1}}U \equiv U_{--}U_{++} - q^{\frac{1}{2}}U_{-+}U_{+-} = \mathbb{I}\,,\\
&\tilde{U}_{--}\tilde{U}_{-+} = q^{-\frac{1}{2}}\tilde{U}_{-+}\tilde{U}_{--}\,, \quad \tilde{U}_{--}\tilde{U}_{+-} = q^{-\frac{1}{2}}\tilde{U}_{+-}\tilde{U}_{--}\,, \quad \tilde{U}_{-+}\tilde{U}_{++} = q^{-\frac{1}{2}}\tilde{U}_{++}\tilde{U}_{-+}\,,\\
&\tilde{U}_{+-}\tilde{U}_{++} = q^{-\frac{1}{2}}\tilde{U}_{++}\tilde{U}_{+-}\,, [\tilde{U}_{--},\tilde{U}_{++}] = (q^{\frac{1}{2}}-q^{-\frac{1}{2}})\tilde{U}_{-+}\tilde{U}_{+-}\,, \quad [\tilde{U}_{-+},\tilde{U}_{+-}] = 0\,,\\
&\det\nolimits_{q}\tilde{U} \equiv \tilde{U}_{--}\tilde{U}_{++} - q^{-\frac{1}{2}}\tilde{U}_{-+}\tilde{U}_{+-} = \mathbb{I}\,.
\end{aligned}$$

Referring to Definition 4.1.2, we conclude that U is an $\mathrm{SU}_{q^{-1}}(2)$ quantum matrix and $\tilde{U}$ is an $\mathrm{SU}_q(2)$ quantum matrix.

Using the Jordan map (5.5), the commutation relations between the $\mathcal{U}_q(\mathfrak{su}(2))$ generators and the quantum spinors

$$\begin{aligned}
\mathbf{t}^{\epsilon}_{\pm}K = q^{\mp\frac{1}{4}}K\mathbf{t}^{\epsilon}_{\pm}\,, \quad \boldsymbol{\tau}^{\epsilon}_{\pm}K = q^{\mp\frac{1}{4}}K\boldsymbol{\tau}^{\epsilon}_{\pm}\,, \quad \tilde{\mathbf{t}}^{\epsilon}_{\pm}\tilde{K} = q^{\mp\frac{1}{4}}\tilde{K}\tilde{\mathbf{t}}^{\epsilon}_{\pm}\,, \quad \widetilde{\boldsymbol{\tau}}^{\epsilon}_{\pm}\tilde{K} = q^{\mp\frac{1}{4}}\tilde{K}\widetilde{\boldsymbol{\tau}}^{\epsilon}_{\pm}\,,\\
\mathbf{t}^{\epsilon}_{\mp}J_{\pm} - q^{\pm\frac{1}{4}}J_{\pm}\mathbf{t}^{\epsilon}_{\mp} = K^{-1}\mathbf{t}^{\epsilon}_{\pm}\,, \quad \mathbf{t}_{\mp}J_{\mp} = q^{\pm\frac{1}{4}}J_{\mp}\mathbf{t}^{\epsilon}_{\mp}\,,\\
\boldsymbol{\tau}^{\epsilon}_{\mp}J_{\pm} - q^{\mp\frac{1}{4}}J_{\pm}\boldsymbol{\tau}^{\epsilon}_{\mp} = K\boldsymbol{\tau}^{\epsilon}_{\pm}\,, \quad \boldsymbol{\tau}^{\epsilon}_{\mp}J_{\mp} = q^{\mp\frac{1}{4}}J_{\mp}\boldsymbol{\tau}^{\epsilon}_{\mp}\,,\\
\tilde{\mathbf{t}}^{\epsilon}_{\mp}\tilde{J}_{\pm} - q^{\pm\frac{1}{4}}\tilde{J}_{\pm}\tilde{\mathbf{t}}^{\epsilon}_{\mp} = \tilde{K}^{-1}\tilde{\mathbf{t}}^{\epsilon}_{\pm}\,, \quad \tilde{\mathbf{t}}_{\mp}\tilde{J}_{\mp} = q^{\pm\frac{1}{4}}\tilde{J}_{\mp}\tilde{\mathbf{t}}^{\epsilon}_{\mp}\,,\\
\widetilde{\boldsymbol{\tau}}^{\epsilon}_{\mp}\tilde{J}_{\pm} - q^{\mp\frac{1}{4}}\tilde{J}_{\pm}\widetilde{\boldsymbol{\tau}}^{\epsilon}_{\mp} = \tilde{K}\widetilde{\boldsymbol{\tau}}^{\epsilon}_{\pm}\,, \quad \widetilde{\boldsymbol{\tau}}^{\epsilon}_{\mp}\tilde{J}_{\mp} = q^{\mp\frac{1}{4}}\tilde{J}_{\mp}\widetilde{\boldsymbol{\tau}}^{\epsilon}_{\mp}\,,
\end{aligned} \tag{5.24}$$

one can show that the commutation relations in (4.16) are satisfied given the definition of the quantum holonomies (5.21), (5.22) and the quantum fluxes (4.20). □

Flux vectors. We can also reconstruct the quantization of the vectors X and $X^{\rm op}$ from (2.40) in terms of the quantum spinors. They become $\mathcal{U}_q(\mathfrak{su}(2))$ and $\mathcal{U}_{q^{-1}}(\mathfrak{su}(2))$ vector operators respectively, *i.e.* spin 1 tensor operators. The $\mathcal{U}_q(\mathfrak{su}(2))$ quantum vectors can be built from the $\mathcal{U}_q(\mathfrak{su}(2))$ spinors $\mathbf{t}^\epsilon$ and $\tilde{\mathbf{t}}^\epsilon$ and the $\mathcal{U}_{q^{-1}}(\mathfrak{su}(2))$ vectors can be built from the $\mathcal{U}_{q^{-1}}(\mathfrak{su}(2))$ spinors $\boldsymbol{\tau}^\epsilon$ and $\widetilde{\boldsymbol{\tau}}^\epsilon$.

According to the q-WCG coupling, one can define the $\mathcal{U}_q(\mathfrak{su}(2))$ right adjoint vectors as

$$\mathbf{X}_A = \sum_{\substack{m,n=\pm\frac{1}{2}\\ m+n=A}} {}_qC^{\frac{1}{2}\ \frac{1}{2}\ 1}_{-m\ -n\ -A}\mathbf{t}^+_m\mathbf{t}^-_n\,, \quad A=0,\pm1\,. \tag{5.25}$$

In components they read

$$\mathbf{X}_0 = {}_q\, C^{\frac{1}{2}\ \frac{1}{2}\ 1}_{\frac{1}{2}\ -\frac{1}{2}\ 0}\mathbf{t}^+_-\mathbf{t}^-_+ + {}_qC^{\frac{1}{2}\ \frac{1}{2}\ 1}_{-\frac{1}{2}\ \frac{1}{2}\ 0}\mathbf{t}^+_+\mathbf{t}^-_- = \frac{1}{\sqrt{[2]}}\left(q^{\frac{1}{2}}J_+J_- - q^{-\frac{1}{2}}J_-J_+\right)\,,$$
$$\mathbf{X}_{-1} = {}_qC^{\frac{1}{2}\ \frac{1}{2}\ 1}_{\frac{1}{2}\ \frac{1}{2}\ 1}\mathbf{t}^+_-\mathbf{t}^-_- = -J_-K^{-1}\,, \quad \mathbf{X}_1 = {}_qC^{\frac{1}{2}\ \frac{1}{2}\ 1}_{-\frac{1}{2}\ -\frac{1}{2}\ -1}\mathbf{t}^+_+\mathbf{t}^-_+ = J_+K^{-1}\,.$$

It is easy to check that they behave as a vector under the action of $\mathcal{U}_q(\mathfrak{su}(2))$

$$J_\pm \blacktriangleright \mathbf{X}_A = \sqrt{[1\mp A][1\pm A+1]}\,\mathbf{X}_{A\pm1}\,, \quad K\blacktriangleright\mathbf{X}_A = q^{-\frac{A}{2}}\mathbf{X}_A\,, \tag{5.26}$$

so that the Wigner-Eckart theorem applies and gives the matrix elements of $\mathbf{X}_A$ in the irreducible representation $\mathcal{V}^j$,

$$\langle j,n|\mathbf{X}_A|j,m\rangle = N_j\,{}_qC^{j\ 1\ j}_{n\ -A\ m}\,, \text{ with } N_j = \sqrt{\frac{[2j][2j+2]}{[2]}}\,. \tag{5.27}$$

Similarly, one defines the $\mathcal{U}_{q^{-1}}(\mathfrak{su}(2))$ vector as

$$\mathbf{X}^{\rm op}_A = \sum_{\substack{m,n=\pm\frac{1}{2}\\ m+n=A}} {}_{q^{-1}}C^{\frac{1}{2}\ \frac{1}{2}\ 1}_{-m\ -n\ -A}\boldsymbol{\tau}^+_m\boldsymbol{\tau}^-_n\,, \quad A=0,\pm1\,, \tag{5.28}$$

whose components are

$$\mathbf{X}^{\rm op}_0 = {}_{q^{-1}}\, C^{\frac{1}{2}\ \frac{1}{2}\ 1}_{\frac{1}{2}\ -\frac{1}{2}\ 0}\boldsymbol{\tau}^+_-\boldsymbol{\tau}^-_+ + {}_{q^{-1}}\, C^{\frac{1}{2}\ \frac{1}{2}\ 1}_{-\frac{1}{2}\ \frac{1}{2}\ 0}\boldsymbol{\tau}^+_+\boldsymbol{\tau}^-_- = \frac{1}{\sqrt{[2]}}\left(q^{-\frac{1}{2}}J_+J_- - q^{\frac{1}{2}}J_-J_+\right)\,,$$
$$\mathbf{X}^{\rm op}_{-1} = {}_{q^{-1}}\, C^{\frac{1}{2}\ \frac{1}{2}\ 1}_{\frac{1}{2}\ \frac{1}{2}\ 1}\boldsymbol{\tau}^+_-\boldsymbol{\tau}^-_- = -J_-K\,, \quad \mathbf{X}^{\rm op}_1 = {}_{q^{-1}}\, C^{\frac{1}{2}\ \frac{1}{2}\ 1}_{-\frac{1}{2}\ -\frac{1}{2}\ -1}\boldsymbol{\tau}^+_+\boldsymbol{\tau}^-_+ = J_+K\,.$$

They are indeed $\mathcal{U}_{q^{-1}}(\mathfrak{su}(2))$ vectors since

$$J_\pm \blacktriangleright \mathbf{X}^{\rm op}_A = \sqrt{[1\mp A][1\pm A+1]}\,\mathbf{X}_{A\pm 1}\,, \quad K\blacktriangleright \mathbf{X}^{\rm op}_A = q^{-\frac{A}{2}}\mathbf{X}^{\rm op}_A\,, \tag{5.29}$$

and from the Wigner-Eckart theorem,

$$\langle j,n|\mathbf{X}^{\rm op}_A|j,m\rangle = N_{j\,q^{-1}}C^{j\ 1\ j}_{n\ -A\ m}\,,\ \text{with}\ N_j = \sqrt{\frac{[2j][2j+2]}{[2]}}\,. \tag{5.30}$$

One can see that $\mathbf{X}$ and $\mathbf{X}^{\rm op}$ are the natural quantization the classical deformed vectors $\vec{X}$ and $\vec{X}^{\rm op}$ as defined in (2.40). The tilde sector of vectors $\tilde{\mathbf{X}}$ and $\tilde{\mathbf{X}}^{\rm op}$ can also be built in the same way from $\tilde{\mathbf{t}}^\epsilon$ and $\widetilde{\boldsymbol{\tau}}^\epsilon$ respectively. In addition, higher spin quantum vectors of $\mathcal{U}_q(\mathfrak{su}(2))$ and $\mathcal{U}_{q^{-1}}(\mathfrak{su}(2))$ types can be built with the q-WCG coefficient in a similar method.

5.3 Flipping the ribbon

In the following, we will omit the index ϵ on the spinor operators as it is not relevant for the present discussion. We introduce the operator $\mathfrak{M}$ associated to changing the orientation of a link of Γ, which is a quantum version of $\mathfrak{m}$ defined in (3.19).

(a) The reference ribbon.

(b) The flipped ribbon.

Figure 5.2: Flipping the reference ribbon due to the change of orientation of the link e is equivalent to the spinor flip $\widetilde{\boldsymbol{\tau}} \to \boldsymbol{\tau}, \quad \tilde{\mathbf{t}} \to \mathbf{t}$.

When changing the orientation of a link as shown in 5.2, we have the following involutive transformation on the spinor operators

$$\widetilde{\boldsymbol{\tau}} \to \boldsymbol{\tau}, \quad \tilde{\mathbf{t}} \to \mathbf{t}. \tag{5.31}$$

Since the tilde and non-tilde spinors are classically the same, and since the quantization map is the same for both (5.12), we can define

$$\mathfrak{M}(\mathbf{t}) = \tilde{\mathbf{t}}, \qquad \mathfrak{M}(\tilde{\mathbf{t}}) = \mathbf{t}, \qquad \mathfrak{M}(\boldsymbol{\tau}) = \widetilde{\boldsymbol{\tau}}, \qquad \mathfrak{M}(\widetilde{\boldsymbol{\tau}}) = \boldsymbol{\tau}, \tag{5.32}$$

and just like we did classically, we can lift $\mathfrak{M}$ to the q-bosons by setting

$$\mathfrak{M}(a) = \tilde{a}, \qquad \mathfrak{M}(a^\dagger) = \tilde{a}^\dagger, \qquad \mathfrak{M}(b) = \tilde{b}, \qquad \mathfrak{M}(b^\dagger) = \tilde{b}^\dagger, \tag{5.33}$$

and requiring that $\mathfrak{M}$ is an involution. By applying $\mathfrak{M}$ to (5.5), one finds

$$\mathfrak{M}(J_\pm) = \tilde{J}_\pm, \qquad \mathfrak{M}(\tilde{J}_\pm) = J_\pm, \qquad \mathfrak{M}(K) = \tilde{K}, \qquad \mathfrak{M}(\tilde{K}) = K. \tag{5.34}$$

It is then possible to find $\mathfrak{M}(L)$ in terms of $\tilde{L}$,

$$\mathfrak{M}(L) = \begin{pmatrix} \tilde{K}^{-1} & 0 \\ -q^{\frac{1}{4}}(q^{\frac{1}{2}} - q^{-\frac{1}{2}})\tilde{J}_+ & \tilde{K} \end{pmatrix} = S(\tilde{L}) \tag{5.35}$$

where S is the antipode of $\mathcal{U}_q(\mathfrak{su}(2))$. Similarly, one finds $I(\tilde{L}) = \overline{S}(L)$ with $\overline{S}$ being the antipode of $\mathcal{U}_{q^{-1}}(\mathfrak{su}(2))$. Indeed, $S(\overline{S}(L)) \equiv L$ and $\overline{S}(S(\tilde{L})) \equiv \tilde{L}$, consistently with the fact that I is an involution.

The same can be applied to U. Parametrize the matrix elements of U and $\tilde{U}$ as well as their antipode to be (See Definition 4.1.2 for definition of the Hopf algebra $\mathrm{SU}_q(2)$.)

$$U = \begin{pmatrix} U_{--} & U_{-+} \\ U_{+-} & U_{++} \end{pmatrix} \in \mathrm{SU}_{q^{-1}}(2)\,, \quad \overline{S}(U) = \begin{pmatrix} U_{++} & -q^{-\frac{1}{2}}U_{-+} \\ -q^{\frac{1}{2}}U_{+-} & U_{--} \end{pmatrix}, \tag{5.36}$$

$$\tilde{U} = \begin{pmatrix} \tilde{U}_{--} & \tilde{U}_{-+} \\ \tilde{U}_{+-} & \tilde{U}_{++} \end{pmatrix} \in \mathrm{SU}_q(2)\,, \quad S(\tilde{U}) = \begin{pmatrix} \tilde{U}_{++} & -q^{\frac{1}{2}}\tilde{U}_{-+} \\ -q^{-\frac{1}{2}}\tilde{U}_{+-} & \tilde{U}_{--} \end{pmatrix}, \tag{5.37}$$

where we have used $\overline{S}$ to denote the antipode for $\mathrm{SU}_{q^{-1}}(2)$. We define the operator $\mathfrak{M}$ acting on the generators $U_{--}, U_{-+}, U_{+-}, U_{++}$ of U and generators $\tilde{U}_{--}, \tilde{U}_{-+}, \tilde{U}_{+-}, \tilde{U}_{++}$ of $\tilde{U}$ as

$$\begin{aligned} &\mathfrak{M}(U_{--}) = \tilde{U}_{++}\,, \quad \mathfrak{M}(U_{-+}) = -q^{\frac{1}{2}}\tilde{U}_{-+}\,, \quad \mathfrak{M}(U_{+-}) = -q^{-\frac{1}{2}}\tilde{U}_{+-}\,, \quad \mathfrak{M}(U_{++}) = \tilde{U}_{--}\,, \\ &\mathfrak{M}(\tilde{U}_{--}) = U_{++}\,, \quad \mathfrak{M}(\tilde{U}_{-+}) = -q^{-\frac{1}{2}}U_{-+}\,, \quad \mathfrak{M}(\tilde{U}_{+-}) = -q^{\frac{1}{2}}U_{+-}\,, \quad \mathfrak{M}(\tilde{U}_{++}) = U_{--}\,, \end{aligned} \tag{5.38}$$

where $\mathfrak{M}$ is indeed an involution. We then have

$$\mathfrak{M}(U) = S(\tilde{U})\,, \quad \mathfrak{M}(\tilde{U}) = \overline{S}(U)\,. \tag{5.39}$$

Recall that one can reconstruct these quantum holonomies in terms of the quantum spinors in the way as in (5.21) and (5.22) which copy here.

$$U_{AB} = (-1)^{\frac{1}{2}-B} q^{\frac{B}{2}} \sum_{\epsilon=\pm} \boldsymbol{\tau}^{\epsilon}_{A} \tilde{\mathbf{t}}^{\epsilon}_{-B} \frac{1}{[N+1]} \in \mathrm{SU}_{q^{-1}}(2)\,,$$
$$\tilde{U}_{AB} = \frac{1}{[\tilde{N}+1]} (-1)^{\frac{1}{2}+B} q^{-\frac{B}{2}} \sum_{\epsilon=\pm} \mathbf{t}^{\epsilon}_{A} \widetilde{\boldsymbol{\tau}}^{\epsilon}_{-B} \in \mathrm{SU}_{q}(2)\,.$$

The matrix element of the antipodes of U and $\tilde{U}$ defined in (5.37) can be equivalently written as

$$(\overline{S}(U))_{AB} = (-1)^{B-A} q^{\frac{A-B}{2}} U_{-B\,-A} = \frac{1}{[N+1]} (-1)^{\frac{1}{2}+B} q^{-\frac{B}{2}} \sum_{\epsilon} \tilde{\mathbf{t}}^{\epsilon}_{A} \boldsymbol{\tau}^{\epsilon}_{-B}\,, \tag{5.40}$$
$$(S(\tilde{U}))_{AB} = (-1)^{A-B} q^{\frac{B-A}{2}} \tilde{U}_{-B\,-A} = (-1)^{\frac{1}{2}-B} q^{\frac{B}{2}} \sum_{\epsilon} \widetilde{\boldsymbol{\tau}}^{\epsilon}_{A} \mathbf{t}^{\epsilon}_{-B} \frac{1}{[\tilde{N}+1]}\,. \tag{5.41}$$

Then (5.39) can be deduced from (5.32).

Therefore, we have a complete map for quantum objects in terms of flipping the ribbons. We can now focus only on one orientation for a ribbon and use the involution map $\mathfrak{M}$ to deduce the results after the change of orientation.

5.4 The $\mathcal{R}$-matrix as parallel transport

In the classical construction, the different spinors are related through parallel transport by the AN(2) holonomies. We will see that their quantum counterparts, the spinor operators, are related by $\mathrm{AN}_q(2)$ holonomies. We expect to have two possible cases, either lower triangular or upper triangular.

Parallel transport within a ribbon. The covariant and braided-covariant, classical, spinors of a *single* ribbon are related to one another by AN(2) parallel transport in (3.26)

and the first equation of (3.40).

$$L\boldsymbol{\tau}^\epsilon = \begin{pmatrix} K^{-1}\boldsymbol{\tau}^\epsilon_- \\ -(q^{\frac{3}{4}}-q^{-\frac{1}{4}})J_+\boldsymbol{\tau}^\epsilon_- + K\boldsymbol{\tau}^\epsilon_+ \end{pmatrix} = q^{\frac{1+\epsilon}{4}} q^{\epsilon\frac{N}{4}} \mathbf{t}^\epsilon \,, \tag{5.42a}$$

$$\tilde{L}\tilde{\mathbf{t}}^\epsilon = \begin{pmatrix} \tilde{K}\tilde{\mathbf{t}}^\epsilon_- \\ (q^{\frac{1}{4}}-q^{-\frac{3}{4}})\tilde{J}_+\tilde{\mathbf{t}}^\epsilon_- + \tilde{K}^{-1}\tilde{\mathbf{t}}^\epsilon_+ \end{pmatrix} = q^{-\epsilon\frac{\tilde{N}}{4}} q^{-\frac{1+\epsilon}{4}} \widetilde{\boldsymbol{\tau}}^\epsilon \,, \tag{5.42b}$$

$$\overline{S}(L)\mathbf{t}^\epsilon = \begin{pmatrix} K\mathbf{t}^\epsilon_- \\ (q^{\frac{1}{4}}-q^{-\frac{3}{4}})J_+\mathbf{t}^\epsilon_- + K^{-1}\mathbf{t}^\epsilon_+ \end{pmatrix} = q^{-\frac{1+\epsilon}{4}} q^{-\epsilon\frac{N}{4}} \boldsymbol{\tau}^\epsilon \,, \tag{5.42c}$$

$$S(\tilde{L})\widetilde{\boldsymbol{\tau}}^\epsilon = \begin{pmatrix} \tilde{K}^{-1}\widetilde{\boldsymbol{\tau}}^\epsilon_- \\ -(q^{\frac{3}{4}}-q^{-\frac{1}{4}})\tilde{J}_+\widetilde{\boldsymbol{\tau}}^\epsilon_- + \tilde{K}\widetilde{\boldsymbol{\tau}}^\epsilon_+ \end{pmatrix} = q^{\epsilon\frac{\tilde{N}}{4}} q^{\frac{1+\epsilon}{4}} \tilde{\mathbf{t}}^\epsilon \,. \tag{5.42d}$$

One can take the complex conjugate of these relations and get equivalently,

$$(-1)^{\frac{1}{2}-A} q^{\frac{A}{2}} \mathbf{t}^\epsilon_{-A} = q^{\epsilon\frac{N}{4}} q^{\frac{\epsilon-2}{4}} (-1)^{\frac{1}{2}-B} q^{-\frac{B}{2}} \boldsymbol{\tau}^\epsilon_{-B} \left(L^\dagger\right)_B{}^A \,, \tag{5.43a}$$

$$(-1)^{\frac{1}{2}-A} q^{-\frac{A}{2}} \boldsymbol{\tau}^\epsilon_{-A} = q^{-\epsilon\frac{N}{4}} q^{\frac{2-\epsilon}{4}} (-1)^{\frac{1}{2}-B} q^{\frac{B}{2}} \mathbf{t}^\epsilon_{-B} \left(\overline{S}(L)^\dagger\right)_B{}^A \,, \tag{5.43b}$$

$$(-1)^{\frac{1}{2}-A} q^{-\frac{A}{2}} \widetilde{\boldsymbol{\tau}}^\epsilon_{-A} = q^{-\epsilon\frac{\tilde{N}}{4}} q^{\frac{2-\epsilon}{4}} (-1)^{\frac{1}{2}-B} q^{\frac{B}{2}} \tilde{\mathbf{t}}^\epsilon_{-B} \left(\tilde{L}^\dagger\right)_B{}^A \,, \tag{5.43c}$$

$$(-1)^{\frac{1}{2}-A} q^{\frac{A}{2}} \tilde{\mathbf{t}}^\epsilon_{-A} = q^{\epsilon\frac{\tilde{N}}{4}} q^{\frac{\epsilon-2}{4}} (-1)^{\frac{1}{2}-B} q^{-\frac{B}{2}} \widetilde{\boldsymbol{\tau}}^\epsilon_{-B} \left(S(\tilde{L})^\dagger\right)_B{}^A \,. \tag{5.43d}$$

To get (5.43) from (5.42a) and (5.42d), we have used the formulas for taking the complex conjugating of spinor components

$$\begin{aligned} (\mathbf{t}^\epsilon_A)^\dagger &= \epsilon(-1)^{\frac{1}{2}-A} q^{\frac{A}{2}} \mathbf{t}^{-\epsilon}_{-A} \,, \quad (\boldsymbol{\tau}^\epsilon_A)^\dagger = \epsilon(-1)^{\frac{1}{2}-A} q^{-\frac{A}{2}} \boldsymbol{\tau}^{-\epsilon}_{-A} \,, \\ \left(\tilde{\mathbf{t}}^\epsilon_A\right)^\dagger &= \epsilon(-1)^{\frac{1}{2}-A} q^{\frac{A}{2}} \tilde{\mathbf{t}}^{-\epsilon}_{-A} \,, \quad (\widetilde{\boldsymbol{\tau}}^\epsilon_A)^\dagger = \epsilon(-1)^{\frac{1}{2}-A} q^{-\frac{A}{2}} \widetilde{\boldsymbol{\tau}}^{-\epsilon}_{-A} \,, \end{aligned} \tag{5.44}$$

and the commutation relation of the factor $q^{\epsilon\frac{N}{4}}$ or $q^{\epsilon\frac{\tilde{N}}{4}}$ with the spinor components

$$q^{\epsilon\frac{N}{4}} \mathbf{t}^{\epsilon'}_A = q^{\frac{\epsilon\epsilon'}{4}} \mathbf{t}^{\epsilon'}_A q^{\epsilon\frac{N}{4}} \,, \quad q^{\epsilon\frac{N}{4}} \boldsymbol{\tau}^{\epsilon'}_A = q^{\frac{\epsilon\epsilon'}{4}} \boldsymbol{\tau}^{\epsilon'}_A q^{\epsilon\frac{N}{4}} \,, \quad q^{\epsilon\frac{\tilde{N}}{4}} \tilde{\mathbf{t}}^{\epsilon'}_A = q^{\frac{\epsilon\epsilon'}{4}} \tilde{\mathbf{t}}^{\epsilon'}_A q^{\epsilon\frac{\tilde{N}}{4}} \,, \quad q^{\epsilon\frac{\tilde{N}}{4}} \widetilde{\boldsymbol{\tau}}^{\epsilon'}_A = q^{\frac{\epsilon\epsilon'}{4}} \widetilde{\boldsymbol{\tau}}^{\epsilon'}_A q^{\epsilon\frac{\tilde{N}}{4}} \,. \tag{5.45}$$

This quantum version of the parallel transport works within a single ribbon, see fig.5.2a. Let us now consider what happens when dealing with more ribbons.

Spinors for many ribbons. We are interested in defining spinor operators when dealing with many ribbons. We focus on a ribbon graph Γ_{rib} where the graph Γ is an N_v-valent node v with N_v links ordered and labeled as e_1 and e_N going counterclockwise. The

ribbon graph $\Gamma_{\rm rib}$ is an N_v-gon $R(v)$ surrounded by N_v ribbons $R(e_n)$, $n \in \{1, \cdots, N_v\}$. Once more, we do not consider the index ϵ which does not bring anything to the present discussion. For the ribbon $R(e_n)$, we introduce

$$\widetilde{\boldsymbol{\tau}}_n = \mathbb{I} \otimes \cdots \otimes \widetilde{\boldsymbol{\tau}} \otimes \cdots \otimes \mathbb{I}, \quad \tilde{\mathbf{t}}_n = \mathbb{I} \otimes \cdots \otimes \tilde{\mathbf{t}} \otimes \cdots \otimes \mathbb{I}. \tag{5.46}$$

These objects, $\widetilde{\boldsymbol{\tau}}_n$ or $\tilde{\mathbf{t}}_n$, are built using permutations, starting respectively from $\widetilde{\boldsymbol{\tau}}_1$ or $\tilde{\mathbf{t}}_1$. However, the permutation is not consistent with the coproduct if it is non-co-commutative. Consequently, due to the non-co-commutativity of the coproducts of $\mathcal{U}_q(\mathfrak{su}(2))$ and $\mathcal{U}_{q^{-1}}(\mathfrak{su}(2))$, these objects are not spinor operators, except $\widetilde{\boldsymbol{\tau}}_1$ and $\tilde{\mathbf{t}}_1$.

We now want to define spinor operators, that is objects transforming covariantly under the $\mathcal{U}_q(\mathfrak{su}(2))$ and $\mathcal{U}_{q^{-1}}(\mathfrak{su}(2))$ adjoint actions. To make the distinction between the objects living on the n^{th} leg, $\widetilde{\boldsymbol{\tau}}_n$ or $\tilde{\mathbf{t}}_n$, and the spinor operators, we will denote ${}^{(n)}\widetilde{\boldsymbol{\tau}}$ and ${}^{(n)}\tilde{\mathbf{t}}$, the objects transforming respectively as a $\mathcal{U}_{q^{-1}}(\mathfrak{su}(2))$ and $\mathcal{U}_q(\mathfrak{su}(2))$ spinor operators. The construction of the spinor operators on different Hilbert spaces is usually done using the braiding induced by the $\mathcal{R}$-matrix [179].

As a consequence the usual construction of spinor operators (or any tensor operators) is in terms of the $\mathcal{R}$-matrix. There are two ways to define such a spinor operator. Explicitly, we use $\mathcal{R}^{-1}_{ij}$ or $\mathcal{R}_{ji}$ to define the $\mathcal{U}_{q^{-1}}(\mathfrak{su}(2))$ tensor operator ${}^{(n)}\widetilde{\boldsymbol{\tau}}$.

$$\begin{aligned} {}^{(n)}\widetilde{\boldsymbol{\tau}}_A &= \mathcal{R}^{-1}_{n-1,n}\mathcal{R}^{-1}_{n-2,n}\cdots\mathcal{R}^{-1}_{2n}\mathcal{R}^{-1}_{1n}(\widetilde{\boldsymbol{\tau}}_n)_A\mathcal{R}_{1n}\mathcal{R}_{2n}\cdots\mathcal{R}_{n-2,n}\mathcal{R}_{n-1,n}\otimes\mathbb{I}\otimes\cdots & (5.47a)\\ \text{or}\quad {}^{(n)}\widetilde{\boldsymbol{\tau}}_A &= \mathcal{R}_{n,n-1}\mathcal{R}_{n,n-2}\cdots\mathcal{R}_{n2}\mathcal{R}_{n1}(\widetilde{\boldsymbol{\tau}}_n)_A\mathcal{R}^{-1}_{n1}\mathcal{R}^{-1}_{n2}\cdots\mathcal{R}^{-1}_{n,n-2}\mathcal{R}^{-1}_{n,n-1}\otimes\mathbb{I}\otimes\cdots & (5.47b)\end{aligned}$$

The two formulas of (5.47) are proportional to each other with the proportionality coefficient being a function of the norms $N_1, \cdots, N_n$ which commutes with the $\mathcal{U}_q(\mathfrak{su}(2))$ (or $\mathcal{U}_{q^{-1}}(\mathfrak{su}(2))$) generators. Similarly, we use $\mathcal{R}_{ij}$ or $\mathcal{R}^{-1}_{ji}$ to define the $\mathcal{U}_q(\mathfrak{su}(2))$ tensor operator ${}^{(n)}\tilde{\mathbf{t}}$

$$\begin{aligned} {}^{(n)}\tilde{\mathbf{t}}_A &= \mathcal{R}_{n-1,n}\mathcal{R}_{n-2,n}\cdots\mathcal{R}_{2n}\mathcal{R}_{1n}(\tilde{\mathbf{t}}_n)_A\mathcal{R}^{-1}_{1n}\mathcal{R}^{-1}_{2n}\cdots\mathcal{R}^{-1}_{n-2,n}\mathcal{R}^{-1}_{n-1,n}\otimes\mathbb{I}\otimes\cdots & (5.48a)\\ \text{or}\quad {}^{(n)}\tilde{\mathbf{t}}_A &= \mathcal{R}^{-1}_{n,n-1}\mathcal{R}^{-1}_{n,n-2}\cdots\mathcal{R}^{-1}_{n2}\mathcal{R}^{-1}_{n1}(\tilde{\mathbf{t}}_n)_A\mathcal{R}_{n1}\mathcal{R}_{n2}\cdots\mathcal{R}_{n,n-2}\mathcal{R}_{n,n-1}\otimes\mathbb{I}\otimes\cdots & (5.48b)\end{aligned}$$

We now show that these $\mathcal{U}_{q^{-1}}(\mathfrak{su}(2))$ spinors (resp. $\mathcal{U}_q(\mathfrak{su}(2))$ spinors) can be equivalently obtained by using the quantum parallel transport induced by $\tilde{L}$ (resp. $S(\tilde{L})$) or $S(\tilde{L})^\dagger$ (resp. $\tilde{L}^\dagger$).

Braiding as parallel transport. Let us focus first on the case with all ribbons $R(e_n)$ oriented in the same way corresponding to incoming links in the associated graph. We focus on the N_v-gon $R(v)$.

Proposition 5.4.1. *The braiding induced by the $\mathcal{R}$-matrix can be seen as a parallel transport.*

$$\begin{aligned}
{}^{(n)}\widetilde{\boldsymbol{\tau}}_A &= \mathcal{R}^{-1}_{n-1,n}\mathcal{R}^{-1}_{n-2,n}\cdots\mathcal{R}^{-1}_{2n}\mathcal{R}^{-1}_{1n}(\widetilde{\boldsymbol{\tau}}_n)_A\mathcal{R}_{1n}\mathcal{R}_{2n}\cdots\mathcal{R}_{n-2,n}\mathcal{R}_{n-1,n}\otimes\mathbb{I}\otimes\cdots \\
&= (\tilde{L}\otimes\cdots\otimes\tilde{L}\otimes\widetilde{\boldsymbol{\tau}}_n)_A\otimes\mathbb{I}\otimes\cdots \qquad (5.49)\\
&= \tilde{L}_A{}^{A_2}\otimes\tilde{L}_{A_2}{}^{A_3}\otimes\cdots\otimes\widetilde{\boldsymbol{\tau}}_{A_{n-1}}\otimes\mathbb{I}\otimes\cdots, \\
{}^{(n)}\widetilde{\boldsymbol{\tau}}_A &= \mathcal{R}_{n,n-1}\mathcal{R}_{n,n-2}\cdots\mathcal{R}_{n2}\mathcal{R}_{n1}(\widetilde{\boldsymbol{\tau}}_n)_A\mathcal{R}^{-1}_{n1}\mathcal{R}^{-1}_{n2}\cdots\mathcal{R}^{-1}_{n,n-2}\mathcal{R}^{-1}_{n,n-1}\otimes\mathbb{I}\otimes\cdots \\
\textit{or}\qquad &= (S(\tilde{L})^\dagger\otimes\cdots\otimes S(\tilde{L})^\dagger\otimes\widetilde{\boldsymbol{\tau}}_n)_A\otimes\mathbb{I}\otimes\cdots \qquad (5.50)\\
&= (S(\tilde{L})^\dagger)_A{}^{A_2}\otimes(S(\tilde{L})^\dagger)_{A_2}{}^{A_3}\otimes\cdots\otimes\widetilde{\boldsymbol{\tau}}_{A_{n-1}}\otimes\mathbb{I}\otimes\cdots,
\end{aligned}$$

$$\begin{aligned}
{}^{(n)}\tilde{\mathbf{t}}_A &= \mathcal{R}_{n-1,n}\mathcal{R}_{n-2,n}\cdots\mathcal{R}_{2n}\mathcal{R}_{1n}(\tilde{\mathbf{t}}_n)_A\mathcal{R}^{-1}_{1n}\mathcal{R}^{-1}_{2n}\cdots\mathcal{R}^{-1}_{n-2,n}\mathcal{R}^{-1}_{n-1,n}\otimes\mathbb{I}\otimes\cdots \\
&= (S(\tilde{L})\otimes\cdots\otimes S(\tilde{L})\otimes\tilde{\mathbf{t}}_n)_A\otimes\mathbb{I}\otimes\cdots \qquad (5.51)\\
&= S(\tilde{L})_A{}^{A_2}\otimes S(\tilde{L})_{A_2}{}^{A_3}\otimes\cdots\otimes\tilde{\mathbf{t}}_{A_{n-1}}\otimes\mathbb{I}\otimes\cdots. \\
{}^{(n)}\tilde{\mathbf{t}}_A &= \mathcal{R}^{-1}_{n,n-1}\mathcal{R}^{-1}_{n,n-2}\cdots\mathcal{R}^{-1}_{n2}\mathcal{R}^{-1}_{n1}(\tilde{\mathbf{t}}_n)_A\mathcal{R}_{n1}\mathcal{R}_{n2}\cdots\mathcal{R}_{n,n-2}\mathcal{R}_{n,n-1}\otimes\mathbb{I}\otimes\cdots \\
\textit{or}\qquad &= (\tilde{L}^\dagger\otimes\cdots\otimes\tilde{L}^\dagger\otimes\tilde{\mathbf{t}}_n)_A\otimes\mathbb{I}\otimes\cdots \qquad (5.52)\\
&= (\tilde{L}^\dagger)_A{}^{A_2}\otimes(\tilde{L}^\dagger)_{A_2}{}^{A_3}\otimes\cdots\otimes\tilde{\mathbf{t}}_{A_{n-1}}\otimes\mathbb{I}\otimes\cdots.
\end{aligned}$$

The proof is lengthy and we give it in Proof B.3.2.

Geometric interpretation. We have just shown that the braiding induced by the $\mathcal{R}$-matrix can be explicitly written as a parallel transport along the ribbons using $AN_q(2)$ or $AN_{q^{-1}}(2)$ holonomies[2]. Indeed, equations (5.49) – (5.52) tell us that the algebraic definition of a tensor operator written in terms of the $\mathcal{R}$-matrix can be replaced by a definition which has a very natural geometrical interpretation when working with ribbons.

Let's illustrate the geometrical definition of the tensor operator ${}^{(n)}\widetilde{\boldsymbol{\tau}}$ given in (5.49) in terms of parallel transports by $\tilde{L}$'s. We put consecutively the ribbons, so that they share a node. Let us deal again with the case where all the links are incoming. The construction is illustrated in fig.5.3.

[2]Recall the matrix elements of $AN_q(2)$ and $AN_{q^{-1}}(2)$ are given by the generators of $\mathcal{U}_q(\mathfrak{su}(2))$.

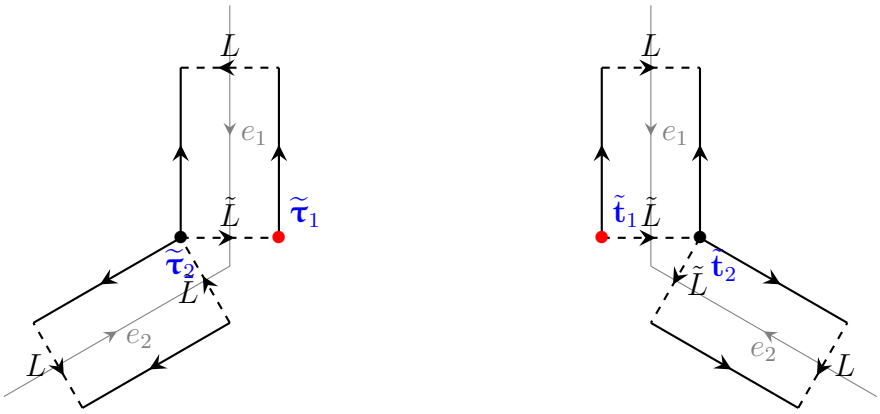

Figure 5.3: The choice of cilium is given by the red bullet. In 5.3a, the orientation is anti-clockwise, while in 5.3b, the orientation is clock-wise. This choice matters since we usually order the tensor product from left to right.

The first step consists in identifying a reference point. This corresponds to choosing a *base corner*. We naturally choose the reference point to sit on the ribbon $R(e_1)$. The construction of the spinor operators will depend on the orientation chosen for the ordering of the ribbons: counterclockwise or clockwise starting from $R(e_1)$. Indeed, the source point can be the left- or right-end point. (Left- or right-end point is specified by sitting at the node in Γ and looking towards the outgoing direction of the relevant link.) Let us choose first the right end point to be our base corner as in fig.5.3a (the node in red). This means that ${}^{(1)}\widetilde{\boldsymbol{\tau}}$ is the reference spinor. We choose to order the ribbons counter-clockwise which is the orientation consistent with the definition of the spinors given in Proposition 5.4.1.

Indeed, the parallel transport by $\tilde{L}$ indicates that we take $\widetilde{\boldsymbol{\tau}}_2$ – which sits at the left-end point of $R(e_1)$ since the right-end point of $R(e_2)$ is identified with the left-end point of $R(e_1)$ – and transport it to the reference point.

We proceed recursively with other ribbons. The object $\widetilde{\boldsymbol{\tau}}_3$ sitting at the right-end point of $R(e_3)$ which is identified with the left end point of $R(e_2)$. We can transport $\widetilde{\boldsymbol{\tau}}_3$ using $\tilde{L}$ to ${}^{(2)}\widetilde{\boldsymbol{\tau}}$, and so on and so forth.

Therefore, the geometrical construction of the spinor operator ${}^{(n)}\widetilde{\boldsymbol{\tau}}$ is obtained by parallel transporting $\widetilde{\boldsymbol{\tau}}_n$, which sits at the right-end point of ribbon $R(e_n)$, along the ribbon short sides using the $\tilde{L}$'s to go from the right-end point to the left-end point of each ribbon until reaching the reference point (the right-end point of $R(e_1)$).

If instead, we choose the base corner to be at the left-end point of ribbon 1, this means we use as a reference $\tilde{\mathbf{t}}$. This means that we order/add ribbons now in a clockwise manner. This is illustrated in the fig.5.3b.

Now let us discuss the case when the links do not have the same orientations.

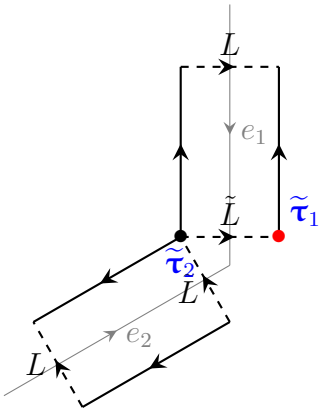

(a) We transport $\widetilde{\boldsymbol{\tau}}_2$ using $\tilde{L}$ to the base corner (in red) to define a spinor ${}^{(2)}\widetilde{\boldsymbol{\tau}}$.

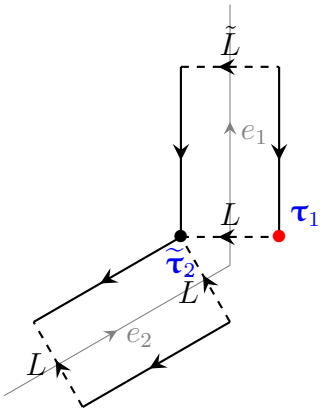

(b) We transport $\widetilde{\boldsymbol{\tau}}_2$ using $\overline{S}(L) = \tilde{L}$ to the base corner (in red) to recover a spinor ${}^{(2)}\widetilde{\boldsymbol{\tau}}$.

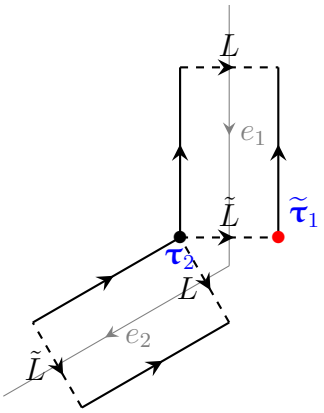

(c) We transport $\boldsymbol{\tau}_2$ using $\tilde{L}$ to the base corner (in red) to recover spinor ${}^{(2)}\boldsymbol{\tau}$.

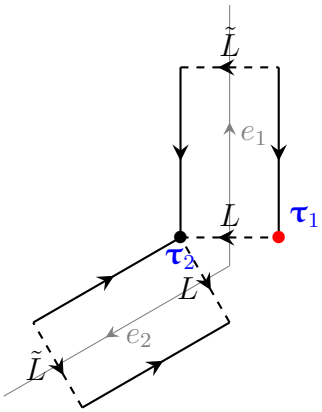

(d) We transport $\boldsymbol{\tau}_2$ using $\overline{S}(L) = \tilde{L}$ to the base corner (in red) to define a spinor ${}^{(2)}\boldsymbol{\tau}$.

Figure 5.4: The choice of base corner, the right-end point of ribbon 1, is given by the red bullet. In each case, we transport the relevant spinor living on right-end point of ribbon 2 using the holonomy in ribbon 1. We recover the same spinor in each case as in the un-flipped case.

Flipping ribbons, again. We again drop the ϵ spinor decoration since it does not bring anything to the present discussion. As discussed in section 5.3, when we flip the orientation of the ribbon, the exchange of variables is performed by I such that

$$I(\mathbf{t}) = \tilde{\mathbf{t}}, \quad I(\boldsymbol{\tau}) = \widetilde{\boldsymbol{\tau}}, \quad I(L) = S(\tilde{L}), \quad I(\tilde{L}) = \overline{S}(L). \tag{5.53}$$

When flipping the orientation of a link in Proposition 5.4.1, it is thus enough to apply the operator I, but only to the factor of the tensor product which corresponds to this link.

For instance, consider $n = 2$ and reverse the orientation of the link 2 only (not 1). Then applying I on ribbon 2 (which we henceforth denote I_2) to the last line of (5.49) gives

$${}^{(2)}\boldsymbol{\tau}_A = I_2(\tilde{L}_A{}^B \otimes \widetilde{\boldsymbol{\tau}}_B) = \tilde{L}_A{}^B \otimes I(\widetilde{\boldsymbol{\tau}}_B) = \tilde{L}_A{}^B \otimes \boldsymbol{\tau}_B \tag{5.54}$$

and to the last line of (5.51),

$${}^{(2)}\mathbf{t}_A = S(\tilde{L})_A{}^B \otimes \mathbf{t}_B. \tag{5.55}$$

The geometric picture is as follows. The first relation (5.54) consists in the case where the base corner is at the right-end point. Because ribbon 2 is flipped, we have $\boldsymbol{\tau}_2$ that stands at the right-end point of ribbon 2 which is identified with the left-end point of ribbon 1. We then parallel transport $\boldsymbol{\tau}_2$ using $\tilde{L}$ on the sector 1 (See Figure 5.4c). The same applies for ${}^{(2)}\mathbf{t}_A$, when the base corner is taken as the left-end point.

Consider now the case where it is ribbon 1 which is flipped (outgoing) but ribbon 2 is *not* (it is incoming), see Figure 5.4b. We thus apply I to the first factor of the tensor product in the last lines of (5.49) and (5.51),

$${}^{(2)}\widetilde{\boldsymbol{\tau}}_A = I_1(\tilde{L}_A{}^B \otimes \widetilde{\boldsymbol{\tau}}_B) = \overline{S}(L)_A{}^B \otimes \widetilde{\boldsymbol{\tau}}_B, \qquad {}^{(2)}\tilde{\mathbf{t}}_A = S(I(\tilde{L}))_A{}^B \otimes \tilde{\mathbf{t}}_B = L_A{}^B \otimes \tilde{\mathbf{t}}_B. \tag{5.56}$$

In the first case, we take the base corner to be the right-end point of ribbon 1, which is decorated by the spinor $\boldsymbol{\tau}_1$. On the right-end point of ribbon 2, identified with the left-end point of ribbon 1, we have $\widetilde{\boldsymbol{\tau}}_2$. We can define a spinor operator by transporting $\widetilde{\boldsymbol{\tau}}_2$ to the base corner through $\overline{S}(L)$, that is $(\overline{S}(L))_A{}^B \otimes \widetilde{\boldsymbol{\tau}}_B$.

When both ribbon 1 and ribbon 2 are flipped, see figure 5.4d, we use the map I_{12} which flips the sectors 1 and 2. As we just discussed, we can define the spinor

$${}^{(2)}\boldsymbol{\tau}_A = I_{12}(\tilde{L}_A{}^B \otimes \widetilde{\boldsymbol{\tau}}_B) = \overline{S}(L)_A{}^B \otimes \boldsymbol{\tau}_B, \qquad {}^{(2)}\mathbf{t}_A = I_{12}(S((\tilde{L}))_A{}^B \otimes \tilde{\mathbf{t}}_B) = L_A{}^B \otimes \mathbf{t}_B. \tag{5.57}$$

We still take the right-end point of ribbon 1 as the reference point, we have now $\boldsymbol{\tau}_1$ sitting at the base corner. At the right-end point of the ribbon 2, coinciding with the left-end

point of ribbon 1, we have $\boldsymbol{\tau}_2$. We can define a spinor operator by transporting $\boldsymbol{\tau}_2$ to the base corner through $\overline{S}(L)$, that is $(\overline{S}(L))_A{}^B \otimes \boldsymbol{\tau}_B$.

To summarize, *the definition of the spinor operator on different ribbons does not depend on the orientation of the links*, since for example $\tilde{L}$ and $\overline{S}(L)$ are the same operators and so are $\widetilde{\boldsymbol{\tau}}$ and $\boldsymbol{\tau}$. So (5.57) is the same as (5.54) and (5.55).

5.5 Scalar observables

We will now proceed to the quantization of the observables defined in Section 3.4. The first part of this section has already appeared in [80, 81, 39]. The spinors are promoted to spinor operators as we have discussed previously. The scalar product is obtained by contracting with Clebsch-Gordan coefficients projecting the tensor product of two spin 1/2 representations to the trivial representation.

Proposition 5.5.1. *The quantization of the general observable (3.65) living on the links e_i and e_j with $i \leq j$ is given by, up to some overall normalization constant,*

$$\mathbf{E}^{\epsilon_i,\epsilon_j}_{e_ie_j} = \begin{cases} \sum_A (-1)^{\frac{1}{2}+A} q^{-\frac{A}{2}} {}^{(i)}\widetilde{\boldsymbol{\tau}}^{\epsilon_i}_{-A} {}^{(j)}\widetilde{\boldsymbol{\tau}}^{\epsilon_j}_{A} \text{ for } o_i = o_j = -1 \\ \sum_A (-1)^{\frac{1}{2}-A} q^{-\frac{A}{2}} {}^{(i)}\boldsymbol{\tau}^{-\epsilon_i}_{-A} {}^{(j)}\widetilde{\boldsymbol{\tau}}^{\epsilon_j}_{A} \text{ for } o_i = -o_j = -1 \\ \sum_A (-1)^{\frac{1}{2}+A} q^{\frac{A}{2}} {}^{(i)}\widetilde{\boldsymbol{\tau}}^{\epsilon_i}_{-A} {}^{(j)}\boldsymbol{\tau}^{-\epsilon_j}_{A} \text{ for } o_i = -o_j = 1 \\ \sum_A (-1)^{\frac{1}{2}-A} q^{\frac{A}{2}} {}^{(i)}\boldsymbol{\tau}^{-\epsilon_i}_{-A} {}^{(j)}\boldsymbol{\tau}^{-\epsilon_j}_{A} \text{ for } o_i = o_j = 1 \end{cases} . \tag{5.58}$$

Since the quantum operators $\boldsymbol{\tau}^\epsilon$ and $\widetilde{\boldsymbol{\tau}}^\epsilon$ have the same matrix element, or as we discussed in section 5.3 the spinors are invariant under the flip of the ribbon, *the observables for the different orientations in Proposition 5.5.1 are actually the same*[3]. A natural question to enquire is the algebra that they satisfy, if they satisfy one. One can indeed check that if we were to build observables from the fluxes, the algebra of observables would not close (even with no quantum deformation [118]). The great advantage of using spinor variables is that they provide a closed algebra of observables [118, 98, 120]. In the non-deformed case, the algebra of observables is given in terms of the $\mathfrak{so}^*(2n)$ Lie algebra [120] where n here stands for the number of links meeting at the node of Γ.

[3]We remind the readers that the observable defined in (5.58) is not the same as in [42] for different orientations. Here the $\mathbf{E}_{ij}$'s are defined in the same way for different orientations of e_i and e_j, while they are defined differently in [42] for a uniform action on the intertwiners for different orientation cases.

If we denote the generators of $\mathfrak{so}^*(2n)$ by $e_{ij}, f_{ij}, \tilde{f}_{ij}, i, j = 1, \cdots, n$, their commutation relations are

$$\begin{aligned}&[e_{ij}, e_{kl}] = \delta_{jk}e_{il} - \delta_{il}e_{kj}\,, \quad [e_{ij}, f_{kl}] = \delta_{il}f_{jk} - \delta_{ik}f_{jl}\,, \quad [e_{ij}, g_{kl}] = \delta_{jk}g_{il} - \delta_{jl}g_{ik}\,,\\ &[f_{ij}, g_{kl}] = \delta_{jl}e_{ki} + \delta_{ik}e_{lj} - \delta_{jk}e_{li} - \delta_{il}e_{kj}\,, \quad [f_{ij}, f_{kl}] = [g_{ij}, g_{kl}] = 0\,.\end{aligned} \tag{5.59}$$

We can identify $\mathfrak{u}(n)$ as a sub-Lie algebra of $\mathfrak{so}^*(2n)$ which is generated by $\{e_{ij}\}$.

We want to show now that a similar statement holds in the deformed case, *i.e.* we have a deformation of the $\mathfrak{so}^*(2n)$ algebra which contains a deformation of the $\mathfrak{u}(n)$ algebra. The deformation of the $\mathfrak{u}(n)$ algebra was already identified in [81] using the $\mathcal{R}$-matrix formalism. We extend here the construction to have the full deformation of $\mathfrak{so}^*(2n)$. We are first going to recover the deformed substructure $\mathcal{U}_q(\mathfrak{u}(n))$ then the full deformed algebra $\mathcal{U}_q(\mathfrak{so}^*(2n))$.

Given a semi-simple Lie algebra, its deformation is given in terms of the Serre-Chevalley relations [58]. The (Cartan-Weyl) generators are constructed by induction.

We have constructed a set of observables using the spinor parametrization. As we discussed, we can obtain different parametrizations because we can use different types of parallel transport, either L or $S(L)^\dagger$. Hence in terms of the spinor parameterization, we also have some arbitrariness in terms of the explicit expression of the observables. We know that at the classical level these observables form the algebra $\mathfrak{so}^*(2n)$. Hence we could apply the Serre-Chevalley induction for the deformed case. The goal is then to relate this construction to the parameterization in terms of the spinors. We are going to show that *the Serre-Chevalley construction picks exclusively the parallel transport induced by* $S(L)^\dagger$. Let us recall more details on the Serre-Chevalley induction process to fix the notations.

The definition of the $\mathcal{U}_q(\mathfrak{u}(n))$ from the Cartan-Weyl generators $\mathcal{E}_{ij}$ is as follows [33]. We first specify the Chevalley set of generators containing $n-1$ raising, $n-1$ lowering and $n-1$ diagonal generators, denoted respectively as $\mathcal{E}_{i,i+1}$, $\mathcal{E}_{i,i-1}$, and $\mathcal{E}_i$, which satisfy the following commutation relations

$$\begin{gathered}[\mathcal{E}_i, \mathcal{E}_j] = 0\,, \quad [\mathcal{E}_i, \mathcal{E}_{j,j+1}] = (\delta_{ij} - \delta_{i,j+1})\mathcal{E}_{j,j+1}\,, \quad [\mathcal{E}_i, \mathcal{E}_{j+1,j}] = (\delta_{i,j+1} - \delta_{ij})\mathcal{E}_{j+1,j}\,,\\ [\mathcal{E}_{i,i+1}, \mathcal{E}_{j+1,j}] = \delta_{ij}[\mathcal{E}_i - \mathcal{E}_{i+1}]\,.\end{gathered} \tag{5.60}$$

The remaining Cartan-Weyl generators $\mathcal{E}_{ij}$ and $\mathcal{E}_{ji}$ with $j > i+1$ are defined recursively as follows.

$$\mathcal{E}_{ij} := q^{\frac{N_{j-1}}{2}}\left(\mathcal{E}_{i,j-1}\mathcal{E}_{j-1,j} - q^{\frac{1}{2}}\mathcal{E}_{j-1,j}\mathcal{E}_{i,j-1}\right)\,, \tag{5.61a}$$

$$\mathcal{E}_{ji} := q^{-\frac{N_{j-1}}{2}}\left(\mathcal{E}_{j,j-1}\mathcal{E}_{j-1,i} - q^{-\frac{1}{2}}\mathcal{E}_{j-1,i}\mathcal{E}_{j,j-1}\right)\,. \tag{5.61b}$$

By the Jordan map, the Chevalley set can be defined in terms of the q-bosons $(a_i, a_i^\dagger, b_i, b_i^\dagger)$:

$$\left|\begin{array}{l} \mathcal{E}_{i,i+1} = a_i^\dagger a_{i+1} q^{\frac{N_{b_i}-N_{b_{i+1}}}{4}} + b_i^\dagger b_{i+1} q^{\frac{-N_{a_i}+N_{a_{i+1}}}{4}}\,, \\ \mathcal{E}_{i+1,i} = a_i a_{i+1}^\dagger q^{\frac{N_{b_i}-N_{b_{i+1}}}{4}} + b_i b_{i+1}^\dagger q^{\frac{-N_{a_i}+N_{a_{i+1}}}{4}}\,, \end{array}\right. \qquad \mathcal{E}_i = N_i + 1\,, \tag{5.62}$$

and other generators in terms of the q-bosons can be deduced from (5.61). We can then identify directly the relations between the $\mathcal{U}_q(\mathfrak{u}(n))$ Chevalley set of generators and the quadratic operators constructed from the deformed quantum spinors. They simply are

$$\mathbf{E}^{+,-}_{i,i+1} = \mathcal{E}_{i,i+1}\,, \quad \mathbf{E}^{-,+}_{i,i+1} = \mathcal{E}_{i+1,i}\,, \quad \mathbf{E}^{+,-}_{i,i} = [\mathcal{E}_i - 1]\,, \quad \mathbf{E}^{-,+}_{i,i} = [\mathcal{E}_i + 1]\,. \tag{5.63}$$

For the remaining Cartan-Weyl generators in terms of the quantum spinors, one can make use of the quantum fluxes to connect the spinors from distanced sites. The result is given in the following proposition.

Proposition 5.5.2. *The Cartan-Weyl generators $\mathcal{E}_{i,i+p}$ and $\mathcal{E}_{i+p,i}$ of $\mathcal{U}_q(\mathfrak{u}(n))$ for any $p \in \mathbb{N}^+$ can be expressed with the quantum spinors at sites i and $i+p$ and the quantum fluxes for ribbon links connecting them. Explicitly, they can be written as*

$$\mathcal{E}_{i,i+p} = q^{\frac{\sum_{k=1}^{p-1} N_{i+k}}{4}} \sum_{\substack{A_i, A_{i+1}, \\ \cdots, A_{i+p}}} (-1)^{\frac{1}{2}+A_i} q^{\frac{A_i}{2}} \tilde{\mathbf{t}}^+_{i,-A_i} \prod_{k=1}^{p-1} (S(\tilde{L}_{i+k})^\dagger)_{A_{i+k-1}}{}^{A_{i+k}} \widetilde{\boldsymbol{\tau}}^-_{i+p,A_{i+p-1}}\,, \tag{5.64}$$

$$\mathcal{E}_{i+p,i} = q^{-\frac{\sum_{k=1}^{p-1} N_{i+k}}{4}} \sum_{\substack{A_i, A_{i+1}, \\ \cdots, A_{i+p}}} (-1)^{\frac{1}{2}-A_i} q^{\frac{A_i}{2}} \tilde{\mathbf{t}}^-_{i,-A_i} \prod_{k=1}^{p-1} (S(\tilde{L}_{i+k})^\dagger)_{A_{i+k-1}}{}^{A_{i+k}} \widetilde{\boldsymbol{\tau}}^+_{i+p,A_{i+p-1}}\,. \tag{5.65}$$

Proof. Notice that the following relations are satisfied.

$$\widetilde{\boldsymbol{\tau}}^-_{i,A} \tilde{\mathbf{t}}^+_{i,B} - q^{\frac{1}{2}} \tilde{\mathbf{t}}^+_{i,B} \widetilde{\boldsymbol{\tau}}^-_{i,A} = q^{-\frac{N_i}{4}} (-1)^{\frac{1}{2}-B} q^{\frac{B}{2}} \left(S(\tilde{L}_i)^\dagger\right)_A{}^{-B} \equiv q^{-\frac{N_i}{4}} (-1)^{\frac{1}{2}+A} q^{-\frac{A}{2}} \left(\tilde{L}_i^\dagger\right)_B{}^{-A}\,, \tag{5.66a}$$

$$\tilde{\mathbf{t}}^-_{i,A} \widetilde{\boldsymbol{\tau}}^+_{i,B} - q^{-\frac{1}{2}} \widetilde{\boldsymbol{\tau}}^+_{i,B} \tilde{\mathbf{t}}^-_{i,A} = q^{\frac{N_i}{4}} (-1)^{\frac{1}{2}+A} q^{\frac{A}{2}} \left(S(\tilde{L}_i)^\dagger\right)_B{}^{-A} = q^{\frac{N_i}{4}} (-1)^{\frac{1}{2}-B} q^{-\frac{B}{2}} \left(\tilde{L}_i^\dagger\right)_A{}^{-B}\,. \tag{5.66b}$$

Using the scalar operator of two spinors at the same corner to define the $\mathcal{U}_q(\mathfrak{u}(n))$ generator

$$\mathcal{E}_{i,i+1} = \sum_{A_i = \pm\frac{1}{2}} (-1)^{\frac{1}{2}+A_i} q^{\frac{A_i}{2}} \tilde{\mathbf{t}}^+_{i,-A_i} \widetilde{\boldsymbol{\tau}}^-_{i+1,A_i}\,, \quad \mathcal{E}_{i+1,i} = \sum_{A_i = \pm\frac{1}{2}} (-1)^{\frac{1}{2}-A_i} q^{\frac{A_i}{2}} \tilde{\mathbf{t}}^-_{i,-A_i} \widetilde{\boldsymbol{\tau}}^+_{i+1,A_i}\,, \tag{5.67}$$

and the induction, one can show the validity of (5.64) and (5.65). □

We extend the construction to include all the different types of observables and verify that the observables $\mathbf{E}_{ij}^{\epsilon_i,\epsilon_j}$ are the generators of $\mathcal{U}_q(\mathfrak{so}^*(2n))$, which is the q-deformation of the algebra $\mathfrak{so}^*(2n)$ [120]. Denote for different sectors ϵ_i and ϵ_j for the quadratic operator $\mathbf{E}_{ij}^{\epsilon_i,\epsilon_j}$ as

$$\begin{aligned}
&\mathcal{E}_{i,i} \equiv \mathcal{E}_i := N_i + 1\,, \quad \mathcal{E}_{i,i+p} := \mathbf{E}_{i,i+p}^{+,-}\,, \qquad \mathcal{E}_{i+p,i} := \mathbf{E}_{i,i+p}^{-,+}\,, \\
&\mathcal{F}_{i,i+p} := \mathbf{E}_{i,i+p}^{-,-}\,, \qquad \mathcal{F}_{i+p,i} := -\mathcal{F}_{i,i+p}\,, \quad \mathcal{G}_{i,i+p} := -\mathbf{E}_{i,i+p}^{+,+}\,, \quad \mathcal{G}_{i+p,i} := -\mathcal{G}_{i,i+p}\,.
\end{aligned} \tag{5.68}$$

Proposition 5.5.3. *The operators $\mathcal{F}_{i,i+p}$ and $\mathcal{G}_{i,i+p}$ with $p > 1$ defined in (5.68) satisfy the recursion relations in terms of $\mathcal{E}_{ij}$ as follows.*

$$\begin{aligned}
\mathcal{F}_{i,i+p} &= q^{\frac{N_{i+p-1}}{2}} \left(\mathcal{F}_{i,i+p-1}\mathcal{E}_{i+p-1,i+p} - q^{\frac{1}{2}} \mathcal{E}_{i+p-1,i+p}\mathcal{F}_{i,i+p-1} \right) \\
&= \left(\mathcal{F}_{i+1,i+p}\mathcal{E}_{i+1,i} - q^{-\frac{1}{2}} \mathcal{E}_{i+1,i}\mathcal{F}_{i+1,i+p} \right)\,,
\end{aligned} \tag{5.69a}$$

$$\begin{aligned}
\mathcal{G}_{i,i+p} &= q^{-\frac{N_{i+p-1}}{2}} \left(\mathcal{E}_{i+p,i+p-1}\mathcal{G}_{i,i+p-1} - q^{-\frac{1}{2}} \mathcal{G}_{i,i+p-1}\mathcal{E}_{i+p,i+p-1} \right) \\
&= \left(\mathcal{E}_{i,i+1}\mathcal{G}_{i+1,i+p} - q^{\frac{1}{2}} \mathcal{G}_{i+1,i+p}\mathcal{E}_{i,i+1} \right)\,.
\end{aligned} \tag{5.69b}$$

The operators $\mathcal{E}_{i,i+1}$, $\mathcal{F}_{i,i+1}$ and $\mathcal{G}_{i,i+1}$ defined in (5.68) form the generators of $\mathcal{U}_q(\mathfrak{so}^*(2n))$ which is a closed algebra. These generators satisfy (5.60) and the following commutation relations.

$$\begin{aligned}
&\mathcal{E}_{i,i+1}\mathcal{F}_{j,j+1} - q^{-\frac{1}{2}}\mathcal{F}_{j,j+1}\mathcal{E}_{i,i+1} = \delta_{i,j+1} q^{-\frac{\mathcal{E}_i}{2}} \mathcal{F}_{i+1,i-1}\,, \\
&q^{-\frac{1}{2}}\mathcal{E}_{i+1,i}\mathcal{F}_{j,j+1} - \mathcal{F}_{j,j+1}\mathcal{E}_{i+1,i} = -\delta_{i,j-1}\mathcal{F}_{i,i+2}\,, \\
&\mathcal{E}_{i,i+1}\mathcal{G}_{j,j+1} - q^{\frac{1}{2}}\mathcal{G}_{j,j+1}\mathcal{E}_{i,i+1} = \delta_{i,j-1}\mathcal{G}_{i,i+2}\,, \\
&q^{\frac{1}{2}}\mathcal{E}_{i+1,i}\mathcal{G}_{j,j+1} - \mathcal{G}_{j,j+1}\mathcal{E}_{i+1,i} = -\delta_{i,j+1} q^{\frac{\mathcal{E}_i}{2}} \mathcal{G}_{i+1,i-1}\,, \\
&[\mathcal{E}_i, \mathcal{F}_{j,j+1}] = -(\delta_{ij} + \delta_{i,j+1})\mathcal{F}_{j,j+1}\,, \quad [\mathcal{E}_i, \mathcal{G}_{j,j+1}] = (\delta_{ij} + \delta_{i,j+1})\mathcal{G}_{j,j+1}\,, \\
&[\mathcal{F}_{i,i+1}, \mathcal{G}_{j,j+1}] = \delta_{ij}\left([\mathcal{E}_i + \mathcal{E}_{i+1}]\right) - \delta_{i,j-1}\mathcal{E}_{i+2,i} - \delta_{i,j+1}\mathcal{E}_{i-1,i+1}\,, \\
&[\mathcal{F}_{i,i+1}, \mathcal{F}_{j,j+1}] = [\mathcal{G}_{i,i+1}, \mathcal{G}_{j,j+1}] = 0\,.
\end{aligned} \tag{5.70}$$

The first two lines can be seen directly from (5.69). The rest of the commutation relations can be calculated with the definition (5.68) of the generators and the relation between the spinors and the flux as shown in (5.66). The commutation relations (5.70) are consistent with (5.59) when $q \to 1$, and it is in this sense that we view the operators $\mathcal{E}_{i,i+1}$, $\mathcal{F}_{i,i+1}$ and $\mathcal{G}_{i,i+1}$ as the generators of $\mathcal{U}_q(\mathfrak{so}^*(2n))$.

In this chapter, we have revisited the q-deformed LQG in terms of the quantum spinors. We have extended the spinor formalism whose classical setup was initiated in [79] and the quantum aspect was touched in [81]. We have shown how all the regular variables of LQG, namely the flux and the holonomy are defined in the deformed case and can be expressed in terms of the spinor operators which are the fundamental building blocks to build the observables. We were able to recover the fundamental observables, defined in terms of the spinor operators which are local objects, associated with a node of the graph. This algebra is a deformation of the $\mathfrak{so}^*(2n)$ algebra where n is the number of links at the node of interest.

This framework was instrumental to study the dynamical aspects in the context of 3D gravity with a cosmological constant, which we will illustrate in the next chapter. See also the work [42] by the author and collaborators. In particular, it allows us to connect the canonical approach (LQG) to the spinfoam models using recursion relations.

Another important aspect we recovered is the interpretation of braiding in terms of parallel transport. In a way, this is not so surprising as the ribbon structure shares a lot of similarities with integrable systems where the L operators (or T operators in the standard notation of integrable systems) and the $\mathcal{R}$-matrix have appeared [184]. This geometric interpretation provides a more intuitive framework than using the R-matrix to do calculations. It was extensively used for example in [42] as it rendered the calculations much more amenable.

Chapter 6

Hamiltonian constraint in spinor representation

Having described the kinematics of the q-deformed LQG in terms of spinors, we now study the dynamics and physical states that solve the Hamiltonian constraint. Since 3D gravity is a topological theory, the physical states ought to be topological invariant.

On the other hand, knowing the physical states helps connecting LQG with other quantum gravity approaches. For instance, in the case of $\Lambda = 0$, it has been shown by Noui and Perez in [162] that the scalar products of physical spin network states defined in LQG are given by the Ponzano-Regge amplitudes from the spinfoam model [173, 22, 21, 164, 138].

It has been shown in [43, 44] that the Hamiltonian constraint translates in the spin network basis as *difference equations* on the coefficients of the physical states. These difference equations should really be seen as Wheeler-DeWitt equations for 3D LQG. In particular, they are solved by spin network evaluations, which is consistent with the Ponzano-Regge model.

Therefore, it is natural to expect that the spinfoam amplitude for $\Lambda \neq 0$ can be reproduced by solving the Hamiltonian constraint in the LQG model with a non-vanishing Λ. Such a spinfoam model is the Turaev-Viro model [204]. It is known to provide the partition function of 3D gravity in Euclidean signature with a positive cosmological constant [10]. It is expressed as a sum of states in $\mathrm{SU}_q(2)$ representation, with q a root of unity encoding the cosmological constant. It is thus a q-deformation of the Ponzano-Regge model, further providing a regularization through a natural cut-off on representations when replacing $\mathrm{SU}(2)$ with $\mathrm{SU}_q(2)$. The large spin limit of the q-6j symbol matches the Regge calculus for curved tetrahedra [199]. The Turaev-Viro model thus provides an example of the interplay

between the cosmological constant, curved geometries and the quantum group deformation of Lie groups.

On the LQG side, the Hamiltonian takes a more complicated form when the cosmological constant is non-zero, so much so that even how to discretize it has been unclear and it seems to evade traditional LQG methods. It has nevertheless been conjectured for a long time that the quantum theory ought to be described by quantum groups, as expected from the spin foam model [192, 190, 49, 150, 191]. One (indirect) way to relate 3D LQG with a $\lambda \neq 0$ to the Turaev-Viro model is to take the Chern-Simons formulation of 3D gravity and consider the Witten-Reshetikhin-Turaev path integral $\mathcal{Z}_{WRT}(\mathcal{M})$ on a 3-manifold $\mathcal{M}$ with the Chern-Simons actions with opposite levels, say k and $-k$. It has been well-known that the Turaev-Viro state sum matches such path integral as $\mathcal{Z}_{TV}(\mathcal{M}) = |\mathcal{Z}_{WRT}(\mathcal{M})|^2$ [207, 205].

A more direct way to bridge the two quantum gravity approaches — LQG and spinfoam models — is to consider the q-deformed LQG model. In fact, this model provides a natural starting point to construct the Hamiltonian constraint that describes 3D homogeneously curved geometries built from 2D curved building blocks. This is because in this model, the kinematical phase space, hence the kinematical Hilbert space, is solved by the Gauss constraint that encodes the cosmological constant [80].

In [39], the dynamics of the kinematical states has been investigated, using the same techniques as in [43], *i.e.* by building a Hamiltonian constraint out of the flatness constraints. It can be classically interpreted as generating displacements of the vertices of the triangulation [38]. At the quantum level, the Hamiltonian constraints give rise to *difference equations*, which can therefore be considered as Wheeler-DeWitt equations in the spin network basis. [39] considers the (simple) case of the boundary of the tetrahedron, and showed that the solution to those difference equations is the q-6j symbol, which is consistent with the amplitude in the Turaev-Viro model (when the parameter q is extended to be real). This result thus gives a new connection between the LQG and the spinfoam approaches for $\Lambda \neq 0$ case.

Here we are interested in using the spinorial formalism introduced in Chapter 3 and Chapter 5 instead of holonomies and fluxes, and further extracting all building blocks for the transition amplitudes, *i.e.* going beyond the case of the tetrahedron from [39]. In Chapter 4 and 5 (which are based on [41]), we have revisited all kinematical aspects of the q-deformed LQG model in detail, and in the spinor representation. In particular, the quantization of the deformed spinors are performed in terms of q-bosons. We have also used those q-bosons to define the invariant operators. These operators will be needed for quantizing the Hamiltonian constraint in spinor variables.

This chapter is based on the work in [42] by the author and collaborators. In Section 6.1, we construct the spinorial representation of the flatness constraints in terms of the deformed spinors, following [41], and construct the classical Hamiltonian constraints. We then perform the quantization in Section 6.2. This is where in particular we find the difference equations encoding the Wheeler-DeWitt equations in the spin network basis. Then in Section 6.3, we study how solutions to the difference equations are related under Pachner moves, thereby providing the building blocks for the transition amplitudes *à la* Turaev-Viro. We collect some of the lengthy proofs in Appendix B.4.

6.1 Classical Hamiltonian constraint

Defining the kinematical phase space (*resp.* kinematical Hilbert space), we did impose the Gauss constraint. Gravity has another set of constraints, the flatness constraints. The flatness constraints generate (deformed) translations. We need to impose the flatness constraint to define the physical phase space (*resp.* physical Hilbert space). In this section, we express these flatness constraints in terms of the deformed spinors. This allows us to define scalar constraints in terms of the scalar products of the deformed spinors, whose quantization has been analyzed in the last chapter.

Consider a face f surrounded by d links. Choose a random link of reference and denote it e_1, then $e_2, \dots, e_d$ are the links encountered counter-clockwise around f. For all possible orientations of the links $e_1, \dots, e_d$ on the boundary of f, the SU(2) matrices $u_{e_i v}$ are all counter-clockwise, where v denotes the target node of e_i when e_i is oriented counter-clockwisely, pictured in fig.6.1. The flatness constraint on f reads

$$u_{e_d v_1} \cdots u_{e_2 v_3} u_{e_1 v_2} = \mathbb{I}\,, \tag{6.1}$$

as pictured in fig.6.1.

Let us rewrite the holonomies for one ribbon in terms of the deformed spinors which is graphically illustrated in fig.3.3.

$$u = \frac{|\tau\rangle[\tilde{t}| - |\tau]\langle\tilde{t}|}{\sqrt{\langle\tau|\tau\rangle\langle\tilde{t}|\tilde{t}\rangle}}\,, \qquad \tilde{u} = \frac{|t\rangle[\tilde{\tau}| - |t]\langle\tilde{\tau}|}{\sqrt{\langle t|t\rangle\langle\tilde{\tau}|\tilde{\tau}\rangle}}\,, \tag{6.2}$$

with $N_0 + N_1 = \tilde{N}_0 + \tilde{N}_1$.

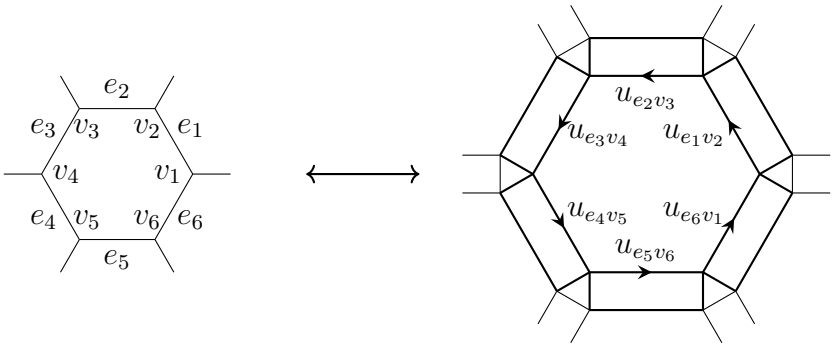

Figure 6.1: When considering ribbon links and ribbon nodes, the face on the left bounded by links $e_1, \cdots, e_6$ becomes bounded by long links on the right. All matrices $u_{e_i v_{i+1}}, i = 1, \cdots, 6$ are oriented counter-clockwise around the face.

In order to write the holonomies in a uniform way, we introduce the notations that is different from those in Chapter 3 as follows.

$$\begin{aligned} t_A^- &:= (-1)^{\frac{1}{2}+A} t_A, \\ t_A^+ &:= \bar{t}_{-A}, \end{aligned} \qquad \text{and} \qquad \begin{aligned} \tilde{t}_A^- &:= (-1)^{\frac{1}{2}+A} \tilde{t}_A\,, \\ \tilde{t}_A^+ &:= \bar{\tilde{t}}_{-A}\,. \end{aligned} \tag{6.3}$$

for $A = \pm 1/2$. Similar but exchanged notations are used for τ and $\tilde{\tau}$,

$$\begin{aligned} \tau_A^- &:= \tau_A\,, \\ \tau_A^+ &:= (-1)^{\frac{1}{2}-A} \bar{\tau}_{-A}\,, \end{aligned} \qquad \text{and} \qquad \begin{aligned} \tilde{\tau}_A^- &:= \tilde{\tau}_A\,, \\ \tilde{\tau}_A^+ &:= (-1)^{\frac{1}{2}-A} \bar{\tilde{\tau}}_{-A}\,. \end{aligned} \tag{6.4}$$

For reference, we explicitly write the spinors and dual spinors with those notations in a footnote[1]. The norms read

$$\begin{aligned} \langle t|t\rangle &= \tfrac{1}{2} \textstyle\sum_{\epsilon=\pm} \sum_{A=\pm\frac{1}{2}} \epsilon (-1)^{\frac{1}{2}+A}\, t_A^\epsilon t_{-A}^{-\epsilon}\,, \quad & \langle \tilde{t}|\tilde{t}\rangle &= \tfrac{1}{2} \textstyle\sum_{\epsilon=\pm} \sum_{A=\pm\frac{1}{2}} \epsilon (-1)^{\frac{1}{2}+A}\, \tilde{t}_A^\epsilon \tilde{t}_{-A}^{-\epsilon}\,, \\ \langle \tau|\tau\rangle &= \tfrac{1}{2} \textstyle\sum_{\epsilon=\pm} \sum_{A=\pm\frac{1}{2}} \epsilon (-1)^{\frac{1}{2}+A}\, \tau_A^\epsilon \tau_{-A}^{-\epsilon}\,, \quad & \langle \tilde{\tau}|\tilde{\tau}\rangle &= \tfrac{1}{2} \textstyle\sum_{\epsilon=\pm} \sum_{A=\pm\frac{1}{2}} \epsilon (-1)^{\frac{1}{2}+A}\, \tilde{\tau}_A^\epsilon \tilde{\tau}_{-A}^{-\epsilon}\,. \end{aligned}$$

[1]

$$\begin{aligned} |t\rangle &= \begin{pmatrix} t_-^- \\ -t_+^- \end{pmatrix}, & |t] &= \begin{pmatrix} -t_-^+ \\ t_+^+ \end{pmatrix}, & |\tilde{t}\rangle &= \begin{pmatrix} \tilde{t}_-^- \\ -\tilde{t}_+^- \end{pmatrix}, & |\tilde{t}] &= \begin{pmatrix} -\tilde{t}_-^+ \\ \tilde{t}_+^+ \end{pmatrix}, \\ \langle t| &= \begin{pmatrix} t_+^+, & t_-^+ \end{pmatrix}, & [t| &= \begin{pmatrix} t_+^-, & t_-^- \end{pmatrix}, & \langle \tilde{t}| &= \begin{pmatrix} \tilde{t}_+^+, & \tilde{t}_-^+ \end{pmatrix}, & [\tilde{t}| &= \begin{pmatrix} \tilde{t}_+^-, & \tilde{t}_-^- \end{pmatrix}, \\ |\tau\rangle &= \begin{pmatrix} \tau_-^- \\ \tau_+^- \end{pmatrix}, & |\tau] &= \begin{pmatrix} \tau_-^+ \\ \tau_+^+ \end{pmatrix}, & |\tilde{\tau}\rangle &= \begin{pmatrix} \tilde{\tau}_-^- \\ \tilde{\tau}_+^- \end{pmatrix}, & |\tilde{\tau}] &= \begin{pmatrix} \tilde{\tau}_-^+ \\ \tilde{\tau}_+^+ \end{pmatrix}, \\ \langle \tau| &= \begin{pmatrix} \tau_+^+, & -\tau_-^+ \end{pmatrix}, & [\tau| &= \begin{pmatrix} -\tau_+^-, & \tau_-^- \end{pmatrix}, & \langle \tilde{\tau}| &= \begin{pmatrix} \tilde{\tau}_+^+, & -\tilde{\tau}_-^+ \end{pmatrix}, & [\tilde{\tau}| &= \begin{pmatrix} -\tilde{\tau}_+^-, & \tilde{\tau}_-^- \end{pmatrix}, \end{aligned} \tag{6.5}$$

where the subscripts $A = \pm\frac{1}{2}$ have been notated as $A = \pm$ for simplicity.

and the holonomies

$$u_{AB} = -\frac{1}{\sqrt{\langle\tau|\tau\rangle\langle\tilde{t}|\tilde{t}\rangle}} \sum_{\epsilon=\pm} \epsilon \tau_A^\epsilon \tilde{t}_{-B}^\epsilon \qquad \tilde{u}_{AB}^{-1} = \frac{1}{\sqrt{\langle\tilde{\tau}|\tilde{\tau}\rangle\langle t|t\rangle}} \sum_{\epsilon=\pm} \epsilon\ \tilde{\tau}_A^\epsilon t_{-B}^\epsilon \tag{6.6}$$

Using the notations (6.3) and (6.4), we can give a uniform expression for the four possible scalar products at fixed orientations. For example, when both links are outgoing,

$$E^{\epsilon_2,\epsilon_1}_{e_2e_1} := \sum_{A=\pm 1/2} \tau^{\epsilon_2}_{2,-A} t^{\epsilon_1}_{1,A} = \begin{cases} \langle t_2|\tau_1] & \text{for } \epsilon_1 = +, \epsilon_2 = + \\ \langle t_2|\tau_1\rangle & \text{for } \epsilon_1 = -, \epsilon_2 = + \\ [t_2|\tau_1] & \text{for } \epsilon_1 = +, \epsilon_2 = - \\ [t_2|\tau_1\rangle & \text{for } \epsilon_1 = -, \epsilon_2 = - \end{cases}. \tag{6.7}$$

The other orientations are obtained by changing τ_1 to $\tilde{\tau}_1$ and/or t_2 to $\tilde{t}_2$ as described in Section 3.4. The invariant is still denoted $E^{\epsilon_2,\epsilon_1}_{e_2,e_1}$.

It will be convenient to encode all orientations and have a fully uniform way of writing the invariant. We orient the wedge (containing the two links e_1 and e_2 and the node they incident to, shown in red in the left panel of fig.6.1) between e_1 and e_2 to be counter-clockwise. We say that the orientation o_i of e_i for $i = 1, 2$ is positive if it matches that of the wedge, and negative otherwise[2]. We denote the spinors meeting there as t_{e_1v} and t_{e_2v} according to

	t_{e_1v}
$o_1 = 1$	$\tilde{\tau}_1$
$o_1 = -1$	τ_1

	t_{e_2v}
$o_2 = 1$	t_2
$o_2 = -1$	$\tilde{t}_2$

(6.8)

so that

$$E^{\epsilon_2,\epsilon_1}_{e_2e_1} = \begin{cases} \langle t_{e_2v}|t_{e_1v}] & \text{for } \epsilon_1 = +, \epsilon_2 = + \\ \langle t_{e_2v}|t_{e_1v}\rangle & \text{for } \epsilon_1 = -, \epsilon_2 = + \\ [t_{e_2v}|t_{e_1v}] & \text{for } \epsilon_1 = +, \epsilon_2 = - \\ [t_{e_2v}|t_{e_1v}\rangle & \text{for } \epsilon_1 = -, \epsilon_2 = - \end{cases} \tag{6.9}$$

By plugging u and $\tilde{u}$ from (6.2) into the flatness constraint (6.1), one obtains a spinorial expression of the constraint. Then by taking the matrix elements of the constraints between different spinors, we get some scalar constraints which we call *Hamiltonian constraints*. They are the κ-deformed versions of [44].

[2]The convention for the orientation o_i is indeed different from that used in constructing the scalar products, see *e.g.* (3.60), since we are now referring to the orientation of a face instead of that of a ribbon node.

We first write the Hamiltonian constraints generally, *i.e.* on faces of arbitrary lengths, then specialize them to the case of faces of length 3.

The Hamiltonian on a face of arbitrary degree

Let f be a face of length d. We will introduce a constraint, derived from the flatness constraint, for every pair of links (e, e') around f. Label the links counter-clockwise around f as $e_1, \dots, e_d$. Without loss of generality, we set the pair (e, e') which labels our function to (e_1, e_k) for $k \in \{2, \dots, d\}$. Label the nodes around f as $v_1, \dots, v_d$ counter-clockwise, such that e_i is incident to v_i and v_{i+1}, for $i = 1, \dots, d \mod d$, as shown in fig.6.2. We assume that f visits each node and link exactly once (as when Γ is dual to a simplicial complex), so that all e_i's and v_i's are distinct. By convention, we denote the orientation

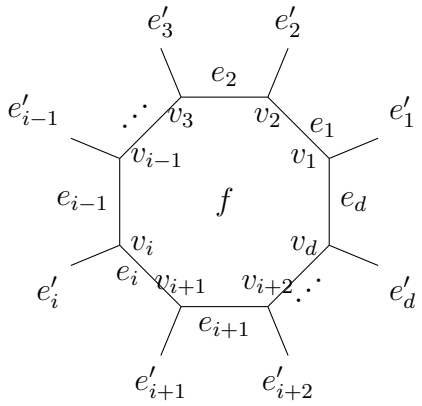

Figure 6.2: A sunny graph with links $e_1, \cdots, e_d$ counterclockwise oriented around the face f. Each triple of links (e_i, e_{i-1}, e'_i) are incident to a node v_i.

$o_i = 1$ if e_i is counter-clockwise and $o_i = -1$ elsewise (this is the relative orientation of the link with respect to the counter-clockwise orientation of f). With the notation u_{ev} introduced earlier, the flatness constraint reads $u_{e_d v_1} \cdots u_{e_2 v_3} u_{e_1 v_2} = \mathbb{I}$ in SU(2). In order to simplify the notations a bit, we will use

$$u_{e_i f} := u_{e_i v_{i+1}} = \begin{cases} \tilde{u}_{e_i}^{-1}\,, & \text{if } o_1 = 1\,, \\ u_{e_i}\,, & \text{if } o_1 = -1\,. \end{cases} \tag{6.10}$$

Furthermore we denote as $t_{e_i v_i}$ the spinor along the long side of $R(e_i)$ which is incident to both f and v_i. It is determined by the orientation of e_i,

$$\begin{aligned} o_i = 1 \quad &\Rightarrow \quad t_{e_i v_i} = t_{e_i} \quad \text{and} \quad t_{e_i v_{i+1}} = \tilde{\tau}_{e_i} \,, \\ o_i = -1 \quad &\Rightarrow \quad t_{e_i v_i} = \tilde{t}_{e_i} \quad \text{and} \quad t_{e_i v_{i+1}} = \tau_{e_i} \,. \end{aligned} \tag{6.11}$$

Notice that we can combine the parallel transport relations (3.49) with the notations (6.3), (6.4) to relate the spinors which are on both ends of the long side of e_i incident to f,

$$t^{\epsilon_i}_{e_i v_i, -A} = -o_i \sum_{B=\pm 1/2} t^{-\epsilon_i}_{e_i v_{i+1}, -B} (-1)^{\frac{1}{2}+B} \, u_{e_i f, BA} \,, \quad t^{\epsilon_i}_{e_i v_{i+1}, A} = o_i \sum_{B=\pm 1/2} u_{e_i f, AB} \, (-1)^{\frac{1}{2}+B} t^{-\epsilon_i}_{e_i v_i, B} \,. \tag{6.12}$$

The flatness constraint on f is thus $u_{e_d f} \cdots u_{e_1 f} = \mathbb{I}$. Assume momentarily that all links are counter-clockwise. Then, $\tilde{u}^{-1}_{e_d} \cdots \tilde{u}^{-1}_{e_1} = \mathbb{I}$ implies for all k

$$[t_{e_k}| \tilde{u}^{-1}_{e_{k-1}} \cdots \tilde{u}^{-1}_{e_2} |\tilde{\tau}_{e_1}\rangle = [t_{e_k}| \tilde{u}_{e_k} \tilde{u}_{e_{k+1}} \cdots \tilde{u}_{e_d} \tilde{u}_{e_1} |\tilde{\tau}_{e_1}\rangle = \langle \tilde{\tau}_{e_k}| \tilde{u}_{e_{k+1}} \cdots \tilde{u}_{e_d} |t_{e_1}] \,. \tag{6.13}$$

In the first equality, we have used the constraint itself, while in the second equality we have used the parallel transport relations on the links e_1 and e_k. By then rewriting $\tilde{u}_{1_1}, \ldots, \tilde{u}_{e_d}$ with (6.2), one obtains the following result: a constraint written as a sum of products of scalar invariants living on the nodes around the face. Obviously, one can change $[t_{e_k}|$ to $\langle t_{e_k}|$ and $|\tilde{\tau}_{e_1}\rangle$ to $|\tilde{\tau}_{e_1}]$ without changing that result (qualitatively). Similarly, one should be able to write this function for arbitrarily chosen link orientations. The notations we have introduced will help us write it in the most generic way.

Going back to arbitrary link orientations around f, we consider

$$E^{\epsilon_1, \epsilon_k}_{e_1 \to e_k} = \sum_{A,B=\pm 1/2} t^{\epsilon_k}_{e_k v_k, -A} \left(u_{e_{k-1} f} \cdots u_{e_2 f} \right)_{AB} t^{\epsilon_1}_{e_1 v_2, B} \tag{6.14}$$

as the generalization of the left hand side of (6.13). Using the parallel transport relations (6.12), it reads

$$E^{\epsilon_1, \epsilon_k}_{e_1 \to e_k} = -o_1 o_k \sum_{C,D=\pm 1/2} t^{-\epsilon_k}_{e_k v_{k+1}, -C} (-1)^{\frac{1}{2}-C} \left(u_{e_k f} u_{e_{k-1} f} \cdots u_{e_2 f} u_{e_1 f} \right)_{CD} (-1)^{\frac{1}{2}-D} t^{-\epsilon_1}_{e_1 v_1, D} \,. \tag{6.15}$$

If the flatness constraint holds, the holonomy going counter-clockwise from e_1 to e_k can then be replaced with the holonomy the other way around f, *i.e.* clockwise. We thus define

$$E^{\epsilon_1, \epsilon_k}_{e_1 \leftarrow e_k} = \sum_{A,B=\pm 1/2} t^{-\epsilon_1}_{e_1 v_1, -A} \left(u_{e_d f} \cdots u_{e_{k+1} f} \right)_{AB} t^{-\epsilon_k}_{e_k v_{k+1}, B} \,. \tag{6.16}$$

So if the flatness constraint holds, then

$$E^{\epsilon_1,\epsilon_k}_{e_1\to e_k} + o_1 o_k E^{\epsilon_1,\epsilon_k}_{e_1\leftarrow e_k} = 0. \tag{6.17}$$

Indeed, using the flatness constraint in (6.15) we get

$$E^{\epsilon_1,\epsilon_k}_{e_1\to e_k} = -o_1 o_k \sum_{C,D=\pm 1/2} t^{-\epsilon_k}_{e_k v_{k+1},-C}(-1)^{\frac{1}{2}-C}\big(u_{e_d f}\cdots u_{e_{k+1}f}\big)^{-1}_{CD}(-1)^{\frac{1}{2}-D} t^{-\epsilon_1}_{e_1 v_1,D}\,. \tag{6.18}$$

For any matrix $g \in \mathrm{SU}(2)$, the matrix elements of the inverse can be written $g^{-1}_{CD} = (-1)^{\frac{1}{2}-D} g_{-D-C}(-1)^{\frac{1}{2}-C}$. This can be used to transform the above expression into $o_1 o_k E^{\epsilon_1,\epsilon_k}_{e_1\leftarrow e_k}$. The last step to define our Hamiltonian constraints is to rewrite $E^{\epsilon_1,\epsilon_k}_{e_1\to e_k}$ and $E^{\epsilon_1,\epsilon_k}_{e_1\leftarrow e_k}$ in terms of scalars like (6.9). The matrix elements of the holonomies are indeed

$$u_{e_i f, A_{i+1}A_i} = o_i \frac{1}{N_{e_i}} \sum_{\epsilon_i=\pm} \epsilon_i \; t^{\epsilon_i}_{e_i v_{i+1},A_{i+1}} \; t^{\epsilon_i}_{e_i v_i,-A_i}\,, \tag{6.19}$$

$$\text{with}\quad N_{e_i} = \frac{1}{2}\sqrt{\sum_{\epsilon_i,\epsilon'_i=\pm}\sum_{A,B=\pm 1/2} \epsilon\epsilon'(-1)^{\frac{1}{2}+A}(-1)^{\frac{1}{2}+B}\, t^{\epsilon_i}_{e_i,v_{i+1},A} t^{-\epsilon_i}_{e_i v_{i+1},-A}\, t^{\epsilon'_i}_{e_i,v_i,B} t^{-\epsilon'_i}_{e_i v_i,-B}}\,, \tag{6.20}$$

so that one can re-organize the products over the nodes instead of links,

$$E^{\epsilon_1,\epsilon_k}_{e_1\to e_k} = \sum_{\substack{\epsilon_2,\dots,\epsilon_{k-1}=\pm\\ A_2,\dots,A_k=\pm 1/2}} \left(\prod_{i=2}^{k-1}\frac{o_i\epsilon_i}{N_{e_i}}\right)\left(\prod_{i=2}^{k} t^{\epsilon_i}_{e_i v_i,-A_i} t^{\epsilon_{i-1}}_{e_{i-1}v_i,A_i}\right), \tag{6.21}$$

$$E^{\epsilon_1,\epsilon_k}_{e_1\leftarrow e_k} = (-1)^{d-k} \sum_{\substack{\epsilon_{k+1},\dots,\epsilon_d=\pm\\ A_{k+1},\dots,A_{d+1}=\pm 1/2}} \left(\prod_{i=k+1}^{d}\frac{o_i\epsilon_i}{N_{e_i}}\right)\left(\prod_{i=k+1}^{d+1} t^{-\epsilon_i}_{e_i v_i,-A_i} t^{-\epsilon_{i-1}}_{e_{i-1}v_i,A_i}\right). \tag{6.22}$$

We can now use the scalar products, which are quadratic invariants, defined in (6.9), which encodes all four scalar products of the two spinors meeting at v_i, *i.e.*

$$E^{\epsilon_i,\epsilon_{i-1}}_{e_i e_{i-1}} = \sum_{A=\pm 1/2} t^{\epsilon_i}_{e_i v_i,-A} t^{\epsilon_{i-1}}_{e_{i-1}v_i,A} = \begin{cases} \langle t_{e_i v_i}|t_{e_{i-1}v_i}] & \text{for } \epsilon_i=+,\epsilon_{i-1}=+\\ \langle t_{e_i v_i}|t_{e_{i-1}v_i}\rangle & \text{for } \epsilon_i=+,\epsilon_{i-1}=-\\ [t_{e_i v_i}|t_{e_{i-1}v_i}] & \text{for } \epsilon_i=-,\epsilon_{i-1}=+\\ [t_{e_i v_i}|t_{e_{i-1}v_i}\rangle & \text{for } \epsilon_i=-,\epsilon_{i-1}=-, \end{cases} \tag{6.23}$$

where the spinors $t_{e_i v_i}$ and $t_{e_{i-1}v_{i-1}}$ are given by the rule (6.11) according to the orientations. This leads us to the following definition of the Hamiltonian constraints.

Definition 6.1.1. *Let f be a face of degree d, with links labeled by $e_1, \dots, e_d$ counterclockwise around f. A Hamiltonian is associated to f and a pair of links along f with a sign attached to each of them. Without loss of generality, the pair can be chosen to be (e_1, e_k) with signs $(\epsilon_1, \epsilon_k) \in \{+,-\}^2$, for $k \in \{2, \dots, d\}$, and the Hamiltonian is*

$$h^{\epsilon_1,\epsilon_k}_{f,e_1,e_k} = \sum_{\epsilon_2,\dots,\epsilon_{k-1}=\pm} \left(\prod_{i=2}^{k} \frac{o_i \epsilon_i}{N_{e_i}} E^{\epsilon_i,\epsilon_{i-1}}_{e_i e_{i-1}} \right) + (-1)^{d-k} \epsilon_1 \epsilon_k \frac{N_{e_1}}{N_{e_k}} \sum_{\epsilon_{k+1},\dots,\epsilon_d=\pm} \left(\prod_{i=k+1}^{d+1} \frac{o_i \epsilon_i}{N_{e_i}} E^{-\epsilon_i,-\epsilon_{i-1}}_{e_i e_{i-1}} \right). \tag{6.24}$$

The Hamiltonian constraint (6.24) captures the flatness constraint completely with all choices of pairs (e_1, e_k) and of signs (ϵ_1, ϵ_k). The proof is the same as in the vector case at $\kappa = 0$, see [43].

Application to faces of degree three

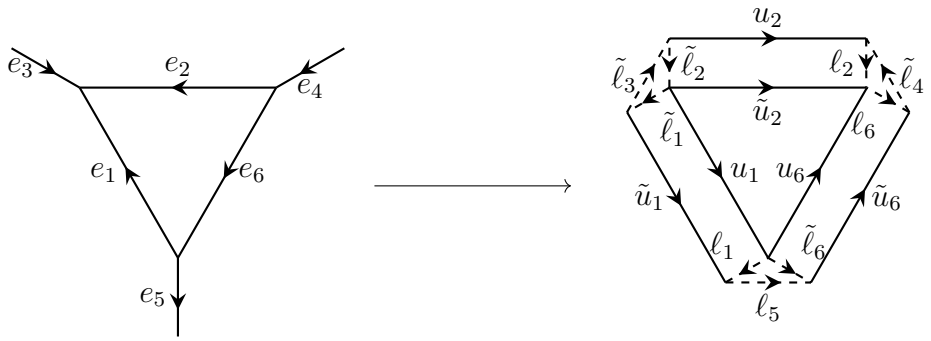

Figure 6.3: On the left, a triangular face with its adjacent links. On the right, we have shown the ribbon graph it gives rise to.

Let us discuss more explicitly the case of triangular faces. We use the notations and orientations of fig.6.3 as an example. In particular $o_1 = o_6 = -1$ and $o_2 = 1$. Here there are three choices of pairs of links (which label the Hamiltonians (6.24)), which correspond to the three nodes of the face.

On a node, say between the links e_2 and e_6, there are four invariant quantities quadratic

in the spinors, $\langle t_2|\tau_6\rangle, \langle t_2|\tau_6], [t_2|\tau_6\rangle, [t_2|\tau_6]$ which are encoded in the scalar product (6.9),

$$E_{26}^{\epsilon_2,\epsilon_6} = \sum_{A=\pm 1/2} t_{2,-A}^{\epsilon_2} \tau_{6,A}^{\epsilon_6} = \begin{cases} \langle t_2|t_6] & \text{for } \epsilon_2 = \epsilon_6 = +, \\ \langle t_2|t_6\rangle & \text{for } \epsilon_2 = -\epsilon_6 = +, \\ [t_2|t_6] & \text{for } \epsilon_2 = -\epsilon_6 = -, \\ [t_2|t_6\rangle & \text{for } \epsilon_2 = \epsilon_6 = -\,. \end{cases} \tag{6.25}$$

Similarly at the nodes between e_1, e_2 and e_6, e_1,

$$E_{12}^{\epsilon_1,\epsilon_2} = \sum_{A=\pm 1/2} \tilde{t}_{1,-A}^{\epsilon_1} \tilde{\tau}_{2,A}^{\epsilon_2}, \qquad E_{61}^{\epsilon_6,\epsilon_1} = \sum_{A=\pm 1/2} \tilde{t}_{6,-A}^{\epsilon_6} \tau_{1,A}^{\epsilon_1}\,. \tag{6.26}$$

The flatness constraint $\tilde{u}_2 u_1^{-1} u_6^{-1} = \mathbb{I}$ implies that if $|\tau_6\rangle$ and $|\tau_6]$ are transported around the face via $\tilde{u}_2 u_1^{-1} u_6^{-1}$, the above quadratic quantities are left unchanged, that is

$$\begin{aligned} \langle t_2|\tilde{u}_2 u_1^{-1} u_6^{-1}|\tau_6\rangle &= \langle t_2|\tau_6\rangle\,, & \langle t_2|\tilde{u}_2 u_1^{-1} u_6^{-1}|\tau_6] &= \langle t_2|\tau_6]\,, \\ [t_2|\tilde{u}_2 u_1^{-1} u_6^{-1}|\tau_6\rangle &= [t_2|\tau_6\rangle\,, & [t_2|\tilde{u}_2 u_1^{-1} u_6^{-1}|\tau_6] &= [t_2|\tau_6]\,. \end{aligned} \tag{6.27}$$

Similarly at the nodes where e_1, e_2 and e_6, e_1 meet respectively,

$$\begin{aligned} \langle \tilde{t}_1|u_1^{-1} u_6^{-1} \tilde{u}_2|\tilde{\tau}_2\rangle &= \langle \tilde{t}_1|\tilde{\tau}_2\rangle\,, & \langle \tilde{t}_6|u_6^{-1} \tilde{u}_2 u_1^{-1}|\tau_1\rangle &= \langle \tilde{t}_6|\tau_1\rangle\,, \\ \langle \tilde{t}_1|u_1^{-1} u_6^{-1} \tilde{u}_2|\tilde{\tau}_2] &= \langle \tilde{t}_1|\tilde{\tau}_2]\,, & \langle \tilde{t}_6|u_6^{-1} \tilde{u}_2 u_1^{-1}|\tau_1] &= \langle \tilde{t}_6|\tau_1]\,, \\ [\tilde{t}_1|u_1^{-1} u_6^{-1} \tilde{u}_2|\tilde{\tau}_2\rangle &= [\tilde{t}_1|\tilde{\tau}_2\rangle\,, & [\tilde{t}_6|u_6^{-1} \tilde{u}_2 u_1^{-1}|\tau_1\rangle &= [\tilde{t}_6|\tau_1\rangle\,, \\ [\tilde{t}_1|u_1^{-1} u_6^{-1} \tilde{u}_2|\tilde{\tau}_2] &= [\tilde{t}_1|\tilde{\tau}_2]\,, & [\tilde{t}_6|u_6^{-1} \tilde{u}_2 u_1^{-1}|\tau_1] &= [\tilde{t}_6|\tau_1]\,. \end{aligned} \tag{6.28}$$

In fact, this set of constraints can be seen as projecting the constraint $\tilde{u}_2 u_1^{-1} u_6^{-1} = \mathbb{I}$ onto a basis. Therefore, as long as those vectors are generic (hence linearly independent), this whole set is equivalent to $\tilde{u}_2 u_1^{-1} u_6^{-1} = \mathbb{I}$.

Let us consider the constraint $\langle t_2|\tilde{u}_2 u_1^{-1} u_6^{-1}|\tau_6] - \langle t_2|\tau_6]$ and rewrite it like in (6.24). Use the parallel transport relations $u_6^{-1}|\tau_6] = -|\tilde{t}_6\rangle$ and $\langle t_2|\tilde{u}_2 = [\tilde{\tau}_2|$ which gives $\langle t_2|\tilde{u}_2 u_1^{-1} u_6^{-1}|\tau_6] = -[\tilde{\tau}_2|u_1^{-1}|\tilde{t}_6\rangle = [\tilde{t}_6|u_1|\tilde{\tau}_2\rangle$. Then use $u_1 = \frac{1}{N_{e_1}}(|\tau_1\rangle[\tilde{t}_1| - |\tau_1]\langle\tilde{t}_1|)$ so that the constraint becomes

$$\begin{aligned} \langle t_2|\tilde{u}_2 u_1^{-1} u_6^{-1}|\tau_6] - \langle t_2|\tau_6] &= \frac{1}{N_{e_1}}\big([\tilde{t}_6|\tau_1\rangle[\tilde{t}_1|\tilde{\tau}_2\rangle - [\tilde{t}_6|\tau_1]\langle\tilde{t}_1|\tilde{\tau}_2\rangle\big) - \langle t_2|\tau_6] \\ &= -\frac{1}{N_{e_1}} \sum_{\epsilon=\pm} \epsilon\, E_{61}^{-,\epsilon} E_{12}^{\epsilon,-} - E_{26}^{+,+} \end{aligned} \tag{6.29}$$

which is exactly the specialization of (6.24) to $d = 3$, $k = 2$, $o_1 = o_6 = -o_2 = -1$ and $\epsilon_2 = \epsilon_6 = +$,

$$h_{e_2e_6}^{\epsilon_2,\epsilon_6} = E_{26}^{\epsilon_2,\epsilon_6} + \frac{1}{N_{e_1}} \sum_{\epsilon_1=\pm} \epsilon_1 E_{12}^{\epsilon_1,-\epsilon_2} E_{61}^{-\epsilon_6,\epsilon_1} \,. \tag{6.30}$$

where we recall that $N_{e_1} = \sqrt{\langle \tau_1 | \tau_1 \rangle \langle \tilde{t}_1 | \tilde{t}_1 \rangle}$.

This way, the Hamiltonian constraint does not involve holonomy variables anymore like in (6.27), but only the scalar products of spinors.

6.2 Quantum Hamiltonian constraint

We now proceed to the quantization of the system. The aim is to quantize the Hamiltonian constraints (6.24) and solve them at the quantum level. This requires quantizing the quadratic invariant $E_{e_ie_{i-1}}^{\epsilon_i,\epsilon_{i-1}}$. Recall that, before enforcing the Gauss constraints, space of states is $\bigoplus_{\{j_e\}} \bigotimes_e \mathcal{V}_{j_e} \otimes \mathcal{V}_{j_e}^*$, where $\mathcal{V}_{j_e}$ is associated to the target end of e and $\mathcal{V}_{j_e}^*$ to its source. At each node v, the Gauss constraint enforces a projection of the tensor product of the vectors meeting at v onto the trivial representation. If the links meeting at v are denoted $e_1, \dots, e_n$, the space of intertwiners, which we uniformly denote as $\mathrm{Inv}(j_{e_1v} \otimes \cdots \otimes j_{e_nv})$, is the invariant subspace of the tensor product $\mathcal{V}_{j_{e_1}} \otimes \cdots \otimes \mathcal{V}_{j_{e_n}}$ if all e_i's are incoming at v, and we dualize to $\mathcal{V}_{j_{e_i}}^*$ if e_i is outgoing at v. In the case of trivalent nodes, the invariant space $\mathrm{Inv}(j_{e_1v} \otimes j_{e_2v} \otimes j_{e_3v})$ is one-dimensional. Therefore, the kinematical Hilbert space is given by the invariant

$$\mathcal{H}_{\mathrm{kin}} = \bigoplus_{\{j_e \in \mathbb{N}/2\}} \bigotimes_v \mathrm{Inv}(j_{e_1v} \otimes \cdots \otimes j_{e_nv}) \,. \tag{6.31}$$

Recall that a basis of $\mathcal{H}_{\mathrm{kin}}$ is formed by the spin network state

$$|\{j_e, i_v\}\rangle = \bigotimes_v i_{j_{e_1v} \cdots j_{e_nv}} \tag{6.32}$$

where $i_{j_{e_1v} \cdots j_{e_n(v)v}} \in \mathrm{Inv}(j_{e_1v} \otimes \cdots \otimes j_{e_nv})$ is an intertwiner. A kinematical state $|\psi\rangle$ thus can be written as the expansion under such a basis,

$$|\psi\rangle = \sum_{\{j_e\}} \sum_{\{i_v\}} \psi(\{j_e, i_v\}) \; |\{j_e, i_v\}\rangle. \tag{6.33}$$

with

$$|\{j_e, i_v\}\rangle = \bigotimes_v i_{j_{e_1v} \cdots j_{e_nv}} \tag{6.34}$$

The scalar observable and its action on the intertwiner. The quantization of the quadratic invariant (6.9), $E^{\epsilon_2,\epsilon_1}_{e_2e_1}$ has been introduced in (5.58). We are particularly interested in its action on the intertwiner for a three-valent graph. While $E^{\epsilon_2,\epsilon_1}_{e_2e_1}$ would be independent of orientations, the vector space on which it acts does depend on orientations ($\mathcal{V}_j^*$ versus $\mathcal{V}_j$). Therefore the action on an intertwiner would in fact depend explicitly on the orientations. Instead, we decide to perform the quantization so that its action on intertwiners is independent of orientations. Therefore, we will not use (5.58) directly here, but instead a more complicated definition of $\mathbf{E}^{\epsilon_2,\epsilon_1}_{e_2e_1}$ whose expression depends on the orientation of e_1 and e_2.

The way we define such an operator is to change the spinor operator to its q^{-1} version when flipping the orientation. Obviously, this exchanges the $\mathbf{t}$'s with the $\boldsymbol{\tau}$'s. However, we prefer to keep the same letter for the spinor operator because we think exchanging $\mathbf{t}$'s with $\boldsymbol{\tau}$'s could be confusing in the ribbon picture. We therefore define $\overline{\mathbf{t}^{\epsilon}} := \boldsymbol{\tau}^{\epsilon}$ and same with the tildes, and eventually

$$\begin{aligned}\mathbf{E}^{\epsilon_2,\epsilon_1}_{e_2e_1} &= -o_1\sqrt{[2]}(-1)^{\frac{1-o_1}{2}\frac{1+\epsilon_1}{2}}(-1)^{\frac{1-o_2}{2}\frac{1+\epsilon_2}{2}}\sum_{A=\pm\frac12} {}_{q^{o_1}}C^{\frac12\ \frac12\ 0}_{A\,-A\,0}\,\mathbf{T}^{o_1\epsilon_1}_{e_1v,A}\otimes\mathbf{T}^{-o_2\epsilon_2}_{e_2v,-A}\\ &= \begin{cases}\sum_{A=\pm\frac12}(-1)^{\frac12-A}q^{\frac{A}{2}}\epsilon_2\,\tilde{\mathbf{t}}^{\epsilon_1}_A\otimes\tilde{\boldsymbol{\tau}}^{\epsilon_2}_{-A} & \text{for } -o_1=o_2=-1\\ \sum_{A=\pm\frac12}(-1)^{\frac12+A}q^{\frac{A}{2}}\tilde{\mathbf{t}}^{\epsilon_1}_A\otimes\overline{\boldsymbol{\tau}^{-\epsilon_2}_{-A}} & \text{for } o_1=o_2=1\\ \sum_{A=\pm\frac12}(-1)^{\frac12-A}q^{-\frac{A}{2}}\epsilon_1\epsilon_2\,\overline{\mathbf{t}^{-\epsilon_1}_A}\otimes\tilde{\boldsymbol{\tau}}^{\epsilon_2}_{-A} & \text{for } -o_1=-o_2=1\\ \sum_{A=\pm\frac12}(-1)^{\frac12+A}q^{-\frac{A}{2}}\epsilon_1\,\overline{\mathbf{t}^{-\epsilon_1}_A}\otimes\overline{\boldsymbol{\tau}^{-\epsilon_2}_{-A}} & \text{for } -o_1=o_2=1\end{cases},\end{aligned} \tag{6.35}$$

where $\mathbf{T}^{-o_2\epsilon_2}_{e_2v,A}=\mathbf{t}^{\epsilon_2}_{e_2v,A}$ if $o_2=-1$ while $\mathbf{T}^{-o_2\epsilon_2}_{e_2v,A}=\overline{\mathbf{t}^{-\epsilon_2}_{e_2v,A}}$ if $o_2=1$, and similarly for $\mathbf{T}^{o_1\epsilon_1}_{e_1v,A}$. We then extend this definition to the space $\mathrm{Inv}(j_{e_1v}\otimes\cdots\otimes j_{e_nv})$ of invariant vectors at v by tensoring with the identity as necessary. It comes

$$\mathbf{E}^{\epsilon_2,\epsilon_1}_{e_2e_1}\,i_{j_1j_2j_3}=\sqrt{[d_{j_1}][d_{j_2}][d_{l_1}][d_{l_2}]}\delta_{l_1,j_1+\frac{\epsilon_1}{2}}\delta_{l_2,j_2+\frac{\epsilon_2}{2}}\begin{Bmatrix}l_1 & j_1 & \frac12\\ j_2 & l_2 & j_3\end{Bmatrix}_q(-1)^{l_1+l_2+j_3}i_{l_1l_2j_3}\,, \tag{6.36}$$

It thus maps the interwtiner space $\mathrm{Inv}(j_1\otimes j_2\otimes j_3)$ to $\mathrm{Inv}(l_1\otimes l_2\otimes j_3)$.

This definition also works for two links e_i, e_{i+1} sharing a node in $\mathrm{Inv}(j_{e_1v}\otimes\cdots\otimes j_{e_nv})$, for $i=1,\dots,n-1$. In the trivalent case, this gives $E^{\epsilon_3,\epsilon_2}_{e_3e_2}i_{j_1j_2j_3}$ exactly as in (6.36) with $e_1\to e_2, e_2\to e_3, e_3\to e_1$

$$\mathbf{E}^{\epsilon_3,\epsilon_2}_{e_3e_2}\,i_{j_1j_2j_3}=\sqrt{[d_{j_2}][d_{j_3}][d_{l_2}][d_{l_3}]}\delta_{l_2,j_2+\frac{\epsilon_2}{2}}\delta_{l_3,j_3+\frac{\epsilon_3}{2}}\begin{Bmatrix}l_2 & j_2 & \frac12\\ j_3 & l_3 & j_1\end{Bmatrix}_q(-1)^{l_2+l_3+j_1}i_{j_1l_2l_3}. \tag{6.37}$$

For the case $i = n$, *i.e.* $E^{\epsilon_1,\epsilon_n}_{e_1 e_n}$, the definition has to be amended to obtain an invariant operator [41] and eventually one finds the same expression for $E^{\epsilon_1,\epsilon_3}_{e_1 e_3} i_{j_1 j_2 j_3}$ as (6.36) with the appropriate permutation of the indices, *i.e.*

$$\mathbf{E}^{\epsilon_1,\epsilon_3}_{e_1 e_3}\, i_{j_1 j_2 j_3} = \sqrt{[d_{j_3}][d_{j_1}][d_{l_3}][d_{l_1}]}\delta_{l_3, j_3+\frac{\epsilon_3}{2}}\delta_{l_1, j_1+\frac{\epsilon_1}{2}} \left\{ \begin{array}{ccc} l_3 & j_3 & \frac{1}{2} \\ j_1 & l_1 & j_2 \end{array} \right\}_q (-1)^{l_3+l_1+j_2} i_{l_1 j_2 l_3}. \quad (6.38)$$

Quantize the Hamiltonian constraint. We now need to quantize the classical Hamiltonian (6.24) as a well-defined operator on $\mathcal{H}_{\rm kin}$ (defined in (6.31)). The first step is obviously to use the quantization map described in the previous section turning the observables $E^{\epsilon_i,\epsilon_{i-1}}_{e_i e_{i-1}}$ into operators $\mathbf{E}^{\epsilon_i,\epsilon_{i-1}}_{e_i e_{i-1}}$ as in (6.35). The second step is concerned with quantization ambiguities. Indeed, factors N_{e_i} appear in (6.24) and they are expected to be diagonal on the spin network basis, as a function of j_{e_i} only in fact. Notice however that the operators $E^{\epsilon_2,\epsilon_1}_{e_2 e_1}$ change the spins of the links e_1, e_2 by $\epsilon_1/2$ and $\epsilon_2/2$. There are therefore ordering ambiguities, the result differing according to whether N_{e_i} is before or after some operators E which changes j_{e_i}. We found an ordering, see below, which ultimately leads to a topological model, which would presumably not be true for other orderings.

Let us introduce

$$\mathbf{h}^{\epsilon_1,\epsilon_p}_{f,e_1,e_p} = \frac{1}{\mathbf{N}_{e_1 v_2}} \left(\sum_{\substack{\epsilon_2,\dots,\\ \epsilon_{p-1}=\pm}} \prod_{i=2}^{p} \mathbf{E}^{\epsilon_i,\epsilon_{i-1}}_{e_i e_{i-1}} \frac{o_i \epsilon_i}{\mathbf{N}_{e_i v_i}} \right) + \frac{(-1)^{d-p}\epsilon_1\epsilon_p}{\mathbf{N}_{e_p v_{p+1}}} \left(\sum_{\substack{\epsilon_{p+1},\dots,\\ \epsilon_d=\pm}} \prod_{i=p+1}^{d+1} \mathbf{E}^{-\epsilon_i,-\epsilon_{i-1}}_{e_i e_{i-1}} \frac{o_i \epsilon_i}{\mathbf{N}_{e_i v_i}} \right), \quad (6.39)$$

where $\mathbf{N}_{e_i v_i}$ is diagonal on $\mathcal{V}_{j_{e_i}}$ (or its dual), $\mathbf{N}_{e_i v_i}|j_{e_i}, m_{e_i}\rangle = [d_{j_{e_i}}]|j_{e_i}, m_{e_i}\rangle$. We include the node v_i in the notation because here $\mathbf{N}_{e_i v_i}$ only acts on the space of intertwiners at v_i, where e_i and e_{i-1} meet. As already discussed, the ordering is important because $[\mathbf{N}_{e_i v_i}, \mathbf{E}^{\epsilon_{i-1},\epsilon_i}_{e_{i-1} e_i}] \neq 0$. However $[\mathbf{N}_{e_i v_i}, \mathbf{E}^{\epsilon_i,\epsilon_{i+1}}_{e_i e_{i+1}}] = 0$ by definition, so that the operators $\mathbf{E}^{\epsilon_i,\epsilon_{i-1}}_{e_i e_{i-1}} \frac{o_i \epsilon_i}{\mathbf{N}_{e_i v_i}}$ which act on the space of intertwiners at v_i commute with one another. Here $\mathbf{N}_{e_i v_i}$ is placed to the right of $\mathbf{E}^{\epsilon_i,\epsilon_{i-1}}_{e_i e_{i-1}}$, which is also the case if one reconstructs the quantum holonomies from the quantum spinors [41].

However, the operator $\mathbf{h}^{\epsilon_1,\epsilon_p}_{f,e_1,e_p}$ as such is not defined on $\mathcal{H}_{\rm kin}$. Indeed, a state in $\mathcal{H}_{\rm kin}$ is a superposition of spin network states which assigns a spin to each link along with the space $\mathcal{V}_j$ to the target end and V_j^* to the source end. Say the link e_1 gets the spin j_1.

Then the first term of the above operator acts on e_1 with $\mathbf{E}^{\epsilon_2,\epsilon_1}_{e_2e_1}$ which shifts the spin j_1 to $j_1+\epsilon_1/2$, on the intertwiner which sits at the node where e_1 and e_2 meet. It thus maps $\mathcal{V}_{j_1}$ to $\mathcal{V}_{j_1+\epsilon_1/2}$, or $\mathcal{V}^*_{j_1}$ to $\mathcal{V}^*_{j_1+\epsilon_1/2}$ depending on orientations, but not both, i.e. it does not shift j_1 at the node where e_d and e_1 meet. Therefore the operator brings the state out of $\mathcal{H}_{\text{kin}}$.

Similarly, the second term of $\mathbf{h}^{\epsilon_1,\epsilon_p}_{f,e_1,e_p}$ acts on e_1 through $\mathbf{E}^{-\epsilon_1,-\epsilon_d}_{e_1e_d}$. This shifts j_1 to $j_1-\epsilon_1/2$ at the node where e_d, e_1 meet. If $\mathbf{E}^{\epsilon_2,\epsilon_1}_{e_2e_1}$ in the first term acted on $\mathcal{V}_{j_1}$, then this operator acts on $V^*_{j_1}$ (or the other way around).

We thus turn $\mathbf{h}^{\epsilon_1,\epsilon_p}_{f,e_1,e_p}$ into a well-defined operator on $\mathcal{H}_{\text{kin}}$ by multiplying it by a product of operators $\mathbf{E}^{\epsilon_i,\epsilon_{i-1}}_{e_ie_{i-1}}$ so that the intertwiners of both ends of the same link have the same spin. Notice that the first term in (6.39) only contains the shift operators for $i=2,\cdots,p$, one can add $\mathbf{E}^{\epsilon_i,\epsilon_{i-1}}_{e_ie_{i-1}}$ for all the remaining nodes, *i.e.* $i=p+1,\cdots,d+1$, so that the spin changes for both ends of each link are the same. For the second term in (6.39), adding these shift operators also shift all the spins $j_i-\epsilon_i/2$ to j_i thus drags the state back in $\mathcal{H}_{\text{kin}}$. This is the method which was already used in [44] for constructing the quantum Hamiltonian in the spinor representation in the flat case.

Definition 6.2.1. *We define the quantum Hamiltonian on the face f, labeled by the pair of links (e_1,e_p), to be*

$$\mathbf{H}^{\epsilon_1,\epsilon_p,\epsilon_{p+1},\ldots,\epsilon_d}_{f,e_1,e_p}=\left[\prod_{i=p+1}^{d+1}\mathbf{E}^{\epsilon_i,\epsilon_{i-1}}_{e_ie_{i-1}}\right]\mathbf{h}^{\epsilon_1,\epsilon_p}_{f,e_1,e_p}. \tag{6.40}$$

Compared to the operator (6.39), the quantum Hamiltonian defined as such not only depends on ϵ_1 and ϵ_p, but also $\epsilon_{p+1},\cdots,\epsilon_{d+1}$. The physical Hilbert space is spanned by the physical states which are the solutions to the quantum Hamiltonian. In the spin representation, the coefficients of these physical spin network states satisfy a set of difference equations, which is stated in the following theorem.

Theorem 6.2.2. *The constraint*

$$\forall k_e \qquad \langle\{k_e\}|\ \mathbf{H}^{\epsilon_1,\epsilon_p,\epsilon_{p+1},\ldots,\epsilon_d}_{f,e_1,e_p}\ |\psi\rangle=0, \tag{6.41}$$

is equivalent to the following set of difference equations *on the spin network coefficients*

$\psi(k_1, k_2, \cdots, k_d, \{k_e\}_{e\notin\partial f})$ *of* $|\psi\rangle$,

$$\sum_{\tilde\epsilon_2,\dots,\tilde\epsilon_{p-1}=\pm}\left(\prod_{i=2}^{p} A_{o_i}^{\tilde\epsilon_i,\tilde\epsilon_{i-1}}(k_i,k_{i-1},l_i)\right)$$
$$\psi(k_1-\frac{\epsilon_1}{2},k_2-\frac{\tilde\epsilon_2}{2},\dots,k_{p-1}-\frac{\tilde\epsilon_{p-1}}{2},k_p-\frac{\epsilon_p}{2},\dots,k_d-\frac{\epsilon_d}{2},\{k_e\}_{e\notin\partial f})$$
$$+(-1)^{d-p}\alpha^{\epsilon_1,\epsilon_p}(k_1,k_p)\sum_{\tilde\epsilon_{p+1},\dots,\tilde\epsilon_d=\pm}\left(\prod_{i=p+1}^{d+1} B_{o_i}^{\tilde\epsilon_i,\tilde\epsilon_{i-1}}(k_i-\frac{\epsilon_i}{2},k_{i-1}-\frac{\epsilon_{i-1}}{2},l_i)\right)$$
$$\psi(k_1,\dots,k_p,k_{p+1}-\frac{\epsilon_{p+1}}{2}+\frac{\tilde\epsilon_{p+1}}{2},\dots,k_d-\frac{\epsilon_d}{2}+\frac{\tilde\epsilon_d}{2},\{k_e\}_{e\notin\partial f})=0. \quad (6.42)$$

Here

- $l_1,\dots,l_d$ *are the spins carried by the links* $e'_1,\dots,e'_d$ *incident to* f*, see fig.6.2.*
- *By definition,* $\tilde\epsilon_1=\epsilon_1,\tilde\epsilon_p=\epsilon_p$*, while* $\epsilon_{p+1},\dots,\epsilon_d$ *are fixed.*
- *The coefficients are*

$$A_{o_i}^{\tilde\epsilon_i,\tilde\epsilon_{i-1}}(k_i,k_{i-1},l_i)=o_i\tilde\epsilon_i[d_{k_i}](-1)^{k_i+k_{i-1}+l_i}\begin{Bmatrix} k_i & k_i-\frac{\tilde\epsilon_i}{2} & \frac12\\ k_{i-1}-\frac{\tilde\epsilon_{i-1}}{2} & k_{i-1} & l_i\end{Bmatrix}_q, \quad (6.43)$$

$$B_{o_i}^{\tilde\epsilon_i,\tilde\epsilon_{i-1}}(k_i,k_{i-1},l_i)=o_i\tilde\epsilon_i[d_{k_i}](-1)^{k_i+k_{i-1}+l_i}\begin{Bmatrix} k_i & k_i+\frac{\tilde\epsilon_i}{2} & \frac12\\ k_{i-1}+\frac{\tilde\epsilon_{i-1}}{2} & k_{i-1} & l_i\end{Bmatrix}_q, \quad (6.44)$$

$$\alpha^{\epsilon_1,\epsilon_p}(k_1,k_p)=\epsilon_1\epsilon_p\frac{[d_{k_p}]}{[d_{k_1-\frac{\epsilon_1}{2}}]}. \quad (6.45)$$

Before we prove this theorem, we first discuss some properties of the constraint (6.42). Those constraints are recursions on the physical states. They generalize the one found in [44] for a triangular face. Improving on [43], the differences are shifts of the spins by 1/2 instead of 1. Moreover, link orientations are kept arbitrary.

Those constraints have two types of contributions: the *A-terms* and the *B-terms*. Notice that $\mathbf{h}_{f,e_1,e_p}^{\epsilon_1,\epsilon_p}$ contains all the operators $\mathbf{E}_{e_ie_{i-1}}^{\tilde\epsilon_i,\tilde\epsilon_{i-1}}$ exactly once, for $i=1,\dots,d$. Whether an operator $\mathbf{E}_{e_ie_{i-1}}^{\tilde\epsilon_i,\tilde\epsilon_{i-1}}$ gives rise to an A-term or a B-term depends on the choice of the reference links e_1 and e_p around f. It is important that the coefficients $A_{o_i}^{\tilde\epsilon_i,\tilde\epsilon_{i-1}}(k_i,k_{i-1},l_i)$ and $B_{o_i}^{\tilde\epsilon_i,\tilde\epsilon_{i-1}}(k_i,k_{i-1},l_i)$ are *local*: they only depend on the spins incident to the node. As

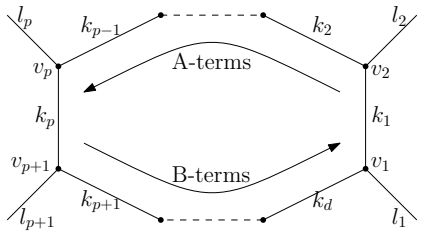

Figure 6.4: The schematic representation of the quantum constraint (6.42) with its A-terms and B-terms associated to the nodes around the face.

a consequence, for example, if one considers another constraint on the same face with e_q, $q < p$, chosing e_1 as reference link, then the coefficients $A_{o_i}^{\tilde{\epsilon}_i,\tilde{\epsilon}_{i-1}}(k_i, k_{i-1}, l_i)$ for $i = 1, \dots, q$ would be the same as those appearing above, and similarly for the B-terms. The structure of the constraint is schematically pictured in fig.6.4.

By exchanging the role of e_1 with e_p, the A-terms become the B-terms and vice versa. The constraint obtained this way is equivalent to (6.42), as we now show. First, evaluate (6.42) on $k_1 + \epsilon_1/2, \dots, k_d + \epsilon_d/2$, and then flip the signs of all the ϵ_i and $\tilde{\epsilon}_i$. That gives the constraint

$$\begin{aligned}
\sum_{\tilde{\epsilon}_2,\dots,\tilde{\epsilon}_{p-1}=\pm} \Big(\prod_{i=2}^{p} A_{o_i}^{-\tilde{\epsilon}_i,-\tilde{\epsilon}_{i-1}}(k_i - \frac{\epsilon_i}{2}, k_{i-1} - \frac{\epsilon_{i-1}}{2}, l_i) \Big) \\
\psi\Big(k_1, k_2 - \frac{\epsilon_2}{2} + \frac{\tilde{\epsilon}_2}{2}, \dots, k_{p-1} - \frac{\epsilon_{p-1}}{2} + \frac{\tilde{\epsilon}_{p-1}}{2}, k_p, \dots, k_d, \{k_e\}_{e\not\in\partial f}\Big) \\
+ (-1)^{d-p} \alpha^{\epsilon_1,\epsilon_p}(k_1 - \frac{\epsilon_1}{2}, k_p - \frac{\epsilon_p}{2}) \sum_{\tilde{\epsilon}_{p+1},\dots,\tilde{\epsilon}_d=\pm} \Big(\prod_{i=p+1}^{d+1} B_{o_i}^{-\tilde{\epsilon}_i,-\tilde{\epsilon}_{i-1}}(k_i, k_{i-1}, l_i) \Big) \\
\psi\Big(k_1 - \frac{\epsilon_1}{2}, \dots, k_p - \frac{\epsilon_p}{2}, k_{p+1} - \frac{\tilde{\epsilon}_{p+1}}{2}, \dots, k_d - \frac{\tilde{\epsilon}_d}{2}, \{k_e\}_{e\not\in\partial f}\Big) = 0\,. \quad (6.46)
\end{aligned}$$

We then use the key relation between the coefficients A and B,

$$B_{o_i}^{\tilde{\epsilon}_i,\tilde{\epsilon}_{i-1}}(k_i, k_{i-1}, l_i) = -A_{o_i}^{-\tilde{\epsilon}_i,-\tilde{\epsilon}_{i-1}}(k_i, k_{i-1}, l_i) \quad (6.47)$$

to get

$$(-1)^p \sum_{\tilde\epsilon_2,\dots,\tilde\epsilon_{p-1}=\pm} \left(\prod_{i=2}^{p} B_{o_i}^{\tilde\epsilon_i,\tilde\epsilon_{i-1}}(k_i-\frac{\epsilon_i}{2},k_{i-1}-\frac{\epsilon_{i-1}}{2},l_i)\right)$$
$$\psi\Big(k_1,k_2-\frac{\epsilon_2}{2}+\frac{\tilde\epsilon_2}{2},\dots,k_{p-1}-\frac{\epsilon_{p-1}}{2}+\frac{\tilde\epsilon_{p-1}}{2},k_p,\dots,k_d,\{k_e\}_{e\notin\partial f}\Big)$$
$$+\alpha^{\epsilon_1,\epsilon_p}(k_1-\frac{\epsilon_1}{2},k_p-\frac{\epsilon_p}{2}) \sum_{\tilde\epsilon_{p+1},\dots,\tilde\epsilon_d=\pm} \left(\prod_{i=p+1}^{d+1} A_{o_i}^{\tilde\epsilon_i,\tilde\epsilon_{i-1}}(k_i,k_{i-1},l_i)\right)$$
$$\psi\Big(k_1-\frac{\epsilon_1}{2},\dots,k_p-\frac{\epsilon_p}{2},k_{p+1}-\frac{\tilde\epsilon_{p+1}}{2},\dots,k_d-\frac{\tilde\epsilon_d}{2},\{k_e\}_{e\notin\partial f}\Big)=0, \quad (6.48)$$

where we recognize the matrix element $\langle\{k_e\}|\mathbf{H}_{f,e_p,e_1}^{\epsilon_1,\epsilon_2,\dots,\epsilon_p}|\psi\rangle$ and have shown the equivalence

$$\langle\{k_e\}|\mathbf{H}_{f,e_p,e_1}^{\epsilon_p,\epsilon_1,\epsilon_2,\dots,\epsilon_{p-1}}|\psi\rangle=0 \quad\Leftrightarrow\quad \langle\{k_e\}|\ \mathbf{H}_{f,e_1,e_p}^{\epsilon_1,\epsilon_p,\epsilon_{p+1},\dots,\epsilon_d}\ |\psi\rangle=0. \quad (6.49)$$

The proof of Theorem 6.2.2 is given in Proof B.4.1.

The dependence of ψ on the orientations is given by the following lemma.

Lemma 6.2.3. *If $|\psi\rangle$, with spin network coefficients $\psi(\{j_e\})$, satisfies all the constraints (6.42) for given link orientations $\{o_e\}$, then $(-1)^{2j^*}\psi(\{j_e\})$ satisfies all the constraints on the same graph with reversed orientation $-o_{e^*}$ on the link e^*.*

Proof. Consider the constraint (6.42) on the fixed face f. If $e^*\notin\partial f$, multiplication by $(-1)^{2j^*}$ does not change anything. If $e^*\equiv e_s\in\{e_2,\dots,e_{p-1}\}$, then the coefficient $A_{o_s}^{\tilde\epsilon_s,\tilde\epsilon_{s-1}}(k_s,k_{s-1},l_s)$ changes sign. Moreover, it is the only one that depends on o_s. The state coefficient on the first line of (6.42) changes from $\psi(k_1-\epsilon_1,\dots,k_{e_p}-\tilde\epsilon_p,\dots)$ to $(-1)^{2k_s+1}\psi(k_1-\epsilon_1,\dots,k_p-\tilde\epsilon_p,\dots)$ since $(-1)^{\tilde\epsilon_s}=-1$. Moreover, the coefficients B's are independent of the orientation o_s and the state coefficient on the second line changes from $\psi(k_1,\dots,k_p,\dots)$ to $(-1)^{2k_s}\psi(k_1,\dots,k_p,\dots)$. Factorizing $(-1)^{2k_s}$ from the equation reveals that only the first line is modified, by $-o_s\times(-1)=o_s$. The constraint therefore still holds. If $e^*\equiv e_s\in\{e_{p+1},\cdots,e_{d+1}\}$, the coefficient $B_{o_s}^{\tilde\epsilon_s,\tilde\epsilon_{s-1}}(k_s-\frac{\epsilon_s}{2},k_{s-1}-\frac{\epsilon_{s-1}}{2},l_s)$ changes sign while the coefficients A's remain unchanged. The same analysis leads to the same conclusion.

The argument is the same for all links in the boundary of f, since the orientation of any of those links appears in a single coefficient of the equation. □

Having defined the quantum Hamiltonian, the next task is to find the solutions to this constraint, which are the physical states. In fact, one can justify a physical state by showing (the discrete version of) the diffeomorphism invariance of the state. This is done by performing Pachner moves which we describe in the next section.

6.3 Pachner moves

Pachner moves [167] are the change of triangulation of a manifold by keeping the boundary triangulation fixed. In the graph picture, that is equivalent to keeping the xlinks piercing the boundary fixed. Sequences of Pachner moves are then the combinatorial equivalent of manifold diffeomorphism. In this section, we show show how to relate physical states on triangulations which are related by Pachner moves. This is an extension of [162] to q real (using Hamiltonian constraints instead of projection on flat connections). In two dimensions, there are two types of Pachner moves, the $3-1$ moves and the $2-2$ moves (as well as their inverses). We state the relations of the spin network coefficients in the theorems below and leave the proofs in Appendix B.4

2-2 Pachner move. The 2-2 Pachner move changes a portion of the graph into another one as follows,

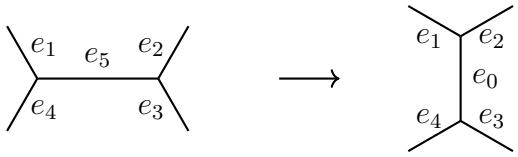

(6.50)

We denote the initial graph which contains the left-hand side as Γ_i, and the final graph which contains the right-hand side as Γ_f. The orientation of all links are left arbitrary.

Theorem 6.3.1. *Let $|\psi_f\rangle$ on Γ_f be defined in the spin network basis by*

$$\begin{aligned}&\psi_f(j_1,j_2,j_3,j_4,j_0,\dots)\\&\quad=(-1)^{j_1+j_2+j_3+j_4}[d_{j_0}]\sum_{j_5}(-1)^{(1-o_5)j_5+(1-o_0)j_0}\begin{Bmatrix}j_1&j_2&j_0\\j_3&j_4&j_5\end{Bmatrix}_q\psi_i(j_1,j_2,j_3,j_4,j_5,\dots)\,.\end{aligned}\tag{6.51}$$

where the ellipses denote spins which are the same on both sides (for links which are not affected by the move). Then $|\psi_i\rangle$ is a state which satisfies all the constraints on Γ_i if and only if $|\psi_f\rangle$ satisfies all the constraints on Γ_f.

Since the 2-2 move is its own inverse, there is a symmetry between both sides of the move. This must translate into a symmetry which exchanges the role of $|\psi_i\rangle$ and $|\psi_f\rangle$ in (6.51). This is indeed true thanks to the orthonormality of the q-6j symbols,

$$\sum_{j_5}[d_{j_5}][d_{j_0}]\begin{Bmatrix}j_1&j_2&j_0\\j_3&j_4&j_5\end{Bmatrix}_q\begin{Bmatrix}j_1&j_2&j_0'\\j_3&j_4&j_5\end{Bmatrix}_q=\delta_{j_0,j_0'}\,,\tag{6.52}$$

which transforms (6.51) into

$$\psi_i(j_1, j_2, j_3, j_4, j_5, \dots) = (-1)^{j_1+j_2+j_3+j_4}[d_{j_5}] \sum_{j_0'} (-1)^{(1-o_5)j_5+(1-o_0)j_0'} \begin{Bmatrix} j_1 & j_2 & j_0' \\ j_3 & j_4 & j_5 \end{Bmatrix}_q \psi_f(j_1, j_2, j_3, j_4, j_0', \dots) \,. \tag{6.53}$$

The proof of Theorem 6.3.1 is given in Proof B.4.2.

Removing a link. Consider two adjacent faces F and f, separated by a link e_0. We consider the move which consists in removing e_0 (as well as its two end nodes). By performing a series of 2-2 Pachner moves (6.50), we can always assume that f is triangular,

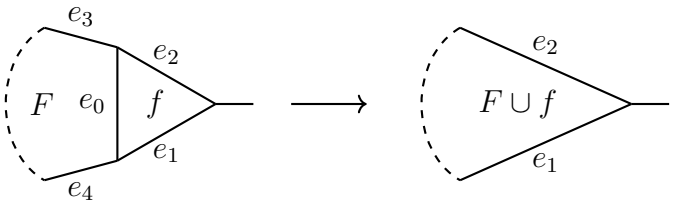

(6.54)

If $|\psi_i\rangle$ is a state which satisfies all the constraints before the link removal, we want to describe how it transforms through the move.

Theorem 6.3.2. *$|\psi_f\rangle$ with spin network coefficients*

$$\psi_f(j_1, j_2, \dots) = (-1)^{(1+o_1)j_1+(1+o_2)j_2} \sqrt{[d_{j_1}]\,[d_{j_2}]}\, \psi_i(0, j_1, j_2, j_2, j_1, \dots) \tag{6.55}$$

is a solution of the constraints on the graph after the link removal. Here o_1, o_2 are the orientations of the links e_1, e_2 with respect to f (counter-clockwise oriented) and $\psi(j_0, j_1, j_2, j_3, j_4, \dots)$ is the spin network coefficient of $|\psi_i\rangle$.

In other words, $|\psi_i\rangle$ gives rise to a solution of the constraints on Γ_f, obtained by keeping only its $j_0 = 0$ components. We will use this relation to study the 3-1 Pachner move. The proof of Theorem 6.3.2 is given in Proof. B.4.3.

3-1 Pachner move. The 3-1 Pachner move removes a triangular face from the graph and replaces it with a node. The links incident to the face become incident to the node,

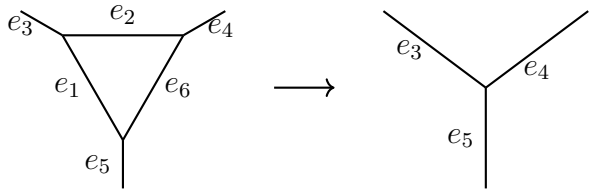

(6.56)

The orientation of all the links are left arbitrary.

Theorem 6.3.3. *If $|\psi_i\rangle$ is a state on the initial graph Γ_i which satisfy all the constraints, then its spin network coefficients can be written*

$$\begin{aligned}&\psi_i(j_1, j_2, j_3, j_4, j_5, j_6, \dots)\\ &\quad = (-1)^{(1+o_1)j_1+(1+o_2)j_2+(1+o_6)j_6}(-1)^{j_3+j_4+j_5}\begin{Bmatrix} j_1 & j_2 & j_3 \\ j_4 & j_5 & j_6 \end{Bmatrix}_q \psi_f(j_3, j_4, j_5, \dots)\,.\end{aligned} \tag{6.57}$$

where $\psi_f(j_3, j_4, j_5, \dots)$ are the spin network coefficients of a state $|\psi_f\rangle$ which satisfies all the constraints on the final graph Γ_f.

We recognize that (6.57) is consistent with the result in [162] when $q = 1$. The proof of Theorem 6.3.3 is given in Proof B.4.4.

In this chapter, we have built up the Hamiltonian constraint for the q-deformed LQG model, obtained from the flatness constraints (6.1). We have written them with the deformed spinors and performed the quantization following the method introduced in the last chapter, or in more detail in [41]. The result is a direct generalization of the quantum Hamiltonian constraints derived in [44] for flat space. By studying the way the solutions to the quantum constraints change under Pachner moves, we provide a generalization of the Noui-Perez transition amplitudes [162] to $q \neq 1$ real: the transition amplitudes are the coefficients relating the physical states in the spin network basis under Pachner moves. Here, they clearly lead to a Turaev-Viro model for q real. It is a topological model (with the same finiteness issues as the $q = 1$ version, the Ponzano-Regge model).

Our method is radically different from [162] however and maybe more in the spirit of LQG. On its way to linking the q-deformed LQG to spin foams, our method derives Wheeler-DeWitt equations as difference equations on the spin network coefficients of the states, see Equation (6.42). In the flat case, the Hamiltonian constraint can be interpreted

as displacements of the nodes of the triangulation [38]. Our difference equations (6.42) are quantum implementations of those symmetries.

Although our constraints are in fact derived from the flatness constraints, we believe that this approach is promising to study both how to incorporate the cosmological constant in 4D and how to write interesting dynamics for curved 4D geometries. A first step in the continuous theory has been initiated in [119].

Chapter 7

Spinors in the spinfoam model

The spinors and their quantization defined in Chapter 3 and 5 can not only be used in the LQG framework but also in other quantum gravity theories. Finally in this chapter, we use the quantum spinors to revisit another quantum gravity model - the spinfoam model (see *e.g.* [21, 168, 138] for review), which is also a background-independent and non-perturbative approach to quantum gravity. We focus on the $\Lambda = 0$ case in this chapter.

Unlike the LQG, the spinfoam model is a covariant formalism that can be understood as a discrete version of gravity path integral. In 3D (in Euclidean signature), the spinfoam model is called the Ponzano-Regge model [174] for $\Lambda = 0$ and the Turaev-Viro model [204] for $\Lambda > 0$, where the latter is a q-deformation of the former with q root of unity. For $\Lambda < 0$, one can extend the result from the Turaev-Viro model to q real.

Such a path-integral formalism, which can be viewed as describing all possible histories of 2D spatial geometries along "time", can be separated into local geometrical amplitudes associated to individual simplicies of the triangulated spacetime manifold. The original Ponzano-Regge model is formulated in terms of the SU(2) irreducible representations. When considering the recoupling theory, the triangular inequalities for the representations bring computational difficulties. As an example, the vertex amplitude of the Ponzano-Regge model, associated to a tetrahedron (whose 3D dual is a vertex), is given by the so-called "$6j$-symbols" from the recoupling theory of SU(2). The exact formula of the $6j$-symbols consists of nonlinear iterations and sums spin labels, thus are hard to compute. The problem is often circumvented by looking at the semi-classical limit, which is more controllable but we are then led far from the microscopic scale.

Alternatively, one can use the spinorial representation. Roughly speaking, it is to replace the $6j$-symbols with some "spinor symbols" reflecting the local quantum geometries,

which naturally turn the amplitude expression from an infinite sum into an integral function of the spinor fields. In this way, understanding the behaviour of the amplitude turns into function(al) analysis. It is expected to be a better route to approach the quantum regime. The use of spinors in spinfoam models is not new. They were used to define the SU(2) coherent states, which were applied to construct the EPRL-FK spinfoam model [82, 96, 141]. However, the role of spinors was not yet unravelled therein.

The coherent states were then recasted with spinors in the U(n) formulation of LQG (see *e.g.* [98, 99, 50]), Further development of coherent intertwiners [75] makes it possible to eliminate spins and only spinors are left in the description. It has been used to construct the spinfoam model in a holomorphic fashion [74, 76], and the invariance of the path integral under Pachner moves was also well-understood [26, 59]. The drawbacks of this holomorphic spinfoam model lie in, on one hand, that the locality of amplitudes is not restored as in the original spinfoam using $6j$-symbols, and, on the other hand, that SU(2) holonomies and/or spins are still explicit in the expression, which makes it hard to extract the true geometrical information carried by the spinors.

The goal of this chapter is to further construct a spinfoam model purely in terms of spinors, which also admits the locality of amplitudes. In other words, the desired path integral is able to be decoupled into products of local amplitudes, as functions of spinors only, associated to local geometry which possesses an analogous structure as in the original Ponzano-Regge amplitude. This would allow us to identify the geometrical interpretation of the local amplitudes and the gluing process.

A natural spinorial substitute of the $6j$-symbol is the generating function of the $6j$-symbols [45]. As a generating function, it brings the benefit that the analysis can be transferred from discrete series to continuous functions (possibly with poles). Different generating functions are distinct by different weights. A careful choice of weights allows us to write a generating function in closed form and thus is well-controlled. Such a generating function does exist. It is called the Schwinger's generating function (SGF) of the $6j$-symbols, and it was found early in the 60s by Schwinger [187] and then reconstructed by Bargmann [28] using a Gaussian integral. The SGF is in the form of a rational function and carries a large family of symmetries as it involves only the loop structure. It came into notice in the spinorial reconstruction of LQG [93, 44, 45, 37], in which it is identified as a new spin network state spanning the loop Hilbert space. Bearing in mind the link between LQG and the spinfoam approach, this construction manifestly opens a route to a new spinfoam model [93, 132]. It is expected that the computational complexity of the vertex amplitudes would be diminished compared to the $6j$-symbols.

The geometrical interpretation of the SGF was discovered by the stationary analysis

at the large scale limit [46], which shows that only the conformal geometry information is stored in the SGF while the scale information is washed out. This provides a new way of seeing the spinfoam amplitude as gluing scale-invariant blocks and it is potentially a better starting point for studying the coarse-graining behaviour of quantum gravity in the spinfoam approach. Coarse-graining, or renormalization, of different spinfoam models has been considered both theoretically and numerically (see *e.g.* a recent review [193]). It is a useful tool to bridge the microscopic theory to the observational scale and prove its viability, and also one of the standard ways to approach the boundary structure and understand the bulk/boundary holography from the point of view of quantum gravity. (See [139] for a discussion on the relation of coarse-graining and holography in LQG.) Moreover, the striking duality of the SGF and the 2D Ising model [37] provides a brand new route to analyze the spinfoam properties using tools from the Ising model, whose coarse-graining behaviour is better understood. On the other hand, a change in vertex amplitude draws our attention to the boundary dependence of the spinfoam path integral as the local vertex amplitude is the quantum counterpart of the discrete boundary action. We will investigate the boundary action consistent with the new vertex amplitude.

This chapter is based on [137] by the author and E. Livine. In Section 7.1, we review the original Ponzano-Regge state-sum model. We start from the classical theory with a boundary term. The state-sum result can be derived in different ways. In one way, one defines the spinfoam vertex amplitude as the trivial evaluation of the boundary projected spin network state, which reveals the relation between the spinfoam model and LQG. In Section 7.2, we briefly review the SGF as the evaluation of the spin network defined by gluing coherent intertwiners associated to each node. We then construct a new spinfoam path integral with the SGF as the new vertex amplitude and prove that the result of the original spinfoam can be recovered by deforming the edge and face amplitudes. The topological invariance can be proven by writing the SGF, or more generally the newly defined spin network state for a general three-valent graph, into a Gaussian integral. This section contains the main results of this chapter. In Section 7.3, we analyze the geometrical interpretation of the newly developed state-integral model. We first look into the symmetries and the geometrical interpretation of the SGF, which describes the local geometry of each unit 3D block, and then the geometrical interpretation of the edge amplitude, which exposes the gluing process of neighbouring blocks in building the global geometry. We compare the new spinfoam model with the original one from their geometrical interpretation and their classical correspondence.

7.1 The Ponzano-Regge state-sum for 3D quantum gravity

In this section, we review the Ponzano-Regge model [174], which is written as a state-sum formula. At this stage, it is important to take the boundary terms into account.

Let us consider the first-order action with a boundary term

$$S[\mathbf{e},\omega]=\int_{\mathcal{M}}\mathrm{Tr}(\mathbf{e}\wedge F(\omega))+\int_{\partial\mathcal{M}}\mathrm{Tr}(\mathbf{e}\wedge\omega)\,. \tag{7.1}$$

This boundary term is the first-order version of the GHY term as shown in (1.18) (we take $s=+$ in this chapter). The path integral is an integration over the gauge equivalent class of the bulk configuration subject to an admissible boundary condition ∂,

$$Z[\mathcal{M},\partial]=\int\mathcal{D}\omega_{\mathrm{B}}\int\mathcal{D}\mathbf{e}_{\mathrm{B}}\,\exp\left(iS[\mathbf{e},\omega]\right)=C[\partial\mathcal{M},\partial]\int\mathcal{D}\omega_{\mathrm{B}}\,\delta(F(\omega_{\mathrm{B}}))\,, \tag{7.2}$$

where $C[\partial\mathcal{M},\partial]$ is a term that depends on the boundary condition and the subscript "B" denotes the configuration in the bulk.

The quantization program proceeds firstly with the triangulation of the spacetime, then with the discretization of variables so that they are concentrated on the simplices of a particular dimension, similar to what we did in the canonical framework. What is different here is that, in the spinfoam model, we consider the triangulation of a 3D manifold.

For consistency purpose, we apply the terminology and notation introduced in Section 2.2 for 0,1,2-simplices and their 2D duals. We now also fix the terminology and notation for 3-simplices and their 3D dual as follows. Upon the 3D triangulation, denoted as $\mathbf{T}$, of $\mathcal{M}$, a 3-simplex is a tetrahedron, denoted as T. Again, a triangle is denoted as $\triangle$; an edge is denoted as $\bar{e}$; a vertex is denoted as $\bar{v}$. What we call a "spinfoam" is the oriented dual 2-complex of $\mathbf{T}$ and we denote it as $\mathbf{T}^*$. In the dual picture, a dual plaquette f^* is dual to one edge $\bar{e}$, an oriented dual edge e^* is dual to one triangle $\triangle$, and a dual vertex v^* is dual to one tetrahedron T. The boundary ∂T of T contains 4 triangles, 6 edges and 4 vertices and it is topologically isomorphic to a two-sphere. When e^* is on the boundary of f^*, we denote $e^*\in\partial f^*$ The same notation and terminology will be used for the spinfoam dual to a general cellular decomposition $\mathbf{C}$ whenever in need, in which case a triangle is generalized to a plaquette denoted as $\bar{f}$.

Moreover, we will intensively make use of oriented graphs on $\partial\mathcal{M}$ when $\mathcal{M}$ is topologically isomorphic to a 3-ball and is triangulated to a tetrahedron T. We are particularly

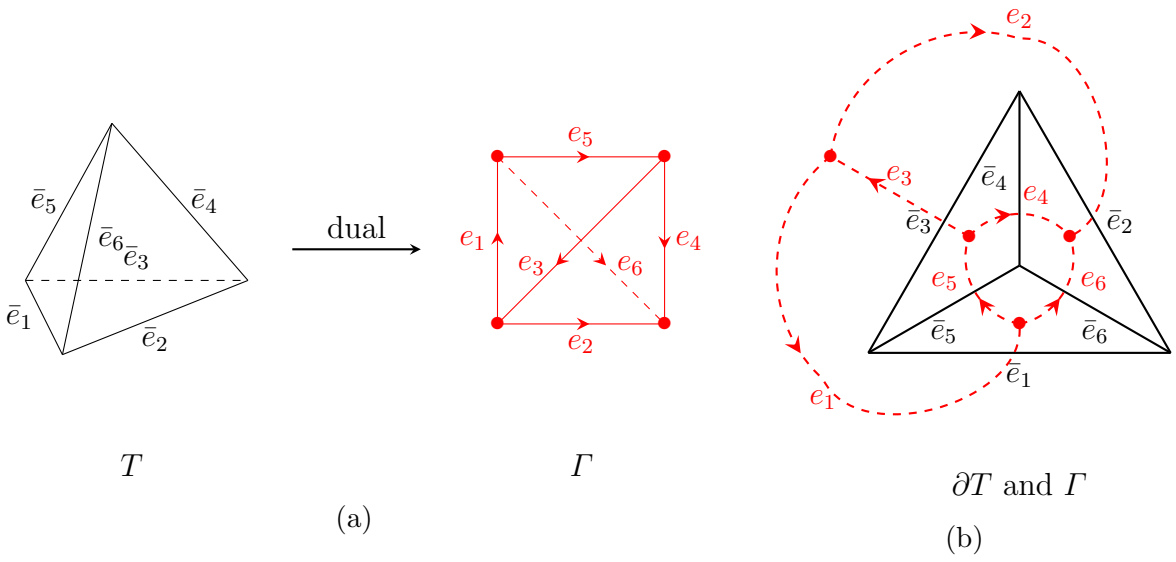

Figure 7.1: (a) From the tetrahedron T to the boundary dual graph $\Gamma \equiv (\partial T)^*$: each triangle $\triangle \subset T$ is replaced by a node $v \subset \Gamma$ and each edge $\bar{e}_i \subset T$ by a link $e_i \subset \Gamma$. The graph Γ also has the combinatorics of a tetrahedron. (b) Combination of ∂T (*in black*), which is the top view projection of the left panel, and its dual graph Γ (*in red*).

interested in the graph $\Gamma \equiv (\partial T)^*$ dual to ∂T, which has the combinatorics of a tetrahedron. It is illustrated in fig.7.1.

In the following, we will introduce the logic of the spinfoam model in Subsection 7.1.1 starting from the path integral (7.2) and the triangularization of $\mathcal{M}$, after which we specialize in the Ponzano-Regge model in Subsection 7.1.2, which is based on the irreducible representation of SU(2). We will derive the Ponzano-Regge state-sum expression in two ways, first from the discretized path integral expression and then from the local amplitude ansatz. The former method is more standard, but the latter is what we will follow when using spinors to re-formulate the Ponzano-Regge model. The Ponzano-Regge model is topological invariant, as it can be checked by performing the Pachner moves.

7.1.1 Spinfoam model as a product of local amplitudes

The idea of spinfoam is to write the path integral (7.2), which reduces to the flatness condition in the bulk, in a discrete fashion that encodes the local geometrical information. As (7.2) integrates out the triads and reduces to a function of the connection in the bulk, it

is natural to define the discrete variables related to the connection. With the triangulation of $\mathcal{M}$ and its dual skeleton at hand, we assign an SU(2) group element g_{e^*} called holonomy to each dual edge e^*, which encodes the discrete information of the connection. The reverse of the dual edge orientation maps g_{e^*} to its inverse $g_{e^*}^{-1}$. Inspired by lattice gauge theory, the curvature is naturally defined by the path-ordered product of holonomies for a dual plaquette with a randomly selected starting dual vertex. For the $\mathbf{e}_\partial$ field on the boundary, applying the same technique as in LQG, it is discretized to be the flux variable $X_{\bar{e}}$, which is an $\mathfrak{su}(2)$ Lie algebra object, assigned to each edge $\bar{e} \in \partial\mathcal{M}$ on the discretized boundary. This leads to the discrete version of (7.2),

$$Z_{\mathbf{T}}[\mathcal{M}, \partial\mathcal{M}] = C_{\mathbf{T}}[\partial\mathcal{M}, \partial] \int_{\mathrm{SU}(2)} \prod_{e^* \notin (\partial\mathcal{M})^*} \mathrm{d}g_{e^*} \prod_{f^*} \delta(\overrightarrow{\prod}_{e^* \in \partial f^*} g_{e^*}) \,, \tag{7.3}$$

where the measure $\mathrm{d}g$ is the Haar measure of SU(2), and the delta distribution on the SU(2) group imposes the group element in the argument to be identity. The discrete flatness is thus understood as the trivial holonomy associated to each dual plaquette. $Z_{\mathbf{T}}[\partial\mathcal{M}, \partial]$ depends on the discrete boundary condition. Upon quantization, these boundary condition becomes boundary states, thus the quantization of (7.2) will depend on the boundary states ψ_Γ on the graph Γ, which is the dual of the boundary triangulation.

The spinfoam machinery to achieve localization consist in expressing the delta distribution in (7.3) as a plane wave of SU(2) in a certain representation, which is then decomposed into a product of plane waves localized in different cells. In other words, it consists in constructing the spinfoam path integral, also understood as the total amplitude, with a product of local amplitudes associated to dual vertices, dual edges and dual plaquettes, capturing the (admissible) local representations and local intertwiners, and then sum over all possible local configurations. It is called the *local spinfoam ansatz*, which postulates that one can formally decompose the total amplitude into

$$Z_{\mathbf{T}}[\mathcal{M}, \psi_\Gamma^{\rho}] = \sum_{\rho_{\mathrm{B}}, \iota_{\mathrm{B}}} \prod_{f^*} \mathcal{A}_{f^*} \prod_{e^*} \mathcal{A}_{e^*} \prod_{v^*} \mathcal{A}_{v^*} \,, \tag{7.4}$$

where ρ and ι denote the representation and the intertwiner respectively, and the sum of representations is only over those associated to the bulk (denoted with the subscript "B")[1]. The boundary state ψ_Γ^{ρ} encodes the representation ρ associated to the boundary graph Γ, which is left in the expression of the total amplitude. The summation symbol was used as we assumed the representations ρ are discrete, which will no longer be the case when we

[1]The total amplitude expression (7.4) can be directly generalized to a general cell decomposition.

consider the spinfoam model with spinor representation in Section 7.2. In the latter case, the summation symbol is changed to the integration symbol.

The edge amplitude $\mathcal{A}_{e^*}$ and the face amplitude[2] $\mathcal{A}_{f^*}$ are both kinematical. The former describes the gluing of adjacent 3-simplices, while the latter is there in order to compensate the factors to recover the delta distribution in (7.3), whose contribution dominates only in the quantum regime. In contrast, the vertex amplitude $\mathcal{A}_{v^*}$ contains the dynamical information of the spinfoam, thus deserves a deeper investigation.

7.1.2 The Ponzano-Regge amplitudes

The Ponzano-Regge model [174] is a realization of (7.4) based on the triangulation of the manifold, where ρ is given by the SU(2) irreducible representation labelled by spin $j \in \mathbb{N}/2$. j is interpreted into the edge length suggested by the (flat) LQG framework [182]. The vertex amplitude of the Ponzano-Regge state-sum geometrically describes the 3D geometry of the tetrahedron it is associated to, and an edge amplitude describes how two neighbouring tetrahedra are glued together.

We start from the discrete path integral (7.3) and work on the dual picture. $\delta(g_{f^*})$ can be decomposed over the SU(2) spin representations using the Peter-Weyl theorem,

$$\delta(g_{f^*}) = \sum_{j_{f^*}} d_{j_{f^*}} \chi^{j_{f^*}}(g_{f^*}) \,, \tag{7.5}$$

where $d_j \equiv 2j+1$ is the dimension of the spin j representation space $\mathcal{V}^j$ and $\chi^j(g) = \mathrm{Tr} D^j(g)$ the character of g in the spin j representation, formulated as the trace of the Wigner matrix $D^j(g)$ of g in the j representation. Thus equivalently in the triangulation picture, each edge $\bar{e}$ is dressed with a spin $j_{\bar{e}}$. When decomposing $\delta(g_{f^*})$ into spin representations, one has an SU(2) group integration for each dual edge e^*, which is dual to a triangle, of 3 copies of the Wigner matrix $D^{j_i}(g)$ $(i = 1 \cdots n)$. This is the projector, also called intertwiner $\mathbb{I}_{\mathcal{H}} = |\mathcal{I}\rangle\langle\mathcal{I}|$, of the kinematical Hilbert space onto the SU(2)-invariant Hilbert space $\mathrm{Inv}_{\mathrm{SU(2)}}\left(\mathcal{V}^{j_1} \otimes \mathcal{V}^{j_2} \otimes \mathcal{V}^{j_3}\right) \bigotimes \mathrm{Inv}_{\mathrm{SU(2)}}\left(\mathcal{V}^{*j_1} \otimes \mathcal{V}^{*j_2} \otimes \mathcal{V}^{*j_3}\right)$. One of the benefits of working on a triangulation over a general cell decomposition is that the intertwiners for 3-valent nodes are one-dimensional[3], which simplify greatly the formulas. In particular, the integration of g_{e^*} for the three Wigner matrices appearing in the discrete path integral

[2] Although we use the terminology that an f^* is a dual plaquette, we denote $\mathcal{A}_{f^*}$ as a face amplitude to be consistent with the literature.

simply becomes

$$\int_{\mathrm{SU}(2)} \mathrm{d}g_{e^*}\, D^{j_1}_{m_1n_1}(g_{e^*}) D^{j_2}_{m_2n_2}(g_{e^*}) D^{j_3}_{m_3n_3}(g_{e^*}) = \begin{pmatrix} j_1 & j_2 & j_3 \\ m_1 & m_2 & m_3 \end{pmatrix} \begin{pmatrix} j_1 & j_2 & j_3 \\ n_1 & n_2 & n_3 \end{pmatrix}, \quad (7.6)$$

which is the product of two normalized *Clebsh-Gordan coefficients*, or equivalently the $3jm$*-symbols*. A combinatorial choice of re-coupling of the $3jm$-symbols gives $6j$*-symbol*, which is associated to a tetrahedron T, or equivalently a dual vertex v^*. For a tetrahedron with the notation in fig.7.1 and each edge $\bar{e}_i$ dressed with a spin j_i, the $6j$-symbol is given by

$$\begin{Bmatrix} j_1 & j_2 & j_3 \\ j_4 & j_5 & j_6 \end{Bmatrix} = \sum_{m_i} (-1)^{\sum_{i=1}^6 (j_i - m_i)} \begin{pmatrix} j_1 & j_2 & j_3 \\ m_1 & m_2 & -m_3 \end{pmatrix} \begin{pmatrix} j_1 & j_5 & j_6 \\ -m_1 & m_5 & m_6 \end{pmatrix} \begin{pmatrix} j_4 & j_2 & j_6 \\ -m_4 & -m_2 & -m_6 \end{pmatrix} \begin{pmatrix} j_4 & j_5 & j_3 \\ m_4 & -m_5 & m_3 \end{pmatrix}. \quad (7.7)$$

It ends up with a state-sum formulation of the discrete partition function (7.3), *i.e.* the *Ponzano-Regge state-sum model*,

$$Z_{\mathbf{T}}[\mathcal{M}, \psi^j_\Gamma] = \sum_{\{j_{f^*}\}} \prod_{f^*} (-1)^{2j_{f^*}} d_{j_{f^*}} \prod_{e^*} (-1)^{\sum_{i=1}^3 j_i} \prod_{v^*} \begin{Bmatrix} j_1 & j_2 & j_3 \\ j_4 & j_5 & j_6 \end{Bmatrix}_{v^*}. \quad (7.8)$$

It easily reads that the vertex amplitude $\mathcal{A}_{v^*}$ is the $6j$-symbol associated to the tetrahedron dual to v^*, and the edge amplitude $\mathcal{A}_{e^*}$ is a sign given by the spins on the sides of the triangle dual to e^*, and the face amplitude $\mathcal{A}_{f^*}$ is the dimension $d_{j_{f^*}}$ of the spin representation space associated to the plaquette f^*. See *e.g.* [30] for detailed explanation of the sign factors. When there's no boundary, the edge amplitude term can be absorbed in the vertex amplitude [30], then the state-sum can be written as

$$Z_{\mathbf{T}}[\mathcal{M}] = \sum_{\{j_{f^*}\}} \prod_{f^*} (-1)^{2j_{f^*}} d_{j_{f^*}} \prod_{v^*} (-1)^{\sum_{i=1}^6 j_i} \begin{Bmatrix} j_1 & j_2 & j_3 \\ j_4 & j_5 & j_6 \end{Bmatrix}_{v^*}. \quad (7.9)$$

Geometrically, the vertex amplitude describes a tetrahedron with edge lengths specified by the spins in the $6j$-symbol. The edge amplitude determines that the gluing of two adjacent tetrahedra is performed by matching the side lengths of the triangles, thus the full 2D geometrical information of the triangles. This trivial way of gluing can be viewed as resulting from the flatness of the manifold, imposed by $\delta(g_{\bar{e}})$ for all the edges of the

triangulation. The face amplitude is simply a weight factor, which is important only in the quantum regime.

A locally-holographic amplitude. Instead of splitting a delta distribution into local amplitudes as above, one can start from the local amplitude ansatz (7.4) and construct first the vertex amplitudes and then recover total amplitude (7.3) by choosing the edge and face amplitudes. This is feasible because a vertex amplitude $\mathcal{A}_{v^*}$ can also be realized by the evaluation of the spin network state as discussed in the following.

Consider a triangulation of $\mathcal{M}$ whose boundary is a union of 2-simplices. We construct an oriented graph Γ dual to this boundary made up with E links e's, V nodes v's and F faces f's. On Γ, we associate a spin j_e to each oriented link e and an intertwiner ι^v to each node v as we did in normal LQG.

An intertwiner can be viewed as an SU(2)-invariant map from the Cartesian product of the spin representation spaces (or the dual spin representation space), associated to the links incident to the same node, to the trivial space:

$$\iota^v_{(j_e)} : \left(\bigotimes_{e|s(e)=v} \mathcal{V}^{j_e}\right) \otimes \left(\bigotimes_{e|t(e)=v} \mathcal{V}^{j_e *}\right) \to 0\,, \tag{7.10}$$

where $s(e)$ and $t(e)$ respectively denote the source and target node of the link e. Or equivalently, the basis of the intertwiner can be written as the tensor product of the magnetic basis followed by a group averaging

$$\iota^v_{(j_e)}(m_e)|0\rangle = \int_{\mathrm{SU}(2)} \mathrm{d}h_v \left(\bigotimes_{e|t(e)=v} \langle j_e, n_e|\, h_v^{-1}\right) \otimes \left(\bigotimes_{e|s(e)=v} h_v\, |j_e, m_e\rangle\right)\,, \tag{7.11}$$

which is indeed SU(2)-invariant. Finally, the spin network state $s_\Gamma^{(j_e,\iota_v)}$ on Γ is simply defined as the tensor product of the intertwiners. Conventionally the spin network state is evaluated on the group elements $\{g_e\} \in \mathrm{SU}(2)^E$ associated to the links, thus

$$s_\Gamma^{\{j_e,\iota_v\}}(g_e) = \sum_{m_e,n_e} \prod_e \langle j_e, m_e|g_e|j_e, n_e\rangle \prod_v \langle \otimes_{e|t(e)=v}\, j_e, n_e|\iota^v_{(j_e)}|\, \otimes_{e|s(e)=v}\, j_e, m_e\rangle\,. \tag{7.12}$$

[3]For a general cell decomposition, an edge is dual to an n-gon, where $n \geq 3$. When $n > 3$, we need to consider intertwiners that are higher dimensional. Then one can decompose the intertwiner into a particular a basis and write $\mathbb{1}_{\mathcal{H}} = \sum_a |\mathcal{I}_a\rangle\langle\mathcal{I}_a|$. See *e.g.* [137] for a discussion.

Its evaluation on the identity $s_\Gamma^{(j_e,\iota_v)}(\mathbb{I})$ plays the role of the vertex amplitude $\mathcal{A}_{v^*}(j_e,\iota_v)$ of the spinfoam partition function (7.4) and it describes the 2D boundary quantum geometry of an elementary 3-simplex, which is a tetrahedron.

In short, the spinfoam can be viewed as a gluing, under certain gluing conditions, of "bubbles" which are homogeneously two-spheres dressed with spin network evaluation. When working on the spin network states, the gluing condition is to identify the shape and size of the glued boundaries, *i.e.* they have the same spins on the glued links. The spinfoam can thus be written as

$$Z_{\mathbf{C}}[\mathcal{M},\psi^j_{\Gamma\subset\partial\mathcal{M}}]=\sum_{\{j_{f^*}\}}\prod_{f^*}(-1)^{2j_{f^*}}d_{j_{f^*}}\prod_{e^*}\mathrm{Sign}(\iota_{e^*})\prod_{v^*}s_{v^*}^{\{j_e,\iota_v\}}(\mathbb{I})\,, \tag{7.13}$$

where $s_{v^*}^{\{j_e,\iota_v\}}(\mathbb{I})$ is the spin network evaluation on each bubble, and the edge amplitude $\mathrm{Sign}(\iota_{e^*})$ is a sign depending on the spins of the intertwiner on (the node dual to) the shared plaquette dual to the edge e^*. The exact value of this sign depends on the choice of basis of the intertwiner.

For a triangulation, each boundary is made up of a triangle and thus Γ is identically three-valent, in which case the intertwiner is one-dimensional and thus uniquely defined under a chosen basis. In this case, the spin network evaluation is simply a $3nj$-symbol. The smallest three-valent graph embedded on a two-sphere is indeed a tetrahedron graph $\Gamma=(\partial T)^*$, as illustrated in fig.7.1. The spin network state trivially evaluated on a tetrahedron graph gives a $6j$-symbol[4],

$$s_{\mathrm{tet}}^{\{j_e\}}(\mathbb{I})=\begin{Bmatrix} j_1 & j_2 & j_3\\ j_4 & j_5 & j_6\end{Bmatrix}\,, \tag{7.14}$$

which is exactly the vertex amplitude we obtained through decomposing the delta distribution on SU(2). This is the Ponzano-Regge state-sum for the simplest triangulation of a 3-ball (with no summation at all), describing the boundary quantum geometry of a tetrahedron. In the semi-classical limit, seen from scaling j to λj and taking $\lambda\to\infty$, the $6j$-symbol is given by the Hartle-Sorkin action [129] in Regge calculus for a tetrahedron in terms of the edge lengths and dihedral angles:

$$\begin{Bmatrix} \lambda j_1 & \lambda j_2 & \lambda j_3\\ \lambda j_4 & \lambda j_5 & \lambda j_6\end{Bmatrix}\xrightarrow{\lambda\to\infty}\frac{1}{\sqrt{12\pi V}}\cos\left(S_{\mathrm{HS}}(\{\lambda j_e+\frac{1}{2}\})+\frac{\pi}{4}\right)\,,$$
$$\text{with}\quad S_{\mathrm{HS}}(\{\ell_e\})=\sum_{e=1}^{6}\ell_e\Theta_e\,, \tag{7.15}$$

[4]We have ignored the notation ι^v for the intertwiners on the left-hand side for simplicity. The intertwiners are implicit in the definition of the $6j$-symbol.

where Θ_e is the dihedral angle around the edge $\bar{e}$ (dual to link e) and V is the volume of the tetrahedron with edge length $\ell_e = \lambda j_e + \frac{1}{2}, e = 1, \cdots, 6$. This asymptotic was postulated by Ponzano and Regge [174] and proven in different methods [180, 186, 102, 29]. The Hartle-Sorkin action (7.15) is the discrete version the GHY boundary term [129]:

$$\int_{\partial\mathcal{M}} \mathrm{d}^2\sqrt{h}K \xrightarrow{\text{discretize}} \sum_{e\in\partial\mathcal{M}} \ell_e\Theta_e\,. \tag{7.16}$$

For general $3nj$-symbols, the semi-classical limit also encodes the geometry of the boundary 2-cell it describes [69]. The reproduction of the vertex amplitude with the boundary states exposes the fact that the vertex amplitude is a local-holographic amplitude, encoding only the boundary data of the 3-cell it is associated to. The gluing process for two adjacent 3-cells can be understood as smearing the data on the shared boundaries. In this way, the degrees of freedom on the shared boundaries become gauge through gluing, and the only physical degrees of freedom are on the union of the un-glued boundaries, *i.e.* the cellular decomposition of $\partial\mathcal{M}$. This is exactly why the bulk part of the amplitude is independent of the cellular decomposition.limit.

Topological invariance of the Ponzano-Regge model from Pachner moves. The Ponzano-Regge state-sum formula

$$Z_{\mathbf{T}}[\mathcal{M}, \psi_\Gamma^j] = C_{\mathbf{T}}[\partial\mathcal{M}] \int_{\mathrm{SU}(2)} \prod_{e^*\notin(\partial\mathcal{M})^*} \mathrm{d}g_{e^*} \prod_{f^*} \delta(\overrightarrow{\prod}_{e^*\in\partial f^*} g_{e^*}) \tag{7.17}$$

$$= \sum_{\{j_{f^*}\}} \prod_{f^*} (-1)^{2j_{f^*}} d_{j_{f^*}} \prod_{e^*} (-1)^{\sum_{i=1}^3 j_i} \prod_{v^*} \begin{Bmatrix} j_1 & j_2 & j_3 \\ j_4 & j_5 & j_6 \end{Bmatrix}_{v^*} \tag{7.18}$$

is invariant under the Pachner moves in the bulk [163], which is evidence that the amplitude is independent of the bulk configuration and only depends on the boundary states. In 3D, there are two types of Pachner moves, namely the $2-3$ moves and the $1-4$ moves as shown in fig.7.2. To prove the topological invariance, one can either start from the group formulation (7.17) and apply the change of variable method or start from the spin formulation (7.18) and apply the recursion relation of $6j$-symbols [105]. It deserves to be mentioned here that adding a vertex inside a tetrahedron in the $1-4$ Pachner move (fig.7.2b) leads to a divergent amplitude. The divergence comes from $\sum_J d_J^2 = \delta_{\mathrm{SU}(2)}(\mathbb{I})$ whose degree depends on the topology only (see [30, 47, 48] for discussion.) Regularization was originally performed by introducing a cut-off on spin J [174]. It was then realized that the divergence corresponds to the $\mathfrak{su}(2)$ gauge that generates the translational symmetry

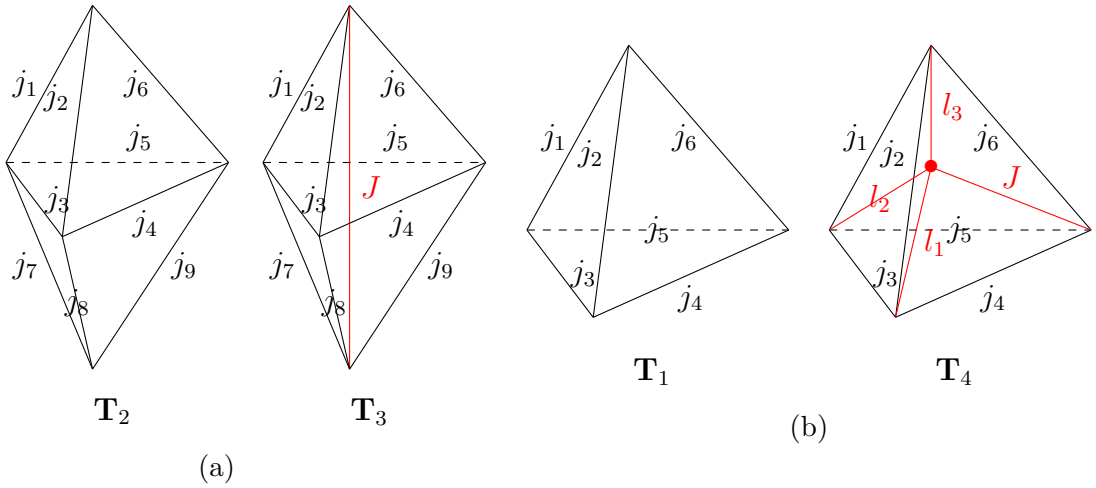

Figure 7.2: (a) 2-3 Pachner move: adding an internal edge. (b) 1-4 Pachner move: adding an internal vertex.

of the internal vertex thus the regularization can be performed by a partial gauge fixing procedure [103, 104].

In the Ponzano-Regge state-sum (7.18), the boundary data are the lengths of the one-skeleton encoded in the $6j$-symbols. Therefore, the path integral constructed as such depends on the boundary metric and thus the length scale. The scale invariance of the bulk is merely obtained by the summation of the spin labels.

In the next section, we will study a scale-invariant path integral even with boundary configurations. To this end, it is natural to choose a scale-invariant boundary state, then one can define a scale-invariant vertex amplitude as the evaluation of this new quantum state on the boundary of an elementary 3-cell. These states should encode the conformal geometry, *i.e.* angles, of the triangulation of the boundary surface. Technically, to define such a conformal boundary quantum state means to find an "alternative" representation of SU(2) that can be geometrically interpreted as angles. Given a different formulation of the partition function from (7.18), the recursion relation of $6j$-symbols would be replaced by other identities in order to reproduce the topological invariance, which will be the case illustrated in Subsection 7.2.5.

7.2 A new coherent state-integral

The "alternative" representation we are going to apply is the spinor representation of SU(2) [143], developed from the U(n) formulation of LQG [75, 99, 50]. The quantum states under this representation are called the *coherent spin network states* (see below) [44]. After a concise review of its general construction, we will specialize in the coherent spin network state of a tetrahedron graph, whose evaluation on identity after changing the weight gives the SGF [187, 28]. We will construct the Ponzano-Regge model in a new formalism with spinor variables, where the SGF serves as the vertex amplitude. Similar to the original one, it can also be seen as built with local amplitudes associated to the elementary bubbles.

7.2.1 Scaleless spin network states and generating function

Let us introduce the SU(2) spin coherent state (or the SU(2) coherent state for short) *à la* Perelomov, denoted as $|j,\zeta\rangle$ with a fixed spin $j \in \mathbb{N}/2$ and a spinor $|\zeta\rangle := \begin{pmatrix} \zeta^- \\ \zeta^+ \end{pmatrix} \in \mathbb{C}^2$ introduced in Chapter 3.

To this end, one needs to quantize the classical spinor components $\zeta^A, \bar{\zeta}^A$. Upon quantization, the spinors become the annihilation operators $\zeta^A \to a^A$ and the creation operator $\bar{\zeta}^A \to a^{A\dagger}$ such that satisfies the commutator

$$[a^A, a^{B\dagger}] = \delta^{AB}\,, \quad [a^A, a^B] = [a^{A\dagger}, a^{B\dagger}] = 0\,. \tag{7.19}$$

This being said, the phase space for an n-valent node is quantized to be a set of $2n$ harmonic oscillators. The commutators naturally inherit from the Poisson brackets (3.15). Indeed, (7.19) is the $q = 1$ version of the deformed commutation relation (5.2). It is natural to obtain the Fock states $|n^-, n^+\rangle_{\text{HO}}$ which diagonalize the occupation number operator $N^A := a^{A\dagger}a^A$

$$N^A|n^-, n^+\rangle_{\text{HO}} = n^A|n^-, n^+\rangle_{\text{HO}}\,. \tag{7.20}$$

This basis is equivalent to the magnetic number basis $|j, m\rangle \in \mathcal{V}^j$ with the relation between the eigenvalue as

$$j = \frac{1}{2}(n^- + n^+)\,, \quad m = \frac{1}{2}(n^- - n^+)\,. \tag{7.21}$$

The action of $(a^A, a^{B\dagger})$ on the magnetic number basis allows the jumping between different

spin representations. Explicitly,

$$a^A|j,m\rangle = \sqrt{j+(-1)^A m}\,|j-\frac{1}{2},m-\frac{1}{2}+A\rangle\,, \tag{7.22a}$$

$$a^{A\dagger}|j,m\rangle = \sqrt{j+(-1)^A m+1}\,|j+\frac{1}{2},m+\frac{1}{2}-A\rangle\,, \tag{7.22b}$$

which is the $q=1$ version of (5.9).

The state $|j,\zeta\rangle$ is a superposition state of a pair of harmonic oscillators $|n^0,n^1\rangle_{\rm HO}$, identified with a magnetic number basis $|j,m\rangle \in \mathcal{V}^j$ by the relation (7.21) and reads

$$|j,\zeta\rangle := \frac{(\zeta^A a^{A\dagger})^{2j}}{\sqrt{(2j)!}}|0\rangle \equiv \sum_{m=-j}^{j}\sqrt{\frac{(2j)!}{(j+m)!(j-m)!}}(\zeta^-)^{j+m}(\zeta^+)^{j-m}|j,m\rangle\,, \tag{7.23}$$

where $a^{A\dagger}$ is the creation operator acting on the oscillator n^A, $A=\pm$. This is the state that admits the generalized minimal uncertainty given by the dispersion of the SU(2) Casimir [140]. The norm is easily computed $\langle j,\zeta|j,\zeta\rangle = \langle\zeta|\zeta\rangle^{2j}$. For a fixed spin j, $|j,\zeta\rangle$ serves as an alternative orthonormal basis spanning the representation space $\mathcal{V}^j$. We refer to [143] for more details.

By the definition of the coherent state basis through the magnetic number basis (7.23), it is easy to find that a^A acts on $|j,\zeta\rangle$ as a multiplication operator while $a^{A\dagger}$ acts as a derivative operator on $|j,\zeta\rangle$, *i.e.*

$$a^A|j,\zeta\rangle = \sqrt{2j}\,\zeta^A\,|j-\frac{1}{2},\zeta\rangle\,,\quad a^{A\dagger}|j,\zeta\rangle = \frac{1}{\sqrt{2j+1}}\frac{\partial}{\partial\zeta^A}\,|j+\frac{1}{2},\zeta\rangle\,, \tag{7.24}$$

thus a^A decreases the spin by $1/2$ as well as multiplying the state by ζ^A, while $a^{A\dagger}$ increases the spin by $1/2$ and derives the state by ζ^A.

We also introduce a dual SU(2) coherent state $[j,\zeta| \equiv \langle j,\varsigma\zeta|$ in terms of a dual spinor $[\zeta| = \langle\varsigma\zeta| := \begin{pmatrix} -\zeta^+, & \zeta^- \end{pmatrix}$, which is also holomorphic ζ^A, living in the dual representation space $\mathcal{V}^{j*}$ (see (3.2)). a^A acts on $[j,\zeta|$ as the creation operator while $a^{A\dagger}$ acts as the annihilation operator,

$$[j,\zeta|\,a^A = -\epsilon^{AB}\frac{1}{\sqrt{2j+1}}\frac{\partial}{\partial\zeta^B}\,[j+\frac{1}{2},\zeta|\,,\quad [j,\zeta|\,a^{A\dagger} = -\epsilon^{AB}\sqrt{2j}\,\zeta^B\,[j-\frac{1}{2},\zeta|\,. \tag{7.25}$$

Consider an oriented graph Γ with E oriented links e's, V nodes v's and F faces f's. We dress each link e with a spin j_e, and associate a spinor $|\zeta_e\rangle$ to the source $s(e)$ of e

and another spinor $|\tilde{\zeta}_e]$ to the target $t(e)$. For an n-valent node v, we can construct an intertwiner living in the tensor space $\left(\bigotimes_{e|s(e)=v}\mathcal{V}^{j_e}\right)\otimes\left(\bigotimes_{e|t(e)=v}\mathcal{V}^{j_e^*}\right)$ by SU(2)-group averaging the tensor product of the SU(2) holomorphic coherent states, *i.e.*

$$\iota^v_{(j_e)}(\zeta_e)\,|0\rangle := \int_{\mathrm{SU}(2)}\mathrm{d}g_v\left(\bigotimes_{e|t(e)=v}[j_e,\tilde{\zeta}_e|\,g_v^{-1}\right)\otimes\left(\bigotimes_{e|s(e)=v}g_v\,|j_e,\zeta_e\rangle\right). \tag{7.26}$$

This is called the *Livine-Speziale (LS) coherent intertwiner*, first introduced in [140] (see also [99]) and used to define the EPRL-FK spinfoam models [82, 141]. It is also closely related to the U(n) coherent states which are by definition covariant under the U(n) action [99].

(7.11) and (7.26) are simply projections of a general SU(2) intertwiner on different bases, the former on the magnetic number basis while the latter on the coherent state basis. Equipped with the intertwiners (7.26), one can define a spin network state evaluated on SU(2) group elements $\{g_e\}$ as a holomorphic function of the spinors:

$$s_\Gamma^{\{j_e,\zeta_e,\tilde{\zeta}_e\}}(g_e)=\int_{\mathrm{SU}(2)^V}\prod_v\mathrm{d}h_v\prod_e[j_e,\tilde{\zeta}_e|\,h_{t(e)}^{-1}\,g_e\,h_{s(e)}\,|j_e,\zeta_e\rangle\,. \tag{7.27}$$

It is also possible to eliminate the spins and define an intertwiner associated to a node v with only spinor labels, which can be viewed as a generating function of the LS coherent intertwiners (7.26) with a chosen series of weight [45]. The simplest weight is $\frac{1}{\prod_{e\in v}\sqrt{(2j_e)!}}$, which defines the *coherent intertwiner*[5],

$$\iota^v(\zeta_e)=\sum_{\{j_e\}}\frac{1}{\prod_{e\in v}\sqrt{(2j_e)!}}\iota^v_{(j_e)}(\zeta_e)\,. \tag{7.28}$$

It is indeed an SU(2) invariant state in $\bigoplus_{\{j_e\}}\left(\bigotimes_{e|s(e)=v}\mathcal{V}^{j_e}\right)\otimes\left(\bigotimes_{e|t(e)=v}\mathcal{V}^{j_e^*}\right)$. We associate a coherent intertwiner to each node and glue them along links associated with SU(2) holonomies. The gluing is performed in the standard way, *i.e.* taking $\langle k,n|j,m\rangle=\delta_{jk}\delta_{mn}$. The result defines the coherent spin network state [45]

$$\begin{aligned}s_\Gamma^{\mathrm{cohe}}(g_e)&=\sum_{\{j_e\}}\int_{\mathrm{SU}(2)^V}\prod_v\mathrm{d}h_v\prod_e\frac{1}{(2j_e)!}[j_e,\tilde{\zeta}_e|\,h_{t(e)}^{-1}\,g_e\,h_{s(e)}\,|j_e,\zeta_e\rangle\\&=\int_{\mathrm{SU}(2)^V}\prod_v\mathrm{d}h_v\prod_e e^{[\tilde{\zeta}_e|h_{t(e)}^{-1}\,g_e\,h_{s(e)}|\zeta_e\rangle}\,.\end{aligned} \tag{7.29}$$

A slightly different choice of weight[6], which we will focus on in this chapter is $\frac{(J_v+1)!}{\prod_{e\in v}\sqrt{(2j_e)!}}$, where $J_v \equiv \sum_{e\in v} j_e$ is the sum of spins on the links incident to v. It defines the *scaleless intertwiner* (as we will see in the next subsection that it encodes the scale-invariant geometry of a 3-cell boundary):

$$\iota_v^{\mathfrak{sl}}(\zeta_e) = \sum_{\{j_e\}} \frac{(J_v+1)!}{\prod_{e\in v}\sqrt{(2j_e)!}} \iota^v_{(j_e)}(\zeta_e)\,. \tag{7.30}$$

Again, we associate a scaleless intertwiner to each node and glue them in the same way as the coherent intertwiner. We define it as the *scaleless spin network state* :

$$s_\Gamma^{\mathfrak{sl}}(g_e) = \sum_{\{j_e\}} \prod_v \frac{(J_v+1)!}{\prod_{e\in v}(2j_e)!} \int_{\mathrm{SU}(2)^V} \prod_v \mathrm{d}h_v \prod_e [j_e, \tilde{\zeta}_e|\, h^{-1}_{t(e)}\, g_e\, h_{s(e)}\, |j_e, \zeta_e\rangle\,. \tag{7.31}$$

It can be viewed as a generating function of the spin network state (7.12). The use of spinors shifts the view of building blocks of quantum geometries from the links to the nodes, which is also the spirit behind the construction of the U(n) coherent states [99, 50, 75].

The LQG kinematical Hilbert space $L_2(\mathrm{SU}(2),\mathrm{d}g)^E//\mathrm{SU}(2)^V$, where the symplectic reduction is due to the Gauss constraints performed on the nodes, is usually understood as spanned by the spin network states labelled by spins. The quantization of the spinorial phase space allows us to span the same Hilbert space by the coherent or scaleless spin network states labelled by spinors. To this end, we also need to introduce a Haar measure. It is given by the Haar measure $\mathrm{d}\mu(\zeta)$ of the Bargmann space $\mathcal{F}_2 = L_2^{\mathrm{hol}}(\mathbb{C}^2,\mathrm{d}\mu)$, the space of holomorphic squared integrable functions, over the spinor variables [143]:

$$\mathrm{d}\mu(\zeta) := \frac{1}{\pi^2} e^{-\langle\zeta|\zeta\rangle} \mathrm{d}\zeta^-\mathrm{d}\zeta^+\,. \tag{7.32}$$

It is a measure which is invariant under the SU(2) transformation $\mathrm{d}\mu(g\zeta) = \mathrm{d}\mu(\zeta)$, $\forall\, g \in \mathrm{SU}(2)$. The space $\mathcal{F}_2$ can be decomposed into the direct sum of d_j-dimensional subspace: $\mathcal{F}_2 = \oplus_{j\in\mathbb{N}/2}\mathcal{V}^j$, with the orthonormal basis of each spin j subspace given by

$$e^j_m(\zeta) := \frac{(\zeta^-)^{j+m}(\zeta^+)^{j-m}}{\sqrt{(j+m)!(j-m)!}} |j,m\rangle\,. \tag{7.33}$$

[5]The term "coherent intertwiner" was used to denote the LS coherent intertwiner (7.26) for short in some literature. We remind the readers that these two terms have distinct definitions in this article, following [45].

[6]Other choices of weight lead to different generating functions, which would be useful for different interests. See *e.g.* [45] for a discussion and the application of other generating functions with alternative weights.

The Hilbert space of one link is thus equivalently given by $\mathcal{H}_e = \mathcal{F}_2 \times \mathcal{F}_2 // \mathrm{U}(1)$, with U(1) given by the norm matching constraint (3.8) which is first class. One can find more details for the Bargmann space reconstruction of the Hilbert space in [143]. By taking the closure constraint for nodes into consideration, we conclude that the Hilbert space spanned by the coherent or scaleless spin network states can be represented as $L_2^{\mathrm{hol}}(\mathbb{C}^2, \mathrm{d}\mu)^{2E} // (\mathrm{SU}(2)^V \times \mathrm{U}(1)^E)$.

Above we have defined the coherent intertwiners, coherent spin network states, scaleless intertwiners and scaleless spin network states for a general graph. The goal is to use these notions to define a new vertex amplitude in terms of spinors in the Ponzano-Regge model. To this end, we will work on a three-valent graph in the next subsection. More specifically, we will study the tetrahedron graph as shown in fig.7.1 and study the evaluation of the scaleless spin network state on this simple graph.

7.2.2 The holomorphic $\{12\zeta^{\times 2}\}$ symbol

In this subsection and the next, we will fix the cellular decomposition of $\mathcal{M}$ to be a triangulation unless specified and intensively work on the tetrahedron graph $\Gamma = (\partial T)^*$ that is a 2D dual graph of the boundary two-skeleton of a tetrahedron T. The simplicity it brings helps to quantify the scaleless intertwiners (7.30) and the scaleless spin network functions (7.31). On the other hand, it turns out that the scaleless spin network state for a tetrahedron graph, when evaluated on the identity, possesses a closed form, which is known as the SGF.

For a three-valent graph, the intertwiner (7.26) for each node is one-dimensional, thus it must be proportional to the $3jm$-symbol. The exact relation is well-known [206], with the proportionality coefficient given by a holomorphic polynomial of degree J_v. Consider three outgoing links (e_1, e_2, e_3) meeting at the node v, we denote the total spin as $J_{123} = j_1 + j_2 + j_3$. Then one gets

$$\iota^v_{j_1 j_2 j_3}(\zeta_1, \zeta_2, \zeta_3) = P_{j_1 j_2 j_3}(\zeta_1, \zeta_2, \zeta_3)\, \iota^v_{j_1 j_2 j_3}\,, \tag{7.34}$$

with

$$P_{j_1 j_2 j_3}(\zeta_1, \zeta_2, \zeta_3) = \frac{\triangle(j_1 j_2 j_3)}{(J_{123}+1)!} \left(\prod_{e=1}^{3} \sqrt{(2j_e)!} \right) [\zeta_1|\zeta_2\rangle^{J_{123}-2j_3}\, [\zeta_2|\zeta_3\rangle^{J_{123}-2j_1}\, [\zeta_3|\zeta_1\rangle^{J_{123}-2j_2}\,, \tag{7.35}$$

where $\triangle(j_1j_2j_3)$ is the quantum triangle coefficient defined as

$$\triangle(j_1j_2j_3)=\sqrt{\frac{(J_{123}+1)!}{(j_1+j_2-j_3)!(j_1+j_3-j_2)!(j_2+j_3-j_1)!}}\,. \tag{7.36}$$

The scaleless intertwiner (7.30) for the node with incident links (e_1,e_2,e_3) outgoing reads

$$\iota_v^{\mathfrak{sl}}(\zeta_1,\zeta_2,\zeta_3)=\sum_{j_1,j_2,j_3}\frac{(J_{123}+1)!}{\prod_{e=1}^3\sqrt{(2j_e)!}}\iota^v_{j_1j_2j_3}(\zeta_1,\zeta_2,\zeta_3)\,, \tag{7.37}$$

which is an invariant vector on $\otimes_{e=1}^3(\oplus_{j_e}\mathcal{V}^{j_e})$, and is also a generating function of the $3jm$-symbol.

The proportionality coefficient (7.35) remains unchanged when some links are incoming (except that in this case, we denote the spinor on an incoming link with a tilde). For instance, for a node with links e_1, e_2 incoming and link e_3 outgoing, the relation reads

$$\iota^v_{j_1^*j_2^*j_3}(\tilde\zeta_1,\tilde\zeta_2,\zeta_3)=P_{j_1j_2j_3}(\tilde\zeta_1,\tilde\zeta_2,\zeta_3)\,\iota^v_{j_1^*j_2^*j_3}\,. \tag{7.38}$$

The scaleless spin network state for the tetrahedron graph naturally follows except that there is a sign ambiguity as the graph is odd-valent. The reason is that the sign of the intertwiner (7.34) would be changed under exchanging any pair of spinors in the argument, thus it is necessary to fix the ordering of links incident to a node in order to specify (the sign of) the definition of the scaleless spin network function. In practice, it is enough to fix a cyclic order $\prec$ for each node. We apply the same notation as in fig.2.6 for the ordering of links incident to the same node. For an ordering $(e\prec e',e'\prec,e'',e''\prec e)$, we fix an ordered holomorphic polynomial $P^{\prec}_{j_ej_{e'}j_{e''}}(\zeta_e,\zeta_{e'},\zeta_{e''})$ to be

$$P^{\prec}_{j_ej_{e'}j_{e''}}(\zeta_e,\zeta_{e'},\zeta_{e''})=\frac{\triangle(j_ej_{e'}j_{e''})}{(J_v+1)!}\left(\prod_{e\in v}\sqrt{(2j_e)!}\right)\,[\zeta_e|\zeta_{e'}\rangle^{J_v-2j_{e''}}\,[\zeta_{e'}|\zeta_{e''}\rangle^{J_v-2j_e}\,[\zeta_{e''}|\zeta_e\rangle^{J_v-2j_{e'}}\,. \tag{7.39}$$

We have ignored the tilde of spinors for incoming links for simplicity and unification. Consider again a tetrahedron graph as in fig.7.1, it can be naturally embedded in a 2-sphere, which generates the cyclic order for all the nodes at once. The scaleless spin network function is then uniquely defined as

$$\mathcal{S}^{\{\zeta_e,\tilde\zeta_e\}}_{\rm tet}(g_e)=\sum_{j_1,\cdots,j_6}\frac{\prod_{v=1}^4(J_v+1)!}{\prod_{e=1}^6(2j_e)!}s^{\{j_e,\zeta_e,\tilde\zeta_e\}}_{\rm tet}(g_e)\,, \tag{7.40}$$

with

$$s_{\rm tet}^{\{j_e,\zeta_e,\tilde\zeta_e\}}(g_e) = \int_{{\rm SU}(2)^4} \prod_{v=1}^4 {\rm d}h_v \prod_{e=1}^6 [j_e,\tilde\zeta_e|\, h_{t(e)}^{-1}\, g_e\, h_{s(e)}\, |j_e,\zeta_e\rangle$$
$$= P^{\prec}_{j_1j_2j_3}(\zeta_1,\zeta_2,\zeta_3) P^{\prec}_{j_1j_5j_6}(\tilde\zeta_1,\tilde\zeta_5,\zeta_6) P^{\prec}_{j_3j_4j_5}(\tilde\zeta_3,\tilde\zeta_4,\zeta_5) P^{\prec}_{j_2j_4j_6}(\tilde\zeta_2,\tilde\zeta_6,\zeta_4)\, s_{\rm tet}^{\{j_e,\iota_v\}}(g_e) \tag{7.41}$$

being the special case of (7.27) for a tetrahedron graph, which can be factorized, as shown in the second line of (7.41), into the standard spin network function independent of the spinors, and a holomorphic polynomial independent of the arguments $\{g_e\}$. In particular, its evaluation on identity gives a holomorphic "$\{12\zeta^{\times 2}\}$ symbol", known as Schwinger's generating function of the $6j$-symbols (SGF), which is a function of 12 spinors thus 24 complex variables,

$$\mathcal{S}_{\rm tet}^{\mathfrak{sl}}(\{\zeta_e,\tilde\zeta_e\}) = \mathcal{S}_{\rm tet}^{\{\zeta_e,\tilde\zeta_e\}}(\mathbb{I})$$
$$= \sum_{j_1\cdots j_6} \left[\prod_{v=1}^4 \sqrt{\frac{(J_v+1)!}{\prod_{e\in v}(J_v-2j_e)!}}\right] \left\{\begin{array}{ccc} j_1 & j_2 & j_3 \\ j_4 & j_5 & j_6 \end{array}\right\} \prod_{v=1}^4 \prod_{\substack{e,\,e',\,e''\in v,\\ e\prec e'}} [\zeta_e|\zeta_{e'}\rangle^{J_v-2j_{e''}}\,. \tag{7.42}$$

It was first found to be of the closed form by Schwinger [187, 28, 44]. (See also [37] for the deduction from the duality between the 2D Ising model and the Ponzano-Regge model). It is in a form of a scaleless function:

$$\mathcal{S}(\{\zeta_e,\tilde\zeta_e\}) \equiv \mathcal{S}_{\rm tet}^{\mathfrak{sl}}(\{\zeta_e,\tilde\zeta_e\}) = G(\{\zeta_e,\tilde\zeta_e\})^{-2}\,,$$
$$G(\{\zeta_e,\tilde\zeta_e\}) = 1 + \sum_{\mathcal{L}} \prod_{v\subset\mathcal{L},\, e\prec e'} [\zeta_e|\zeta_{e'}\rangle = 1 + \sum_{\triangle^*} \prod_{\substack{v\,\subset\,\triangle^*\\ e\,\prec\, e'}} [\zeta_e|\zeta_{e'}\rangle + \sum_{\square^*} \prod_{\substack{v\,\subset\,\square^*\\ e\,\prec\, e'}} [\zeta_e|\zeta_{e'}\rangle\,, \tag{7.43}$$

where $\mathcal{L}$'s denote the loops in the tetrahedron graph, including three-cycles $\triangle^*$'s and four-cycles $\square^*$'s. The scaleless spin network states can be used to describe the kinematical information in the Hilbert space of quantum geometry. By the continuous nature of the spinor arguments in a scaleless spin network state, the dynamics given by the Wheeler de-Witt equation would be translated into a differential equation of the SGF [44], rather than a recursion relation as for the $6j$-symbols when we consider the spin network states [43].

Symmetries of the SGF. The loop structure (7.43) of the SGF brings a large number of degrees of symmetry. Compared to a $6j$-symbol which has only 6 real variables, the SGF has 12 independent spinors, thus 24 complex or 48 real variables, in its argument. The symmetries would allow us to work on a smaller set of variables. Firstly, the SGF (7.42) is explicitly written only in terms of the inner product $[\zeta_e|\zeta_{e'}\rangle$ of spinors, which is by definition invariant under the $\mathrm{SL}(2,\mathbb{C})$ action that acts covariantly on the spinors

$$g_v \triangleright |\zeta'_e\rangle = g_v|\zeta'_e\rangle\,, \quad g_v \triangleright [\zeta_e| = [\zeta_e|g_v^{-1}\,, \quad e,e' \in v\,, \quad g_v \in \mathrm{SL}(2,\mathbb{C})\,. \tag{7.44}$$

Thus the spinors form a set with 12 complex or 24 real variables. Secondly, notice that the exact evaluation (7.43) takes the form as cycles, a (complex) rescaling of the spinor $\zeta_e \to \alpha\zeta_e$ ($\alpha \in \mathbb{C}\backslash\{0\}$) on one end of each link and an "anti-rescaling" of the spinor $\tilde{\zeta}_e \to \frac{1}{\alpha}\tilde{\zeta}_e$ on the other end leaves the SGF unchanged. Therefore, the symmetries of the SGF can be expressed as

$$\mathcal{S}(\{\zeta_e^v, \tilde{\zeta}_e^{v'}\}) = \mathcal{S}(\{g_v\,\zeta_e^v, g_{v'}\,\tilde{\zeta}_e^{v'}\}) = \mathcal{S}(\{\alpha_e\,\zeta_e^v, \alpha_e^{-1}\tilde{\zeta}_e^{v'}\})\,, \quad \forall\, g_v \in \mathrm{SL}(2,\mathbb{C})\,, \forall\, \alpha_e \in \mathbb{C}\backslash\{0\}\,. \tag{7.45}$$

In words, the SGF is invariant under the $\mathrm{SL}(2,\mathbb{C})$ gauge transformation, one for each node hence a total of 12 complex degrees of freedom, and anti-scale transformation, one for each link hence a total of 6 complex degrees of freedom. These symmetries form the full redundant degrees of freedom in the 12 spinors, leaving 6 complex degrees of freedom in the SGF. The same redundancy appears when we use the spinor representation to describe the scaleless spin network states for a general graph. It is thus possible to change the argument variables of the SGF to a smaller set. We will see in Subsection 7.3.1 that a change of variables will make it clear to see the geometrical information given by this scaleless spin network state.

7.2.3 The Ponzano-Regge model in terms of coherent blocks

We now turn our attention back to the Ponzano-Regge model. We aim to decompose the discrete path integral

$$Z_{\mathbf{T}}[\mathcal{M},\partial\mathcal{M}] = C_{\mathbf{T}}[\partial\mathcal{M}] \int_{\mathrm{SU}(2)} \prod_{e^*\notin\partial\mathcal{M}} \mathrm{d}g_{e^*} \prod_{f^*} \delta(\overrightarrow{\prod}_{e^*\in\partial f^*} g_{e^*})$$

into the product of vertex, edge and face amplitudes encoding local quantum geometries through the spinor representation labels, so that the global quantum geometry can be

understood as gluing elementary blocks with local geometry information stored in these spinor variables. The total amplitude should be written alternatively in the form as

$$\mathcal{A}_{\mathbf{T}}[\mathcal{M},\psi_\Gamma^{\text{cohe}}]=\int[\mathrm{d}\mu(\zeta)]\prod_{f^*}\mathcal{A}_{f^*}[\zeta_{f^*}]\prod_{e^*}\mathcal{A}_{e^*}[\zeta_{e^*}]\prod_{v^*}\mathcal{A}_{v^*}[\zeta_{v^*}]\,, \tag{7.46}$$

where $\psi_\Gamma^{\text{cohe}}$ is the boundary coherent spin network state and $\mathrm{d}\mu(\zeta):=\frac{1}{\pi^2}e^{-\langle\zeta|\zeta\rangle}\mathrm{d}\zeta^-\mathrm{d}\zeta^+$ is the Haar measure of spinors. With the use of spinors, therefore, the amplitude would be written as a "state-integral" instead of state-sum.

Let us first introduce the notations we will use in the state-integral formulas both in Proposition 7.2.1 and 7.2.2. For the vertex amplitude, we denote the spinors (or dual spinors) on the source $s(e)$ and target $t(e)$ of a link e as ζ_e and $\tilde{\zeta}_e$ respectively. For the edge amplitude of a dual edge e^*, we consider the node v in a triangle shared by two adjacent tetrahedra. Therefore, spinors on v have two independent copies, one from the tetrahedron dual to $s(e^*)$ and the other from the tetrahedron dual to $t(e^*)$. For a link $e\in v$, we denote the two spinors from the two tetrahedra respectively as $\zeta_e^{s(e^*)}$ and $\zeta_e^{t(e^*)}$. For the face amplitude, we consider a dual face f^* whose boundary loop connects $n(\geq 3)$ tetrahedra. One needs to choose randomly a node on the boundary of one of these tetrahedra, say T_1. We denote the spinor on this node that will contribute to this face amplitude as ζ^{f^*,T_1}. See an illustration in fig.7.3.

Proposition 7.2.1. *The spinfoam model can be expressed as an integral in terms of coherent blocks*

$$\mathcal{A}_{\mathbf{T}}[\mathcal{M},\psi_\Gamma^{cohe}]=\int[\mathrm{d}\mu(\zeta)]\prod_{f^*}\mathcal{A}_{f^*}[\zeta_{f^*}]\prod_{e^*}\mathcal{A}_{e^*}[\zeta_{e^*}]\prod_{v^*}\mathcal{A}_{v^*}[\zeta_{v^*}]$$

with the vertex, edge and face amplitude written as

$$\mathcal{A}_{v^*}=s_{tet}^{cohe}(\mathbb{I})=\int_{\mathrm{SU}(2)^4}\prod_{v=1}^{4}\mathrm{d}h_v\,e^{\sum_{e=1}^{6}[\tilde{\zeta}_e|h_{t(e)}^{-1}h_{s(e)}|\zeta_e\rangle}\,, \tag{7.47}$$

$$\mathcal{A}_{e^*}=e^{\sum_{e\in v}\langle\zeta_e^{s(e^*)}|\zeta_e^{t(e^*)}]}\,, \tag{7.48}$$

$$\mathcal{A}_{f^*}=\langle\zeta^{f^*,T_1}|\zeta^{f^*,T_1}\rangle-1\,. \tag{7.49}$$

For sake of simplicity of the main text, we leave the proof B.5.1 in Appendix B.5.

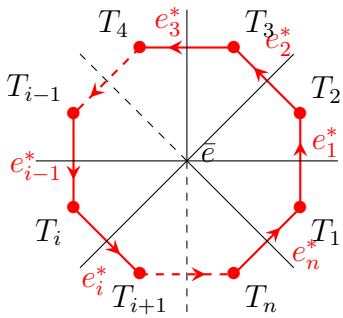

Figure 7.3: A dual face *(in red)* dual to the edge $\bar{e}$ surrounded by a loop $(e_1^* e_2^* \cdots e_n^* e_1^*)$, with e_i^* dual to triangle $\triangle_i$. Two adjacent tetrahedra T_i and T_{i+1} (identifying $T_{n+1} \equiv T_1$) are glued along the triangle $\triangle_i$.

A similar state-integral model for 4D BF theory was explicitly constructed in [74]. The vertex amplitude constructed above no longer depends on the spins, thus it is expected to be irrelevant to the size of the tetrahedron it is associated to. The drawback of this construction is that the SU(2) group elements are still included in the formula other than spinors, making it hard to single out the geometrical information stored in the spinors themselves. Thus in the next subsection, we promote the integral expression of the Ponzano-Regge amplitude in terms of different blocks so that only spinors are left in the integral expression.

7.2.4 A new Ponzano-Regge state-integral formula

To get rid of the SU(2) group integral in the vertex amplitude, we replace the vertex amplitude by the SGF. We apply the idea that the vertex amplitude can be provided by the spin network state evaluation on the boundary of a tetrahedron. Therefore, the SGF, as the scaleless spin network evaluation, is a natural replacement of the $6j$-symbol. Notice that the SGF can be expressed as a group integral similar to (7.29)[44]

$$\mathcal{S}(\{\zeta_e, \tilde{\zeta}_e\}) = \sum_{j_1 \cdots j_6} \left(\prod_{v=1}^{4} (J_v + 1)! \int_{\mathrm{SU}(2)} \mathrm{d}h_v \right) \prod_{e=1}^{6} \frac{1}{(2j_e)!} [j_e, \tilde{\zeta}_e | h_{t(e)}^{-1} h_{s(e)} | j_e, \zeta_e \rangle \,. \tag{7.50}$$

The difference is the factor $(J_v + 1)!$ for each node. This can be cancelled out by modifying the edge amplitude, and the result is given in the following proposition. The notations are the same as in Proposition 7.2.1.

Proposition 7.2.2. *The spinfoam model can be expressed as a state-integral*

$$\mathcal{A}_{\mathbf{T}}[\mathcal{M},\psi_\Gamma^{\mathfrak{sl}}]=\int[\mathrm{d}\mu(\zeta)]\prod_{f^*}\mathcal{A}_{f^*}[\zeta_{f^*}]\prod_{e^*}\mathcal{A}_{e^*}[\zeta_{e^*}]\prod_{v^*}\mathcal{A}_{v^*}[\zeta_{v^*}]$$

with the vertex, edge and face amplitude written as

$$\mathcal{A}_{v^*}=\mathcal{S}_{v^*}^{\mathfrak{sl}}(\{\zeta_e,\tilde{\zeta}_e\})=\frac{1}{(1+\sum_{\mathcal{L}}\prod_{v\subset\mathcal{L},\,e\prec e'}[\zeta_e|\zeta_{e'}\rangle)^2} \tag{7.51}$$

$$\mathcal{A}_{e^*}=\sum_{k=0}^{\infty}\frac{1}{(k+1)!^2(2k)!}\left(\sum_{e\in v}\langle\zeta_e^{s(e^*)}|\xi_e^{t(e^*)}]\right)^{2k}={}_0F_3(;2,2,\frac{1}{2};\frac{\left(\sum_{e\in v}\langle\zeta_e^{s(e^*)}|\xi_e^{t(e^*)}]\right)^2}{4}) \tag{7.52}$$

$$\mathcal{A}_{f^*}=\langle\zeta^{f^*,T_1}|\zeta^{f^*,T_1}\rangle-1\,. \tag{7.53}$$

$\psi_\Gamma^{\mathfrak{sl}}$ is the boundary scaleless spin network state.

The proof of this proposition is rather technical and is given in Proof B.5.2.

To summarize, Proposition 7.2.2 is a re-grouped version of Proposition 7.2.1. In order to have a simple vertex amplitude with a nice geometrical interpretation, the edge amplitude becomes more complicated. However, we will see in Subsection 7.3.2 that this new edge amplitude also possesses a nice geometrical interpretation that is compatible with that of the new vertex amplitude (7.51).

7.2.5 Topological invariance of the Ponzano-Regge state-integral model

The topological invariance of the new Ponzano-Regge state-integral formula can be proven by performing the $2-3$ and $1-4$ Pachner moves. To do this, one can either express the vertex amplitude (7.51) into the explicit form as the generating function of the $6j$-symbols (7.42) then use the recursion relation of the $6j$-symbols [206], or work on the spinors variables to prove the invariance of total amplitude under Pachner moves. The former approach is rather straightforward hence here we only illustrate the latter approach.

We consider in this section the gluing of general 3-cells through triangles and show that the resulting total amplitude after gluing is given by the boundary scaleless spin network state on the union boundary, which means that the state-integral model is topological invariant.

We will show it through three different types of gluing which serve as the elementary steps to glue disjoint 3-cells. The first type is to glue two 3-cells through one triangle with no extra internal edge produced (Proposition 7.2.4). The second type is to glue two adjacent triangles sharing one edge on the boundary of one 3-cell and produce one extra internal edge (Proposition 7.2.5). The third type is to glue two adjacent triangles sharing two edges on the boundary of one 3-cell and produce two internal edges and one internal vertex (Proposition 7.2.6). The topological invariance of the Ponzano-Regge state-integral model, which can be directly derived by analyzing the total amplitude under a combination of these three types of gluing without changing the topological nature of the 3-cell, is a natural conclusion (Corollary 7.2.7).

The scaleless spin network state for a three-valent graph can be expressed into a Gaussian integral [28, 37]. Let us introduce an auxiliary spinor $|\gamma_{ve}\rangle = \begin{pmatrix} \gamma_{ve}^- \\ \gamma_{ve}^+ \end{pmatrix} \in \mathbb{C}^2$ attached to each half link e attached to node v with the same spinor measure $\mathrm{d}\mu(\gamma_{ev}) = \frac{1}{\pi^2}\mathrm{d}\gamma_{ve}^-\mathrm{d}\bar{\gamma}_{ve}^-\mathrm{d}\gamma_{ve}^+\mathrm{d}\bar{\gamma}_{ve}^+ e^{-\langle\gamma_{ev}|\gamma_{ev}\rangle}$. The dual auxiliary spinor is defined in the same way as z's, *i.e.* $|\gamma_{ev}] = \begin{pmatrix} -\bar{\gamma}_{ev}^+ \\ \bar{\gamma}_{ev}^- \end{pmatrix}$. To unify the notation, we denote the new spinors at the source $s(e)$ and target $t(e)$ of a link e as γ_e and $\tilde{\gamma}_e$. Consider a general 3-cell $\mathbf{C}$ whose boundary $\partial\mathbf{C}$ is made up by jointed triangles whose dual graph $(\partial\mathbf{C})^*$ is a (closed) three-valent graph. The correspondent scaleless spin network state is [37]

$$\mathcal{S}^{\mathfrak{sl}}_{\partial\mathbf{C}}(\{\zeta_e,\tilde{\zeta}_e\}) = \int\left(\prod_e \mathrm{d}\mu(\gamma_e)\mathrm{d}\mu(\tilde{\gamma}_e)\right) e^{\sum_e\langle\gamma_e|\tilde{\gamma}_e]+\sum_\alpha[\zeta_{s(\alpha)}|\zeta_{t(\alpha)}\rangle[\gamma_{s(\alpha)}|\gamma_{t(\alpha)}\rangle}\,, \tag{7.54}$$

where α is the angle formed by two links $s(\alpha)$ and $t(\alpha)$ incident to a same node with the cyclic order $s(\alpha)\prec t(\alpha)$. We denote $\alpha\in v$ if $s(\alpha),t(\alpha)\in v$. Clearly (7.54) contains a link-term $e^{\sum_e\langle\gamma_e|\tilde{\gamma}_e]}$ and an angle-term $e^{\sum_\alpha[\zeta_{s(\alpha)}|\zeta_{t(\alpha)}\rangle[\gamma_{s(\alpha)}|\gamma_{t(\alpha)}\rangle}$.

Lemma 7.2.3. *Arbitrary gluing of 3-cells through triangles can be separated into a sequence of the following three types of gluing:*

- **Type I***: identifying three edges of two disjoint triangles, each on the boundary of one 3-cell (fig.7.4a), whose result is one 3-cell with no extra internal edges produced (fig.7.4b);*
- **Type II***: identifying the two remaining edges of two adjacent triangles sharing one edge on the boundary of one 3-cell (fig7.5a), whose result is one 3-cell with one extra internal edge produced (fig.7.5b);*

- **Type III**: *identifying the remaining edge of two adjacent triangles sharing two edges on the boundary of one 3-cell (fig.7.6a), whose result is one 3-cell with two extra internal edges and one internal vertex produced (fig.7.6b).*

We consider separately these three types of gluing and analyze the total amplitude after gluing. The formulas given are formal but notations are consistent with the corresponding figures and the proofs, which we leave in Appendix B.5.

Proposition 7.2.4. *For gluing of Type I, the scaleless spin network states $\mathcal{S}^{\mathfrak{sl}}_{\partial\mathbf{C}_1}, \mathcal{S}^{\mathfrak{sl}}_{\partial\mathbf{C}_2}$ on the boundaries $\partial\mathbf{C}_1, \partial\mathbf{C}_2$ of two 3-cells $\mathbf{C}_1, \mathbf{C}_2$ glued with an edge amplitude $\mathcal{A}_{e^*}^{\partial\mathbf{C}_1\cap\partial\mathbf{C}_2}$ in the form of (7.52) produces a scaleless spin network state $\mathcal{S}^{\mathfrak{sl}}_{\partial(\mathbf{C}_1\cup\mathbf{C}_2)}$ on the union boundary $\partial(\mathbf{C}_1\cup\mathbf{C}_2)$ after gluing. The gluing process is symbolically expressed as (referring to the spinor notation in fig.7.4)*

$$\mathcal{S}^{\mathfrak{sl}}_{\partial(\mathbf{C}_1\cup\mathbf{C}_2)} = \int \left(\prod_{e,c\in\partial\mathbf{C}_1\cap\partial\mathbf{C}_2} \mathrm{d}\mu(\zeta_e)\mathrm{d}\mu(\tilde{\xi}_c)\right) \mathcal{S}^{\mathfrak{sl}}_{\partial\mathbf{C}_1}(\{\zeta_e,\tilde{\zeta}_e\})\, \mathcal{A}_{e^*}^{\partial\mathbf{C}_1\cap\partial\mathbf{C}_2}\, \mathcal{S}^{\mathfrak{sl}}_{\partial\mathbf{C}_2}(\{\xi_c,\tilde{\xi}_c\})\,. \quad (7.55)$$

The proof is given in Proof B.5.3.

Proposition 7.2.5. *For gluing of Type II, the scaleless spin network state $\mathcal{S}^{\mathfrak{sl}}_{\partial\mathbf{C}}$ on the boundary $\partial\mathbf{C}$ of a 3-cell $\mathbf{C}$ glued with an edge amplitude $\mathcal{A}_{e^*}^{\triangle_1\cap\triangle_2=\bar{e}}$ of the form (7.52), which is for two adjacent triangles $\triangle_1, \triangle_2 \in \partial\mathbf{C}$ sharing one edge $\bar{e}$, and one face amplitude $\mathcal{A}^{\bar{e}}_{f^*}$, which is for the shared edge $\bar{e}$, produces a scaleless spin network state $\mathcal{S}^{\mathfrak{sl}}_{\partial\mathbf{C}'}$ on the resulting 3-cell boundary $\partial\mathbf{C}'$. It is symbolically expressed as*

$$\mathcal{S}^{\mathfrak{sl}}_{\partial\mathbf{C}'} = \int \left(\prod_{e\in\triangle_1\cup\triangle_2} \mathrm{d}\mu(\zeta_e)\right) \mathcal{S}^{\mathfrak{sl}}_{\partial\mathbf{C}}\, \mathcal{A}_{e^*}^{\triangle_1\cap\triangle_2=\bar{e}}\, \mathcal{A}^{\bar{e}}_{f^*}\,. \quad (7.56)$$

The proof is given in Proof B.5.4.

Define a function of the face amplitude, which is defined with the spinor ζ sitting on the base node, as

$$G(\mathcal{A}_{f^*}(\zeta)) := e^{-(1+\mathcal{A}_{f^*}(\zeta))} = e^{-\langle\zeta|\zeta\rangle}\,. \quad (7.57)$$

We then have the following proposition.

Proposition 7.2.6. *For gluing of Type III, the scaleless spin network state $\mathcal{S}^{\mathfrak{sl}}_{\partial\mathbf{C}}$ on the boundary $\partial\mathbf{C}$ of a 3-cell $\mathbf{C}$ glued with an edge amplitude $\mathcal{A}_{e^*}^{\triangle_1\cap\triangle_2=\{\bar{e}_1,\bar{e}_2\}}$ in the form of (7.52), which is for two adjacent triangles $\triangle_1, \triangle_2 \in \partial\mathbf{C}$ sharing two edges $\bar{e}_1, \bar{e}_2$, a face*

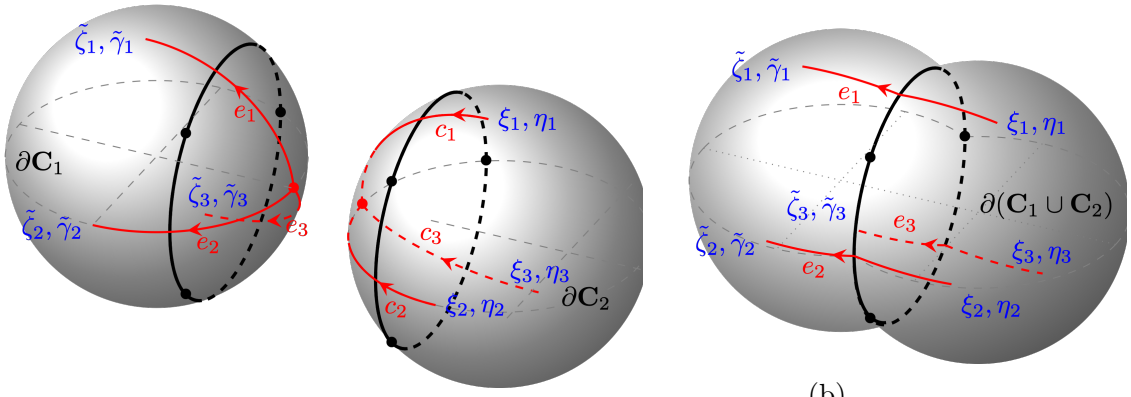

(a) (b)

Figure 7.4: (a) Before gluing of two 3-cells $\mathbf{C}_1$ and $\mathbf{C}_2$ *(visualized as 2-spheres)* through identifying the left and right triangles *(in thick, each visualized as a circle embedding in the corresponding 2-sphere with three vertices on it)*. The links *(in red)*, each dual to one side of a triangle is assigned spinor information. Fix the orientation of the links $e_{1,2,3}$ on the left triangle to be outgoing, the sources are assigned the spinors $\zeta_{1,2,3}$ and the auxiliary spinors $\gamma_{1,2,3}$ (not shown in the figure for clear visualization) and the targets are assigned the spinors $\tilde{\zeta}_{1,2,3}$ and the auxiliary spinors $\tilde{\gamma}_{1,2,3}$; also fix the orientation of the links $c_{1,2,3}$ on the right triangle to be ingoing, the sources are assigned the spinors $\xi_{1,2,3}$ and the auxiliary spinors $\eta_{1,2,3}$ and the targets are assigned the spinors $\tilde{\xi}_{1,2,3}$ and the auxiliary spinors $\tilde{\eta}_{1,2,3}$ (not shown in the figure for clear visualization). (b) After gluing two 3-cells $\mathbf{C}_1$ and $\mathbf{C}_2$ *(visualized as a double bubble)* . The spinor information in the bulk is integrated out and only the spinors on the union boundary $\partial(\mathbf{C}_1 \cup \mathbf{C}_2)$ are left.

amplitude $\mathcal{A}_{f^*}^{\bar{e}_1}$ *in the form of* (7.53)*, which is for one of the shared edge* $\bar{e}_1$*, and the function* $G(\mathcal{A}_{f^*}^{\bar{e}_2})$ *of the face amplitude for the other shared edge* $\bar{e}_2$ *in the form of* (7.57)*, produces a scaleless spin network state* $\mathcal{S}^{\mathfrak{sl}}_{\partial \mathbf{C}'}$ *on the resulting 3-cell boundary* $\partial \mathbf{C}'$*. It is symbolically expressed as*

$$\mathcal{S}^{\mathfrak{sl}}_{\partial \mathbf{C}'} = \int \left(\prod_{e \tilde{\in} \triangle_1 \cup \triangle_2} \mathrm{d}\mu(\zeta_e) \right) \mathcal{S}^{\mathfrak{sl}}_{\partial \mathbf{C}} \, \mathcal{A}_{e^*}^{\triangle_1 \cap \triangle_2 = \{\bar{e}_1, \bar{e}_2\}} \, \mathcal{A}_{f^*}^{\bar{e}_1} \, G(\mathcal{A}_{f^*}^{\bar{e}_2}) \,, \tag{7.58}$$

where the $e \tilde{\in} \triangle_1 \cup \triangle_2$ *denotes that the integral is for all the spinors on (the dual node of) the two triangles* $\triangle_1$ *and* $\triangle_2$ *except the one defining the face amplitude* $\mathcal{A}_{f^*}^{\bar{e}_2}$*.*

The proof is given in Proof B.5.5.

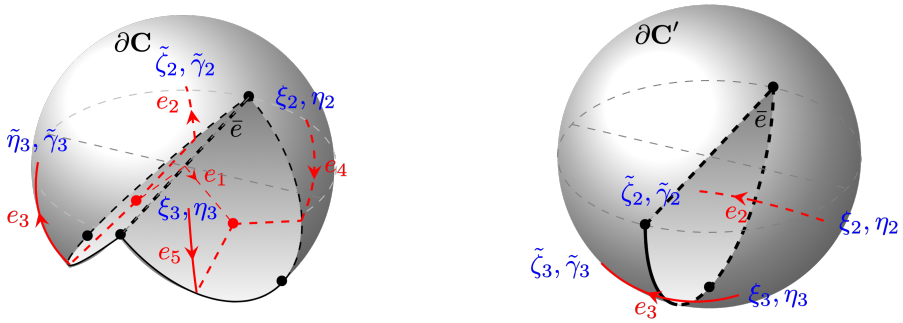

(a) (b)

Figure 7.5: Gluing two adjacent triangles *(in thick, each visualized as a semicircle and one edge connecting the two ends)* sharing one edge $\bar{e}$ on one continuous boundary *(visualized as the boundary of a 3-ball removing a lemon slice)*. (a) Before gluing: The left triangle is dual to a node with three links $e_{1,2,3}$ outgoing, while the right triangle is dual to the other node with three links $e_{1,4,5}$ incoming. For e_1, the source is assigned ζ_1, γ_1 and the target is assigned $\tilde{\xi}_1, \tilde{\eta}_1$. For links $e_{2,3}$, the sources are assigned $\zeta_{2,3}, \gamma_{2,3}$ and the targets are assigned $\tilde{\zeta}_{2,3}, \tilde{\gamma}_{2,3}$. For links $e_{4,5}$, the source are assigned $\xi_{2,3}, \eta_{2,3}$ and the targets are assigned $\tilde{\xi}_{2,3}, \tilde{\eta}_{2,3}$. (Only part of the spinors are shown for clear visualization). (b) After gluing: The shared edge $\bar{e}$ becomes internal and the other two edges from different triangles collapse *(in thick)*. Spinor information in the bulk is integrated out and only the spinors on the resulting boundary (as shown) are left.

Note that (7.58) is a finite equation because we did not perform the integration over ζ_2. The dependence of the final result on z_2 is removed simply by $\delta(g)$. If one replaces $G(\mathcal{A}_{f^*}^{\bar{e}_2})$ by $\mathcal{A}_{f^*}^{\bar{e}_2}(\zeta_2)$ and further integrate ζ_2 on the right hand side, one gets a delta distribution of SU(2) group evaluated on the identity on the left hand side, *i.e.*

$$\mathcal{S}^{\mathfrak{sl}}_{\partial\mathbf{C}'}\,\delta_{\mathrm{SU}(2)}(\mathbb{I}) = \int \left(\prod_{e\in\triangle_1\cup\triangle_2} \mathrm{d}\mu(\zeta_e)\right) \mathcal{S}^{\mathfrak{sl}}_{\partial\mathbf{C}} \cdot \mathcal{A}_{e^*}^{\triangle_1\cap\triangle_2=\{\bar{e}_1,\bar{e}_2\}} \cdot \mathcal{A}_{f^*}^{\bar{e}_1} \cdot \mathcal{A}_{f^*}^{\bar{e}_2}\,, \tag{7.59}$$

which diverges and the divergence corresponds to the translational symmetry of the extra internal vertex produced after gluing as in the original Ponzano-Regge state-sum model [103, 104]. In the state-sum model, this divergence can be eliminated by fixing the spin (thus edge length, say $\ell_{\bar{e}}$,) of one internal edge incident to this internal vertex. In a similar spirit, (7.58) can be viewed as the gauge-fixing version of (7.59) which fixes one spinor ζ_2

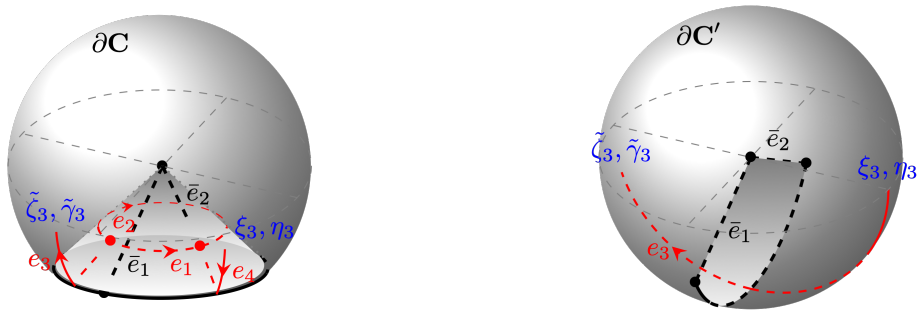

(a) (b)

Figure 7.6: Gluing of the two adjacent triangles *(in thick, each visualized as a semicircle and two edges incident to the origin of the 3-ball)* sharing two edges on one continuous boundary *(visualized as the boundary of a 3-ball removing a solid cone)*. (a) Before gluing: The left triangle is dual to one node with three links $e_{1,2,3}$ outgoing, while the right triangle is dual to the other node with three links $e_{1,2,4}$ ingoing. $s(e_1)$ *(resp.* $t(e_1)$*)* is assigned ζ_1, γ_1 *(resp.* $\tilde{\xi}_1, \tilde{\eta}_1$*)*, $s(e_2)$ *(resp.* $t(e_2)$*)* is assigned ζ_2, γ_2 *(resp.* $\tilde{\xi}_2, \tilde{\eta}_2$*)*, $s(e_3)$ *(resp.* $t(e_3)$*)* is assigned ζ_3, γ_3 *(resp.* $\tilde{\zeta}_3, \tilde{\gamma}_3$*)*, and $s(e_4)$ *(resp.* $t(e_4)$*)* is assigned ξ_3, η_3 *(resp.* $\tilde{\xi}_3, \tilde{\eta}_3$*)*. (only part of the spinors are shown for clear visualization). (b) After gluing: The shared edges become internal and one extra internal vertex (the origin of the 3-ball) is created. The remaining edge from different triangles collapses and lives on the resulting boundary. Spinor information in the bulk is integrated out and only the spinors on the resulting boundary, *i.e.* $\tilde{\zeta}_3, \tilde{\gamma}_3$ and ξ_3, η_3, are left.

in the bulk. Another way of gauge fixing is to gauge fix (the norm of) the inner product $|[\zeta_1|\zeta_2\rangle|$ of the two spinors ζ_1, ζ_2 used to define the face amplitude $\mathcal{A}_{f^*}^{\bar{e}_1}$ and $\mathcal{A}_{f^*}^{\bar{e}_2}$, which encodes the angle information of the triangle dual to the node that ζ_1, ζ_2 lives on (see Section 7.3.1 below). This can be seen by rewriting $\delta_{\mathrm{SU}(2)}(\mathbb{I})$ in terms of $|[\zeta_1|\zeta_2\rangle|$ as

$$\begin{aligned}\delta_{\mathrm{SU}(2)}(\mathbb{I}) &= \int_{\mathrm{SU}(2)} \mathrm{d}g \int \mathrm{d}\mu(\zeta_1)\mathrm{d}\mu(\zeta_2)\,(\langle\zeta_1|\zeta_1\rangle - 1)(\langle\zeta_2|\zeta_2\rangle - 1)e^{\langle\zeta_1|g|\zeta_1\rangle}e^{\langle\zeta_2|g|\zeta_2\rangle} \\ &= \int \mathrm{d}\mu(\zeta_1)\mathrm{d}\mu(\zeta_2)\,(\langle\zeta_1|\zeta_1\rangle - 1)(\langle\zeta_2|\zeta_2\rangle - 1)e^{|[\zeta_1|\zeta_2\rangle|^2}\,.\end{aligned} \tag{7.60}$$

One can straightforwardly conclude from Lemma 7.2.3 and Proposition 7.2.4, 7.2.5, 7.2.6 the following corollary.

Corollary 7.2.7. *The Ponzano-Regge state-integral formula given in Proposition 7.2.2 is topological invariant. This means the total amplitude is independent of the bulk configuration and is equal to the boundary scaleless spin network state upon gauge fixings, one for each internal vertex.*

In particular, in the $2-3$ Pachner move, the gluing of two tetrahedra is of Type I; the gluing of three tetrahedra includes three steps, two of which are of Type I and the other is of Type II. In the $1-4$ Pachner move, the gluing of four tetrahedra includes six steps, three of which are of Type I, two of which are of Type II and the remaining one is of Type III.

7.3 Geometric interpretation of the state-integral

Spins are geometrically interpreted as lengths thus the geometrical meaning of the original Ponzano-Regge state-sum is rather simple as reviewed above. In contrast, the geometrical interpretation of spinors, or the inner product of spinors which are used in the new Ponzano-Regge state-integral described in Proposition 7.2.2, is not as apparent. To understand how the new model describes the geometry, we analyze in this section separately the geometrical information of the tetrahedron described by the new vertex amplitude, and that of the gluing process described by the new edge amplitude.

7.3.1 Poles of the $\{12\zeta^{\times 2}\}$ symbol

In this subsection, we come back to the tetrahedron graph and look into the geometrical interpretation of the SGF. To this end, we rewrite the SGF in terms of the new variables, namely the *angle couplings* and the *link couplings*. They are both invariant under the $\mathrm{SL}(2,\mathbb{C})$ gauge transformation of spinors and the latter is further invariant under the anti-scale transformation (see (7.45)) thus forming a minimum set of variables.

At the first glance, since the SGF encodes the summation of spins, which geometrically represent lengths of the one-skeleton of a tetrahedron, the length information is expected to be washed out and it leaves the rest of the geometrical information, thus angles. Angle information of a tetrahedron includes internal angles of triangles (called internal angles for short) on the boundary of the tetrahedron and the dihedral angles between each pair of triangles. By taking the large j limit of the $6j$-symbols, we will find that these angle information are exactly stored in the norms and phases of the 6 independent link couplings.

We will first regroup the scalar products of spinors in the expression of the SGF (7.43) into an expression in terms of the link couplings. Through a stationary analysis of the new SGF expression, we acknowledge that the link couplings capture the internal angles of triangles in their real part and the dihedral angles between triangles in their imaginary part. This establishes our expectation that the SGF describes the quantum conformal geometry of a tetrahedron.

From angle couplings to link couplings. Each pair of links incident to the same node form an angle. We define the angle coupling $X_{ee'}$ by the (holomorphic) inner product of the spinors associated to the pair of links (e, e') with the order $e \prec e'$ as

$$X_{ee'} \equiv X_{e'e} := [\zeta_e|\zeta_{e'}\rangle = |X_{ee'}|e^{i\Phi_{ee'}}\,, \quad e \prec e'\,, \quad e, e' \in v\,, \quad \Phi_{ee'} \in [0, \pi)\,. \tag{7.61}$$

We have separated the norm $|X_{ee'}|$ and the phase $\Phi_{ee'}$ of the angle coupling. These angle couplings can be grouped to form the link couplings Y_e's [37] such that

$$\prod_{v\in\Gamma} \prod_{e,e',e''\in v} X_{ee'}^{J_v - 2j_{e''}} = \prod_{e\in\Gamma} Y_e^{2j_e}\,. \tag{7.62}$$

Consider two three-valent nodes connected with an oriented link e, where e_1, e_2 are the other two links incident to the source $s(e)$ of the link e, and $\tilde{e}_1, \tilde{e}_2$ are the two other links incident to the target $t(e)$, as shown in fig.7.7. The link coupling Y_e is expressed in terms of the angle couplings as

$$Y_e \equiv |Y_e|e^{i\Psi_e} = \sqrt{\frac{[\zeta_e|\zeta_{e_1}\rangle[\zeta_{e_2}|\zeta_e\rangle}{[\zeta_{e_1}|\zeta_{e_2}\rangle} \frac{[\tilde{\zeta}_e|\zeta_{\tilde{e}_1}\rangle[\zeta_{\tilde{e}_2}|\tilde{\zeta}_e\rangle}{[\zeta_{\tilde{e}_1}|\zeta_{\tilde{e}_2}\rangle}} = \sqrt{\frac{X_{ee_1}X_{ee_2}}{X_{e_1e_2}} \frac{X_{e\tilde{e}_1}X_{e\tilde{e}_2}}{X_{\tilde{e}_1\tilde{e}_2}}}\,, \quad \Psi_e \in [0, \pi)\,. \tag{7.63}$$

The norm $|Y_e|$ and the phase Ψ_e of the link coupling read explicitly

$$|Y_e| = \sqrt{\frac{|X_{ee_1}||X_{ee_2}|}{|X_{e_1e_2}|} \frac{|X_{e\tilde{e}_1}||X_{e\tilde{e}_2}|}{|X_{\tilde{e}_1\tilde{e}_2}|}}\,,$$
$$\Psi_e = \mod\left(\frac{1}{2}(\Phi_{ee_1} + \Phi_{ee_2} - \Phi_{e_1e_2} + \Phi_{e\tilde{e}_1} + \Phi_{e\tilde{e}_2} - \Phi_{\tilde{e}_1\tilde{e}_2}), \pi\right)\,. \tag{7.64}$$

It will be convenient to introduce the "shared" spins for angles on the same node as

$$k_{ee'} := J_v - 2j_{e''}\,, \quad k_{e'e''} := J_v - 2j_e\,, \quad k_{e''e} := J_v - 2j_{e'}\,,$$
$$\text{where } J_v = j_e + j_{e'} + j_{e''} \text{ and } e, e', e'' \in v\,. \tag{7.65}$$

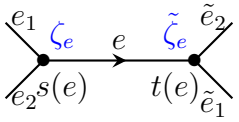

Figure 7.7: Two three-valent nodes $s(e)$ and $t(e)$ connected by an oriented link e. links e, e_1, e_2 are incident to $s(e)$, and links $e, \tilde{e}_1, \tilde{e}_2$ are incident to $t(e)$.

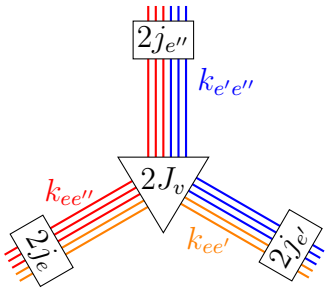

Figure 7.8: Thicken the links e, e', e'' incident to the node v into threads. Each thread carries a spin $\frac{1}{2}$ and the number of threads for each link is twice of the spin value it is dressed with. The shared spins $k_{ee'}$ can be viewed as the number of threads shared by the links e and e'. Similarly for $k_{ee''}$ and $k_{e'e''}$.

$k_{ee'}$ can be understood as the number of threads (equal to twice of the spin value) shared by the links e and e', as illustrated in fig.7.8.

These shared spins are not independent. Referring to the relative position of the edges $e, e_1, e_2, \tilde{e}_1, \tilde{e}_2$ shown in fig.7.7, the constraint for $k_{ee'}$'s is

$$k_{ee_1} + k_{ee_2} = k_{e\tilde{e}_1} + k_{e\tilde{e}_2} = 2j_e\,, \quad \forall e\,. \tag{7.66}$$

Therefore, we have six constraints for 12 shared spins $k_{ee'}$'s, which results in 6 independent shared spins as expected.

Let us recall the SGF (7.42) written with the angle and link couplings,

$$\mathcal{S}(\{X_{ee'}\}) = \sum_{j_1\cdots j_6}\left[\prod_{v=1}^{4}\sqrt{\frac{(J_v+1)!}{\prod_{e,e'\in v}k_{ee'}!}}\right]\left\{\begin{array}{ccc} j_1 & j_2 & j_3 \\ j_4 & j_5 & j_6\end{array}\right\}\prod_{v=1}^{4}\left(\prod_{e,e'\in v}X_{ee'}^{k_{ee'}}\right)\,, \tag{7.67}$$

or

$$\mathcal{S}(\{Y_e\}) = \sum_{j_1\cdots j_6}\left[\prod_{v=1}^{4}\sqrt{\frac{(J_v+1)!}{\prod_{e,e'\in v}k_{ee'}!}}\right]\left\{\begin{array}{ccc} j_1 & j_2 & j_3 \\ j_4 & j_5 & j_6\end{array}\right\}\prod_{e=1}^{6}Y_e^{2j_e}\,. \tag{7.68}$$

For any loop $\mathcal{L}$, the following equality holds

$$\prod_{v\in\mathcal{L}} X^v_{ee'} = \prod_{e\in\mathcal{L}} Y_e\,, \tag{7.69}$$

thus (7.43) can also be written in two ways

$$\mathcal{S}(\{\zeta_e,\tilde{\zeta}_e\}) = G(\{\zeta_e,\tilde{\zeta}_e\})^{-2}\,,\quad G(\{\zeta_e,\tilde{\zeta}_e\}) = 1+\sum_{\mathcal{L}}\prod_{e,e'\in v\subset\mathcal{L}} X_{ee'} = 1+\sum_{\mathcal{L}}\prod_{e\subset\mathcal{L}} Y_e\,. \tag{7.70}$$

Link couplings at the stationary point. Now that we have the expression of the SGF in terms of the link couplings, we would like to apply the stationary analysis at the large j limit of the SGF to look into the poles. We first take the Stirling approximation of the factorials:

$$n!\sim\sqrt{2\pi n}\left(\frac{n}{e}\right)^n = e^{n\ln n+O(n)}\,. \tag{7.71}$$

When $V^2>0$, the $6j$-symbol represents a tetrahedron embedded in the 3D Euclidean space. It reads [174]

$$\left\{\begin{array}{ccc} j_1 & j_2 & j_3\\ j_4 & j_5 & j_6\end{array}\right\}\sim\frac{1}{\sqrt{12\pi V}}\cos\left(\sum_{e=1}^6\ell_e\Theta_e+\frac{\pi}{4}\right)\,, \tag{7.72}$$

where $\ell_e=j_e+\frac{1}{2}$ is the edge length of the edge $\bar{e}$, V the volume of the tetrahedron with edge lengths $\{\ell_e\}$ calculated by the Cayley-Menger determinant, and Θ_e the external dihedral angle about the edge $\bar{e}$, *i.e.* the angle between the outward normals to the faces sharing the edge $\bar{e}$ [7]. The large j limit of the SGF (7.68) is thus [46]

$$\begin{aligned}\mathcal{S}^{\mathfrak{sl}}(\{Y_e\}) &= \sum_{j_1\cdots j_6}\left[\prod_{v=1}^4\sqrt{\frac{(J_v+1)!}{\prod_{e,e'\in v}k_{ee'}!}}\right]\left\{\begin{array}{ccc} j_1 & j_2 & j_3\\ j_4 & j_5 & j_6\end{array}\right\}\prod_{e=1}^6 Y_e^{2j_e}\\ &\sim\sum_{\{j_e\}} e^{\sum_{v=1}^4\frac{1}{2}\left(J_v\ln J_v-\sum_{e,e'\in v}k_{ee'}\ln k_{ee'}\right)}e^{\sum_{e=1}^6 2j_e(\ln|Y_e|+i\Psi_e)}\frac{1}{2\sqrt{12\pi V}}\sum_{\epsilon=\pm}e^{i\epsilon\left(\sum_{e=1}^6\ell_e\Theta_e+\frac{\pi}{4}\right)}\\ &=\sum_{\epsilon=\pm}\sum_{\{j_e\}}\frac{1}{2\sqrt{12\pi V}}e^{\mathcal{S}_\epsilon(\{Y_e,j_e\})}\,.\end{aligned} \tag{7.73}$$

[7] Note that the edges of the tetrahedron T are denoted as $\bar{e}$'s and the links of the tetrahedron graph $\Gamma=(\partial T)^*$ dual to the boundary of T are denoted as e's. It is on the links of Γ where we associate spin labels $\{j_e\}$, but they represent the lengths of the edges $\bar{e}$'s on T which are dual to e's. We denote the length ℓ_e and dihedral angle Θ_e with subscript e instead of $\bar{e}$ to avoid a mixture of notation in the same equation as much as possible in the main text.

In the second line, we have used $\cos\left(\sum_{e=1}^{6}\ell_e\Theta_e+\frac{\pi}{4}\right)=\frac{1}{2}\sum_{\epsilon=\pm}e^{i\epsilon\left(\sum_{e=1}^{6}\ell_e\Theta_e+\frac{\pi}{4}\right)}$.

As the volume V grows polynomially with the spins, its derivative of spin will contribute to the sub-leading correction of the stationary point. Therefore, to the leading order, one simply needs to consider the stationary point of the exponent term $\mathcal{S}_\epsilon(\{Y_e,j_e\})$ of the SGF.

The real and imaginary part of $\mathcal{S}_\epsilon$ can be rewritten as

$$\mathrm{Re}[\mathcal{S}_\epsilon(\{Y_e,j_e\})]=\sum_{v=1}^{4}\frac{1}{2}\left[J_v\ln J_v-\sum_{e,e'\in v}k_{ee'}\ln k_{ee'}\right]+\sum_{e=1}^{6}j_e\ln|Y_e|^2\,, \tag{7.74}$$

$$\mathrm{Im}[\mathcal{S}_\epsilon(\{Y_e,j_e\})]=\sum_{e=1}^{6}\left[j_e(2\Psi_e+\epsilon\Theta_e)+\frac{1}{2}\epsilon\Theta_e\right]+\epsilon\frac{\pi}{4}\,. \tag{7.75}$$

Thanks to the Schläfli identity, $\sum_e^6 j_e\frac{\partial\Theta_e}{\partial j_e}=0$, the phase term has a simple derivative expression $\frac{\partial\sum_e j_e\Theta_e}{\partial j_e}=\Theta_e$. The saddle point $\frac{\partial\mathcal{S}_\epsilon}{\partial j_e}$ can be separated into the real part and the imaginary part. Using some trigonometry relations, the result reads (neglecting sub-leading contributions)[37, 46]

$$\frac{\partial\mathrm{Re}[\mathcal{S}_\epsilon]}{\partial j_e}=0\ \rightarrow\ |Y_e|^2\sim\sqrt{\frac{k_{ee_1}k_{ee_2}}{k_{e_1e_2}J_{s(e)}}}\sqrt{\frac{k_{e\tilde{e}_1}k_{e\tilde{e}_2}}{k_{\tilde{e}_1\tilde{e}_2}J_{t(e)}}}\equiv\tan\frac{\phi_{s(e)}}{2}\tan\frac{\phi_{t(e)}}{2}\,, \tag{7.76}$$

$$\frac{\partial\mathrm{Im}[\mathcal{S}_\epsilon]}{\partial j_e}=0\ \rightarrow\ \Psi_e=-\frac{\epsilon}{2}\Theta_e\,. \tag{7.77}$$

we have identified the length of edge $\bar{e}$ with the spin values j_e as $j_e\gg\frac{1}{2}$. $\phi_{s(e)}$ is the internal angle opposite to the edge $\bar{e}$ in the triangle dual to the source node $s(e)$ of the link e, similarly for $\phi_{t(e)}$, as shown in fig.7.9. The saddle point corresponds to the pole of the SGF, which is also the Fisher zero for the Ising partition function on a tetrahedron graph [46]. It clearly expresses the conformal geometry of the (classical limit of) the tetrahedron: The norm of the link coupling $|Y_e|$ corresponds to the pair of internal angles $\left(\phi_{s(e)},\phi_{t(e)}\right)$ opposite to the edge $\bar{e}$ in the two triangles meeting at $\bar{e}$, while the phase Ψ_e corresponds to half of the external dihedral angle about the edge $\bar{e}$.

According to the relation (7.64) between (the norms of) the angle and link couplings and (7.76), one can also write , at the saddle point $\partial\mathcal{S}_\epsilon/\partial j_e=0$, that

$$\frac{|X_{ee'}||X_{ee''}|}{|X_{e'e''}|}\sim\tan\frac{\phi_{e'e''}}{2}\,,\quad\frac{|X_{e'e}||X_{e'e''}|}{|X_{ee''}|}\sim\tan\frac{\phi_{ee''}}{2}\,,\quad\frac{|X_{e''e}||X_{e''e'}|}{|X_{ee'}|}\sim\tan\frac{\phi_{ee'}}{2}\,, \tag{7.78}$$

where $\phi_{ee''}\,,\phi_{ee''}\,,\phi_{ee'}$ are the angles of a triangle as shown in fig.7.10. To determine the shape of a tetrahedron, one merely needs the norm of the couplings or the phase of the couplings. For sake of simplicity, we will make use of the norms only.

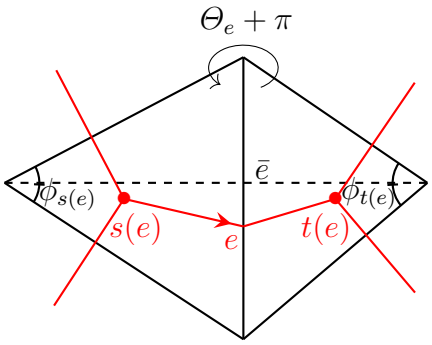

Figure 7.9: Two (unplanar) triangles sharing one edge $\bar{e}$ and its 2D oriented dual graph (*in red*). The node $s(e)$ is dual to the left triangle and $t(e)$ dual to the right one. $\phi_{s(e)}$ and $\phi_{t(e)}$ are the internal angle opposite to the edge $\bar{e}$ within the left and right triangle respectively. Their relation with the norm of the link coupling at the saddle point is given in (7.76). Θ_e is the external dihedral angle about the edge $\bar{e}$. Its relation with the phase of the link coupling at the saddle point is given in (7.77).

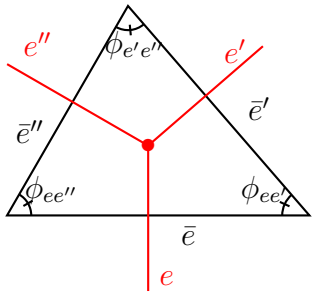

Figure 7.10: Three links (*in red*) e, e', e'' meeting at one node. The triangle (*in black*) dual to the node is bounded by edges $\bar{e}, \bar{e}', \bar{e}''$. (In fact, there is no one-to-one map from the link couplings to angle couplings. We have chosen a "geometric gauge" for the angle couplings which has the most local sense. See [137] for details.) The length of the edge $\bar{e}$ is given by the spin j_e, similarly for $\bar{e}'$ and $\bar{e}''$. The angle formed by links $\bar{e}, \bar{e}'$ is $\phi_{ee'}$. Similarly for $\phi_{e'e''}$ and $\phi_{ee''}$.

7.3.2 Propagator and geometric gluing

We have shown that the SGF describes the local conformal geometry of each elementary 3D block in the Ponzano-Regge state-integral. Since the scales of the building blocks are not fixed, the gluing process becomes non-trivial compared to the original Ponzano-Regge state-sum model, where the gluing is performed by matching the full boundary geometry

— both the shape and size of the glued triangles — of the blocks. This new way of gluing is described by this new edge amplitude

$$\mathcal{A}_{e^*} = {}_0F_3(;2,2,\frac{1}{2};\frac{\left(\sum_{e\in v}\langle\zeta_e^{s(e^*)}|\xi_e^{t(e^*)}]\right)^2}{4})$$

To gain a global picture of the state-integral model, we here analyze the geometrical meaning of the edge amplitude.

The edge amplitude is also called the propagator and it describes how two neighbouring tetrahedra are glued. Note that the measure of the spinors $\mathrm{d}\mu(\zeta) \equiv \mathrm{d}^4\zeta\, e^{-\langle\zeta|\zeta\rangle}$ includes a Gaussian weight, it is necessary to take it into account so that the norm $|P(\{\zeta_e\},\{\xi_e\})|$ of the propagator remains finite (we have assumed that $\{\zeta_e\}$ are from the tetrahedron dual to $s(e^*)$ and $\{\xi_e\}$ are from that dual to $t(e^*)$ and omit the superscript for simplicity). We rewrite the propagator as

$$P(\{\zeta_e\},\{\xi_e\}) = {}_0F_3(;2,2,\frac{1}{2};\frac{\mathbf{z}^2}{4})e^{-\mathbf{r}^2}\,,\quad \mathbf{z} = \sum_{e\in v}\langle\zeta_e|\xi_e]\,,\quad \mathbf{r}^2 := \sum_{e\in v}\left(\langle\zeta_e|\zeta_e\rangle + \langle\xi_e|\xi_e\rangle\right)\,. \tag{7.79}$$

Similar to the vertex amplitude, we are interested in the stationary points of the propagator (7.79). It turns out that the stationary point(s) for the propagator (7.79) forces the two triangles to be glued to have the same shape. This is guaranteed by the following proposition.

Proposition 7.3.1. *The vanishing derivative by $\{\bar{\xi}_e\}$ of $P(\{\zeta_e\},\{\xi_e\})$ defined in (7.79) demands that*

$$|[\zeta_e|\zeta_{e'}\rangle| = |[\xi_e|\xi_{e'}\rangle|\,,\quad |[\zeta_{e'}|\zeta_{e''}\rangle| = |[\xi_{e'}|\xi_{e''}\rangle|\,,\quad |[\zeta_{e''}|\zeta_e\rangle| = |[\xi_{e''}|\xi_e\rangle|\,. \tag{7.80}$$

where ζ_e and ξ_e are spinors associated to the links dual to edges to be glued. Likewise for $\zeta_{e'}$ and $\xi_{e'}$ as well as $\zeta_{e''}$ and $\xi_{e''}$.

(7.80) means that the angle couplings $X_{ee'}\,, X_{e'e''}\,, X_{e''e}$ from both triangles have the same norm. According to the stationary analysis for the angle coupling norms (7.78), we conclude that the gluing is picked when the shapes of the triangle to be glued are the same. The proof of Proposition 7.3.1 is given in Proof B.5.6.

In summary, the Ponzano-Regge state-integral model as constructed above encodes only the conformal geometry of the triangulation blocks either in the vertex amplitudes or the edge amplitudes. A vertex amplitude $\mathcal{A}_{v^*}$ describes the shape of the tetrahedron dual to

v^*; an edge amplitude $\mathcal{A}_{e^*}$ describes that two adjacent tetrahedra can be glued together by identifying the shape of two triangles, each from one of the tetrahedra. When there exists a boundary $\partial\mathcal{M}$ of the manifold, the total amplitude built in this way encodes also the conformal geometry on the triangulation of $\partial\mathcal{M}$ since the boundary structure is described by the scaleless spin network state $\psi^{\mathfrak{sl}}_{\gamma}$.

7.3.3 Ponzano-Regge state-integral versus state-sum model

Let us recall the original spinfoam state-sum and the new spinfoam state-integral expression,

$$\begin{aligned}\mathcal{A}_{\mathbf{T}}[\mathcal{M},\psi_\Gamma] &= \sum_{\{j_{f^*}\}}\prod_{f^*} d_{j_{f^*}} \prod_{e^*}(-1)^{\sum_{i=1}^3 j_i}\prod_{v^*}\left\{\begin{array}{ccc} j_1 & j_2 & j_3 \\ j_4 & j_5 & j_6\end{array}\right\}_{v^*}\\ &= \int [\mathrm{d}\mu(\zeta)]\prod_{f^*}\left(\langle\zeta^{f^*}|\zeta^{f^*}\rangle - 1\right)\prod_{e^*}{}_0F_3(;2,2,\frac{1}{2};\frac{\left(\sum_{e\in v}\langle\zeta_e^{s(e^*)}|\xi_e^{t(e^*)}]\right)^2}{4})\prod_{v^*}\mathcal{S}^{\mathfrak{sl}}_{v^*}(\{\zeta_e^{v^*},\tilde{\zeta}_e^{v^*}\})\,.\end{aligned} \tag{7.81}$$

In the state-sum expression, when no boundary is present, the edge amplitude can be absorbed into the vertex amplitude, while the edge amplitude is always explicit in the state-integral expression. This leads to two different ways to understand spinfoam. In the former model, after choosing a triangulation $\mathbf{T}$ of $\mathcal{M}$, we first associate the representation data (spins) on the one-skeleton of $\mathbf{T}$ then construct the vertex and face amplitudes with these representation data. In the latter model, in contrast, we first isolate all the elementary blocks, *i.e.* tetrahedra, after the triangulation then associate the representation data (spinors) to the boundary of each isolated block, followed by constructing vertex amplitude for each isolated block, edge amplitude through gluing these elementary blocks and finally face amplitude for each edge after gluing.

One may also absorb the edge amplitude into the vertex amplitude for the state-integral by integrating out, with no loss of generality, the spinors $\{\xi_e^{t(e^*)}\}$ from the target tetrahedron in each gluing. We have not found a close form for this expression, unfortunately. Furthermore, since the vertex amplitude is no longer trivial, it would be changed after this absorption, which potentially changes the geometrical interpretation.

On the other hand, leaving the edge amplitude un-absorbed allows us to separate the data from different blocks so that the saddle point analysis can be done for each vertex amplitude independently. Moreover, the saddle point analysis on the vertex amplitudes is

compatible with that on the edge amplitudes. The saddle point of each vertex amplitude (7.76) relates the spinor configuration to spins within a single block, while the saddle point of the edge amplitudes (7.80) relates the spinors from different blocks. These saddle points can be obtained simultaneously and the result effectively relates the (ratios of) spins from different blocks (with spinors as the mediums).

Geometrically, the gluing condition in the state-integral model is looser compared to that in the state-sum model, since the former only requires that the triangles to be glued have the same shape while the latter restricts that the triangles should be of the same shape and size. At the first glance, it seems the state-integral allows more configurations and should produce a different total amplitude. However, the size un-matched configurations can not survive under the spinor integration, thus the total amplitude comes only from the size-wise and shape-wise matched configurations, same as the case of the state-sum model. We have used the same property of the spinor integration in constructing the state-integral to move the contour integral from the vertex amplitude (7.47) to the edge amplitude (7.52).

Another difference between the state-sum and state-integral models is the source of the divergence in the expressions. In the state-sum model, the vertex amplitude damps as $j^{-3/2}$. The divergence comes from the infinite sum of the spin labels and the total amplitude diverges as $\sqrt{j}$. In the state-integral model, in contrast, the integration does not lead to divergence thanks to the Gaussian weight while the vertex amplitudes give divergence since there are poles in the vertex amplitudes. This is because the vertex amplitude, as a generating function of the $6j$-symbols, contains the summation of spins, thus the divergence can be viewed as from the large spin contribution. To see that it is the case, we Taylor expand the vertex amplitude and look at the pole,

$$\mathcal{A}_{v^*} = \frac{1}{(1+x)^2} = \sum_{j\in\mathbb{N}/2} (2j+1)(-x)^{2j} \xrightarrow{x=-1} \sum_{j\in\mathbb{N}/2} (2j+1)\,,$$

where x denotes the cycle-sums as given in (7.43). This illustrates that the divergence of the vertex amplitude in the state-integral model is also given by large spins, which is consistent with the state-sum model.

In this chapter, we have introduced a new framework of the spinfoam model for 3D quantum gravity based on the spinor representation of SU(2). The continuum nature of spinor variables allows us to represent the spinfoam as a state-integral, rather than a state-sum in the original Ponzano-Regge model where the spin representation of SU(2) is used. The integral expression would probably make the computation of *e.g.* correlations and transition amplitudes more controllable. More importantly, the state-integral framework inherits the scale-invariant nature of pure gravity in 3D. It describes a quantum gravity model with

scale-invariant boundary quantum geometry, which can be seen as an integration over the conformal classes of boundary geometry. We expect that this framework would serve as a better starting point to study the coarse-graining or renormalization behaviour of 3D quantum gravity, and would be useful to investigate the quasi-local CFT/gravity duality.

This can be seen as the first step toward applying (the quantization of) the deformed spinors introduced in Chapter 3 to the 3D spinfoam model with a non-vanishing Λ. It would be interesting to see if the deformed spinors can be used to construct the spinfoam that recovers the Turaev-Viro model [204], whose building blocks are the q-deformed $6j$-symbols. Along the line of the construction in this chapter, one of the first things to do can be to construct the "q-deformed scaleless spin network state" on the hyperbolic geometry. We expect that the spinorial framework of LQG and the spinfoam model can be generalized to a q-deformed version with the use of a quantum group in the mathematical construction and describe a quantum gravity with a non-vanishing cosmological constant.

Chapter 8

Summary and outlooks

Summary of results

Let us now summarize what we have done in this thesis. The inclusion of a cosmological constant Λ has not been well-understood in the LQG framework. In this thesis, we tackle the question in a simplified setting — three space-time dimension in the Euclidean signature. This allows us to do exact computations and provide guidance to discover new principles and mathematical structures for four-dimensional LQG.

We formulated the q-deformed LQG model for $\Lambda < 0$ in a mathematically rigorous way. In the classical model, the q-deformed loop gravity phase space structure in terms of the holonomies and fluxes is described by the Heisenberg double of SU(2) or AN(2) in the language of Lie bialgebra. The quantization process follows the Dirac quantization programme and the intrinsic mathematical relations between some quantum groups and Lie bialgebras. That is, a Lie bialgebra can be seen as the infinitesimal notion of some quantum group. The deformation parameter q encodes the value of the cosmological constant and it allows us to recover the 3D LQG model with $\Lambda = 0$ straightforwardly at the $q \to 1$ limit. Thanks to the work [72] on the continuous theory and the discretization process, the q-deformed LQG model is well-defined unambiguously from first principle. This suggests a new mathematical framework to construct LQG and provides an invitation for generalization to the 4D case.

We also reformulated the q-deformed LQG in terms of deformed spinors that live on nodes of a (ribbon) graph. Using these variables, we recover perfectly the classical and quantum structures given by the holonomies and fluxes. These spinors are good candidates for constructing local observables. We showed that this is indeed the case and provided a

geometrical way to construct these observables consistent with the q-deformed LQG model. We discovered, for the first time at least in the LQG community to our knowledge, that the quantum $\mathcal{R}$-matrix — in general understood as a mathematical structure of a quantum group — encodes geometrical information. It opens a window to introduce techniques and methodologies from other fields *e.g.* integrable lattice models [147, 84, 178] to improve our understanding of the quantum structure of LQG.

The local observables constructed from the deformed spinors were further used to construct the quantum Hamiltonian constraint of the q-deformed LQG, which is a q-deformed version of the Hamiltonian constraint for the LQG with $\Lambda = 0$ [44] in a straightforward way. This allows us to find the physical states easily. We justified the solutions through their invariance under Pachner moves. This analysis of the dynamical aspect of the q-deformed LQG completes the program neatly.

Finally, as another application of spinors, we used spinors to rewrite the 3D spinfoam model in a conformal way. That is the building blocks of local amplitudes only capture the local conformal geometries. As a first step, we work on the $\Lambda = 0$ case where the spinfoam model is the Ponzano-Regge model. We were able to reformulate the Ponzano-Regge amplitude as a state-integral instead of a state-sum in the standard formula. We analyzed the geometrical interpretation of different amplitudes in detail and systematically gave the construction of a global amplitude from local ones. It would be fascinating to see how this can be generalized to spinfoam models with $\Lambda \neq 0$ using the deformed spinors introduced in the q-deformed LQG framework.

Future explorations

This thesis has only focused on a specific case of LQG — 3D Euclidean signature with $\Lambda < 0$. Despite the completeness of the model in this situation, there is indeed a lot to explore. We list a few of them below.

- **Generalize the construction to $\Lambda > 0$ case and the Lorentzian signature.** According to the equivalence of the first-order 3D gravity and the Chern-Simons theory, it has been well-known that quantization of 3D gravity with a positive cosmological constant in the Euclidean signature would lead to $\mathcal{U}_q(\mathfrak{su}(2))$ with q root of unity. This is also the symmetry of the Turaev-Viro model. When q is taken to be a root of unity, $\mathcal{U}_q(\mathfrak{su}(2))$ is a quasi-Hopf algebra and its mathematical structures are not the same as those of $\mathcal{U}_q(\mathfrak{su}(2))$ with q real. Taking the infinitesimal limit, one should deal with a quasi-bialgebra structure [203, 127]. It would be interesting to investigate how it can lead to the spherical geometry and its similarity and difference

from the structure we have described in this thesis. Moreover, the quantum group relevant to Lorentzian 3D gravity with a non-vanishing Λ is $\mathcal{U}(\mathfrak{sl}(2,\mathbb{R}))$ with q real or root of unity depending on the sign of the cosmological constant. Exploring the quantum structure of these cases can help us to understand better the BTZ black hole especially the calculation of its entropy from the LQG point of view [110].

- **Relate the q-deformed LQG to other quantum gravity approaches.** For the case of $\Lambda = 0$, different 3D quantum gravity approaches namely LQG, spinfoam models and combinatorial quantization have been shown to be consistent [105, 162, 152]. It is not clear if the consistency can be extended to the $\Lambda \neq 0$. The q-deformed LQG model provides a way to connect LQG and the combinatorial quantization. Our work has shown explicitly this connection at the classical level. To complete the bridge, one needs to analyze the quantum theory as well.

  On the other hand, the Turaev-Viro model only possesses a spin representation expression. This impedes us to interpret the spinfoam as a discrete path integral of gravity as in the $\Lambda = 0$ case. The q-deformed LQG framework we constructed in this thesis has a classical discrete theory consistent with the continuous action in terms of a change of variables. This seems to be able to lead us to a path-integral expression of the Turaev-Viro model. If such an expression can be found (see [116] for a recent work on it), it would allow us to study the quantum field theory aspect of spinfoam and extend it to one with particle insertion as it was done in the $\Lambda = 0$ case [97].

- **Relate the q-deformed LQG to quantum statistical models.** It was found in [68] that 3D quantum gravity with $\Lambda = 0$ in the spinfoam framework can be mapped to some quantum statistical models *e.g.* the six-vertex model (or ice-type model) and the loop models. For instance, to map to the six-vertex, one works on a spin network state with each link carrying a $1/2$ representation. The six-vertex model has a (rather hidden) $\mathcal{U}_q(\mathfrak{su}(2))$ symmetry which can be seen in the form of the $\mathcal{R}$-matrix [183]. The deformation parameter q is related to the anisotropy in the Hamiltonian of the XXZ spin chain model, which is deeply related to the six-vertex model. (See *e.g.* [136] and references therein for details on the six-vertex model and the XXZ model.) The transfer matrices in the six-vertex model play the same role as the quantum holonomies we define in Chapter 4. Using this correspondence, one could give a gravitational interpretation to the six-vertex model. It would be interesting to investigate how the geometrical interpretation of the $\mathcal{R}$-matrix we present in this thesis can play a role in this correspondence and possible correspondences with other quantum statistical models.

- **Include point particles in q-deformed LQG.** 3D gravity coupling to point

particles can be done in its metric formalism [52, 62] or the Chern-Simons formalism [61]. Adding particles to the system would change the topological nature. As there are no gravitational waves in 3D, the particles only change the geometries localized at their positions. It is well-known that the masses of particles give rise to curvature and the spins give rise to torsion of the geometry. It seems natural to interpret the inclusion of particles in the q-deform loop gravity model by relaxing the Gauss constraint and the flatness constraint at the location of particles. A systematic analysis starting from the continuous action is needed to justify this intuition. To build the Hilbert space of the quantum theory coupling to particles, a well-studied way in LQG with $\Lambda = 0$ is to consider the same representation for particle degrees of freedom as that of the quantum geometry [161]. It is interesting to see if the same method can be applied to our framework or if new treatments need to be introduced. The coupling with particles would allow us to construct Dirac observables, *e.g.* distance between particles, hence relate to physical processes.

- **Extend to 4D LQG with $\Lambda \neq 0$.** The ribbon framework also opens a new way to consider LQG with $\Lambda \neq 0$ in 4D, which might unravel how (if it does) the cosmological constant is encoded in the quantum group structure in the real physical situation. One possible way to generalize the ribbon in 4D is to consider 2-groups. This was recently introduced [13, 121, 117], where the Drinfeld double was generalized to the notion of 2-Drinfeld double in terms of 2-groups. Along with this storyline, the spinor should be generalized to some notion of "2-spinor". It would be interesting to investigate how to build such objects and construct local observables out of them. It remains an unsolved problem whether quantum group symmetries would appear in 4D quantum gravity. It is also possible that the quantum group symmetries emerging in the 3D case is only due to the topological nature of 3D gravity. Nevertheless, one can still start from a topological setting in 4D then impose constraint to describe gravity as done in the spinfoam models [21, 168, 138, 82, 96, 141]. Quantum group structure would still be expected to appear in the topological setting. Then the question is whether imposing the quantum constraint would change or break the quantum group structure.

References

[1] B. P. Abbott et al. Observation of Gravitational Waves from a Binary Black Hole Merger. *Phys. Rev. Lett.*, 116(6):061102, 2016.

[2] A. Achucarro and P. K. Townsend. A Chern-Simons Action for Three-Dimensional anti-De Sitter Supergravity Theories. *Phys. Lett. B*, 180:89, 1986.

[3] K. S. Ahluwalia. Fundamentals of poisson lie groups with application to the classical double. 10 1993.

[4] Kazunori Akiyama et al. First M87 Event Horizon Telescope Results. I. The Shadow of the Supermassive Black Hole. *Astrophys. J. Lett.*, 875:L1, 2019.

[5] Kazunori Akiyama et al. First Sagittarius A* Event Horizon Telescope Results. I. The Shadow of the Supermassive Black Hole in the Center of the Milky Way. *Astrophys. J. Lett.*, 930(2):L12, 2022.

[6] A. Yu. Alekseev and L. D. Faddeev. A involution and dynamics for the q deformed quantum top. *Zap. Nauchn. Semin.*, 200:3–16, 1992.

[7] Anton Yu. Alekseev, Harald Grosse, and Volker Schomerus. Combinatorial quantization of the Hamiltonian Chern-Simons theory. *Commun. Math. Phys.*, 172:317–358, 1995.

[8] Anton Yu. Alekseev, Harald Grosse, and Volker Schomerus. Combinatorial quantization of the Hamiltonian Chern-Simons theory. 2. *Commun. Math. Phys.*, 174:561–604, 1995.

[9] Jan Ambjorn and R. Loll. Nonperturbative Lorentzian quantum gravity, causality and topology change. *Nucl. Phys. B*, 536:407–434, 1998.

[10] Francis Archer and Ruth M. Williams. The Turaev-Viro state sum model and three-dimensional quantum gravity. *Phys. Lett. B*, 273:438–444, 1991.

[11] Jácome Armas. *Conversations on Quantum Gravity*. Cambridge University Press, 2021.

[12] Richard L. Arnowitt, Stanley Deser, and Charles W. Misner. The Dynamics of general relativity. *Gen. Rel. Grav.*, 40:1997–2027, 2008.

[13] Seth K. Asante, Bianca Dittrich, Florian Girelli, Aldo Riello, and Panagiotis Tsimiklis. Quantum geometry from higher gauge theory. *Class. Quant. Grav.*, 37(20):205001, 2020.

[14] A. Ashtekar, J. Baez, A. Corichi, and Kirill Krasnov. Quantum geometry and black hole entropy. *Phys. Rev. Lett.*, 80:904–907, 1998.

[15] Abhay Ashtekar and Eugenio Bianchi. A short review of loop quantum gravity. *Rept. Prog. Phys.*, 84(4):042001, 2021.

[16] Abhay Ashtekar and Jorge Pullin. *Loop Quantum GRavity: the first 30 years*, volume 4. World Scientific, 2017.

[17] Abhay Ashtekar and Jorge Pullin. The overview chapter in loop quantum gravity: The first 30 years. *arXiv preprint arXiv:1703.07396*, 2017.

[18] Abhay Ashtekar and Parampreet Singh. Loop Quantum Cosmology: A Status Report. *Class. Quant. Grav.*, 28:213001, 2011.

[19] Scott Axelrod, Steve Della Pietra, and Edward Witten. Geometric quantization of Chern-Simons gauge theory. *J. Diff. Geom.*, 33(3):787–902, 1991.

[20] P. Baekler, E. W. Mielke, and F. W. Hehl. Dynamical symmetries in topological 3-D gravity with torsion. *Nuovo Cim. B*, 107:91–110, 1992.

[21] J. C. Baez. An Introduction to Spin Foam Models of BF Theory and Quantum Gravity. *Lect. Notes Phys.*, 543:25–93, 2000.

[22] John C. Baez. Spin foam models. *Class. Quant. Grav.*, 15:1827–1858, 1998.

[23] Benjamin Bahr and Bianca Dittrich. (Broken) Gauge Symmetries and Constraints in Regge Calculus. *Class. Quant. Grav.*, 26:225011, 2009.

[24] Benjamin Bahr and Bianca Dittrich. Improved and Perfect Actions in Discrete Gravity. *Phys. Rev. D*, 80:124030, 2009.

[25] Maximo Banados, Thorsten Brotz, and Miguel E. Ortiz. Boundary dynamics and the statistical mechanics of the (2+1)-dimensional black hole. *Nucl. Phys. B*, 545:340–370, 1999.

[26] Andrzej Banburski, Lin-Qing Chen, Laurent Freidel, and Jeff Hnybida. Pachner moves in a 4d Riemannian holomorphic Spin Foam model. *Phys. Rev. D*, 92(12):124014, 2015.

[27] Dror Bar-Natan and Edward Witten. Perturbative expansion of Chern-Simons theory with noncompact gauge group. *Commun. Math. Phys.*, 141:423–440, 1991.

[28] V. Bargmann. On the Representations of the Rotation Group. *Rev. Mod. Phys.*, 34:829–845, 1962.

[29] John W. Barrett and T. J. Foxon. Semiclassical limits of simplicial quantum gravity. *Class. Quant. Grav.*, 11:543–556, 1994.

[30] John W. Barrett and Ileana Naish-Guzman. The Ponzano-Regge model. *Class. Quant. Grav.*, 26:155014, 2009.

[31] Katrin Becker, Melanie Becker, and John H Schwarz. *String theory and M-theory: A modern introduction*. Cambridge University Press, 2006.

[32] Per Berglund, Laurent Freidel, Tristan Hubsch, Jerzy Kowalski-Glikman, Robert G. Leigh, David Mattingly, and Djordje Minic. Infrared Properties of Quantum Gravity: UV/IR Mixing, Gravitizing the Quantum – Theory and Observation. In *2022 Snowmass Summer Study*, 2 2022.

[33] L.C. Biedenharn and M.A. Lohe. *Quantum group symmetry and q tensor algebras*. World Scientific, 11 1996.

[34] Matthias Blau and George Thompson. A New Class of Topological Field Theories and the Ray-singer Torsion. *Phys. Lett. B*, 228:64–68, 1989.

[35] Matthias Blau and George Thompson. Topological Gauge Theories of Antisymmetric Tensor Fields. *Annals Phys.*, 205:130–172, 1991.

[36] Martin Bojowald and Hugo A. Morales-Tecotl. Cosmological Applications of Loop Quantum Gravity. *Lect. Notes Phys.*, 646:421–462, 2004.

[37] Valentin Bonzom, Francesco Costantino, and Etera R. Livine. Duality between Spin networks and the 2D Ising model. *Commun. Math. Phys.*, 344(2):531–579, 2016.

[38] Valentin Bonzom and Bianca Dittrich. Dirac's discrete hypersurface deformation algebras. *Class. Quant. Grav.*, 30:205013, 2013.

[39] Valentin Bonzom, Maïté Dupuis, and Florian Girelli. Towards the turaev-viro amplitudes from a hamiltonian constraint. *Physical Review D*, 90(10):104038, 2014.

[40] Valentin Bonzom, Maité Dupuis, Florian Girelli, and Etera R Livine. Deformed phase space for 3d loop gravity and hyperbolic discrete geometries. *arXiv preprint arXiv:1402.2323*, 2014.

[41] Valentin Bonzom, Maïté Dupuis, Florian Girelli, and Qiaoyin Pan. Local Observables in $SU_q(2)$ Lattice Gauge Theory. 5 2022.

[42] Valentin Bonzom, Maïté Dupuis, and Qiaoyin Pan. Spinor Representation of the Hamiltonian Constraint in 3D LQG with a Non-zero Cosmological Constant. 11 2021.

[43] Valentin Bonzom and Laurent Freidel. The Hamiltonian constraint in 3d Riemannian loop quantum gravity. *Class. Quant. Grav.*, 28:195006, 2011.

[44] Valentin Bonzom and Etera R. Livine. A New Hamiltonian for the Topological BF phase with spinor networks. *J. Math. Phys.*, 53:072201, 2012.

[45] Valentin Bonzom and Etera R. Livine. Generating Functions for Coherent Intertwiners. *Class. Quant. Grav.*, 30:055018, 2013.

[46] Valentin Bonzom and Etera R. Livine. Self-duality of the 6j-symbol and Fisher zeros for the Tetrahedron. 5 2019.

[47] Valentin Bonzom and Matteo Smerlak. Bubble divergences from cellular cohomology. *Lett. Math. Phys.*, 93:295–305, 2010.

[48] Valentin Bonzom and Matteo Smerlak. Bubble divergences from twisted cohomology. *Commun. Math. Phys.*, 312:399–426, 2012.

[49] Roumen Borissov, Seth Major, and Lee Smolin. The geometry of quantum spin networks. *Classical and Quantum Gravity*, 13(12):3183, 1996.

[50] Enrique F. Borja, Laurent Freidel, Inaki Garay, and Etera R. Livine. U(N) tools for Loop Quantum Gravity: The Return of the Spinor. *Class. Quant. Grav.*, 28:055005, 2011.

[51] J. David Brown and M. Henneaux. Central Charges in the Canonical Realization of Asymptotic Symmetries: An Example from Three-Dimensional Gravity. *Commun. Math. Phys.*, 104:207–226, 1986.

[52] E. Buffenoir and K. Noui. Unfashionable observations about three-dimensional gravity. 5 2003.

[53] E. Buffenoir, K. Noui, and P. Roche. Hamiltonian quantization of Chern-Simons theory with SL(2,C) group. *Class. Quant. Grav.*, 19:4953, 2002.

[54] Steven Carlip. Conformal field theory, (2+1)-dimensional gravity, and the BTZ black hole. *Class. Quant. Grav.*, 22:R85–R124, 2005.

[55] Steven Carlip and Steven Jonathan Carlip. *Quantum gravity in 2+ 1 dimensions*, volume 50. Cambridge University Press, 2003.

[56] Ali H. Chamseddine, Alain Connes, and Viatcheslav Mukhanov. Geometry and the Quantum: Basics. *JHEP*, 12:098, 2014.

[57] Ali H. Chamseddine, Alain Connes, and Viatcheslav Mukhanov. Quanta of Geometry: Noncommutative Aspects. *Phys. Rev. Lett.*, 114(9):091302, 2015.

[58] Vyjayanthi Chari, Andrew Pressley, et al. *A guide to quantum groups*. Cambridge university press, 1995.

[59] Lin-Qing Chen. *Amplitudes in the Spin Foam Approach to Quantum Gravity*. PhD thesis, Perimeter Inst. Theor. Phys., 2017.

[60] Shiin-Shen Chern and James Simons. Characteristic forms and geometric invariants. *Annals Math.*, 99:48–69, 1974.

[61] Philipp de Sousa Gerbert. On spin and (quantum) gravity in (2+1)-dimensions. *Nucl. Phys. B*, 346:440–472, 1990.

[62] Stanley Deser and R. Jackiw. Three-Dimensional Cosmological Gravity: Dynamics of Constant Curvature. *Annals Phys.*, 153:405–416, 1984.

[63] Stanley Deser, R. Jackiw, and Gerard 't Hooft. Three-Dimensional Einstein Gravity: Dynamics of Flat Space. *Annals Phys.*, 152:220, 1984.

[64] Stanley Deser and P. van Nieuwenhuizen. Nonrenormalizability of the Quantized Dirac-Einstein System. *Phys. Rev. D*, 10:411, 1974.

[65] Eric D'Hoker and Daniel Z. Freedman. Supersymmetric gauge theories and the AdS / CFT correspondence. In *Theoretical Advanced Study Institute in Elementary Particle Physics (TASI 2001): Strings, Branes and EXTRA Dimensions*, pages 3–158, 1 2002.

[66] C. di Bartolo, F. Nori, R. Gambini, and A. Trias. Loop Space Quantum Formulation of Free Electromagnetism. *Lett. Nuovo Cim.*, 38:497, 1983.

[67] Bianca Dittrich. Diffeomorphism symmetry in quantum gravity models. *Adv. Sci. Lett.*, 2:151, 10 2008.

[68] Bianca Dittrich, Christophe Goeller, Etera Livine, and Aldo Riello. Quasi-local holographic dualities in non-perturbative 3d quantum gravity I – Convergence of multiple approaches and examples of Ponzano–Regge statistical duals. *Nucl. Phys. B*, 938:807–877, 2019.

[69] R. J. Dowdall, Henrique Gomes, and Frank Hellmann. Asymptotic analysis of the Ponzano-Regge model for handlebodies. *J. Phys. A*, 43:115203, 2010.

[70] Fay Dowker. Introduction to causal sets and their phenomenology. *Gen. Rel. Grav.*, 45(9):1651–1667, 2013.

[71] Maïté Dupuis, Laurent Freidel, and Florian Girelli. Discretization of 3d gravity in different polarizations. *Phys. Rev. D*, 96(8):086017, 2017.

[72] Maïté Dupuis, Laurent Freidel, Florian Girelli, Abdulmajid Osumanu, and Julian Rennert. On the origin of the quantum group symmetry in 3d quantum gravity. 6 2020.

[73] Maïté Dupuis, Florian Girelli, and Etera R Livine. Deformed spinor networks for loop gravity: towards hyperbolic twisted geometries. *General Relativity and Gravitation*, 46(11):1802, 2014.

[74] Maite Dupuis and Etera R. Livine. Holomorphic Simplicity Constraints for 4d Spinfoam Models. *Class. Quant. Grav.*, 28:215022, 2011.

[75] Maite Dupuis and Etera R. Livine. Revisiting the Simplicity Constraints and Coherent Intertwiners. *Class. Quant. Grav.*, 28:085001, 2011.

[76] Maite Dupuis and Etera R. Livine. Holomorphic Simplicity Constraints for 4d Riemannian Spinfoam Models. *J. Phys. Conf. Ser.*, 360:012046, 2012.

[77] Maïté Dupuis, Etera R. Livine, and Qiaoyin Pan. q-deformed 3D Loop Gravity on the Torus. *Class. Quant. Grav.*, 37(2):025017, 2020.

[78] Maite Dupuis, James P. Ryan, and Simone Speziale. Discrete gravity models and Loop Quantum Gravity: a short review. *SIGMA*, 8:052, 2012.

[79] Maité Dupuis, Florian Girelli, and Etera R. Livine. Deformed Spinor Networks for Loop Gravity: Towards Hyperbolic Twisted Geometries. *Gen. Rel. Grav.*, 46(11):1802, 2014.

[80] Maïté Dupuis and Florian Girelli. Quantum hyperbolic geometry in loop quantum gravity with cosmological constant. *Phys. Rev. D*, 87(12):121502, 2013.

[81] Maïté Dupuis and Florian Girelli. Observables in Loop Quantum Gravity with a cosmological constant. *Phys. Rev. D*, 90(10):104037, 2014.

[82] Jonathan Engle, Etera Livine, Roberto Pereira, and Carlo Rovelli. LQG vertex with finite Immirzi parameter. *Nucl. Phys. B*, 799:136–149, 2008.

[83] Jonathan Engle, Karim Noui, Alejandro Perez, and Daniele Pranzetti. Black hole entropy from an SU(2)-invariant formulation of Type I isolated horizons. *Phys. Rev. D*, 82:044050, 2010.

[84] L. D. Faddeev, E. K. Sklyanin, and L. A. Takhtajan. The Quantum Inverse Problem Method. 1. *Teor. Mat. Fiz.*, 40:194–220, 1979.

[85] V. V. Fock and A. A. Rosly. Poisson structure on moduli of flat connections on Riemann surfaces and r matrix. *Am. Math. Soc. Transl.*, 191:67–86, 1999.

[86] Daniel S. Freed, Michael J. Hopkins, Jacob Lurie, and Constantin Teleman. Topological Quantum Field Theories from Compact Lie Groups. In *A Celebration of Raoul Bott's Legacy in Mathematics*, 5 2009.

[87] Laurent Freidel. Group field theory: An Overview. *Int. J. Theor. Phys.*, 44:1769–1783, 2005.

[88] Laurent Freidel, Marc Geiller, and Daniele Pranzetti. Edge modes of gravity. Part I. Corner potentials and charges. *JHEP*, 11:026, 2020.

[89] Laurent Freidel, Marc Geiller, and Daniele Pranzetti. Edge modes of gravity. Part II. Corner metric and Lorentz charges. *JHEP*, 11:027, 2020.

[90] Laurent Freidel, Marc Geiller, and Daniele Pranzetti. Edge modes of gravity. Part III. Corner simplicity constraints. *JHEP*, 01:100, 2021.

[91] Laurent Freidel, Florian Girelli, and Barak Shoshany. 2+1D Loop Quantum Gravity on the Edge. *Phys. Rev. D*, 99(4):046003, 2019.

[92] Laurent Freidel, Christophe Goeller, and Etera R. Livine. The quantum gravity disk: Discrete current algebra. *J. Math. Phys.*, 62(10):102303, 2021.

[93] Laurent Freidel and Jeff Hnybida. On the exact evaluation of spin networks. *J. Math. Phys.*, 54:112301, 2013.

[94] Laurent Freidel, Jerzy Kowalski-Glikman, Robert G. Leigh, and Djordje Minic. Quantum gravity phenomenology in the infrared. *Int. J. Mod. Phys. D*, 30(14):2141002, 2021.

[95] Laurent Freidel and Kirill Krasnov. Discrete space-time volume for three-dimensional BF theory and quantum gravity. *Class. Quant. Grav.*, 16:351–362, 1999.

[96] Laurent Freidel and Kirill Krasnov. A New Spin Foam Model for 4d Gravity. *Class. Quant. Grav.*, 25:125018, 2008.

[97] Laurent Freidel and Etera R. Livine. Ponzano-Regge model revisited III: Feynman diagrams and effective field theory. *Class. Quant. Grav.*, 23:2021–2062, 2006.

[98] Laurent Freidel and Etera R. Livine. The Fine Structure of SU(2) Intertwiners from U(N) Representations. *J. Math. Phys.*, 51:082502, 2010.

[99] Laurent Freidel and Etera R. Livine. U(N) Coherent States for Loop Quantum Gravity. *J. Math. Phys.*, 52:052502, 2011.

[100] Laurent Freidel and Etera R. Livine. Bubble networks: framed discrete geometry for quantum gravity. *Gen. Rel. Grav.*, 51(1):9, 2019.

[101] Laurent Freidel, Etera R. Livine, and Daniele Pranzetti. Gravitational edge modes: from Kac–Moody charges to Poincaré networks. *Class. Quant. Grav.*, 36(19):195014, 2019.

[102] Laurent Freidel and David Louapre. Asymptotics of 6j and 10j symbols. *Class. Quant. Grav.*, 20:1267–1294, 2003.

[103] Laurent Freidel and David Louapre. Diffeomorphisms and spin foam models. *Nucl. Phys. B*, 662:279–298, 2003.

[104] Laurent Freidel and David Louapre. Ponzano-Regge model revisited I: Gauge fixing, observables and interacting spinning particles. *Class. Quant. Grav.*, 21:5685–5726, 2004.

[105] Laurent Freidel and David Louapre. Ponzano-Regge model revisited II: Equivalence with Chern-Simons. 10 2004.

[106] Laurent Freidel, Roberto Oliveri, Daniele Pranzetti, and Simone Speziale. Extended corner symmetry, charge bracket and Einstein's equations. *JHEP*, 09:083, 2021.

[107] Laurent Freidel, Roberto Oliveri, Daniele Pranzetti, and Simone Speziale. The Weyl BMS group and Einstein's equations. *JHEP*, 07:170, 2021.

[108] Laurent Freidel and Simone Speziale. Twisted geometries: A geometric parametrisation of SU(2) phase space. *Phys. Rev.*, D82:084040, 2010.

[109] Laurent Freidel and Jonathan Ziprick. Spinning geometry = Twisted geometry. *Class. Quant. Grav.*, 31(4):045007, 2014.

[110] Ernesto Frodden, Marc Geiller, Karim Noui, and Alejandro Perez. Statistical Entropy of a BTZ Black Hole from Loop Quantum Gravity. *JHEP*, 05:139, 2013.

[111] R. Gambini and A. Trias. Second Quantization of the Free Electromagnetic Field as Quantum Mechanics in the Loop Space. *Phys. Rev. D*, 22:1380, 1980.

[112] Rodolfo Gambini and Antoni Trias. Gauge Dynamics in the C Representation. *Nucl. Phys. B*, 278:436–448, 1986.

[113] Marc Geiller, Christophe Goeller, and Nelson Merino. Most general theory of 3d gravity: Covariant phase space, dual diffeomorphisms, and more. *JHEP*, 02:120, 2021.

[114] Amit Ghosh and Daniele Pranzetti. CFT/Gravity Correspondence on the Isolated Horizon. *Nucl. Phys. B*, 889:1–24, 2014.

[115] G. W. Gibbons and S. W. Hawking. Action Integrals and Partition Functions in Quantum Gravity. *Phys. Rev. D*, 15:2752–2756, 1977.

[116] Florian Girelli and Matteo Laudonio. Group field theory on quantum groups. 5 2022.

[117] Florian Girelli, Matteo Laudonio, and Panagiotis Tsimiklis. Polyhedron phase space using 2-groups: κ-Poincaré as a Poisson 2-group. 5 2021.

[118] Florian Girelli and Etera R. Livine. Reconstructing quantum geometry from quantum information: Spin networks as harmonic oscillators. *Class. Quant. Grav.*, 22:3295–3314, 2005.

[119] Florian Girelli, Abdulmajid Osumanu, and Wolfgang Wieland. Canonical transformations generated by the boundary volume: unimodular and non-abelian teleparallel gravity. 1 2021.

[120] Florian Girelli and Giuseppe Sellaroli. SO*(2N) coherent states for loop quantum gravity. *J. Math. Phys.*, 58(7):071708, 2017.

[121] Florian Girelli and Panagiotis Tsimiklis. Discretization of 4d Poincaré BF theory: from groups to 2-groups. 5 2021.

[122] William M Goldman. Invariant functions on lie groups and hamiltonian flows of surface group representations. *Inventiones mathematicae*, 85(2):263–302, 1986.

[123] Daniel Grumiller, Wout Merbis, and Max Riegler. Most general flat space boundary conditions in three-dimensional Einstein gravity. *Class. Quant. Grav.*, 34(18):184001, 2017.

[124] Daniel Grumiller and Max Riegler. Most general AdS_3 boundary conditions. *JHEP*, 10:023, 2016.

[125] Hal M. Haggard, Muxin Han, Wojciech Kamiński, and Aldo Riello. SL(2,C) Chern–Simons theory, a non-planar graph operator, and 4D quantum gravity with a cosmological constant: Semiclassical geometry. *Nucl. Phys. B*, 900:1–79, 2015.

[126] Hal M. Haggard, Muxin Han, Wojciech Kamiński, and Aldo Riello. Four-dimensional Quantum Gravity with a Cosmological Constant from Three-dimensional Holomorphic Blocks. *Phys. Lett. B*, 752:258–262, 2016.

[127] Hal M. Haggard, Muxin Han, and Aldo Riello. Encoding Curved Tetrahedra in Face Holonomies: Phase Space of Shapes from Group-Valued Moment Maps. *Annales Henri Poincare*, 17(8):2001–2048, 2016.

[128] Daniel Harlow and Jie-Qiang Wu. Covariant phase space with boundaries. *JHEP*, 10:146, 2020.

[129] J.B. Hartle and R. Sorkin. Boundary Terms in the Action for the Regge Calculus. *Gen. Rel. Grav.*, 13:541–549, 1981.

[130] Stephen W. Hawking, Malcolm J. Perry, and Andrew Strominger. Soft Hair on Black Holes. *Phys. Rev. Lett.*, 116(23):231301, 2016.

[131] Stephen W. Hawking, Malcolm J. Perry, and Andrew Strominger. Superrotation Charge and Supertranslation Hair on Black Holes. *JHEP*, 05:161, 2017.

[132] Jeff Hnybida. Spin Foams Without Spins. *Class. Quant. Grav.*, 33(20):205003, 2016.

[133] Gary T. Horowitz. Exactly Soluble Diffeomorphism Invariant Theories. *Commun. Math. Phys.*, 125:417, 1989.

[134] Claus Kiefer. Why quantum gravity? In *Approaches to fundamental physics*, pages 123–130. Springer, 2007.

[135] Yvette Kosmann-Schwarzbach. Lie bialgebras, poisson lie groups and dressing transformations. In *Integrability of nonlinear systems*, pages 104–170. Springer, 1997.

[136] Jules Lamers. A pedagogical introduction to quantum integrability, with a view towards theoretical high-energy physics. *PoS*, Modave2014:001, 2015.

[137] Etera Livine and Qiaoyin Pan. 3D quantum gravity from scale invariant blocks. in preparation.

[138] Etera R. Livine. The Spinfoam Framework for Quantum Gravity. Other thesis, 10 2010.

[139] Etera R. Livine. From Coarse-Graining to Holography in Loop Quantum Gravity. *EPL*, 123(1):10001, 2018.

[140] Etera R. Livine and Simone Speziale. A New spinfoam vertex for quantum gravity. *Phys. Rev. D*, 76:084028, 2007.

[141] Etera R. Livine and Simone Speziale. Consistently Solving the Simplicity Constraints for Spinfoam Quantum Gravity. *EPL*, 81(5):50004, 2008.

[142] Etera R. Livine and Johannes Tambornino. Loop gravity in terms of spinors. *J. Phys. Conf. Ser.*, 360:012023, 2012.

[143] Etera R. Livine and Johannes Tambornino. Spinor Representation for Loop Quantum Gravity. *J. Math. Phys.*, 53:012503, 2012.

[144] Etera R. Livine and Johannes Tambornino. Holonomy Operator and Quantization Ambiguities on Spinor Space. *Phys. Rev. D*, 87(10):104014, 2013.

[145] R. Loll. Quantum Gravity from Causal Dynamical Triangulations: A Review. *Class. Quant. Grav.*, 37(1):013002, 2020.

[146] D. Lovelock. The Einstein tensor and its generalizations. *J. Math. Phys.*, 12:498–501, 1971.

[147] S. Majid. Quasitriangular Hopf Algebras and Yang-Baxter Equations. *Int. J. Mod. Phys. A*, 5:1–91, 1990.

[148] Shahn Majid. *Foundations of quantum group theory*. Cambridge university press, 2000.

[149] Shahn Majid. Quantum groups and noncommutative geometry. *J. Math. Phys.*, 41:3892–3942, 2000.

[150] Seth Major and Lee Smolin. Quantum deformation of quantum gravity. *Nucl. Phys. B*, 473:267–290, 1996.

[151] Stanley Mandelstam. Quantization of the gravitational field. *Annals Phys.*, 19:25–66, 1962.

[152] C. Meusburger and K. Noui. The Hilbert space of 3d gravity: quantum group symmetries and observables. *Adv. Theor. Math. Phys.*, 14(6):1651–1715, 2010.

[153] Eckehard W. Mielke and Peter Baekler. Topological gauge model of gravity with torsion. *Phys. Lett. A*, 156:399–403, 1991.

[154] Charles W Misner, Kip S Thorne, and John Archibald Wheeler. *Gravitation*. Princeton University Press, 2017.

[155] V. Moncrief. Reduction of the Einstein equations in (2+1)-dimensions to a Hamiltonian system over Teichmuller space. *J. Math. Phys.*, 30:2907–2914, 1989.

[156] Horatiu Nastase. Introduction to AdS-CFT. 12 2007.

[157] M. Niedermaier. The Asymptotic safety scenario in quantum gravity: An Introduction. *Class. Quant. Grav.*, 24:R171–230, 2007.

[158] K. Noui, A. Perez, and D. Pranzetti. Canonical quantization of non-commutative holonomies in 2+1 loop quantum gravity. *JHEP*, 10:036, 2011.

[159] K. Noui, A. Perez, and D. Pranzetti. Non-commutative holonomies in 2+1 LQG and Kauffman's brackets. *J. Phys. Conf. Ser.*, 360:012040, 2012.

[160] Karim Noui. Three Dimensional Loop Quantum Gravity: Particles and the Quantum Double. *J. Math. Phys.*, 47:102501, 2006.

[161] Karim Noui and Alejandro Perez. Three-dimensional loop quantum gravity: Coupling to point particles. *Class. Quant. Grav.*, 22:4489–4514, 2005.

[162] Karim Noui and Alejandro Perez. Three-dimensional loop quantum gravity: Physical scalar product and spin foam models. *Class. Quant. Grav.*, 22:1739–1762, 2005.

[163] Hirosi Ooguri. Partition functions and topology changing amplitudes in the 3-D lattice gravity of Ponzano and Regge. *Nucl. Phys. B*, 382:276–304, 1992.

[164] Daniele Oriti. Space-time geometry from algebra: Spin foam models for nonperturbative quantum gravity. *Rept. Prog. Phys.*, 64:1703–1756, 2001.

[165] Daniele Oriti. Quantum gravity as a quantum field theory of simplicial geometry. pages 101–126, 12 2005.

[166] Daniele Oriti. The Group field theory approach to quantum gravity. pages 310–331, 7 2006.

[167] Udo Pachner. Pl homeomorphic manifolds are equivalent by elementary shellings. *European journal of Combinatorics*, 12(2):129–145, 1991.

[168] Alejandro Perez. The Spin Foam Approach to Quantum Gravity. *Living Rev. Rel.*, 16:3, 2013.

[169] Alejandro Perez and Daniele Pranzetti. On the regularization of the constraints algebra of Quantum Gravity in 2+1 dimensions with non-vanishing cosmological constant. *Class. Quant. Grav.*, 27:145009, 2010.

[170] P. Podles and S. L. Woronowicz. Quantum deformation of Lorentz group. *Commun. Math. Phys.*, 130:381–431, 1990.

[171] Joseph Polchinski. *String theory: Volume 1, an introduction to the bosonic string*. Cambridge university press, 1998.

[172] Joseph Polchinski. *String theory: Volume 2, superstring theory and beyond*. Cambridge university press, 1998.

[173] Giorgio Ponzano and Tullio Regge. Semiclassical limit of racah coefficients. Technical report, Princeton Univ., NJ, 1969.

[174] Giorgio Ponzano and Tullio Eugenio Regge. Semiclassical limit of racah coefficients. 1968.

[175] C Quesne. Sets of covariant and contravariant spinors for SUq(2) and alternative quantizations. *Journal of Physics A: Mathematical and General*, 26(6):L299–L306, mar 1993.

[176] Ana-Maria Raclariu. Lectures on Celestial Holography. 7 2021.

[177] N. Reshetikhin and V. G. Turaev. Invariants of three manifolds via link polynomials and quantum groups. *Invent. Math.*, 103:547–597, 1991.

[178] Ana L. Retore. Introduction to classical and quantum integrability. *J. Phys. A*, 55(17):173001, 2022.

[179] V. Rittenberg and M. Scheunert. Tensor operators for quantum groups and applications. *J. Math. Phys.*, 33:436–445, 1992.

[180] Justin Roberts. Classical 6j-symbols and the tetrahedron. *Geom. Topol.*, 3(1):21–66, 1999.

[181] Carlo Rovelli. Notes for a brief history of quantum gravity. In *Recent developments in theoretical and experimental general relativity, gravitation and relativistic field theories. Proceedings, 9th Marcel Grossmann Meeting, MG'9, Rome, Italy, July 2-8, 2000. Pts. A-C*, pages 742–768, 2000.

[182] Carlo Rovelli. *Quantum gravity*. Cambridge university press, 2004.

[183] H. Saleur and J. B. Zuber. Integrable lattice models and quantum groups. In *Spring School on String Theory and Quantum Gravity (to be followed by 3 day Workshop)*, 4 1990.

[184] H. Saleur and J.B. Zuber. Integrable lattice models and quantum groups. *CEA-CONF–10358*, 1990.

[185] Bernd J. Schroers. Quantum gravity and non-commutative spacetimes in three dimensions: a unified approach. *Acta Phys. Polon. Supp.*, 4:379–402, 2011.

[186] Klaus Schulten and Roy G Gordon. Semiclassical approximations to 3 j-and 6 j-coefficients for quantum-mechanical coupling of angular momenta. *Journal of Mathematical Physics*, 16(10):1971–1988, 1975.

[187] J Schwinger. On angular momentum, usaec report nyo-3071 (1952); reprinted in lc biedenharn and h. van dam,(editors), quantum theory of angular momentum, 1965.

[188] Barak Shoshany. *At the Corner of Space and Time*. PhD thesis, U. Waterloo (main), 2019.

[189] Barak Shoshany. Dual 2+1D Loop Quantum Gravity on the Edge. *Phys. Rev. D*, 100(2):026003, 2019.

[190] Lee Smolin. Linking topological quantum field theory and nonperturbative quantum gravity. *J. Math. Phys.*, 36:6417–6455, 1995.

[191] Lee Smolin. Quantum gravity with a positive cosmological constant. 9 2002.

[192] Lee Smolin and Chopin Soo. The Chern-Simons invariant as the natural time variable for classical and quantum cosmology. *Nucl. Phys. B*, 449:289–316, 1995.

[193] Sebastian Steinhaus. Coarse graining spin foam quantum gravity – a review. 7 2020.

[194] A. Stern and I. Yakushin. Deformation quantization of the isotropic rotator. *Mod. Phys. Lett. A*, 10:399–408, 1995.

[195] Andrew Strominger. Lectures on the Infrared Structure of Gravity and Gauge Theory. 3 2017.

[196] Sumati Surya. Directions in Causal Set Quantum Gravity. 3 2011.

[197] Gerard 't Hooft. An algorithm for the poles at dimension four in the dimensional regularization procedure. *Nucl. Phys. B*, 62:444–460, 1973.

[198] Gerard 't Hooft and M. J. G. Veltman. One loop divergencies in the theory of gravitation. *Ann. Inst. H. Poincare Phys. Theor. A*, 20:69–94, 1974.

[199] Yuka U Taylor and Christopher T Woodward. 6 j symbols for u_q ($mathfraksl_2$) and non-euclidean tetrahedra. *Selecta Mathematica*, 11(3):539–571, 2006.

[200] Thomas Thiemann. Modern canonical quantum general relativity. 2001.

[201] Thomas Thiemann. Loop Quantum Gravity: An Inside View. *Lect. Notes Phys.*, 721:185–263, 2007.

[202] Thomas Thiemann. *Modern canonical quantum general relativity*. Cambridge University Press, 2008.

[203] Thomas Treloar. The symplectic geometry of polygons in the 3-sphere, 2000.

[204] V. G. Turaev and O. Y. Viro. State sum invariants of 3 manifolds and quantum 6j symbols. *Topology*, 31:865–902, 1992.

[205] Vladimir Turaev and Alexis Virelizier. On two approaches to 3-dimensional tqfts. *arXiv preprint arXiv:1006.3501*, 2010.

[206] D. A. Varshalovich, A. N. Moskalev, and V. K. Khersonskii. *Quantum theory of angular momentum*. World Scientific, 1988.

[207] Kevin Walker. On witten's 3-manifold invariants. *preprint*, 116, 1991.

[208] Steven Weinberg. Ultraviolet divergences in quantum theories of gravitation. In *General relativity*. 1979.

[209] Edward Witten. (2+1)-Dimensional Gravity as an Exactly Soluble System. *Nucl. Phys. B*, 311:46, 1988.

[210] Edward Witten. Quantum Field Theory and the Jones Polynomial. *Commun. Math. Phys.*, 121:351–399, 1989.

[211] Edward Witten. Anti de sitter space and holography. *arXiv preprint hep-th/9802150*, 1998.

[212] James York. Boundary terms in the action principles of general relativity. *Found. Phys.*, 16:249–257, 1986.

[213] S. C. Zhang, T. H. Hansson, and S. Kivelson. An effective field theory model for the fractional quantum hall effect. *Phys. Rev. Lett.*, 62:82–85, 1988.

APPENDICES

Appendix A

Mathematical frameworks

In this appendix chapter, we summarize the construction of the Heisenberg double and its quantization, which serve as the mathematical framework for building the LQG phase space and the Hilbert space. We only give the definition of concepts and their properties used in the current article. Proofs and more detailed illustrations can be found in the textbooks of Lie bialgebra and Hopf algebra *e.g.* [135, 148, 58]. The notations in this chapter mainly follow [148].

A.1 Heisenberg double and Drinfeld double

Definition A.1.1 (Lie bialgebra)**.** *A Lie bialgebra is a pair* $(\mathfrak{g}, \delta)$ *over field* $\mathbb{K}$ *consisting of a Lie algebra* $\mathfrak{g}$ *whose structure is given by a Lie bracket* $[\,,\,]_{\mathfrak{g}} : \mathfrak{g} \otimes \mathfrak{g} \to \mathfrak{g}$*, and a 1-cocycle* $\delta : \mathfrak{g} \to \mathfrak{g} \otimes \mathfrak{g}$ *on* $\mathfrak{g}$ *which defines the Lie bracket* $[\,,\,]_{\mathfrak{g}^*} : \mathfrak{g}^* \otimes \mathfrak{g}^* \to \mathfrak{g}^*$ *of the dual Lie algebra* $\mathfrak{g}^*$ *such that*

$$\langle [\xi, \eta]_{\mathfrak{g}^*}, x \rangle = \langle \xi \otimes \eta, \delta(x) \rangle \,, \quad \forall x \in \mathfrak{g} \,,\, \xi, \eta \in \mathfrak{g}^* \,, \tag{A.1}$$

where $\langle\,,\,\rangle : \mathfrak{g}^* \otimes \mathfrak{g} \to \mathbb{K}$ *is the dual map.*

Thus a Lie bialgebra contains the information of the Lie algebra therein and its dual. We consider here the case where $\mathfrak{g}$ is finite-dimensional, then so is $\mathfrak{g}^*$. Accordingly, one can also define the dual $(\mathfrak{g}^*, \delta_*)$ of the Lie bialgebra $(\mathfrak{g}, \delta)$ with the cocycle $\delta_* : \mathfrak{g}^* \to \mathfrak{g}^* \otimes \mathfrak{g}^*$ defined as

$$\langle \xi, [x, y]_{\mathfrak{g}} \rangle = \langle \delta_*(\xi), x \otimes y \rangle \,, \quad \forall x, y \in \mathfrak{g} \,,\, \xi \in \mathfrak{g}^* \,. \tag{A.2}$$

When (A.1) and (A.2) are satisfied, we say that the Lie algebras $\mathfrak{g}$ and $\mathfrak{g}^*$ form a *dual pair* whose duality is defined through a given dual map $\langle\,,\,\rangle : \mathfrak{g}^* \otimes \mathfrak{g} \to \mathbb{K}$.

Given the generators $e_i \in \mathfrak{g}\,, f^i \in \mathfrak{g}^*$, the dual map is given by the bilinear map $\langle e_i, f^j\rangle = \delta_i^j$. $[\,,\,]_{\mathfrak{g}}$ and δ_* give the structure constants α_{ij}^k of $\mathfrak{g}$ while δ and $[\,,\,]_{\mathfrak{g}^*}$ give the structure constant β_k^{ij} of $\mathfrak{g}^*$ as follows.

$$[e_i, e_j] = \alpha_{ij}^k e_k\,, \quad \delta(e_k) = \beta_k^{ij} e_j \otimes e_k\,, \quad [f^i, f^j] = \beta_k^{ij} f^k\,, \quad \delta_*(f^k) = \alpha_{ij}^k f^j \otimes f^k\,. \tag{A.3}$$

When δ can be written as the coboundary $\delta = \partial r$ of some 1-cochain $r \in \mathfrak{g} \otimes \mathfrak{g}$, the Lie bialgebra is called a *coboundary Lie bialgebra*, denoted as $(\mathfrak{g}, r)$. We have only considered this case in the main text. Use the notation $r \equiv r_{12} = \sum r_{[1]} \otimes r_{[2]}$. Then the transpose of r is $r_{21} := \sum r_{[2]} \otimes r_{[1]}$. More generally, $r_{ij} = \sum \mathbb{I} \otimes \cdots \otimes \mathbb{I} \otimes r_{[1]} \otimes \mathbb{I} \otimes \cdots \otimes \mathbb{I} \otimes r_{[2]} \otimes \mathbb{I} \otimes \cdots \otimes \mathbb{I}$ $(i \neq j)$ with $r_{[1]}$ in the i-th vector space and $r_{[2]}$ in the j-th vector space. Then $\partial\delta = r$ means

$$\delta(x) = \sum [x, r_{[1]}] \otimes r_{[2]} + r_{[1]} \otimes [x, r_{[2]}]\,. \tag{A.4}$$

Definition A.1.2 (quasitriangular Lie bialgebra)**.** *A Lie bialgebra $(\mathfrak{g}, \delta)$ is called quasitriangular if the r-matrix $r \in \mathfrak{g} \otimes \mathfrak{g}$ such that $\delta = \partial r$ satisfies the following conditions:*

1. *The symmetric part $r_s = \frac{1}{2}(r + r_{21})$ of r is $\mathfrak{g}$-invariant and*
2. *r satisfies*

$$(\mathbb{I} \otimes \delta) r = [r_{13}, r_{12}]\,, \quad (\delta \otimes \mathbb{I}) r = [r_{13}, r_{23}]\,. \tag{A.5}$$

Either of the conditions in (A.5) implies that r satisfies the *classical Yang-Baxter equation* (CYBE), *i.e.*

$$[r_{12}, r_{13}] + [r_{12}, r_{23}] + [r_{13}, r_{23}] = 0\,. \tag{A.6}$$

Additionally, if the symmetric part r_s of r is non-degenerate, the Lie bialgebra is said to be *factorizable*.

The r-matrix defining the coboundary Lie bialgebra can be viewed as a map $r : \mathbb{K} \to \mathfrak{g} \otimes \mathfrak{g}$. Due to the duality map, r can also be seen as a map $r : \mathfrak{g}^* \otimes \mathfrak{g}^* \to \mathbb{K}$. This leads to the definition of the *dual quasitriangular Lie bialgebra*.

Definition A.1.3 (dual quasitriangular Lie bialgebra)**.** *A dual quasitriangular Lie bialgebra is a pair $(\mathfrak{h}, \delta)$ consisting of a Lie algebra $\mathfrak{h}$ and a 1-cocycle $\delta = \partial r$ which is the*

coboundary of a map $r : \mathfrak{h} \otimes \mathfrak{h} \to \mathbb{K}$ *satisfying the following conditions*

$$[\xi, \eta] = \sum \xi_{[1]} r(\xi_{[2]} \otimes \eta) + \eta_{[1]} r(\xi \otimes \eta_{[2]}) \,, \tag{A.7}$$

$$r(\xi \otimes [\eta, \zeta]) = \sum r(\xi_{[1]} \otimes \zeta) r(\xi_{[2]} \otimes \zeta) \,, \tag{A.8}$$

$$r([\xi, \eta] \otimes \zeta) = \sum r(\xi \otimes \zeta_{[1]}) r(\eta \otimes \zeta_{[2]}) \,, \quad \forall \xi, \eta, \zeta \in \mathfrak{h} \,, \tag{A.9}$$

where $\delta(\xi) = \sum \xi_{[1]} \otimes \xi_{[2]}$*, and the symmetric part of* r *is* $\mathfrak{h}$*-invariant.*

It is straightforward to check that r satisfies the condition

$$\sum r(\xi \otimes \eta_{[1]}) r(\eta_{[2]} \otimes \zeta) + r(\xi_{[1]} \otimes \eta) r(\xi_{[2]} \otimes \zeta) + r(\xi \otimes \zeta_{[1]}) r(\eta \otimes \zeta_{[2]}) = 0 \,. \tag{A.10}$$

The duality between a quasitriangular Lie bialgebra and a dual quasitriangular Lie bialgebra is in the sense of the same r-matrix and that (A.7) is the dual of (A.4), (A.8) and (A.9) are the dual of (A.5). Accordingly, (A.10) is the dual of the CYBE (A.6).

We do not need the concept of the dual quasitriangular Lie bialgebra in the main text except for its quantum deformation which will be given below.

On the vector space $\mathfrak{g} \oplus \mathfrak{g}^*$, one can build another Lie bialgebra with $\mathfrak{g}$ and $\mathfrak{g}^*$ as the subalgebras. The adjoint actions $\mathrm{ad}_x \in \mathrm{End}(\mathfrak{g})$ and $\mathrm{ad}_\xi \in \mathrm{End}(\mathfrak{g}^*)$ on the subalgebras are defined by $\mathrm{ad}_x y = [x, y]_\mathfrak{g} \,, \mathrm{ad}_\xi \eta = [\xi, \eta]_{\mathfrak{g}^*} \,, \forall x, y \in \mathfrak{g} \,, \xi, \eta \in \mathfrak{g}^*$. In addition, we can define $\mathrm{ad}_x^* \in \mathrm{End}(\mathfrak{g}^*)$ and $\mathrm{ad}_\xi^* \in \mathrm{End}(\mathfrak{g})$ through the duality of $\mathfrak{g}$ and $\mathfrak{g}^*$ as

$$\langle \xi, \mathrm{ad}_x y \rangle = -\langle \mathrm{ad}_x^* \xi, y \rangle \,, \quad \langle \mathrm{ad}_\xi \eta, x \rangle = -\langle \eta, \mathrm{ad}_\xi^* x \rangle \,, \quad \forall x, y \in \mathfrak{g} \,, \xi, \eta \in \mathfrak{g}^* \,. \tag{A.11}$$

Definition A.1.4 (classical double)**.** *A classical double* $(\mathfrak{d}(\mathfrak{g}), \delta_\mathfrak{d})$ *of* $\mathfrak{g}$ *is a quasitriangular Lie bialgebra with the Lie algebra* $\mathfrak{d} = \mathfrak{g} \bowtie \mathfrak{g}^*$ *on the vector space* $\mathfrak{g} \oplus \mathfrak{g}^*$ *whose structure is given by* $[\,,\,]_\mathfrak{d} : \mathfrak{d} \otimes \mathfrak{d} \to \mathfrak{d}$ *which acts on the Lie algebra elements as*

$$[x, y]_\mathfrak{d} = [x, y]_\mathfrak{g} \,, \quad [\xi, \eta]_\mathfrak{d} = [\xi, \eta]_{\mathfrak{g}^*} \,, \quad [x, \xi]_\mathfrak{d} = ad_x^* \xi - ad_\xi^* x \,, \quad \forall x, y \in \mathfrak{g} \,, \xi, \eta \in \mathfrak{g}^* \,, \tag{A.12}$$

and the cocycle structure is given by

$$\delta_\mathfrak{d}(X) = [X \otimes X, r] \,, \quad X \in \mathfrak{d} \,, \quad r \in \mathfrak{g} \otimes \mathfrak{g}^* \subset \mathfrak{d}(\mathfrak{g}) \otimes \mathfrak{d}(\mathfrak{g}) \,, \quad \partial r = \delta_\mathfrak{d} \,. \tag{A.13}$$

The dimensions of $\mathfrak{g}$ and $\mathfrak{g}^*$ are necessarily the same. Given the basis $e_i \in \mathfrak{g}$ and $f^j \in \mathfrak{g}^*$, the r-matrix and the Poisson structure in (A.12) can be written explicitly as

$$r = \sum_i e_i \otimes f^i \,, \quad [e_i, e_j] = \alpha_{ij}^k e_k \,, \quad [f^i, f^j] = \beta_k^{ij} f^k \,, \quad [e_i, f^j] = \beta_i^{jk} e_k - \alpha_{ik}^j f^k \,. \tag{A.14}$$

We will denote the double as $\mathfrak{d}(\mathfrak{g})$, or simply $\mathfrak{d}$, and omit the cocycle. The double of quasitriangular Lie bialgebra can be exponentiated to form a double of Lie group, which leads to the following definition.

Definition A.1.5 (Heisenberg double)**.** *Exponentiating the double $\mathfrak{d}(\mathfrak{g})$, we get a Lie group $\mathcal{D}(G) \sim G \bowtie G^*$. A Heisenberg double is a pair $(\mathcal{D}(G), \pi_H)$ consisting of the Lie group $\mathcal{D}(G)$ generated by the double $\mathfrak{d}(\mathfrak{g})$ and a Poisson bivector $\pi_H : \mathcal{D} \to \mathcal{D} \otimes \mathcal{D}$ which defines the Poisson brackets of $\mathcal{D}$ as*

$$\pi_H(d) \equiv \{d_1, d_2\} = -r_{21} d_1 d_2 + d_1 d_2 r \,, \quad \forall d \in \mathcal{D} \,, \tag{A.15}$$

where $d_1 = d \otimes \mathbb{I}$, $d_2 = \mathbb{I} \otimes d$ and the r-matrix r inherits from $\mathfrak{d}(\mathfrak{g})$.

The fact that the symmetric part r_s of the r-matrix is the Casimir, *i.e.* $[r_s, d_1 d_2] = 0$ implies that the Poisson bracket (A.15) can be equivalently written as

$$\{d_1, d_2\} = r d_1 d_2 - d_1 d_2 r_{21} \,. \tag{A.16}$$

Exchanging the role of $\mathfrak{g}$ and $\mathfrak{g}^*$, the double $\mathfrak{d}$ can be viewed as the double of $\mathfrak{g}^*$ with the r-matrix $\tilde{r} = r_{21} = \sum_i f^i \otimes e_i \in \mathfrak{g}^* \otimes \mathfrak{g}$ and $\tilde{r}_{21} = r$, so as the Heisenberg double $\mathcal{D}(G^*) \sim G^* \bowtie G$. Another similar and relevant notion is the *Drinfeld double* $(\mathcal{D}(G), \pi_D)$ which is defined with the same Lie group $\mathcal{D}(G)$ but a different Poisson bivector

$$\pi_D(d) = [r, d_1 d_2] \,. \tag{A.17}$$

One of the most essential differences lies in the fact that the Drinfeld double is a Poisson-Lie group while the Heisenberg double is not, and the Heisenberg double is a symplectic space while the Drinfeld double is not.

A.2 Quasi-triangular Hopf algebra

Definition A.2.1 (quasitriangular Hopf algebra)**.** *A quasitriangular Hopf algebra is a pair $(H, \mathcal{R})$ consisting of a Hopf algebra H and an invertible quantum $\mathcal{R}$-matrix $\mathcal{R} \in H \otimes H$ satisfying the following properties*

$$(\triangle \otimes \mathbb{I})\mathcal{R} = \mathcal{R}_{13}\mathcal{R}_{23} \,, \tag{A.18}$$

$$(\mathbb{I} \otimes \triangle)\mathcal{R} = \mathcal{R}_{13}\mathcal{R}_{12} \,, \tag{A.19}$$

$$\sigma \circ \triangle h = \mathcal{R}(\triangle h)\mathcal{R}^{-1} \,, \quad \forall h \in H \,, \tag{A.20}$$

where $\triangle$ is the coproduct of H and σ is the permutation operator which acts on elements in tensor space as $\sigma(a \otimes b) = b \otimes a$.

The inverse of the $\mathcal{R}$-matrix can be obtained by

$$\mathcal{R}^{-1} = (S \otimes \mathbb{I})\mathcal{R}\,, \tag{A.21}$$

where S is the antipode of H. One can show from (A.19) and (A.20) that $\mathcal{R}$ satisfies the QYBE

$$\mathcal{R}_{12}\mathcal{R}_{13}\mathcal{R}_{23} = \mathcal{R}_{23}\mathcal{R}_{13}\mathcal{R}_{12}\,. \tag{A.22}$$

We denote the result of the coproduct acting on a Hopf algebra element as $\triangle(h) = \sum h_{(1)} \otimes h_{(2)}\,, h \in H$.

Definition A.2.2 (dual quasitriangular Hopf algebra)**.** *A dual quasitriangular Hopf algebra is a pair $(A, \mathcal{R})$ consisting of a Hopf algebra A and an invertible map $\mathcal{R} : A \otimes A \to \mathbb{K}$ such that*

$$\mathcal{R}(ab \otimes c) = \sum \mathcal{R}(a \otimes c_{(1)})\mathcal{R}(b \otimes c_{(2)})\,, \tag{A.23}$$

$$\mathcal{R}(a \otimes bc) = \sum \mathcal{R}(a_{(1)} \otimes c)\mathcal{R}(a_{(2)} \otimes b)\,, \tag{A.24}$$

$$\sum b_{(1)}a_{(1)}\mathcal{R}(a_{(2)} \otimes b_{(2)}) = \sum \mathcal{R}(a_{(1)} \otimes b_{(1)})a_{(2)}b_{(2)}\,, \quad \forall a, b, c \in A\,. \tag{A.25}$$

$(H, \mathcal{R})$ and $(A, \mathcal{R})$ are dual in the sense of the same $\mathcal{R}$-matrix and that (A.23) is the dual of (A.18), (A.24) is the dual of (A.19) and (A.25) is the dual of (A.20).

Two Hopf algebras H, A are said to form a dual pair if there is a bilinear map $\langle\,,\,\rangle : A \otimes H \to \mathbb{K}$ satisfying the conditions

$$\langle ab, h\rangle = \langle a \otimes b, \triangle(h)\rangle\,, \quad \langle \triangle(a), h \otimes g\rangle = \langle a, hg\rangle\,, \quad \langle \mathbb{I}, h\rangle = \epsilon(h)\,, \quad \langle a, \mathbb{I}\rangle = \epsilon(a)\,, \quad \forall a, b \in A\,,\ h, g \in H\,, \tag{A.26}$$

where ϵ is the counit.

We are particularly interested in a dual quasitriangular type of bialgebra which is generated by identity and the coordinate functions $T = \{t^i{}_j\}$ on the space of $n \times n$ matrices M_n. The coproduct and counit are then given by

$$\triangle(T) = T \otimes T\,, \quad \epsilon(T) = \mathbb{I}\,, \quad i.e. \quad \triangle(t^i{}_j) = \sum_k t^i{}_k \otimes t^k{}_j\,, \quad \epsilon(t^i{}_j) = \delta^i_j\,. \tag{A.27}$$

Given a Hopf algebra A of this type and an invertible $\mathcal{R}$-matrix $\mathcal{R}$, a matrix $R \in M_n \otimes M_n$ defined as

$$R = \mathcal{R}(T \otimes T)\,, \quad i.e. \quad R^{i\ k}_{\ j\ l} = \mathcal{R}(t^i{}_j \otimes t^k{}_l) \tag{A.28}$$

is invertible and satisfies the QYBE (A.22). The following relation also holds in A.

$$RT_1T_2 = T_2T_1R\,, \tag{A.29}$$

where $T_1 = T \otimes \mathbb{I}\,, T_2 = \mathbb{I} \otimes T$. Reversely, one can define a Hopf algebra $A(R)$ generated by identity and T satisfying (A.27) with R satisfying (A.29). This is called the *associated matrix Hopf algebra*, and $(A(R), \mathcal{R})$ with $\mathcal{R}$ obtained by inverting (A.28) is a dual quasitriangular Hopf algebra.

Given a dual quasitriangular Hopf algebra $(A(R), \mathcal{R})$, we want to build a quasitriangular Hopf algebra $(H, \mathcal{R})$ where H is dual paired with $A(R)$ via the bilinear map

$$\langle T \otimes T, \mathcal{R}\rangle = R\,. \tag{A.30}$$

With this bilinear map, elements $Q^{\pm} = \{(q^{\pm})^i{}_j\}$ defined by

$$Q^+ := (\mathbb{I} \otimes T)(\mathcal{R}) \equiv \sum \mathcal{R}_{(1)}\langle T, \mathcal{R}_{(2)}\rangle\,, \quad Q^- = (T \otimes \mathbb{I})(\mathcal{R}^{-1}) \equiv \sum \mathcal{R}_{(2)}\langle T, \mathcal{R}_{(1)}\rangle \tag{A.31}$$

belong to H, where we have used the notation $\mathcal{R} = \sum \mathcal{R}_{(1)} \otimes \mathcal{R}_{(2)}$. The coproduct and counit are given by

$$\triangle(Q^{\pm}) = Q^{\pm} \otimes Q^{\pm}\,, \quad \epsilon(Q^{\pm}) = \mathbb{I}\,, \quad i.e. \quad \triangle((q^{\pm})^i{}_j) = \sum_k (q^{\pm})^i{}_k \otimes (q^{\pm})^k{}_j\,, \quad \epsilon((q^{\pm}))^i = \delta^i_j\,. \tag{A.32}$$

Applying the definition (A.31) and properties of a quasitriangular Hopf algebra (A.18) and (A.19), one can show that the following relations hold in H.

$$Q_1^{\pm}Q_2^{\pm}R = RQ_2^{\pm}Q_1^{\pm}\,, \quad Q_1^-Q_2^+R = RQ_2^+Q_1^-\,, \tag{A.33}$$

where $Q_1^{\pm} = Q^{\pm} \otimes \mathbb{I}\,, Q_2^{\pm} = \mathbb{I} \otimes Q^{\pm}$. The pairing can be characterized by the bilinear form between T and $Q^{\pm}$ as

$$\langle T_1, Q_2^+\rangle = R\,, \quad \langle T_1, Q_2^-\rangle = R_{21}^{-1}\,, \quad i.e. \quad \langle t^i{}_j, (q^+)^k{}_l\rangle = R^{i\ k}_{j\ l}\,, \quad \langle t^i{}_j, (q^-)^k{}_l\rangle = (R^{-1})^{i\ k}_{j\ l}\,. \tag{A.34}$$

The classical theory described in the previous subsection is the first order limit of the quantum theory. Explicitly, the relation between the quantum $\mathcal{R}$-matrix and the classical r-matrix, and the relation between the quantum coproduct $\triangle$ and classical cocycle δ are given by

$$\mathcal{R} = \mathbb{I} \otimes \mathbb{I} + i\hbar r + O(\hbar^2)\,, \quad \triangle - \sigma \circ \triangle = i\hbar\delta + O(\hbar^2)\,. \tag{A.35}$$

Then the (dual) quasitriangular Lie bialgebra is the linear $\hbar$ order of the (dual) quasitriangular Hopf algebra, which can be seen from *e.g.* the following relations of the conditions in their definitions.

$$\begin{array}{ccc} (\triangle \otimes \mathbb{I})\mathcal{R} = \mathcal{R}_{13}\mathcal{R}_{23} & \longrightarrow & (\delta \otimes \mathbb{I})r = [r_{13}, r_{23}] \\ (\mathbb{I} \otimes \triangle)\mathcal{R} = \mathcal{R}_{13}\mathcal{R}_{12} & \longrightarrow & (\mathbb{I} \otimes \delta)r = [r_{13}, r_{12}] \\ \sigma \circ \triangle = \mathcal{R}\triangle\mathcal{R}^{-1} & \longrightarrow & \delta = \partial r \end{array} . \tag{A.36}$$

The kind of (dual) quasitriangular Hopf algebra used in the main text is the deformation $\mathcal{U}_q(\mathfrak{g})$ of a universal enveloping algebra $\mathcal{U}(\mathfrak{g})$, where $q = e^{\kappa\hbar}(\kappa \in \mathbb{R})$ is the deformation parameter and the classical limit is given by $\hbar \to 0$ thus $q \to 1$.

Appendix B

Examples and calculation details

In this appendix chapter, we collect some calculation details for the results in the main text and illustration of a toy model for the loop gravity model.

B.1 Explicit Poisson brackets for Heisenberg double $\mathrm{SL}(2,\mathbb{C})$

In this section, we give the Poisson brackets for the SU(2) holonomies $(u, \tilde{u})$ and the AN(2) fluxes $(\ell, \tilde{\ell})$ of the phase space described in Subsection 2.3.1. The Poisson brackets read

$$\begin{aligned}
&\{\ell_1, \ell_2\} = -[r_{21}, \ell_1\ell_2]\,, \quad \{\ell_1, u_2\} = -\ell_1 r_{21} u_2\,, \quad \{u_1, \ell_2\} = \ell_2 r u_1\,, \quad \{u_1, u_2\} = -[r, u_1 u_2]\,,\\
&\{\tilde{\ell}_1, \tilde{\ell}_2\} = [r_{21}, \tilde{\ell}_1\tilde{\ell}_2]\,, \quad \{\tilde{\ell}_1, \tilde{u}_2\} = -\tilde{u}_2 r_{21}\tilde{\ell}_1\,, \quad \{\tilde{u}_1, \tilde{\ell}_2\} = \tilde{u}_1 r\tilde{\ell}_2\,, \quad \{\tilde{u}_1, \tilde{u}_2\} = [r, \tilde{u}_1\tilde{u}_2]\,,\\
&\{\ell_1, \tilde{u}_2\} = -r_{21}\ell_1\tilde{u}_2\,, \quad \{\tilde{\ell}_1, u_2\} = -\tilde{\ell}_1 u_2 r_{21}\,, \quad \{u_1, \tilde{\ell}_2\} = \tilde{\ell}_2 u_1 r\,, \quad \{\tilde{u}_1, \ell_2\} = r\tilde{u}_1\ell_2\,,\\
&\{\tilde{\ell}_1, \ell_2\} = 0\,, \qquad \{\tilde{u}_1, u_2\} = 0\,.
\end{aligned} \tag{B.1}$$

It is important to note that (B.1) is not enough to describe the full Poisson structure. Notice that the $\mathfrak{an}(2)$ Lie algebra is preserved under $\ell \to (\ell^\dagger)^{-1}, \rho^i \to -(\rho^i)^\dagger$, one can

switch $r \to -r^\dagger = r_{21}$ in (B.1) and write the Poisson brackets

$$
\begin{array}{|l|l|l|}
\hline
\{\ell_1^\dagger, \ell_2\} = -\ell_1^\dagger r \ell_2 + \ell_2 r \ell_1^\dagger \,, & \{\ell_1^\dagger, \ell_2^\dagger\} = [r_{21}, \ell_1^\dagger \ell_2^\dagger] \,, & \{\ell_1^\dagger, u_2\} = -r\ell_1^\dagger u_2 \,, \\
\{\ell_1, \ell_2^\dagger\} = -\ell_1 r_{21} \ell_2^\dagger + \ell_2^\dagger r_{21} \ell_1 \,, & \{\ell_1^\dagger, \tilde{\ell}_2\} = 0 \,, & \{u_1, \ell_2^\dagger\} = r_{21} u_1 \ell_2^\dagger \,, \\
\hline
\{\ell_1^\dagger, \tilde{u}_2\} = -\ell_1^\dagger r \tilde{u}_2 \,, & \{\tilde{\ell}^\dagger, \tilde{\ell}_2\} = \tilde{\ell}_1^\dagger r \tilde{\ell}_2 - \tilde{\ell}_2 r \tilde{\ell}_1^\dagger \,, & \{\tilde{\ell}_1^\dagger, \ell_2\} = 0 \,, \\
\{\tilde{u}_1, \ell_2^\dagger\} = \ell_2^\dagger r_{21} \tilde{u}_1 \,, & \{\tilde{\ell}_1, \tilde{\ell}_2^\dagger\} = \tilde{\ell}_1 r_{21} \tilde{\ell}_2^\dagger - \tilde{\ell}_2^\dagger r_{21} \tilde{\ell}_1 \,, & \{\tilde{\ell}_1^\dagger, \tilde{\ell}_2^\dagger\} = -[r_{21}, \tilde{\ell}_1^\dagger \tilde{\ell}_2^\dagger] \,, \\
\hline
\{\tilde{\ell}_1^\dagger, u_2\} = -u_2 r \tilde{\ell}_1^\dagger \,, & \{\tilde{\ell}_1^\dagger, \tilde{u}_2\} = -\tilde{\ell}_1^\dagger \tilde{u}_2 r \,, & \\
\{u_1, \tilde{\ell}_2^\dagger\} = u_1 r_{21} \tilde{\ell}_2^\dagger \,, & \{\tilde{u}_1, \tilde{\ell}_2^\dagger\} = \tilde{u}_1 \tilde{\ell}_2^\dagger r_{21} \,. & \\
\hline
\end{array}
\tag{B.2}
$$

We parametrize them into 2×2 matrices

$$
\ell = \begin{pmatrix} \lambda & 0 \\ z & \lambda^{-1} \end{pmatrix} , \quad \tilde{\ell} = \begin{pmatrix} \tilde{\lambda} & 0 \\ \tilde{z} & \tilde{\lambda}^{-1} \end{pmatrix} , \quad u = \begin{pmatrix} \alpha & -\bar{\beta} \\ \beta & \bar{\alpha} \end{pmatrix} , \quad \tilde{u} = \begin{pmatrix} \tilde{\alpha} & -\bar{\tilde{\beta}} \\ \tilde{\beta} & \bar{\tilde{\alpha}} \end{pmatrix} , \tag{B.3}
$$

where $\lambda, \tilde{\lambda} \in \mathbb{R}^+$ and other parameters are complex. With this parametrization, the Poisson

brackets in (B.1) and (B.2) are explicitly

$$
\begin{aligned}
&\{\lambda,z\}=\tfrac{i\kappa}{2}\lambda z\,, && \{\lambda,\bar z\}=-\tfrac{i\kappa}{2}\lambda\bar z\,, && \{z,\bar z\}=i\kappa(\lambda^2-\lambda^{-2})\,,\\
&\{\alpha,\beta\}=-\tfrac{i\kappa}{2}\alpha\beta\,, && \{\alpha,\bar\beta\}=-\tfrac{i\kappa}{2}\alpha\bar\beta\,, && \{\alpha,\bar\alpha\}=i\kappa\beta\bar\beta\,,\\
&\{\bar\alpha,\beta\}=\tfrac{i\kappa}{2}\bar\alpha\beta\,, && \{\bar\alpha,\bar\beta\}=\tfrac{i\kappa}{2}\bar\alpha\bar\beta\,, && \{\beta,\bar\beta\}=0\,,\\
&\{\lambda,\alpha\}=-\tfrac{i\kappa}{4}\lambda\alpha,\,, && \{\lambda,\bar\alpha\}=\tfrac{i\kappa}{4}\lambda\bar\alpha\,, && \{\lambda,\beta\}=\tfrac{i\kappa}{4}\lambda\beta\,,\\
&\{\lambda,\bar\beta\}=-\tfrac{i\kappa}{4}\lambda\bar\beta\,, && \{z,\beta\}=\tfrac{i\kappa}{4}z\beta\,, && \{z,\bar\alpha\}=\tfrac{i\kappa}{4}z\bar\alpha\,,\\
&\{z,\alpha\}=-\tfrac{i\kappa}{4}\left(z\alpha+4\lambda^{-1}\beta\right)\,, && \{z,\bar\beta\}=-\tfrac{i\kappa}{4}\left(z\bar\beta-4\lambda^{-1}\bar\alpha\right)\,, && \{\bar z,\alpha\}=-\tfrac{i\kappa}{4}\bar z\alpha\,,\\
&\{\bar z,\bar\beta\}=-\tfrac{i\kappa}{4}\bar z\bar\beta\,, && \{\bar z,\bar\alpha\}=\tfrac{i\kappa}{4}(\bar z\bar\alpha+4\lambda^{-1}\bar\beta)\,, && \{\bar z,\beta\}=\tfrac{i\kappa}{4}(\bar z\beta-4\lambda^{-1}\alpha)\,,
\end{aligned}
$$

$$
\begin{aligned}
&\{\tilde\lambda,\tilde z\}=-\tfrac{i\kappa}{2}\tilde\lambda\tilde z\,, && \{\tilde\lambda,\bar{\tilde z}\}=\tfrac{i\kappa}{2}\tilde\lambda\bar{\tilde z}\,, && \{\tilde z,\bar{\tilde z}\}=-i\kappa(\tilde\lambda^2-\tilde\lambda^{-2})\,,\\
&\{\tilde\alpha,\tilde\beta\}=\tfrac{i\kappa}{2}\tilde\alpha\tilde\beta\,, && \{\tilde\alpha,\bar{\tilde\beta}\}=\tfrac{i\kappa}{2}\tilde\alpha\bar{\tilde\beta}\,, && \{\tilde\alpha,\bar{\tilde\alpha}\}=-i\kappa\tilde\beta\bar{\tilde\beta}\,,\\
&\{\bar{\tilde\alpha},\tilde\beta\}=-\tfrac{i\kappa}{2}\bar{\tilde\alpha}\tilde\beta\,, && \{\bar{\tilde\alpha},\bar{\tilde\beta}\}=-\tfrac{i\kappa}{2}\bar{\tilde\alpha}\bar{\tilde\beta}\,, && \{\tilde\beta,\bar{\tilde\beta}\}=0\,,\\
&\{\tilde\lambda,\tilde\alpha\}=-\tfrac{i\kappa}{4}\tilde\lambda\tilde\alpha\,, && \{\tilde\lambda,\bar{\tilde\alpha}\}=\tfrac{i\kappa}{4}\tilde\lambda\bar{\tilde\alpha}\,, && \{\tilde\lambda,\tilde\beta\}=-\tfrac{i\kappa}{4}\tilde\lambda\tilde\beta\,,\\
&\{\tilde\lambda,\bar{\tilde\beta}\}=\tfrac{i\kappa}{4}\tilde\lambda\bar{\tilde\beta}\,, && \{\tilde z,\tilde\alpha\}=\tfrac{i\kappa}{4}\tilde z\tilde\alpha\,, && \{\tilde z,\tilde\beta\}=\tfrac{i\kappa}{4}\tilde z\tilde\beta\,,\\
&\{\tilde z,\bar{\tilde\alpha}\}=-\tfrac{i\kappa}{4}(\tilde z\bar{\tilde\alpha}+4\tilde\lambda\tilde\beta)\,, && \{\tilde z,\bar{\tilde\beta}\}=-\tfrac{i\kappa}{4}(\tilde z\bar{\tilde\beta}-4\tilde\lambda\tilde\alpha)\,, && \{\bar{\tilde z},\bar{\tilde\alpha}\}=-\tfrac{i\kappa}{4}\bar{\tilde z}\bar{\tilde\alpha}\,,\\
&\{\bar{\tilde z},\bar{\tilde\beta}\}=-\tfrac{i\kappa}{4}\bar{\tilde z}\bar{\tilde\beta}\,, && \{\bar{\tilde z},\tilde\alpha\}=\tfrac{i\kappa}{4}(\bar{\tilde z}\tilde\alpha+4\tilde\lambda\bar{\tilde\beta})\,, && \{\bar{\tilde z},\tilde\beta\}=\tfrac{i\kappa}{4}(\bar{\tilde z}\tilde\beta-4\lambda\bar{\tilde\alpha})\,,
\end{aligned}
$$

$$
\begin{aligned}
&\{\lambda,\tilde\alpha\}=-\tfrac{i\kappa}{4}\lambda\tilde\alpha\,, && \{\lambda,\bar{\tilde\alpha}\}=\tfrac{i\kappa}{4}\lambda\bar{\tilde\alpha}\,, && \{\lambda,\tilde\beta\}=\tfrac{i\kappa}{4}\lambda\tilde\beta\,,\\
&\{\lambda,\bar{\tilde\beta}\}=-\tfrac{i\kappa}{4}\lambda\bar{\tilde\beta}\,, && \{z,\bar{\tilde\alpha}\}=-\tfrac{i\kappa}{4}z\bar{\tilde\alpha}\,, && \{z,\tilde\beta\}=-\tfrac{i\kappa}{4}z\tilde\beta\,,\\
&\{z,\tilde\alpha\}=\tfrac{i\kappa}{4}(z\tilde\alpha-4\lambda\tilde\beta)\,, && \{z,\bar{\tilde\beta}\}=\tfrac{i\kappa}{4}(z\bar{\tilde\beta}+4\lambda\bar{\tilde\alpha})\,, && \{\bar z,\tilde\alpha\}=\tfrac{i\kappa}{4}\bar z\tilde\alpha\,,\\
&\{\bar z,\bar{\tilde\beta}\}=\tfrac{i\kappa}{4}\bar z\bar{\tilde\beta}\,, && \{\bar z,\tilde\beta\}=-\tfrac{i\kappa}{4}(\bar z\tilde\beta+4\lambda\tilde\alpha)\,, && \{\bar z,\bar{\tilde\alpha}\}=-\tfrac{i\kappa}{4}(\bar z\bar{\tilde\alpha}-4\lambda\bar{\tilde\beta})\,,
\end{aligned}
$$

$$
\begin{aligned}
&\{\tilde\lambda,\alpha\}=-\tfrac{i\kappa}{4}\tilde\lambda\alpha\,, && \{\tilde\lambda,\bar\alpha\}=\tfrac{i\kappa}{4}\tilde\lambda\bar\alpha\,, && \{\tilde\lambda,\beta\}-\tfrac{i\kappa}{4}\tilde\lambda\beta\,,\\
&\{\tilde\lambda,\bar\beta\}=\tfrac{i\kappa}{4}\tilde\lambda\bar\beta\,, && \{\tilde z,\alpha\}=-\tfrac{i\kappa}{4}\tilde z\alpha\,, && \{\tilde z,\beta\}=-\tfrac{i\kappa}{4}\tilde z\beta\,,\\
&\{\tilde z,\bar\alpha\}=\tfrac{i\kappa}{4}(\tilde z\bar\alpha-4\tilde\lambda^{-1}\beta)\,, && \{\tilde z,\bar\beta\}=\tfrac{i\kappa}{4}(\tilde z\bar\beta+4\tilde\lambda^{-1}\alpha)\,, && \{\bar{\tilde z},\bar\beta\}=\tfrac{i\kappa}{4}\bar{\tilde z}\bar\beta\,,\\
&\{\bar{\tilde z},\bar\alpha\}=\tfrac{i\kappa}{4}\bar{\tilde z}\bar\alpha\,, && \{\bar{\tilde z},\beta\}=-\tfrac{i\kappa}{4}(\bar{\tilde z}\beta+4\tilde\lambda^{-1}\bar\alpha)\,, && \{\bar{\tilde z},\alpha\}=-\tfrac{i\kappa}{4}(\bar{\tilde z}\alpha-4\tilde\lambda^{-1}\bar\beta)\,,
\end{aligned}
\tag{B.4}
$$

and others vanish. These explicit Poisson brackets are used to check the validity of the spinor parametrization in Chapter 3.

B.2 An example: q-deformed loop gravity on a torus

In this section, we apply the q-deformed loop gravity framework described in Section 2.3, with the deformed holonomy-flux phase space provided with the $\mathrm{SL}(2,\mathbb{C})$ Poisson brackets, to the simple case of the torus. A torus is a genus-2 2D manifold thus a graph on the torus can have at most two independent non-contractable loops. We will see that those loops can be assigned the physical observables that form a Goldman bracket. The phase space can also be obtained by a gauge fixing from a fat graph following the recipe given in Section 2.4. We are not repeating the process but refer interested readers to [77].

Ribbon graph on the torus: We draw a basic graph for the 2-torus, with two links wrapping around the torus meeting at a single node and surrounding a single face as illustrated on the left panel of fig.B.1. The corresponding ribbon graph is depicted on the right panel of fig.B.1, dressed with AN(2) fluxes and SU(2) holonomies. The ribbon

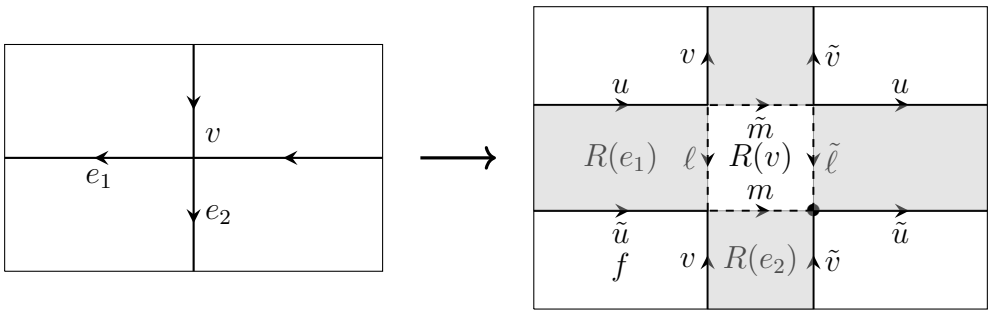

Figure B.1: The same graph as in fig.2.7 The ribbon constraints for the ribbons $R(e_1)$ and $R(e_2)$ give the relations between the AN(2) fluxes at the source and target of the ribbons: $\mathcal{R}^{(\ell)} = \ell u \tilde{\ell}^{-1} \tilde{u}^{-1} = \mathbb{I}$ and $\mathcal{R}^{(m)} = m v \tilde{m}^{-1} \tilde{v}^{-1} = \mathbb{I}$. The Gauss constraint $\mathcal{G} = m \ell \tilde{m}^{-1} \tilde{\ell}^{-1} = \mathbb{I}$ is a AN(2) flatness around the ribbon node $R(v)$ while the holonomy flatness constraint $\mathcal{F} = \tilde{u}^{-1} v u \tilde{v}^{-1} = \mathbb{I}$ is the SU(2) flatness around the face f.

graph defines four faces, noted $R(e_1)$, $R(e_2)$, $R(v)$ and f. The face $R(v)$ is a ribbon node, the face f is the face defined by the graph, while the two shaded faces, $R(e_1)$ and $R(e_2)$, are the two ribbons. The horizontal ribbon is decorated by the variables $u, \tilde{u} \in \mathrm{SU}(2)$ along the long links and $\ell, \tilde{\ell} \in \mathrm{AN}(2)$ on the short links. The vertical ribbon is decorated by the variables $v, \tilde{v} \in \mathrm{SU}(2)$ along the long links and $m, : w \in \mathrm{AN}(2)$ on the short links. The variables associated to the two ribbons, $(\ell, u, \tilde{\ell}, \tilde{u})$ and $(m, v, \tilde{m}, \tilde{v})$, Poisson-commute with each other. And each set of ribbon variables is provided with the Poisson brackets, (2.35), (2.36) and (2.38), defined above from the symplectic structure on $\mathrm{SL}(2,\mathbb{C})$ as the Heisenberg double $\mathrm{SU}(2) \bowtie \mathrm{AN}(2)$.

The ribbon constraints on the two ribbons are

$$\mathcal{R}^{(\ell)} = \ell u \tilde{\ell}^{-1} \tilde{u}^{-1} = \mathbb{I}\,, \quad \mathcal{R}^{(m)} = m v \tilde{m}^{-1} \tilde{v}^{-1} = \mathbb{I}\,. \tag{B.5}$$

The constraint algebra: The two loops around the faces $R(v)$ and f define the Gauss constraint and the SU(2) flatness constraint, which we both root at the same corner around the central node of the graph, as drawn on the right panel of fig.B.1:

$$\mathcal{G} = m \ell \tilde{m}^{-1} \tilde{\ell}^{-1} = \mathbb{I}\,, \quad \mathcal{F} = \tilde{u}^{-1} v u \tilde{v}^{-1} = \mathbb{I}\,. \tag{B.6}$$

Imposing the ribbon constraints, the Gauss and the SU(2) flatness constraints, amounts to imposing the $\mathrm{SL}(2,\mathbb{C})$ flatness around the four faces of the ribbon graph. As a consequence, the ordered oriented product of SU(2) and AN(2) group elements along any path on the ribbon graph does not depend on the path itself but simply on where it starts and ends, as for a flat connection theory.

The Poisson brackets of the closure and flatness constraints form a closed algebra and therefore define a system of first class constraints:

$$\{\mathcal{F}_1, \mathcal{G}_2\} = \mathcal{G}_2 r \mathcal{F}_1 - \mathcal{F}_1 r \mathcal{G}_2\,, \quad \{\mathcal{G}_1, \mathcal{G}_2\} = -[r_{21}, \mathcal{G}_1 \mathcal{G}_2]\,, \quad \{\mathcal{F}_1, \mathcal{F}_2\} = -[r, \mathcal{F}_1 \mathcal{F}_2]\,. \tag{B.7}$$

As described above, $\mathcal{G}$ generates the SU(2) gauge transformations and $\mathcal{F}$ generates the translational gauge transformations. We now identify Dirac observables, that Poisson-commute with both the Gauss and flatness constraints.

$\mathrm{SL}(2,\mathbb{C})$ **Holonomies and physical observables:** From the structure of the ribbon graph, it is clear that the $\mathrm{SL}(2,\mathbb{C})$ group elements running along the ribbons, and used to define the symplectic structure, $D = \ell u$ and $D' = mv$ do not start and end at the same point. It seems more natural to introduce $\mathrm{SL}(2,\mathbb{C})$ holonomies that wrap around the cycles of the torus and come back to their initial point. We introduce $\mathrm{SL}(2,\mathbb{C})$ holonomies rooted at a corner[1] around the graph node, as drawn on fig.B.2:

$$A = \tilde{\ell}^{-1} \tilde{v}\,, \qquad B = m^{-1} \tilde{u}^{-1}\,, \qquad A, B \in \mathrm{SL}(2,\mathbb{C})\,. \tag{B.8}$$

First, A and B contain all the information about the holonomy-flux variables around the ribbons (once we assume the ribbon flatness constraints). They are not the $\mathrm{SL}(2,\mathbb{C})$

[1] We could consider the $\mathrm{SL}(2,\mathbb{C})$ holonomies rooted at any corner. This would not change anything, as long as the two $\mathrm{SL}(2,\mathbb{C})$ holonomies are rooted at the point.

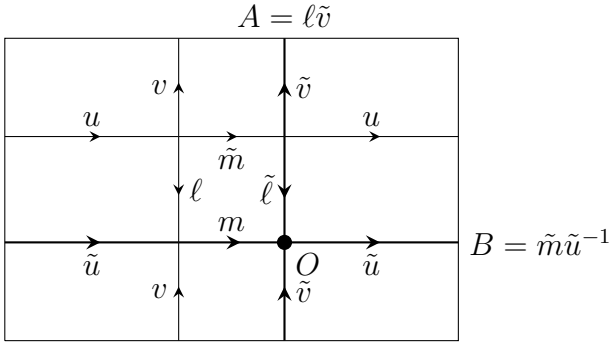

Figure B.2: $\mathrm{SL}(2,\mathbb{C})$ holonomies rooted at the node O. Having chosen the root node around the central polygon and the face for both SU(2) and AN(2) gauge transformations, these two sets of gauge transformations are combined into a single set of $\mathrm{SL}(2,\mathbb{C})$ gauge transformations. Then $\mathrm{SL}(2,\mathbb{C})$ holonomies going around loops starting and ending at that root node simply transform under the $\mathrm{SL}(2,\mathbb{C})$ action by conjugation and allow to define simple Wilson loop observables.

group elements, $D = \ell u$ and $D' = mv$, around the ribbons but mix the AN(2) fluxes and SU(2) holonomies of the different ribbons.

Second, their Poisson brackets form a closed algebra expressed in terms of the r-matrix:

$$\{A_1, A_2\} = [r_{21}, A_1 A_2]\,, \quad \{B_1, B_2\} = -[r_{21}, B_1 B_2]\,, \quad \{A_1, B_2\} = A_1 r_{21} B_2 + B_2 r A_1\,. \tag{B.9}$$

Third, the AN(2) Gauss constraint $\mathcal{G}$ and the SU(2) flatness constraint $\mathcal{F}$ can be repackaged in a single $\mathrm{SL}(2,\mathbb{C})$ flatness constraint, implying that the two $\mathrm{SL}(2,\mathbb{C})$ holonomies A and B commute:

$$\mathcal{G} = \mathcal{F} = \mathbb{I} \quad \Longleftrightarrow \quad \mathcal{C} := ABA^{-1}B^{-1} = \mathbb{I}\,. \tag{B.10}$$

This is exactly the $\mathrm{SL}(2,\mathbb{C})$ constraint for a flat $\mathrm{SL}(2,\mathbb{C})$ connection on the torus, as arising in the Chern-Simons phase space and its combinatorial quantization [7, 8]. However, due to the non-trivial braiding between AN(2) and SU(2) group elements which is reflected in the non-trivial commutator between the constraints $\mathcal{G}$ and $\mathcal{F}$, the Poisson brackets of the $\mathrm{SL}(2,\mathbb{C})$ constraint $\mathcal{C}$ have a more complicated form than the closed algebra (B.7) formed by $\mathcal{G}$ and $\mathcal{F}$:

$$\{\mathcal{C}_1, \mathcal{C}_2\} = [r_{21}, \mathcal{C}_1\mathcal{C}_2] + A_2 B_2 [r, \mathcal{C}_1] A_2^{-1} B_2^{-1} - A_1 B_1 [r_{21}, \mathcal{C}_2] A_1^{-1} B_1^{-1} \sim 0\,. \tag{B.11}$$

Finally, the two holonomies A and B are rooted at the same node. Their gauge transformations are straightforward. Under both the SU(2) gauge transformations and the

AN(2) gauge transformations for their components [77], the $\mathrm{SL}(2,\mathbb{C})$ holonomies A and B transform under the action by conjugation:

$$A, B \xmapsto{g\in \mathrm{SU}(2)} gAg^{-1},\, gBg^{-1}\,, \qquad\qquad A, B \xmapsto{b\in \mathrm{AN}(2)} bAb^{-1},\, bBb^{-1}\,. \tag{B.12}$$

Moreover, one can check that the $\mathrm{SL}(2,\mathbb{C})$ flatness constraint $ABA^{-1}B^{-1} = \mathbb{I}$, together with the Poisson brackets (B.9), generates these gauge transformations. This means that Dirac observables, invariant under both rotation and translation gauge transformations, are simply the components of A and B invariant under conjugation by $\mathrm{SL}(2,\mathbb{C})$. This leaves us with the two complex Dirac observables given by the two Wilson loops, $\mathrm{Tr}A$ and $\mathrm{Tr}B$. We can compute their Poisson bracket using the bracket $\{A_1, B_2\}$:

$$\begin{aligned}\{\mathrm{Tr}A, \mathrm{Tr}B\} &= \mathrm{Tr}\left(A_1 B_2 (r + r_{21})\right) = -2i\kappa (\mathrm{Tr}A\tau^a)\,(\mathrm{Tr}B\tau^a) \\ &= i\kappa\left(\mathrm{Tr}(AB) - \frac{1}{2}\mathrm{Tr}A\,\mathrm{Tr}B\right)\,,\end{aligned} \tag{B.13}$$

We recognize the Goldman bracket for gauge-invariant functions on the moduli space $\mathrm{Hom}(\pi, \mathrm{SL}(2,\mathbb{C}))/\mathrm{SL}(2,\mathbb{C})$, π being the fundamental group of the surface, with the bilinear map identified with (2.30) up to a constant: $\mathcal{B}(M,N) = \kappa\,\mathrm{Im}(\mathrm{Tr}(MN))$ for $M, N \in \mathfrak{sl}(2,\mathbb{C})$ [122]. This is the desired result since upon imposing constraints on all the faces A and B indeed live on the space of flat connections, thus the Wilson loops $\mathrm{Tr}A$ and $\mathrm{Tr}B$ are the projection on the corresponding moduli space.

Therefore, we have shown that the q-deformed loop gravity phase space, provided with non-abelian AN(2) Gauss constraints and SU(2) flatness constraints, can be reformulated as a phase space of discrete $\mathrm{SL}(2,\mathbb{C})$ connections with a simple Poisson bracket (B.9) and $\mathrm{SL}(2,\mathbb{C})$ flatness constraints (B.10). The physical phase space is then the moduli space of flat $\mathrm{SL}(2,\mathbb{C})$ connection with the expected Goldman bracket.

B.3 Proofs on the deformed spinors in Chapter 3 and Chapter 5

In this appendix, we collect some lengthy proofs of propositions on the classical and quantum deformed spinors in Chapter 3 and Chapter 5.

Proof B.3.1 (Proof of Proposition 3.4.1).

We prove this proposition using the following induction result of the SU(2) transformation for any function f from [40][2].

$$-\kappa^{-1}\left(\prod_{k=1}^{n}\Lambda_k^{-2}\right)\{\mathrm{Tr}W\mathcal{G}\mathcal{G}^\dagger,f\}\equiv-\kappa^{-1}\sum_{k=1}^{n}\Lambda_k^{-2}\mathrm{Tr}W^{(k+1)}\{\ell_{e_k,v}\ell^\dagger_{e_k,v},f\}\,,$$

$$\text{with}\quad\left|\begin{array}{l}W^{(k)}=-\Lambda_k^{-2}\ell^\dagger_{e_k,v}W^{(k+1)}\ell_{e_k,v}\\ W^{(n+1)}\equiv W=\begin{pmatrix}2\epsilon_z & \epsilon_-\\ \epsilon_+ & 0\end{pmatrix}\end{array}\right.\,, \tag{B.14}$$

and the Poisson brackets

$$\begin{array}{l|l}\{\Lambda_i^2,t^\epsilon_{e_iv,A}\}=(-1)^{\frac{1}{2}-A}\frac{i\kappa}{2}\Lambda_i^2t^\epsilon_{e_iv,A}\,, & \left|\begin{array}{l}\{\Lambda_{i\mathfrak{Z}i},t^\epsilon_{e_iv,-}\}=-i\kappa\Lambda_i^2t^\epsilon_{e_iv,+}\,,\\ \{\Lambda_{i\mathfrak{Z}i},t^\epsilon_{e_iv,+}\}=0\,,\\ \{\Lambda_{i\bar{\mathfrak{Z}}i},t^\epsilon_{e_iv,-}\}=0\\ \{\Lambda_{i\bar{\mathfrak{Z}}i},t^\epsilon_{e_iv,+}\}=-i\kappa\Lambda_i^2t^\epsilon_{e_iv,-}\,,\end{array}\right.\\ \{\Lambda_i^2,\tau^\epsilon_{e_iv,A}\}=(-1)^{\frac{1}{2}-A}\frac{i\kappa}{2}\Lambda_i^2\tau^\epsilon_{e_iv,A}\,, & \left|\begin{array}{l}\{\Lambda_{i\mathfrak{Z}i},\tau^\epsilon_{e_iv,-}\}=-\frac{i\kappa}{2}\Lambda_{i\mathfrak{Z}i}\tau^\epsilon_{e_iv,-}-i\kappa\tau^\epsilon_+\,,\\ \{\Lambda_{i\mathfrak{Z}i},\tau^\epsilon_{e_iv,+}\}=\frac{i\kappa}{2}\Lambda_{i\mathfrak{Z}i}\tau^\epsilon_{e_iv,+}\,,\\ \{\Lambda_{i\bar{\mathfrak{Z}}i},\tau^\epsilon_{e_iv,-}\}=-\frac{i\kappa}{2}\Lambda_{i\bar{\mathfrak{Z}}i}\tau^\epsilon_{e_iv,-}\,,\\ \{\Lambda_{i\bar{\mathfrak{Z}}i},\tau^\epsilon_{e_iv,+}\}=\frac{i\kappa}{2}\Lambda_{i\bar{\mathfrak{Z}}i}\tau^\epsilon_{e_iv,+}-i\kappa\tau^\epsilon_{e_iv,-}\,.\end{array}\right.\end{array} \tag{B.15}$$

The braided matrix $W^{(k)}$ reads explicitly

$$W^{(k)}=\begin{pmatrix}2\epsilon_z^{(k)} & \epsilon_-^{(k)}\\ \epsilon_+^{(k)} & 0\end{pmatrix} \tag{B.16}$$

where the vector components of $\vec{\epsilon}^{(k)}$ are defined inductively in (3.59) or explicitly

$$\epsilon_\pm^{(k)}=\left(\prod_{i=k}^{n}\Lambda_i^{-2}\right)\epsilon_\pm\,,\quad \epsilon_z^{(k)}=\epsilon_z+\frac{1}{2}\sum_{i=k}^{n}\left(\prod_{j=i}^{n}\Lambda_j^{-2}\right)(\epsilon_-\Lambda_{i\mathfrak{Z}i}+\epsilon_+\Lambda_{i\bar{\mathfrak{Z}}i})\,. \tag{B.17}$$

[2]We use different convention from [40] thus the expressions look different.

Expanding the right-hand side of (B.14), the SU(2) transformation for $t^{\epsilon}_{e_i v,A}$ is

$$\begin{aligned}\delta_\epsilon t^{\epsilon}_{e_i v} &= -\kappa^{-1}\Lambda_i^{-2}\left(2\epsilon_z^{(i-1)}\{\Lambda_i^2, t^{\epsilon}_{e_i v}\} + \epsilon_-^{(i+1)}\{\Lambda_i \mathfrak{z}_i, t^{\epsilon}_{e_i v}\} + \epsilon_+^{(i+1)}\{\Lambda_i \bar{\mathfrak{z}}_i, t^{\epsilon}_{e_i v}\}\right) \\ &= \begin{pmatrix} \epsilon_z^{(i+1)} & \epsilon_-^{(i+1)} \\ \epsilon_+^{(i+1)} & -\epsilon_z^{(i+1)} \end{pmatrix} t^{\epsilon}_{e_i v}\,, \end{aligned} \tag{B.18}$$

$$\begin{aligned}\delta_\epsilon \tau^{\epsilon}_{e_i v} &= -\kappa^{-1}\Lambda_i^{-2}\left(2\epsilon_z^{(i+1)}\{\Lambda_i^2, \tau^{\epsilon}_{e_i v}\} + \epsilon_-^{(i+1)}\{\Lambda_i \mathfrak{z}_i, \tau^{\epsilon}_{e_i v}\} + \epsilon_+^{(i+1)}\{\Lambda_i \bar{\mathfrak{z}}_i, \tau^{\epsilon}_{e_i v}\}\right) \\ &= \begin{pmatrix} \epsilon_z^{(i)} & \epsilon_-^{(i)} \\ \epsilon_+^{(i)} & -\epsilon_z^{(i)} \end{pmatrix} \tau^{\epsilon}_{e_i v}\,, \end{aligned} \tag{B.19}$$

where the right-hand sides of both equations above are calculated via (3.59) and (B.15). We have therefore proved (3.58). □

Proof B.3.2 (Proof of Proposition 5.4.1).

For notational convenience, we remove the tildes of the generators of $\mathcal{U}_q(\mathfrak{su}(2))$ in the tilde sector. We consider (5.49) at $n = 2$. Then from the last line,

$${}^{(2)}\widetilde{\boldsymbol{\tau}} = \begin{pmatrix} K \otimes \widetilde{\boldsymbol{\tau}}_- \\ q^{-\frac{1}{4}}(q^{\frac{1}{2}} - q^{-\frac{1}{2}})J_+ \otimes \widetilde{\boldsymbol{\tau}}_- + K^{-1} \otimes \widetilde{\boldsymbol{\tau}}_+ \end{pmatrix}. \tag{B.20}$$

We will show that the first line, *i.e.* $\mathcal{R}_{12}^{-1}(\mathbb{I} \otimes \widetilde{\boldsymbol{\tau}})\mathcal{R}_{12}$ gives the same object. By using (5.5) and (5.12) to express the generators of $\mathcal{U}_q(\mathfrak{su}(2))$ and the spinors in terms of the q-harmonic oscillators, we find

$$J_z\widetilde{\boldsymbol{\tau}}_+ = \widetilde{\boldsymbol{\tau}}_+\big(J_z + \frac{1}{2}\big), \qquad J_+\widetilde{\boldsymbol{\tau}}_+ = q^{-\frac{1}{4}}\widetilde{\boldsymbol{\tau}}_+ J_+, \qquad J_-\widetilde{\boldsymbol{\tau}}_+ = q^{-\frac{1}{4}}\big(\widetilde{\boldsymbol{\tau}}_+ J_- - K\widetilde{\boldsymbol{\tau}}_-\big) \tag{B.21}$$

and

$$J_z\widetilde{\boldsymbol{\tau}}_- = \widetilde{\boldsymbol{\tau}}_-\big(J_z - \frac{1}{2}\big), \qquad J_-\widetilde{\boldsymbol{\tau}}_- = q^{\frac{1}{4}}\widetilde{\boldsymbol{\tau}}_- J_-, \qquad J_+\widetilde{\boldsymbol{\tau}}_- = q^{\frac{1}{4}}\big(\widetilde{\boldsymbol{\tau}}_- J_+ - K\widetilde{\boldsymbol{\tau}}_+\big). \tag{B.22}$$

It leads to the commutation relations

$$[KJ_\pm, \widetilde{\boldsymbol{\tau}}_\mp] = -q^{\pm\frac{1}{4}}K^2\widetilde{\boldsymbol{\tau}}_\pm, \qquad [KJ_\pm, \widetilde{\boldsymbol{\tau}}_\pm] = 0. \tag{B.23}$$

Consider the first line of (5.49) for $A = -$, then

Let us apply these commutation relations to (5.49) for instance. Consider first $n = 2$. Use the definition (4.3) of the $\mathcal{R}$-matrix, then we can compute $\mathcal{R}_{12}^{-1}(\mathbb{I} \otimes \widetilde{\boldsymbol{\tau}}_-)$ directly.

$$
\begin{aligned}
&\mathcal{R}_{12}^{-1}(\mathbb{I} \otimes \widetilde{\boldsymbol{\tau}}_-) \\
=&q^{-J_z \otimes J_z} \sum_{n=0}^{\infty} \frac{(1-q)^n}{[n]!} q^{-\frac{n(n-1)}{4}} \left(K^{-1} J_+\right)^n \otimes (K J_-)^n \, \widetilde{\boldsymbol{\tau}}_- \\
=&q^{-J_z \otimes J_z} \sum_{n=0}^{\infty} \frac{(1-q)^n}{[n]!} q^{-\frac{n(n-1)}{4}} \left(K^{-1} J_+\right)^n \otimes \widetilde{\boldsymbol{\tau}}_- \, (K J_-)^n \\
=&q^{-J_z \otimes J_z} (\mathbb{I} \otimes \widetilde{\boldsymbol{\tau}}_-) \sum_{n=0}^{\infty} \frac{(1-q)^n}{[n]!} q^{-\frac{n(n-1)}{4}} \left(K^{-1} J_+\right)^n \otimes (K J_-)^n \\
=&(\mathbb{I} \otimes \widetilde{\boldsymbol{\tau}}_-) q^{-J_z \otimes (J_z - \frac{1}{2})} \sum_{n=0}^{\infty} \frac{(1-q)^n}{[n]!} q^{-\frac{n(n-1)}{4}} \left(K^{-1} J_+\right)^n \otimes (K J_-)^n \\
=&(K \otimes \widetilde{\boldsymbol{\tau}}_-) \mathcal{R}_{12}^{-1} \equiv (\tilde{L} \otimes \widetilde{\boldsymbol{\tau}})_- \mathcal{R}_{12}^{-1} \,,
\end{aligned}
\tag{B.24}
$$

as desired. Computing $\mathcal{R}_{12}^{-1}(\mathbb{I} \otimes \widetilde{\boldsymbol{\tau}}_+)$ takes more work as KJ_- and $\widetilde{\boldsymbol{\tau}}_+$ do not commute. Indeed, each time we put KJ_- to the right of $\widetilde{\boldsymbol{\tau}}_+$, we get an extra term $-q^{\frac{1}{2}} K^2 \widetilde{\boldsymbol{\tau}}_-$. This gives

$$
\begin{aligned}
(K J_-)^n \widetilde{\boldsymbol{\tau}}_+ &= \widetilde{\boldsymbol{\tau}}_+ (K J_-)^n - q^{-\frac{1}{4}} \sum_{k=0}^{n-1} K^2 \widetilde{\boldsymbol{\tau}}_- q^k (K J_-)^{n-1} \\
&= \widetilde{\boldsymbol{\tau}}_+ (K J_-)^n - q^{-\frac{1}{4}} \frac{1-q^n}{1-q} K^2 \widetilde{\boldsymbol{\tau}}_- (K J_-)^{n-1}
\end{aligned}
\tag{B.25}
$$

by using $J_-^k K^2 = q^k K^2 J_-^k$. We can thus write

$$
\begin{aligned}
&\mathcal{R}_{12}^{-1}(\mathbb{I}\otimes\widetilde{\boldsymbol{\tau}}_+)\\
=&q^{-J_z\otimes J_z}\,(\mathbb{I}\otimes\widetilde{\boldsymbol{\tau}}_+)\sum_{n=0}^{\infty}\frac{(1-q)^n}{[n]!}q^{-\frac{n(n-1)}{4}}\left(K^{-1}J_+\right)^n\otimes(KJ_-)^n-q^{-\frac{1}{4}}q^{-J_z\otimes J_z}\left(K^{-1}J_+\otimes K^2\widetilde{\boldsymbol{\tau}}_-\right)\\
&\sum_{n=0}^{\infty}\frac{(1-q)^{n-1}}{[n-1]!}q^{-\frac{(n-1)(n-2)}{4}}\frac{(1-q)}{[n]}q^{-\frac{(n-1)}{2}}\frac{1-q^n}{1-q}\left((K^{-1}J_+)^{n-1}\otimes(KJ_-)^{n-1}\right)\\
=&(\mathbb{I}\otimes\widetilde{\boldsymbol{\tau}}_+)\,q^{-J_z\otimes(J_z+\frac{1}{2})}\sum_{n=0}^{\infty}\frac{(1-q)^n}{[n]!}q^{-\frac{n(n-1)}{4}}\left(K^{-1}J_+\right)^n\otimes(KJ_-)^n\\
&+(q^{\frac{3}{4}}-q^{-\frac{1}{4}})\left(K^{-1}J_+\otimes K^2\widetilde{\boldsymbol{\tau}}_-\right)q^{-(J_z+1)\otimes(J_z-\frac{1}{2})}\\
&\sum_{n=1}^{\infty}\frac{(1-q)^{n-1}}{[n-1]!}q^{-\frac{(n-1)(n-2)}{4}}\left((K^{-1}J_+)^{n-1}\otimes(KJ_-)^{n-1}\right)\\
=&(K^{-1}\otimes\widetilde{\boldsymbol{\tau}}_+)\mathcal{R}_{12}^{-1}+q^{\frac{1}{2}}(q^{\frac{3}{4}}-q^{-\frac{1}{4}})\left(K^{-1}J_+K\otimes K^2\widetilde{\boldsymbol{\tau}}_-K^{-2}\right)\mathcal{R}_{12}^{-1}\\
=&\left(K^{-1}\otimes\widetilde{\boldsymbol{\tau}}_++(q^{\frac{1}{4}}-q^{-\frac{3}{4}})J_+\otimes\widetilde{\boldsymbol{\tau}}_-\right)\mathcal{R}_{12}^{-1}\equiv(\tilde{L}\otimes\widetilde{\boldsymbol{\tau}})_+\mathcal{R}_{12}^{-1}\,.
\end{aligned}
\tag{B.26}
$$

The generalization to any n is straightforward as

$$
\begin{aligned}
{}^{(n)}\widetilde{\boldsymbol{\tau}}_A&=\mathcal{R}_{n-1,n}^{-1}\mathcal{R}_{n-2,n}^{-1}\cdots\mathcal{R}_{2n}^{-1}R_{1n}^{-1}(\widetilde{\boldsymbol{\tau}}_n)_AR_{1n}\mathcal{R}_{2n}\cdots\mathcal{R}_{n-2,n}\mathcal{R}_{n-1,n}\\
&=(\tilde{L}_A{}^{A_2}\otimes\mathbb{I}\otimes\cdots)\mathcal{R}_{n-1,n}^{-1}\mathcal{R}_{n-2,n}^{-1}\cdots\mathcal{R}_{2n}^{-1}(\widetilde{\boldsymbol{\tau}}_n)_{A_2}\mathcal{R}_{2n}\cdots\mathcal{R}_{n-2,n}\mathcal{R}_{n-1,n}\\
&=(\tilde{L}_A{}^{A_2}\otimes\tilde{L}_{A_2}{}^{A_3}\otimes\mathbb{I}\otimes\cdots)\mathcal{R}_{n-1,n}^{-1}\mathcal{R}_{n-2,n}^{-1}\cdots\mathcal{R}_{3n}^{-1}(\widetilde{\boldsymbol{\tau}}_n)_{A_3}\mathcal{R}_{3n}\cdots\mathcal{R}_{n-2,n}\mathcal{R}_{n-1,n}\\
&=\cdots=\tilde{L}_A{}^{A_2}\otimes\tilde{L}_{A_2}{}^{A_3}\otimes\cdots\otimes\widetilde{\boldsymbol{\tau}}_{A_{n-1}}\otimes\mathbb{I}\otimes\cdots\,.
\end{aligned}
\tag{B.27}
$$

Therefore, we have proved (5.49). Equations (5.50)-(5.52) can be proven using the same method. Useful commutation relations are as follows.

$$
J_z^nJ_\pm=J_\pm(J_z\pm1)^n\,,\quad
\left|\begin{array}{l}
[\tilde{K}^{-1}\tilde{J}_\pm,\tilde{\mathbf{t}}_\mp^\epsilon]=-q^{\mp\frac{1}{4}}\tilde{K}^{-2}\tilde{\mathbf{t}}_\pm^\epsilon\\
[\tilde{K}^{-1}\tilde{J}_\pm,\tilde{\mathbf{t}}_\pm^\epsilon]=0\\
\tilde{K}^2\tilde{\mathbf{t}}_\mp^\epsilon=q^{\mp\frac{1}{2}}\tilde{\mathbf{t}}_\mp^\epsilon\tilde{K}^2\\
\tilde{J}_z^n\tilde{\mathbf{t}}_\mp^\epsilon=\tilde{\mathbf{t}}_\mp^\epsilon(\tilde{J}_z\mp\frac{1}{2})^n
\end{array}\right.,\quad
\left|\begin{array}{l}
[\tilde{K}\tilde{J}_\pm,\widetilde{\boldsymbol{\tau}}_\mp^\epsilon]=-q^{\pm\frac{1}{4}}\tilde{K}^2\widetilde{\boldsymbol{\tau}}_\pm^\epsilon\\
[\tilde{K}\tilde{J}_\pm,\widetilde{\boldsymbol{\tau}}_\pm^\epsilon]=0\\
\tilde{K}^2\widetilde{\boldsymbol{\tau}}_\mp^\epsilon=q^{\mp\frac{1}{2}}\widetilde{\boldsymbol{\tau}}_\mp^\epsilon\tilde{K}^2\\
\tilde{J}_z^n\widetilde{\boldsymbol{\tau}}_\mp^\epsilon=\widetilde{\boldsymbol{\tau}}_\mp^\epsilon(\tilde{J}_z\mp\frac{1}{2})^n
\end{array}\right.\,.
$$

□

B.4 Proofs of theorems in Chapter 6

Proof B.4.1 (Proof of Theorem 6.2.2.).

There are two types of terms in (6.40), whose action on spin network states is now presented. First,

$$\prod_{i=p+1}^{d+1} \mathbf{E}^{\epsilon_i,\epsilon_{i-1}}_{e_i e_{i-1}} \frac{1}{\mathbf{N}_{e_1 v_2}} \left(\prod_{i=2}^{p} \mathbf{E}^{\epsilon_i,\epsilon_{i-1}}_{e_i e_{i-1}} \frac{o_i \epsilon_i}{\mathbf{N}_{e_i v_i}} \right) |\{j_e\}\rangle = \frac{1}{[d_{k_1}]} \prod_{i=2}^{p} \frac{o_i \epsilon_i}{[d_{j_i}]}$$

$$\prod_{i=2}^{d+1} \delta_{k_i, j_i + \frac{\epsilon_i}{2}} [d_{k_i}][d_{j_i}] (-1)^{k_i + k_{i-1} + l_i} \begin{Bmatrix} k_i & k_i - \frac{\epsilon_i}{2} & \frac{1}{2} \\ k_{i-1} - \frac{\epsilon_{i-1}}{2} & k_{i-1} & l_i \end{Bmatrix}_q |\{k_i\}_{i=1,\dots,d}, \{j_e\}_{e \notin \partial f}\rangle \,, \quad \text{(B.28)}$$

where we have applied the action (6.36) of $\mathbf{E}^{\epsilon_i,\epsilon_{i-1}}_{e_i e_{i-1}}$ on the intertwiner $i_{j_{i-1} j_i l_i}$ at the node where $e_{i-1}\,, e_i$ and e_i' meet for all $i = 1, \cdots, d$. Each operator $1/\mathbf{N}_{e_i v_i}$ acts before the shift operator $\mathbf{E}^{\epsilon_i,\epsilon_{i-1}}_{e_i e_{i-1}}$ thus the result picks up a factor $1/[d_{j_i}]$. For $i = 1, \dots, d$, the spin j_i is shifted to $j_i + \frac{\epsilon_i}{2}$ after the action of $\mathbf{E}^{\epsilon_i,\epsilon_{i-1}}_{e_i e_{i-1}}$. The spins of of links not on the boundary of the face f remain unchanged. In addition, $\frac{1}{\mathbf{N}_{e_1 v_2}}$ acts after $\mathbf{E}^{\epsilon_2,\epsilon_1}_{e_2 e_1}$ thus the result picks up the factor $1/[d_{k_1}]$. As each link is incident to two nodes, the assigned spin shows up in two intertwiners thus the term $\sqrt{[d_{k_i}][d_{j_i}]}$ appears twice in the result, which gives the factor $[d_{k_i}][d_{j_i}]$. The q-$6j$ symbols and the sign factors naturally follows from (6.36).

Secondly,

$$\begin{aligned}
&\prod_{i=p+1}^{d+1} \mathbf{E}^{\epsilon_i,\epsilon_{i-1}}_{e_i e_{i-1}} \frac{1}{\mathbf{N}_{e_p v_{p+1}}} \left(\prod_{i=p+1}^{d+1} \mathbf{E}^{-\tilde{\epsilon}_i,-\tilde{\epsilon}_{i-1}}_{e_i e_{i-1}} \frac{o_i \epsilon_i}{\mathbf{N}_{e_i v_i}} \right) |\{j_e\}\rangle \\
&= \frac{1}{[d_{j_p - \frac{\tilde{\epsilon}_p}{2}}]} \prod_{i=p+1}^{d+1} \frac{o_i \epsilon_i}{[d_{j_i}]} \delta_{k_i, j_i - \frac{\tilde{\epsilon}_i}{2} + \frac{\epsilon_i}{2}} (-1)^{k_i - \frac{\epsilon_i}{2} + k_{i-1} - \frac{\epsilon_{i-1}}{2} + l_i} (-1)^{k_i + k_{i-1} + l_i} [d_{j_i - \frac{\tilde{\epsilon}_i}{2}}][d_{j_{i-1} - \frac{\tilde{\epsilon}_{i-1}}{2}}] \\
&\quad \sqrt{[d_{j_i}][d_{k_i}][d_{j_{i-1}}][d_{k_{i-1}}]} \begin{Bmatrix} k_i - \frac{\epsilon_i}{2} & j_i & \frac{1}{2} \\ j_{i-1} & k_{i-1} - \frac{\epsilon_{i-1}}{2} & l_i \end{Bmatrix}_q \begin{Bmatrix} k_i - \frac{\epsilon_i}{2} & k_i & \frac{1}{2} \\ k_{i-1} & k_{i-1} - \frac{\epsilon_{i-1}}{2} & l_i \end{Bmatrix}_q \\
&\quad |\{j_i\}_{i=1,\dots,p}, \{k_i\}_{i=p+1,\dots,d}, \{j_e\}_{e \notin \partial f}\rangle \\
&= \frac{[d_{k_p}]}{[d_{k_1}][d_{k_1 - \frac{\epsilon_1}{2}}]} \prod_{i=p+1}^{d+1} o_i \epsilon_i \delta_{k_i, j_i - \frac{\tilde{\epsilon}_i}{2} + \frac{\epsilon_i}{2}} (-1)^{k_i - \frac{\epsilon_i}{2} + k_{i-1} - \frac{\epsilon_{i-1}}{2} + l_i} (-1)^{k_i + k_{i-1} + l_i} [d_{k_i - \frac{\epsilon_i}{2}}]^2 [d_{k_i}] \\
&\begin{Bmatrix} k_i - \frac{\epsilon_i}{2} & j_i & \frac{1}{2} \\ j_{i-1} & k_{i-1} - \frac{\epsilon_{i-1}}{2} & l_i \end{Bmatrix}_q \begin{Bmatrix} k_i - \frac{\epsilon_i}{2} & k_i & \frac{1}{2} \\ k_{i-1} & k_{i-1} - \frac{\epsilon_{i-1}}{2} & l_i \end{Bmatrix}_q |\{j_i\}_{i=1,\dots,p}, \{k_i\}_{i=p+1,\dots,d}, \{j_e\}_{e \notin \partial f}\rangle \,.
\end{aligned} \quad \text{(B.29)}$$

Here, two shift operators act on each site for $i = p+1, \cdots, d+1$ and we denote $k_i = j_i - \frac{\tilde{\epsilon}_i}{2} + \frac{\epsilon_i}{2}$. The first shift operator $\mathbf{E}_{e_i e_{i-1}}^{-\tilde{\epsilon}_i, -\tilde{\epsilon}_{i-1}}$ (in the bracket) acts on the spin network state and shifts j_i and j_{i-1} to $j_i - \tilde{\epsilon}_i/2$ and $j_{i-1} - \tilde{\epsilon}_{i-1}/2$ respectively. It also gives the first q-6j symbol in the third line and the term $(-1)^{k_i - \frac{\epsilon_i}{2} + k_{i-1} - \frac{\epsilon_{i-1}}{2} + l_i} \sqrt{[d_{j_i}][d_{j_{i-1}}][d_{j_i - \frac{\tilde{\epsilon}_i}{2}}][d_{j_{i-1} - \frac{\tilde{\epsilon}_{i-1}}{2}}]}$. The result picks up a factor $1/[d_{j_i}]$ by the action of $1/\mathbf{N}_{e_i v_i}$ before the shift operator. In addition, $1/\mathbf{N}_{e_p v_{p+1}}$ acts on the spin network state after $\mathbf{E}_{e_{p+1} e_p}^{-\tilde{\epsilon}_{p+1}, -\tilde{\epsilon}_p}$ and thus brings a factor $1/[d_{j_p - \frac{\tilde{\epsilon}_p}{2}}]$. The action of the second shift operator $\mathbf{E}_{e_i e_{i-1}}^{\epsilon_i, \epsilon_{i-1}}$ shifts the spins $j_i - \tilde{\epsilon}_i/2$ and $j_{i-1} - \tilde{\epsilon}_{i-1}/2$ to k_i and k_{i-1} respectively and brings the second q-6j symbol in the third line as well as the term $(-1)^{k_i + k_{i-1} + l_i} \sqrt{[d_{k_i}][d_{k_{i-1}}][d_{k_i - \frac{\epsilon_i}{2}}][d_{k_{i-1} - \frac{\epsilon_{i-1}}{2}}]}$. Note that the spin $j_1 = k_1$ and $j_p = k_p$ are kept unchanged in the result as $\epsilon_1 = \tilde{\epsilon}_1$ and $\epsilon_p = \tilde{\epsilon}_p$. The last equality is the rearrangement of the result.

Putting them together, using the orthogonality of the spin network states, $\langle \{k_e\} | \{j_e\} \rangle \propto \prod_e \delta_{k_e, j_e}$ and eliminating the common terms

$$\frac{1}{[d_{k_1}]} \prod_{i=p+1}^{d+1} [d_{k_i - \frac{\epsilon_i}{2}}][d_{k_i}] (-1)^{k_i + k_{i-1} + l_i} \begin{Bmatrix} k_i & k_i - \frac{\epsilon_i}{2} & \frac{1}{2} \\ k_{i-1} - \frac{\epsilon_{i-1}}{2} & k_{i-1} & l_i \end{Bmatrix}_q$$

leads to the expected difference equations. □

Proof B.4.2 (Proof of Theorem 6.3.1)**.**

There are four faces involved in the move on each side. Clearly, $|\psi_i\rangle$ and $|\psi_f\rangle$ satisfy the same constraints associated to faces which are not among those four. Therefore, we can focus on the four faces involved in the move, and for symmetry reasons, we can simply look at the constraints on two faces: the face f_{12} which has e_1, e_2 in its boundary, and the face f_{14} which has e_1, e_4 in its boundary.

Face f_{12}. It has a different boundary on Γ_f and Γ_i, due to the disappearance of e_5. On Γ_i, there are constraints where $\mathbf{E}_{e_5 e_1}^{\epsilon_5, \epsilon_1}$ and $\mathbf{E}_{e_2 e_5}^{\epsilon_2, \epsilon_5}$ are both among the A-terms of the constraint (6.42). Let us denote the two reference edges (e_1 and e_k in (6.42)) e and e', which may be e_1 and/or e_2. Then the difference equations (6.42) read

$$\sum_{\{\tilde{\epsilon}\}} \Big(\prod_{\substack{e \to e' \\ \text{c.c.}}} A \Big) \sum_{\tilde{\epsilon}_5 = \pm} A_{o_5}^{\tilde{\epsilon}_5, \tilde{\epsilon}_1}(k_5, k_1, k_4) A_{o_2}^{\tilde{\epsilon}_2, \tilde{\epsilon}_5}(k_2, k_5, k_3) \psi_i \Big(k_1 - \frac{\tilde{\epsilon}_1}{2}, k_2 - \frac{\tilde{\epsilon}_2}{2}, k_3, k_4, k_5 - \frac{\tilde{\epsilon}_5}{2}, \dots \Big)$$
$$+ (-1)^{d_{12,i} - d_{ee'}} \alpha^{\epsilon_e, \epsilon_{e'}}(k_e, k_{e'}) \sum_{\{\tilde{\epsilon}\}} \Big(\prod_{\substack{e' \to e \\ \text{c.c.}}} B \Big) \psi_i(k_1, k_2, k_3, k_4, k_5, \dots) = 0, \quad \text{(B.30)}$$

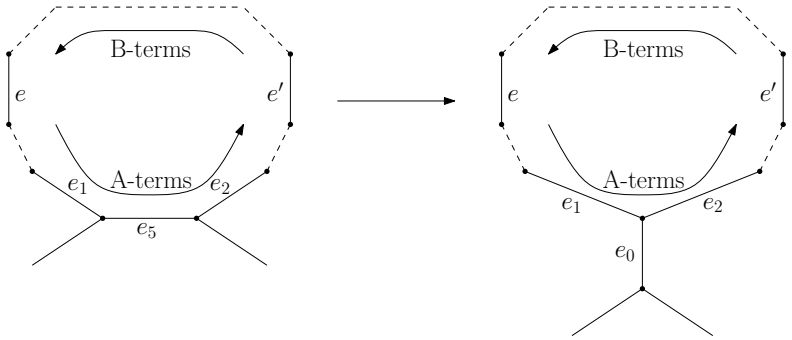

Figure B.3: A graphical representation of (B.30) on the LHS and (B.31) on the RHS.

where $d_{12,i}$ denotes the number of boundary edges of f_{12} in Γ_i and $d_{ee'}$ the number of edges from e to e' counter-clockwise. Notice that $\tilde{\epsilon}_1$ (respectively $\tilde{\epsilon}_2$) is fixed if $e = e_1$ (respectively if $e' = e_2$) and summed over otherwise. We have indicated in ψ_i only the spins which are involved in the move.

We have written $\sum_{\{\tilde{\epsilon}\}}(\prod_{e \underset{\text{c.c.}}{\to} e'} A)$ and $\sum_{\{\tilde{\epsilon}\}}(\prod_{e' \underset{\text{c.c.}}{\to} e} B)$ schematically the coefficients of the equation which are associated to corners *not* involved in the move. Here $\sum_{\{\tilde{\epsilon}\}}(\prod_{e \underset{\text{c.c.}}{\to} e'} A)$ is the product of the A-terms over the corners from e to e' going counter-clockwise, except for the two corners with e_5, whose A-terms are distinguished. Then $\sum_{\{\tilde{\epsilon}\}}(\prod_{e' \underset{\text{c.c.}}{\to} e} B)$ is the product of the B-terms over the corners from e' to e counter-clockwise. This is depicted in the Fig.B.3.

On the other hand, a state on Γ_f must also satisfy a constraint along the face f_{12} with the two reference edges e and e'. It reads

$$\langle \{k_e\}_{\Gamma_f} | \mathbf{H}_{f_{12},e,e'} | \psi_f \rangle \propto \sum_{\{\tilde{\epsilon}\}} \Big(\prod_{e \underset{\text{c.c.}}{\to} e'} A \Big) A_{o_2}^{\epsilon_2,\epsilon_1}(k_2,k_1,k_0) \psi_f\Big(k_1 - \frac{\tilde{\epsilon}_1}{2}, k_2 - \frac{\tilde{\epsilon}_2}{2}, k_3, k_4, k_0, \dots\Big)$$
$$+ (-1)^{d_{12,i}-d_{ee'}+1} \alpha^{\epsilon_e,\epsilon_{e'}}(k_e,k_{e'}) \sum_{\{\tilde{\epsilon}\}} \Big(\prod_{e' \underset{\text{c.c.}}{\to} e} B \Big) \psi_f(k_1,k_2,k_3,k_4,k_0,\dots). \quad \text{(B.31)}$$

There is also a constraint where $\mathbf{E}_{e_1 e_2}^{\tilde{\epsilon}_1,\tilde{\epsilon}_2}$ gives rise to a B-term, but as we have shown this is equivalent to the above constraint. Here it is important that the products of the A-terms and B-terms over all corners except the one where e_1 and e_2 meet are the same as in (B.30). The reason is obviously that those terms are local and the 2-2 move does not involve their corners. As in (B.30), $\tilde{\epsilon}_1$ and $\tilde{\epsilon}_2$ may be fixed or summed over.

We now plug (6.51) into (B.31) to check that it vanishes, provided the constraint (B.30) holds. First compute, with $j_{1,2} := k_{1,2} - \frac{\tilde{\epsilon}_{1,2}}{2}$,

$$A_{o_2}^{\tilde{\epsilon}_2,\tilde{\epsilon}_1}(k_2,k_1,k_0)\psi_f(j_1,j_2,k_3,k_4,k_0,\dots)$$
$$= o_2\tilde{\epsilon}_2[d_{k_2}][d_{k_0}]\sum_{j_5}(-1)^{(1-o_5)j_5+(1-o_0)k_0}(-1)^{j_1+j_2+k_3+k_4}(-1)^{k_0+k_1+k_2}$$
$$\begin{Bmatrix} k_1 & j_1 & \frac{1}{2} \\ j_2 & k_2 & k_0 \end{Bmatrix}_q \begin{Bmatrix} j_1 & j_2 & k_0 \\ k_3 & k_4 & j_5 \end{Bmatrix}_q \psi_i(j_1,j_2,k_3,k_4,j_5,\dots)\,. \quad \text{(B.32)}$$

The Biedenharn-Elliott identity on q-6j symbols gives precisely

$$(-1)^{j_1+j_2+k_3+k_4}(-1)^{k_0+k_1+k_2}\begin{Bmatrix} k_1 & j_1 & \frac{1}{2} \\ j_2 & k_2 & k_0 \end{Bmatrix}_q \begin{Bmatrix} j_1 & j_2 & k_0 \\ k_3 & k_4 & j_5 \end{Bmatrix}_q$$
$$= \sum_{k_5}[d_{k_5}](-1)^{k_5+j_5+\frac{1}{2}}\begin{Bmatrix} k_1 & k_2 & k_0 \\ k_3 & k_4 & k_5 \end{Bmatrix}_q \begin{Bmatrix} k_1 & j_1 & \frac{1}{2} \\ j_5 & k_5 & k_4 \end{Bmatrix}_q \begin{Bmatrix} k_5 & j_5 & \frac{1}{2} \\ j_2 & k_2 & k_3 \end{Bmatrix}_q\,. \quad \text{(B.33)}$$

Setting $j_5 = k_5 - \frac{\tilde{\epsilon}_5}{2}$ to change the summation over j_5 to one over $\tilde{\epsilon}_5$ (there are no other values of j_5 allowed by the triangular inequalities on the q-6j symbol), we get

$$A_{o_2}^{\epsilon_2,\epsilon_1}(k_2,k_1,k_0)\psi_f(j_1,j_2,k_3,k_4,k_0,\dots) = o_2\epsilon_2[d_{k_2}][d_{k_0}]\sum_{k_5,\tilde{\epsilon}_5}(-1)^{(1-o_5)j_5+(1-o_0)k_0}(-1)^{k_5+j_5+\frac{1}{2}}$$
$$[d_{k_5}]\begin{Bmatrix} k_1 & k_2 & k_0 \\ k_3 & k_4 & k_5 \end{Bmatrix}_q \begin{Bmatrix} k_1 & j_1 & \frac{1}{2} \\ j_5 & k_5 & k_4 \end{Bmatrix}_q \begin{Bmatrix} k_5 & j_5 & \frac{1}{2} \\ j_2 & k_2 & k_3 \end{Bmatrix}_q \psi_i(j_1,j_2,k_3,k_4,j_5,\dots)\,. \quad \text{(B.34)}$$

Using $\epsilon_5 = (-1)^{\frac{1}{2}+j_5-k_5}$, we find $(-1)^{k_5+j_5+\frac{1}{2}} = \epsilon_5(-1)^{2k_5}$. We also use $(-1)^{(1-o_5)j_5} = o_5(-1)^{(1-o_5)k_5}$ and notice that a q-6j symbol can be factored. Thus,

$$\langle\{k_e\}_{\Gamma_f}|\mathbf{H}_{f_{12},e,e'}|\psi_f\rangle \propto \sum_{k_5,\tilde{\epsilon}_5}(-1)^{(1-o_5)k_5+(1-o_0)k_0}(-1)^{k_1+k_2+k_3+k_4}\begin{Bmatrix} k_1 & k_2 & k_0 \\ k_3 & k_4 & k_5 \end{Bmatrix}_q [d_{k_0}]$$
$$\Bigg(\sum_{\{\tilde{\epsilon}\}}\Big(\prod_{\substack{e\to e' \\ \text{c.c.}}} A\Big)o_5\epsilon_5[d_{k_5}](-1)^{2k_5}(-1)^{k_1+k_2+k_3+k_4}o_2\epsilon_2[d_{k_2}]\begin{Bmatrix} k_1 & j_1 & \frac{1}{2} \\ j_5 & k_5 & k_4 \end{Bmatrix}_q \begin{Bmatrix} k_5 & j_5 & \frac{1}{2} \\ j_2 & k_2 & k_3 \end{Bmatrix}_q$$
$$\psi_i(j_1,j_2,k_3,k_4,j_5,\dots) + (-1)^{d_{12,i}-d_{ee'}}\alpha^{\epsilon_e,\epsilon_{e'}}(k_e,k_{e'})\sum_{\{\tilde{\epsilon}\}}\Big(\prod_{\substack{e'\to e \\ \text{c.c.}}} B\Big)\psi_i(k_1,k_2,k_3,k_4,k_5,\dots)\Bigg)\,. \quad \text{(B.35)}$$

We now recognize the coefficients in (B.30),

$$\langle\{k_e\}_{\Gamma_f}|\mathbf{H}_{f_{12},e,e'}|\psi_f\rangle \propto \sum_{k_5}(-1)^{(1-o_5)k_5+(1-o_0)k_0}(-1)^{k_1+k_2+k_3+k_4}\begin{Bmatrix}k_1 & k_2 & k_0\\ k_3 & k_4 & k_5\end{Bmatrix}_q [d_{k_0}]$$
$$\Bigg(\sum_{\{\tilde\epsilon\}}\Big(\prod_{\substack{e\to e'\\ \text{c.c.}}} A\Big)\sum_{\tilde\epsilon_5=\pm} A^{\tilde\epsilon_5,\tilde\epsilon_1}_{o_5}(k_5,k_1,k_4)A^{\tilde\epsilon_2,\tilde\epsilon_5}_{o_2}(k_2,k_5,k_3)\psi_i(j_1,j_2,k_3,k_4,j_5,\dots)$$
$$+(-1)^{d_{12,i}-d_{ee'}}\alpha^{\epsilon_e,\epsilon_{e'}}(k_e,k_{e'})\sum_{\{\tilde\epsilon\}}\Big(\prod_{\substack{e'\to e\\ \text{c.c.}}} B\Big)\psi_i(k_1,k_2,k_3,k_4,k_5,\dots)\Bigg), \quad \text{(B.36)}$$

and conclude that (B.31) vanished provided (B.30) and (6.51).

Face f_{14}. We now perform the same analysis on the constraints which act on the face f_{14}. We use the same notation as for the face f_{12}, *i.e.* let e and e' be two reference edges around f_{14} and consider the Hamiltonian constraints associated to them on Γ_i and Γ_f. On Γ_i, the Hamiltonians contain the operator $\mathbf{E}^{\epsilon_1,\epsilon_4}_{e_1e_4}$, which without loss of generality can be considered to give rise to an A-term. The constraints on the spin network coefficients of $|\psi_i\rangle$ read

$$\sum_{\{\tilde\epsilon\}}\Big(\prod_{\substack{e\to e'\\ \text{c.c.}}} A\Big)A^{\tilde\epsilon_1,\tilde\epsilon_4}_{o_1}(k_1,k_4,k_5)\psi_i(j_1,k_2,k_3,j_4,k_5,\dots)$$
$$+(-1)^{d_{14,i}-d_{ee'}}\alpha^{\epsilon_e,\epsilon_{e'}}(k_e,k_{e'})\sum_{\{\tilde\epsilon\}}\Big(\prod_{\substack{e'\to e\\ \text{c.c.}}} B\Big)\psi_i(k_1,k_2,k_3,k_4,k_5,\dots)=0, \quad \text{(B.37)}$$

with $j_1 = k_1 - \tilde\epsilon_1/2, j_4 = k_4 - \tilde\epsilon_4/2$. The sign $\tilde\epsilon_1$ (respectively $\tilde\epsilon_4$) is fixed if $e = e_1$ (respectively if $e' = e_4$) and summed over otherwise. Here, $\prod_{\substack{e\to e'\\ \text{c.c.}}} A$ is the product of the A-terms from e to e' counter-clockwise, except for the one on the corner of e_1, e_4 which has been singled out. As for $\prod_{\substack{e'\to e\\ \text{c.c.}}} B$, it is the product of the B-terms going counter-clockwise from e' to e.

On Γ_f, we need to look at two types of constraints. Either the operators $\mathbf{E}^{\tilde\epsilon_0,\tilde\epsilon_4}_{e_0e_4}$ and $\mathbf{E}^{\tilde\epsilon_1,\tilde\epsilon_0}_{e_1e_0}$ which enter $\mathbf{H}_{f_{14},e,e'}$ on Γ_f both contribute to A-terms of the constraint (or both to B-terms but this is the same), or one gives rise to an A-term and the other one to a B-term.

In case they both give rise to A-terms, we are in the same situation as in our previous analysis on the face f_{12}, with the role of Γ_i and Γ_f exchanged. Since the relation (6.51) between $|\psi_f\rangle$ and $|\psi_i\rangle$ can be inverted with the same form, we have nothing to prove.

If $\mathbf{E}^{\tilde\epsilon_0,\tilde\epsilon_4}_{e_0e_4}$ contributes to a B-term, and $\mathbf{E}^{\tilde\epsilon_1,\tilde\epsilon_0}_{e_1e_0}$ contributes to an A-term, this means that $e_0 = e$ is a reference edge chosen for the constraint. The Hamiltonians of this type on Γ_f are $\mathbf{H}^{\epsilon_0,\epsilon_{e'},\dots,\epsilon_4}_{f_{14},e_0,e'}$ and they are labeled by signs for all the edges from e' to e_0 counter-clockwise. The matrix elements read

$$\langle\{k_e\}_{\Gamma_f}|\mathbf{H}^{\epsilon_0,\epsilon_{e'},\dots,\epsilon_4}_{f_{14},e_0,e'}|\psi_f\rangle \propto \sum_{\{\tilde\epsilon\}}\Big(\prod_{\substack{e_1\to e'\\ \text{c.c.}}} A\Big)A^{\tilde\epsilon_1,\epsilon_0}_{o_1}(k_1,k_0,k_2)\psi_f(j_1,k_2,k_3,j_4,j_0,\dots)$$
$$+(-1)^{d_{14,f}-d_{e_0e'}}\alpha^{\epsilon_0,\epsilon_{e'}}(k_0,k_{e'})\sum_{\{\tilde\epsilon\}}\Big(\prod_{\substack{e'\to e_4\\ \text{c.c.}}} B\Big)B^{\epsilon_0,\tilde\epsilon_4}_{o_0}(j_0,j_4,k_3)\psi_f(k_1,k_2,k_3,l_4,k_0,\dots)\,, \quad \text{(B.38)}$$

where ϵ_0 is fixed (but $\tilde\epsilon_4$ only is if $e' = e_4$) and $j_{0,4} = k_{0,4} - \epsilon_{0,4}/2$, and $l_4 = j_4 + \tilde\epsilon_4/2$.

We now plug (6.51) into the above matrix elements. We first look at the A-term,

$$A^{\epsilon_1,\epsilon_0}_{o_1}(k_1,k_0,k_2)\psi_f(j_1,k_2,k_3,j_4,j_0,\dots) = [d_{j_0}]\sum_{k_5} o_1\epsilon_1[d_{k_1}](-1)^{(1-o_5)k_5+(1-o_0)j_0}$$
$$(-1)^{k_0+k_1+k_2}(-1)^{j_1+k_2+k_3+j_4}\begin{Bmatrix} j_1 & k_2 & j_0\\ k_3 & j_4 & k_5\end{Bmatrix}_q\begin{Bmatrix} k_1 & j_1 & \frac12\\ j_0 & k_0 & k_2\end{Bmatrix}_q\psi_i(j_1,k_2,k_3,j_4,k_5,\dots). \quad \text{(B.39)}$$

The relevant Biedenharn-Elliott identity is

$$(-1)^{k_0+k_1+k_2+j_0+j_1+k_3+k_5}\begin{Bmatrix} j_1 & k_2 & j_0\\ k_3 & j_4 & k_5\end{Bmatrix}_q\begin{Bmatrix} k_1 & j_1 & \frac12\\ j_0 & k_0 & k_2\end{Bmatrix}_q$$
$$=\sum_{l_4}[d_{l_4}](-1)^{j_4+l_4+\frac12}\begin{Bmatrix} j_4 & l_4 & \frac12\\ k_1 & j_1 & k_5\end{Bmatrix}_q\begin{Bmatrix} j_4 & l_4 & \frac12\\ k_0 & j_0 & k_3\end{Bmatrix}_q\begin{Bmatrix} k_1 & k_2 & k_0\\ k_3 & l_4 & k_5\end{Bmatrix}_q. \quad \text{(B.40)}$$

As for the B-term,

$$\sum_{l_4} B^{\epsilon_0,\tilde\epsilon_4}_{o_0}(j_0,j_4,k_3)\psi_f(k_1,k_2,k_3,l_4,k_0,\dots) = \sum_{k_5,l_4} o_0\epsilon_0[d_{j_0}][d_{k_0}](-1)^{j_0+k_3+j_4}$$
$$(-1)^{(1-o_5)k_5+(1-o_0)k_0}(-1)^{k_1+k_2+k_3+l_4}\begin{Bmatrix} j_4 & l_4 & \frac12\\ k_0 & j_0 & k_3\end{Bmatrix}_q\begin{Bmatrix} k_1 & k_2 & k_0\\ k_3 & l_4 & k_5\end{Bmatrix}_q\psi_i(k_1,k_2,k_3,l_4,k_5,\dots). \quad \text{(B.41)}$$

We recognize the two same q-6j symbols as in the Biendenharn-Elliott identity above. We can thus factor them out, so that the matrix elements of the Hamiltonian are proportional to

$$\begin{aligned}\langle\{k_e\}_{\Gamma_f}|\mathbf{H}^{\epsilon_0,\epsilon_{e'},\dots,\epsilon_4}_{f_{14},e_0,e'}|\psi_f\rangle \propto \sum_{k_5,l_4}(-1)^{j_0+k_3+j_4}(-1)^{(1-o_5)k_5+(1-o_0)k_0}\begin{Bmatrix} j_4 & l_4 & \frac{1}{2}\\ k_0 & j_0 & k_3\end{Bmatrix}_q\\ (-1)^{k_1+k_2+k_3+l_4}\begin{Bmatrix} k_1 & k_2 & k_0\\ k_3 & l_4 & k_5\end{Bmatrix}_q [d_{j_0}]\Bigg(\sum_{\{\tilde\epsilon\}}\Big(\prod_{e_1\underset{\text{c.c.}}{\to}e'}A\Big)o_0o_1\epsilon_1[d_{k_1}][d_{l_4}](-1)^{k_2+j_4-j_0-k_5}\\ (-1)^{j_4+l_4+\frac{1}{2}}(-1)^{j_0+k_3+j_4}(-1)^{k_1+k_2+k_3+l_4}\begin{Bmatrix} j_4 & l_4 & \frac{1}{2}\\ k_1 & j_1 & k_5\end{Bmatrix}_q \times\psi_i(j_1,k_2,k_3,j_4,k_5,\dots)\\ +(-1)^{d_{14,f}-d_{e_0e'}}\alpha^{\epsilon_0,\epsilon_{e'}}(k_0,k_{e'})\sum_{\{\tilde\epsilon\}}\Big(\prod_{e'\underset{\text{c.c.}}{\to}e_4}B\Big)o_0\epsilon_0[d_{k_0}]\psi_i(k_1,k_2,k_3,l_4,k_5,\dots)\Bigg)\end{aligned}\tag{B.42}$$

It now suffices to show that the expression into brackets vanishes thanks to (B.37). Let us take care of the signs:

$$\begin{aligned}(-1)^{k_2+j_4-j_0-k_5}(-1)^{j_4+l_4+\frac{1}{2}}(-1)^{j_0+k_3+j_4}(-1)^{k_1+k_2+k_3+l_4}\\ =(-1)^{2(k_2-k_5+k_3)}(-1)^{4j_4}(-1)^{\frac{1+\tilde\epsilon_4}{2}}(-1)^{k_1+l_4+k_5}=-\tilde\epsilon_4(-1)^{k_1+l_4+k_5}\,.\end{aligned}$$

Replace the sign factor in the bracket, we get

$$\begin{aligned}-\sum_{\{\tilde\epsilon\}}\Big(\prod_{e_1\underset{\text{c.c.}}{\to}e'}A\Big)o_0o_1\epsilon_1[d_{k_1}][d_{l_4}](-1)^{j_1-k_1+j_4-l_4}(-1)^{j_1+l_4+k_5+\frac{1}{2}}\begin{Bmatrix} j_4 & l_4 & \frac{1}{2}\\ k_1 & j_1 & k_5\end{Bmatrix}_q\\ \psi_i(j_1,k_2,k_3,j_4,k_5,\dots)+(-1)^{d_{14,f}-d_{e_0e'}}\alpha^{\epsilon_0,\epsilon_{e'}}(k_0,k_{e'})\sum_{\{\tilde\epsilon\}}\Big(\prod_{e'\underset{\text{c.c.}}{\to}e_4}B\Big)o_0\epsilon_0[d_{k_0}]\end{aligned}$$

$$\begin{aligned}\psi_i(k_1,k_2,k_3,l_4,k_5,\dots)=-o_0\tilde\epsilon_4[d_{l_4}]\Bigg(\sum_{\{\tilde\epsilon\}}\Big(\prod_{e_1\underset{\text{c.c.}}{\to}e'}A\Big)A^{\epsilon_1,\tilde\epsilon_4}_{o_1}(k_1,l_4,k_5)\psi_i(j_1,k_2,k_3,j_4,k_5,\dots)\\ +(-1)^{d_{14,i}-d_{e_4e'}}\alpha^{\tilde\epsilon_4,\epsilon_{e'}}(l_4,k_{e'})\sum_{\{\tilde\epsilon\}}\Big(\prod_{e'\underset{\text{c.c.}}{\to}e_4}B\Big)\psi_i(k_1,k_2,k_3,l_4,k_5,\dots)\Bigg).\end{aligned}\tag{B.43}$$

The expression into brackets on the RHS is exactly the constraint (B.37) on Γ_i with the choice $e=e_4$ of reference edge and arbitrary $\tilde\epsilon_4$ fixed. □

Proof B.4.3 (Proof of Theorem 6.3.2)**.**

Consider two reference edges e, e' in $F \cup f$, and the associated constraint such that $\mathbf{E}^{\tilde{\epsilon}_1,\tilde{\epsilon}_2}_{e_1 e_2}$ is an A-term (without loss of generality since A- and B-terms can be exchanged). Its matrix elements $\langle\{k_e\}|\mathbf{H}_{F\cup f,e,e'}|\psi_f\rangle$ read

$$\langle\{k_e\}|\mathbf{H}_{F\cup f,e,e'}|\psi_f\rangle \propto \sum_{\{\tilde{\epsilon}\}} \Big(\prod_{\substack{e\to e'\\ \text{c.c.}}} A\Big) A^{\tilde{\epsilon}_2,\tilde{\epsilon}_1}_{o_2}(k_2,k_1,l_2)\psi_f(j_1,j_2,\dots) + (-1)^{d_f-d_{ee'}}\alpha^{\epsilon_e,\epsilon_{e'}}(k_e,k_{e'})\sum_{\{\tilde{\epsilon}\}}\Big(\prod_{\substack{e'\to e\\ \text{c.c.}}} B\Big)\psi_f(k_1,k_2,\dots), \quad \text{(B.44)}$$

with $j_{1,2} = k_{1,2} - \tilde{\epsilon}_{1,2}/2$, and d_f denotes the number of boundary edges surrounding $F \cup f$. Here, $\prod_{\substack{e\to e'\\ \text{c.c.}}} A$ is the product of the A-terms from e to e' counter-clockwise, except for the one on the corner of e_1, e_2 which has been singled out. We will show those matrix elements vanish as soon as the constraints on f and on F are both satisfied on $|\psi_i\rangle$, given (6.55).

On f, we have the constraint, for fixed ϵ_1, ϵ_2, and $j_{1,2} = k_{1,2} - \epsilon_{1,2}/2$,

$$\begin{aligned} &B^{-\epsilon_2,-\epsilon_1}_{o_2}(k_2,k_1,l_2)\psi_i(k_0,j_1,j_2,k_3,k_4,\dots)\\ &= \alpha^{\epsilon_1,\epsilon_2}(k_1,k_2)\sum_{\epsilon_0=\pm} A^{\epsilon_0,-\epsilon_2}_{o_{0,f}}(k_0,j_2,k_3)A^{-\epsilon_1,\epsilon_0}_{o_1}(j_1,k_0,k_4)\psi_i(k_0-\frac{\epsilon_0}{2},k_1,k_2,k_3,k_4,\dots), \end{aligned} \quad \text{(B.45)}$$

where $o_{0,f}$ is the orientation of e_0 relative to f. On F there is a constraint similar to (B.44), from the Hamiltonians $\mathbf{H}_{F,e,e'}$ with the same signs ϵs. It reads,

$$\begin{aligned} \sum_{\{\tilde{\epsilon}\}}\Big(\prod_{\substack{e\to e'\\ \text{c.c.}}} A\Big)\sum_{\tilde{\epsilon}_0=\pm} &A^{\tilde{\epsilon}_0,\tilde{\epsilon}_4}_{o_{0,F}}(k_0,k_4+\frac{\tilde{\epsilon}_4}{2},k_1)A^{\tilde{\epsilon}_3,\tilde{\epsilon}_0}_{o_3}(k_3+\frac{\tilde{\epsilon}_3}{2},k_0,k_2)\\ &\psi_i(k_0-\frac{\tilde{\epsilon}_0}{2},k_1,k_2,k_3-\frac{\tilde{\epsilon}_3}{2},k_4-\frac{\tilde{\epsilon}_4}{2},\dots)\\ &+(-1)^{d_f-d_{ee'}}\alpha^{\epsilon_e,\epsilon_{e'}}(k_e,k_{e'})\sum_{\{\tilde{\epsilon}\}}\Big(\prod_{\substack{e'\to e\\ \text{c.c.}}} B\Big)\psi_i(k_0,k_1,k_2,k_3,k_4,\dots)=0\,, \end{aligned} \quad \text{(B.46)}$$

where $o_{0,F}$ is the orientation of e_0 as the boundary of F, which is opposite to $o_{0,f}$. Here $\tilde{\epsilon}_4$ (respectively $\tilde{\epsilon}_3$) is fixed if $e = e_4$ (respectively if $e' = e_3$) and summed over otherwise.

We now specialise (B.45) and (B.46) to $k_0 = 0$, where they simplify a lot. First, that enforces $\epsilon_0 = -$ in (B.45) and $\tilde{\epsilon}_0 = -$ in (B.46), so that those sums reduce to a single term.

In (B.46) we further take $k_3 = k_2$ and $k_4 = k_1$. All q-6j-symbols with a spin equal to 0 can be evaluated as $\left\{ \begin{smallmatrix} j_1 & k_1 & \frac{1}{2} \\ \frac{1}{2} & 0 & k_4 \end{smallmatrix} \right\}_q = \delta_{j_1,k_4}(-1)^{j_1+k_1+\frac{1}{2}}/\sqrt{[2][d_{j_1}]}$.

As a consequence, (B.45) gives

$$B_{o_2}^{-\epsilon_2,-\epsilon_1}(k_2,k_1,l_2)\psi_i(0,j_1,j_2,j_2,j_1,\dots) \\ = -\alpha^{\epsilon_1,\epsilon_2}(k_1,k_2)o_{0,f}o_1\epsilon_2\frac{[d_{j_1}]}{[2]\sqrt{[d_{j_1}][d_{j_2}]}}\psi_i(\frac{1}{2},k_1,k_2,j_2,j_1,\dots), \quad \text{(B.47)}$$

where $k_3 = j_2$ and $k_4 = j_1$ on the last term is enforced by the special evaluations of the q-6j-symbols with a spin 0. (B.46) gives

$$\sum_{\{\tilde{\epsilon}\}}\Big(\prod_{\substack{e\to e'\\ \text{c.c.}}} A\Big)o_{0,f}o_3\epsilon_1\frac{[d_{k_2}]}{[2]\sqrt{[d_{k_1}][d_{k_2}]}}\psi_i(\frac{1}{2},k_1,k_2,j_2,j_1,\dots) \\ + (-1)^{d_f-d_{ee'}}\alpha^{\epsilon_e,\epsilon_{e'}}(k_e,k_{e'})\sum_{\{\tilde{\epsilon}\}}\Big(\prod_{\substack{e'\to e\\ \text{c.c.}}} B\Big)\psi_i(0,k_1,k_2,k_2,k_1,\dots) = 0\,. \quad \text{(B.48)}$$

The term $\psi_i(\frac{1}{2},k_1,k_2,j_2,j_1,\dots)$ can be eliminated using (B.47). Moreover we turn the B-coefficient of this equation into an A-coefficient using $-A_{o_2}^{\epsilon_2,\epsilon_1}(k_2,k_1,l_2) = B_{o_2}^{-\epsilon_2,-\epsilon_1}(k_2,k_1,l_2)$. It is then enough to recognize ψ_f as given in (6.55) to obtain that (B.44) vanishes.

□

Proof B.4.4 (Proof of Theorem 6.3.3)**.**

Let us write the constraints on the triangular face. There is one constraint for each pair of edges of the boundary. For the pair (e_2,e_6), for instance, one gets

$$\sum_{\epsilon_1=\pm} A_{o_1}^{\epsilon_1,\epsilon_2}(k_1,k_2,k_3)A_{o_6}^{\epsilon_6,\epsilon_1}(k_6,k_1,k_5)\psi_i(j_1,j_2,k_3,k_4,k_5,j_6,\dots) \\ + \alpha^{\epsilon_2,\epsilon_6}(k_2,k_6)B_{o_2}^{\epsilon_2,\epsilon_6}(j_2,j_6,k_4)\psi_i(k_1,k_2,k_3,k_4,k_5,k_6,\dots) = 0\,. \quad \text{(B.49)}$$

Here $j_i = k_i - \epsilon_i/2$, for $i = 1,2,6$. The coefficients are

$$A_{o_1}^{\epsilon_1,\epsilon_2}(k_1,k_2,k_3) = o_1\epsilon_1[d_{k_1}](-1)^{k_1+k_2+k_3}\begin{Bmatrix} k_1 & j_1 & \frac{1}{2} \\ j_2 & k_2 & k_3 \end{Bmatrix}_q, \\ A_{o_6}^{\epsilon_6,\epsilon_1}(k_6,k_1,k_5) = o_6\epsilon_6[d_{k_6}](-1)^{k_1+k_5+k_6}\begin{Bmatrix} k_6 & j_6 & \frac{1}{2} \\ j_1 & k_1 & k_5 \end{Bmatrix}_q, \quad \text{(B.50)} \\ B_{o_2}^{\epsilon_2,\epsilon_6}(j_2,j_6,k_4) = o_2\epsilon_2[d_{j_2}](-1)^{j_2+k_4+j_6}\begin{Bmatrix} k_6 & j_6 & \frac{1}{2} \\ j_2 & k_2 & k_4 \end{Bmatrix}_q.$$

We thus have the recursion

$$\sum_{\epsilon_1=\pm} o_1 o_2 o_6 [d_{k_1}] (-1)^{2k_1+k_2+k_3+k_5+k_6+\frac{1-\epsilon_1}{2}+\frac{\epsilon_2}{2}+\frac{\epsilon_6}{2}} \begin{Bmatrix} k_1 & j_1 & \frac{1}{2} \\ j_2 & k_2 & k_3 \end{Bmatrix}_q \begin{Bmatrix} k_6 & j_6 & \frac{1}{2} \\ j_1 & k_1 & k_5 \end{Bmatrix}_q$$
$$\psi_i(j_1, j_2, k_3, k_4, k_5, j_6, \dots) + (-1)^{k_2+k_4+k_6} \begin{Bmatrix} k_6 & j_6 & \frac{1}{2} \\ j_2 & k_2 & k_4 \end{Bmatrix}_q \psi_i(k_1, k_2, k_3, k_4, k_5, k_6, \dots) = 0, \tag{B.51}$$

and similarly for the pairs (e_1, e_2), (e_6, e_1). A similar result for the flat case was found in [44], where q is set to 1. Those recursions determine the dependence of ψ_i on j_1, j_2, j_6 up to a single initial condition. As the recursion involve three terms, it may seem like several initial conditions are required. However, at $k_1 = 0$, only two terms are left in the recursion, as shown in (B.47). This means that from the initial condition $\psi_i(0, k_3, k_3, k_4, k_5, k_5)$, one gets $\psi_i(\frac{1}{2}, k_3 - \epsilon_2/2, k_3, k_4, k_5, k_5 - \epsilon_6/2)$. Then this determines ψ_i for arbitrary k_1, k_2, k_6. The result is known to be

$$\psi_i(k_1, k_2, k_3, k_4, k_5, k_6, \dots) = \begin{Bmatrix} k_1 & k_2 & k_3 \\ k_4 & k_5 & k_6 \end{Bmatrix}_q \phi(k_3, k_4, k_5, \dots), \tag{B.52}$$

where $\phi(k_3, k_4, k_5, \dots)$ is independent of k_1, k_2, k_6. To determine ϕ, we set $k_1 = 0$,

$$\begin{aligned} \phi(k_3, k_4, k_5, \dots) &= \begin{Bmatrix} 0 & k_3 & k_3 \\ k_4 & k_5 & k_5 \end{Bmatrix}_q^{-1} \psi_i(0, k_3, k_3, k_4, k_5, k_5, \dots) \\ &= (-1)^{k_3+k_4+k_5} \sqrt{[d_{k_3}][d_{k_5}]} \psi_i(0, k_3, k_3, k_4, k_5, k_5, \dots). \end{aligned} \tag{B.53}$$

We conclude with Theorem 6.3.2. □

B.5 Proofs of propositions in Chapter 7

Proof B.5.1 (Proof of Proposition 7.2.1)**.**

Recall that the coherent spin network state for a tetrahedron graph is

$$\sum_{\{j_e\}} s^{\text{cohe}}_{\text{tet}}(g_e) = \int_{\text{SU}(2)^4} \prod_{v=1}^{4} \mathrm{d}h_v \, e^{\sum_{e=1}^{6} [\tilde{\zeta}_e | h_{t(e)}^{-1} g_e h_{s(e)} | \zeta_e \rangle}. \tag{B.54}$$

The evaluation on identity gives the vertex amplitude (7.47). To glue the vertex amplitudes associated to adjacent tetrahedra, we make use of the identity in the representation space $\mathcal{V}^j \otimes \mathcal{V}^{*j}$ spanned by the coherent states [143]

$$\mathbb{I}_{\mathcal{V}^j\otimes\mathcal{V}^{*j}} = \frac{1}{(2j)!}\int \mathrm{d}\mu(\zeta)|j,\zeta\rangle\langle j,\zeta| = \frac{1}{(2j)!}\int \mathrm{d}\mu(\zeta)|j,\zeta][j,\zeta|\,. \tag{B.55}$$

To do the gluing, we will use the following identity,

$$\begin{aligned}
&\int \mathrm{d}\mu(\xi_1)\int \mathrm{d}\mu(\xi_2)\, e^{[\zeta|g|\xi_1\rangle+\langle\xi_1|\xi_2]+[\xi_2|h|\zeta'\rangle}\\
=&\sum_{j,k,l\in\mathbb{N}/2}\frac{1}{(2j)!(2k)!(2l)!}\int \mathrm{d}\mu(\xi_1)\int \mathrm{d}\mu(\xi_2)\,[j,\zeta|g|j,\xi_1\rangle\langle k,\xi_1|k,\xi_2][l,\xi_2|h|l,\zeta'\rangle\\
=&\sum_{j\in\mathbb{N}/2}\frac{1}{(2j)!}[j,\zeta|gh|j,\zeta'\rangle = e^{[\zeta|gh|\zeta'\rangle}\,.
\end{aligned}$$

We have used (B.55) to obtained the third line. This product rule can be applied to contract terms between adjacent tetrahedra, say T_1 and T_2, connected with the triangle whose 2D dual is a node v, while 3D dual is an oriented dual edge e^*. Say the source dual vertex $s(e^*)$ is dual to T_1 and the target $t(e^*)$ is dual to T_2. Consider the graphs $(\partial T_1)^*$ and $(\partial T_2)^*$ both including the node v. To identify the triangles from T_1 and T_2 is to identify the three links $e, e', e'' \in v$ from the two graphs. However, the spinors associated to links from different graphs are different. For instance, consider a link $e \in v$, the spinor $\zeta_e^{T_1}$ (or $\zeta_e^{s(e^*)}$ with the dual language) on $(\partial T_1)^*$ is not the same as $\zeta_e^{T_2}$ (or $\zeta_e^{t(e^*)}$) on $(\partial T_2)^*$. Integrating over the relevant terms from vertex amplitudes of $s(e^*)$ and $t(e^*)$, and the edge amplitude of e^*, one gets (we write only integration for one link e for short)

$$\begin{aligned}
&\int \mathrm{d}\mu(\zeta_e^{s(e^*)})\int \mathrm{d}\mu(\zeta_e^{t(e^*)})\, e^{[\zeta^{v_1}|\left(h_{v_1}^{T_1}\right)^{-1}h_v^{T_1}|\zeta_e^{s(e^*)}\rangle}\, e^{\langle\zeta_e^{s(e^*)}|\zeta_e^{t(e^*)}]}\, e^{[\zeta^{t(e^*)}|\left(h_v^{T_2}\right)^{-1}h_{v_2}^{T_2}|\zeta^{v_2}\rangle}\\
=&e^{[\zeta^{v_1}|\left(h_{v_1}^{T_1}\right)^{-1}h_v^{T_1}\left(h_v^{T_2}\right)^{-1}h_{v_2}^{T_2}|\zeta^{v_2}\rangle} = e^{[\zeta^{v_1}|\left(h_{v_1}^{T_1}\right)^{-1}h_v h_{v_2}^{T_2}|\zeta^{v_2}\rangle}\,,
\end{aligned} \tag{B.56}$$

with $h_v \equiv h_v^{T_1}\left(h_v^{T_2}\right)^{-1}$.

The contraction (B.56) can be repeatedly performed along a closed chain $(e_1^*e_2^*...e_n^*e_1^*) \in T^*$ (or equivalently $(\triangle_1\triangle_2\cdots\triangle_n\triangle_1 \in T)$ surrounding an edge $\bar{e}$ shared by n tetrahedra, as illustrated in fig.7.3. The edge amplitude can be absorbed into the vertex amplitudes. As a result, one simply flips of the spinors $[\zeta_e^{t(e^*)}|$ associated to the target $t(e^*)$ of e^* to

their dual $\langle\zeta_e^{t(e^*)}|$ and identify the spinors for the same link from different tetrahedra. In this way, then the gluing of a close chain of tetrahedra reads

$$\int\prod_{i=1}^{n}\mathrm{d}\mu(\zeta^{v_i})e^{\langle\zeta^{v_1}|\left(h_{v_1}^{T_1}\right)^{-1}h_{v_2}^{T_1}|\zeta^{v_2}\rangle+\langle\zeta^{v_2}|\left(h_{v_2}^{T_2}\right)^{-1}h_{v_3}^{T_2}|\zeta^{v_3}\rangle+\cdots+\langle\zeta^{v_n}|\left(h_{v_n}^{T_n}\right)^{-1}h_{v_1}^{T_n}|\zeta^{v_1}\rangle}$$
$$=\int\mathrm{d}\mu(\zeta^{v_1})e^{\langle\zeta^{v_1}|G_{\bar{e}}|\zeta^{v_1}\rangle}\quad(B.57)$$

with $G_{\bar{e}}\equiv\left(h_{v_1}^{T_1}\right)^{-1}h_{v_2}h_{v_3}\cdots h_{v_n}h_{v_1}^{T_n}$. Different from the magnetic number basis, each dual plaquette is weighted by a factor $\langle\zeta^{v_1}|G_{\bar{e}}|\zeta^{v_1}\rangle$ depending on the the spinor attached to the (randomly chosen) base node v_1 and the Wilson loop around the dual plaquette, or a factor $(\langle\zeta^{v_1}|\zeta^{v_1}\rangle-1)$ (or $(\langle\zeta^{f^*,T_1}|\zeta^{f^*,T_1}\rangle-1)$ depending only on the spinor attached to the v_1 [74]. At the end of the day, one gets the partition function expressed as

$$\begin{aligned}Z_{\mathbf{T}}[\mathcal{M},\partial\mathcal{M}]&=\int_{\mathrm{SU}(2)}\left(\prod_{v\in\Gamma}\mathrm{d}h_v\right)\prod_{f^*\in\mathbf{T}^*}\int\mathrm{d}\mu(\zeta^{v_1})(1+\langle\zeta^{v_1}|G_{\bar{e}}|\zeta^{v_1}\rangle)e^{\langle\zeta^{v_1}|G_{\bar{e}}|\zeta^{v_1}\rangle}\\&=\int_{\mathrm{SU}(2)}\left(\prod_{v\in\Gamma}\mathrm{d}h_v\right)\prod_{f^*\in\mathbf{T}^*}\int\mathrm{d}\mu(\zeta^{v_1})(\langle\zeta^{v_1}|\zeta^{v_1}\rangle-1\rangle)e^{\langle\zeta^{v_1}|G_{\bar{e}}|\zeta^{v_1}\rangle}\\&=\left(\int_{\mathrm{SU}(2)}\prod_{\triangle\in T}\mathrm{d}h_{\triangle}\right)\prod_{\bar{e}\in\mathbf{T}}\delta(G_{\bar{e}})=\left(\int_{\mathrm{SU}(2)}\prod_{e^*}\mathrm{d}g_{e^*}\right)\prod_{f^*}\delta(\overrightarrow{\prod}_{e^*\in\partial f^*}g_{e^*})\,,\end{aligned}\quad(B.58)$$

where an integration by part is used to get the second line. This matches the results by using the spin network basis as shown in Subsection 7.1.2. □

Proof B.5.2 (Proof of Proposition 7.2.2)**.**

This is a re-arrangement of the vertex amplitude and edge amplitude compared to (7.47)-(7.49). The difference between (7.47) and (7.51) is a factorial factor. We first apply the identity

$$\frac{1}{(n-1)!}=\frac{1}{2\pi i}\oint_{|s|=r_0}\mathrm{d}s\frac{e^s}{s^n}\quad(B.59)$$

to rewrite the vertex amplitude (7.47) so that it is related to the SGF (7.50):

$$s_{\mathrm{tet}}^{\mathrm{cohe}}(\mathbb{l})=\sum_{j_1\cdots j_6}\left(\prod_{v=1}^{4}\frac{1}{2\pi i}\oint\mathrm{d}s_v\frac{e^{s_v}}{s_v^{J_v+2}}(J_v+1)!\int_{\mathrm{SU}(2)}\mathrm{d}h_v\right)\prod_{e=1}^{6}\frac{1}{(2j_e)!}[j_e,\zeta_e|h_{t(e)}^{-1}h_{s(e)}|j_e,\tilde{\zeta}_e\rangle\,.\quad(B.60)$$

Then we expand the exponential of the edge amplitude (7.48)

$$e^{\sum_{e\in v}\langle\zeta_e^{s(e^*)}|\zeta_e^{t(e^*)}]} = \sum_{k_1\cdots k_3\in\mathbb{N}/2}\prod_{e\in v}\frac{\langle k_e,\zeta_e^{s(e^*)}|k_e,\zeta_e^{t(e^*)}]}{(2k_e)!}\,. \tag{B.61}$$

The spinor integration in the total amplitude expression will select $k_e \equiv j_e$, $\forall e$ from (B.60) and (B.61), thus we are safe to redefine $J_v = \sum_{e\in v} k_e$. This moves the contour integral from the vertex amplitude to the edge amplitude, leaving the vertex amplitude purely given by the SGF. As such, each edge amplitude absorbs two contour integrals, one from the tetrahedron $s(e^*)$ and the other from $t(e^*)$, and is written as

$$\begin{aligned}
\mathcal{A}_{e^*}(\{\zeta_e\},\{w_e\}) &= \frac{1}{(2\pi i)^2}\oint \mathrm{d}s\oint \mathrm{d}t\,\frac{e^{s+t}}{(st)^2}\sum_{k_1\cdots k_3\in\mathbb{N}/2}\prod_{e\in v}\frac{1}{(st)^{k_e}}\frac{\langle k_e,\zeta_e^{s(e^*)}|k_e,\zeta_e^{t(e^*)}]}{(2k_e)!}\\
&= \frac{1}{(2\pi i)^2}\oint \mathrm{d}s\oint \mathrm{d}t\,\frac{1}{(st)^2}e^{s+t+\frac{1}{\sqrt{st}}\sum_{e\in v}\langle\zeta_e^{s(e^*)}|\xi_e^{t(e^*)}]}\\
&= \frac{1}{(2\pi i)^2}\oint \mathrm{d}s\oint \mathrm{d}t\sum_{k,m,n\in\mathbb{N}}\frac{1}{k!m!n!}s^{k-2-\frac{n}{2}}\,t^{m-2-\frac{n}{2}}\left(\sum_{e\in v}\langle\zeta_e^{s(e^*)}|\xi_e^{t(e^*)}]\right)^k\\
&= \sum_{k=0}^{\infty}\frac{1}{(k+1)!^2(2k)!}\left(\sum_{e\in v}\langle\zeta_e^{s(e^*)}|\xi_e^{t(e^*)}]\right)^{2k}\\
&= {}_0F_3(;2,2,\frac{1}{2};\frac{\left(\sum_{e\in v}\langle\zeta_e^{s(e^*)}|\xi_e^{t(e^*)}]\right)^2}{4})
\end{aligned} \tag{B.62}$$

thus (7.52). We have used the identity $\langle k_e,\zeta_e^{s(e^*)}|k_e,\zeta^{t(e^*)}] \equiv \langle\zeta_e^{s(e^*)}|\xi_e^{t(e^*)}]^{2k_e}$ to get the second line. To arrived at the fourth line, we have identified n with $2k-2$ and m with k followed with a change of variable $k\to k+1$ since $\frac{1}{2\pi i}\oint \mathrm{d}t\,t^n = 1$ for $n=-1$ and zero otherwise. □

Proof B.5.3 (Proof of Proposition 7.2.4)**.**

Let us write explicitly, using the definition of the scaleless spin network state (7.54), the relevant part of the right-hand side of (7.55) in terms of the spinors on the two triangles to be glued (see fig.7.4a). Denote the links on (the dual of) the boundary $\partial\mathbf{C}_1$ of the left 3-cell as e's. For each link e, the source $s(e)$ (*resp.* target $t(e)$) is assigned a spinor ζ_e (*resp.* $\tilde{\zeta}_e$) and an auxiliary spinor γ_e (*resp.* $\tilde{\gamma}_e$). Also, denote the links on (the dual of)

the boundary $\partial\mathbf{C}_2$ of the right 3-cell as c's. For each link c, the source $s(c)$ (*resp.* target $t(c)$) is assigned a spinor ξ_c (*resp.* $\tilde{\xi}_c$) and an auxiliary spinor η_c (*resp.* $\tilde{\eta}_c$). With no loss of generality, we can fix the orientation of the relevant links. We fix that the links e_1, e_2, e_3 on the left triangle are outgoing from the node dual to the left triangle and c_1, c_2, c_3 are incoming towards the node dual to the right triangle. Let $\mathbf{C}_1$ to be the source of the dual edge dual to the glued triangle and $\mathbf{C}_2$ the target, then the edge amplitude for the gluing is

$$\mathcal{A}_{e^*}^{\partial\mathbf{C}_1\cap\partial\mathbf{C}_2} = {}_0F_3(;2,2,\frac{1}{2};\frac{\left(\sum_{e=1}^3\langle\zeta_e|\tilde{\xi}_e]\right)^2}{4}) = \sum_{k=0}^{\infty}\frac{1}{(k+1)!^2(2k)!}\left(\sum_{e=1}^3\langle\zeta_e|\tilde{\xi}_e]\right)^{2k}.$$

The right hand side of (7.55) reads

$$\begin{aligned}
&\int\left(\prod_{e'}\mathrm{d}\mu(\gamma_{e'})\mathrm{d}\mu(\tilde{\gamma}_{e'})\prod_{c'}\mathrm{d}\mu(\eta_{c'})\mathrm{d}\mu(\tilde{\eta}_{c'})\right)\\
&\exp\left[\sum_{e'}\langle\gamma_{e'}|\tilde{\gamma}_{e'}]+\sum_{c'}\langle\eta_{c'}|\tilde{\eta}_{c'}]+\sum_{\alpha'}[\zeta_{s(\alpha')}|\zeta_{t(\alpha')}\rangle[\gamma_{s(\alpha')}|\gamma_{t(\alpha')}\rangle+\sum_{\beta'}[\xi_{s(\beta')}|\xi_{t(\beta')}\rangle[\eta_{s(\beta')}|\eta_{t(\beta')}\rangle\right]\\
&\int\left(\prod_{e=1}^3\mathrm{d}\mu(\gamma_e)\mathrm{d}\mu(\tilde{\eta}_e)\right)e^{\sum_{e=1}^3(\langle\gamma_e|\tilde{\gamma}_e]+\langle\eta_e|\tilde{\eta}_e])}\int\left(\prod_{e=1}^3\mathrm{d}\mu(\zeta_e)\mathrm{d}\mu(\tilde{\xi}_e)\right)\\
&\exp\left[\sum_{\substack{e,e'=1,2,3\\ e\prec e'}}[\zeta_e|\zeta_{e'}\rangle[\gamma_e|\gamma_{e'}\rangle+[\tilde{\xi}_e|\tilde{\xi}_{e'}\rangle[\tilde{\eta}_e|\tilde{\eta}_{e'}\rangle\right]\left(\sum_{l\in\mathbb{N}}\frac{1}{(l+1)!^2(2l)!}\left(\sum_{e=1}^3\langle\zeta_e|\tilde{\xi}_e]\right)^{2l}\right).
\end{aligned}\tag{B.63}$$

We have denoted the irrelevant part with primes in the first line. The second line till the first term in the fourth line is the part of $\mathcal{S}^{\mathfrak{sl}}_{\partial\mathbf{C}_1}(\{\zeta_e,\tilde{\zeta}_e\})$ and $\mathcal{S}^{\mathfrak{sl}}_{\partial\mathbf{C}_2}(\{\xi_c,\tilde{\xi}_c\})$ relevant to the triangles to be glued. The last term in the fourth line is the edge amplitude gluing $\mathbf{C}_1$ and $\mathbf{C}_2$. We first perform the spinor integration for $\zeta_{1,2,3}$ and $\tilde{\xi}_{1,2,3}$.

Let us introduce the complex triples, following Bargmann's trick [28],

$$\begin{aligned}
&a=(\zeta_1^-,\zeta_2^-,\zeta_3^-),\quad b=(\zeta_1^+,\zeta_2^+,\zeta_3^+),\quad c=(\tilde{\xi}_1^-,\tilde{\xi}_2^-,\tilde{\xi}_3^-),\quad d=(\tilde{\xi}_1^+,\tilde{\xi}_2^+,\tilde{\xi}_3^+),\\
&\alpha=(\gamma_1^-,\gamma_2^-,\gamma_3^-),\quad \beta=(\gamma_1^+,\gamma_2^+,\gamma_3^+),\quad \sigma=(\tilde{\eta}_1^-,\tilde{\eta}_2^-,\tilde{\eta}_3^-),\quad \rho=(\tilde{\eta}_1^+,\tilde{\eta}_2^+,\tilde{\eta}_3^+).
\end{aligned}\tag{B.64}$$

$\bar{a}=(\bar{a}_1,\bar{a}_2,\bar{a}_3)^T$ is the conjugate of a, and we denote the measure for the a as $\mathrm{d}\mu_3(a)=\frac{1}{\pi^3}\mathrm{d}a_1\mathrm{d}\bar{a}_1\mathrm{d}a_2\mathrm{d}\bar{a}_2\mathrm{d}a_3\mathrm{d}\bar{a}_3$. Likewise for $b,c,d,\alpha,\beta,\sigma,\rho$. For simplicity, we also denote $\Xi=$

$\alpha \times \beta = ([\xi_2|\xi_3\rangle, [\gamma_3|\gamma_1\rangle, [\gamma_1|\gamma_2\rangle)$ and $\Psi = \sigma \times \rho = ([\tilde{\eta}_2|\tilde{\eta}_3\rangle, [\tilde{\eta}_3|\tilde{\eta}_1\rangle, [\tilde{\eta}_1|\tilde{\eta}_2\rangle$. We then arrange them in the matrices

$$\mathbf{A} = \begin{pmatrix} \Xi_1 & \Xi_2 & \Xi_3 \\ a_1 & a_2 & a_3 \\ b_1 & b_2 & b_3 \end{pmatrix}, \quad \mathbf{B} = \begin{pmatrix} \Psi_1 & \Psi_2 & \Psi_3 \\ c_1 & c_2 & c_3 \\ d_1 & d_2 & d_3 \end{pmatrix}, \quad \mathbf{\Gamma} = \begin{pmatrix} 0 & 0 & 0 \\ 0 & 0 & -1 \\ 0 & 1 & 0 \end{pmatrix}. \tag{B.65}$$

One can thus rewrite the integral of $\zeta_{1,2,3}$ and $\tilde{\xi}_{1,2,3}$ in the second and third lines of (B.63) in a compact way:

$$\begin{aligned} &\frac{1}{(2\pi i)^2}\oint \mathrm{d}t \oint \mathrm{d}s \frac{e^{s+t}}{(st)^2} \int \left(\prod_{e=1}^{3} \mathrm{d}\mu(\zeta_e)\mathrm{d}\mu(\tilde{\xi}_e)\right) e^{\det \mathbf{A}+\det \mathbf{B}+\frac{1}{\sqrt{st}}\mathrm{Tr}(\mathbf{A}^\dagger \mathbf{\Gamma} \bar{\mathbf{B}})} \\ =&\frac{1}{(2\pi i)^2}\oint \mathrm{d}t \oint \mathrm{d}s \frac{e^{s+t}}{(st)^2} \int \mathrm{d}\mu_3(a)\mathrm{d}\mu_3(b)\mathrm{d}\mu_3(c)\mathrm{d}\mu_3(d) \\ &e^{-\bar{a}\cdot a-\bar{b}\cdot b-\bar{c}\cdot c-\bar{d}\cdot d} e^{(\Xi\times b)\cdot a+(\Psi\times d)\cdot c} e^{\frac{1}{\sqrt{st}}(\bar{b}\cdot\bar{c}-\bar{a}\cdot\bar{d})}, \end{aligned} \tag{B.66}$$

where we have used the contour integral expression for the inverse Gamma function $\frac{1}{(l+1)!} = \frac{1}{2\pi i}\oint \mathrm{d}t \frac{e^t}{t^{l+2}}$. One can calculate this Gaussian integral for a, b, c, d one by one. Note that for a complex n-ple bfv and a complex $n \times n$ matrix A whose Hermitian part is positive definite, one has the Gaussian integral

$$\int \mathrm{d}\mu_n(\mathbf{v}) e^{-\bar{\mathbf{v}}\cdot A\mathbf{v}+\mathbf{u}\cdot\mathbf{v}+\mathbf{u}'\cdot\bar{\mathbf{v}}} = \det A^{-1} e^{\mathbf{u}\cdot A^{-1}\mathbf{u}'}, \tag{B.67}$$

where $\mathbf{u}$ and $\mathbf{u}'$ are independent n-ples.

After integrating out a, b, c, one can use (B.67) to perform the remaining integral for d:

$$\int \mathrm{d}\mu_3(d)\, e^{-\bar{d}\cdot d}\, e^{\frac{1}{st}(\Psi\times\bar{d})\cdot(\Xi\times d)} = \int \mathrm{d}\mu_3(d)\, e^{\bar{d}\cdot(\mathbb{I}-\frac{M}{st})d} = \frac{1}{\det(\mathbb{I}-\frac{M}{st})} = \frac{1}{(1-\frac{\Psi\cdot\Xi}{st})^2}, \tag{B.68}$$

where the matrix M has entries

$$M_{ij} = (\Psi\cdot\Xi)\delta_{ij} - \Psi_i\Xi_j, \quad i,j = 1,2,3 \tag{B.69}$$

so that $\bar{d}\cdot Md = (\Psi\cdot\Xi)(\bar{d}\cdot d) - (\Psi\cdot d)(\Xi\cdot\bar{d}) = (\Psi\times\bar{d})\cdot(\Xi\times d)$. The explicit form of $\Psi\cdot\Xi$ is

$$\begin{aligned} \Psi\cdot\Xi =&(\alpha\times\beta)\cdot(\sigma\times\rho) = (\alpha\cdot\sigma)(\beta\cdot\rho) - (\alpha\cdot\rho)(\beta\cdot\sigma) \\ =&[\gamma_1|\gamma_2\rangle[\tilde{\eta}_1|\tilde{\eta}_2\rangle + [\gamma_2|\gamma_3\rangle[\tilde{\eta}_2|\tilde{\eta}_3\rangle + [\gamma_3|\gamma_1\rangle[\tilde{\eta}_3|\tilde{\eta}_1\rangle. \end{aligned} \tag{B.70}$$

Now we perform the counter integral to complete the integration in (B.66):

$$\begin{aligned}
&\frac{1}{(2\pi i)^2}\oint \mathrm{d}t \oint \mathrm{d}s \frac{e^{s+t}}{(st)^2}\frac{1}{(1-\frac{\Psi\cdot\Xi}{st})^2}\\
=&\frac{1}{(2\pi i)^2}\oint \mathrm{d}t \oint \mathrm{d}s \sum_{m,n,k=0}^{\infty}\frac{k+1}{m!n!}\frac{s^m t^n}{s^2t^2}\left(\frac{\Psi\cdot\Xi}{st}\right)^k\\
=&\sum_{k=0}^{\infty}\frac{1}{k!(k+1)!}(\Psi\cdot\Xi)^k\\
=&C_1(\Psi\cdot\Xi)\,,
\end{aligned} \tag{B.71}$$

where $C_1(z)$ is the Bessel-Clifford function of order one. A Bessel-Clifford function of order n expands as $C_n(x) := \sum_{k=0}^{\infty}\frac{x^k}{k!(k+n)!}$. The explicit form (B.70) of $\Psi\cdot\Xi$ allows us to express $C_1(\Psi\cdot\Xi)$ into an SU(2) integral by the following beautiful identity [37]

$$\int_{\mathrm{SU}(2)}\mathrm{d}g\, e^{\sum_i[\zeta_i|g|\tilde{\zeta}_i\rangle} = \sum_{k=0}^{\infty}\frac{1}{k!(k+1)!}\left(\sum_{i<j}[\zeta_i|\zeta_j\rangle[\tilde{\zeta}_i|\tilde{\zeta}_j\rangle\right)^k\,,\quad \forall\zeta_i,\tilde{\zeta}_i\in\mathbb{C}^2\,. \tag{B.72}$$

Therefore,

$$C_1(\Psi\cdot\Xi) = \int_{\mathrm{SU}(2)}\mathrm{d}g\, e^{\sum_{e=1}^3[\gamma_e|g|\tilde{\eta}_e\rangle}\,. \tag{B.73}$$

We next combine this result with the integral of the auxiliary spinors in the second line of (B.63). It is straightforward to calculate that

$$\begin{aligned}
&\int_{\mathrm{SU}(2)}\mathrm{d}g\int\left(\prod_{e=1}^3\mathrm{d}\mu(\gamma_e)\mathrm{d}\mu(\tilde{\eta}_e)\right)e^{\sum_{e=1}^3(\langle\eta_e|\tilde{\eta}_e]+[\tilde{\eta}_e|g|\gamma_e\rangle+\langle\gamma_e|\tilde{\gamma}_e])}\\
=&\int_{\mathrm{SU}(2)}\mathrm{d}g\, e^{\sum_{e=1}^3\langle\eta_e|g|\tilde{\gamma}_e]}
\end{aligned} \tag{B.74}$$

Finally, one performs the SU(2) transformation with g on all the auxiliary spinors $(\gamma_e,\tilde{\gamma}_e)\to(g\gamma_e\,, g\tilde{\gamma}_e)$ from $\mathbf{C}_1$, which preserves the inner products $\langle\gamma_{e'}|\tilde{\gamma}_{e'}]$ and $[\gamma_{s(\alpha')}|\gamma_{t(\alpha')}\rangle$ of the irrelevant auxiliary spinors (see the first line of (B.63)). Thanks to the SU(2)-invariant property of the spinor Haar measure, one can rewrite (B.74) into $\int_{\mathrm{SU}(2)}\mathrm{d}g\, e^{\sum_{e=1}^3\langle\eta_e|\tilde{\gamma}_e]} = e^{\sum_{e=1}^3\langle\eta_e|\tilde{\gamma}_e]}$, which is exactly the link term for a general scaleless spin network state (see (7.54) and fig.7.4b). Combining this result with the irrelevant part in the first line of (B.63), one arrives at a scaleless spin network state $\mathcal{S}^{\mathfrak{sl}}_{\partial(\mathbf{C}_1\cup\mathbf{C}_2)}$ on the union boundary $\mathbf{C}_1\cup\mathbf{C}_2$ after gluing. □

Proof B.5.4 (Proof of Proposition 7.2.5)**.**

Before gluing, the 3-cell boundary $\partial\mathbf{C}$ and the dual graph is as shown in fig.7.5a. The right-hand side of (7.56) reads (we again denote the irrelevant part with primes.)

$$\int \left(\prod_{e'} \mathrm{d}\mu(\gamma_{e'}) \prod_{e'} \mathrm{d}\mu(\tilde{\gamma}_{e'})\right) e^{\sum_{e'}\langle\gamma_{e'}|\tilde{\gamma}_{e'}]+\sum_{\alpha'}[\zeta_{s(\alpha')}|\zeta_{t(\alpha')}\rangle[\gamma_{s(\alpha')}|\gamma_{t(\alpha')}\rangle}$$
$$\int \left(\prod_{e=1}^{3} \mathrm{d}\mu(\gamma_e)\mathrm{d}\mu(\tilde{\eta}_e)\right) e^{\langle\gamma_1|\tilde{\eta}_1]+\sum_{e=1}^{2}(\langle\gamma_e|\tilde{\gamma}_e]+\langle\eta_e|\tilde{\eta}_e])}$$
$$\int \left(\prod_{e=1}^{3} \mathrm{d}\mu(\zeta_e)\mathrm{d}\mu(\tilde{\xi}_e)\right) \exp\left[\sum_{\substack{e,e'=1,2,3\\ e\prec e'}} [\zeta_e|\zeta_{e'}\rangle[\gamma_e|\gamma_{e'}\rangle + [\tilde{\xi}_e|\tilde{\xi}_{e'}\rangle[\tilde{\eta}_e|\tilde{\eta}_{e'}\rangle\right]$$
$$\left(\sum_{l\in\mathbb{N}} \frac{1}{(l+1)!^2(2l)!}\left(\sum_{e=1}^{3}\langle\zeta_e|\tilde{\xi}_e]\right)^{2l}\right)(\langle\zeta_1|\zeta_1\rangle - 1)\,. \quad \text{(B.75)}$$

With no loss of generality, we have fixed the half links incident to the left node to be outgoing and denote the spinors and auxiliary spinors on these half links to be $\zeta_{1,2,3}$ and $\gamma_{1,2,3}$ respectively, and fixed the half links incident to the right node to be incoming and denote the spinors and auxiliary spinors on these half links to be $\tilde{\xi}_{1,2,3}$ and $\tilde{\eta}_{1,2,3}$ respectively. The difference of the relevant integral in (B.75) (the last three lines) from that in (B.63) are the terms $e^{\langle\gamma_1|\tilde{\eta}_1]}$, since the two auxiliary spinors ξ_1 and $\tilde{\eta}_1$ are from the same link e_1, and $(\langle\zeta_1|\zeta_1\rangle - 1)$ which is the face amplitude on edge $\bar{e}$ given that the left node is chosen to be the base node.

We now claim that the face amplitude $(\langle\zeta_1|\zeta_1\rangle - 1)$ can be replaced by $(\langle\gamma_1|\gamma_1\rangle - 1)$ without changing the amplitude. To prove that, we first rewrite $e^{\langle\gamma_1|\tilde{\eta}_1]}$ by introducing two intermediate spinor integrals,

$$e^{\langle\gamma_1|\tilde{\eta}_1]} = \int \mathrm{d}\mu(\tilde{\gamma}_1)\mathrm{d}\mu(\eta_1) e^{\langle\gamma_1|\tilde{\gamma}_1]+\langle\eta_1|\tilde{\eta}_1]}\, e^{[\tilde{\gamma}_1|\eta_1\rangle} \quad \text{(B.76)}$$

so that the second line in (B.75) can be expressed in a symmetric way:

$$\int \mathrm{d}\mu(\tilde{\gamma}_1)\mathrm{d}\mu(\eta_1) e^{[\tilde{\gamma}_1|\eta_1\rangle} \int \left(\prod_{e=1}^{3} \mathrm{d}\mu(\gamma_e)\mathrm{d}\mu(\tilde{\eta}_e)\right) e^{\sum_{e=1}^{3}(\langle\gamma_e|\tilde{\gamma}_e]+\langle\eta_e|\tilde{\eta}_e])}\,. \quad \text{(B.77)}$$

We next notice for the edge amplitude that each term of the summation is a homogenous holomorphic polynomial of spinors $\zeta_{1,2,3}$ and $\tilde{\xi}_{1,2,3}$ of order $2l$. Each term of order $2l$ can survive under the spinor integration only by matching with a homogenous anti-holomorphic polynomial of spinors $\zeta_{1,2,3}$ and $\tilde{\xi}_{1,2,3}$ of order $2l$. This means we can safely move the term $\sum_{l\in\mathbb{N}}\frac{1}{(l+1)!^2}$ from the last line of (B.75) to the third line, then the last two lines become

$$\begin{aligned}
&\int\left(\prod_{e=1}^{3}\mathrm{d}\mu(\zeta_e)\mathrm{d}\mu(\tilde{\xi}_e)\right)\sum_{k\in\mathbb{N}}\frac{1}{k!}\left(\sum_{\substack{e,e'=1,2,3\\ e\prec e'}}[\zeta_e|\zeta_{e'}\rangle[\gamma_e|\gamma_{e'}\rangle+[\tilde{\xi}_e|\tilde{\xi}_{e'}\rangle[\tilde{\eta}_e|\tilde{\eta}_{e'}\rangle\right)^k\delta_{k,2l}\\
&\left(\sum_{l\in\mathbb{N}}\frac{1}{(l+1)!^2(2l)!}\left(\sum_{e=1}^{3}\langle\zeta_e|\tilde{\xi}_e]\right)^{2l}\right)(\langle\zeta_1|\zeta_1\rangle-1)\\
=&\int\left(\prod_{e=1}^{3}\mathrm{d}\mu(\zeta_e)\mathrm{d}\mu(\tilde{\xi}_e)\right)\sum_{l\in\mathbb{N}}\frac{1}{(l+1)!^2(2l)!}\left(\sum_{\substack{e,e'=1,2,3\\ e\prec e'}}[\zeta_e|\zeta_{e'}\rangle[\gamma_e|\gamma_{e'}\rangle+[\tilde{\xi}_e|\tilde{\xi}_{e'}\rangle[\tilde{\eta}_e|\tilde{\eta}_{e'}\rangle\right)^{2l}\\
&e^{\sum_{e=1}^{3}\langle\zeta_e|\tilde{\xi}_e]}(\langle\zeta_1|\zeta_1\rangle-1)\,.
\end{aligned}\tag{B.78}$$

Now the third line in (B.78) is a summation of homogenous holomorphic polynomial of the auxiliary spinors $\xi_{1,2,3}$ and $\tilde{\eta}_{1,2,3}$, each of order $2l$. For the same reason, one can further move the term $\sum_{l\in\mathbb{N}}\frac{1}{(l+1)!^2}$ to the second line of (B.75). We also separate $zeta_e$ and $\tilde{\xi}_e$ in the last line of (B.78) by adding six intermediate spinor integral over $\tilde{\zeta}_{1,2,3}$ and $\xi_{1,2,3}$. As a result, the last three lines of (B.75) can be rewritten as

$$\begin{aligned}
&\int\mathrm{d}\mu(\tilde{\gamma}_1)\mathrm{d}\mu(\eta_1)e^{[\tilde{\gamma}_1|\eta_1\rangle}\int\left(\prod_{e=1}^{3}\mathrm{d}\mu(\gamma_e)\mathrm{d}\mu(\tilde{\eta}_e)\right)\sum_{l\in\mathbb{N}}\frac{1}{(l+1)!^2(2l)!}\left(\sum_{e=1}^{3}(\langle\gamma_e|\tilde{\gamma}_e]+\langle\eta_e|\tilde{\eta}_e])\right)^{2l}\\
&\int\left(\prod_{e=1}^{3}\mathrm{d}\mu(\zeta_e)\mathrm{d}\mu(\tilde{\xi}_e)\right)\exp\left[\sum_{\substack{e,e'=1,2,3\\ e\prec e'}}[\zeta_e|\zeta_{e'}\rangle[\gamma_e|\gamma_{e'}\rangle+[\tilde{\xi}_e|\tilde{\xi}_{e'}\rangle[\tilde{\eta}_e|\tilde{\eta}_{e'}\rangle\right]\\
&\int\left(\prod_{e=1}^{3}\mathrm{d}\mu(\tilde{\zeta}_e)\mathrm{d}\mu(w_e)\right)e^{\sum_{e=1}^{3}[\tilde{\zeta}_e|\xi_e\rangle}\,e^{\sum_{e=1}^{3}\langle\zeta_e|\tilde{\zeta}_e]+\langle\xi_3|\tilde{\xi}_e]}(\langle\zeta_1|\zeta_1\rangle-1)\,.
\end{aligned}\tag{B.79}$$

We now realize from comparing (B.79) and the last three lines of (B.75) that $\xi_{1,2,3}$ and $z_{1,2,3}$ take the exchanged expressions. This means one can simply replace the face amplitude $(\langle z_1|z_1\rangle - 1)$ in (B.75) with $(\langle \xi_1|\xi_1\rangle - 1)$ without changing the total amplitude. This allows us to use the same Bargmann's trick as in (B.64)-(B.71) as well as the identity (B.73) so that the last three lines of (B.75) arrives at

$$\begin{aligned}
&\int \mathrm{d}\mu(\tilde{\gamma}_1)\mathrm{d}\mu(\eta_1)\mathrm{d}\mu(\gamma_1) e^{[\tilde{\gamma}_1|\eta_1\rangle} \int_{\mathrm{SU}(2)} \mathrm{d}g\, e^{\langle\gamma_1|\tilde{\gamma}_1] + \langle\eta_1|g|\gamma_1\rangle}\, e^{\langle\eta_2|g|\tilde{\gamma}_2] + \langle\eta_3|g|\tilde{\gamma}_3]} (\langle\gamma_1|\gamma_1\rangle - 1) \\
&= \int_{\mathrm{SU}(2)} \mathrm{d}g \int \mathrm{d}\mu(\gamma_1)(\langle\gamma_1|\gamma_1\rangle - 1) e^{\langle\gamma_1|g|\gamma_1\rangle} e^{\langle\eta_2|g|\tilde{\gamma}_2] + \langle\eta_3|g|\tilde{\gamma}_3]} \\
&= \int_{\mathrm{SU}(2)} \mathrm{d}g\, \delta(g)\, e^{\langle\eta_2|g|\tilde{\gamma}_2] + \langle\eta_3|g|\tilde{\gamma}_3]} = e^{\langle\eta_2|\tilde{\gamma}_2] + \langle\eta_3|\tilde{\gamma}_3]}\,,
\end{aligned} \tag{B.80}$$

which is the link-term for a general scaleless spin network state. To arrive at the third line of (B.80), we have used the identity for delta distribution on SU(2)

$$\delta(g) = \int \mathrm{d}\mu(\zeta)(\langle\zeta|\zeta\rangle - 1) e^{\langle\zeta|g|\zeta\rangle}\,. \tag{B.81}$$

Combining the result of (B.80) and the irrelevant part in the first line of (B.75), one arrives at a scaleless spin network state $\mathcal{S}^{\mathfrak{sl}}_{\partial\mathbf{C}'}$ on the 3-cell boundary $\partial\mathbf{C}'$ after gluing. □

Proof B.5.5 (Proof of Proposition 7.2.6)**.**

This gluing can be visualized as collapsing a cone into a triangle bounded with two edges connecting the apex and two points on the base circle, as shown in fig.7.6a. With no loss of generality, we again consider half links associated to one of the nodes (the left one in fig.7.6a) are outgoing and are assigned the spinors $\zeta_{1,2,3}$ and half-links associated to the other node are incoming and are assigned spinors $\tilde{\xi}_{1,2,3}$. With this setting, it is not hard to get a similar expression for the relevant part of the right-hand side of (7.58) as in (B.80) after integrating out $\zeta_{1,2,3}$, $\tilde{\xi}_{1,2,3}$ and other auxiliary spinors, which takes the form (we use here the spinors $zeta_{1,2}$ instead of the auxiliary spinors $\gamma_{1,2}$ as in (B.80) which does not change the final result.)

$$\begin{aligned}
&\int_{\mathrm{SU}(2)} \mathrm{d}g \int \mathrm{d}\mu(z_1)(\langle z_1|z_1\rangle - 1)\, e^{\langle z_1|g|z_1\rangle}\, e^{\langle z_2|g|z_2\rangle - \langle z_2|z_2\rangle} e^{\langle\eta_4|g|\tilde{\xi}_3]} \\
=&\int_{\mathrm{SU}(2)} \mathrm{d}g\, \delta(g) e^{\langle z_2|g|z_2\rangle - \langle z_2|z_2\rangle} e^{\langle\eta_4|\tilde{\xi}_3]} \\
=&e^{\langle\eta_4|\tilde{\xi}_3]}\,.
\end{aligned} \tag{B.82}$$

The result is again the link-term for the general scaleless spin network state. Together with the irrelevant part of the right-hand side of (7.58), we arrive at the scaleless spin network state for the 3-cell boundary after gluing, thus the left-hand side of (7.58). □

Proof B.5.6 (Proof of Proposition 7.3.1)**.**

We consider $w_{e,e',e''}$ with $e, e', e'' \in v$ to be the configurations of the propagator and obtain the stationary points by the vanishing derivative of $\bar{w}_{e,e',e''}$. For instance, the derivatives of $\bar{w}_e^{0,1}$ give

$$\begin{aligned}
\frac{\partial P(\{\zeta_e\},\{\xi_e\})}{\partial \bar{\xi}_e^0} &= \bar{\zeta}_e^1 \sum_{k=0}^{\infty} \frac{2k}{(k+1)!^2(2k)!} \mathbf{z}^{2k-1} e^{-\mathbf{r}^2} - \xi_e^0 \, {}_0F_3(;2,2,\frac{1}{2};\frac{\mathbf{z}^2}{4}) e^{-\mathbf{r}^2} \\
&= \bar{\zeta}_e^1 \, {}_0F_3(;3,3,\frac{3}{2};\frac{\mathbf{z}^2}{4})\, \mathbf{z}\, e^{-\mathbf{r}^2} - \xi_e^0 \, {}_0F_3(;2,2,\frac{1}{2};\frac{\mathbf{z}^2}{4}) e^{-\mathbf{r}^2} = 0\,, \\
\frac{\partial P(\{\zeta_e\},\{\xi_e\})}{\partial \bar{\xi}_e^1} &= -\bar{\zeta}_e^0 \sum_{k=0}^{\infty} \frac{2k}{(k+1)!^2(2k)!} \mathbf{z}^{2k-1} e^{-\mathbf{r}^2} - \xi_e^1 \, {}_0F_3(;2,2,\frac{1}{2};\frac{\mathbf{z}^2}{4}) e^{-\mathbf{r}^2} \\
&= -\bar{\zeta}_e^0 \, {}_0F_3(;3,3,\frac{3}{2};\frac{\mathbf{z}^2}{4})\, \mathbf{z}\, e^{-\mathbf{r}^2} - \xi_e^1 \, {}_0F_3(;2,2,\frac{1}{2};\frac{\mathbf{z}^2}{4}) e^{-\mathbf{r}^2} = 0\,.
\end{aligned}$$

This saddle point formula is valid for the spinors $\xi_e, \xi_{e'}, \xi_{e''}$ associated to three links incident to the same node, thus there are totally six such formulas, which can be summarized as follows. Denote $A := {}_0F_3(;3,3,\frac{3}{2};\frac{\mathbf{z}^2}{4})\, \mathbf{z}\, e^{-\mathbf{r}^2}$ and $B := {}_0F_3(;2,2,\frac{1}{2};\frac{\mathbf{z}^2}{4}) e^{-\mathbf{r}^2}$, then

$$\left|\begin{array}{lcll} A|\zeta_e] & + & B|\xi_e\rangle & = 0 \\ A|\zeta_{e'}] & + & B|\xi_{e'}\rangle & = 0 \\ A|\zeta_{e''}] & + & B|\xi_{e''}\rangle & = 0 \end{array}\right| \quad \longrightarrow \quad \left|\begin{array}{lcl} B^2[\xi_e|\xi_{e'}\rangle & = & A^2\langle\zeta_e|\zeta_{e'}] \\ B^2[\xi_{e'}|\xi_{e''}\rangle & = & A^2\langle\zeta_{e'}|\zeta_{e''}] \\ B^2[\xi_{e''}|\xi_e\rangle & = & A^2\langle\zeta_{e''}|\zeta_e] \end{array}\right| . \tag{B.83}$$

The corresponding angle coupling from different tetrahedra have the same ratio A^2/B^2. Recall the stationary analysis for the angle coupling norms in (7.78). According to the trigonometric identity

$$\tan\frac{\phi_{ee'}}{2}\tan\frac{\phi_{e'e''}}{2} + \tan\frac{\phi_{e'e''}}{2}\tan\frac{\phi_{e''e}}{2} + \tan\frac{\phi_{e''e}}{2}\tan\frac{\phi_{ee'}}{2} = 1\,, \tag{B.84}$$

the angle coupling norms satisfy the closure constraint $|X_{ee'}|^2 + |X_{e'e''}|^2 + |X_{ee''}|^2 = 1$, thus

$$\begin{aligned}
|B|^4 &= |B|^4 \left(|[\xi_e|\xi_{e'}\rangle|^2 + |[\xi_{e'}|\xi_{e''}\rangle|^2 + |[\xi_{e''}|\xi_e\rangle|^2\right) \\
&= |A|^4 \left(|\langle\zeta_e|\zeta_{e'}]|^2 + |\langle\zeta_{e'}|\zeta_{e''}]|^2 + |\langle\zeta_{e''}|\zeta_e]|^2\right) = |A|^4\,.
\end{aligned} \tag{B.85}$$

Taking the norm of the right equations in (B.83), we arrive at (7.80).

□